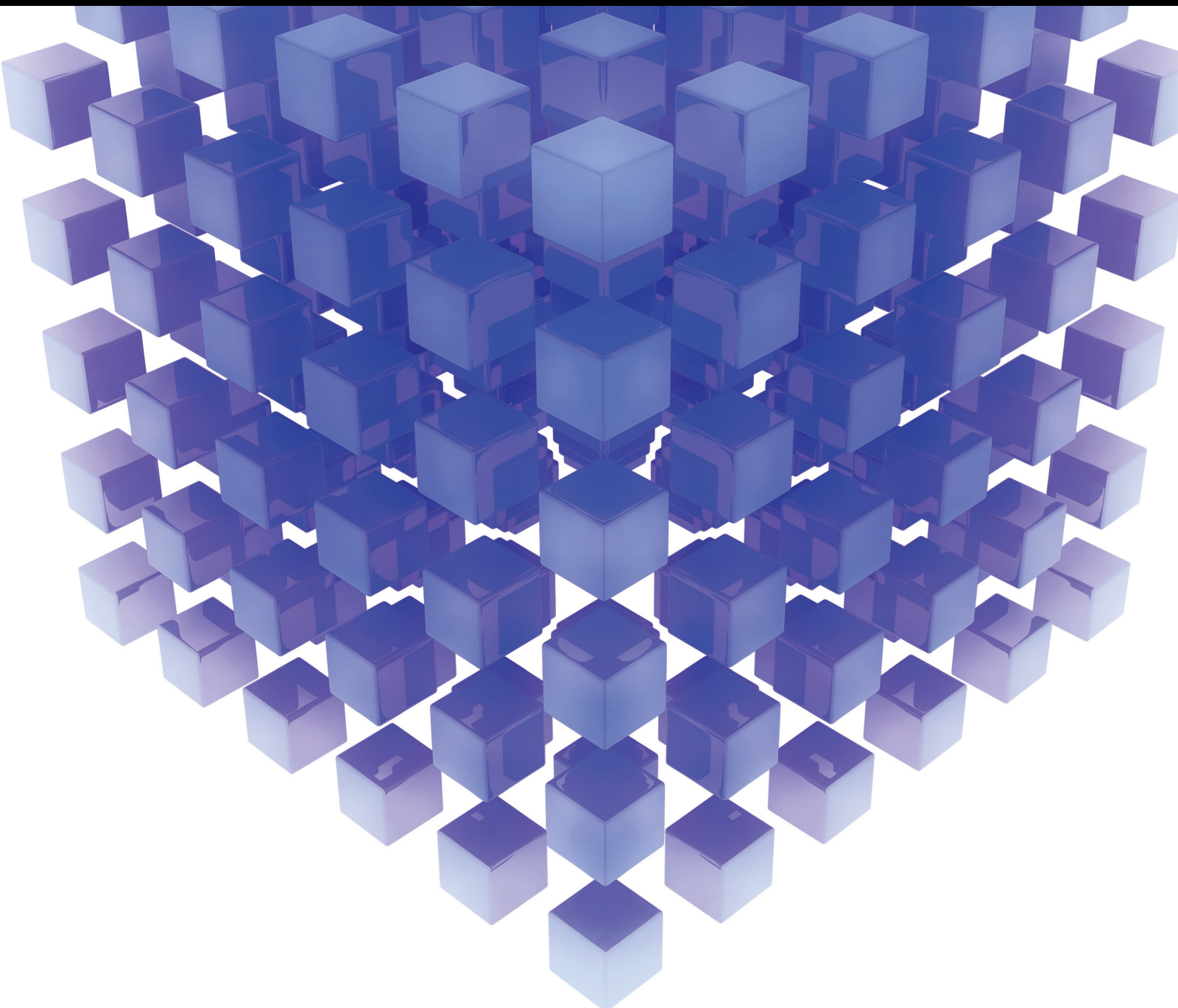


Intelligent Target Detection in Complex Scene Image

Lead Guest Editor: Kai Guo

Guest Editors: Hengchang Jing and Sivakumar B





Intelligent Target Detection in Complex Scene Image

Mathematical Problems in Engineering

Intelligent Target Detection in Complex Scene Image

Lead Guest Editor: Kai Guo


Guest Editors: Hengchang Jing and Sivakumar B



Copyright © 2023 Hindawi Limited. All rights reserved.

This is a special issue published in “Mathematical Problems in Engineering.” All articles are open access articles distributed under the Creative Commons Attribution License, which permits unrestricted use, distribution, and reproduction in any medium, provided the original work is properly cited.

Chief Editor

Guangming Xie , China

Academic Editors

Kumaravel A , India
Waqas Abbasi, Pakistan
Mohamed Abd El Aziz , Egypt
Mahmoud Abdel-Aty , Egypt
Mohammed S. Abdo, Yemen
Mohammad Yaghoub Abdollahzadeh
Jamalabadi , Republic of Korea
Rahib Abiyev , Turkey
Leonardo Acho , Spain
Daniela Addessi , Italy
Arooj Adeel , Pakistan
Waleed Adel , Egypt
Ramesh Agarwal , USA
Francesco Aggogeri , Italy
Ricardo Aguilar-Lopez , Mexico
Afaq Ahmad , Pakistan
Naveed Ahmed , Pakistan
Elias Aifantis , USA
Akif Akgul , Turkey
Tareq Al-shami , Yemen
Guido Ala, Italy
Andrea Alaimo , Italy
Reza Alam, USA
Osamah Albahri , Malaysia
Nicholas Alexander , United Kingdom
Salvatore Alfonzetti, Italy
Ghous Ali , Pakistan
Nouman Ali , Pakistan
Mohammad D. Aliyu , Canada
Juan A. Almendral , Spain
A.K. Alomari, Jordan
José Domingo Álvarez , Spain
Cláudio Alves , Portugal
Juan P. Amezcua-Sanchez, Mexico
Mukherjee Amitava, India
Lionel Amodeo, France
Sebastian Anita, Romania
Costanza Arico , Italy
Sabri Arik, Turkey
Fausto Arpino , Italy
Rashad Asharabi , Saudi Arabia
Farhad Aslani , Australia
Mohsen Asle Zaem , USA

Andrea Avanzini , Italy
Richard I. Avery , USA
Viktor Avrutin , Germany
Mohammed A. Awadallah , Malaysia
Francesco Aymerich , Italy
Sajad Azizi , Belgium
Michele Bacciocchi , Italy
Seungik Baek , USA
Khaled Bahlali, France
M.V.A Raju Bahubalendruni, India
Pedro Balaguer , Spain
P. Balasubramaniam, India
Stefan Balint , Romania
Ines Tejado Balsera , Spain
Alfonso Banos , Spain
Jerzy Baranowski , Poland
Tudor Barbu , Romania
Andrzej Bartoszewicz , Poland
Sergio Baselga , Spain
S. Caglar Baslamisli , Turkey
David Bassir , France
Chiara Bedon , Italy
Azeddine Beghdadi, France
Andriette Bekker , South Africa
Francisco Beltran-Carbajal , Mexico
Abdellatif Ben Makhlof , Saudi Arabia
Denis Benasciutti , Italy
Ivano Benedetti , Italy
Rosa M. Benito , Spain
Elena Benvenuti , Italy
Giovanni Berselli, Italy
Michele Betti , Italy
Pietro Bia , Italy
Carlo Bianca , France
Simone Bianco , Italy
Vincenzo Bianco, Italy
Vittorio Bianco, Italy
David Bigaud , France
Sardar Muhammad Bilal , Pakistan
Antonio Bilotta , Italy
Sylvio R. Bistafa, Brazil
Chiara Boccaletti , Italy
Rodolfo Bontempo , Italy
Alberto Borboni , Italy
Marco Bortolini, Italy

Paolo Boscariol, Italy
Daniela Boso , Italy
Guillermo Botella-Juan, Spain
Abdesselem Boulkroune , Algeria
Boulaïd Boulkroune, Belgium
Fabio Bovenga , Italy
Francesco Braghin , Italy
Ricardo Branco, Portugal
Julien Bruchon , France
Matteo Bruggi , Italy
Michele Brun , Italy
Maria Elena Bruni, Italy
Maria Angela Butturi , Italy
Bartłomiej Błachowski , Poland
Dhanamjayulu C , India
Raquel Caballero-Águila , Spain
Filippo Cacace , Italy
Salvatore Caddemi , Italy
Zuowei Cai , China
Roberto Caldelli , Italy
Francesco Cannizzaro , Italy
Maosen Cao , China
Ana Carpio, Spain
Rodrigo Carvajal , Chile
Caterina Casavola, Italy
Sara Casciati, Italy
Federica Caselli , Italy
Carmen Castillo , Spain
Inmaculada T. Castro , Spain
Miguel Castro , Portugal
Giuseppe Catalanotti , United Kingdom
Alberto Cavallo , Italy
Gabriele Cazzulani , Italy
Fatih Vehbi Celebi, Turkey
Miguel Cerrolaza , Venezuela
Gregory Chagnon , France
Ching-Ter Chang , Taiwan
Kuei-Lun Chang , Taiwan
Qing Chang , USA
Xiaoheng Chang , China
Prasenjit Chatterjee , Lithuania
Kacem Chehdi, France
Peter N. Cheimets, USA
Chih-Chiang Chen , Taiwan
He Chen , China
























Kebing Chen , China
Mengxin Chen , China
Shyi-Ming Chen , Taiwan
Xizhong Chen , Ireland
Xue-Bo Chen , China
Zhiwen Chen , China
Qiang Cheng, USA
Zeyang Cheng, China
Luca Chiapponi , Italy
Francisco Chicano , Spain
Tirivanhu Chinyoka , South Africa
Adrian Chmielewski , Poland
Seongim Choi , USA
Gautam Choubey , India
Hung-Yuan Chung , Taiwan
Yusheng Ci, China
Simone Cinquemani , Italy
Roberto G. Citarella , Italy
Joaquim Ciurana , Spain
John D. Clayton , USA
Piero Colajanni , Italy
Giuseppina Colicchio, Italy
Vassilios Constantoudis , Greece
Enrico Conte, Italy
Alessandro Contento , USA
Mario Cools , Belgium
Gino Cortellessa, Italy
Carlo Cosentino , Italy
Paolo Crippa , Italy
Erik Cuevas , Mexico
Guozeng Cui , China
Mehmet Cunkas , Turkey
Giuseppe D'Aniello , Italy
Peter Dabnichki, Australia
Weizhong Dai , USA
Zhifeng Dai , China
Purushothaman Damodaran , USA
Sergey Dashkovskiy, Germany
Adiel T. De Almeida-Filho , Brazil
Fabio De Angelis , Italy
Samuele De Bartolo , Italy
Stefano De Miranda , Italy
Filippo De Monte , Italy

José António Fonseca De Oliveira
Correia , Portugal
Jose Renato De Sousa , Brazil
Michael Defoort, France
Alessandro Della Corte, Italy
Laurent Dewasme , Belgium
Sanku Dey , India
Gianpaolo Di Bona , Italy
Roberta Di Pace , Italy
Francesca Di Puccio , Italy
Ramón I. Diego , Spain
Yannis Dimakopoulos , Greece
Hasan Dinçer , Turkey
José M. Domínguez , Spain
Georgios Dounias, Greece
Bo Du , China
Emil Dumic, Croatia
Madalina Dumitriu , United Kingdom
Premraj Durairaj , India
Saeed Eftekhari Azam, USA
Said El Kafhali , Morocco
Antonio Elipse , Spain
R. Emre Erkmen, Canada
John Escobar , Colombia
Leandro F. F. Miguel , Brazil
FRANCESCO FOTI , Italy
Andrea L. Facci , Italy
Shahla Faisal , Pakistan
Giovanni Falsone , Italy
Hua Fan, China
Jianguang Fang, Australia
Nicholas Fantuzzi , Italy
Muhammad Shahid Farid , Pakistan
Hamed Faruqi, Iran
Yann Favennec, France
Fiorenzo A. Fazzolari , United Kingdom
Giuseppe Fedele , Italy
Roberto Fedele , Italy
Baowei Feng , China
Mohammad Ferdows , Bangladesh
Arturo J. Fernández , Spain
Jesus M. Fernandez Oro, Spain
Francesco Ferrise, Italy
Eric Feulvarch , France
Thierry Floquet, France

Eric Florentin , France
Gerardo Flores, Mexico
Antonio Forcina , Italy
Alessandro Formisano, Italy
Francesco Franco , Italy
Elisa Francomano , Italy
Juan Frausto-Solis, Mexico
Shujun Fu , China
Juan C. G. Prada , Spain
HECTOR GOMEZ , Chile
Matteo Gaeta , Italy
Mauro Gaggero , Italy
Zoran Gajic , USA
Jaime Gallardo-Alvarado , Mexico
Mosè Gallo , Italy
Akemi Gálvez , Spain
Maria L. Gandarias , Spain
Hao Gao , Hong Kong
Xingbao Gao , China
Yan Gao , China
Zhiwei Gao , United Kingdom
Giovanni Garcea , Italy
José García , Chile
Harish Garg , India
Alessandro Gasparetto , Italy
Stylianios Georgantzinou, Greece
Fotios Georgiades , India
Parviz Ghadimi , Iran
Ştefan Cristian Gherghina , Romania
Georgios I. Giannopoulos , Greece
Agathoklis Giaralis , United Kingdom
Anna M. Gil-Lafuente , Spain
Ivan Giorgio , Italy
Gaetano Giunta , Luxembourg
Jefferson L.M.A. Gomes , United Kingdom
Emilio Gómez-Déniz , Spain
Antonio M. Gonçalves de Lima , Brazil
Qunxi Gong , China
Chris Goodrich, USA
Rama S. R. Gorla, USA
Veena Goswami , India
Xunjie Gou , Spain
Jakub Grabski , Poland

Antoine Grall , France
George A. Gravvanis , Greece
Fabrizio Greco , Italy
David Greiner , Spain
Jason Gu , Canada
Federico Guarracino , Italy
Michele Guida , Italy
Muhammet Gul , Turkey
Dong-Sheng Guo , China
Hu Guo , China
Zhaoxia Guo, China
Yusuf Gurefe, Turkey
Salim HEDDAM , Algeria
ABID HUSSANAN, China
Quang Phuc Ha, Australia
Li Haitao , China
Petr Hájek , Czech Republic
Mohamed Hamdy , Egypt
Muhammad Hamid , United Kingdom
Renke Han , United Kingdom
Weimin Han , USA
Xingsi Han, China
Zhen-Lai Han , China
Thomas Hanne , Switzerland
Xinan Hao , China
Mohammad A. Hariri-Ardebili , USA
Khalid Hattaf , Morocco
Defeng He , China
Xiao-Qiao He, China
Yanchao He, China
Yu-Ling He , China
Ramdane Hedjar , Saudi Arabia
Jude Hemanth , India
Reza Hemmati, Iran
Nicolae Herisanu , Romania
Alfredo G. Hernández-Díaz , Spain
M.I. Herreros , Spain
Eckhard Hitzer , Japan
Paul Honeine , France
Jaromir Horacek , Czech Republic
Lei Hou , China
Yingkun Hou , China
Yu-Chen Hu , Taiwan
Yunfeng Hu, China
Can Huang , China
Gordon Huang , Canada
Linsheng Huo , China
Sajid Hussain, Canada
Asier Ibeas , Spain
Orest V. Iftime , The Netherlands
Przemyslaw Ignaciuk , Poland
Giacomo Innocenti , Italy
Emilio Insfran Pelozo , Spain
Azeem Irshad, Pakistan
Alessio Ishizaka, France
Benjamin Ivorra , Spain
Breno Jacob , Brazil
Reema Jain , India
Tushar Jain , India
Amin Jajarmi , Iran
Chiranjibe Jana , India
Łukasz Jankowski , Poland
Samuel N. Jator , USA
Juan Carlos Jáuregui-Correa , Mexico
Kandasamy Jayakrishna, India
Reza Jazar, Australia
Khalide Jbilou, France
Isabel S. Jesus , Portugal
Chao Ji , China
Qing-Chao Jiang , China
Peng-fei Jiao , China
Ricardo Fabricio Escobar Jiménez , Mexico
Emilio Jiménez Macías , Spain
Maolin Jin, Republic of Korea
Zhuo Jin, Australia
Ramash Kumar K , India
BHABEN KALITA , USA
MOHAMMAD REZA KHEDMATI , Iran
Viacheslav Kalashnikov , Mexico
Mathiyalagan Kalidass , India
Tamas Kalmar-Nagy , Hungary
Rajesh Kaluri , India
Jyottheswara Reddy Kalvakurthi, India
Zhao Kang , China
Ramani Kannan , Malaysia
Tomasz Kapitaniak , Poland
Julius Kaplunov, United Kingdom
Konstantinos Karamanos, Belgium
Michal Kawulok, Poland

Irfan Kaymaz , Turkey
Vahid Kayvanfar , Qatar
Krzysztof Kecik , Poland
Mohamed Khader , Egypt
Chaudry M. Khalique , South Africa
Mukhtaj Khan , Pakistan
Shahid Khan , Pakistan
Nam-Il Kim, Republic of Korea
Philipp V. Kiryukhantsev-Korneev ,
Russia
P.V.V Kishore , India
Jan Koci , Czech Republic
Ioannis Kostavelis , Greece
Sotiris B. Kotsiantis , Greece
Frederic Kratz , France
Vamsi Krishna , India
Edyta Kucharska, Poland
Krzysztof S. Kulpa , Poland
Kamal Kumar, India
Prof. Ashwani Kumar , India
Michal Kunicki , Poland
Cedrick A. K. Kwuimy , USA
Kyandoghere Kyamakya, Austria
Ivan Kyrchei , Ukraine
Márcio J. Lacerda , Brazil
Eduardo Lalla , The Netherlands
Giovanni Lancioni , Italy
Jaroslaw Latalski , Poland
Hervé Laurent , France
Agostino Lauria , Italy
Aimé Lay-Ekuakille , Italy
Nicolas J. Leconte , France
Kun-Chou Lee , Taiwan
Dimitri Lefebvre , France
Eric Lefevre , France
Marek Lefik, Poland
Yaguo Lei , China
Kauko Leiviskä , Finland
Ervin Lenzi , Brazil
ChenFeng Li , China
Jian Li , USA
Jun Li , China
Yueyang Li , China
Zhao Li , China































Zhen Li , China
En-Qiang Lin, USA
Jian Lin , China
Qibin Lin, China
Yao-Jin Lin, China
Zhiyun Lin , China
Bin Liu , China
Bo Liu , China
Heng Liu , China
Jianxu Liu , Thailand
Lei Liu , China
Sixin Liu , China
Wanquan Liu , China
Yu Liu , China
Yuanchang Liu , United Kingdom
Bonifacio Llamazares , Spain
Alessandro Lo Schiavo , Italy
Jean Jacques Loiseau , France
Francesco Lolli , Italy
Paolo Lonetti , Italy
António M. Lopes , Portugal
Sebastian López, Spain
Luis M. López-Ochoa , Spain
Vassilios C. Loukopoulos, Greece
Gabriele Maria Lozito , Italy
Zhiguo Luo , China
Gabriel Luque , Spain
Valentin Lychagin, Norway
YUE MEI, China
Junwei Ma , China
Xuanlong Ma , China
Antonio Madeo , Italy
Alessandro Magnani , Belgium
Toqeer Mahmood , Pakistan
Fazal M. Mahomed , South Africa
Arunava Majumder , India
Sarfranz Nawaz Malik, Pakistan
Paolo Manfredi , Italy
Adnan Maqsood , Pakistan
Muazzam Maqsood, Pakistan
Giuseppe Carlo Marano , Italy
Damijan Markovic, France
Filipe J. Marques , Portugal
Luca Martinelli , Italy
Denizar Cruz Martins, Brazil

Francisco J. Martos , Spain
Elio Masciari , Italy
Paolo Massioni , France
Alessandro Mauro , Italy
Jonathan Mayo-Maldonado , Mexico
Pier Luigi Mazzeo , Italy
Laura Mazzola, Italy
Driss Mehdi , France
Zahid Mehmood , Pakistan
Roderick Melnik , Canada
Xiangyu Meng , USA
Jose Merodio , Spain
Alessio Merola , Italy
Mahmoud Mesbah , Iran
Luciano Mescia , Italy
Laurent Mevel , France
Constantine Michailides , Cyprus
Mariusz Michta , Poland
Prankul Middha, Norway
Aki Mikkola , Finland
Giovanni Minafò , Italy
Edmondo Minisci , United Kingdom
Hiroyuki Mino , Japan
Dimitrios Mitsotakis , New Zealand
Ardashir Mohammadzadeh , Iran
Francisco J. Montáns , Spain
Francesco Montefusco , Italy
Gisele Mophou , France
Rafael Morales , Spain
Marco Morandini , Italy
Javier Moreno-Valenzuela , Mexico
Simone Morganti , Italy
Caroline Mota , Brazil
Aziz Moukrim , France
Shen Mouquan , China
Dimitris Mourtzis , Greece
Emiliano Mucchi , Italy
Taseer Muhammad, Saudi Arabia
Ghulam Muhiuddin, Saudi Arabia
Amitava Mukherjee , India
Josefa Mula , Spain
Jose J. Muñoz , Spain
Giuseppe Muscolino, Italy
Marco Mussetta , Italy

Hariharan Muthusamy, India
Alessandro Naddeo , Italy
Raj Nandkeolyar, India
Keivan Navaie , United Kingdom
Soumya Nayak, India
Adrian Neagu , USA
Erivelton Geraldo Nepomuceno , Brazil
AMA Neves, Portugal
Ha Quang Thinh Ngo , Vietnam
Nhon Nguyen-Thanh, Singapore
Papakostas Nikolaos , Ireland
Jelena Nikolic , Serbia
Tatsushi Nishi, Japan
Shanzhou Niu , China
Ben T. Nohara , Japan
Mohammed Nouari , France
Mustapha Nourelfath, Canada
Kazem Nouri , Iran
Ciro Núñez-Gutiérrez , Mexico
Włodzimierz Ogryczak, Poland
Roger Ohayon, France
Krzysztof Okarma , Poland
Mitsuhiro Okayasu, Japan
Murat Olgun , Turkey
Diego Oliva, Mexico
Alberto Olivares , Spain
Enrique Onieva , Spain
Calogero Orlando , Italy
Susana Ortega-Cisneros , Mexico
Sergio Ortobelli, Italy
Naohisa Otsuka , Japan
Sid Ahmed Ould Ahmed Mahmoud , Saudi Arabia
Taoreed Owolabi , Nigeria
EUGENIA PETROPOULOU , Greece
Arturo Pagano, Italy
Madhumangal Pal, India
Pasquale Palumbo , Italy
Dragan Pamučar, Serbia
Weifeng Pan , China
Chandan Pandey, India
Rui Pang, United Kingdom
Jürgen Pannek , Germany
Elena Panteley, France
Achille Paolone, Italy

George A. Papakostas , Greece
Xosé M. Pardo , Spain
You-Jin Park, Taiwan
Manuel Pastor, Spain
Pubudu N. Pathirana , Australia
Surajit Kumar Paul , India
Luis Payá , Spain
Igor Pažanin , Croatia
Libor Pekař , Czech Republic
Francesco Pellicano , Italy
Marcello Pellicciari , Italy
Jian Peng , China
Mingshu Peng, China
Xiang Peng , China
Xindong Peng, China
Yuxing Peng, China
Marzio Pennisi , Italy
Maria Patrizia Pera , Italy
Matjaz Perc , Slovenia
A. M. Bastos Pereira , Portugal
Wesley Peres, Brazil
F. Javier Pérez-Pinal , Mexico
Michele Perrella, Italy
Francesco Pesavento , Italy
Francesco Petrini , Italy
Hoang Vu Phan, Republic of Korea
Lukasz Pieczonka , Poland
Dario Piga , Switzerland
Marco Pizzarelli , Italy
Javier Plaza , Spain
Goutam Pohit , India
Dragan Poljak , Croatia
Jorge Pomares , Spain
Hiram Ponce , Mexico
Sébastien Poncet , Canada
Volodymyr Ponomaryov , Mexico
Jean-Christophe Ponsart , France
Mauro Pontani , Italy
Sivakumar Poruran, India
Francesc Pozo , Spain
Aditya Rio Prabowo , Indonesia
Anchasa Pramuanjaroenkij , Thailand
Leonardo Primavera , Italy
B Rajanarayan Prusty, India

Krzysztof Puszynski , Poland
Chuan Qin , China
Dongdong Qin, China
Jianlong Qiu , China
Giuseppe Quaranta , Italy
DR. RITU RAJ , India
Vitomir Racic , Italy
Carlo Rainieri , Italy
Kumbakonam Ramamani Rajagopal, USA
Ali Ramazani , USA
Angel Manuel Ramos , Spain
Higinio Ramos , Spain
Muhammad Afzal Rana , Pakistan
Muhammad Rashid, Saudi Arabia
Manoj Rastogi, India
Alessandro Rasulo , Italy
S.S. Ravindran , USA
Abdolrahman Razani , Iran
Alessandro Reali , Italy
Jose A. Reinoso , Spain
Oscar Reinoso , Spain
Haijun Ren , China
Carlo Renno , Italy
Fabrizio Renno , Italy
Shahram Rezapour , Iran
Ricardo Rianza , Spain
Francesco Riganti-Fulginei , Italy
Gerasimos Rigatos , Greece
Francesco Ripamonti , Italy
Jorge Rivera , Mexico
Eugenio Roanes-Lozano , Spain
Ana Maria A. C. Rocha , Portugal
Luigi Rodino , Italy
Francisco Rodríguez , Spain
Rosana Rodríguez López, Spain
Francisco Rossomando , Argentina
Jose de Jesus Rubio , Mexico
Weiguo Rui , China
Rubén Ruiz , Spain
Ivan D. Rukhlenko , Australia
Dr. Eswaramoorthi S. , India
Weichao SHI , United Kingdom
Chaman Lal Sabharwal , USA
Andrés Sáez , Spain

Bekir Sahin, Turkey
Laxminarayan Sahoo , India
John S. Sakellariou , Greece
Michael Sakellariou , Greece
Salvatore Salamone, USA
Jose Vicente Salcedo , Spain
Alejandro Salcido , Mexico
Alejandro Salcido, Mexico
Nunzio Salerno , Italy
Rohit Salgotra , India
Miguel A. Salido , Spain
Sinan Salih , Iraq
Alessandro Salvini , Italy
Abdus Samad , India
Sovan Samanta, India
Nikolaos Samaras , Greece
Ramon Sancibrian , Spain
Giuseppe Sanfilippo , Italy
Omar-Jacobo Santos, Mexico
J Santos-Reyes , Mexico
José A. Sanz-Herrera , Spain
Musavarah Sarwar, Pakistan
Shahzad Sarwar, Saudi Arabia
Marcelo A. Savi , Brazil
Andrey V. Savkin, Australia
Tadeusz Sawik , Poland
Roberta Sburlati, Italy
Gustavo Scaglia , Argentina
Thomas Schuster , Germany
Hamid M. Sedighi , Iran
Mijanur Rahaman Seikh, India
Tapan Senapati , China
Lotfi Senhadji , France
Junwon Seo, USA
Michele Serpilli, Italy
Silvestar Šesnić , Croatia
Gerardo Severino, Italy
Ruben Sevilla , United Kingdom
Stefano Sfarra , Italy
Dr. Ismail Shah , Pakistan
Leonid Shaikhet , Israel
Vimal Shanmuganathan , India
Prayas Sharma, India
Bo Shen , Germany
Hang Shen, China

Xin Pu Shen, China
Dimitri O. Shepelsky, Ukraine
Jian Shi , China
Amin Shokrollahi, Australia
Suzanne M. Shontz , USA
Babak Shotorban , USA
Zhan Shu , Canada
Angelo Sifaleras , Greece
Nuno Simões , Portugal
Mehakpreet Singh , Ireland
Piyush Pratap Singh , India
Rajiv Singh, India
Seralathan Sivamani , India
S. Sivasankaran , Malaysia
Christos H. Skiadas, Greece
Konstantina Skouri , Greece
Neale R. Smith , Mexico
Bogdan Smolka, Poland
Delfim Soares Jr. , Brazil
Alba Sofi , Italy
Francesco Soldovieri , Italy
Raffaele Solimene , Italy
Yang Song , Norway
Jussi Sopanen , Finland
Marco Spadini , Italy
Paolo Spagnolo , Italy
Ruben Specogna , Italy
Vasilios Spitas , Greece
Ivanka Stamova , USA
Rafał Stanisławski , Poland
Miladin Stefanović , Serbia
Salvatore Strano , Italy
Yakov Strelniker, Israel
Kangkang Sun , China
Qiuqin Sun , China
Shuaishuai Sun, Australia
Yanchao Sun , China
Zong-Yao Sun , China
Kumarasamy Suresh , India
Sergey A. Suslov , Australia
D.L. Suthar, Ethiopia
D.L. Suthar , Ethiopia
Andrzej Swierniak, Poland
Andras Szekrenyes , Hungary
Kumar K. Tamma, USA

Yong (Aaron) Tan, United Kingdom
Marco Antonio Taneco-Hernández , Mexico
Lu Tang , China
Tianyou Tao, China
Hafez Tari , USA
Alessandro Tasora , Italy
Sergio Teggi , Italy
Adriana del Carmen Téllez-Anguiano , Mexico
Ana C. Teodoro , Portugal
Efstathios E. Theotokoglou , Greece
Jing-Feng Tian, China
Alexander Timokha , Norway
Stefania Tomasiello , Italy
Gisella Tomasini , Italy
Isabella Torricollo , Italy
Francesco Tornabene , Italy
Mariano Torrisi , Italy
Thang nguyen Trung, Vietnam
George Tsiatas , Greece
Le Anh Tuan , Vietnam
Nerio Tullini , Italy
Emilio Turco , Italy
Ilhan Tuzcu , USA
Efstratios Tzirtzilakis , Greece
FRANCISCO UREÑA , Spain
Filippo Ubertini , Italy
Mohammad Uddin , Australia
Mohammad Safi Ullah , Bangladesh
Serdar Ulubeyli , Turkey
Mati Ur Rahman , Pakistan
Panayiotis Vafeas , Greece
Giuseppe Vairo , Italy
Jesus Valdez-Resendiz , Mexico
Eusebio Valero, Spain
Stefano Valvano , Italy
Carlos-Renato Vázquez , Mexico
Martin Velasco Villa , Mexico
Franck J. Vernerey, USA
Georgios Veronis , USA
Vincenzo Vespri , Italy
Renato Vidoni , Italy
Venkatesh Vijayaraghavan, Australia

Anna Vila, Spain
Francisco R. Villatoro , Spain
Francesca Vipiana , Italy
Stanislav Vitek , Czech Republic
Jan Vorel , Czech Republic
Michael Vynnycky , Sweden
Mohammad W. Alomari, Jordan
Roman Wan-Wendner , Austria
Bingchang Wang, China
C. H. Wang , Taiwan
Dagang Wang, China
Guoqiang Wang , China
Huaiyu Wang, China
Hui Wang , China
J.G. Wang, China
Ji Wang , China
Kang-Jia Wang , China
Lei Wang , China
Qiang Wang, China
Qingling Wang , China
Weiwei Wang , China
Xinyu Wang , China
Yong Wang , China
Yung-Chung Wang , Taiwan
Zhenbo Wang , USA
Zhibo Wang, China
Waldemar T. Wójcik, Poland
Chi Wu , Australia
Qihong Wu, China
Yuqiang Wu, China
Zhibin Wu , China
Zhizheng Wu , China
Michalis Xenos , Greece
Hao Xiao , China
Xiao Ping Xie , China
Qingzheng Xu , China
Binghan Xue , China
Yi Xue , China
Joseph J. Yame , France
Chuanliang Yan , China
Xinggang Yan , United Kingdom
Hongtai Yang , China
Jixiang Yang , China
Mijia Yang, USA
Ray-Yeng Yang, Taiwan

Zaoli Yang , China
Jun Ye , China
Min Ye , China
Luis J. Yebra , Spain
Peng-Yeng Yin , Taiwan
Muhammad Haroon Yousaf , Pakistan
Yuan Yuan, United Kingdom
Qin Yuming, China
Elena Zaitseva , Slovakia
Arkadiusz Zak , Poland
Mohammad Zakwan , India
Ernesto Zambrano-Serrano , Mexico
Francesco Zammori , Italy
Jessica Zangari , Italy
Rafal Zdunek , Poland
Ibrahim Zeid, USA
Nianyin Zeng , China
Junyong Zhai , China
Hao Zhang , China
Haopeng Zhang , USA
Jian Zhang , China
Kai Zhang, China
Lingfan Zhang , China
Mingjie Zhang , Norway
Qian Zhang , China
Tianwei Zhang , China
Tongqian Zhang , China
Wenyu Zhang , China
Xianming Zhang , Australia
Xuping Zhang , Denmark
Yinyan Zhang, China
Yifan Zhao , United Kingdom
Debao Zhou, USA
Heng Zhou , China
Jian G. Zhou , United Kingdom
Junyong Zhou , China
Xueqian Zhou , United Kingdom
Zhe Zhou , China
Wu-Le Zhu, China
Gaetano Zizzo , Italy
Mingcheng Zuo, China

Contents

Retracted: Optimization of Plane Image Color Enhancement Processing Based on Computer Vision Virtual Reality

Mathematical Problems in Engineering

Retraction (1 page), Article ID 9757931, Volume 2023 (2023)

Retracted: Research and Implementation of Association Analysis of Agricultural Insurance Based on Data Mining Algorithm

Mathematical Problems in Engineering

Retraction (1 page), Article ID 9843130, Volume 2023 (2023)

Retracted: Design of Regression Model for MultiParameter Evaluation of English Pronunciation Quality

Mathematical Problems in Engineering

Retraction (1 page), Article ID 9832149, Volume 2023 (2023)

Retracted: Application of Multimedia Tilt Photogrammetry Technology Based on Unmanned Aerial Vehicle in Geological Survey

Mathematical Problems in Engineering

Retraction (1 page), Article ID 9816709, Volume 2023 (2023)

Retracted: Research on the Financial Support Performance Evaluation of Big Data Industry Development

Mathematical Problems in Engineering

Retraction (1 page), Article ID 9785276, Volume 2023 (2023)

Retracted: Application of 3D Laser Virtual Imaging Technology in Combined Building Interactive Modeling

Mathematical Problems in Engineering

Retraction (1 page), Article ID 9863979, Volume 2023 (2023)

Retracted: Trajectory Tracking of Soccer Motion Based on Multiobject Detection Algorithm

Mathematical Problems in Engineering

Retraction (1 page), Article ID 9838593, Volume 2023 (2023)

Retracted: Nontarget Suppression in Ball Sports Multitarget-Tracking Task

Mathematical Problems in Engineering

Retraction (1 page), Article ID 9808650, Volume 2023 (2023)

Retracted: Application of Multi-Measurement Vector Based on the Wireless Sensor Network in Mechanical Fault Diagnosis

Mathematical Problems in Engineering

Retraction (1 page), Article ID 9798267, Volume 2023 (2023)

Retracted: Video Image Processing Method Based on Cloud Platform Massive Data and Virtual Reality

Mathematical Problems in Engineering

Retraction (1 page), Article ID 9790875, Volume 2023 (2023)

Retracted: Construction of Heritage Digital Resource Platform Based on Digital Twin Technology

Mathematical Problems in Engineering

Retraction (1 page), Article ID 9780602, Volume 2023 (2023)

Retracted: Monitoring and Analysis of Cotton Planting Parameters in Multiareas Based on Multisensor

Mathematical Problems in Engineering

Retraction (1 page), Article ID 9759103, Volume 2023 (2023)

Retracted: Layout Simulation of Prefabricated Building Construction Based on the Markov Model

Mathematical Problems in Engineering

Retraction (1 page), Article ID 9754613, Volume 2023 (2023)

Retracted: Simulation of Video Image Fault Tolerant Coding Transmission in Digital Multimedia

Mathematical Problems in Engineering

Retraction (1 page), Article ID 9846392, Volume 2023 (2023)

Retracted: Design of the Violin Performance Evaluation System Based on Mobile Terminal Technology

Mathematical Problems in Engineering

Retraction (1 page), Article ID 9842526, Volume 2023 (2023)

Retracted: Analysis on Innovation Path of Business Administration Based on Artificial Intelligence

Mathematical Problems in Engineering

Retraction (1 page), Article ID 9836169, Volume 2023 (2023)

Retracted: Application of Cloud Computing Combined with GIS Virtual Reality in Construction Process of Building Steel Structure

Mathematical Problems in Engineering

Retraction (1 page), Article ID 9835319, Volume 2023 (2023)

Retracted: Financial Accounting Information Data Analysis System Based on Internet of Things

Mathematical Problems in Engineering

Retraction (1 page), Article ID 9835289, Volume 2023 (2023)

Retracted: Construction of Hotel Resource Information Platform Based on the Internet of Things Technology

Mathematical Problems in Engineering

Retraction (1 page), Article ID 9831291, Volume 2023 (2023)

Retracted: Parameter Identification of 3D Elastic-Plastic Model for Tunnel Engineering Based on Improved Genetic Algorithm

Mathematical Problems in Engineering

Retraction (1 page), Article ID 9828940, Volume 2023 (2023)

Contents

Retracted: Application of Data Image Encryption Technology in Computer Network Information Security

Mathematical Problems in Engineering

Retraction (1 page), Article ID 9828503, Volume 2023 (2023)

Retracted: Analysis of the Influencing Factors of Urban Sports Brand Sales Volume Based on AHP

Mathematical Problems in Engineering

Retraction (1 page), Article ID 9823237, Volume 2023 (2023)

Retracted: Analysis of Financial Management Target Architecture Based on ISM Model

Mathematical Problems in Engineering

Retraction (1 page), Article ID 9817695, Volume 2023 (2023)

Retracted: Recommendation Model of Tourist Attractions Based on Deep Learning

Mathematical Problems in Engineering

Retraction (1 page), Article ID 9813074, Volume 2023 (2023)

Retracted: Application of Sensor-Based Intelligent Wearable Devices in Information Physical Education

Mathematical Problems in Engineering

Retraction (1 page), Article ID 9802782, Volume 2023 (2023)

Retracted: Automatic Scoring Model of Japanese Interpretation Based on Semantic Scoring

Mathematical Problems in Engineering

Retraction (1 page), Article ID 9791361, Volume 2023 (2023)

Retracted: Parameter Optimization of Educational Network Ecosystem Based on BERT Deep Learning Model

Mathematical Problems in Engineering

Retraction (1 page), Article ID 9790809, Volume 2023 (2023)

Retracted: Application of Neural Network Sample Training Algorithm in Regional Economic Management

Mathematical Problems in Engineering

Retraction (1 page), Article ID 9780809, Volume 2023 (2023)

Retracted: Intelligent Application of Data Mining Model in Chinese International Education

Mathematical Problems in Engineering

Retraction (1 page), Article ID 9762136, Volume 2023 (2023)

Retracted: Design of English Translation Model Based on Recurrent Neural Network

Mathematical Problems in Engineering

Retraction (1 page), Article ID 9760613, Volume 2023 (2023)

Retracted: Vectorization Analysis of Cultural Creative Design Based on the Recognition Model of Virtual Reality Technology

Mathematical Problems in Engineering

Retraction (1 page), Article ID 9757016, Volume 2023 (2023)

Retracted: Based on Virtual Reality Technology Research on Innovation and Design of Ceramic Painting Products

Mathematical Problems in Engineering

Retraction (1 page), Article ID 9754140, Volume 2023 (2023)

Retracted: Volunteer Service Participation Emergency Management Information Collection Platform Based on Big Data Technology

Mathematical Problems in Engineering

Retraction (1 page), Article ID 9896741, Volume 2023 (2023)

Retracted: Remote Human-Computer Interaction and STEM Teacher Online Training Based on Embedded Internet of Things

Mathematical Problems in Engineering

Retraction (1 page), Article ID 9891419, Volume 2023 (2023)

Retracted: Application of Wireless Sensor Network Data Fusion Technology in Mechanical Fault Diagnosis

Mathematical Problems in Engineering

Retraction (1 page), Article ID 9874528, Volume 2023 (2023)

Retracted: The Influence of Brand Visual Communication on Consumer Psychology Based on Deep Learning

Mathematical Problems in Engineering

Retraction (1 page), Article ID 9867964, Volume 2023 (2023)

Retracted: E-Commerce Data Access Control and Encrypted Storage Based on Internet of Things

Mathematical Problems in Engineering

Retraction (1 page), Article ID 9867250, Volume 2023 (2023)

Retracted: Distributed 3D Environment Design System Based on Color Image Model

Mathematical Problems in Engineering

Retraction (1 page), Article ID 9848703, Volume 2023 (2023)

Retracted: Data Analysis and Optimization of English Reading Corpus Based on Feature Extraction

Mathematical Problems in Engineering

Retraction (1 page), Article ID 9836304, Volume 2023 (2023)

Retracted: Analysis of Passenger Flow Characteristics of Urban Rail Transit Based on Spatial Data Dynamic Analysis Technology

Mathematical Problems in Engineering

Retraction (1 page), Article ID 9806035, Volume 2023 (2023)


Contents

Retracted: Intelligent Optimization of the Financial Sharing Path Based on Accounting Big Data

Mathematical Problems in Engineering


Retraction (1 page), Article ID 9768039, Volume 2023 (2023)

Optimization of Physical Education Course Resource Allocation Model Based on Deep Belief Network

Lili Sun 

Research Article (8 pages), Article ID 8457760, Volume 2023 (2023)

[Retracted] Design of Regression Model for MultiParameter Evaluation of English Pronunciation Quality

Ke Chen 


Research Article (7 pages), Article ID 7288443, Volume 2023 (2023)

[Retracted] Vectorization Analysis of Cultural Creative Design Based on the Recognition Model of Virtual Reality Technology

Ying Yang  and Zili Xu



Research Article (7 pages), Article ID 8930240, Volume 2022 (2022)

[Retracted] Intelligent Optimization of the Financial Sharing Path Based on Accounting Big Data

Zhongmin Zhang 


Research Article (8 pages), Article ID 1310994, Volume 2022 (2022)

[Retracted] Analysis of Passenger Flow Characteristics of Urban Rail Transit Based on Spatial Data Dynamic Analysis Technology

Yan Zhang  and Ningchuan Li 


Research Article (9 pages), Article ID 1601169, Volume 2022 (2022)

The Application of Genetic Algorithm in the Optimal Design of Landscape Space Environment

Zhao Liu 


Research Article (12 pages), Article ID 8768974, Volume 2022 (2022)

[Retracted] Nontarget Suppression in Ball Sports Multitarget-Tracking Task

Manchao Li and Liying Zhang 

Research Article (8 pages), Article ID 6848195, Volume 2022 (2022)

[Retracted] Parameter Optimization of Educational Network Ecosystem Based on BERT Deep Learning Model

Sha Tao 


Research Article (9 pages), Article ID 3119014, Volume 2022 (2022)

Application Analysis of Artificial Intelligence Algorithms in Image Processing

Lei Feng 


Research Article (10 pages), Article ID 7382938, Volume 2022 (2022)

[Retracted] The Influence of Brand Visual Communication on Consumer Psychology Based on Deep Learning

Hui Wang 


Research Article (8 pages), Article ID 9599943, Volume 2022 (2022)

[Retracted] Analysis on Innovation Path of Business Administration Based on Artificial Intelligence

Ben Lu 

Research Article (7 pages), Article ID 6790836, Volume 2022 (2022)

[Retracted] Volunteer Service Participation Emergency Management Information Collection Platform Based on Big Data Technology

Daqing Wang 


Research Article (8 pages), Article ID 6813463, Volume 2022 (2022)

[Retracted] Construction of Hotel Resource Information Platform Based on the Internet of Things Technology

Yi Meng 

Research Article (8 pages), Article ID 4898550, Volume 2022 (2022)

[Retracted] Distributed 3D Environment Design System Based on Color Image Model

Kang Huai , Longjiao Ni, Miaomiao Zhu, and Huihui Zhou


Research Article (6 pages), Article ID 9268632, Volume 2022 (2022)

[Retracted] Application of Wireless Sensor Network Data Fusion Technology in Mechanical Fault Diagnosis

Xinle Zhao , Zuhui Shen, and Zhisheng Jing


Research Article (8 pages), Article ID 5707210, Volume 2022 (2022)

[Retracted] Design of the Violin Performance Evaluation System Based on Mobile Terminal Technology

Yixuan Lin 

Research Article (7 pages), Article ID 8269007, Volume 2022 (2022)

[Retracted] Layout Simulation of Prefabricated Building Construction Based on the Markov Model

Xin Jiao 



Research Article (7 pages), Article ID 6882522, Volume 2022 (2022)

Gearbox Fault Diagnosis Based on a Sparse Principal Component-Generalized Regression Neural Network

Yimo Wang  and Yajun Han

Research Article (6 pages), Article ID 1406676, Volume 2022 (2022)


[Retracted] E-Commerce Data Access Control and Encrypted Storage Based on Internet of Things

Yue He  and Wanda Hu 

Research Article (7 pages), Article ID 4547002, Volume 2022 (2022)

Contents

[Retracted] Analysis of the Influencing Factors of Urban Sports Brand Sales Volume Based on AHP

Mingyue Zhang, Yuxin Wu, and Xiaolong Zhou 


Research Article (7 pages), Article ID 9625049, Volume 2022 (2022)

[Retracted] Research on the Financial Support Performance Evaluation of Big Data Industry Development

Wenyu Fu, Jingfeng Zhao , Changming Wang, and Xiaobin Zhou


Research Article (9 pages), Article ID 1972726, Volume 2022 (2022)

[Retracted] Simulation of Video Image Fault Tolerant Coding Transmission in Digital Multimedia

Feng Li 

Research Article (7 pages), Article ID 4657091, Volume 2022 (2022)

[Retracted] Financial Accounting Information Data Analysis System Based on Internet of Things

Yulin Bi 


Research Article (6 pages), Article ID 6162504, Volume 2022 (2022)

[Retracted] Application of Multi-Measurement Vector Based on the Wireless Sensor Network in Mechanical Fault Diagnosis

Wei Kang 


Research Article (7 pages), Article ID 2390119, Volume 2022 (2022)

[Retracted] Automatic Scoring Model of Japanese Interpretation Based on Semantic Scoring

Qin Wang 


Research Article (7 pages), Article ID 3299549, Volume 2022 (2022)

[Retracted] Data Analysis and Optimization of English Reading Corpus Based on Feature Extraction

Nengwei Fan 



Research Article (7 pages), Article ID 1746329, Volume 2022 (2022)

A Genetic Algorithm Model for Human Resource Management Optimization in the Internet Marketing Era

Yi Li and Wang Linna 


Research Article (9 pages), Article ID 6931386, Volume 2022 (2022)

An Enhanced Triadic Color Scheme for Content-Based Image Retrieval

S. K. B. Sangeetha , Sandeep Kumar Mathivanan, Thanapal Pandi, K. Arivu selvan, Prabhu Jayagopal, and Gemmachis Teshite Dalu 

Research Article (6 pages), Article ID 5736630, Volume 2022 (2022)

[Retracted] Analysis of Financial Management Target Architecture Based on ISM Model

Yulin Bi 

Research Article (8 pages), Article ID 3416671, Volume 2022 (2022)

[Retracted] Remote Human-Computer Interaction and STEM Teacher Online Training Based on Embedded Internet of Things

Xinning Wu  and Qian Zhang


Research Article (8 pages), Article ID 2896481, Volume 2022 (2022)

[Retracted] Recommendation Model of Tourist Attractions Based on Deep Learning

Xinquan Cheng  and Wenlong Su


Research Article (7 pages), Article ID 9080818, Volume 2022 (2022)

[Retracted] Intelligent Application of Data Mining Model in Chinese International Education

Feng Wu 


Research Article (7 pages), Article ID 9171551, Volume 2022 (2022)

[Retracted] Trajectory Tracking of Soccer Motion Based on Multiobject Detection Algorithm

Yuping Xie 


Research Article (8 pages), Article ID 3602074, Volume 2022 (2022)

[Retracted] Application of Sensor-Based Intelligent Wearable Devices in Information Physical Education

Wanjun Chen 

Research Article (7 pages), Article ID 5075425, Volume 2022 (2022)

[Retracted] Design of English Translation Model Based on Recurrent Neural Network

Xiaohui Wang 

Research Article (7 pages), Article ID 5177069, Volume 2022 (2022)

[Retracted] Application of Neural Network Sample Training Algorithm in Regional Economic Management

Yan He 


Research Article (7 pages), Article ID 7666331, Volume 2022 (2022)

[Retracted] Parameter Identification of 3D Elastic-Plastic Model for Tunnel Engineering Based on Improved Genetic Algorithm

Xiaoma Dong  and Lifei Chen


Research Article (8 pages), Article ID 8305175, Volume 2022 (2022)

[Retracted] Application of Multimedia Tilt Photogrammetry Technology Based on Unmanned Aerial Vehicle in Geological Survey

Wenyu Li 

Research Article (6 pages), Article ID 4616119, Volume 2022 (2022)


Application of Deep Learning Intelligent Laser Scanning Technology in Mural Digitization

Zhiming Dong 


Research Article (9 pages), Article ID 8439616, Volume 2022 (2022)

Contents

[Retracted] Monitoring and Analysis of Cotton Planting Parameters in Multiareas Based on Multisensor

Zehua Fan, Nannan Zhang, Desheng Wang, Jinhu Zhi, and Xuedong Zhang 
Research Article (8 pages), Article ID 7013745, Volume 2022 (2022)

[Retracted] Application of Cloud Computing Combined with GIS Virtual Reality in Construction Process of Building Steel Structure

Yugang Dong , Haozhi Sui, and Lei Zhu
Research Article (8 pages), Article ID 4299756, Volume 2022 (2022)


[Retracted] Construction of Heritage Digital Resource Platform Based on Digital Twin Technology

Haomei Jia  and Jing Yan
Research Article (8 pages), Article ID 4361135, Volume 2022 (2022)

[Retracted] Optimization of Plane Image Color Enhancement Processing Based on Computer Vision Virtual Reality

Renzheng Xue , Ming Liu, and Zuozheng Lian
Research Article (7 pages), Article ID 9404874, Volume 2022 (2022)

Analysis of China's Regional Economic Competitiveness, Regionalization, and Spatial Aggregation Characteristics Based on Density Clustering Algorithm

Jinglin He  and Rixing Liu
Research Article (11 pages), Article ID 2610711, Volume 2022 (2022)




[Retracted] Research and Implementation of Association Analysis of Agricultural Insurance Based on Data Mining Algorithm

Wen Shao 
Research Article (8 pages), Article ID 3690346, Volume 2022 (2022)

[Retracted] Application of 3D Laser Virtual Imaging Technology in Combined Building Interactive Modeling

Xiaoqiu Ma , Ge Shang, Dandan Liu, and Donglei Ju
Research Article (8 pages), Article ID 8048269, Volume 2022 (2022)


[Retracted] Video Image Processing Method Based on Cloud Platform Massive Data and Virtual Reality

Ming Liu , Renzheng Xue , and Xiaoye Li 
Research Article (7 pages), Article ID 2802901, Volume 2022 (2022)

[Retracted] Application of Data Image Encryption Technology in Computer Network Information Security

Li Li 
Research Article (7 pages), Article ID 8963756, Volume 2022 (2022)

[Retracted] Based on Virtual Reality Technology Research on Innovation and Design of Ceramic Painting Products

Yong Jiang 

Research Article (7 pages), Article ID 4421769, Volume 2022 (2022)

Retraction

Retracted: Optimization of Plane Image Color Enhancement Processing Based on Computer Vision Virtual Reality

Mathematical Problems in Engineering

Received 5 December 2023; Accepted 5 December 2023; Published 6 December 2023

Copyright © 2023 Mathematical Problems in Engineering. This is an open access article distributed under the Creative Commons Attribution License, which permits unrestricted use, distribution, and reproduction in any medium, provided the original work is properly cited.

This article has been retracted by Hindawi, as publisher, following an investigation undertaken by the publisher [1]. This investigation has uncovered evidence of systematic manipulation of the publication and peer-review process. We cannot, therefore, vouch for the reliability or integrity of this article.

Please note that this notice is intended solely to alert readers that the peer-review process of this article has been compromised.

Wiley and Hindawi regret that the usual quality checks did not identify these issues before publication and have since put additional measures in place to safeguard research integrity.

We wish to credit our Research Integrity and Research Publishing teams and anonymous and named external researchers and research integrity experts for contributing to this investigation.

The corresponding author, as the representative of all authors, has been given the opportunity to register their agreement or disagreement to this retraction. We have kept a record of any response received.

References

- [1] R. Xue, M. Liu, and Z. Lian, "Optimization of Plane Image Color Enhancement Processing Based on Computer Vision Virtual Reality," *Mathematical Problems in Engineering*, vol. 2022, Article ID 9404874, 7 pages, 2022.

Retraction

Retracted: Research and Implementation of Association Analysis of Agricultural Insurance Based on Data Mining Algorithm

Mathematical Problems in Engineering

Received 5 December 2023; Accepted 5 December 2023; Published 6 December 2023

Copyright © 2023 Mathematical Problems in Engineering. This is an open access article distributed under the Creative Commons Attribution License, which permits unrestricted use, distribution, and reproduction in any medium, provided the original work is properly cited.

This article has been retracted by Hindawi, as publisher, following an investigation undertaken by the publisher [1]. This investigation has uncovered evidence of systematic manipulation of the publication and peer-review process. We cannot, therefore, vouch for the reliability or integrity of this article.

Please note that this notice is intended solely to alert readers that the peer-review process of this article has been compromised.

Wiley and Hindawi regret that the usual quality checks did not identify these issues before publication and have since put additional measures in place to safeguard research integrity.

We wish to credit our Research Integrity and Research Publishing teams and anonymous and named external researchers and research integrity experts for contributing to this investigation.

The corresponding author, as the representative of all authors, has been given the opportunity to register their agreement or disagreement to this retraction. We have kept a record of any response received.

References

- [1] W. Shao, "Research and Implementation of Association Analysis of Agricultural Insurance Based on Data Mining Algorithm," *Mathematical Problems in Engineering*, vol. 2022, Article ID 3690346, 8 pages, 2022.

Retraction

Retracted: Design of Regression Model for MultiParameter Evaluation of English Pronunciation Quality

Mathematical Problems in Engineering

Received 5 December 2023; Accepted 5 December 2023; Published 6 December 2023

Copyright © 2023 Mathematical Problems in Engineering. This is an open access article distributed under the Creative Commons Attribution License, which permits unrestricted use, distribution, and reproduction in any medium, provided the original work is properly cited.

This article has been retracted by Hindawi, as publisher, following an investigation undertaken by the publisher [1]. This investigation has uncovered evidence of systematic manipulation of the publication and peer-review process. We cannot, therefore, vouch for the reliability or integrity of this article.

Please note that this notice is intended solely to alert readers that the peer-review process of this article has been compromised.

Wiley and Hindawi regret that the usual quality checks did not identify these issues before publication and have since put additional measures in place to safeguard research integrity.

We wish to credit our Research Integrity and Research Publishing teams and anonymous and named external researchers and research integrity experts for contributing to this investigation.

The corresponding author, as the representative of all authors, has been given the opportunity to register their agreement or disagreement to this retraction. We have kept a record of any response received.

References

- [1] K. Chen, "Design of Regression Model for MultiParameter Evaluation of English Pronunciation Quality," *Mathematical Problems in Engineering*, vol. 2023, Article ID 7288443, 7 pages, 2023.

Retraction

Retracted: Application of Multimedia Tilt Photogrammetry Technology Based on Unmanned Aerial Vehicle in Geological Survey

Mathematical Problems in Engineering

Received 5 December 2023; Accepted 5 December 2023; Published 6 December 2023

Copyright © 2023 Mathematical Problems in Engineering. This is an open access article distributed under the Creative Commons Attribution License, which permits unrestricted use, distribution, and reproduction in any medium, provided the original work is properly cited.

This article has been retracted by Hindawi, as publisher, following an investigation undertaken by the publisher [1]. This investigation has uncovered evidence of systematic manipulation of the publication and peer-review process. We cannot, therefore, vouch for the reliability or integrity of this article.

Please note that this notice is intended solely to alert readers that the peer-review process of this article has been compromised.

Wiley and Hindawi regret that the usual quality checks did not identify these issues before publication and have since put additional measures in place to safeguard research integrity.

We wish to credit our Research Integrity and Research Publishing teams and anonymous and named external researchers and research integrity experts for contributing to this investigation.

The corresponding author, as the representative of all authors, has been given the opportunity to register their agreement or disagreement to this retraction. We have kept a record of any response received.

References

- [1] W. Li, "Application of Multimedia Tilt Photogrammetry Technology Based on Unmanned Aerial Vehicle in Geological Survey," *Mathematical Problems in Engineering*, vol. 2022, Article ID 4616119, 6 pages, 2022.

Retraction

Retracted: Research on the Financial Support Performance Evaluation of Big Data Industry Development

Mathematical Problems in Engineering

Received 5 December 2023; Accepted 5 December 2023; Published 6 December 2023

Copyright © 2023 Mathematical Problems in Engineering. This is an open access article distributed under the Creative Commons Attribution License, which permits unrestricted use, distribution, and reproduction in any medium, provided the original work is properly cited.

This article has been retracted by Hindawi, as publisher, following an investigation undertaken by the publisher [1]. This investigation has uncovered evidence of systematic manipulation of the publication and peer-review process. We cannot, therefore, vouch for the reliability or integrity of this article.

Please note that this notice is intended solely to alert readers that the peer-review process of this article has been compromised.

Wiley and Hindawi regret that the usual quality checks did not identify these issues before publication and have since put additional measures in place to safeguard research integrity.

We wish to credit our Research Integrity and Research Publishing teams and anonymous and named external researchers and research integrity experts for contributing to this investigation.

The corresponding author, as the representative of all authors, has been given the opportunity to register their agreement or disagreement to this retraction. We have kept a record of any response received.

References

- [1] W. Fu, J. Zhao, C. Wang, and X. Zhou, "Research on the Financial Support Performance Evaluation of Big Data Industry Development," *Mathematical Problems in Engineering*, vol. 2022, Article ID 1972726, 9 pages, 2022.

Retraction

Retracted: Application of 3D Laser Virtual Imaging Technology in Combined Building Interactive Modeling

Mathematical Problems in Engineering

Received 26 September 2023; Accepted 26 September 2023; Published 27 September 2023

Copyright © 2023 Mathematical Problems in Engineering. This is an open access article distributed under the Creative Commons Attribution License, which permits unrestricted use, distribution, and reproduction in any medium, provided the original work is properly cited.

This article has been retracted by Hindawi following an investigation undertaken by the publisher [1]. This investigation has uncovered evidence of one or more of the following indicators of systematic manipulation of the publication process:

- (1) Discrepancies in scope
- (2) Discrepancies in the description of the research reported
- (3) Discrepancies between the availability of data and the research described
- (4) Inappropriate citations
- (5) Incoherent, meaningless and/or irrelevant content included in the article
- (6) Peer-review manipulation

The presence of these indicators undermines our confidence in the integrity of the article's content and we cannot, therefore, vouch for its reliability. Please note that this notice is intended solely to alert readers that the content of this article is unreliable. We have not investigated whether authors were aware of or involved in the systematic manipulation of the publication process.

Wiley and Hindawi regrets that the usual quality checks did not identify these issues before publication and have since put additional measures in place to safeguard research integrity.

We wish to credit our own Research Integrity and Research Publishing teams and anonymous and named external researchers and research integrity experts for contributing to this investigation.

The corresponding author, as the representative of all authors, has been given the opportunity to register their agreement or disagreement to this retraction. We have kept a record of any response received.

References

- [1] X. Ma, G. Shang, D. Liu, and D. Ju, "Application of 3D Laser Virtual Imaging Technology in Combined Building Interactive Modeling," *Mathematical Problems in Engineering*, vol. 2022, Article ID 8048269, 8 pages, 2022.

Retraction

Retracted: Trajectory Tracking of Soccer Motion Based on Multiobject Detection Algorithm

Mathematical Problems in Engineering

Received 26 September 2023; Accepted 26 September 2023; Published 27 September 2023

Copyright © 2023 Mathematical Problems in Engineering. This is an open access article distributed under the Creative Commons Attribution License, which permits unrestricted use, distribution, and reproduction in any medium, provided the original work is properly cited.

This article has been retracted by Hindawi following an investigation undertaken by the publisher [1]. This investigation has uncovered evidence of one or more of the following indicators of systematic manipulation of the publication process:

- (1) Discrepancies in scope
- (2) Discrepancies in the description of the research reported
- (3) Discrepancies between the availability of data and the research described
- (4) Inappropriate citations
- (5) Incoherent, meaningless and/or irrelevant content included in the article
- (6) Peer-review manipulation

The presence of these indicators undermines our confidence in the integrity of the article's content and we cannot, therefore, vouch for its reliability. Please note that this notice is intended solely to alert readers that the content of this article is unreliable. We have not investigated whether authors were aware of or involved in the systematic manipulation of the publication process.

Wiley and Hindawi regrets that the usual quality checks did not identify these issues before publication and have since put additional measures in place to safeguard research integrity.

We wish to credit our own Research Integrity and Research Publishing teams and anonymous and named external researchers and research integrity experts for contributing to this investigation.

The corresponding author, as the representative of all authors, has been given the opportunity to register their agreement or disagreement to this retraction. We have kept a record of any response received.

References

- [1] Y. Xie, "Trajectory Tracking of Soccer Motion Based on Multiobject Detection Algorithm," *Mathematical Problems in Engineering*, vol. 2022, Article ID 3602074, 8 pages, 2022.

Retraction

Retracted: Nontarget Suppression in Ball Sports Multitarget-Tracking Task

Mathematical Problems in Engineering

Received 26 September 2023; Accepted 26 September 2023; Published 27 September 2023

Copyright © 2023 Mathematical Problems in Engineering. This is an open access article distributed under the Creative Commons Attribution License, which permits unrestricted use, distribution, and reproduction in any medium, provided the original work is properly cited.

This article has been retracted by Hindawi following an investigation undertaken by the publisher [1]. This investigation has uncovered evidence of one or more of the following indicators of systematic manipulation of the publication process:

- (1) Discrepancies in scope
- (2) Discrepancies in the description of the research reported
- (3) Discrepancies between the availability of data and the research described
- (4) Inappropriate citations
- (5) Incoherent, meaningless and/or irrelevant content included in the article
- (6) Peer-review manipulation

The presence of these indicators undermines our confidence in the integrity of the article's content and we cannot, therefore, vouch for its reliability. Please note that this notice is intended solely to alert readers that the content of this article is unreliable. We have not investigated whether authors were aware of or involved in the systematic manipulation of the publication process.

In addition, our investigation has also shown that one or more of the following human-subject reporting requirements has not been met in this article: ethical approval by an Institutional Review Board (IRB) committee or equivalent, patient/participant consent to participate, and/or agreement to publish patient/participant details (where relevant).

Wiley and Hindawi regrets that the usual quality checks did not identify these issues before publication and have since put additional measures in place to safeguard research integrity.

We wish to credit our own Research Integrity and Research Publishing teams and anonymous and named external researchers and research integrity experts for contributing to this investigation.

The corresponding author, as the representative of all authors, has been given the opportunity to register their agreement or disagreement to this retraction. We have kept a record of any response received.

References

- [1] M. Li and L. Zhang, "Nontarget Suppression in Ball Sports Multitarget-Tracking Task," *Mathematical Problems in Engineering*, vol. 2022, Article ID 6848195, 8 pages, 2022.

Retraction

Retracted: Application of Multi-Measurement Vector Based on the Wireless Sensor Network in Mechanical Fault Diagnosis

Mathematical Problems in Engineering

Received 26 September 2023; Accepted 26 September 2023; Published 27 September 2023

Copyright © 2023 Mathematical Problems in Engineering. This is an open access article distributed under the Creative Commons Attribution License, which permits unrestricted use, distribution, and reproduction in any medium, provided the original work is properly cited.

This article has been retracted by Hindawi following an investigation undertaken by the publisher [1]. This investigation has uncovered evidence of one or more of the following indicators of systematic manipulation of the publication process:

- (1) Discrepancies in scope
- (2) Discrepancies in the description of the research reported
- (3) Discrepancies between the availability of data and the research described
- (4) Inappropriate citations
- (5) Incoherent, meaningless and/or irrelevant content included in the article
- (6) Peer-review manipulation

The presence of these indicators undermines our confidence in the integrity of the article's content and we cannot, therefore, vouch for its reliability. Please note that this notice is intended solely to alert readers that the content of this article is unreliable. We have not investigated whether authors were aware of or involved in the systematic manipulation of the publication process.

Wiley and Hindawi regrets that the usual quality checks did not identify these issues before publication and have since put additional measures in place to safeguard research integrity.

We wish to credit our own Research Integrity and Research Publishing teams and anonymous and named external researchers and research integrity experts for contributing to this investigation.

The corresponding author, as the representative of all authors, has been given the opportunity to register their agreement or disagreement to this retraction. We have kept a record of any response received.

References

- [1] W. Kang, "Application of Multi-Measurement Vector Based on the Wireless Sensor Network in Mechanical Fault Diagnosis," *Mathematical Problems in Engineering*, vol. 2022, Article ID 2390119, 7 pages, 2022.

Retraction

Retracted: Video Image Processing Method Based on Cloud Platform Massive Data and Virtual Reality

Mathematical Problems in Engineering

Received 26 September 2023; Accepted 26 September 2023; Published 27 September 2023

Copyright © 2023 Mathematical Problems in Engineering. This is an open access article distributed under the Creative Commons Attribution License, which permits unrestricted use, distribution, and reproduction in any medium, provided the original work is properly cited.

This article has been retracted by Hindawi following an investigation undertaken by the publisher [1]. This investigation has uncovered evidence of one or more of the following indicators of systematic manipulation of the publication process:

- (1) Discrepancies in scope
- (2) Discrepancies in the description of the research reported
- (3) Discrepancies between the availability of data and the research described
- (4) Inappropriate citations
- (5) Incoherent, meaningless and/or irrelevant content included in the article
- (6) Peer-review manipulation

The presence of these indicators undermines our confidence in the integrity of the article's content and we cannot, therefore, vouch for its reliability. Please note that this notice is intended solely to alert readers that the content of this article is unreliable. We have not investigated whether authors were aware of or involved in the systematic manipulation of the publication process.

Wiley and Hindawi regrets that the usual quality checks did not identify these issues before publication and have since put additional measures in place to safeguard research integrity.

We wish to credit our own Research Integrity and Research Publishing teams and anonymous and named external researchers and research integrity experts for contributing to this investigation.

The corresponding author, as the representative of all authors, has been given the opportunity to register their agreement or disagreement to this retraction. We have kept a record of any response received.

References

- [1] M. Liu, R. Xue, and X. Li, "Video Image Processing Method Based on Cloud Platform Massive Data and Virtual Reality," *Mathematical Problems in Engineering*, vol. 2022, Article ID 2802901, 7 pages, 2022.

Retraction

Retracted: Construction of Heritage Digital Resource Platform Based on Digital Twin Technology

Mathematical Problems in Engineering

Received 26 September 2023; Accepted 26 September 2023; Published 27 September 2023

Copyright © 2023 Mathematical Problems in Engineering. This is an open access article distributed under the Creative Commons Attribution License, which permits unrestricted use, distribution, and reproduction in any medium, provided the original work is properly cited.

This article has been retracted by Hindawi following an investigation undertaken by the publisher [1]. This investigation has uncovered evidence of one or more of the following indicators of systematic manipulation of the publication process:

- (1) Discrepancies in scope
- (2) Discrepancies in the description of the research reported
- (3) Discrepancies between the availability of data and the research described
- (4) Inappropriate citations
- (5) Incoherent, meaningless and/or irrelevant content included in the article
- (6) Peer-review manipulation

The presence of these indicators undermines our confidence in the integrity of the article's content and we cannot, therefore, vouch for its reliability. Please note that this notice is intended solely to alert readers that the content of this article is unreliable. We have not investigated whether authors were aware of or involved in the systematic manipulation of the publication process.

Wiley and Hindawi regrets that the usual quality checks did not identify these issues before publication and have since put additional measures in place to safeguard research integrity.

We wish to credit our own Research Integrity and Research Publishing teams and anonymous and named external researchers and research integrity experts for contributing to this investigation.

The corresponding author, as the representative of all authors, has been given the opportunity to register their agreement or disagreement to this retraction. We have kept a record of any response received.

References

- [1] H. Jia and J. Yan, "Construction of Heritage Digital Resource Platform Based on Digital Twin Technology," *Mathematical Problems in Engineering*, vol. 2022, Article ID 4361135, 8 pages, 2022.

Retraction

Retracted: Monitoring and Analysis of Cotton Planting Parameters in Multiareas Based on Multisensor

Mathematical Problems in Engineering

Received 26 September 2023; Accepted 26 September 2023; Published 27 September 2023

Copyright © 2023 Mathematical Problems in Engineering. This is an open access article distributed under the Creative Commons Attribution License, which permits unrestricted use, distribution, and reproduction in any medium, provided the original work is properly cited.

This article has been retracted by Hindawi following an investigation undertaken by the publisher [1]. This investigation has uncovered evidence of one or more of the following indicators of systematic manipulation of the publication process:

- (1) Discrepancies in scope
- (2) Discrepancies in the description of the research reported
- (3) Discrepancies between the availability of data and the research described
- (4) Inappropriate citations
- (5) Incoherent, meaningless and/or irrelevant content included in the article
- (6) Peer-review manipulation

The presence of these indicators undermines our confidence in the integrity of the article's content and we cannot, therefore, vouch for its reliability. Please note that this notice is intended solely to alert readers that the content of this article is unreliable. We have not investigated whether authors were aware of or involved in the systematic manipulation of the publication process.

Wiley and Hindawi regrets that the usual quality checks did not identify these issues before publication and have since put additional measures in place to safeguard research integrity.

We wish to credit our own Research Integrity and Research Publishing teams and anonymous and named external researchers and research integrity experts for contributing to this investigation.

The corresponding author, as the representative of all authors, has been given the opportunity to register their agreement or disagreement to this retraction. We have kept a record of any response received.

References

- [1] Z. Fan, N. Zhang, D. Wang, J. Zhi, and X. Zhang, "Monitoring and Analysis of Cotton Planting Parameters in Multiareas Based on Multisensor," *Mathematical Problems in Engineering*, vol. 2022, Article ID 7013745, 8 pages, 2022.

Retraction

Retracted: Layout Simulation of Prefabricated Building Construction Based on the Markov Model

Mathematical Problems in Engineering

Received 26 September 2023; Accepted 26 September 2023; Published 27 September 2023

Copyright © 2023 Mathematical Problems in Engineering. This is an open access article distributed under the Creative Commons Attribution License, which permits unrestricted use, distribution, and reproduction in any medium, provided the original work is properly cited.

This article has been retracted by Hindawi following an investigation undertaken by the publisher [1]. This investigation has uncovered evidence of one or more of the following indicators of systematic manipulation of the publication process:

- (1) Discrepancies in scope
- (2) Discrepancies in the description of the research reported
- (3) Discrepancies between the availability of data and the research described
- (4) Inappropriate citations
- (5) Incoherent, meaningless and/or irrelevant content included in the article
- (6) Peer-review manipulation

The presence of these indicators undermines our confidence in the integrity of the article's content and we cannot, therefore, vouch for its reliability. Please note that this notice is intended solely to alert readers that the content of this article is unreliable. We have not investigated whether authors were aware of or involved in the systematic manipulation of the publication process.

Wiley and Hindawi regrets that the usual quality checks did not identify these issues before publication and have since put additional measures in place to safeguard research integrity.

We wish to credit our own Research Integrity and Research Publishing teams and anonymous and named external researchers and research integrity experts for contributing to this investigation.

The corresponding author, as the representative of all authors, has been given the opportunity to register their agreement or disagreement to this retraction. We have kept a record of any response received.

References

- [1] X. Jiao, "Layout Simulation of Prefabricated Building Construction Based on the Markov Model," *Mathematical Problems in Engineering*, vol. 2022, Article ID 6882522, 7 pages, 2022.

Retraction

Retracted: Simulation of Video Image Fault Tolerant Coding Transmission in Digital Multimedia

Mathematical Problems in Engineering

Received 8 August 2023; Accepted 8 August 2023; Published 9 August 2023

Copyright © 2023 Mathematical Problems in Engineering. This is an open access article distributed under the Creative Commons Attribution License, which permits unrestricted use, distribution, and reproduction in any medium, provided the original work is properly cited.

This article has been retracted by Hindawi following an investigation undertaken by the publisher [1]. This investigation has uncovered evidence of one or more of the following indicators of systematic manipulation of the publication process:

- (1) Discrepancies in scope
- (2) Discrepancies in the description of the research reported
- (3) Discrepancies between the availability of data and the research described
- (4) Inappropriate citations
- (5) Incoherent, meaningless and/or irrelevant content included in the article
- (6) Peer-review manipulation

The presence of these indicators undermines our confidence in the integrity of the article's content and we cannot, therefore, vouch for its reliability. Please note that this notice is intended solely to alert readers that the content of this article is unreliable. We have not investigated whether authors were aware of or involved in the systematic manipulation of the publication process.

Wiley and Hindawi regrets that the usual quality checks did not identify these issues before publication and have since put additional measures in place to safeguard research integrity.

We wish to credit our own Research Integrity and Research Publishing teams and anonymous and named external researchers and research integrity experts for contributing to this investigation.

The corresponding author, as the representative of all authors, has been given the opportunity to register their agreement or disagreement to this retraction. We have kept a record of any response received.

References

- [1] F. Li, "Simulation of Video Image Fault Tolerant Coding Transmission in Digital Multimedia," *Mathematical Problems in Engineering*, vol. 2022, Article ID 4657091, 7 pages, 2022.

Retraction

Retracted: Design of the Violin Performance Evaluation System Based on Mobile Terminal Technology

Mathematical Problems in Engineering

Received 8 August 2023; Accepted 8 August 2023; Published 9 August 2023

Copyright © 2023 Mathematical Problems in Engineering. This is an open access article distributed under the Creative Commons Attribution License, which permits unrestricted use, distribution, and reproduction in any medium, provided the original work is properly cited.

This article has been retracted by Hindawi following an investigation undertaken by the publisher [1]. This investigation has uncovered evidence of one or more of the following indicators of systematic manipulation of the publication process:

- (1) Discrepancies in scope
- (2) Discrepancies in the description of the research reported
- (3) Discrepancies between the availability of data and the research described
- (4) Inappropriate citations
- (5) Incoherent, meaningless and/or irrelevant content included in the article
- (6) Peer-review manipulation

The presence of these indicators undermines our confidence in the integrity of the article's content and we cannot, therefore, vouch for its reliability. Please note that this notice is intended solely to alert readers that the content of this article is unreliable. We have not investigated whether authors were aware of or involved in the systematic manipulation of the publication process.

Wiley and Hindawi regrets that the usual quality checks did not identify these issues before publication and have since put additional measures in place to safeguard research integrity.

We wish to credit our own Research Integrity and Research Publishing teams and anonymous and named external researchers and research integrity experts for contributing to this investigation.

The corresponding author, as the representative of all authors, has been given the opportunity to register their agreement or disagreement to this retraction. We have kept a record of any response received.

References

- [1] Y. Lin, "Design of the Violin Performance Evaluation System Based on Mobile Terminal Technology," *Mathematical Problems in Engineering*, vol. 2022, Article ID 8269007, 7 pages, 2022.

Retraction

Retracted: Analysis on Innovation Path of Business Administration Based on Artificial Intelligence

Mathematical Problems in Engineering

Received 8 August 2023; Accepted 8 August 2023; Published 9 August 2023

Copyright © 2023 Mathematical Problems in Engineering. This is an open access article distributed under the Creative Commons Attribution License, which permits unrestricted use, distribution, and reproduction in any medium, provided the original work is properly cited.

This article has been retracted by Hindawi following an investigation undertaken by the publisher [1]. This investigation has uncovered evidence of one or more of the following indicators of systematic manipulation of the publication process:

- (1) Discrepancies in scope
- (2) Discrepancies in the description of the research reported
- (3) Discrepancies between the availability of data and the research described
- (4) Inappropriate citations
- (5) Incoherent, meaningless and/or irrelevant content included in the article
- (6) Peer-review manipulation

The presence of these indicators undermines our confidence in the integrity of the article's content and we cannot, therefore, vouch for its reliability. Please note that this notice is intended solely to alert readers that the content of this article is unreliable. We have not investigated whether authors were aware of or involved in the systematic manipulation of the publication process.

Wiley and Hindawi regrets that the usual quality checks did not identify these issues before publication and have since put additional measures in place to safeguard research integrity.

We wish to credit our own Research Integrity and Research Publishing teams and anonymous and named external researchers and research integrity experts for contributing to this investigation.

The corresponding author, as the representative of all authors, has been given the opportunity to register their agreement or disagreement to this retraction. We have kept a record of any response received.

References

- [1] B. Lu, "Analysis on Innovation Path of Business Administration Based on Artificial Intelligence," *Mathematical Problems in Engineering*, vol. 2022, Article ID 6790836, 7 pages, 2022.

Retraction

Retracted: Application of Cloud Computing Combined with GIS Virtual Reality in Construction Process of Building Steel Structure

Mathematical Problems in Engineering

Received 8 August 2023; Accepted 8 August 2023; Published 9 August 2023

Copyright © 2023 Mathematical Problems in Engineering. This is an open access article distributed under the Creative Commons Attribution License, which permits unrestricted use, distribution, and reproduction in any medium, provided the original work is properly cited.

This article has been retracted by Hindawi following an investigation undertaken by the publisher [1]. This investigation has uncovered evidence of one or more of the following indicators of systematic manipulation of the publication process:

- (1) Discrepancies in scope
- (2) Discrepancies in the description of the research reported
- (3) Discrepancies between the availability of data and the research described
- (4) Inappropriate citations
- (5) Incoherent, meaningless and/or irrelevant content included in the article
- (6) Peer-review manipulation

The presence of these indicators undermines our confidence in the integrity of the article's content and we cannot, therefore, vouch for its reliability. Please note that this notice is intended solely to alert readers that the content of this article is unreliable. We have not investigated whether authors were aware of or involved in the systematic manipulation of the publication process.

Wiley and Hindawi regrets that the usual quality checks did not identify these issues before publication and have since put additional measures in place to safeguard research integrity.

We wish to credit our own Research Integrity and Research Publishing teams and anonymous and named external researchers and research integrity experts for contributing to this investigation.

The corresponding author, as the representative of all authors, has been given the opportunity to register their

agreement or disagreement to this retraction. We have kept a record of any response received.

References

- [1] Y. Dong, H. Sui, and L. Zhu, "Application of Cloud Computing Combined with GIS Virtual Reality in Construction Process of Building Steel Structure," *Mathematical Problems in Engineering*, vol. 2022, Article ID 4299756, 8 pages, 2022.

Retraction

Retracted: Financial Accounting Information Data Analysis System Based on Internet of Things

Mathematical Problems in Engineering

Received 8 August 2023; Accepted 8 August 2023; Published 9 August 2023

Copyright © 2023 Mathematical Problems in Engineering. This is an open access article distributed under the Creative Commons Attribution License, which permits unrestricted use, distribution, and reproduction in any medium, provided the original work is properly cited.

This article has been retracted by Hindawi following an investigation undertaken by the publisher [1]. This investigation has uncovered evidence of one or more of the following indicators of systematic manipulation of the publication process:

- (1) Discrepancies in scope
- (2) Discrepancies in the description of the research reported
- (3) Discrepancies between the availability of data and the research described
- (4) Inappropriate citations
- (5) Incoherent, meaningless and/or irrelevant content included in the article
- (6) Peer-review manipulation

The presence of these indicators undermines our confidence in the integrity of the article's content and we cannot, therefore, vouch for its reliability. Please note that this notice is intended solely to alert readers that the content of this article is unreliable. We have not investigated whether authors were aware of or involved in the systematic manipulation of the publication process.

Wiley and Hindawi regrets that the usual quality checks did not identify these issues before publication and have since put additional measures in place to safeguard research integrity.

We wish to credit our own Research Integrity and Research Publishing teams and anonymous and named external researchers and research integrity experts for contributing to this investigation.

The corresponding author, as the representative of all authors, has been given the opportunity to register their agreement or disagreement to this retraction. We have kept a record of any response received.

References

- [1] Y. Bi, "Financial Accounting Information Data Analysis System Based on Internet of Things," *Mathematical Problems in Engineering*, vol. 2022, Article ID 6162504, 6 pages, 2022.

Retraction

Retracted: Construction of Hotel Resource Information Platform Based on the Internet of Things Technology

Mathematical Problems in Engineering

Received 8 August 2023; Accepted 8 August 2023; Published 9 August 2023

Copyright © 2023 Mathematical Problems in Engineering. This is an open access article distributed under the Creative Commons Attribution License, which permits unrestricted use, distribution, and reproduction in any medium, provided the original work is properly cited.

This article has been retracted by Hindawi following an investigation undertaken by the publisher [1]. This investigation has uncovered evidence of one or more of the following indicators of systematic manipulation of the publication process:

- (1) Discrepancies in scope
- (2) Discrepancies in the description of the research reported
- (3) Discrepancies between the availability of data and the research described
- (4) Inappropriate citations
- (5) Incoherent, meaningless and/or irrelevant content included in the article
- (6) Peer-review manipulation

The presence of these indicators undermines our confidence in the integrity of the article's content and we cannot, therefore, vouch for its reliability. Please note that this notice is intended solely to alert readers that the content of this article is unreliable. We have not investigated whether authors were aware of or involved in the systematic manipulation of the publication process.

Wiley and Hindawi regrets that the usual quality checks did not identify these issues before publication and have since put additional measures in place to safeguard research integrity.

We wish to credit our own Research Integrity and Research Publishing teams and anonymous and named external researchers and research integrity experts for contributing to this investigation.

The corresponding author, as the representative of all authors, has been given the opportunity to register their agreement or disagreement to this retraction. We have kept a record of any response received.

References

- [1] Y. Meng, "Construction of Hotel Resource Information Platform Based on the Internet of Things Technology," *Mathematical Problems in Engineering*, vol. 2022, Article ID 4898550, 8 pages, 2022.

Retraction

Retracted: Parameter Identification of 3D Elastic-Plastic Model for Tunnel Engineering Based on Improved Genetic Algorithm

Mathematical Problems in Engineering

Received 8 August 2023; Accepted 8 August 2023; Published 9 August 2023

Copyright © 2023 Mathematical Problems in Engineering. This is an open access article distributed under the Creative Commons Attribution License, which permits unrestricted use, distribution, and reproduction in any medium, provided the original work is properly cited.

This article has been retracted by Hindawi following an investigation undertaken by the publisher [1]. This investigation has uncovered evidence of one or more of the following indicators of systematic manipulation of the publication process:

- (1) Discrepancies in scope
- (2) Discrepancies in the description of the research reported
- (3) Discrepancies between the availability of data and the research described
- (4) Inappropriate citations
- (5) Incoherent, meaningless and/or irrelevant content included in the article
- (6) Peer-review manipulation

The presence of these indicators undermines our confidence in the integrity of the article's content and we cannot, therefore, vouch for its reliability. Please note that this notice is intended solely to alert readers that the content of this article is unreliable. We have not investigated whether authors were aware of or involved in the systematic manipulation of the publication process.

Wiley and Hindawi regrets that the usual quality checks did not identify these issues before publication and have since put additional measures in place to safeguard research integrity.

We wish to credit our own Research Integrity and Research Publishing teams and anonymous and named external researchers and research integrity experts for contributing to this investigation.

The corresponding author, as the representative of all authors, has been given the opportunity to register their agreement or disagreement to this retraction. We have kept a record of any response received.

References

- [1] X. Dong and L. Chen, "Parameter Identification of 3D Elastic-Plastic Model for Tunnel Engineering Based on Improved Genetic Algorithm," *Mathematical Problems in Engineering*, vol. 2022, Article ID 8305175, 8 pages, 2022.

Retraction

Retracted: Application of Data Image Encryption Technology in Computer Network Information Security

Mathematical Problems in Engineering

Received 8 August 2023; Accepted 8 August 2023; Published 9 August 2023

Copyright © 2023 Mathematical Problems in Engineering. This is an open access article distributed under the Creative Commons Attribution License, which permits unrestricted use, distribution, and reproduction in any medium, provided the original work is properly cited.

This article has been retracted by Hindawi following an investigation undertaken by the publisher [1]. This investigation has uncovered evidence of one or more of the following indicators of systematic manipulation of the publication process:

- (1) Discrepancies in scope
- (2) Discrepancies in the description of the research reported
- (3) Discrepancies between the availability of data and the research described
- (4) Inappropriate citations
- (5) Incoherent, meaningless and/or irrelevant content included in the article
- (6) Peer-review manipulation

The presence of these indicators undermines our confidence in the integrity of the article's content and we cannot, therefore, vouch for its reliability. Please note that this notice is intended solely to alert readers that the content of this article is unreliable. We have not investigated whether authors were aware of or involved in the systematic manipulation of the publication process.

Wiley and Hindawi regrets that the usual quality checks did not identify these issues before publication and have since put additional measures in place to safeguard research integrity.

We wish to credit our own Research Integrity and Research Publishing teams and anonymous and named external researchers and research integrity experts for contributing to this investigation.

The corresponding author, as the representative of all authors, has been given the opportunity to register their agreement or disagreement to this retraction. We have kept a record of any response received.

References

- [1] L. Li, "Application of Data Image Encryption Technology in Computer Network Information Security," *Mathematical Problems in Engineering*, vol. 2022, Article ID 8963756, 7 pages, 2022.

Retraction

Retracted: Analysis of the Influencing Factors of Urban Sports Brand Sales Volume Based on AHP

Mathematical Problems in Engineering

Received 8 August 2023; Accepted 8 August 2023; Published 9 August 2023

Copyright © 2023 Mathematical Problems in Engineering. This is an open access article distributed under the Creative Commons Attribution License, which permits unrestricted use, distribution, and reproduction in any medium, provided the original work is properly cited.

This article has been retracted by Hindawi following an investigation undertaken by the publisher [1]. This investigation has uncovered evidence of one or more of the following indicators of systematic manipulation of the publication process:

- (1) Discrepancies in scope
- (2) Discrepancies in the description of the research reported
- (3) Discrepancies between the availability of data and the research described
- (4) Inappropriate citations
- (5) Incoherent, meaningless and/or irrelevant content included in the article
- (6) Peer-review manipulation

The presence of these indicators undermines our confidence in the integrity of the article's content and we cannot, therefore, vouch for its reliability. Please note that this notice is intended solely to alert readers that the content of this article is unreliable. We have not investigated whether authors were aware of or involved in the systematic manipulation of the publication process.

Wiley and Hindawi regrets that the usual quality checks did not identify these issues before publication and have since put additional measures in place to safeguard research integrity.

We wish to credit our own Research Integrity and Research Publishing teams and anonymous and named external researchers and research integrity experts for contributing to this investigation.

The corresponding author, as the representative of all authors, has been given the opportunity to register their agreement or disagreement to this retraction. We have kept a record of any response received.

References

- [1] M. Zhang, Y. Wu, and X. Zhou, "Analysis of the Influencing Factors of Urban Sports Brand Sales Volume Based on AHP," *Mathematical Problems in Engineering*, vol. 2022, Article ID 9625049, 7 pages, 2022.

Retraction

Retracted: Analysis of Financial Management Target Architecture Based on ISM Model

Mathematical Problems in Engineering

Received 8 August 2023; Accepted 8 August 2023; Published 9 August 2023

Copyright © 2023 Mathematical Problems in Engineering. This is an open access article distributed under the Creative Commons Attribution License, which permits unrestricted use, distribution, and reproduction in any medium, provided the original work is properly cited.

This article has been retracted by Hindawi following an investigation undertaken by the publisher [1]. This investigation has uncovered evidence of one or more of the following indicators of systematic manipulation of the publication process:

- (1) Discrepancies in scope
- (2) Discrepancies in the description of the research reported
- (3) Discrepancies between the availability of data and the research described
- (4) Inappropriate citations
- (5) Incoherent, meaningless and/or irrelevant content included in the article
- (6) Peer-review manipulation

The presence of these indicators undermines our confidence in the integrity of the article's content and we cannot, therefore, vouch for its reliability. Please note that this notice is intended solely to alert readers that the content of this article is unreliable. We have not investigated whether authors were aware of or involved in the systematic manipulation of the publication process.

Wiley and Hindawi regrets that the usual quality checks did not identify these issues before publication and have since put additional measures in place to safeguard research integrity.

We wish to credit our own Research Integrity and Research Publishing teams and anonymous and named external researchers and research integrity experts for contributing to this investigation.

The corresponding author, as the representative of all authors, has been given the opportunity to register their agreement or disagreement to this retraction. We have kept a record of any response received.

References

- [1] Y. Bi, "Analysis of Financial Management Target Architecture Based on ISM Model," *Mathematical Problems in Engineering*, vol. 2022, Article ID 3416671, 8 pages, 2022.

Retraction

Retracted: Recommendation Model of Tourist Attractions Based on Deep Learning

Mathematical Problems in Engineering

Received 8 August 2023; Accepted 8 August 2023; Published 9 August 2023

Copyright © 2023 Mathematical Problems in Engineering. This is an open access article distributed under the Creative Commons Attribution License, which permits unrestricted use, distribution, and reproduction in any medium, provided the original work is properly cited.

This article has been retracted by Hindawi following an investigation undertaken by the publisher [1]. This investigation has uncovered evidence of one or more of the following indicators of systematic manipulation of the publication process:

- (1) Discrepancies in scope
- (2) Discrepancies in the description of the research reported
- (3) Discrepancies between the availability of data and the research described
- (4) Inappropriate citations
- (5) Incoherent, meaningless and/or irrelevant content included in the article
- (6) Peer-review manipulation

The presence of these indicators undermines our confidence in the integrity of the article's content and we cannot, therefore, vouch for its reliability. Please note that this notice is intended solely to alert readers that the content of this article is unreliable. We have not investigated whether authors were aware of or involved in the systematic manipulation of the publication process.

Wiley and Hindawi regrets that the usual quality checks did not identify these issues before publication and have since put additional measures in place to safeguard research integrity.

We wish to credit our own Research Integrity and Research Publishing teams and anonymous and named external researchers and research integrity experts for contributing to this investigation.

The corresponding author, as the representative of all authors, has been given the opportunity to register their agreement or disagreement to this retraction. We have kept a record of any response received.

References

- [1] X. Cheng and W. Su, "Recommendation Model of Tourist Attractions Based on Deep Learning," *Mathematical Problems in Engineering*, vol. 2022, Article ID 9080818, 7 pages, 2022.

Retraction

Retracted: Application of Sensor-Based Intelligent Wearable Devices in Information Physical Education

Mathematical Problems in Engineering

Received 8 August 2023; Accepted 8 August 2023; Published 9 August 2023

Copyright © 2023 Mathematical Problems in Engineering. This is an open access article distributed under the Creative Commons Attribution License, which permits unrestricted use, distribution, and reproduction in any medium, provided the original work is properly cited.

This article has been retracted by Hindawi following an investigation undertaken by the publisher [1]. This investigation has uncovered evidence of one or more of the following indicators of systematic manipulation of the publication process:

- (1) Discrepancies in scope
- (2) Discrepancies in the description of the research reported
- (3) Discrepancies between the availability of data and the research described
- (4) Inappropriate citations
- (5) Incoherent, meaningless and/or irrelevant content included in the article
- (6) Peer-review manipulation

The presence of these indicators undermines our confidence in the integrity of the article's content and we cannot, therefore, vouch for its reliability. Please note that this notice is intended solely to alert readers that the content of this article is unreliable. We have not investigated whether authors were aware of or involved in the systematic manipulation of the publication process.

In addition, our investigation has also shown that one or more of the following human-subject reporting requirements has not been met in this article: ethical approval by an Institutional Review Board (IRB) committee or equivalent, patient/participant consent to participate, and/or agreement to publish patient/participant details (where relevant).

Wiley and Hindawi regrets that the usual quality checks did not identify these issues before publication and have since put additional measures in place to safeguard research integrity.

We wish to credit our own Research Integrity and Research Publishing teams and anonymous and named external

researchers and research integrity experts for contributing to this investigation.

The corresponding author, as the representative of all authors, has been given the opportunity to register their agreement or disagreement to this retraction. We have kept a record of any response received.

References

- [1] W. Chen, "Application of Sensor-Based Intelligent Wearable Devices in Information Physical Education," *Mathematical Problems in Engineering*, vol. 2022, Article ID 5075425, 7 pages, 2022.

Retraction

Retracted: Automatic Scoring Model of Japanese Interpretation Based on Semantic Scoring

Mathematical Problems in Engineering

Received 8 August 2023; Accepted 8 August 2023; Published 9 August 2023

Copyright © 2023 Mathematical Problems in Engineering. This is an open access article distributed under the Creative Commons Attribution License, which permits unrestricted use, distribution, and reproduction in any medium, provided the original work is properly cited.

This article has been retracted by Hindawi following an investigation undertaken by the publisher [1]. This investigation has uncovered evidence of one or more of the following indicators of systematic manipulation of the publication process:

- (1) Discrepancies in scope
- (2) Discrepancies in the description of the research reported
- (3) Discrepancies between the availability of data and the research described
- (4) Inappropriate citations
- (5) Incoherent, meaningless and/or irrelevant content included in the article
- (6) Peer-review manipulation

The presence of these indicators undermines our confidence in the integrity of the article's content and we cannot, therefore, vouch for its reliability. Please note that this notice is intended solely to alert readers that the content of this article is unreliable. We have not investigated whether authors were aware of or involved in the systematic manipulation of the publication process.

Wiley and Hindawi regrets that the usual quality checks did not identify these issues before publication and have since put additional measures in place to safeguard research integrity.

We wish to credit our own Research Integrity and Research Publishing teams and anonymous and named external researchers and research integrity experts for contributing to this investigation.

The corresponding author, as the representative of all authors, has been given the opportunity to register their agreement or disagreement to this retraction. We have kept a record of any response received.

References

- [1] Q. Wang, "Automatic Scoring Model of Japanese Interpretation Based on Semantic Scoring," *Mathematical Problems in Engineering*, vol. 2022, Article ID 3299549, 7 pages, 2022.

Retraction

Retracted: Parameter Optimization of Educational Network Ecosystem Based on BERT Deep Learning Model

Mathematical Problems in Engineering

Received 8 August 2023; Accepted 8 August 2023; Published 9 August 2023

Copyright © 2023 Mathematical Problems in Engineering. This is an open access article distributed under the Creative Commons Attribution License, which permits unrestricted use, distribution, and reproduction in any medium, provided the original work is properly cited.

This article has been retracted by Hindawi following an investigation undertaken by the publisher [1]. This investigation has uncovered evidence of one or more of the following indicators of systematic manipulation of the publication process:

- (1) Discrepancies in scope
- (2) Discrepancies in the description of the research reported
- (3) Discrepancies between the availability of data and the research described
- (4) Inappropriate citations
- (5) Incoherent, meaningless and/or irrelevant content included in the article
- (6) Peer-review manipulation

The presence of these indicators undermines our confidence in the integrity of the article's content and we cannot, therefore, vouch for its reliability. Please note that this notice is intended solely to alert readers that the content of this article is unreliable. We have not investigated whether authors were aware of or involved in the systematic manipulation of the publication process.

Wiley and Hindawi regrets that the usual quality checks did not identify these issues before publication and have since put additional measures in place to safeguard research integrity.

We wish to credit our own Research Integrity and Research Publishing teams and anonymous and named external researchers and research integrity experts for contributing to this investigation.

The corresponding author, as the representative of all authors, has been given the opportunity to register their agreement or disagreement to this retraction. We have kept a record of any response received.

References

- [1] S. Tao, "Parameter Optimization of Educational Network Ecosystem Based on BERT Deep Learning Model," *Mathematical Problems in Engineering*, vol. 2022, Article ID 3119014, 9 pages, 2022.

Retraction

Retracted: Application of Neural Network Sample Training Algorithm in Regional Economic Management

Mathematical Problems in Engineering

Received 8 August 2023; Accepted 8 August 2023; Published 9 August 2023

Copyright © 2023 Mathematical Problems in Engineering. This is an open access article distributed under the Creative Commons Attribution License, which permits unrestricted use, distribution, and reproduction in any medium, provided the original work is properly cited.

This article has been retracted by Hindawi following an investigation undertaken by the publisher [1]. This investigation has uncovered evidence of one or more of the following indicators of systematic manipulation of the publication process:

- (1) Discrepancies in scope
- (2) Discrepancies in the description of the research reported
- (3) Discrepancies between the availability of data and the research described
- (4) Inappropriate citations
- (5) Incoherent, meaningless and/or irrelevant content included in the article
- (6) Peer-review manipulation

The presence of these indicators undermines our confidence in the integrity of the article's content and we cannot, therefore, vouch for its reliability. Please note that this notice is intended solely to alert readers that the content of this article is unreliable. We have not investigated whether authors were aware of or involved in the systematic manipulation of the publication process.

Wiley and Hindawi regrets that the usual quality checks did not identify these issues before publication and have since put additional measures in place to safeguard research integrity.

We wish to credit our own Research Integrity and Research Publishing teams and anonymous and named external researchers and research integrity experts for contributing to this investigation.

The corresponding author, as the representative of all authors, has been given the opportunity to register their agreement or disagreement to this retraction. We have kept a record of any response received.

References

- [1] Y. He, "Application of Neural Network Sample Training Algorithm in Regional Economic Management," *Mathematical Problems in Engineering*, vol. 2022, Article ID 7666331, 7 pages, 2022.

Retraction

Retracted: Intelligent Application of Data Mining Model in Chinese International Education

Mathematical Problems in Engineering

Received 8 August 2023; Accepted 8 August 2023; Published 9 August 2023

Copyright © 2023 Mathematical Problems in Engineering. This is an open access article distributed under the Creative Commons Attribution License, which permits unrestricted use, distribution, and reproduction in any medium, provided the original work is properly cited.

This article has been retracted by Hindawi following an investigation undertaken by the publisher [1]. This investigation has uncovered evidence of one or more of the following indicators of systematic manipulation of the publication process:

- (1) Discrepancies in scope
- (2) Discrepancies in the description of the research reported
- (3) Discrepancies between the availability of data and the research described
- (4) Inappropriate citations
- (5) Incoherent, meaningless and/or irrelevant content included in the article
- (6) Peer-review manipulation

The presence of these indicators undermines our confidence in the integrity of the article's content and we cannot, therefore, vouch for its reliability. Please note that this notice is intended solely to alert readers that the content of this article is unreliable. We have not investigated whether authors were aware of or involved in the systematic manipulation of the publication process.

Wiley and Hindawi regrets that the usual quality checks did not identify these issues before publication and have since put additional measures in place to safeguard research integrity.

We wish to credit our own Research Integrity and Research Publishing teams and anonymous and named external researchers and research integrity experts for contributing to this investigation.

The corresponding author, as the representative of all authors, has been given the opportunity to register their agreement or disagreement to this retraction. We have kept a record of any response received.

References

- [1] F. Wu, "Intelligent Application of Data Mining Model in Chinese International Education," *Mathematical Problems in Engineering*, vol. 2022, Article ID 9171551, 7 pages, 2022.

Retraction

Retracted: Design of English Translation Model Based on Recurrent Neural Network

Mathematical Problems in Engineering

Received 8 August 2023; Accepted 8 August 2023; Published 9 August 2023

Copyright © 2023 Mathematical Problems in Engineering. This is an open access article distributed under the Creative Commons Attribution License, which permits unrestricted use, distribution, and reproduction in any medium, provided the original work is properly cited.

This article has been retracted by Hindawi following an investigation undertaken by the publisher [1]. This investigation has uncovered evidence of one or more of the following indicators of systematic manipulation of the publication process:

- (1) Discrepancies in scope
- (2) Discrepancies in the description of the research reported
- (3) Discrepancies between the availability of data and the research described
- (4) Inappropriate citations
- (5) Incoherent, meaningless and/or irrelevant content included in the article
- (6) Peer-review manipulation

The presence of these indicators undermines our confidence in the integrity of the article's content and we cannot, therefore, vouch for its reliability. Please note that this notice is intended solely to alert readers that the content of this article is unreliable. We have not investigated whether authors were aware of or involved in the systematic manipulation of the publication process.

Wiley and Hindawi regrets that the usual quality checks did not identify these issues before publication and have since put additional measures in place to safeguard research integrity.

We wish to credit our own Research Integrity and Research Publishing teams and anonymous and named external researchers and research integrity experts for contributing to this investigation.

The corresponding author, as the representative of all authors, has been given the opportunity to register their agreement or disagreement to this retraction. We have kept a record of any response received.

References

- [1] X. Wang, "Design of English Translation Model Based on Recurrent Neural Network," *Mathematical Problems in Engineering*, vol. 2022, Article ID 5177069, 7 pages, 2022.

Retraction

Retracted: Vectorization Analysis of Cultural Creative Design Based on the Recognition Model of Virtual Reality Technology

Mathematical Problems in Engineering

Received 8 August 2023; Accepted 8 August 2023; Published 9 August 2023

Copyright © 2023 Mathematical Problems in Engineering. This is an open access article distributed under the Creative Commons Attribution License, which permits unrestricted use, distribution, and reproduction in any medium, provided the original work is properly cited.

This article has been retracted by Hindawi following an investigation undertaken by the publisher [1]. This investigation has uncovered evidence of one or more of the following indicators of systematic manipulation of the publication process:

- (1) Discrepancies in scope
- (2) Discrepancies in the description of the research reported
- (3) Discrepancies between the availability of data and the research described
- (4) Inappropriate citations
- (5) Incoherent, meaningless and/or irrelevant content included in the article
- (6) Peer-review manipulation

The presence of these indicators undermines our confidence in the integrity of the article's content and we cannot, therefore, vouch for its reliability. Please note that this notice is intended solely to alert readers that the content of this article is unreliable. We have not investigated whether authors were aware of or involved in the systematic manipulation of the publication process.

Wiley and Hindawi regrets that the usual quality checks did not identify these issues before publication and have since put additional measures in place to safeguard research integrity.

We wish to credit our own Research Integrity and Research Publishing teams and anonymous and named external researchers and research integrity experts for contributing to this investigation.

The corresponding author, as the representative of all authors, has been given the opportunity to register their agreement or disagreement to this retraction. We have kept a record of any response received.

References

- [1] Y. Yang and Z. Xu, "Vectorization Analysis of Cultural Creative Design Based on the Recognition Model of Virtual Reality Technology," *Mathematical Problems in Engineering*, vol. 2022, Article ID 8930240, 7 pages, 2022.

Retraction

Retracted: Based on Virtual Reality Technology Research on Innovation and Design of Ceramic Painting Products

Mathematical Problems in Engineering

Received 8 August 2023; Accepted 8 August 2023; Published 9 August 2023

Copyright © 2023 Mathematical Problems in Engineering. This is an open access article distributed under the Creative Commons Attribution License, which permits unrestricted use, distribution, and reproduction in any medium, provided the original work is properly cited.

This article has been retracted by Hindawi following an investigation undertaken by the publisher [1]. This investigation has uncovered evidence of one or more of the following indicators of systematic manipulation of the publication process:

- (1) Discrepancies in scope
- (2) Discrepancies in the description of the research reported
- (3) Discrepancies between the availability of data and the research described
- (4) Inappropriate citations
- (5) Incoherent, meaningless and/or irrelevant content included in the article
- (6) Peer-review manipulation

The presence of these indicators undermines our confidence in the integrity of the article's content and we cannot, therefore, vouch for its reliability. Please note that this notice is intended solely to alert readers that the content of this article is unreliable. We have not investigated whether authors were aware of or involved in the systematic manipulation of the publication process.

Wiley and Hindawi regrets that the usual quality checks did not identify these issues before publication and have since put additional measures in place to safeguard research integrity.

We wish to credit our own Research Integrity and Research Publishing teams and anonymous and named external researchers and research integrity experts for contributing to this investigation.

The corresponding author, as the representative of all authors, has been given the opportunity to register their agreement or disagreement to this retraction. We have kept a record of any response received.

References

- [1] Y. Jiang, "Based on Virtual Reality Technology Research on Innovation and Design of Ceramic Painting Products," *Mathematical Problems in Engineering*, vol. 2022, Article ID 4421769, 7 pages, 2022.

Retraction

Retracted: Volunteer Service Participation Emergency Management Information Collection Platform Based on Big Data Technology

Mathematical Problems in Engineering

Received 8 August 2023; Accepted 8 August 2023; Published 9 August 2023

Copyright © 2023 Mathematical Problems in Engineering. This is an open access article distributed under the Creative Commons Attribution License, which permits unrestricted use, distribution, and reproduction in any medium, provided the original work is properly cited.

This article has been retracted by Hindawi following an investigation undertaken by the publisher [1]. This investigation has uncovered evidence of one or more of the following indicators of systematic manipulation of the publication process:

- (1) Discrepancies in scope
- (2) Discrepancies in the description of the research reported
- (3) Discrepancies between the availability of data and the research described
- (4) Inappropriate citations
- (5) Incoherent, meaningless and/or irrelevant content included in the article
- (6) Peer-review manipulation

The presence of these indicators undermines our confidence in the integrity of the article's content and we cannot, therefore, vouch for its reliability. Please note that this notice is intended solely to alert readers that the content of this article is unreliable. We have not investigated whether authors were aware of or involved in the systematic manipulation of the publication process.

Wiley and Hindawi regrets that the usual quality checks did not identify these issues before publication and have since put additional measures in place to safeguard research integrity.

We wish to credit our own Research Integrity and Research Publishing teams and anonymous and named external researchers and research integrity experts for contributing to this investigation.

The corresponding author, as the representative of all authors, has been given the opportunity to register their

agreement or disagreement to this retraction. We have kept a record of any response received.

References

- [1] D. Wang, "Volunteer Service Participation Emergency Management Information Collection Platform Based on Big Data Technology," *Mathematical Problems in Engineering*, vol. 2022, Article ID 6813463, 8 pages, 2022.

Retraction

Retracted: Remote Human-Computer Interaction and STEM Teacher Online Training Based on Embedded Internet of Things

Mathematical Problems in Engineering

Received 8 August 2023; Accepted 8 August 2023; Published 9 August 2023

Copyright © 2023 Mathematical Problems in Engineering. This is an open access article distributed under the Creative Commons Attribution License, which permits unrestricted use, distribution, and reproduction in any medium, provided the original work is properly cited.

This article has been retracted by Hindawi following an investigation undertaken by the publisher [1]. This investigation has uncovered evidence of one or more of the following indicators of systematic manipulation of the publication process:

- (1) Discrepancies in scope
- (2) Discrepancies in the description of the research reported
- (3) Discrepancies between the availability of data and the research described
- (4) Inappropriate citations
- (5) Incoherent, meaningless and/or irrelevant content included in the article
- (6) Peer-review manipulation

The presence of these indicators undermines our confidence in the integrity of the article's content and we cannot, therefore, vouch for its reliability. Please note that this notice is intended solely to alert readers that the content of this article is unreliable. We have not investigated whether authors were aware of or involved in the systematic manipulation of the publication process.

In addition, our investigation has also shown that one or more of the following human-subject reporting requirements has not been met in this article: ethical approval by an Institutional Review Board (IRB) committee or equivalent, patient/participant consent to participate, and/or agreement to publish patient/participant details (where relevant).

Wiley and Hindawi regrets that the usual quality checks did not identify these issues before publication and have since put additional measures in place to safeguard research integrity.

We wish to credit our own Research Integrity and Research Publishing teams and anonymous and named external

researchers and research integrity experts for contributing to this investigation.

The corresponding author, as the representative of all authors, has been given the opportunity to register their agreement or disagreement to this retraction. We have kept a record of any response received.

References

- [1] X. Wu and Q. Zhang, "Remote Human-Computer Interaction and STEM Teacher Online Training Based on Embedded Internet of Things," *Mathematical Problems in Engineering*, vol. 2022, Article ID 2896481, 8 pages, 2022.

Retraction

Retracted: Application of Wireless Sensor Network Data Fusion Technology in Mechanical Fault Diagnosis

Mathematical Problems in Engineering

Received 8 August 2023; Accepted 8 August 2023; Published 9 August 2023

Copyright © 2023 Mathematical Problems in Engineering. This is an open access article distributed under the Creative Commons Attribution License, which permits unrestricted use, distribution, and reproduction in any medium, provided the original work is properly cited.

This article has been retracted by Hindawi following an investigation undertaken by the publisher [1]. This investigation has uncovered evidence of one or more of the following indicators of systematic manipulation of the publication process:

- (1) Discrepancies in scope
- (2) Discrepancies in the description of the research reported
- (3) Discrepancies between the availability of data and the research described
- (4) Inappropriate citations
- (5) Incoherent, meaningless and/or irrelevant content included in the article
- (6) Peer-review manipulation

The presence of these indicators undermines our confidence in the integrity of the article's content and we cannot, therefore, vouch for its reliability. Please note that this notice is intended solely to alert readers that the content of this article is unreliable. We have not investigated whether authors were aware of or involved in the systematic manipulation of the publication process.

Wiley and Hindawi regrets that the usual quality checks did not identify these issues before publication and have since put additional measures in place to safeguard research integrity.

We wish to credit our own Research Integrity and Research Publishing teams and anonymous and named external researchers and research integrity experts for contributing to this investigation.

The corresponding author, as the representative of all authors, has been given the opportunity to register their agreement or disagreement to this retraction. We have kept a record of any response received.

References

- [1] X. Zhao, Z. Shen, and Z. Jing, "Application of Wireless Sensor Network Data Fusion Technology in Mechanical Fault Diagnosis," *Mathematical Problems in Engineering*, vol. 2022, Article ID 5707210, 8 pages, 2022.

Retraction

Retracted: The Influence of Brand Visual Communication on Consumer Psychology Based on Deep Learning

Mathematical Problems in Engineering

Received 8 August 2023; Accepted 8 August 2023; Published 9 August 2023

Copyright © 2023 Mathematical Problems in Engineering. This is an open access article distributed under the Creative Commons Attribution License, which permits unrestricted use, distribution, and reproduction in any medium, provided the original work is properly cited.

This article has been retracted by Hindawi following an investigation undertaken by the publisher [1]. This investigation has uncovered evidence of one or more of the following indicators of systematic manipulation of the publication process:

- (1) Discrepancies in scope
- (2) Discrepancies in the description of the research reported
- (3) Discrepancies between the availability of data and the research described
- (4) Inappropriate citations
- (5) Incoherent, meaningless and/or irrelevant content included in the article
- (6) Peer-review manipulation

The presence of these indicators undermines our confidence in the integrity of the article's content and we cannot, therefore, vouch for its reliability. Please note that this notice is intended solely to alert readers that the content of this article is unreliable. We have not investigated whether authors were aware of or involved in the systematic manipulation of the publication process.

Wiley and Hindawi regrets that the usual quality checks did not identify these issues before publication and have since put additional measures in place to safeguard research integrity.

We wish to credit our own Research Integrity and Research Publishing teams and anonymous and named external researchers and research integrity experts for contributing to this investigation.

The corresponding author, as the representative of all authors, has been given the opportunity to register their agreement or disagreement to this retraction. We have kept a record of any response received.

References

- [1] H. Wang, "The Influence of Brand Visual Communication on Consumer Psychology Based on Deep Learning," *Mathematical Problems in Engineering*, vol. 2022, Article ID 9599943, 8 pages, 2022.

Retraction

Retracted: E-Commerce Data Access Control and Encrypted Storage Based on Internet of Things

Mathematical Problems in Engineering

Received 8 August 2023; Accepted 8 August 2023; Published 9 August 2023

Copyright © 2023 Mathematical Problems in Engineering. This is an open access article distributed under the Creative Commons Attribution License, which permits unrestricted use, distribution, and reproduction in any medium, provided the original work is properly cited.

This article has been retracted by Hindawi following an investigation undertaken by the publisher [1]. This investigation has uncovered evidence of one or more of the following indicators of systematic manipulation of the publication process:

- (1) Discrepancies in scope
- (2) Discrepancies in the description of the research reported
- (3) Discrepancies between the availability of data and the research described
- (4) Inappropriate citations
- (5) Incoherent, meaningless and/or irrelevant content included in the article
- (6) Peer-review manipulation

The presence of these indicators undermines our confidence in the integrity of the article's content and we cannot, therefore, vouch for its reliability. Please note that this notice is intended solely to alert readers that the content of this article is unreliable. We have not investigated whether authors were aware of or involved in the systematic manipulation of the publication process.

Wiley and Hindawi regrets that the usual quality checks did not identify these issues before publication and have since put additional measures in place to safeguard research integrity.

We wish to credit our own Research Integrity and Research Publishing teams and anonymous and named external researchers and research integrity experts for contributing to this investigation.

The corresponding author, as the representative of all authors, has been given the opportunity to register their agreement or disagreement to this retraction. We have kept a record of any response received.

References

- [1] Y. He and W. Hu, "E-Commerce Data Access Control and Encrypted Storage Based on Internet of Things," *Mathematical Problems in Engineering*, vol. 2022, Article ID 4547002, 7 pages, 2022.

Retraction

Retracted: Distributed 3D Environment Design System Based on Color Image Model

Mathematical Problems in Engineering

Received 8 August 2023; Accepted 8 August 2023; Published 9 August 2023

Copyright © 2023 Mathematical Problems in Engineering. This is an open access article distributed under the Creative Commons Attribution License, which permits unrestricted use, distribution, and reproduction in any medium, provided the original work is properly cited.

This article has been retracted by Hindawi following an investigation undertaken by the publisher [1]. This investigation has uncovered evidence of one or more of the following indicators of systematic manipulation of the publication process:

- (1) Discrepancies in scope
- (2) Discrepancies in the description of the research reported
- (3) Discrepancies between the availability of data and the research described
- (4) Inappropriate citations
- (5) Incoherent, meaningless and/or irrelevant content included in the article
- (6) Peer-review manipulation

The presence of these indicators undermines our confidence in the integrity of the article's content and we cannot, therefore, vouch for its reliability. Please note that this notice is intended solely to alert readers that the content of this article is unreliable. We have not investigated whether authors were aware of or involved in the systematic manipulation of the publication process.

Wiley and Hindawi regrets that the usual quality checks did not identify these issues before publication and have since put additional measures in place to safeguard research integrity.

We wish to credit our own Research Integrity and Research Publishing teams and anonymous and named external researchers and research integrity experts for contributing to this investigation.

The corresponding author, as the representative of all authors, has been given the opportunity to register their agreement or disagreement to this retraction. We have kept a record of any response received.

References

- [1] K. Huai, L. Ni, M. Zhu, and H. Zhou, "Distributed 3D Environment Design System Based on Color Image Model," *Mathematical Problems in Engineering*, vol. 2022, Article ID 9268632, 6 pages, 2022.

Retraction

Retracted: Data Analysis and Optimization of English Reading Corpus Based on Feature Extraction

Mathematical Problems in Engineering

Received 1 August 2023; Accepted 1 August 2023; Published 2 August 2023

Copyright © 2023 Mathematical Problems in Engineering. This is an open access article distributed under the Creative Commons Attribution License, which permits unrestricted use, distribution, and reproduction in any medium, provided the original work is properly cited.

This article has been retracted by Hindawi following an investigation undertaken by the publisher [1]. This investigation has uncovered evidence of one or more of the following indicators of systematic manipulation of the publication process:

- (1) Discrepancies in scope
- (2) Discrepancies in the description of the research reported
- (3) Discrepancies between the availability of data and the research described
- (4) Inappropriate citations
- (5) Incoherent, meaningless and/or irrelevant content included in the article
- (6) Peer-review manipulation

The presence of these indicators undermines our confidence in the integrity of the article's content and we cannot, therefore, vouch for its reliability. Please note that this notice is intended solely to alert readers that the content of this article is unreliable. We have not investigated whether authors were aware of or involved in the systematic manipulation of the publication process.

Wiley and Hindawi regrets that the usual quality checks did not identify these issues before publication and have since put additional measures in place to safeguard research integrity.

We wish to credit our own Research Integrity and Research Publishing teams and anonymous and named external researchers and research integrity experts for contributing to this investigation.

The corresponding author, as the representative of all authors, has been given the opportunity to register their agreement or disagreement to this retraction. We have kept a record of any response received.

References

- [1] N. Fan, "Data Analysis and Optimization of English Reading Corpus Based on Feature Extraction," *Mathematical Problems in Engineering*, vol. 2022, Article ID 1746329, 7 pages, 2022.

Retraction

Retracted: Analysis of Passenger Flow Characteristics of Urban Rail Transit Based on Spatial Data Dynamic Analysis Technology

Mathematical Problems in Engineering

Received 1 August 2023; Accepted 1 August 2023; Published 2 August 2023

Copyright © 2023 Mathematical Problems in Engineering. This is an open access article distributed under the Creative Commons Attribution License, which permits unrestricted use, distribution, and reproduction in any medium, provided the original work is properly cited.

This article has been retracted by Hindawi following an investigation undertaken by the publisher [1]. This investigation has uncovered evidence of one or more of the following indicators of systematic manipulation of the publication process:

- (1) Discrepancies in scope
- (2) Discrepancies in the description of the research reported
- (3) Discrepancies between the availability of data and the research described
- (4) Inappropriate citations
- (5) Incoherent, meaningless and/or irrelevant content included in the article
- (6) Peer-review manipulation

The presence of these indicators undermines our confidence in the integrity of the article's content and we cannot, therefore, vouch for its reliability. Please note that this notice is intended solely to alert readers that the content of this article is unreliable. We have not investigated whether authors were aware of or involved in the systematic manipulation of the publication process.

Wiley and Hindawi regrets that the usual quality checks did not identify these issues before publication and have since put additional measures in place to safeguard research integrity.

We wish to credit our own Research Integrity and Research Publishing teams and anonymous and named external researchers and research integrity experts for contributing to this investigation.

The corresponding author, as the representative of all authors, has been given the opportunity to register their agreement or disagreement to this retraction. We have kept a record of any response received.

References

- [1] Y. Zhang and N. Li, "Analysis of Passenger Flow Characteristics of Urban Rail Transit Based on Spatial Data Dynamic Analysis Technology," *Mathematical Problems in Engineering*, vol. 2022, Article ID 1601169, 9 pages, 2022.

Retraction

Retracted: Intelligent Optimization of the Financial Sharing Path Based on Accounting Big Data

Mathematical Problems in Engineering

Received 1 August 2023; Accepted 1 August 2023; Published 2 August 2023

Copyright © 2023 Mathematical Problems in Engineering. This is an open access article distributed under the Creative Commons Attribution License, which permits unrestricted use, distribution, and reproduction in any medium, provided the original work is properly cited.

This article has been retracted by Hindawi following an investigation undertaken by the publisher [1]. This investigation has uncovered evidence of one or more of the following indicators of systematic manipulation of the publication process:

- (1) Discrepancies in scope
- (2) Discrepancies in the description of the research reported
- (3) Discrepancies between the availability of data and the research described
- (4) Inappropriate citations
- (5) Incoherent, meaningless and/or irrelevant content included in the article
- (6) Peer-review manipulation

The presence of these indicators undermines our confidence in the integrity of the article's content and we cannot, therefore, vouch for its reliability. Please note that this notice is intended solely to alert readers that the content of this article is unreliable. We have not investigated whether authors were aware of or involved in the systematic manipulation of the publication process.

Wiley and Hindawi regrets that the usual quality checks did not identify these issues before publication and have since put additional measures in place to safeguard research integrity.

We wish to credit our own Research Integrity and Research Publishing teams and anonymous and named external researchers and research integrity experts for contributing to this investigation.

The corresponding author, as the representative of all authors, has been given the opportunity to register their agreement or disagreement to this retraction. We have kept a record of any response received.

References

- [1] Z. Zhang, "Intelligent Optimization of the Financial Sharing Path Based on Accounting Big Data," *Mathematical Problems in Engineering*, vol. 2022, Article ID 1310994, 8 pages, 2022.

Research Article

Optimization of Physical Education Course Resource Allocation Model Based on Deep Belief Network

Lili Sun 

School of Physical Education, Yunnan Minzu University, Kunming, Yunnan 650500, China

Correspondence should be addressed to Lili Sun; x17201019@stu.ahu.edu.cn

Received 20 August 2022; Revised 23 September 2022; Accepted 3 October 2022; Published 29 April 2023

Academic Editor: B. Sivakumar

Copyright © 2023 Lili Sun. This is an open access article distributed under the Creative Commons Attribution License, which permits unrestricted use, distribution, and reproduction in any medium, provided the original work is properly cited.

In order to meet the optimization needs of physical education curriculum resource allocation, the author proposes a deep belief-based physical education curriculum resource allocation technology. The efficient feature abstraction and feature extraction capabilities of deep belief technology fully explore the interests and preferences of learners on course resources. Because deep belief has strong capabilities in feature detection and feature extraction, it has unique and efficient feature abstraction capabilities for different dimensional attributes of input data; the author proposes a DBN-MCPR model optimization method based on deep belief classification in the MOOC environment. Experimental results show that when the number of iterations reaches about 80, the RMSE of DBN-MCPR trained with the training dataset without learner feature vector is 77.94%, while the RMSE of DBN-MCPR trained with the dataset with learner feature vector is 77.01; DBN-MCPR with full eigenvectors tends to converge after about 40 iterations, while DBN-MCPR without learner eigenvectors starts to converge after about 15 iterations; this result is in line with the characteristics of the internal network structure of DBN. *Conclusion.* This application proves that the technical research based on deep belief can effectively meet the needs of the optimization of physical education curriculum resource allocation.

1. Introduction

With the decline of physical fitness of Chinese students year by year and the continuous deepening of the new curriculum reform, the physical fitness of middle school students has become a basic political task in China, which all shows the importance of Chinese physical education and health courses [1]. In the context of China's basic education reform, the research and application of physical education curriculum resources play a key role in China's physical education work; the reform of the physical education curriculum is mainly reflected in the physical education and health curriculum of each school, and students are the participants of the school physical education class and the object of teaching, which is used to enhance the students' physical fitness. At present, the best way to exercise is to be reflected in the school physical education class, which shows that Chinese physical education teachers should focus on enhancing the physical fitness of students in physical education classes; this way of class not only allows students to exercise

but also cultivates students' love for sports; if the will to persist in exercising is to be greatly improved, it should start from the physical education class, and whether students can persist in exercising independently; it also depends on the role that teachers play in the course of the class. At present, the classrooms of primary and secondary school students still need to rely on the equipment and venue resources in the physical education curriculum resources to complete the teaching goals; this can not only achieve the effect of exercise but also allow students to fully participate in the classroom and then exercise the will quality of students [2].

Accordingly, the problem of the allocation of physical education curriculum resources has been paid more and more attention. The optimal allocation of curriculum resources is a challenge to education from an economy and a learning society and an urgent need for the cultivation and growth of innovative talents. In the course of curriculum reform, the allocation of curriculum resources has become a brand-new research field in education and scientific research. With the continuous advancement of a new round of

college education curriculum reform, the optimal allocation of physical education curriculum resources is attracting attention and discussion in the field of physical education theory and practice; the effective allocation of physical education curriculum resources is an important basis and premise for the achievement of physical education curriculum goals, and it has become more and more people's consensus.

On the basis of limited physical education curriculum resources, optimize the allocation of resources that are conducive to the construction of physical education courses, fully explore the best benefits of physical education curriculum resources with the help of the advantages of college sports resources, and provide a strong and favorable guarantee for improving the comprehensive quality of talents; this is not only an important task of deepening education reform but also the core of improving the utilization rate of China's educational resources, which is of special significance for promoting the reform and development of China's higher education.

2. Literature Review

With the vigorous development of Internet technology, the era of big data is quietly coming, emerging concepts such as artificial intelligence, machine learning, and deep learning are surging, "Internet + education" came into being, and always the trend of the information age is followed [3]. The in-depth combination of Internet technology and education has made MOOC (Massive Open Online Courses) platforms represented by XuetangX, NetEase Cloud Classroom, Guoke, Coursera, and so on, which are strongly impacting the ecology of traditional education and rapidly reshaping the way learners learn. With the digitization and network sharing of educational resources, MOOC platform course resources are increasing day-by-day, and they are increasing at the petabyte level every day. Faced with countless educational resources of varying quality, on the one hand, learners can always discover the course resources they really need; on the other hand, due to the differences in learners' own cognitive ability and knowledge structure, it is difficult for them to correctly identify the content of the resource itself; it is impossible to filter out the learning resources that interest you in a very short period of time, so you lose your direction or choose blindly, wasting more precious time. This leads to the dilemma of rich curriculum resources but difficult-to-select resources, which makes learners have the information trek [4]. Information trek is mainly blamed on the problem of "information overload" caused by too many courses. How to help learners quickly and accurately find suitable learning resources among the rapidly growing MOOC resources is an urgent problem to be solved in the field of educational big data. Therefore, it is very important to study the personalized recommendation system based on course resources.

On the basis of the current research, the author proposes a recommendation method for building a DBN-MCPR personalized model based on deep belief classification in a MOOC environment. The DBN-MCPR recommendation

process mainly includes the following steps: (1) first, according to the multifeatures defined by the learner's interest model, the original feature data that can fully represent the learner's interest preference is collected; (2) second, through a series of data preprocessing operations such as feature mapping, character data digitization, deletion of data that seriously deviates from the normal value, and feature normalization, a standard data set is formed and divided into training set, validation set, and test set; (3) then, the DBN classification model is used to perform feature learning on the training set, and the unsupervised greedy algorithm is used to pretrain each layer of RBM in the DBNs layer-by-layer; finally, the trained DBNs are used as the feature vector input of BP supervised learning; combined with the class label of the course rating, the feature of BP error back propagation is used to fine-tune the entire network; finally, a well-trained DBN personalized recommendation model is formed; (4) the scores of the model is predicted, and course resources with higher predicted scores are recommended to learners in order of their scores from high to low. Figure 1 shows the data preprocessing module.

3. Research Methods

3.1. Basic Model and Overview of Deep Belief Networks. In recent years, with the continuous maturity of deep learning application research, the use of deep learning for resource recommendation has gradually become the mainstream trend [5]. The deep belief network (DBN) is one of the main implementation methods of deep learning. The DBN is a generative model with several layers of latent variables. Latent variables are usually binary, while visible units can be binary or real [6]. Although it is possible to construct DBNs with relatively sparse connections, in general models, each unit in each layer is connected to each unit in each adjacent layer, and there is no connection within a layer. The DBN can be constructed by sequentially stacking several restricted Boltzmann machines (RBMs); the learning process is divided into two stages, that is, the RBM is firstly pretrained layer-by-layer unsupervised and then the entire network is supervised by the back propagation algorithm [7]. The structures of RBM and DBN are shown in Figure 2, respectively.

Given the model parameters $\theta = (w^R, b_v, b_h)$, the joint probability distribution $P(v, h; \theta)$ of the visible layer and the hidden layer is defined by the energy function $E(v, h; \theta)$ as follows:

$$(v, h; \theta) = \frac{1}{Z} e^{-E(v, h; \theta)}. \quad (1)$$

Among them, $Z = \sum_{v, h} e^{-E(v, h; \theta)}$ is the normalization factor, and the marginal distribution of the model about v is as follows:

$$(v; \theta) = \frac{1}{Z} \sum_h e^{-E(v, h; \theta)}. \quad (2)$$

For a Bernoulli (visible layer) distribution-Bernoulli (hidden layer) distributed RBM, the energy function is defined as follows:



FIGURE 1: Data preprocessing module framework (high-end).

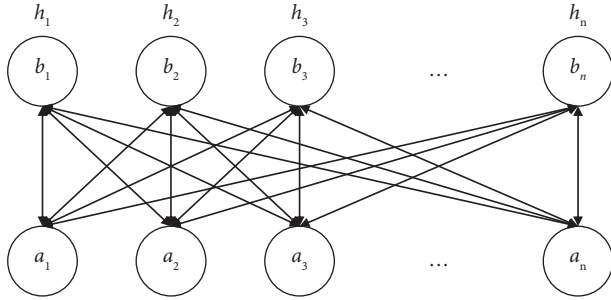


FIGURE 2: RBM structure diagram.

$$E(v, h; \theta) = - \sum_{i=1}^m b_{v_i} v_i - \sum_{j=1}^n b_{h_j} h_j - \sum_{i=1}^m \sum_{j=1}^n v_i w_{ij}^R h_j. \quad (3)$$

Among them, w_{ij}^R is the connection weight of RBM, and b_{v_i} and b_{h_j} represent the bias of visible layer nodes and hidden layer nodes, respectively. Then, the conditional probability distribution can be expressed as follows:

$$\left(h_j = \frac{1}{v}, \theta \right) = \sigma \left(b_{h_j} + \sum_{i=1}^m v_i w_{ij}^R \right), \quad (4)$$

where $\sigma(\cdot)$ is a sigmoid function.

$$\left(v_i = \frac{1}{h}, \theta \right) = \sigma \left(b_{v_i} + \sum_{j=1}^n w_{ij}^R h_j \right). \quad (5)$$

Since the visible layer and the hidden layer are Bernoulli binary states, the standard for judging their binary probability is often achieved by setting a threshold.

By calculating the gradient of the log-likelihood function $\log P(v; \theta)$, the RBM weight update formula can be obtained as follows:

$$\begin{aligned} w_{ij}^R(\tau + 1) &= w_{ij}^R(\tau) + \eta \Delta w_{ij}^R \\ \Delta w_{ij}^R &= E_{\text{data}}(v_i h_j) - E_{\text{model}}(v_i h_j). \end{aligned} \quad (6)$$

In the formula, τ and η represent the number of iterations and learning rate of the RBM, respectively, and $E_{\text{data}}(v_i h_j)$ and $E_{\text{model}}(v_i h_j)$ represent the expectation of the observed data in the training set and the expectation on the distribution determined by the model, respectively. In particular, RBMs have an interesting property that when trained with maximum likelihood-based learning rules, the update of specific weights connecting two neurons depends

only on the statistics collected by these two neurons under different distributions: $P_{\text{model}}(v)$ and $\hat{P}_{\text{data}}(h/v)$. The rest of the network is involved in shaping these statistics, but the weight parameters can be updated with absolutely no knowledge of the rest of the network or how these statistics were produced. This means that the learning rules are “local,” which makes the RBM’s learning seem to be somewhat biological.

As a deep network model, the DBN has the dual properties of a generative model and a discriminative model. Because the pretraining process of the DBN is mainly used to express the high-order correlation of data or describe the joint statistical distribution of data, it has the characteristics of the generative model [8]. The DBN supervised that tuning process is usually used to classify the intrinsic pattern of the data or describe the posterior distribution of the data, which has the characteristics of a discriminative model. At the same time, as a generative model, the generative adversarial network (GAN) has also received a lot of attention in recent years and has been widely used.

The advantage of the DBN learning model is that by combining many RBMs, taking the feature excitation of the previous layer of RBM as the training data of the next layer, the hidden layer can be learned efficiently. Recurrent neural network’s (RNN) depth can even reach the same length as the input data sequence. In the unsupervised learning mode, the RNN is used to predict future data sequences based on previous data samples, and class information is not used in the learning process [9].

The convolutional neural network (CNN) is another deep learning network with discriminative performance, and each module of it is composed of a convolutional layer and a pooling layer. The convolutional layer shares weights, and the pooling layer downsamples the output of the convolutional layer, reducing the amount of data in the next layer. Studies have found that the application of the CNN is mainly concentrated in the field of computer vision or image recognition, and the effect is relatively good [10]. The applications of the DBN are widely distributed in the fields of computer vision and data modeling and prediction.

In addition, the DBN has many hyperparameters, which can be divided into two following categories: one is the training parameters (such as learning rate and momentum term); the other is the parameters that define the network structure (such as the number of network layers and the number of neurons in each layer). The automatic tuning of

the former belongs to the category of hyperparameter optimization (HO), while the automatic tuning of the latter is generally called neural architecture search (NAS) [11].

3.2. DBN-Based Learner Interest Model Construction

3.2.1. Demographic Characteristics. At present, in the online learning platform in the field of education, most personalized resource recommendation systems usually only consider part of the learner's network behavior information when constructing the learner's interest model, which is unfavorable for fully expressing the learner's interest. Descriptions about a series of natural attributes and social conditions of people are called demographic characteristics, such as gender, age, and education level. In addition, for MOOC platform users, things like the school grade of the learner can also be attributed to demographic information. The introduction of demographic information can effectively solve the cold start problem of new users; when a learner registers a new learning platform, the system does not have any behavior information of the learner; at this time, it is possible to mine and predict the interests and hobbies of learners according to the demographic information of learners, and rational use of demographic characteristics can help improve the recommendation efficiency [12].

3.2.2. Learner Behavior Characteristics. Explicit feedback information refers to information such as grades and evaluations that learners actively give to learning resources after browsing or using resources. It is more objective and specific to reflect some natural attributes of learners on the platform. For example, in the MOOC platform, after a learner has finished learning a certain course resource, the displayed rating of the course reflects the learner's direct preference for the course resource. When learners register on the platform, they manually input some basic information to express the user's interests and hobbies [13].

For example, learners' search, click, comment, share, collection of courses, and learners' behaviors are the image depiction of learners' inner feelings and reflect learners' interest preferences [14]. The extraction of implicit feedback information is done without the learner's awareness and without any additional burden on the learner, and the learner's interest is extracted by analyzing the learner's behavior log files.

3.2.3. Content Attributes and Characteristics of Course Resources. This phenomenon leads to various types of course resources on the MOOC platform, such as document courseware, videos, and exercises. In addition, there are structured, semistructured, and unstructured distinctions in course resources, and they are heterogeneous. At the same time, the curriculum resources in different subjects and grades are also different. The definition and coding rules of the curriculum resource classification system are shown in Table 1 [15]. According to the content characteristics of course resources, the division strategy can express the course

resources themselves well to a certain extent, and these course resource content characteristics can well complement the expression of learners' interest and preference for course resources.

3.3. Personalized Model Recommendation Method Based on DBN Classification

3.3.1. Composition of DBN-MCPR. DBN-MCPR is the key to the study of personalized recommendation for learners; it is mainly composed of four modules, namely, data collection, data preprocessing, feature learning, and rating prediction. The overall service architecture diagram of DBN-MCPR is shown in Figure 3.

3.3.2. DBN-MCPR Training. The quality of the recommendation performance depends on the degree of training the DBN classification model, and training the model to optimize its performance is the key to realizing personalized recommendation. The goal of training the model is to make the mapped data fit the original input data as much as possible after the deep feature abstraction of the DBN. The model training process is divided into unsupervised pre-training and supervised parameter fine-tuning. The DBN-MCPR training process is shown in Figure 4 [16].

In the model training process, the most important work is to determine the final parameter set $\theta = \{W, b, c\}$ of each layer of RBM; since the pretraining process of the DBN can be regarded as training several relatively independent RBMs, the training set is firstly used as the input of the first RBM; the first RBM is fully trained using the CD-k algorithm to save the weights and biases of the visible and hidden layers of the trained RBM. Then, the hidden layer of the first RBM is used as the input of the second RBM; after the second RBM is fully trained, the weights and biases of its visible and hidden layers are saved; this process is repeated until all the parameters defined in the model are trained, and the RBM layer completes the unsupervised pretraining process. Finally, the hidden layer of the last RBM trained is used as the input of the visible layer of BP; combined with the course rating class label, the weights and biases of the entire network are fine-tuned using the BP reverse error propagation algorithm in a supervised manner. Finally, when the training error meets a certain set value, the DBN output layer (i.e., the output layer of BP) is classified by a logistic regression classifier, and the score prediction is finally completed [17].

In the DBN-MCPR training process, the training samples come from the learning behavior information and course ratings generated by the learners on the selected course resources. The "learner-course resource" feature vector and the learner's rating of the course together constitute a sample of the learner; for any course resource that the learner has studied, the corresponding learner sample can be obtained; all samples constitute a huge dataset for training and testing [18, 19]. The number of neurons in the visible layer is set as the attribute dimension of the feature vector of "Learner-Course Resource." In order to improve the recommendation effect of DBN-MCPR, each parameter

TABLE 1: Example table of course resource classification strategy.

Classification strategy	Policy description	Coding rules (part)	
Subject	The educational resources are classified by subject tagging and are represented by unique identifiers	Language	1
		Math	2
		English	3
		Physical education	8
Grade	According to the different knowledge levels, the educational resources are classified according to grades and are represented by unique identifiers	High school	10
		Sophomore	11
		Senior year	12
Type	Classify educational resources by type according to resource type, such as documents, videos, exercises, and discussion posts represented by a unique identifier	Courseware	1
		Video	2
		Exercise	3
Knowledge point	Extract the content features of educational resources, build a knowledge map, and mine user interest points and weak points based on knowledge points represented by a unique identifier	Function	01
		Sequence	02
		Derivative	03

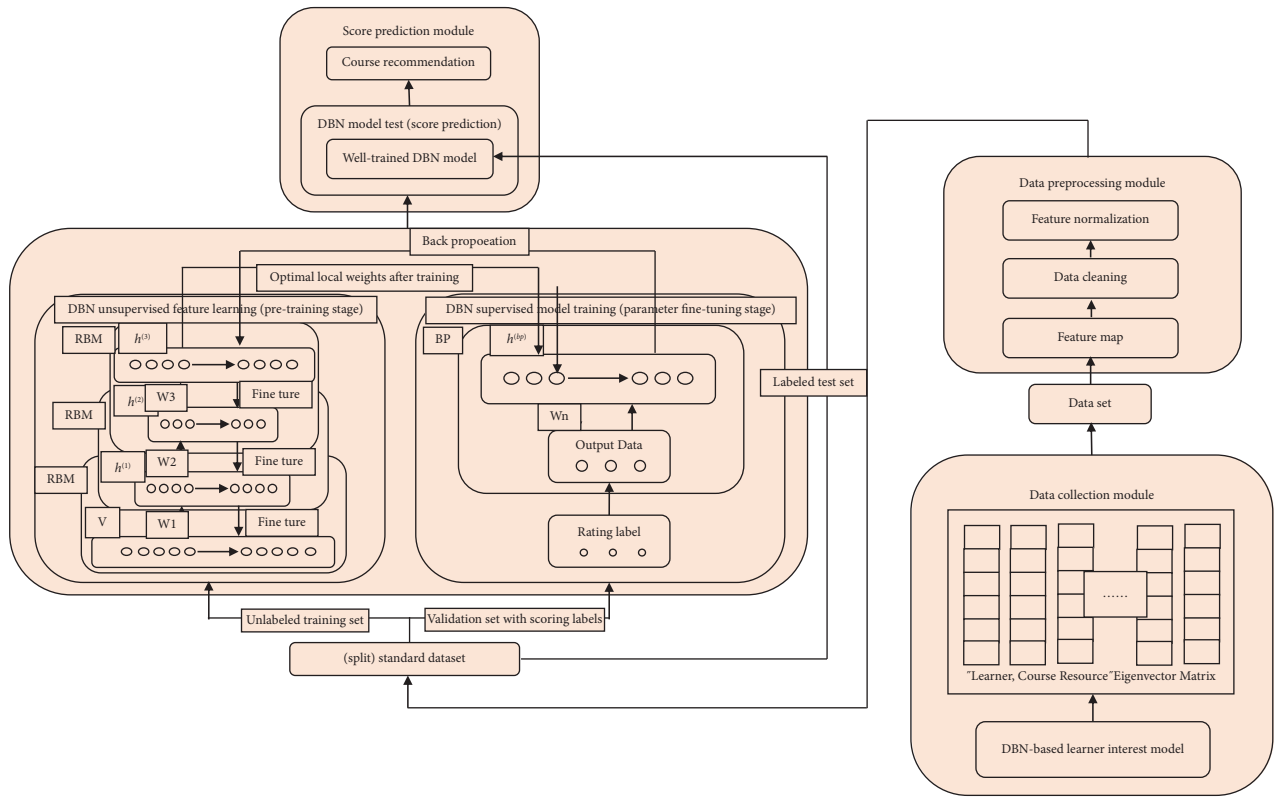


FIGURE 3: DBN-MCPR overall service architecture diagram.

needs to be effectively set before the model runs; the settings generally include the initialization of training parameters and the parameter settings of influence factors.

4. Results Analysis

- (i) Influence of training data set on the recommendation accuracy of DBN-MCPR: considering the complex structural characteristics of the DBN classification model itself, due to its strong feature expression ability, a large amount of data is required to avoid overfitting; if the model is

overfitted, its generalization ability will drop sharply, which will be very detrimental to its training. The authors verify the variation of DBN-MCPR recommendation accuracy with the training dataset by adjusting the size of the training dataset, as shown in Figure 5 [20].

As can be seen from Figure 4, the number of training sets directly affects the recommendation accuracy of DBN-MCPR. Since the smaller the training data set is, the weaker the correlation between the data is, which leads to the easier it is to generate “fragments” of the relationship between

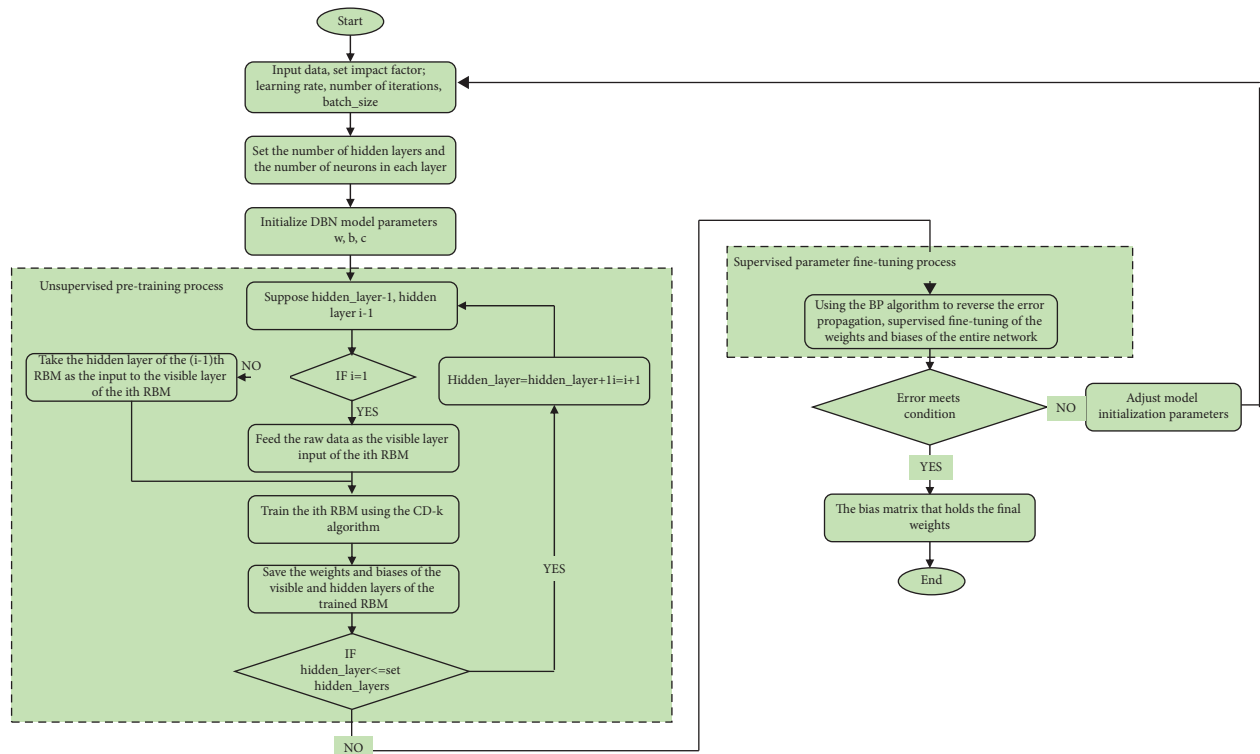


FIGURE 4: DBN-MCPR training process.

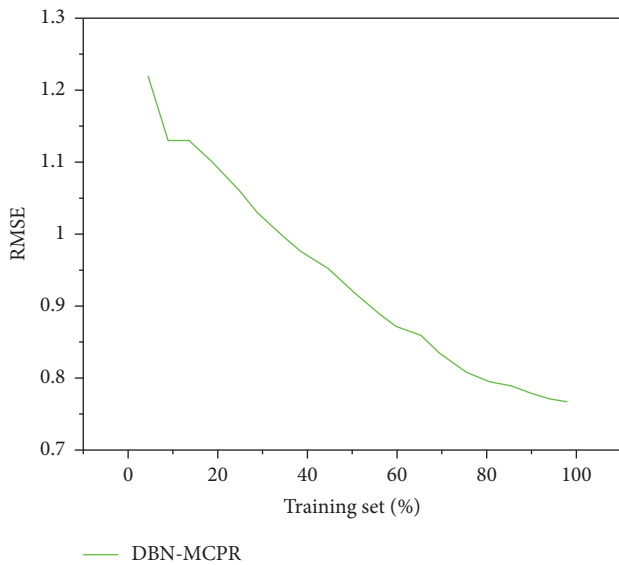


FIGURE 5: The variation of DBN-MCPR recommendation accuracy with the size of the training set.

the samples [21]. In the case of weak correlation between sample information, DBN-MCPR cannot mine the complex relationship between data well, resulting in low recommendation accuracy. As the number of samples in the training data set increases, the correlation between samples becomes more and more abundant, which is more conducive to DBN-MCPR to mine the hidden relationship between samples, so the recommendation accuracy

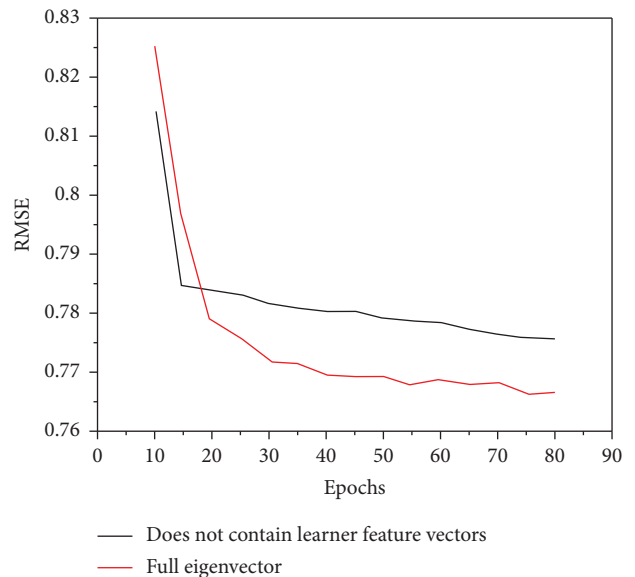


FIGURE 6: Comparison of the influence of full eigenvectors and no learner eigenvectors on the recommendation accuracy of DBN-MCPR.

will be higher. When using the entire training set to train DBN-MCPR, its RMSE is as low as 76.68% [22].

- (2) The influence of learner feature vector on the recommendation accuracy of DBN-MCPR: learner demographics and course resource content attributes together influence learners' interest

preferences; a comparative experiment is set up here to verify the influence of the learner's feature vector on DBN-MCPR and to further verify the effectiveness and practicability of the learner's interest model [23]. Eliminate the relevant demographic feature dimensions and course resource content attribute feature dimensions in each dataset; these attribute dimensions include age, gender, grade, level_of_education, school, course_subject, course_grade, course_knowledge, course_creator, and course_school. Further experiments show that the influence of learner feature vector on the recommendation accuracy of DBN-MCPR is shown in Figure 6 [24].

5. Conclusion

The author proposes a DBN-MCPR model optimization method based on deep belief classification under the MOOC environment, which is mainly based on the efficient feature abstraction and feature extraction capabilities of deep belief technology, fully excavates learners' interests and preferences for course resources, and builds a DBN-MCPR model to test the optimization effect of course resource allocation. From the test results, it can be seen that when the number of iterations reaches about 80, the RMSE of DBN-MCPR trained with the training dataset without learner feature vector is 77.94%, while the RMSE of DBN-MCPR trained with the dataset with learner feature vector is 77.01, the RMSE of DBN-MCPR with full eigenvectors is 1.21% lower than that of DBN-MCPR without learner eigenvectors; it is fully proved that the learner feature vector has a great influence on the prediction accuracy of DBN-MCPR. DBN-MCPR with full eigenvectors tends to converge after about 40 iterations, while DBN-MCPR without learner eigenvectors converges after about 15 iterations; this result is in line with the characteristics of the internal network structure of the DBN, which effectively verifies that the model in this study has a high optimization effect and further proves that the technical model based on deep belief can effectively meet the needs of the optimization of physical education curriculum resource allocation.

Data Availability

The data used to support the findings of this study are available from the corresponding author upon request.

Conflicts of Interest

The author declares that he has no conflicts of interest.

Acknowledgments

The study was supported by the University-Level Educational Reform Project "Research on the Teaching Mode of 1123N New Integrated Curriculum of Health Education in Yunnan Nationalities University," project no. 2021JG-077.

References

- [1] Y. Luo, "Demand-led course construction and teaching resource development and application of practical Chinese in secondary vocational colleges," *Education Teaching Forum*, 2020.
- [2] S. Zheng, "Research on Distance teaching System of English Course Based on Wireless Network technology," *Hindawi Limited*, vol. 2021, Article ID 3275340, 2021.
- [3] J. C. Carey, L. S. Beitelspacher, J. Tosti-Kharas, and E. Swanson, "A resource-efficient modular course design for co-teaching integrated sustainability in higher education: developing the next generation of entrepreneurial leaders," *Entrepreneurship Education and Pedagogy*, vol. 4, no. 2, pp. 169–193, 2020.
- [4] L. N. Dong and J. W. Liu, *Design of security sharing system for online teaching course resources of fine arts specialty International Conference on E-Learning, E-Education, and Online Training*, Springer, Berlin Germany, 2021.
- [5] J. K. Green, "Designing hybrid spaces for learning in higher education health contexts," *Postdigital Science and Education*, vol. 4, no. 1, pp. 93–115, 2022.
- [6] J. Williams, M. J. Davies, B. Sueese, and D. Hunt, "Teachers' experiences of teaching the Australian health and physical education health benefits of physical activity curriculum and the need for greater reality congruence," *Curriculum Perspectives*, vol. 42, no. 1, pp. 27–37, 2022.
- [7] X. Zhu, L. Bao, H. Wang, and N. Zhao, "The train of thought and strategy of Chinese school physical education to cultivate unique minority students' motor quotient in yunnan," *Advances in Physical Education*, vol. 11, no. 04, pp. 481–488, 2021.
- [8] C. Tan and L. Xue, "Application research of big data mining in personalized teaching of internet education platform," *Journal of Physics: Conference Series*, vol. 1992, no. 2, Article ID 022120, 2021.
- [9] S. Wang, T. Sun, X. Qu, and W. Xu, "Online education of atomic physics based on mooc platform," *Journal of Physics: Conference Series*, vol. 1881, no. 3, Article ID 032009, 2021.
- [10] L. C. Redmond and V. J. Howard, "Open educational resource-enabled pedagogy to improve student outcomes in nutrition course," *Journal of Nutrition Education and Behavior*, vol. 53, no. 7, pp. 631–634, 2021.
- [11] R. D. Sushir and D. G. Wakde, "An improved detection of blind image forgery using hybrid deep belief network and adaptive fuzzy clustering," *Multimedia Tools and Applications*, vol. 81, no. 20, pp. 29177–29205, 2022.
- [12] A. Decelle and C. Furtlehner, "Restricted Boltzmann machine: recent advances and mean-field theory," *Chinese Physics B*, vol. 30, no. 4, Article ID 040202, 2021.
- [13] B. Zhou, H. Duan, Q. Wu et al., "Short-term prediction of wind power and its ramp events based on semi-supervised generative adversarial network," *International Journal of Electrical Power & Energy Systems*, vol. 125, no. 2, Article ID 106411, 2021.
- [14] K. E. Arunkumar, D. V. Kalaga, C. M. S. Kumar, M. Kawaji, and T. M. Brenza, "Forecasting of covid-19 using deep layer recurrent neural networks (rnns) with gated recurrent units (grus) and long short-term memory (lstm) cells," *Chaos, Solitons & Fractals*, vol. 146, no. 1, Article ID 110861, 2021.
- [15] Y. N. Fu'Adah, I. Wijayanto, N. K. C. Pratiwi, F. F. Taliningsih, S. Rizal, and M. A. Pramudito, "Automated classification of alzheimer's disease based on mri image processing using convolutional neural network (cnn) with alexnet

- architecture,” *Journal of Physics: Conference Series*, vol. 1844, no. 1, Article ID 012020, 2021.
- [16] B. M. Oloulade, J. Gao, J. Chen, T. Lyu, and R. Al-Sabri, “Graph neural architecture search: a survey,” *Tsinghua Science and Technology*, vol. 27, no. 4, pp. 692–708, 2022.
- [17] C. L. Dobbs, N. K. Caselli, E. Hartzell, C. Flanagan, and Y. Yan, “Understanding middle graders’ language borrowing: how lexical and demographic characteristics predict similarity,” *Reading and Writing*, vol. 35, no. 4, pp. 971–994, 2021.
- [18] G. Lin, F. Liang, W. Pan, and Z. Ming, “Fedrec: federated recommendation with explicit feedback,” *Intelligent Systems, IEEE*, no. 99, p. 1, 2020.
- [19] B. Wang, J. Han, and Y. Cuan, “Improved metric factorization recommendation algorithm based on social networks and implicit feedback,” *Journal of Physics: Conference Series*, vol. 1634, no. 1, Article ID 012037, 2020.
- [20] I. S. Harahap, I. Z. Matondang, E. K. Indah, E. K. Indah, and I. Fitri, “Mapping climate classification of oldeman in agricultural resources management in south tapanuli district,” *IOP Conference Series: Materials Science and Engineering*, vol. 1156, no. 1, Article ID 012002, 2021.
- [21] X. Ruhang, “Efficient clustering for aggregate loads: an unsupervised pretraining based method,” *Energy*, vol. 210, no. 9, Article ID 118617, 2020.
- [22] Y. Guo, C. Zhang, L. Gao, and X. Kang, “Research on Online Teaching Practice Based on Information Technology: A Case Study of the Course “Human Resource Management”online Teaching during the COIVD-19 Pandemic,” in *Proceedings of the 2021 2nd International Conference on Education, Knowledge and Information Management (ICEKIM)*, Xiamen, China, January 2021.
- [23] V. Shah, S. Murthy, J. Warriem, S. Sahasrabudhe, G. Banerjee, and S. Iyer, “Learner-centric mooc model: a pedagogical design model towards active learner participation and higher completion rates,” *Educational Technology Research & Development*, vol. 70, no. 1, pp. 263–288, 2022.
- [24] W. Zhong, K. Xie, Y. Liu, C. Yang, and S. Xie, “Multi-resource allocation of shared energy storage: a distributed combinatorial auction approach,” *IEEE Transactions on Smart Grid*, vol. 11, no. 5, pp. 4105–4115, 2020.

Retraction

Retracted: Design of Regression Model for MultiParameter Evaluation of English Pronunciation Quality

Mathematical Problems in Engineering

Received 5 December 2023; Accepted 5 December 2023; Published 6 December 2023

Copyright © 2023 Mathematical Problems in Engineering. This is an open access article distributed under the Creative Commons Attribution License, which permits unrestricted use, distribution, and reproduction in any medium, provided the original work is properly cited.

This article has been retracted by Hindawi, as publisher, following an investigation undertaken by the publisher [1]. This investigation has uncovered evidence of systematic manipulation of the publication and peer-review process. We cannot, therefore, vouch for the reliability or integrity of this article.

Please note that this notice is intended solely to alert readers that the peer-review process of this article has been compromised.

Wiley and Hindawi regret that the usual quality checks did not identify these issues before publication and have since put additional measures in place to safeguard research integrity.

We wish to credit our Research Integrity and Research Publishing teams and anonymous and named external researchers and research integrity experts for contributing to this investigation.

The corresponding author, as the representative of all authors, has been given the opportunity to register their agreement or disagreement to this retraction. We have kept a record of any response received.

References

- [1] K. Chen, "Design of Regression Model for MultiParameter Evaluation of English Pronunciation Quality," *Mathematical Problems in Engineering*, vol. 2023, Article ID 7288443, 7 pages, 2023.

Research Article

Design of Regression Model for MultiParameter Evaluation of English Pronunciation Quality

Ke Chen ^{1,2}

¹School of International Studies, Hunan Institute of Technology, Hengyang, Hunan 421002, China

²Faculty of Modern Languages and Communication, Universiti Putra Malaysia, Seri Kembangan, Selangor 43400, Malaysia

Correspondence should be addressed to Ke Chen; 201903312@stu.ncwu.edu.cn

Received 11 July 2022; Revised 6 August 2022; Accepted 10 August 2022; Published 29 April 2023

Academic Editor: Hengchang Jing

Copyright © 2023 Ke Chen. This is an open access article distributed under the Creative Commons Attribution License, which permits unrestricted use, distribution, and reproduction in any medium, provided the original work is properly cited.

In order to better evaluate the quality of English pronunciation, this paper proposes a regression model design method based on multiparameter evaluation of English pronunciation quality. This method takes college students' English pronunciation as the research object. Through the combination of various algorithms, a speech recognition model based on a machine learning neural network is constructed with characteristic parameters as input, and a speech quality evaluation model based on multiple regression is constructed with multiparameters such as intonation, speed, rhythm, and intonation as evaluation indicators. The experimental results show that log posterior probability and GOP are good measures of pronunciation standard. When used alone, a higher correlation with manual scores can be obtained, and the correlation of both exceeds 0.5. GOP has the best performance, with a correlation of 0.549. The combination of these two pronunciation standard evaluation features can further improve the evaluation performance, and the correlation degree reaches 0.574. Compared with the GOP algorithm with better performance, the evaluation performance is improved by 4.6%. *Conclusion.* The model provides a scientific basis for oral English speech recognition and objective evaluation of pronunciation quality.

1. Introduction

With the rapid development of computer science and technology, computer English learning has become the norm [1, 2]. In early 2007, the Ministry of Education clarified the standard for computerized English language instruction. Currently, most computer language learning tools focus on memory, writing, and reading and are rarely used in oral instruction. This is because computer speech is very difficult to measure speech. However, in recent years, the use of advanced technology in computer language learning has led to more and more oral English learning, including the assessment of time and sound adjustment by recording the observer's mouth [3]. This technique is helpful to correct learners' pronunciation errors. At the same time, this can help learners, especially second language learners who do not have an environment of speech and practice, to better understand and improve their language. Nowadays, English proficiency assessment has become a standard technology

for computer language learning [4]. In addition, a telephone call test can be used to measure an English oral test, as it lacks the independence of content, more objective and honest. rather than a manual measurement, and can be very effective.

In this context, the design of multiparameter regression model for English pronunciation quality evaluation plays a very important role. Through regression analysis of English pronunciation quality, combined with multiparameter English pronunciation quality standards as a reference, students' English pronunciation quality can be greatly improved.

2. Literature Review

Regression analysis is a mathematical method to deal with the correlation between variables. Its main content is to establish an approximate mathematical expression empirical formula of the correlation between variables by using the

least square method based on the observed test data; The validity of the empirical formula is verified by the correlation test; The established effective empirical formula is applied to predict and control. The practice has proved that using the regression analysis method in economic work is an effective scientific method for better understanding the relationship between economic phenomena, mastering economic laws, and carrying out economic prediction and control [5, 6]. As a global language, English has greatly facilitated the communication of people all over the world. With the deepening of China's integration into the world, people pay more and more attention to the oral English test and students' oral English ability. However, in the traditional English classroom teaching in China, oral English has always been the weakest link. Students' time for oral English training is very limited. Teachers cannot give targeted guidance according to different students' pronunciation, which leads to the poor oral English level of Chinese students. Although most of the students can achieve good results in the written examination based on English vocabulary, grammar and writing, few students can skillfully use English for practical and effective oral communication [7].

The Chinese Academy of Sciences has adopted standards such as accuracy and precision in the measurement of English proficiency. Yi have added guidelines for good telephone measurement and developed good telephone measurement standards that make telephone calls better and more efficient [8]. Ma et al., proposed a pronunciation quality evaluation model independent of phonemes, and the scoring effect is better than other methods [9]. Xh et al., use the wheel as an event after a function in custom language. The correlation coefficient between the automatic score and the manual score was 0.795, and the rating performance improved by 9% [10]. Wagner et al., developed an accurate algorithm for measuring telephone quality based on the ellipse design, which improved the accuracy and efficiency of telephone quality measurement [11]. Wen and Fu have proposed new procedures for assessing oral English and using it in Tsinghua University's English-speaking teaching methods [12]. After testing, the sentence correlation between pass and expert scoring is 0.66, which is better than other scoring algorithms. Bang et al., comprehensively evaluated the oral pronunciation quality of the testees by comparing the speech speed, intonation, stress, intonation, and rhythm of the pronunciation sentence to be tested with the standard language in the corpus and achieved good results [13]. These results provide strong support for the study of computer-aided pronunciation quality assessment.

Based on the above-given research, this paper proposes a method to develop a multiparameter regression model for English pronunciation quality assessment. This method takes English speech pronunciation of college students as the research object, extracts Mel-frequency cepstral feature parameters from the speech signal and uses the feature parameters as input to build a machine learning neural network-based speech recognition model. Based on multiple regression, it is used as an evaluation criterion to create a model for evaluating the quality of spoken English pronunciation. According to the test results, combining the

standard evaluation characteristics of these two pronunciations further improves the evaluation performance, and the correlation reaches 0.574. GOP algorithm and evaluation performance improved by 4.6%. It aims to create a scientific basis for the recognition of spoken English and the objective assessment of pronunciation quality.

3. Research Methods

3.1. Principle of Regression Analysis. Regression analysis methods can be divided into two types according to the number of changes studied: single-variable regression analysis, multivariate regression analysis, and linear regression analysis and nonlinear regression analysis in the form of empirical models. Most nonlinear regression tests can be converted to horizontal tests, and the principle of multiple regression tests is the same as a single test. In terms of regression, this form is just a version of horizontal regression. The empirical formula is defined by the smallest square [14]. In the univariate linear regression analysis, we study the relationship between two variables, one is the common variable x , and the other is the random variable y .

For example, the relationship between the demand for commodities and the number of residents is uncertain. In order to make a purchase and supply plan for a certain commodity throughout the year, the commercial department needs to investigate the demand for such a commodity. Suppose 20 residential areas are investigated, and the relationship between the demand for commodities and the number of residents is listed in Table 1.

How to infer the demand of the whole city and the supply plan of each residential area based on these data? It can be seen from Table 1 that the relationship between Y and X is generally linear, but not completely determined [15]. If there are three settlements with the same population of 600, the demand for commodities is different. Therefore, after the number of people is determined, the demand for goods can not be completely determined. We can only roughly estimate the demand or the range of the demand. That is to say, in addition to the linear influence of X on y , there are other factors on y , forming the randomness (i.e., uncertainty) of Y , which is expressed by the mathematical formula as follows:

$$Y = a + bx + \varepsilon, \quad (1)$$

where ε is called a random term. The problem now is how to use the survey data to eliminate the influence of random factors and find out the linear relationship expression between Y and X . therefore, first draw 20 pairs of data as points on the coordinate plane to get the following line graph, as shown in Figure 1.

From Figure 1, this line is called the regression line of Y to x , and the equation represented by the regression line $Y = a + bx$ is called the regression equation of Y to x .

3.2. Mel Frequency Cepstrum Coefficient. The research on the principle of human ear hearing shows that the sensitivity of human ear to high and low frequency sound signals is different, which is approximately logarithmic. Mel frequency

TABLE 1: Relationship between commodity demand and number of residents.

Settlement No	Number of residents	Commodity demand	Settlement No	Number of residents	Commodity demand
1	100	50	11	700	400
2	200	120	12	750	450
3	300	160	13	800	490
4	300	190	14	800	480
5	400	240	15	850	500
6	500	290	16	850	490
7	550	330	17	900	550
8	600	350	18	950	540
9	600	360	19	950	560
10	600	380	20	1000	610

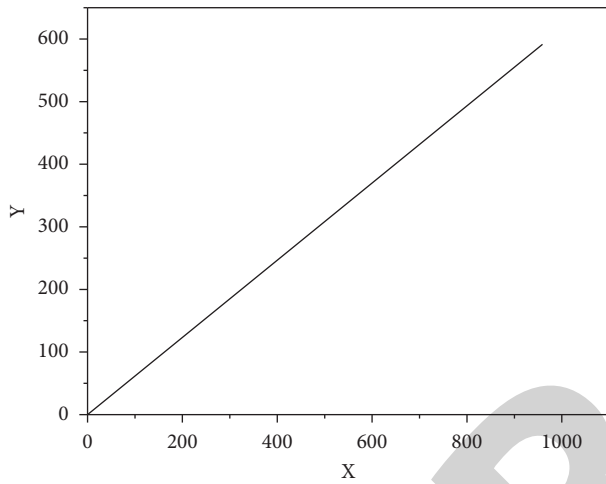


FIGURE 1: Linear relationship between ordinary variables and random variables.

cepstrum coefficients (MFCC) is an acoustic feature that makes full use of the auditory perception characteristics of the human ear. By setting a group of triangular band-pass filters that are nonuniformly distributed along the linear frequency axis, the conversion from linear frequency to Mel frequency is realized, and then the speech signal is processed in the Mel frequency domain.

The conversion relationship from the actual linear frequency f to Mel frequency m is

$$m = 2595 \left(1 + \frac{f}{700} \right). \quad (2)$$

Because MFCC features use Mel frequency, it can better reflect the response of human auditory system than linear frequency. The detailed process of extracting MFCC features from preprocessed speech signals is shown in Figure 2.

Figure 2 shows that for each frame of speech signal after preprocessing, the fast Fourier transform is first performed to obtain the energy distribution on the spectrum. Then, the spectrum is weighted and summed through a group of triangular bandpass filters to convert the spectrum of each frame of speech signal to Mel frequency domain. Then, take the logarithm of Mel filter bank output. Since the filter banks are overlapped, the output energy of each filter is correlated. Then, discrete cosine transform (DCT) is performed on

these logarithmic energies to eliminate the correlation of the output energy of the filter banks. After DCT transformation, 12 Mel cepstrum coefficients and one energy feature can be obtained for each frame of the speech signal, but these parameters only reflect the static characteristics of the speech signal [16]. In order to capture the dynamic characteristics of speech signal at the same time, first-order difference and second-order difference are made for these parameters in turn. After the above processing, the 39 dimensional MFCC feature vector can be extracted from each frame of the speech signal.

3.3. Building a Search Network. After the construction of the knowledge base is completed, in order to align the students' reading pronunciation with the given reading text, a search network should be built according to the information provided by the knowledge base, as shown in Figure 3.

A three-layer search, the first layer is the conjunction that connects the spoken words with some occurrences in the trilingual structure, and the second layer is the phoneme layer that describes the word sequence. Communication words from the telephone dictionary. Phoneme sequences, the third layer is the HMM state layer, which is an acoustic statistical representation of phoneme sequences using the HMM model.

3.4. Construction of Multiparameter Regression Model for English Pronunciation Quality Evaluation

3.4.1. Voice Data Acquisition

(1) *Training Data Set.* In order to verify the effectiveness of the speech recognition model in this study, the speech data are downloaded from the libri speech ASR corpus. The downloaded data set includes 8800 groups of English phonetic data, which are composed of the pronunciation of 10 English words by 88 native speakers aged 10–40 and each word repeated 10 times. The data set is mainly used to train the speech recognition model.

(2) *Test Data Set.* According to the needs of College Students' English audio-visual and oral teaching, this paper establishes a database of test terms. The corpus text materials of this study are derived from the original sound of four movies,



FIGURE 2: MFCC feature extraction flow chart.

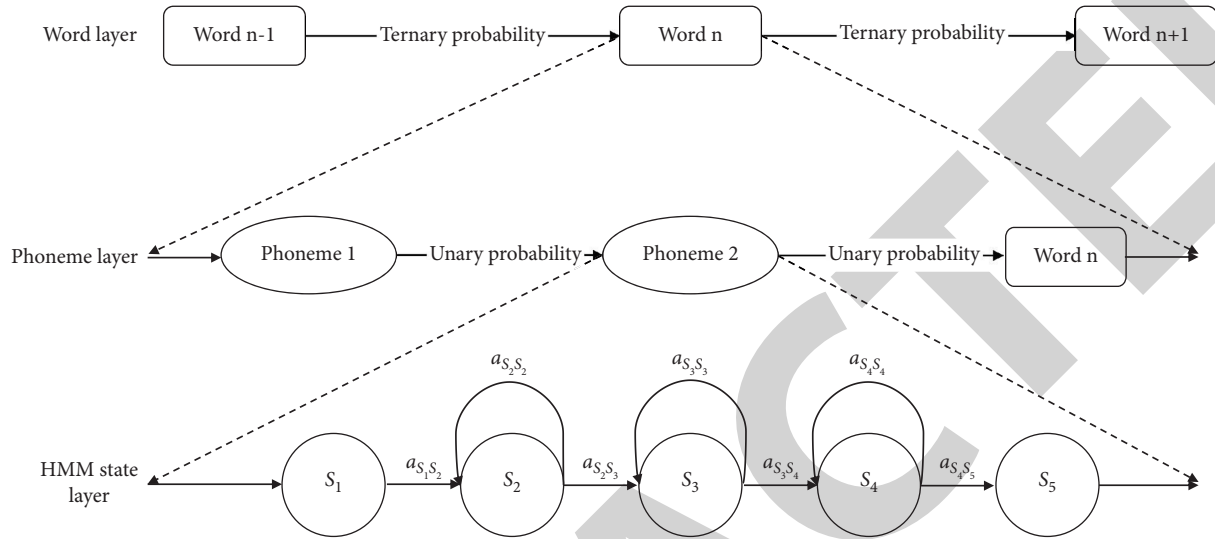


FIGURE 3: Three layer search network.

TABLE 2: Corpus information.

Corpus items	Corpus content
Recorder	300 college students in a college
Source of corpus	Select a segment from each of the four films kung fu panda, hua mulan, truman's world and teddy bear. Under each segment, select 5 representative lines as the reading text, a total of 20 sentences
Recording mode	Each student reads the assigned 20 sentences
Preliminary evaluation method	In order to compare with the followup model evaluation, the designated teacher will first make a preliminary evaluation of the sentence. According to the factors such as pronunciation intonation, rhythm, intonation and speed, the comprehensive evaluation is carried out by using the national CET6 oral test grading standard
Total number of corpora	A total of 6000 wav format speech (16000 hz sampling rate, mono channel, 16 bit quantization), 6000 evaluation data

kung fu panda, Hua Mulan, Truman's world and teddy bear [17]. Some representative phonetic clips are selected as reading materials. Students participating in the test can read aloud and record the corresponding pronunciation. The specific information of the test corpus is shown in Table 2.

3.4.2. English Speech Signal Preprocessing and Feature Extraction. Before speech signal analysis and processing, in order to eliminate the impact of environmental noise, clutter and distortion on signal quality, it is necessary to preprocess it, including pre-emphasis, windowing, endpoint detection, noise filtering, and other operations. Speech signal preprocessing and feature extraction are completed on matlab9.0 platform. MATLAB has corresponding data speech toolbox and digital filter toolbox for the realization of the above functions. Part of the theoretical analysis process is as follows.

Note that, the speech signal is $x(n)$, the output is tested, and the digital speech signal is $y(n)$ after the number. The

main purpose of the speech signal is to emphasize the frequency of speech, eliminate the interference of the lip language, and improve the accuracy of speech frequency [18].

In order to strengthen the voice waveform and weaken the rest of the waveform, the window function is used to process the voice signal. At present, there are three commonly used window functions: hamming window, rectangular window, and hanning window.

Speech exploration is the exploration of the beginning and the end of conversation. There are two methods that are most commonly used: multiple start-ups at the end of the study end and two search-end points at the end. An algorithm for end-to-end detection with two start-ups is usually used to facilitate real-time removal. An algorithm for detecting the end of the end with two starting points must count the speech time: the energy of the short-term short-term and the short-term zero-velocity interactions to calculate check the end of the speech, which can overcome many shortcomings looking forward.

Decomposition of speech signals will eliminate information that does not interfere with speech, and the analysis and processing of speech signals. In this study, the Mel frequency cepstrum coefficient (MFCC), based on listening characteristics, was used to convert speech from the time written to the cepstrum domain and determine speech. The MFCC extraction procedure is shown in Figure 4.

The main extraction algorithms are fast Fourier transform (FFT), Mel filter, logarithmic operation and discrete cosine transform (DCT). MFCC feature parameters will be used as input of speech recognition model.

The language signal pre-emphasis is realized by programming the first-order fir high pass digital filter in the MATLAB system digital filter toolbox. The Hamming window is used to process the voice waveform. The Hamming window is programmed by the window function normalized DTFT amplitude function in the MATLAB system voice toolbox. Voice endpoint detection is realized by voice box function programming in MATLAB system voice toolbox. The speech signal feature extraction process based on Mel frequency cepstrum coefficient is realized by MATLAB and speech toolbox.

3.4.3. Construction of Spoken English Speech Recognition Model and Model Verification. Three machine learning methods, support vector machine, BP neural network, and deep neural network, are used to construct an oral English speech recognition model. The MFCC feature parameters are used as the input of the oral English speech recognition model, and the four most commonly used pronunciation quality evaluation indicators, such as intonation, speech speed, rhythm, and intonation, are used as the output of the model. The model is verified and the speech recognition model with the best performance is selected.

(1) A Model of Spoken English Speech Recognition Based on Support Vector Machine. Support vector machine (SVM) is a supervised learning algorithm in machine learning. It can learn the characteristics of different kinds of known samples and then classify and predict the unknown samples according to the learning results. In this study, SVM algorithm is used to realize speech signal recognition and feature parameter extraction. The kernel algorithm of SVM depends on its kernel function. Kernel function determines the transformation relationship from the inner product in the original dimension to the inner product in the high dimension and directly determines the distribution of samples in the high dimension space. The training data set is used to train SVM, and the trained SVM is used to recognize and verify the parameters of the test data set speech. Before the training data, it is necessary to normalize the feature data to be input into the training set and the test set and then use the feature data in the training set to build SVM. Its parameter settings are as described above and then use the generated SVM prediction model to predict the test set, compare the prediction results with the sentences in the test set, so as to



FIGURE 4: Extraction process of mel frequency cepstrum coefficient.

obtain English speech recognition information and record the corresponding intonation, speed and other speech parameter information [19].

(2) A Model of Spoken English Speech Recognition Based on BP Neural Network. BP neural network has good parallelism, nonlinearity and fault tolerance and has excellent ability of pattern recognition and classification. This study uses a routing neural network consisting of three layers: the input layer, the hidden layer, and the output layer. Commonly used functions are logarithmic operations, logarithmic S-type conversions, and hyperbolic tangent S-type functions.

The input of BP neural network is MFCC characteristic value, the hidden layer adopts activation function, the output is speech recognition information, and records the speech speed, intonation, and other related information. In this study, the BP neural network adopts S-type transformation function, the expected error is set as 0.001, and the number of iterations is set as 200.

(3) Spoken English Speech Recognition Model Based on Res Net Deep Neural Network. The deep residual neural network res net model solves the problems that the traditional convolutional neural network or fully connected network may have more or less information loss and loss during information transmission. Because of its excellent performance, Res Net neural network is used in spoken English speech signal recognition in this study. By training the res net neural network model, the res net neural network model which can recognize speech features is obtained, and then the improved res net neural network model is trained with the new cross feature image training set. The trained neural network has formed a parameter matrix for a single feature and improved the residual block to increase the robustness of the model.

3.4.4. Multiparameter English Pronunciation Quality Evaluation Index and Model Construction

(1) Quantification of Oral English Pronunciation Quality Indicators. In this study, the correlation coefficient between MFCC feature parameters of standard sentences and MFCC feature output from speech recognition model is used as the quantitative index of intonation to judge whether the pronunciation is clear and accurate. The evaluation of speaking speed is quantified by the ratio of standard sentence length to test sentence length. For rhythm evaluation, the pairwise variability index (PVI) proposed by low of Nanyang Technological University in Singapore was used to calculate the rhythm correlation between standard sentences and input sentences.

TABLE 3: Characteristic performance of pronunciation standard evaluation.

Evaluation characteristics	Correlation degree
Logarithmic posterior probability	0.516
GOP	0.549
Pronunciation standard overall performance	0.574

(2) *Construction of Regression Model for Multi Parameter Evaluation of English Pronunciation Quality.* A multiparameter English oral quality analysis model is designed to use multiregression statistical analysis to determine the reliability of the above measurement parameters, as well as bring into account for various parameter parameters such as sound, speed, rhythm, and intonation and their heavy way. Different patterns of different sentences of English speech and pronunciation are considered to be English according to the difference, and the music, fast, music, and music as a difference. The standard English oral measurement model, the coefficient of each measurement, and the values of the model are used in the SPSS assessment analysis.

4. Results and Discussion

In this section, call recognition data effectively assesses students reading English against the call pattern. After testing the performance of the self-measurement function, a support vector regression (SVR) algorithm is used to combine the performance measurement to check the overall performance of the model hu. The performance of the call model measurement is shown in Table 3.

Table 3 shows that the log posterior probability and GOP are good measures of call standardization. If they are used alone, a high correlation with the manual score can be obtained. The correlation between the two exceeds 0.5, and GOP Evaluation has the best performance, with a correlation of 0.549. By combining these two call standard estimation features, the estimation performance is further improved and the correlation reaches 0.574. Compared to the better performing GOP algorithm, the estimation performance is improved by 4.6%. This shows that the multi-parameter regression model for English pronunciation quality assessment has a stronger applicability and can improve the level of spoken English pronunciation of college students [20].

5. Conclusion

This paper proposes several regression models to measure the quality of English speech. Combining the return measurement model and the English language proficiency standard multiple measure, and the English language proficiency standard of the high school students, this model creates a variety of different standards to measure good English, so as to improve the college students' oral English pronunciation level. The experimental results show that log posterior probability and GOP are good measures of pronunciation standard. When used alone, a higher correlation with manual scores can be obtained, and the correlation of both exceeds 0.5. GOP has the best performance, with a

correlation of 0.549. The combination of the standard measurement functions of these two contacts further improves the performance measurement and the correlation level up to 0.574. Performance rating was increased by 4.6% compared to the performance of GOP algorithm. It shows that the multiparameter regression model of English pronunciation quality evaluation is more applicable and can better improve college students' oral English pronunciation.

Data Availability

The data used to support the findings of this study are available from the author upon request.

Conflicts of Interest

The author declares that there are no conflicts of interest.

References

- [1] K. He and H. Feng, "Role status and status-saving behaviour in world politics: the asean case," *International Affairs*, vol. 98, no. 2, pp. 363–381, 2022.
- [2] N. Bogach, E. Boitsova, S. Chernonog et al., "Speech processing for language learning: a practical approach to computer-assisted pronunciation teaching," *Electronics*, vol. 10, no. 3, p. 235, 2021.
- [3] H. Chen and J. Li, "Construction of case-based oral English mobile teaching platform based on mobile virtual technology," *International Journal of Continuing Engineering Education and Life Long Learning*, vol. 31, no. 1, p. 1, 2021.
- [4] A. Bahari, X. Zhang, and Y. Ardasheva, "Establishing a computer-assisted interactive reading model," *Computers & Education*, vol. 172, no. 3, Article ID 104261, 2021.
- [5] M. Yu, Y. Feng, R. Duan, and J. Sun, "Regression analysis of multivariate interval-censored failure time data with informative censoring," *Statistical Methods in Medical Research*, vol. 31, no. 3, pp. 391–403, 2022.
- [6] M. Yu, "Calculation of "two zones" height by empirical formula—shallow 811 working face and shallow 814 working face in bayi mining area of xinhu coal mine," *Advances in Geosciences*, vol. 11, no. 12, pp. 1662–1672, 2021.
- [7] X. Li and H. Yu, "An evaluation model of English teaching effectiveness based on online education," *International Journal of Continuing Engineering Education and Life Long Learning*, vol. 31, no. 1, p. 1, 2021.
- [8] S. P. Yi, "An analysis of emotional English utterances using the prosodic distance between emotional and neutral utterances," *Phonetics and Speech Sciences*, vol. 12, no. 3, pp. 25–32, 2020.
- [9] B. Ma, R. J. Hauer, C. Xu, and W. Li, "Visualizing evaluation model of human perceptions and characteristic indicators of landscape visual quality in urban green spaces by using nomograms," *Urban Forestry and Urban Greening*, vol. 65, no. 3, Article ID 127314, 2021.
- [10] X. Huang, D. Mu, and Z. Li, "Intelligent traffic analysis: a heuristic high-dimensional image search algorithm based on spatiotemporal probability for constrained environments," *Alexandria Engineering Journal*, vol. 59, no. 3, pp. 1413–1423, 2020.
- [11] C. G. Wagner, M. F. Hagan, and A. Baskaran, "Steady states of active brownian particles interacting with boundaries,"

Retraction

Retracted: Vectorization Analysis of Cultural Creative Design Based on the Recognition Model of Virtual Reality Technology

Mathematical Problems in Engineering

Received 8 August 2023; Accepted 8 August 2023; Published 9 August 2023

Copyright © 2023 Mathematical Problems in Engineering. This is an open access article distributed under the Creative Commons Attribution License, which permits unrestricted use, distribution, and reproduction in any medium, provided the original work is properly cited.

This article has been retracted by Hindawi following an investigation undertaken by the publisher [1]. This investigation has uncovered evidence of one or more of the following indicators of systematic manipulation of the publication process:

- (1) Discrepancies in scope
- (2) Discrepancies in the description of the research reported
- (3) Discrepancies between the availability of data and the research described
- (4) Inappropriate citations
- (5) Incoherent, meaningless and/or irrelevant content included in the article
- (6) Peer-review manipulation

The presence of these indicators undermines our confidence in the integrity of the article's content and we cannot, therefore, vouch for its reliability. Please note that this notice is intended solely to alert readers that the content of this article is unreliable. We have not investigated whether authors were aware of or involved in the systematic manipulation of the publication process.

Wiley and Hindawi regrets that the usual quality checks did not identify these issues before publication and have since put additional measures in place to safeguard research integrity.

We wish to credit our own Research Integrity and Research Publishing teams and anonymous and named external researchers and research integrity experts for contributing to this investigation.

The corresponding author, as the representative of all authors, has been given the opportunity to register their agreement or disagreement to this retraction. We have kept a record of any response received.

References

- [1] Y. Yang and Z. Xu, "Vectorization Analysis of Cultural Creative Design Based on the Recognition Model of Virtual Reality Technology," *Mathematical Problems in Engineering*, vol. 2022, Article ID 8930240, 7 pages, 2022.

Research Article

Vectorization Analysis of Cultural Creative Design Based on the Recognition Model of Virtual Reality Technology

Ying Yang ¹ and Zili Xu^{1,2}

¹School of Mechanical and Engineering, Guangzhou College of South China University of Technology, Guangzhou 510800, China

²Faculty of Humanities and Arts, Macau University of Science and Technology, Macau 999078, China

Correspondence should be addressed to Ying Yang; 1706320218@xy.dlpu.edu.cn

Received 9 July 2022; Accepted 1 September 2022; Published 11 October 2022

Academic Editor: Hengchang Jing

Copyright © 2022 Ying Yang and Zili Xu. This is an open access article distributed under the Creative Commons Attribution License, which permits unrestricted use, distribution, and reproduction in any medium, provided the original work is properly cited.

In order to solve the problem of large color matching errors exhibited in the previous color matching system, this study proposes a special color automatic matching system for cultural and creative products based on virtual reality technology. In this study, virtual reality technology (Technology) is applied to the proposed system design. Based on the three-tier architecture, the system framework is designed. The architecture includes a data access layer, a business logic layer, and a presentation layer. The hardware includes a spectrophotometer, a central processing unit, a storage device, and a virtual reality somatosensory interaction device, and the four key devices are introduced in detail. The software part takes the BP neural network algorithm as the core, trains and processes the three color values, constructs the automatic color matching model of cultural and creative products according to the training results, and realizes the logical operation and analysis of the system software. The experimental results show that although there is still a certain error between the color matching of the cultural and creative products output by the system and the actual color matching of the test samples, the maximum absolute error of the matching is relatively small, both of which are less than 0.05, which proves the effectiveness of the research to a certain extent. The error between the 6 groups of actual matching samples and the predicted matching samples is <1.5 , which proves that the color difference is related to human vision, indicating that the matched samples have no color difference and achieve the expected effect. Although there are some errors between the designed system and the expected color matching, the error is small, so the color difference does not affect the visual presentation effect.

1. Introduction

With the continuous improvement of industrialization and the continuous improvement of people's way of life, culture and creative products have become an important part of the culture. The innovative cultural value, retention value, and information transmission value of cultural and creative products have become the core of cultural and creative products. With the advent of the digital age, cultural, and creative products, the carriers of digital technical symbols have emerged, which have the dual characteristics of the integration of technical symbols and digital art. Digital cultural and creative products with technical symbols can not only increase the content and form of cultural and creative products but also conform to the law of the

development of cultural and creative product design. Today, with the rapid development of the digital age, product design with digital technology symbols cannot be avoided by the design industry. The digital age has included a series of information technologies, such as networks and new media virtual simulations. The application of its main technical symbols has brought the possibility of innovation from multiple perspectives. In the future of cultural and creative product design, the integration of digital technology is not only an innovative design but also more likely to become the mainstream form and new media of creative product design in the digital era. Such cultural and creative products are more satisfied with the needs of market users and are also conducive to breakthroughs in the design of cultural and creative products [1, 2]. Exploring the design and research of

cultural and creative products in the digital era can better reflect the value and significance of the combination of the digital era and traditional design in the current society and will contribute to the new development of cultural and creative product design and R&D.

2. Literature Review

Mallika Jecan studied virtual reality technology as purely professional computer technology [3]. Trivedi et al. mentioned virtual reality technology. At the fifth annual meeting of the computer application society of the Chinese Society of Civil Engineering, virtual reality was proposed as one of the three emerging cutting-edge technologies in the world at that time. So far, the Chinese academic circles have paid attention to virtual reality technology [4]. Li and Hou comprehensively introduced the concept, characteristics, short development history, three-dimensional interactive tools, and interactive technology based on the natural skills of virtual reality technology [5]. Liu and Pan started from the technical level, mainly studied the relationship between virtual reality technology and animation art, and paid attention to the changes brought by virtual reality to the animation experience [6]. Gao et al. analyzed the performance technology of virtual reality and thus elaborated the significance of studying virtual reality for vision, hearing, force/touch, and smell/taste [7]. Li et al. regard virtual reality as a core relationship between humans and images and analyze the interaction and symbiosis between humans and images from a macro perspective [8]. Taking “immersion” and “illusion” as clues, this study traces back the historical space of virtual reality fantasy to the frescoes in a mystery villa and discusses the relationship between virtual art and the viewer’s perception and consciousness. Akdere et al. introduced the development process of AR and VR projects, the process of the unity3d software industry, and the application skills of unity3d software interface and nodes so that readers can understand how to use unity3d to develop products [9].

Although many color combinations have been developed, there are no color combinations for commercial and creative products. As a result, there will be some variations of the appropriate colors, there will be significant differences between the product and the ideas and strategies, and the special rules will disappear. Based on this, this material has developed an expert process for automatic color mixing of cultures and creative products to meet the design and implementation requirements of equipment, use virtual (technology) in design, and design consists of four phases: design, hardware design, software development, and system testing.

3. Research Methods

The key to creating a culture and a creative product is how to engage with the culture of the product. It is important to use color to achieve the above goals. Vision is the most sensitive to color. Different colors combine to give a different feel and meaning to the product. Use porcelain as an example: blue

and white porcelain is white and blue, and white represents purity; the green symbolizes spring and energy in Han culture and is good. White glazed porcelain is mainly monochromatic white, and there are many types of white. The higher the whiteness, the stronger the meaning of sweetness and purity. Therefore, once there is a problem with the matching white and the soul of white glazed porcelain will be lost. Different colors can create different visual effects together, and once they are wrongly matched, there will be nondescript phenomena. Therefore, to design good cultural and creative products, virtual reality technology is applied to color matching to help designers “experience” the effect of color matching and adjust the design scheme in time so that the design of cultural and creative products can achieve the expected goal.

3.1. System Framework Design. The automatic color matching system framework of cultural and creative products based on virtual reality technology is designed with reference to the b/s three-tier framework mode, including a data access layer, business logic layer, and presentation layer [10].

3.1.1. Data Access Layer. Be responsible for directly operating the database and adding, deleting, modifying, and searching for data resources. The access layer in this system mainly stores many cultural and creative product samples, color matching schemes, and various operation program codes.

3.1.2. Business Logic Layer. The operation on specific problems, which can also be said to be an operation on the data layer, is the core layer of the entire system [11]. In the system, it is mainly composed of integrated circuit chips, which are responsible for the color matching operations.

3.1.3. Presentation Layer. Generally speaking, it is the interface presented to the user, which is responsible for the successful display of color matching to the user. In the past, the display results of color matching systems were mostly two-dimensional images, lacking an intuitive three-dimensional sense. In the designed system, the display results are mainly displayed through VR technology, which is more intuitive.

3.2. System Hardware Design. The main hardware used in the color automatic matching systems of cultural and creative products based on virtual reality technology includes a spectrophotometer, a central processing unit, a storage device, and a virtual reality somatosensory interaction device. The following is a specific analysis.

3.2.1. Spectrophotometer. The function of the spectrophotometer is to measure the color composition of samples, which is the key to color matching and adjustment. The

spectrophotometer in this system is a CS-580. The equipment features are as follows:

- (1) Color display, true color 2.8 inches, and resolution 320×480
- (2) $\Phi 8/4$ mm two kinds of measuring calibers are suitable for measuring in various scenes
- (3) The interface can use the power adapter for direct charging operation
- (4) Soft rubber buttons are measured at the back of the fuselage, which conforms to the ergonomic design
- (5) The storage capacity of the instrument is 100 standard samples and 20000 samples; it is automatically saved during measurement and records can be cleared

3.2.2. Central Processing Unit. The central processing unit is responsible for the overall control and all operations of the system and is the core part of the system [12]. In this system, an STM32 F429/F439 microcontroller based on ARM[®] Cortex[™]M 4 is selected as the central processor.

3.2.3. Virtual Reality Somatosensory Interaction Device. Virtual reality somatosensory interaction devices are the key to the effectiveness of automatic color matching when users read cultural and creative products. The device is mainly composed of a helmet-mounted display and data sensing gloves. The role of an HMD is to provide users with three-dimensional scenes in virtual reality. The HMD selected in the system is a 3 GLASSESS 2 display. We use a Plug and Play display that does not require drivers and realize voice interaction function through Cortana. The main function of data sensing gloves is to accurately and real time transmit the posture of the human hand to the virtual environment so that users can naturally interact with the establishment of three-dimensional images through gestures, such as opening applications with simple gestures, selecting and adjusting the size of targets, and dragging and dropping holograms, which greatly enhance the interactivity and immersion [13]. The data sensing gloves in this system are Cyberglove II data gloves. The device can measure up to 22 joint angles with high accuracy. It adopts advanced anti-bending induction technology, which can accurately convert the movements of hands and fingers into digital real time joint angle data.

3.2.4. Storage Devices. The main function of the storage device is to store programs and various types of data. Since a large amount of sample data must ensure the accuracy of color matching, it is insufficient to rely only on the memory capacity of the central processor of the system. A storage expansion device is also required in the system [14]. The storage expansion device in the system is BBA-364.

3.3. System Software Program Design. The overall process flow of the software of the automatic color matching system for cultural and creative products based on virtual reality technology is shown in Figure 1.

In the entire system color matching process, the key algorithm is the application of the BP neural network algorithm. For this system, the input value of RGB is three color values of a sample color, and the output value is the proportion of various colors of cultural and creative products, that is, the color scheme [15, 16]. The basic process of creating automatic color schemes of cultures or products based on the BP neural network algorithm is as follows:

Step 1 (prepare the samples): many supporting data models require training BP neural network models. Therefore, the first step in the development of automatic color schemes for cultural or creative products based on the BP neural network algorithm is to develop a model library. The content of the library model should be selected according to the cultural objectives and the creative material.

Step 2 (sample data collection): RGB color characteristic values are collected by a spectrophotometer.

Step 3: standardize RGB color characteristic values. The RGB color characteristic values collected by a spectrophotometer cannot be directly input into a neural network and need to be standardized. The method used is the Premnmx function in MATLAB.

Step 4 (neural network model construction [17]): the problem to be solved by the designed system is the prediction of the color ratio of cultural and creative products.

Creating a neural network is initially divided into two phases: training and experimentation. The sample data are usually divided into two categories, with the most common being used as training models and the smaller ones as test samples. Training: the training sample set is input into the BP neural network model. After the hidden layer transfer function processing, it reaches the output layer. Finally, through the output layer transfer function operation, the color matching scheme of cultural and creative products is obtained [18]. At this time, it is necessary to judge whether the difference between the actual cultural and creative product color matching schemes and the expected cultural and creative product color matching schemes is less than the preset threshold. If the difference is less than the initial one, complete the training of the BP neural network model. If the value difference is greater than the pre-order value, the price difference should be used as the difference between the input value and the weight of each layer to be changed. Constantly, until the weight measurement affects the color contrast of the urine, a concept of culture and creative products to meet demand.

Experiments: test samples were incorporated into a set of BP neural network training models and color models for culture and product development.

The input quantity of BP neural network input layer is shown in the following formula:

$$O_j^{(1)} = x(j), \quad j = 1, 2, 3, 4. \quad (1)$$

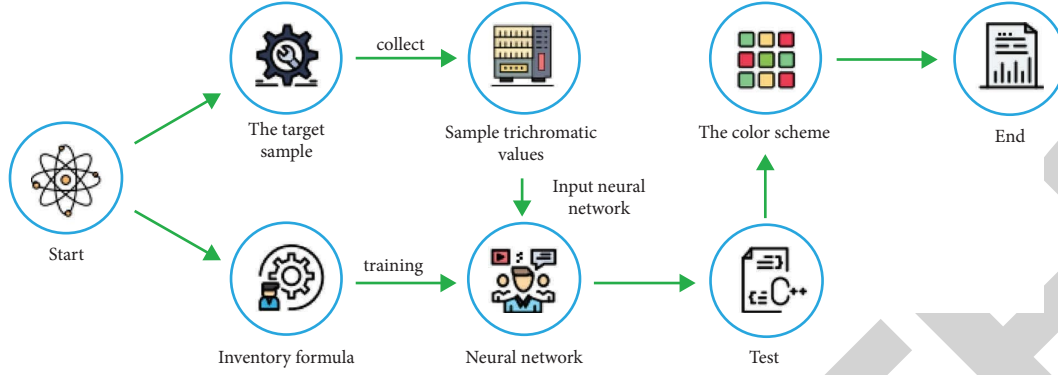


FIGURE 1: Basic process of system color matching.

The input and output quantities of the BP neural network hidden layer are, respectively, shown in formulas (2) and (3):

$$\text{net}_i^{(2)}(k) = \sum_{j=0}^m w_{ij}^{(2)} O_j^{(1)}(k), \quad (2)$$

$$o_i^{(2)}(k) = f[\text{net}_i^{(2)}(k)], \quad i = 1, 2, \dots, 5, \quad (3)$$

where $w_{ij}^{(2)}$ is the weighting coefficient from the input layer to the hidden layer of the BP neural network, and the input layer, hidden layer, and output layers correspond to the above marks (1)–(3), respectively, and M is the number of neuron inputs. A hyperbolic tangent function is adopted as the excitation function for hidden layer neurons:

$$f(x) = \frac{e^x - e^{-x}}{e^x + e^{-x}}. \quad (4)$$

The input and output quantities of BP neural network output layer are, respectively, shown in formulas (5) and (6):

$$\text{net}_i^{(3)}(k) = \sum_{i=0}^q w_{ii}^{(3)} O_i^{(2)}(k), \quad (5)$$

$$o_i^{(3)}(k) = g(\text{net}_i^{(3)}(k)). \quad (6)$$

It is obtained from the following formula:

$$\begin{aligned} o_1^{(3)}(K) &= K_p, \\ o_2^{(3)}(K) &= K_i, \\ o_3^{(3)}(K) &= K, \end{aligned} \quad (7)$$

where $w_{ii}^{(3)}$ is the weighting coefficient from the hidden layer to the output layer and $g(x)$ is the activation function of neurons in the output layer:

$$\begin{aligned} g(x) &= \frac{1 + \tanh(x)}{2} \\ &= \frac{e^x}{e^x + e^{-x}}. \end{aligned} \quad (8)$$

The performance index function is as

$$E(k) = \frac{1}{2}[r(k+1) - y(k+1)]^2. \quad (9)$$

In order to speed up the convergence, an inertia term is added to make the search converge to the global minimum quickly. The formula of the neural network weight coefficient is modified according to the gradient descent method as

$$\Delta\omega_{ii}^{(3)}(k+1) = -\eta \frac{\partial E(k)}{\partial \omega_{ii}^{(3)}} + \alpha \Delta\omega_{ii}^{(3)}(k), \quad (10)$$

where η is the learning rate and α is the momentum factor. (11) can be obtained from (7):

$$\begin{cases} \frac{\partial u(k)}{\partial o_1^{(3)}(k)} = e(k) - e(k-1), \\ \frac{\partial u(k)}{\partial o_2^{(3)}(k)} = e(k), \\ \frac{\partial u(k)}{\partial o_3^{(3)}(k)} = e(k) - 2e(k-1) + e(k-2). \end{cases} \quad (11)$$

Thus, the output layer weight calculation formula (12) of the BP neural network can be obtained:

$$\begin{aligned} \Delta\omega_{ii}^{(3)}(k+1) &= \eta e(k+1) \text{sgn}\left(\frac{\partial y(k+1)}{\partial u(k)}\right) \\ &\quad \frac{\partial u(k)}{\partial o_i^{(3)}(k)} g[\text{net}_i^{(3)}(k)] o_j^{(2)}(k) \\ &\quad + \alpha \Delta\omega_{ii}^{(3)}(k), \quad j = 1, 2, 3, 4, i = 1, 2, 3. \end{aligned} \quad (12)$$

4. Result Analysis

4.1. System Test and Analysis. In order to test the automatic color matching performance of the system, silk fabric is taken as an object for color matching research, and the color

TABLE 1: System test environment.

Name	Parameters
Development language	VRML, HTML, C++
Web application service	Visual Studio 2005
Database	Microsoft SQL Server 2000
Modeling tools	Microsoft Office Visio 2003
Image processing tools	Adobe Photoshop 6.0
Virtual reality software	Pano2VR
Simulation software	Matlab 2.0

TABLE 2: Sample data set (part).

Sample serial number	Sample RGB value			Color scale		
	R	G	B	Brown	White	Red
1-1	150	140	135	5	5	2
1-2	151	77	135	5	5	2
1-3	152	77	138	5	5	2
1-4	149	76	134	5	5	2
1-5	144	77	129	5	5	2
2-1	153	75	140	1	1	5
2-2	135	86	117	1	1	5
2-3	136	85	119	1	1	5
2-4	136	84	118	1	1	5
2-5	135	85	116	4	4	2
3-1	134	86	116	6	6	2
3-2	130	100	109	6	6	2
3-3	127	101	107	6	6	2
3-4	128	96	108	6	6	2
3-5	127	96	107	6	6	2
4-1	128	98	108	3	3	4
4-2	116	82	94	3	3	4
4-3	115	81	93	3	3	4
4-4	113	81	91	3	3	4
4-5	112	81	90	3	3	4

difference in color matching is taken as the inspection standard.

4.1.1. System Test Environment. The system test environment is shown in Table 1.

4.1.2. Test Samples. In this study, 150 types of silk fabrics are selected as objects to build a sample library.

RGB color characteristic values are collected by a spectrophotometer to obtain 150 groups of original sample data sets, which are standardized to obtain training sample sets and inspection sample sets [19]. Among them, 80% of the data is used as the training sample set, and the remaining 20% is used as the test sample set, as shown in Table 2.

4.1.3. Neural Network Parameter Setting. Neural network parameter settings are shown in Table 3.

TABLE 3: Parameter setting table of BP neural network.

Parameters	Value
Network layers	3
Number of nodes in each layer	3
Transfer function	tansig
Output transfer function	purelin
Learning rule function	traingdx
Training error	0.07
Maximum steps of training	2000

4.1.4. System Color Matching Results. The benefits of automatic color schemes for comparison of materials and design based on neural network algorithms are shown in Table 4 (the last 6 groups are selected for explanation).

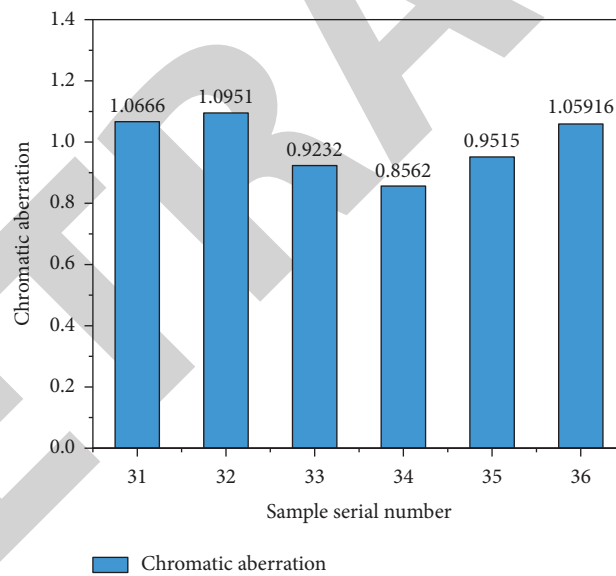
It can be seen from Table 4 that although there is still a certain error between the color matching of cultural and creative product output by the system and the actual color matching of test samples, the maximum absolute error of

TABLE 4: System color matching results (part).

Sample serial number	Actual proportioning			Network output ratio			Maximum absolute error of proportioning
	Brown	White	Red	Brown	White	Red	
31	5	3	2	5.262	2.767	1.764	0.0458
32	4	4	2	4.192	3.501	1.919	0.0196
33	3	5	2	2.530	5.535	2.175	0.0372
34	3	4	3	3.157	3.772	3.071	0.0238
35	3	3	4	3.244	2.813	3.873	0.0304
36	4	3	3	4.141	2.845	3.053	0.0155

TABLE 5: Average values of R , G , and B of actual matching samples and predicted matching samples.

Sample serial number	Actual proportioning			Network output ratio		
	R	G	B	R	G	B
31	87	76	68	85	75	69
32	95	84	77	93	83	75
33	111	98	92	108	95	90
34	96	81	76	97	80	76
35	92	73	69	87	72	67
36	91	76	69	89	71	66

FIGURE 2: Color difference of R , G , and B mean values of actual matching samples and predicted matching samples.

matching is relatively small, both less than 0.05, which proves the effectiveness of the study to a certain extent.

4.1.5. Color Difference Statistical Results. The above research results are not intuitive enough and have little practical reference significance. Therefore, in order to further test the color matching effect of the system, the color difference is used as an indicator for further testing [20, 21]. Color difference detection is used to analyze the color difference after extracting the image color characteristic value. The color difference test results are shown in Table 5 and Figure 2.

It can be seen from Table 5 and Figure 2 that the errors between the 6 groups of actual matching samples and the predicted matching samples R , G , and B are $\Delta E < 1.5$, which proves that the color difference is related to human vision, indicating that the matched samples have no color difference and achieve the expected effect [22, 23].

5. Conclusion

To sum up, the emergence of cultural and creative products has promoted and inherited many traditional cultures. Culture and creative products have been transformed and

Retraction

Retracted: Intelligent Optimization of the Financial Sharing Path Based on Accounting Big Data

Mathematical Problems in Engineering

Received 1 August 2023; Accepted 1 August 2023; Published 2 August 2023

Copyright © 2023 Mathematical Problems in Engineering. This is an open access article distributed under the Creative Commons Attribution License, which permits unrestricted use, distribution, and reproduction in any medium, provided the original work is properly cited.

This article has been retracted by Hindawi following an investigation undertaken by the publisher [1]. This investigation has uncovered evidence of one or more of the following indicators of systematic manipulation of the publication process:

- (1) Discrepancies in scope
- (2) Discrepancies in the description of the research reported
- (3) Discrepancies between the availability of data and the research described
- (4) Inappropriate citations
- (5) Incoherent, meaningless and/or irrelevant content included in the article
- (6) Peer-review manipulation

The presence of these indicators undermines our confidence in the integrity of the article's content and we cannot, therefore, vouch for its reliability. Please note that this notice is intended solely to alert readers that the content of this article is unreliable. We have not investigated whether authors were aware of or involved in the systematic manipulation of the publication process.

Wiley and Hindawi regrets that the usual quality checks did not identify these issues before publication and have since put additional measures in place to safeguard research integrity.

We wish to credit our own Research Integrity and Research Publishing teams and anonymous and named external researchers and research integrity experts for contributing to this investigation.

The corresponding author, as the representative of all authors, has been given the opportunity to register their agreement or disagreement to this retraction. We have kept a record of any response received.

References

- [1] Z. Zhang, "Intelligent Optimization of the Financial Sharing Path Based on Accounting Big Data," *Mathematical Problems in Engineering*, vol. 2022, Article ID 1310994, 8 pages, 2022.

Research Article

Intelligent Optimization of the Financial Sharing Path Based on Accounting Big Data

Zhongmin Zhang 

School of Accounting, Guizhou University of Finance and Economics, Guiyang, Guizhou 550025, China

Correspondence should be addressed to Zhongmin Zhang; 20153201072@m.scnu.edu.cn

Received 15 August 2022; Revised 28 September 2022; Accepted 29 September 2022; Published 11 October 2022

Academic Editor: Hengchang Jing

Copyright © 2022 Zhongmin Zhang. This is an open access article distributed under the Creative Commons Attribution License, which permits unrestricted use, distribution, and reproduction in any medium, provided the original work is properly cited.

In order to solve the problems of inconsistent accounting and untimely accounting information, this paper proposes a research method of intelligent optimization of financial sharing path based on big data of accounting. This paper analyzes the current working situation of the financial sharing service center of large- and medium-sized enterprises and expounds the reasons for the blockchain. The author embeds the blockchain technology in the financial sharing service center, with a view to optimizing the design of the current FSSC's functions in terms of the scope of daily business work, the effectiveness of accounting information processing, and the utilization of financial analysis decisions, and finally analyzes the corporate effect of applying the financial sharing architecture based on blockchain technology. The results show that compared with the financial sharing score under the traditional mode, the financial sharing score under the blockchain technology is higher, and the former is 69.675 points, and the latter is 80.6340 points. From this, we can conclude that financial sharing under blockchain technology has significant advantages. This framework realizes the effective allocation of enterprise information resources through finance to achieve real industry finance integration.

1. Introduction

With the development of economic globalization and information technology, mergers and acquisitions between enterprises are becoming more and more frequent, and the problems of financial cost separation, low efficiency, and poor information quality caused by the expansion of enterprises are becoming more and more obvious. In recent decades, large enterprise groups have grown rapidly. They have established branches and subsidiaries all over the world. The expansion of their scale has increased the pressure of financial management. The repeated financial institutions of branches and subsidiaries have increased the cost of financial management, increased the difficulty of the group's management and control, and their independent financial management rights have led to an increase in the risks of the group's operation and financial management, and shareholders' equity may be damaged [1]. Therefore, large enterprise groups urgently need to find a way out to solve the financial management crisis caused by the above

problems. Financial management activities produce a large amount of data information for enterprises, and its processing efficiency and security restrict the development of large enterprise groups. The financial sharing mode in the 1980s focused on the centralized operation of accounting processing business by establishing a new business unit. Instead of focusing on the tedious basic business processing, enterprise financial managers focused on the core business of the enterprise so as to integrate the internal financial resources of the enterprise, improve the service quality, and enhance customers' satisfaction with financial information [2]. In the new era, with the help of cloud computing technology, the financial sharing mode has greatly improved the data storage capacity and computing capacity in the financial sharing service in the era of big data, and the data security has also been guaranteed, which has provided great help for the integration of financial resources, the reengineering of financial management process, and the improvement of financial business processing efficiency of enterprise groups.

On the basis of this research, this paper proposes a research on the intelligent optimization of financial sharing path based on accounting big data. Combined with the current status analysis of the construction of the financial shared service center, it studies how the blockchain technology can realize the further optimization and design of the financial shared service center and finally analyzes the benefits of a company after applying the financial shared model architecture. It improves the automatic processing of enterprise accounting information and accelerates the use of financial data to make decisions on production, operation, and management of the entire enterprise.

This paper studies and analyzes the financial sharing service platform by using the relevant literature research method, analytic hierarchy process, case analysis method, combined with its operating conditions. Based on the above analysis results, it further concludes the advantages of blockchain technology in the financial sharing platform. First, the concept and characteristics of blockchain technology and financial sharing are sorted out, laying a good theoretical foundation for the next step of research. Secondly, it describes the development status of blockchain technology and financial sharing at home and abroad, analyzes the operation status of its financial sharing service platform, and points out the shortcomings. Finally, the paper analyzes the benefit of the financial sharing mode under the blockchain technology and proposes the implementation guarantee strategy of the financial sharing platform under the blockchain technology.

This paper studies and analyzes the financial sharing service platform by using the relevant literature research method, analytic hierarchy process, case analysis method, combined with its operating conditions. Based on the above analysis results, it further concludes the advantages of blockchain technology in the financial sharing platform. First, the concept and characteristics of blockchain technology and financial sharing are sorted out, laying a good theoretical foundation for the next step of research. Secondly, it describes the development status of blockchain technology and financial sharing at home and abroad, analyzes the operation status of its financial sharing service platform, and points out the shortcomings. Finally, the paper analyzes the benefit of the financial sharing mode under the blockchain technology and proposes the implementation guarantee strategy of the financial sharing platform under the blockchain technology.

2. Literature Review

Mashatan and others believed that shared services belong to an internal activity of an enterprise, which includes a variety of functions, including finance, and marketing. Analyzing relevant activities according to ACCA's professional standards, we can find that some financial activities can be managed through iterative background processes, including accounts receivable and accounts payable [3]. Vikaliana and others analyzed the process of big data audit in the process of analyzing shared services, analyzed the flow direction and preprocessing process of data, and found out the key points that play a theoretical supporting role. These keys enable the

financial sharing model to develop rapidly and effectively [4]. Surjandy and others took Huawei as the object of service when analyzing financial shared services and analyzed the performance of the company from three aspects, all of which will affect the performance of the company. The research results show that the performance of enterprises will be affected by the financial shared service center [5].

Jagadhesan and others believed that the financial shared service model needs to be supported by big data and the Internet. Although the financial process is the most basic content, creating value for the enterprise is the ultimate goal [6]. The financial sharing service model will make the work efficiency of large group companies higher. This model is an innovation of thinking and will be widely used in the future. Hameed and others listed all aspects involved in information system, including credit system, performance management system, and logistics support system. After completing the enterprise financial sharing service, the information system will standardize and professionalize all the contents and make better services at the same time [7].

Bhardwaj and others have studied the security performance of cloud computing technology. In the process of research, they hoped to make a set of very secure audit protocols. This audit protocol can block privacy fraud. If this work can be successfully completed, it will be a very perfect project, which combines storage and computing security smoothly [8]. Yu and others reviewed the current status of cost management in the financial shared service center of Group A and elaborated on the current problems of inability to automatically collect cross-system data, untimely cost accounting, and unreasonable cost analysis and reporting models that are too fixed. Based on robotic process automation (RPA), the cost management process is optimized and improved in terms of cross-system data collection, "cloud procurement platform" construction, and multidimensional comprehensive cost analysis. It is expected to provide a reference for the application of robotic process automation in financial shared service centers [9]. Dong started with the infrastructure of the blockchain, established the infrastructure model and specific optimization path of the financial sharing model, and finally designed the internal and external "double-chain" structure of the financial sharing model based on blockchain technology, hoping to become a financial sharing model. The current development dilemma is looking for a new way out [10]. A multiobjective optimization problem (MOP) usually has more than two objective functions, resulting in an optimal solution based on the Pareto front. Traditional optimization algorithms can no longer meet the needs of industrial applications when dealing with multiobjective optimization problems. With the good performance of evolutionary algorithms in solving complex problems, its application field has also expanded to multiobjective optimization problems. Nie analyzed the Pareto optimal solution and evaluation system of multiobjective optimization problems. The particle swarm optimization (PSO), one of the evolutionary algorithms based on swarm intelligence, is briefly introduced. The combination of particle swarm optimization algorithm and multiobjective optimization is studied [11].

Based on the description of blockchain technology and the analysis of the current situation of the construction of financial sharing service center, this paper studies how blockchain technology can further optimize and design the financial sharing service center and finally analyzes the benefits of a company after applying the financial sharing mode architecture.

3. Research Methods

3.1. Construction Status of the Financial Shared Service Center.

In the new era of industry finance integration, service is to use accounting information to provide help for the operation and decision-making of enterprises. Through the financial sharing service center, enterprises hope to centralize the business information of their branches in various regions to the financial sharing service center so as to carry out unified accounting and data analysis and achieve business data sharing, cost standard accounting, and standardized profit processing. Finally, the effect of saving enterprise financial costs, guiding enterprise budget management, judging possible risks and prompting is achieved. Its operation mode is shown in Figure 1. At present, the services provided by the financial sharing service center can basically realize the functions of synchronizing business information, unified accounting, and timely result feedback of enterprise groups. However, it is still far from the functions of data analysis, business management, and simplified process in the establishment of FSSC objectives.

3.1.1. FSSC Automatic Business Processing Degree.

Financial sharing service is based on the development of data and information technology, and its construction requires a high automation foundation. The higher the level of information automation, the larger the business scope of FSSC processing. At present, although ERP information technology has been fully implemented in enterprises and institutions and the module management of various business information data has been specific to all aspects of financial work, the automation level in financial management is still in the basic stage. As shown in Figure 2, at present, the most widely used automation system in most enterprises is accounts receivable, accounting for 64.19%. Next came the general ledger and a/P, accounting for 28.57% and 23.81%, respectively. This shows that at present, most of the FSSC accounting information has a low degree of automation mainly because it can complete the automatic entry of funds. Then there are general ledger, payables, expenses, taxation, etc.

3.1.2. FSSC Accounting Information Utilization. The focus of enterprise financial management is to integrate the fragmented accounting information and turn the data into effective information based on the whole value chain through special analysis procedures [12, 13]. The ultimate goal of establishing FSSC is to achieve the integration of industry and finance through financial standardization, standardization, and systematic operation and to realize that finance

provides data support and analysis services for enterprise management decisions. However, as shown in Figure 3, the accounting information utilization rate of enterprises that have established FSSC is not high, and the average number of enterprises that can apply data information to budget analysis and financial prediction, cost profit analysis, performance analysis, etc. is not more than 39%. This shows that FSSC has not done enough in information support for enterprise management decisions, especially in customer payment behavior and customer credit risk assessment related to capital risk control.

4. Result Analysis

4.1. Design of Blockchain Technology for the Optimization of Financial Shared Service Mode

4.1.1. Optimization Design of Blockchain Technology on FSSC's Daily Business Scope. At present, most of FSSC's daily work depends on the image scanning and uploading of original vouchers (documents) directly by the financial department of the branch company, such as the documents of daily expenses (reimbursement), and FSSC staff can quickly make financial accounting and pay reimbursement expenses. However, for the work involving many departments and a wide range of businesses, such as the supplier information management data, the procurement department needs to cooperate to complete the image scanning and uploading of the supplier's name, taxpayer identification number, scale, product type, region, and other data. In contrast, the finance department is specialized in this work, and the main job of the procurement department is to carry out procurement tasks, which is cumbersome and heavy workload for them [14].

(1) *Optimization Suggestions.* Embed blockchain into the whole process of business activities. Using blockchain technology, each network port of the whole enterprise is added to the group's internal information receiving and sending network. As long as the branch company has a transaction, it can calculate and transmit data information according to the block mode. As long as it is on the same blockchain, it can be immediately recognized and recorded, and the next time a transaction occurs, continue to record it on the chain one by one [15, 16]. Blockchain will not increase the workload but can solve the problems of large amount of data and cumbersome data, and it is difficult to upload to FSSC completely.

(2) *The Key Point of Optimization.* It is distributed accounting of blockchain. Under blockchain technology, the transmission of information is to link individual block recording the information to a chain connected end to end through the user's encrypted signature and professional verification and become a part of the next piece of information. In this chain, any individual block is an independent and complete information, and each information can be traced back to the previous block [17]. Accounting standards require that the accounting information of the economic business records of enterprises must be kept complete under the condition of ensuring the reliability of accounting

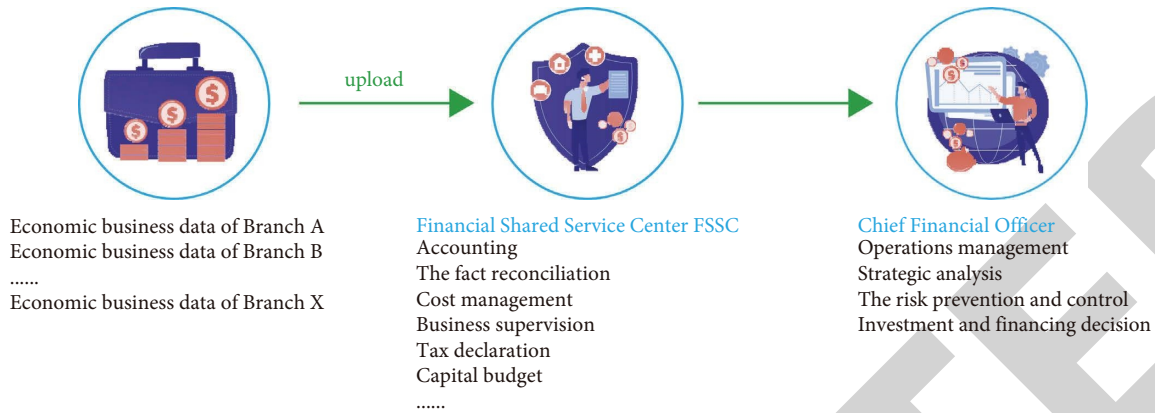


FIGURE 1: Financial FSSC operation mode under the integration of industry and Finance.

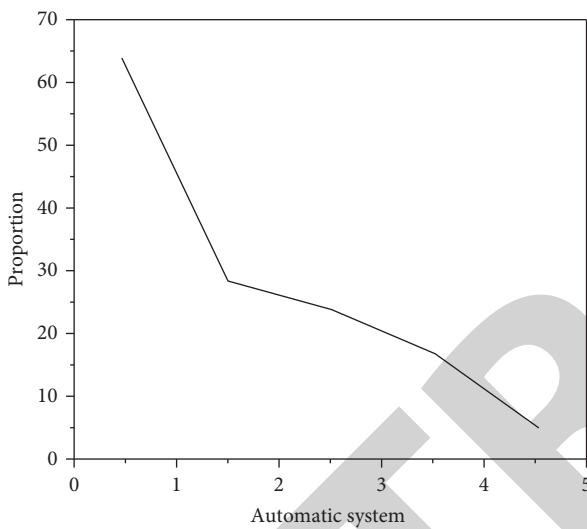


FIGURE 2: Application of the financial shared service center automation system.

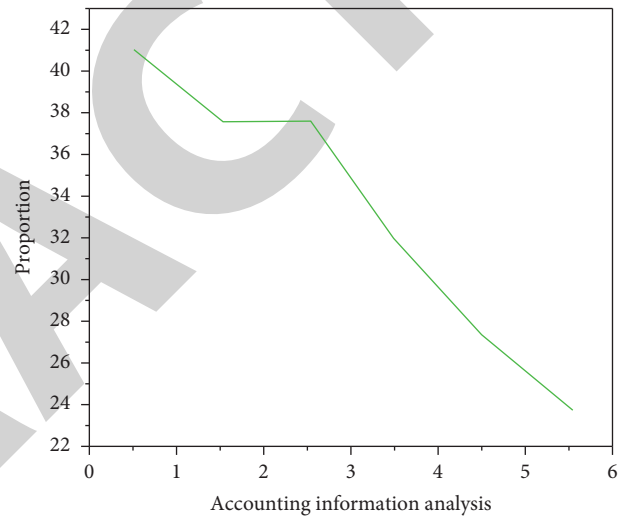


FIGURE 3: Analysis and utilization of accounting information of the financial sharing service center.

information. Under the distributed bookkeeping behavior of blockchain technology, any participant and user of accounting information can obtain all the information of their designated blocks and nest it into the next step, which solves the problem of accounting information being arbitrarily omitted from the technical level.

(3) *Optimization Measures.* It uses the “chain” to realize the instant and complete transmission of information. The occurrence of each business activity of the enterprise, on the one hand, uploads the FSSC in time according to the internal and external vouchers, and on the other hand, transmits one link by one broadcast in the block until all information is transmitted to the FSSC completely and correctly. Taking the sales business as an example, any sales business of an enterprise is stamped and broadcasted to the intranet ports of the enterprise (these ports exist in the financial and supply and marketing departments of the enterprise (group) and its subsidiaries (branches) all over the country, and the data are in a completely transparent perspective) from the beginning of accepting the purchase application and confirming the purchase and sales agreement. With the occurrence of

collection, delivery, and other businesses, multiple blocks covered by multiple time stamps form a “chain” of distributed bookkeeping. Therefore, all information of sales business can be recorded into FSSC in a timely manner. Because the ports of each department of the enterprise are in the blockchain, the purchase and sales contracts and the delivery orders of purchased and sold goods are confirmed to FSSC through the circulation of the corresponding departments. In this way, the content of FSSC processing business is not limited to the expense reimbursement and general ledger processing of the financial department but can be extended to all aspects of supplier (customer) information management, generation cost management, and so on so that the financial information in the industry finance integration is consistent with the business information.

4.1.2. *Optimization Design of Blockchain Technology for FSSC Automatic Processing Business.* At present, the automation level of FSSC processing business is still in the basic stage of current accounts with only a/R and a/P accounts and the automatic processing of expenses, especially the carry

forward of period expenses, and other information automation applications are less [18]. The reason may be that the accounting subjects under the jurisdiction of costs and expenses need secondary judgment, such as whether the wages of workshop directors should be included in management expenses, manufacturing expenses, or production costs.

(1) *Optimization Suggestions.* Use smart contracts to improve the automation of accounting information processing. The smart contract of blockchain is embedded into the accounting information processing system of FSSC. When the images of branches are transmitted to the FSSC Information Center, as long as the information triggers the smart contract, the instructions will be issued to the accounting subjects if the conditions are met. The accounting information system will automatically generate vouchers to complete the accounting of accounts receivable, general ledger, a/P, and even costs and expenses. Only manual auxiliary approval is required.

(2) *Key Point—Smart Contract of Blockchain.* The decentralized nature of blockchain technology eliminates the mistrust of both sides of the transaction in the transmission of accounting information so that the information is completely recorded in both sides of the transaction. Each user port has a copy of the ledger, so there is no need to emphasize that the content of accounting information quality in blockchain is true and complete. Smart contracts are event driven, stateful, and run on a replicated and shared ledger. Traditional contracts require equivalent text confirmation by both parties before signing, while smart contracts are not only defined by code but also enforced. It is completely automatic and cannot be interfered with. When the preprepared account definition and concept conditions are triggered, the smart contract can directly implement the corresponding contract terms and basically realize the forced automatic matching of accounts.

(3) *Optimization Measures-* Automatic matching occurs through smart contracts. After the transaction occurs, FSSC can directly realize the automatic matching of business and accounts through smart contracts and strengthen the foundation of automatic accounting. When a business meeting the management expense dimension occurs, the accounting information system finds the keyword according to the definition of the management expense, automatically matches it into the management expense account through the smart contract, and then enters it into the related detailed account according to the keyword attribution. Then, according to the relationship between the collection and payment and the nature of the account, the accounting information is automatically accounted, so that the business occurrence in the financial integration is financial accounting.

4.1.3. *Blockchain Technology Optimizes the Design of FSSC's Analysis and Prediction Using Accounting Information.* After the establishment of FSSC, enterprises also have a low utilization rate of analysis of accounting information, which

is mainly caused by two reasons: first, the timely and effective accounting information and second, the objective integrity of accounting information. Whether it is financial budget and prediction, cost profit analysis, or performance analysis, or even the customer's credit rating, payment behavior, and credit risk assessment, FSSC needs to obtain all the information of all links involved in the process of enterprise capital movement in time, so as to make comparison, assessment, and prediction.

(1) *Optimization Suggestions.* Blockchain extends into FSSC's large database for real-time sharing. Financial sharing not only enables the sharing of accounting information but also includes all information that occurs in the enterprise [19]. The main support for enterprises to use large databases to complete risk management and control and investment and financing decisions is that large databases can provide early or multistage data comparison, which can be analyzed and studied in combination with the current economic environment. To extend the blockchain technology into the large database of FSSC processed information, we must first solve the trust problem of data information and then make the information of production department, procurement department, and sales department enter the large database at the same time through timely automatic transmission and then use the large database to synchronously complete the comparison, analysis, and evaluation of production, sales, procurement, and even suppliers.

(2) *Key Point: Decentralization and Timing of Blockchain.* The decentralization of blockchain enables the point-to-point transmission of data information, which theoretically does not exist to be forged. It also uses the chain structure marked with time stamps to store data and gives a speed evaluation to each record and calculator on the network side [20]. Therefore, transaction data can be truthfully and timely recorded on the blockchain. Through the real-time timestamp of blockchain, every transaction business can be broadcasted and transmitted in time, which greatly improves the work efficiency and utilization of information users.

(3) *Optimization Measures.* Synchronize real big data analysis with "blocks." When an enterprise's economic business occurs, after the blockchain technology is used as the underlying support and extended into the large database, any transaction related data can be sent to FSSC in real time and also accurately, and cost resources will be virtually shared under the network of the enterprise architecture. From the original indifferent attitude of "obeying the arrangement" and "having nothing to do with me" to the resources and constraints of costs, the branches have changed to the group center and other branches, under the analysis of big data, and quickly obtain the most matching practical information resources, and identify, screen, and utilize them in combination with their own characteristics, so as to realize the optimal allocation of capital costs and time costs of various resources under big data. Similarly, this real-time data through blockchain technology in the big database can also allow managers to integrate and judge

TABLE 1: Pairwise discriminant matrix.

	Customer	Group finance	Enterprise organization process	Other factors
Customer	1	2	2	3
Group finance	1/2	1	2	2
Enterprise organization process	1/2	1/2	1	2
Other factors	1/3	1/2	1/2	1

enterprise resources in a timely manner through changes at any time and even track the operation of ongoing investment projects in the big database to make analysis and prediction, so as to achieve the highest part of industrial and financial integration-guiding business activities with financial information and supporting financial activities with business information.

4.2. Benefit Analysis of a Company's Financial Sharing Mode Framework under Blockchain Technology. In the process of analyzing the financial sharing mode of a company, this paper uses AHP and puts forward four dimensions, namely, information sharing dimension, group financial system dimension, enterprise organization process dimension, and other factor dimension, and each dimension has its corresponding weight. Compare the four dimensions of the two models, then score each dimension, and finally multiply the score and weight to obtain the final conclusion.

Under the analytic hierarchy process, the allocation of performance evaluation indicators is completed under the principle of rationality of weight distribution, and a scientific evaluation system structure is formed. The following table is the overall level weight and judgment matrix. All enterprises' operations are inseparable from the support of customers. Therefore, the customer dimension ranks first in the four dimensions of the standard level, and the group financial dimension and the enterprise organization process dimension rank second, and finally, other factor dimensions. The ultimate purpose of business execution is to obtain economic benefits, and the application of blockchain technology to its financial sharing platform is mainly to optimize its internal processes and reduce internal costs of the enterprise. All these are for customer service, so the customer dimension is the most important. The control of enterprise organization process and group finance are also to adjust from within the group to provide customers with better services. Since ancient times, customer resources have been regarded as the core and foundation of enterprise operation. Based on the above analysis and discussion, we have formulated the Mengniu Dairy index evaluation system to achieve long-term strategic planning.

According to the index system, we sincerely invite a number of scholars in professional fields to score the importance of the index, summarize it according to the scoring results, and then obtain the pairwise discrimination matrix, as shown in Table 1.

Calculate the maximum eigenvalue of the judgment matrix S and get $\lambda_{\max} = 4.0710$. The consistency index is calculated as

TABLE 2: Weight distribution.

Index layer	Weight
Customer	0.4182
Group finance	0.2707
Enterprise organization process	0.1906
Other factors	0.1205

$$\begin{aligned}
 CI &= \frac{\lambda_{\max} - n}{n - 1} \\
 &= \frac{4.0710 - 4}{4 - 1} \\
 &= 0.0237.
 \end{aligned} \tag{1}$$

Average random consistency index $RI = 0.89$. The random consistency ratio is

$$\begin{aligned}
 CR &= \frac{CI}{RI} \\
 &= \frac{0.0237}{0.89} \\
 &= 0.0266 < 0.10.
 \end{aligned} \tag{2}$$

Therefore, the consistency of the results of analytic hierarchy process indicates satisfaction, which means that the distribution of weight coefficients is reasonable. The weight of the index is calculated, as shown in Table 2.

Calculate the maximum characteristic root of the judgment matrix s to get $\lambda_{\max} = 3.0055$ to calculate the consistency index and get

$$\begin{aligned}
 CI &= \frac{\lambda_{\max} - n}{n - 1} \\
 &= \frac{3.0055 - 3}{3 - 1} \\
 &= 0.0028.
 \end{aligned} \tag{3}$$

Mean random concordance indicator $RI = 0.52$. Random consistency ratio is

$$\begin{aligned}
 CR &= \frac{CI}{RI} \\
 &= \frac{0.0028}{0.52} \\
 &= 0.0053 < 0.10.
 \end{aligned} \tag{4}$$

TABLE 3: Expert scoring results.

Index layer	Weight	Index layer	Weight	Scoring of the financial sharing mode in the context of blockchain	Scoring of the traditional financial sharing mode
Customer	0.4182	Customer growth rate	0.4434	93	80
	0.4182	Financial service satisfaction	0.3874	89	73
Group finance	0.2707	Financial sharing cost	0.6608	94	82
	0.2707	Labor cost	0.2081	92	72
Enterprise organization process	0.1906	Business process optimization	0.5954	92	82
	0.1906	Business error rate	0.2764	83	73
Other factors	0.1205	Staff efficiency	0.4126	85	75
	0.1205	Customer satisfaction	0.3275	82	79
	0.1205	Enterprise training fee	0.2599	90	73
Final score				80.6340	69.675

Invite several experts to score, using the hundred mark system scoring method, and invite experts to score the indicators of the financial sharing mode and the financial sharing mode based on blockchain under the traditional mode, so as to obtain the comprehensive weight. The scoring adopts the five grade system, with 100 ~ 90 points as the first grade, 89 ~ 80 points as the second grade, 79 ~ 70 points as the third grade, 69 ~ 60 points as the fourth grade, and below 60 points as the fifth grade. The mean value is obtained based on the sum of the data. Based on the mean value of each grade, the percentile conversion is implemented, and the highest and lowest values of expert scores are removed. Then the mean value is calculated and taken as an integer. Finally, we obtain Table 3.

According to the data in Table 3, for the company, the score of financial sharing mode under blockchain technology is higher than that under the traditional mode, and the former is 69.675 points, while the latter is 80.6340 points. From this, we can conclude that financial sharing under blockchain technology has significant advantages [21].

5. Conclusion

This paper analyzes the basic situation of the current development of financial sharing services in China and the West and finds that financial sharing services have a good development trend but lacks stamina. Then this paper optimizes the design of blockchain technology. With the continuous in-depth research and development of blockchain technology, it can provide more and more help for financial sharing services. In the context of the vigorous development of financial sharing services, the embedding of blockchain technology can solve the problems of enterprises abandoning existing systems and high hardware replacement costs in the process of establishing financial sharing centers, optimize the security, integrity, asymmetry, slowness, and other problems in the exchange and replacement of financial data, improve the degree of automatic processing of enterprise accounting information, and accelerate the pace of using financial data to make production and operation management decisions for the whole enterprise. The further application of blockchain technology in the financial sharing service center also requires the joint efforts of

financial personnel and computer personnel to further realize the business financial integration of enterprises.

In the era of continuous development and progress of information technology, the enterprise financial sharing platform should adapt to the changes of the times and take a high-quality development road of high informatization, automation, and intelligence. Applying blockchain technology to the enterprise financial sharing platform can precisely avoid the defects of the current financial sharing platform, improve the standardization and accuracy of the sharing platform, and respond to the needs of accounting in the new era in terms of scale and timeliness. Blockchain technology has broad market prospects. Today, with the rapid development of information technology, major enterprises should seize the opportunity of development and use blockchain technology to overcome the difficulties of shared services due to changes in the environment. This will enable the financial sharing platform to adapt to the pace of the new era, stand firm, and develop rapidly in the torrent of the times.

Data Availability

The data used to support the findings of this study are available from the author upon request.

Conflicts of Interest

The author declares that there are no conflicts of interest.

References

- [1] J. Simon, D. R. High, B. Wilkinson, T. Mattingly, R. Cantrell, and J. O. V. John, "Managing participation in a monitored system using blockchain technology," *Journal of Intelligent Manufacturing*, vol. 31, no. 8, pp. 1985–2002, 2022.
- [2] B. Sun, Z. Lv, and Q. Li, "Obstetrics nursing and medical health system based on blockchain technology," *Journal of Healthcare Engineering*, vol. 2021, no. 2, 11 pages, Article ID 6631457, 2021.
- [3] A. Mashatan, V. Lemieux, S. H. M. Lee, P. Szufel, and Z. Roberts, "Usurping double-ending fraud in real estate transactions via blockchain technology," *Journal of Database Management*, vol. 32, no. 1, pp. 27–48, 2021.

Retraction

Retracted: Analysis of Passenger Flow Characteristics of Urban Rail Transit Based on Spatial Data Dynamic Analysis Technology

Mathematical Problems in Engineering

Received 1 August 2023; Accepted 1 August 2023; Published 2 August 2023

Copyright © 2023 Mathematical Problems in Engineering. This is an open access article distributed under the Creative Commons Attribution License, which permits unrestricted use, distribution, and reproduction in any medium, provided the original work is properly cited.

This article has been retracted by Hindawi following an investigation undertaken by the publisher [1]. This investigation has uncovered evidence of one or more of the following indicators of systematic manipulation of the publication process:

- (1) Discrepancies in scope
- (2) Discrepancies in the description of the research reported
- (3) Discrepancies between the availability of data and the research described
- (4) Inappropriate citations
- (5) Incoherent, meaningless and/or irrelevant content included in the article
- (6) Peer-review manipulation

The presence of these indicators undermines our confidence in the integrity of the article's content and we cannot, therefore, vouch for its reliability. Please note that this notice is intended solely to alert readers that the content of this article is unreliable. We have not investigated whether authors were aware of or involved in the systematic manipulation of the publication process.

Wiley and Hindawi regrets that the usual quality checks did not identify these issues before publication and have since put additional measures in place to safeguard research integrity.

We wish to credit our own Research Integrity and Research Publishing teams and anonymous and named external researchers and research integrity experts for contributing to this investigation.

The corresponding author, as the representative of all authors, has been given the opportunity to register their agreement or disagreement to this retraction. We have kept a record of any response received.

References

- [1] Y. Zhang and N. Li, "Analysis of Passenger Flow Characteristics of Urban Rail Transit Based on Spatial Data Dynamic Analysis Technology," *Mathematical Problems in Engineering*, vol. 2022, Article ID 1601169, 9 pages, 2022.

Research Article

Analysis of Passenger Flow Characteristics of Urban Rail Transit Based on Spatial Data Dynamic Analysis Technology

Yan Zhang  and Ningchuan Li 

School of Rail Transit, Chengdu Vocational & Technical College of Industry, Chengdu 610218, China

Correspondence should be addressed to Yan Zhang; yzhangdx731026@163.com

Received 24 July 2022; Revised 5 September 2022; Accepted 22 September 2022; Published 10 October 2022

Academic Editor: Kai Guo

Copyright © 2022 Yan Zhang and Ningchuan Li. This is an open access article distributed under the Creative Commons Attribution License, which permits unrestricted use, distribution, and reproduction in any medium, provided the original work is properly cited.

Based on spatial data dynamic analysis technology, the characteristics of urban rail transit passenger flow are analyzed. This study analyzes the passenger flow characteristics of urban rail transit from the perspective of operation and planning by using the dynamic analysis technology of spatial data, combined with social and economic development. Based on the analysis of research data from the study of passenger traffic and passenger traffic data measurement, the characteristics of passenger traffic from urban railways are derived from the time distribution, spatial distribution, and transfer of passengers waiting on the platform. The final length of line 3 is 39.7 m, the passenger volume is 102, with 11 people/day, the passenger flow density is 1.8/2.3, and the high section in peak hours is 2.4/3.2. By considering the various influencing factors, efforts should be made to develop urban rail transit projects to promote the growth of social and economic benefits.

1. Introduction

Urban transportation is one of the most important infrastructure services to maintain the importance of the city and the life of the city [1]. The development of multilevel, three-dimensional, and smart modern transportation will be the goal of urban planning and development. The development of a good transport system with various modes suitable for large, medium, and small passenger transport will be an important measure to achieve the abovementioned goals. Road expansion alone cannot solve the problem of improving traffic in the city. Modern cities need modern transportation that adapts to modern life, create transportation patterns that are coordinated with urban development, and combine the goals of long-term planning with new regulations and developments. We must make a network of roads that are convenient for traffic in the city, gradually improve public transportation services, organically participate in transportation planning, expand the conditions of the use of space, and pay attention to the construction. Public transport will be the basis of rail transport, and metro transport models and trains with large

and medium passengers will be more active. With the rapid development of urban construction, many large cities in China are planning to build large- and medium-volume subway or light rail transit projects. More than 20 big cities have continuously invested a lot of human and material resources to carry out the preliminary work and feasibility study of rail transit project construction to varying degrees, but there are still some problems in project selection, system scale, and construction standards. With the development of the economy, more and more cities plan to build rail transit [2, 3]. Therefore, it is necessary to put forward some guiding construction guidelines and policies, so that macrocontrol can be more scientific and the construction units and consulting and design departments in all regions can establish a relatively unified understanding of the development goals and requirements of urban rail transit so as to avoid the adverse consequences of the wrong guidance of construction standards while stressing the necessity of construction. So, how do you create the conditions for urban rail planning? And how do you get the benefits? Whether it can support the development of the land along the successful line of the plan is a major problem that needs to be solved now.

2. Passenger Flow Analysis during Urban Rail Transit Operation Stage

During the operation of the railway, real-time monitoring of changes in passenger traffic, quality control, and awareness of the changes in passenger rights are the basis for the integration of transportation in the railway [4]. The flow of passengers changes in time and place, which is a reflection of the economy of the city and the characteristics of the railway itself. The basis of passenger identification is to analyze the physical and spatial distribution of passenger traffic.

2.1. Passenger Flow Survey

2.1.1. Flow Is Dynamic. Through the analysis of passenger traffic research data on urban rail traffic, the law of changes in passenger traffic in time and space can be understood [5]. At the same time, the analysis of the operating passenger flow characteristics of the existing lines can also provide reference data for the subsequent implementation of the line or the planned road network of other cities, so as to provide a reference for many aspects such as the control of the line network scale, the adoption and layout of infrastructure projects and equipment, and transportation organization. The types of passenger flow surveys are as follows.

2.1.2. General Education of Passengers. Airline passenger research is a comprehensive study of passenger traffic on all lines, often involving a sample of passenger surveys. Researching passenger vehicles, in general, is time-consuming and intensive and requires many researchers. However, through the collation and statistical analysis of the survey data, we can have a comprehensive and clear understanding of the current situation and the law of passenger flow. A comprehensive passenger flow survey includes an onboard survey and a station survey. The onboard survey is to investigate all passengers getting on and off the train during the whole day operation at the door, and the station survey is to investigate all passengers getting on and off the train during the whole day operation at the station ticket check-in [6]. The latter is often used in the comprehensive passenger flow survey of the rail transit system. Generally, the survey should be carried out for two or three consecutive days. During the whole day of operation, the location and ticket type of all passengers at all stations along the line should be investigated.

2.1.3. Sample Survey of Passengers. A sampling survey uses samples to approximately replace the population, which is conducive to reducing the human, material, and time consumption of passenger flow survey [7]. The sampling survey of passengers' situations is usually carried out with a questionnaire, and the survey content mainly includes two aspects: the composition of passengers and the riding situation. The investigation of passenger composition is generally carried out at the station. The survey content includes age, gender, occupation, residence, and travel purpose. The

survey time can be selected in the operation period with relatively stable passenger flow. The investigation of passengers' riding conditions can be classified according to needs or carried out at a specific time and place. In addition to age, gender, and occupation, the survey content can also include family address, family income, average daily bus times, boarding station and getting off station, the way and time to reach the station, and the way and time to reach the destination after getting off the train.

2.1.4. Section Passenger Flow Survey. Section passenger flow survey is a regular sampling survey of passenger flow, and one or two sections can be selected for the survey. Generally, the maximum passenger flow section is investigated, and the investigators use the direct observation method to investigate the number of passengers in the vehicle [8, 9].

2.1.5. Holiday Passenger Flow Survey. Holiday passenger flow survey is a special passenger flow survey, focusing on the passenger flow during the Spring Festival, New Year's day, national day, weekend holidays, and several folk festivals. The contents of the survey include the vacation arrangements of institutions, schools, enterprises, and other units, the development of urban tourism and entertainment industry, and the changes in the lifestyle of urban residents, which are generally obtained through questionnaires.

2.1.6. Sudden Passenger Flow Survey. The sudden passenger flow survey is mainly a special passenger flow survey conducted for stations with rapid passenger flow distribution, such as cinemas and stadiums. This survey mainly involves the correlation between the scale of cinemas and stadiums and the passenger flow impact degree and duration of nearby rail transit stations.

2.2. Passenger Flow Time Distribution

2.2.1. Hourly Passenger Flow Distribution in a Day. Hourly passenger flow is used to determine the capacity of urban rail transit entrances and exits, channels, and other equipment, and it is the basis for calculating the full-day driving plan and vehicle allocation plan [10]. The hourly passenger flow changes with the rhythm of urban life and fluctuates in a day. The passenger flow at night is scarce, increases gradually before and after dawn, and reaches its peak at the time of going to work and school. Later, the passenger flow decreases gradually, and there is a second peak at the time of going to work or school, and the passenger flow at night decreases gradually. The transportation capacity of rail transit, the route direction, the characteristics of the transportation corridor, and the land use nature of the station are the main factors affecting the distribution of passenger flow in rail transit. Considering the different types of railways with different transport capacities, the following five types of passenger traffic time distribution can be achieved.

(1) *Unidirectional Peak Mode*. When the railway is located where the train track is tidal, or when the area around the station is single, the distribution of passengers at the station is concentrated, and it has the highest alighting and alighting levels in the morning and evening, as shown in Figure 1.

(2) *Bidirectional Peak Mode*. If the station is located in a general service area, the passenger traffic is similar to other modes of transportation. As shown in Figure 2, there are two pairs of combinations in the morning and evening.

(3) *Full Peak Type*. When the rail transit line is located in a highly developed transportation corridor on the land, or the station is located in an area where public buildings and utilities are highly concentrated, then there is no obvious trough in the passenger flow distribution and the two-way boarding and alighting passenger flow is large throughout the day, as shown in Figure 3.

(4) *Peak Type*. The station is located near large public facilities such as stadiums, cinemas, and theatres. At the end of performances or sports competitions, there is a sudden rush hour for a short duration. After a period of time, some other stations may have a sudden drop-off peak, as shown in Figure 4.

(5) *No Peak Mode*. When the railway capacity is low or the station is located in an underdeveloped area, the flow of people is not clearly visible and the two-way passenger flow is low throughout the day, as shown in Figure 5.

For different types of hourly passenger traffic distribution, a one-way distribution of interline passenger traffic inequality can be used to determine the total passenger flow for the day. The formula is as follows:

$$\alpha_1 = \frac{\sum_{t=1}^H P_t / H}{P_{\max}} \quad (1)$$

As α_1 tends to zero, the uncertainty of passenger flow in the one-way intermediate segment increases [11, 12]. When α_1 is small, that is, when the number of passengers in the maximum one-way split time is not equal, a small marshal and a large car arrangement can be used to understand the reasons for transportation organization and marketing; that is, more trains are operated during the peak passenger flow period to meet the passenger transport demand, while in the low passenger flow period, the number of trains is reduced to improve the average load factor of vehicles.

2.2.2. *The Distribution Law of Passenger Flow throughout the Week*. Since people work and rest in a weekly cycle, the regularity of this activity must be reflected in the changes of daily passenger flow in a week. On the rail transit lines with commuting passenger flow, the passenger flow on weekends will be reduced, as shown in Figure 6 [13]. On the rail transit lines connecting commercial outlets and tourist attractions, the passenger flow on weekends tends to increase. In addition, the morning peak hour passenger flow on Mondays and after holidays and the evening peak hour passenger flow on Fridays and before holidays will be larger than that on other weekdays according to the uneven distribution and regular changes of the whole day passenger flow in a week.

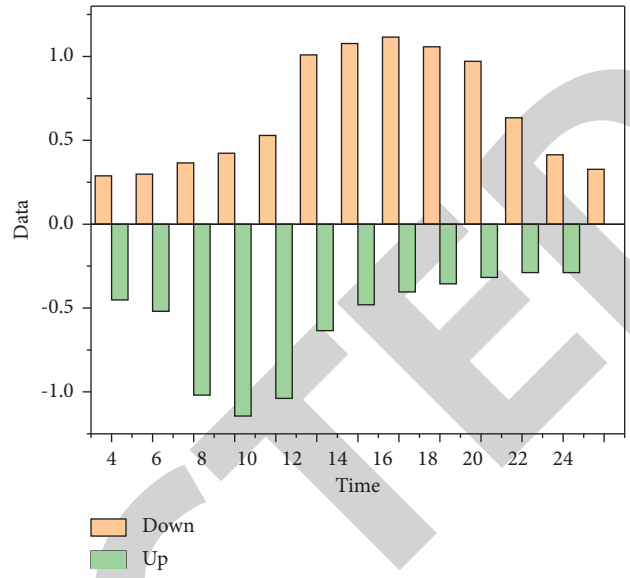


FIGURE 1: One-way peak hour passenger flow distribution.

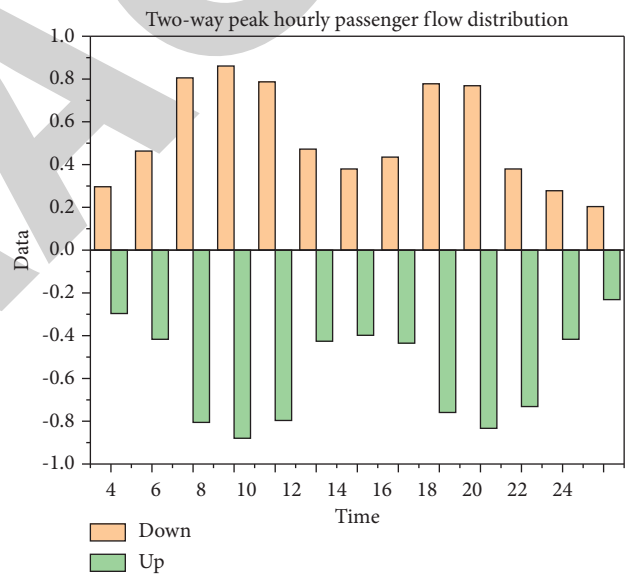


FIGURE 2: Two-way peak hour passenger flow distribution.

2.2.3. *Imbalance of Seasonal or Short-Term Passenger Flow*.

In a year, there is still a seasonal change in passenger flow. For other reasons, the passenger flow in June is usually the lowest throughout the year. The increase in population will increase the passenger flow of rail transit lines when major events are held or the weather changes suddenly [14].

2.3. *Spatial Distribution of Passenger Flow*.

Each line of the urban railway has a different passenger flow and distribution because of its different urban passenger traffic and different land uses along the line [15, 16]. The passenger traffic characteristics of each line can be analyzed from the passenger traffic data during operation.

In the railway line, because of the direction of the passenger traffic, the passenger traffic in the up and down

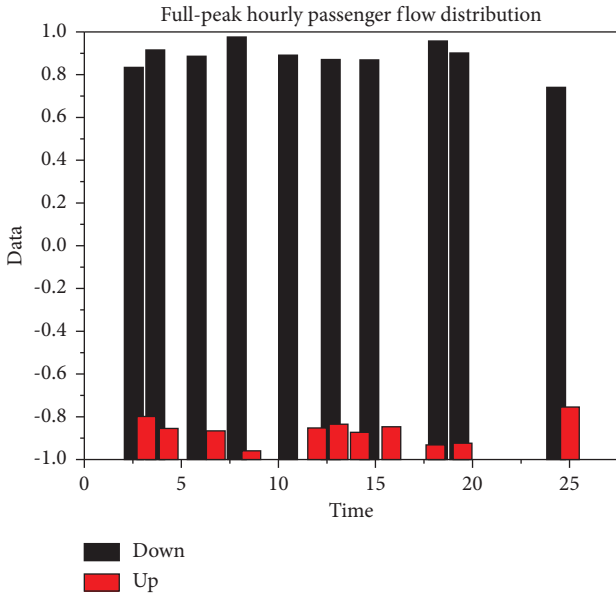


FIGURE 3: Full peak hourly passenger flow distribution.

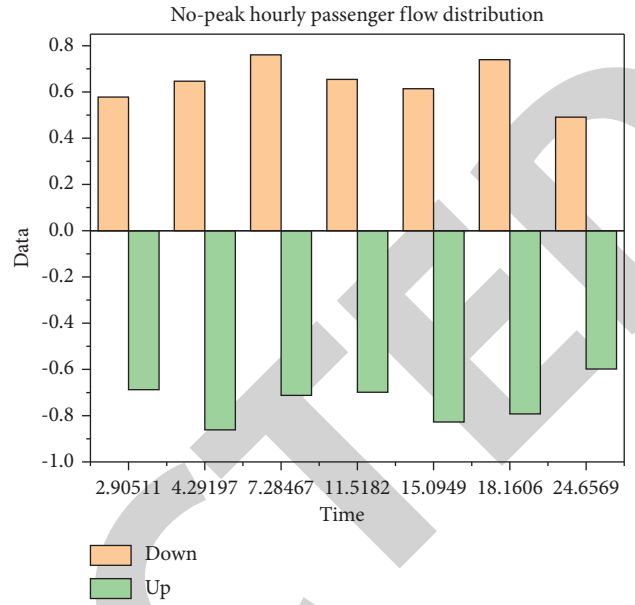


FIGURE 5: Distribution of hourly passenger flow without the peak.

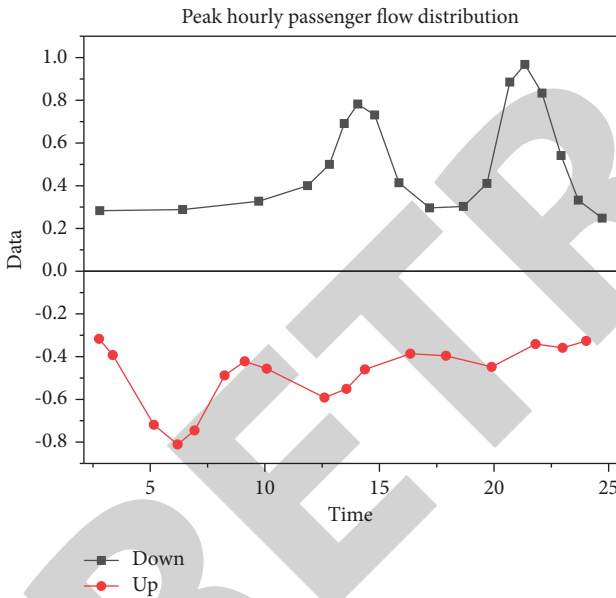


FIGURE 4: Peak hour passenger flow distribution.

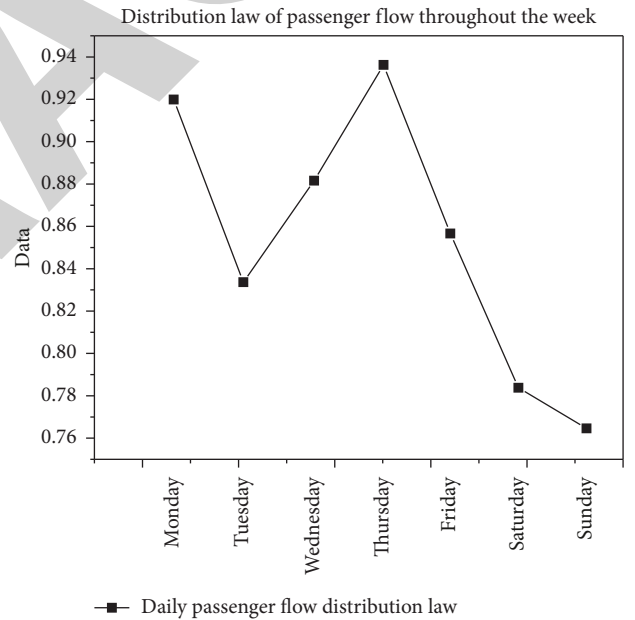


FIGURE 6: Distribution law of passenger flow throughout the day.

directions is usually not equal. On the radial train lines, the disparity between the passenger flow in the upstream and downstream in the morning and in the evening is particularly obvious. The inequality between the upstream and downstream of the railway line can be used to explain the passenger balance between the upstream and downstream of the railway line, and the calculation model is as follows:

$$\alpha_2 = \frac{(P_{\max}^{\text{superior}} + P_{\max}^{\text{down}})}{\max\{P_{\max}^{\text{superior}}, P_{\max}^{\text{down}}\}} \quad (2)$$

The more α_2 tends to zero, the greater the imbalance of passenger flow in the largest section in the upstream and

downstream directions will be [17]. When α_2 is small, that is, when the maximum section passenger flow in the upstream and downstream directions is unbalanced, it is difficult to allocate transport capacity economically and reasonably on the straight line, but measures to arrange different transport capacity on the inner and outer ring lines can be taken on the ring line.

The passenger characteristics of each section are based on the railway lines. Due to the difference in the development of the section that the line passes through, the difference in the distribution point of the passenger flow, and the difference in the number covered, it is important that passengers run on different lines at each station. Each line

segment is not equal [18, 19]. The number of passengers traveling in one direction on each section of the railway can be calculated using the following formula:

$$\alpha_3 = \frac{\sum_{i=1}^K P_i/K}{P_{\max}}. \quad (3)$$

As α_3 approaches zero, the asymmetry of the maximum passenger traffic on one side of the line increases [20]. When α_3 is small, i.e., when there are not enough passengers on one line of the main line, measures can be taken to add trains to sections with large passengers. But it will be difficult to add train sections during peak hours and the addition of train sections will meet new operational and station layout needs. It is not uncommon for the number of passengers at each station of the rail transit line to be uneven or to even vary widely. On many lines, the total boarding and landing volume of stations along the whole line is handled at a few stations. In addition, the formation of new residential areas and the operation of new rail transit lines will also cause great changes in the number of passengers at stations and aggravate new imbalances.

2.4. Distribution of Passengers Waiting on the Platform. It is a periodic dynamic change process from passengers entering the platform to boarding and from passengers getting off the train to leaving the platform. Due to the different functions and passenger distribution status in different periods, the process can be divided into the following three passenger distribution status parts.

In the first state, passengers waiting for the train are evenly distributed before the train arrives at the station. Generally, passengers gradually enter the boarding and landing area of the platform, and the distribution of passengers gradually changes from sparse to dense [21]. As the train did not arrive, passengers had a certain time before taking the bus to find a suitable carriage position or to avoid the crowded situation. In this way, some passengers will move in a small range, which makes the distribution of passengers on the platform tend to be uniform. In this case, the passengers waiting on the platform can be approximately considered as evenly distributed.

The second stage is the assembly state before boarding. When the train pulls in and stops, passengers crowd to both sides of each door to assemble, get out of the door, and wait for the other passengers on the train to get off. The distribution of passengers on both sides of the door is similar to the two sectors.

In the third state, when passengers arrive at the station to get off and pass, the door width can meet the requirements of two people getting off at the same time. In the actual observation, the passengers getting off are not finished, and the passengers getting on have already got on at the same time.

3. Passenger Flow Analysis in Urban Rail Transit Planning Stage

3.1. Passenger Flow Forecast. Passenger transport by high-speed rail mainly includes passenger transport, transfer

passenger transport, and spurred passenger transport. Passenger transport refers to the increase in the passenger flow at train stations and lines, and passenger flow refers to the change in passenger flow because medium- and long-distance passengers often use underground buses and bicycles for rapid transportation. Railways offer the advantages of speed, punctuality, safety, and comfort [22, 23]: with the construction of high-speed railways, the level of service has improved, creating the conditions for cross-regional travel and allowing for a nonstop increase in the number of passengers. Movement of residents: urban riders are highly dependent on urban land use and traffic management. At the same time, according to the rapid and large volume of urban passenger transportation, the railway has changed the access along the railway, which will have some influence on urban planning; for example, it will accelerate the process of urbanization, improving the development of suburbs and land along the railway, thereby affecting the production and distribution of passenger trains. The urban passenger transport structure and the flow direction of urban passenger flow are comprehensively determined by the average travel distance of residents, the service level of transportation facilities, the economic affordability, and values of travelers, as well as the macrocontrol policies adopted by the city. The passenger flow undertaken by rail transit also involves the coordination relationship with other transportation modes in the city. Therefore, the generation, distribution, mode, and route selection of urban passenger flow is not a one-way mechanism, but a dynamic balance mechanism of mutual feedback. Therefore, the formation of rail passenger flow is based on the urban spatial layout, transportation development strategy, the characteristics of various urban passenger transport modes, and the coordination between them, as well as the economic ability of travelers.

Urban rail transit passenger flow forecasting methods can be generally divided into two types: the centralized model and the noncentralized model. The characteristics of the two types of forecasting methods are discussed in the following. The typical representative of the aggregate model is the four-stage traffic prediction model, which is commonly referred to as the “four-stage method.” The basic theory of this model is sufficient, which can not only reflect the relationship between residents’ travel and urban land use data but can also provide feedback on the impact of the interaction of different transportation modes on passenger flow distribution. Based on traffic districts, the four-stage model analyzes the current situation and future traffic conditions of cities according to the four stages of travel generation prediction, distribution prediction, mode division, and traffic allocation. Although in recent decades, the research on the four-stage model has been deepening and there has been a method of combining two or more stages for prediction. However, the idea of grasping the travel characteristics of urban residents from a macroperspective and then predicting and analyzing them in stages is still the same. According to the different positions in the four-stage model, it can be roughly divided into four types of models. A nonaggregate model is called a driving model, which directs

workers to work according to the structure, meaning where the person goes, where to go, the means of transportation to be used, and the way to choose and do things. Statistics is based on trips, modes of transport, and distribution of transport to obtain a model of all transport needs. This model theoretically uses the achievements of modern psychology and introduces the concept of utility. It is based on the theory of maximizing utility. It focuses on traveler behavior. Compared with traditional models, the non-aggregated model has advantages such as good behavior, good intermodel relationships, less sample analysis required for model evaluation, and better temporal and regional variability of the model.

The aggregate model is a kind of traditional traffic demand analysis method based on the aggregate behavior model. Its prediction process includes four stages: trip generation, trip distribution, mode division, and traffic allocation. The nonaggregate model takes the individual traveler rather than the traffic community as the research object and takes the random utility theory and the travel utility maximization theory as the research basis. The two methods are different in terms of analysis unit, model parameter calibration method, the scope of application, policy performance ability, etc. At the same time, there are differences in the use efficiency of data and the possibility of importing independent variables, as shown in Table 1 [24].

3.2. Analysis of Prediction Results. The following are the temporal and spatial distribution characteristics of passenger flow: the time distribution of the whole day passenger volume [25]. The main indicator of passenger transport period distribution is the passenger volume period coefficient, whose value is the ratio of passenger volume in each period to the whole day passenger volume, and the maximum value is the peak hour coefficient. Generally, 7:00-10:00 and 16:00-19:00 are peak hours, and the rest are peak hours. The balance of demand affects the utilization of facilities and equipment and the interval distribution of passenger flow along the whole line. The interval distribution of passenger flow throughout the line determines the train operation organization and operation plan, as shown in Figure 7.

In the process of urban rail transit planning, design, and management, we are very concerned about the relevant passenger flow during peak hours, so it is very necessary to study the travel structure during peak hours. During peak hours, three modes of transportation are mainly used for work travel, bicycle, bus, and car, with a low proportion of walking, and the three modes which are mainly used for school travel are walking, bicycle, and bus. The purpose of travel is that the two travel groups of going to work and school are concentrated in peak hours. In contrast, in peak hours, conventional public transport and rail transit have similar operating characteristics. Their transport capacity quickly reaches saturation or supersaturation with the arrival of peak hours, and the comfort in the carriage gradually deteriorates and then gradually improves with the passing of peak hours. However, there is a big difference in the

attractiveness of rail transit and conventional public transport to travelers. During peak hours, the roads are unobstructed, and the conventional bus is more attractive because of its high convenience and cheaper fares than rail transit. However, with the arrival of peak hours, the roads are gradually crowded, the speed of conventional buses decreases, and the reliability is difficult to guarantee. At this time, the attraction of conventional buses to travelers decreases rapidly. Rail transit also becomes very crowded, and its attraction decreases. However, due to its fast and high reliability, its attraction to travelers will stabilize at a certain level after the decline.

3.3. Passenger Flow Sensitivity Analysis. An urban rail transit network is an orderly and gradual improvement process, which will inevitably produce the passenger flow impact of the subsequent built sections on the completed sections and the subsequent built lines on the existing operating lines. The influence of subsequent lines on the built lines is mainly realized through the transfer station and passenger flow coverage area. Here, another influencing factor is the operation mode. If the lines in the whole network operate in the same line mode, their mutual influence relationship will be greatly different from the independent operation of each line. In order to simplify the analysis process, only the independent operation of each line is discussed here.

Foreign rail transit operation experience shows that most of the users of rail transit are low-income people. Survey data show that more than 90% of the rapid rail transit passengers are former bus passengers, and it is difficult to attract a large number of car and taxi passengers. Therefore, China's rapid rail transit system will mainly attract middle-income bus passengers and passengers who previously used bicycle transportation. The price of train tickets is most important to passengers as middle-income and low-income people are concerned about the cost of daily commuting.

The level of utilization of urban railways is twofold: One is the good internal services of urban railways, such as departure times, car service, and waiting areas. The second is the external location of the city's rail transit business, which affects the system's relative services, such as integration with regular buses and bus service levels. Services in the city's rail transit system are usually run on departures. An increase in departure times will result in longer waiting times for passengers, more passengers on the train at each stop, and more congestion in the carriages, which will directly reduce the level of service. Due to the characteristics and economics of the city railway, it was determined that it can only be used as the main pillar of public transport and that the scope of the network is limited. The passengers have to change doors or walk to the train station, which is inconvenient to go from door to door. Therefore, it is necessary to have a coordinated connection system to play a good role. If the service of conventional public transport reaches a high level, passengers will inevitably choose a more convenient transportation mode when making travel choices and rail transit will lose its advantages.

TABLE 1: Comparison between the nonaggregate model and the aggregate model.

Project	The aggregate model	The nonaggregate model
Investigation unit	Single trip	Single trip
Analysis unit	Residential quarters	Personal
Investigation efficiency	A large number of samples are required	A large number of samples are required
Dependent variable	Cell statistics	Personal selection results
Considering the difficulty of personal attributes	Difficult	Easy

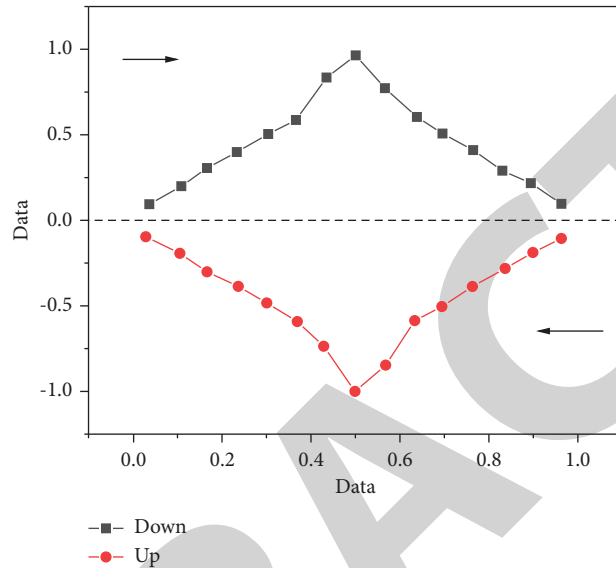


FIGURE 7: Schematic diagram of section distribution of the passenger flow section.

Social activities have a significant impact on passenger flow in the transportation policy. Transportation policy can determine the supply level of transportation macroscopically, thus restricting people’s travel choices. For example, the government issued policies to restrict the use of cars and control the number of cars, which can change the urban traffic structure to a certain extent. We can change people’s willingness to travel and then can change people’s travel habits through slogans and initiatives. For example, putting forward the concept of sustainable development, saving energy and protecting the environment, calling on urban residents to travel by public transportation, and minimizing the travel of individual motor vehicles can also change the travel structure of urban transportation to a certain extent, and this can ultimately affect the passenger flow of rail transit.

On the one hand, the economic level of the city should be able to support the construction cost of rail transit; on the other hand, it also has a direct impact on the scale of passenger flow. Due to the huge construction cost of rail transit, its ticket price is generally higher than that of a conventional bus, so the affordability of passengers to ticket price is the key factor to determine the passenger flow.

3.4. Reliability Analysis of Prediction Results. There are many factors that affect the reliability of the prediction results, and corresponding improvements can be made to the problems

mentioned above, such as continuously improving the city’s traffic planning model and optimizing model parameters, This study starts with the prediction process and the form of prediction results and makes a preliminary exploration on improving the reliability of prediction results.

Table 2 shows the passenger flow forecast results of an urban rail transit. From the data listed in the table, we can find that each forecast value is very accurate, reaching two decimal places. Compared with the problem analysis in the previous section, the prediction results are often far from the actual operation results. Is it necessary and possible to make very accurate data results on such uncertain data? In mathematical statistics, confidence degree and confidence interval are common. If the results of rail transit passenger flow prediction can be made into a form similar to the confidence degree and confidence interval in mathematical statistics, its reliability will be much better than the current single value. The whole prediction process is shown in Figure 8.

The key to the reliability of control data lies in the control of prediction data input and the prediction model method. It is generally believed that the probability distribution of expert opinions conforms to or is close to the normal distribution, which is the main basis for data processing. In quantity processing, the median and upper and lower quarter point methods are often used to process the answers of experts and calculate the expected value and interval of prediction. After expert evaluation of the data, we can get the

TABLE 2: Forecast results of rail transit passenger flow.

Line	Length	Passenger volume	Passenger flow density	The high section in peak hours
Line 1	28.1	132	4.4	3.8
Line 2	43.7	150	3.1	3.6
Line 3	39.7	112	2.3	3.2

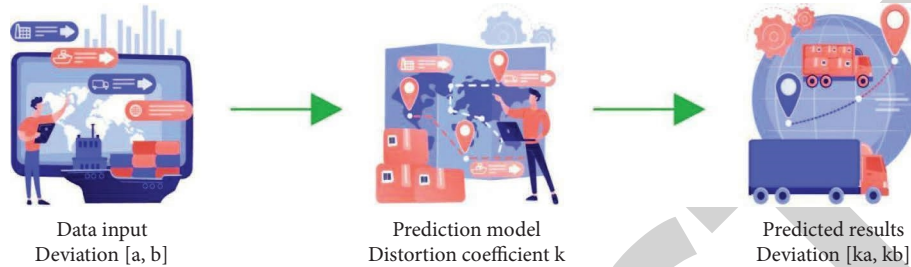


FIGURE 8: Simplified flow of passenger flow forecast.

TABLE 3: Final prediction results.

Line	Length	Passenger volume	Passenger flow density	The high section in peak hours
Line 1	28.1	112, 146	3.8, 4.2	2.8, 3.8
Line 2	43.7	130, 151	2.7, 3.1	2.7, 3.6
Line 3	39.7	102, 121	1.8, 2.3	2.4, 3.2

data input deviation and the distortion coefficient of the prediction model, and then we can obtain the final prediction results, as shown in Table 3.

4. Conclusion

Railways have expanded their services, and the quality of service has improved. During the 13th Five-Year Plan period, railway lines (sections) such as Line 8 (Phases III and IV), West Line 6, and Daxing Airport Line have been put into operation, and further work is up to 172.9 km. The number of suburban railway lines has increased to 4, and the inner city run has reached 364.7 kilometers. By the end of the 13th five-year plan, the total mileage of transport (including suburban railways) had reached 1091.7 kilometers. The rail transit operation organization continues to be optimized. The departure interval of 10 lines is less than 2 minutes, and the reliability of train service is nearly 7 times higher than that at the end of the 12th Five-Year Plan period, realizing the full coverage of the city's rail "one-yard pass" and mobile payment. We should strive to optimize public transport services and must continuously improve the service level. The Third Ring Road, Beijing Tibet expressway, Beijing Hong Kong Macao expressway, Cheng Fu Lu road, and other bus lanes have been completed, and the bus lanes have been gradually connected into a network, with a total mileage of 1005 Lane kilometers. The "master plan of Beijing ground bus network" was issued, and the ground bus lines were continuously optimized. 135 diversified bus lines, including customized shuttle lines, tourist buses, high-speed rail express (Beijing South Railway Station), and hospital

special lines, were newly opened, with a total of 455, which greatly met the diversified travel needs of citizens. The significant improvement of ground bus service level effectively helps citizens' travel convenience.

Data Availability

The labeled data set used to support the findings of this study is available from the corresponding author upon request.

Conflicts of Interest

The authors declare that they have no conflicts of interest.

Acknowledgments

The authors would like to thank the School of Rail Transit, Chengdu Vocational & Technical College of Industry, for their support.

References

- [1] H. Gao, S. Liu, G. Cao, P. Zhao, and P. Zhang, "Big Data Analysis of Beijing Urban Rail Transit Fares Based on Passenger Flow," *IEEE Access*, vol. 8, no. 99, pp. 80049–80062, 2020.
- [2] J. Liu, "Study on passenger flow assignment method of urban rail transit based on improved logit model," *IOP Conference Series: Earth and Environmental Science*, vol. 791, no. 1, Article ID 012051, 2021.
- [3] Y. Jing, H. Hu, S. Guo, X. Wang, and F. Chen, "Short-term prediction of urban rail transit passenger flow in external passenger transport hub based on lstm-lgb-drs," *IEEE*

Research Article

The Application of Genetic Algorithm in the Optimal Design of Landscape Space Environment

Zhao Liu 

Taiyuan Normal University, Jinzhong 030619, China

Correspondence should be addressed to Zhao Liu; liuz@tynu.edu.cn

Received 24 August 2022; Revised 14 September 2022; Accepted 22 September 2022; Published 10 October 2022

Academic Editor: Kai Guo

Copyright © 2022 Zhao Liu. This is an open access article distributed under the Creative Commons Attribution License, which permits unrestricted use, distribution, and reproduction in any medium, provided the original work is properly cited.

Garden landscape not only provides people with places of rest and entertainment, but also protects the natural environment and maintained ecological balance. Although the traditional garden architectural style could retain the classical landscape style, the modern garden facilities and conditions had been greatly improved, and people's expectations for the construction level of garden landscape continued to improve. Therefore, the effect of traditional landscape design could no longer meet the requirements of social development. This article proposed an interactive genetic algorithm-based landscape space environment optimization design method, in order to provide a certain theoretical reference for landscape design. Firstly, by analyzing the relationship between landscape and buildings, the change in people's demand for landscape space environment and the relevant characteristics of landscape, this article expounded on the basic principles and methods that landscape design should follow and gave the problems existing in landscape design. Secondly, the interactive genetic algorithm and its innovative design theory were summarized, and the optimization design method of garden landscape space environment based on interactive genetic algorithm was proposed. Finally, the evaluation index system of landscape spatial environment was constructed, and experimental analysis was carried out with a landscape design as a case. The results showed that compared with the traditional landscape design methods, the design scheme proposed in this article could achieve better evaluation results. The optimization design method of landscape space environment proposed in this article could provide some technical support and theoretical reference for landscape architecture and design.

1. Introduction

With the continuous development of the economy and society, people have higher and higher requirements for production, living, and working environment. As an important part of human settlements and social environment, the development of landscape environment has been widely concerned [1]. Influenced by the development and changes of the times, the current landscape design mainly includes modern landscape planning and traditional landscape planning. Different from traditional landscape design methods, modern landscape design methods and concepts have undergone great changes, for example, in landscape environment design, including landscape architecture, landscape space, landscape culture, and ecology. Although there are many categories of modern landscape architecture,

and the design objectives are also different, due to the increasingly rational human concept and social development, the design concept of landscape architecture mainly follows the principles of saving and environmental protection and meeting people's needs [2, 3]. Traditional landscape design methods have been unable to meet the requirements of modern people and social development. While building modern buildings, we need to consider the matching landscape needs, which undoubtedly brings great challenges to modern landscape space design.

As an important part of modern architectural complex, garden landscape can better provide people with conditions for rest and entertainment, and also provide a guarantee for protecting the natural environment and maintaining ecological balance. On the premise of maintaining the unity with nature, designers usually plan and design the landscape

according to various needs and limited space and environmental conditions. The traditional garden architectural style is more natural, and uses limited space to create the original landscape environment [4]. With the improvement of modern garden facilities and conditions, people's demand and experience for garden landscape are increasing. Therefore, the traditional garden landscape design concept has been unable to meet the requirements of social development.

At present, most garden landscape design is still relatively backward in concept, and designers lack certain innovative thinking. For example, some designers adopt the copying method to simply superimpose or combine the garden landscape materials in order to pursue benefits [5]. The existing landscape design schemes are often difficult to integrate with the development of urban landscape, which not only makes the implementation effect of landscape design boring and single, but also cannot reflect the regional history and culture through the landscape environment. Therefore, based on the innovative design thinking of interactive genetic algorithm, this article puts forward the optimization design scheme of landscape space environment, which provides some technical support for modern landscape design.

2. Related Works

According to the existing research, classical garden design is mostly based on the local environment, with significant regional and personality characteristics. Although the traditional garden landscape is relatively simple in style, it has certain characteristics in the inheritance and integration of culture [6]. For example, many well-preserved classical gardens in China not only record the evolution of society for thousands of years, but also reflect the national cultural characteristics of different periods. This unique garden landscape provides a good idea for promoting the process of social development and the design of modern garden landscape. With the development of the times, more and more deficiencies have been exposed in the design of traditional landscape architecture. Due to the continuous progress of people's understanding and thinking of society, the traditional garden landscape has been insufficient to meet people's various needs [7, 8]. For example, modern architecture requires that the matching garden landscape environment be no longer limited to inheriting history and culture, but needs to meet people's experience of nature and ecological environment. Therefore, the traditional garden landscape design concept must be updated simultaneously.

In a broad sense, garden landscape space means that people experience the space environment of architectural groups through living activities in the living environment, so as to obtain the psychological and physiological satisfaction of the space environment. Landscape space combines space environments of different sizes and forms an environmental system with a certain structure [9]. Therefore, garden space is a broad concept, including landscape space planning, landscape space environment construction. Research shows that the planning of garden landscape space usually needs to

consider people's perception and utilization of space functions and the relationship between them. Most research results show that the construction of landscape space environment should not only consider the layout, form, and function of landscape space, but also combine specific user requirements, existing conditions, and functions to create different levels of space environment for people.

The design of garden landscape needs to follow people's various perceptual needs. Generally, people's perception of landscape space mainly includes static and dynamic [10]. The so-called static perception refers to the various cognitive conditions of landscape space under static conditions. Due to the differences in the size, shape, and color of landscape space at all levels, people have different feelings about landscape space. Therefore, people's static perception of landscape space is usually not limited to spatial entities, but the real impression of spatial components. Designers usually make appropriate adjustments to the landscape space according to people's behavior and use needs [11]. The so-called dynamic perception refers to people's cognition of spatial sequences at different levels. Generally, people's cognition of landscape spatial sequence in the process of sports is related to people's psychology, mood, and other factors. For example, the size, shape, and other elements of landscape space will continue to change with human movement factors, thus affecting people's cognition of landscape space.

Garden space design is a systematic project, in which the landscape forms different visual effects with various functions and styles, and comprehensively reflects the style of garden landscape environment. The research shows that the design of landscape spatial environment cannot be limited to the innovation of landscape individuals, but needs to integrate the landscape environmental design concept into the whole landscape space [12]. The effective integration of individuals into the garden environment system can not only reflect the overall landscape effect, but also realize the function and value of the garden landscape space environment. Some scholars believe that in landscape design, landscape individuals cannot be concentrated in a limited space environment, but can simplify the design of landscape morphology and appropriately increase the dependence and coexistence between different landscape individuals. In the design of garden landscape space, we should not only consider the individual characteristics that constitute the landscape form, but also take into account the correlation between different landscape individuals in terms of function and form, so as to make the garden landscape become an indivisible whole.

3. Basic Theory of Landscape Space Design

3.1. Overview of Garden Landscape

3.1.1. The Relationship between Landscape and Buildings. As the public infrastructure of human life, garden landscape is a combination of garden, green space, landscape, and environment, which can be considered as the art of human living space. On the basis of traditional gardens, through

artificial landscape environment decoration, natural gardens can stand in the landscape environment, thus forming a symbiotic space environment between nature and human beings, so as to meet people's material life and spiritual needs. As a part of garden landscape, architecture is not only used to meet people's living conditions, but also can provide people with a place for rest and entertainment [13]. The shape of the building and the surrounding landscape, green space, vegetation, and so on together constitute the landscape environment for human survival. Although buildings occupy a small space in landscape gardens, they can add human wisdom and art to nature, so that natural gardens can not only become a material landscape for human appreciation, but also become a symbol of people's pursuit of a better life.

The role between buildings and landscape is irreplaceable. They integrate with each other and together form a part of people's production and life. Although the landscape individuals are separated by various buildings in space, if the landscape individuals are not accompanied by buildings, human society may return to its original natural state. On the contrary, if there is a lack of garden green space and landscape environment between buildings, even if the city is full of high-rise buildings, human society is bound in some lifeless small blocks, and a single space makes people's psychology and physiology vulnerable to all kinds of depression. Therefore, buildings and natural landscapes are interdependent and complement each other. The coexistence of garden landscape and modern architecture is not only necessity for the development of human society, but also a symbol for people to explore and create nature.

3.1.2. Human Demand for Space Environment of Garden Landscape. As the main body of buildings and landscape, there is a certain interactive relationship between human beings and the spatial environment of landscape. People's perception of the environment is a comprehensive reflection of the response to the needs of various factors, including people's physiological needs, safety needs, social needs, and self-realization needs [14]. As shown in Figure 1, it describes the hierarchical relationship of human needs for the environment. People's demand for the environment is not limited to the quality of the landscape, but to consider the various needs of the garden space at the same time. As shown in Figure 1, it describes the level of human demand for the spatial environment of garden landscape.

3.1.3. Characteristics of Garden Landscape. Unlike natural landscape or ecological scenic spots, garden landscape has similarities with urban landscape or rural landscape, but it has some characteristics of its own [15]. Firstly, the garden landscape has diversity in terms of its constituent elements. Garden landscape is composed of multiple elements, including tangible, intangible, natural, and man-made elements. Factors such as road arrangement or structure are the main part of garden landscape. Secondly, the landscape is multidimensional from the perspective of time and space. Because the garden landscape has infinity

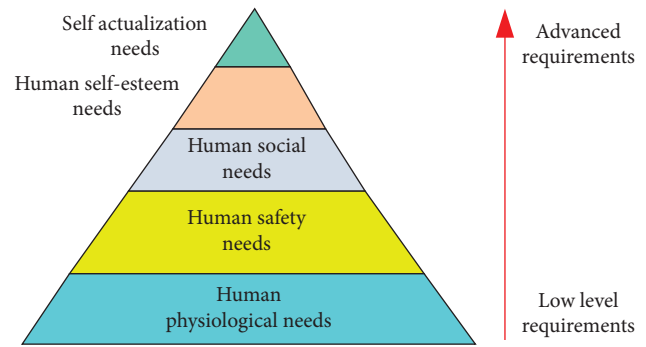


FIGURE 1: The level of human demand for landscape space environment.

in space and continuity in time, the garden landscape has a multidimensional nature of time and space. Thirdly, from the perspective of the main body of the evaluation, the landscape has multidirectionality. Because the design goal of garden landscape has certain directivity, and the evaluation subjects of garden landscape may come from different groups, such as residents, travelers, or operators, the construction of garden landscape often seeks a balance from different groups, that is, to meet the needs of different evaluation subjects as much as possible. Finally, the garden landscape is diverse in terms of the composition of the environment. Different from the design objectives and styles of other works of art or decorative pieces, garden landscapes usually have their own design styles or organizational structures according to their own characteristics to meet the culture, customs, and people's living needs of social development.

3.2. Basic Principles and Methods of Landscape Design

3.2.1. General Principles to be Followed in Landscape Design. When designing the garden landscape, we need to start from people's needs and follow certain design principles. The main thing is to design according to people's different sensory needs of the landscape environment. People's experience of garden landscape space is formed through the perception of the external environment by different organs of the human body. In the design of garden landscape, it is necessary to integrate human vision, hearing, touch, and other different senses into the garden space, so that the designed landscape can fully meet people's various needs [16]. As shown in Figure 2, the principles that should be followed in landscape design are given.

The design of garden landscape is to create a favorable activity space for people's leisure and entertainment. People can perceive the whole landscape space environment through their own senses. Among them, when people enter a certain garden landscape, the eye is the main organ to perceive the landscape form. The perception of the whole landscape environment is first completed through vision, and from it, they experience various elements of the landscape, such as the shape, color, light, and shadow of the landscape.

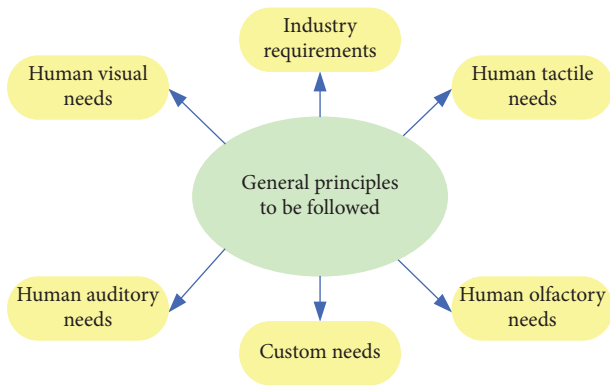


FIGURE 2: Principles to be followed in landscape design.

As an important part of garden landscape, auditory landscape mainly senses all kinds of noises from the external environment through the human ear. Although the scope of the landscape perceived by hearing is less than that of visual space, hearing can not only make people truly feel the landscape environment, but also bring surprise and pleasure to people. Because modern urban life is full of all kinds of noisy sounds, and gradually makes people lose all kinds of primitive scenes endowed by the natural environment, people are eager to perceive the sounds from nature in their spare time, and seek a quiet and relaxed life by listening to the sounds of the garden landscape space environment. For example, in the landscape space environment, the sound of running water, bird calls, and so on can cause the auditory resonance of tourists, so that people can immerse themselves in the natural landscape environment.

The smell produced by the landscape space in the garden environment can make people use their sense of smell to feel the existence of nature. The fragrance of garden landscape in the space environment forms a pleasant microclimate. It not only enables people to obtain a suitable resting environment through appropriate temperature and humidity, but also integrates human beings with the environment, making people feel extremely happy. Among the constituent elements of the landscape, plants, as the soul of the landscape environment, can interact with nature through photosynthesis and adjust the space and climate environment of the landscape, so as to improve people's olfactory needs for the landscape environment. In the garden landscape design, we can plant some *Osmanthus fragrans*, lilies, camphor trees, and other plants to beautify the surrounding environment and create a happy living and leisure place for people.

Garden landscape environment not only needs ornamental plants, but also needs to create conditions for people's experience needs on the tip of the tongue. In order to meet the needs of people picking fruits in nature to obtain taste, some plants with melons and fruits can be planted in the garden landscape. Therefore, in the landscape design, we can provide an experience park for people to pick delicious food, and plant some fruit trees for people to watch and appreciate, so that people can feel that they are returning to the natural life of the countryside. In addition, in terms of

landscape environment design, people can also feel close contact with nature through various landscape modeling, species, and other elements, so that people can feel that they are actually from nature.

3.2.2. Common Methods in Landscape Design. In landscape design, path planning is very important for the design of space environment. Because people mainly feel the garden space through the path, the design of the path in the garden landscape includes the garden square, green space, water corridor, and other landscape elements in addition to the road. In garden landscape, the path can reflect the overall space of the landscape. People's vision can form different observation angles with the change of the path, and then feel the changes brought by the whole garden space. Because the path is composed of multiple elements in the landscape, the path can connect various landscapes into a continuous spatial environment. Taking the path as the main line of viewing, people can organize scattered landscapes into a continuous garden space according to the sequence of activity time. At the same time, the path can help people plan their own viewing clues. With the changes of landscape topography and space, it is easy for people to find their own position and direction in the garden landscape, so that they can quickly become familiar with this garden environment.

From the perspective of garden space, a single space design is mainly surrounded by boundaries. Some boundaries of garden space are relatively clear, while others are not clear enough. The scale of garden space is usually formed by the height and length of the boundary. For example, plants, buildings, or terrain in the landscape can form the height of the boundary, and the distance from the viewer's viewpoint to the boundary object can form the length of the boundary. According to the existing landscape space design research, the size of the garden space mainly depends on the ratio of the length and height of the boundary [17]. For example, spaces dominated by garden buildings are generally designed with a smaller ratio, while spaces dominated by trees or terrain are generally designed with a larger ratio. As shown in Figure 3, the effect of the relationship between human visual angle and landscape space is described.

In landscape design, nodes, as some core parts of the landscape, are the focus of attention in the space environment. If there is a lack of nodes in the landscape space, it will make the garden space lack highlights. The node can be an independent entity or a combination of multiple entities in the landscape, and its location is arbitrary, for example, it can be located inside and outside the space or on the boundary. Nodes and paths together constitute a part of garden space. People can not only change the state of garden space, but also make people feel that the environment is changing by adjusting the location of nodes or the shape of paths. In addition, as the core part of the landscape, signs are the most attractive and symbolic nodes of all landscape elements, usually located in the most prominent position of the landscape space [18]. The design of garden landscape needs to meet people's various needs. Among the elements of garden landscape, people usually pay most attention to the

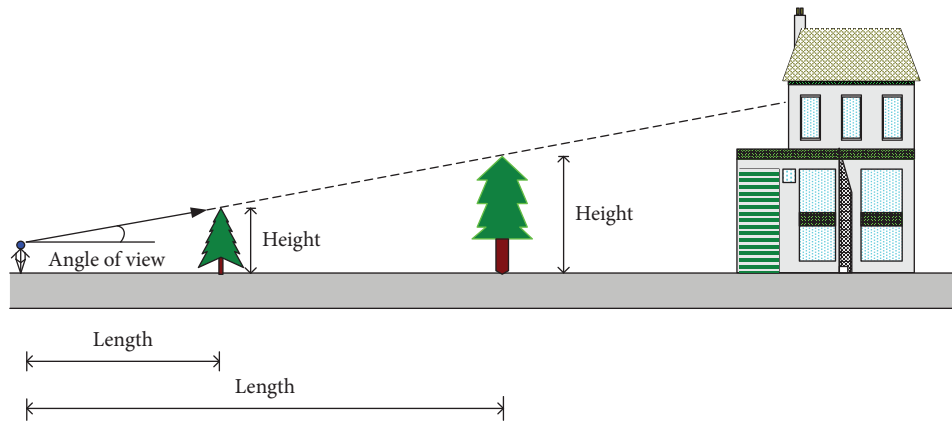


FIGURE 3: The effect diagram of the relationship between human visual angle and landscape space.

symbols of garden landscape. Signs are generally set reasonably according to the distribution of landscape space, roads, and other elements. For example, sculptures, pools, and other landmarks that can enhance the attractiveness of garden landscapes need to consider a variety of factors in the design, so that people can be quickly attracted by landmarks when viewing the landscape environment.

As shown in Figure 4, it describes the comparative effect of the location relationship between garden terrain, buildings, landscape, and people.

3.3. Problems in Landscape Design. Affected by the traditional landscape structure, some designers may lack innovative thinking and blindly follow the inherent garden space mode in the design of modern garden landscape, resulting in the mismatch between landscape design and modern architecture. In order to pursue the economic benefits of landscape, some designers violate the essence of landscape design. The use of some inferior materials not only makes the landscape effect unable to meet the ornamental requirements, but also fails to improve the spatial environment of landscape. In addition, in order to pursue artistic conception innovation, some designers unrealistically formulate landscape design schemes, which not only makes the scheme difficult to implement, but also causes a waste of resources.

In terms of landscape space and environment design, it is still not enough to integrate human demand elements into landscape design. According to the existing research results, at present, due to the lack of theoretical guidance of landscape designers in landscape design, some designers often design according to their own experience or ideas, resulting in the landscape design effect being difficult to meet people's various needs. From the existing landscape design research, designers can fully consider people's physiological needs, psychological needs, and behavioral habits. At present, many landscape designs do not consider the various needs of human scale, which makes the designed landscape environment difficult for people to achieve expectations and happiness.

In addition, in the current landscape space environment design, there are still many problems in the greening, facilities, and characteristics of the landscape. As an important

embodiment of landscape effect, greening is a very important element to create a landscape space environment. The greening effect is often related to the invested funds, local climate and environment, and other factors. Therefore, in order to reduce costs or ignore the limitations of local climate conditions, some designers ignore the greening elements in landscape design, resulting in the lack of natural ecological elements in the landscape space environment, which affects people's leisure and entertainment. The lack of rockeries, fountains, scenic pavilions, and other facilities in the garden landscape, or the unreasonable scale of the facilities, to a certain extent, not only affects the layout of the landscape space, but also makes the garden landscape environment single. As shown in Figure 5, the comparative effect of different proportional relationships between human visual distance and landscape space height is described.

4. Using Interactive Genetic Algorithm to Optimize the Space Environment of Landscape Architecture

4.1. Interactive Genetic Algorithm and Its Innovative Design Theory. Genetic algorithm (GA) is a method used to simulate the genetic and evolutionary processes of related organisms in nature [19]. As an adaptive global optimization method, genetic algorithm is often used to solve some complex system optimization problems. A basic genetic algorithm is usually composed of scheme coding, fitness function solution, operator selection, and other elements. When applying genetic algorithm to solve specific optimization problems, we first need to encode the actual problem and form the corresponding chromosome for computer data processing. Common coding schemes include binary coding, real coding, and tree structure coding. After using genetic algorithm to obtain the target solution of the problem to be optimized, the result needs to be decoded in order to convert it into the corresponding actual optimization solution.

It is known from the evolution process of organisms that individuals with strong adaptability to the environment can continue to reproduce and survive. On the contrary, the organism cannot reproduce or be eliminated by the

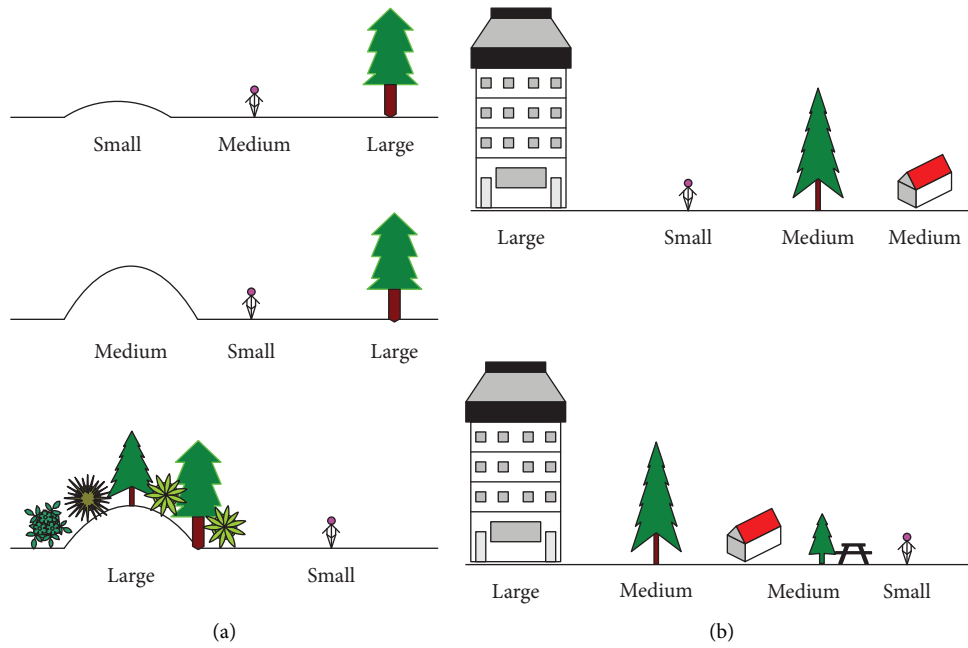


FIGURE 4: Comparative effect of the location relationship between garden terrain, buildings, landscape, and people. (a) The size proportion relationship among terrain, trees, and people. (b) The size proportion relationship among landscape, buildings, and people.

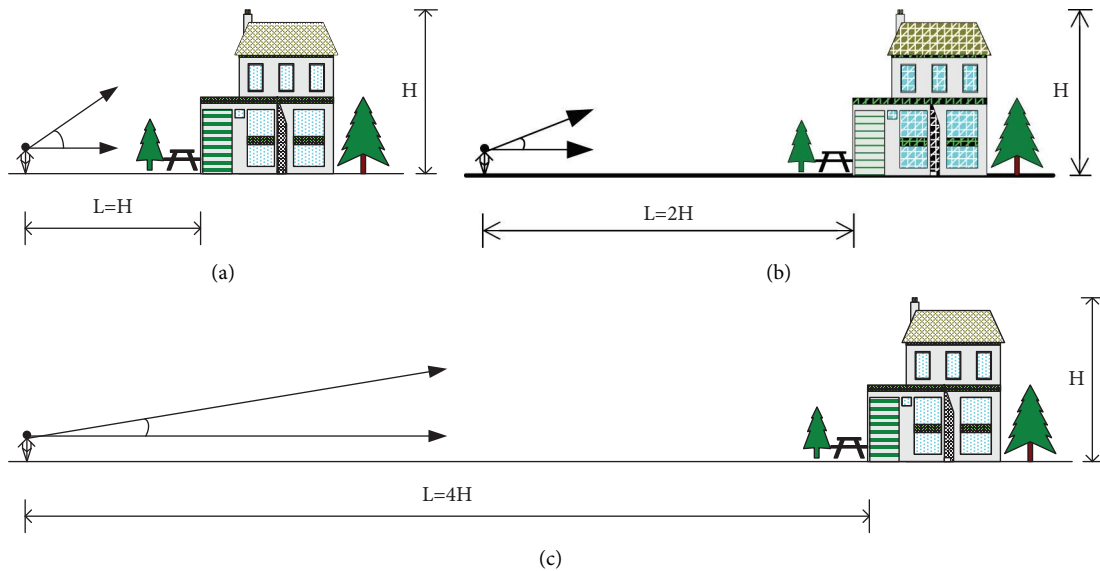


FIGURE 5: Schematic diagram of scale relationship between human visual distance and landscape space height.

environment. In order to reflect this biological law, the fitness function is used in genetic algorithm to calculate the adaptability of biological individuals to the environment, and it is used as the optimization condition. Fitness function is very important for the implementation of genetic algorithm, and directly affects the efficiency of the algorithm and the search for the optimal solution. The construction of fitness function can be determined according to specific problems. For example, for simple optimization problems, the fitness function can be set as the problem to be dealt with, while for complex landscape spatial environment

optimization problems, it is necessary to consider the constituent elements of landscape at the same time, so as to construct the fitness function.

In order to reasonably construct the fitness function to meet the needs of different evaluation subjects, interactive genetic algorithm (IGA) can be used to construct the fitness function on the basis of traditional genetic algorithm [20]. Due to the increase in user participation in the interactive genetic algorithm, the user's evaluation value of individuals can be used as one of the parameters to construct the fitness function, which is also the advantage of interactive genetic

algorithm in innovative design. New individuals generated by machine learning need to be evaluated by users, and then the machine recalculates the fitness of these individuals based on the user evaluation results and using the fitness function. As shown in Figure 6, it is a basic structural diagram of interactive genetic algorithm.

Selection operator is used to simulate the evolution of organisms in the natural environment. The fitness function can be used to obtain the adaptability of individuals to the environment, and the selection operator can be used to select individuals who are able to continue to evolve. In order to avoid local optimization and make the individual evolution process diverse, we can enhance the search scope of the algorithm. For example, by adding a probability factor to the search algorithm, the probability that individuals with strong adaptability will be selected is greater, and the probability that individuals with weak adaptability will be eliminated is greater.

When using the selection operator and selecting different individuals according to fitness, two individuals with small fitness difference can be crossed with a larger probability and the corresponding selection probability can be calculated [21]. The selection probability of the j -th individual can be expressed as follows:

$$f_j = \frac{s_j}{\sum_{k=1}^m s_k}, \quad (1)$$

where m is the number of genetic individuals and s_j is the fitness of the j -th individual.

If s is used to represent fitness and s_j is relative fitness, the cumulative fitness s_p can be expressed as follows:

$$\begin{aligned} s_{p1} &= s_{i1}, \\ s_{pj} &= (s_{p(j-1)} + s_{ij}) \quad j \in [2, n]. \end{aligned} \quad (2)$$

When individual j is selected, its random number r must meet the following conditions:

$$\begin{cases} 0 \leq r < s_{ij}, & j = 1, \\ s_{ij} \leq r < s_{i(j+1)}, & j \in [2, n), \\ s_{ij} \leq r < 0, & j = n. \end{cases} \quad (3)$$

According to the above algorithm, all individuals are selected in turn. When selected, they are removed from the candidate population, and then the relative fitness and cumulative fitness of the remaining unselected individuals are calculated. After each round of selection, the number of next-generation groups and contemporary residual groups should be compared until the number of next-generation groups reaches a specified value, and the selection operator will not be repeated.

Whether the individual obtained by genetic algorithm is optimal or not also needs to be evaluated by using the relevant evaluation system. In order to build a more scientific evaluation system, interactive evaluation method can be used [22]. Because users participate in the evaluation, it is necessary to add user factors to the calculation of individual fitness, and the machine mainly realizes the substantive evaluation of individual fitness through automation.

In the substantive evaluation of individual fitness, the substantive examination result u can be described by the following formula:

$$l_e = \begin{cases} 0, & (u + v = 0), \\ \frac{2uv}{u + v}, & (u + v > 0), \end{cases} \quad (4)$$

where u represents the practicality of the individual, v denotes the innovation of the individual, and u is the harmonic average of u and v .

In order to realize the objective evaluation of individuals, it is necessary to adopt the method of interactive evaluation between users and machines. In the process of interactive evaluation, users and machines constantly screen the practical ability and innovative ability of individuals. Among them, the individuals removed from the population will no longer participate in genetic evolution. At the same time, the result l_f of each interactive evaluation is recorded, and the result will be automatically added to the training set of the classifier, so that the machine has adaptive ability to the evaluation results.

Through the substantive evaluation, interactive evaluation, and automatic evaluation of individuals by machines, the corresponding evaluation values can be obtained. Thus, the fitness function of an individual can be constructed as follows:

$$s = \alpha l_e + \frac{\beta l_f + \gamma l_g}{10}, \quad (5)$$

where l_g is the result of machine automation evaluation, and α , β , and γ represent the weights of l_e , l_f , and γ in turn, which are also parameters of interactive genetic algorithm. Due to $0 \leq l_f \leq 10$ and $0 \leq l_g \leq 10$, it is necessary to normalize them.

As shown in Figure 7, it is the schematic diagram of interactive genetic algorithm module relationship.

4.2. Landscape Environment Optimization Based on Interactive Genetic Algorithm. Because garden space involves many elements and their combinations, such as paths, boundaries, nodes, signs, and so on, each element can be parameterized or characterized in order to optimize the garden landscape space environment by using interactive genetic algorithm. Although feature processing is superior to parametric design to a certain extent, improper feature selection will directly affect the efficiency and landscape effect of landscape design. Parameterized intelligent processing is conducive to optimizing the design scheme. Different design schemes are compared by solving multiple parameters, and then the optimal scheme of landscape design is obtained. Considering that different users have certain subjectivity in the evaluation of landscape design effect, and different evaluation standards will affect the final effect of landscape design, parametric modeling and human-computer interaction can be adopted. Landscape designers can finally achieve the ideal design effect by adjusting parameters when designing the landscape space environment.

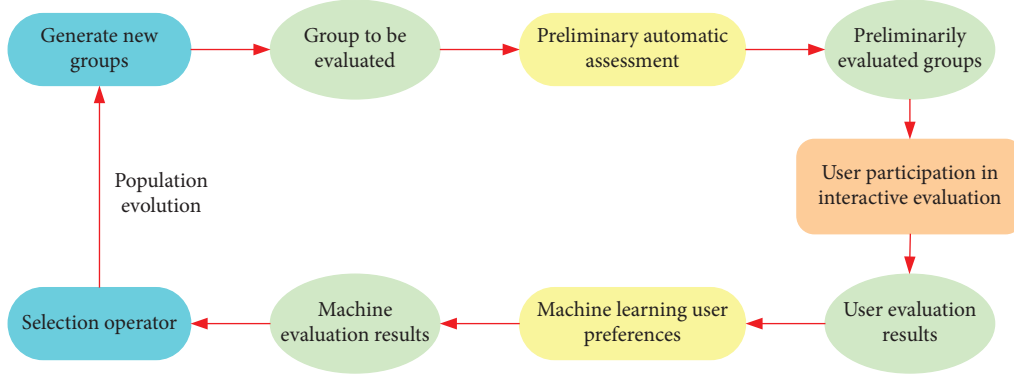


FIGURE 6: Basic structural diagram of interactive genetic algorithm.

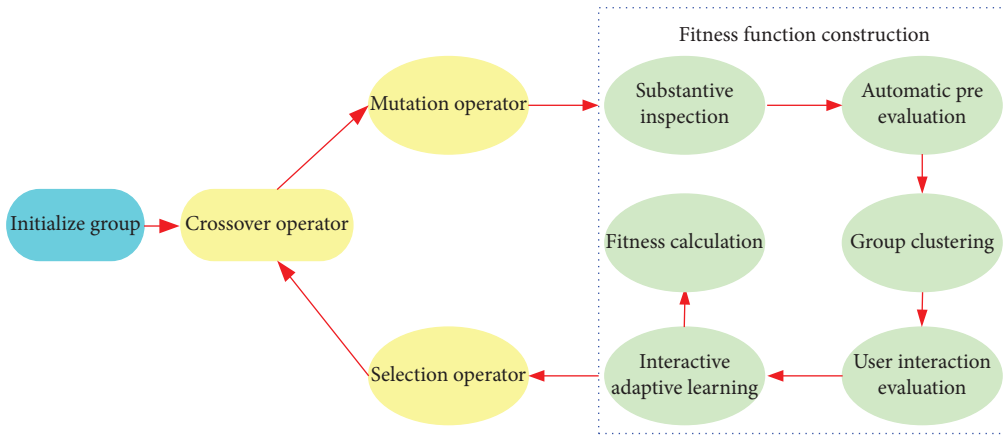


FIGURE 7: Schematic diagram of interactive genetic algorithm module relationship.

It is advisable to adopt the set D of morphological parameters to express the space and environment design of garden landscape, and its form is as follows:

$$D = \{d_1, d_2, \dots, d_N\}, \quad (6)$$

where D is the set of landscape spatial morphological parameters and d_1, d_2, \dots, d_N are the relevant morphological parameters defined by the landscape designer.

An N -dimensional solution space can be constructed from the definition domain of relevant morphological parameters in formula (6). The design process of garden landscape is actually how to find the optimal solution from this space.

Using interactive genetic algorithm can let designers participate in solving the problem of seeking fitness function. Since the idea of the designer is included in the process of problem-solving, the choice of fitness function can be evaluated according to the idea of the designer. Then, with the help of the advantage of genetic algorithm in searching the optimal solution, the final scheme of landscape architecture design can be matched with the personal concept of landscape architects. Affected by the number of population, in order to search the optimal solution comprehensively, quickly, and accurately, genetic algorithm usually requires individuals to provide easily perceived parameters to designers [23]. Therefore, layer-by-layer solution method can

be adopted. As shown in Figure 8, it is the schematic diagram of the layer-by-layer optimization search solution model.

In the layer-by-layer optimization search and solution model, the solution space of landscape design is coded and divided into M layers. Using this hierarchical optimization model, in the corresponding sub-solution space of each layer, the problem to be solved is searched and solved by the interactive genetic algorithm with the participation of designers, and the solution results are treated as the sub-solution space of the next layer. Then, the same method is used to repeat the search and solution process until all parameter values are no longer changed. At this time, the optimization design process of the whole landscape space environment is over.

After dividing the landscape morphology parameter set in formula (6) into M layers, its form is as follows:

$$\begin{cases} D_1 = \{d_1^1, d_2^1, \dots, d_N^1\}, \\ D_2 = \{d_1^2, d_2^2, \dots, d_N^2\}, \\ \vdots \\ D_M = \{d_1^M, d_2^M, \dots, d_N^M\}, \end{cases} \quad (7)$$

where $D = D_1 \cup D_2 \cup \dots \cup D_M$, $N = N_1 + N_2 + \dots + N_M$.

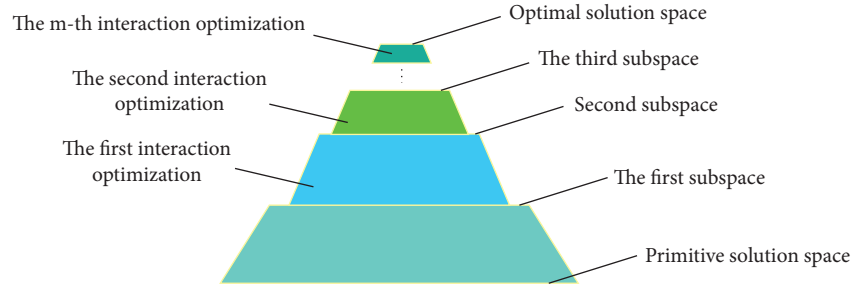


FIGURE 8: Schematic diagram of the layer-by-layer optimization search solution model.

In order to search and solve the landscape morphological parameters layer-by-layer, it is necessary to determine the weight of each morphological parameter, which represents the influence or importance of the morphological parameters in the design scheme. When determining the weight of each morphological parameter layer-by-layer, the larger the parameter weight value, the priority should be given [24]. At the same time, other relevant parameters adjust their weight values accordingly through adaptive methods. The weight coefficient λ_k of morphological parameters can be expressed as follows:

$$\lambda_k = \frac{\delta_k}{\varepsilon_k},$$

$$\delta_k = \sqrt{\frac{\sum_{i=0}^{N_k} (d_i^k - \varepsilon_k)^2}{N_k}}, \quad (8)$$

$$\varepsilon_k = \frac{\sum_{i=0}^{N_k} d_i^k}{N_k},$$

where δ_k indicates the standard deviation of the parameter weight curve, d_i^k represents the mean value of the parameter weight curve, d_i^k is the number of times that the value of parameter k is selected in the i -th interval, and N_k is the number of times that parameter k is selected.

The parameter value $d_{k \max}$ at the peak position of each parameter weight curve can be expressed as follows:

$$d_{k \max} = d_k|_{D=D_{\max}}. \quad (9)$$

According to the above method, the weight values of all morphological parameters can be calculated, and then they can be sorted. Finally, the parameters required for the optimized landscape design scheme can be obtained, and their forms are as follows:

$$D_l = \{d'_1, d'_2, \dots, d'_N\}, \quad (10)$$

where D_l is the sorted set of garden landscape morphological parameters and d'_1, d'_2, \dots, d'_N are the results of arranging the parameters in the initial design scheme according to their weight λ_k from large to small.

5. Experiment and Analysis

In order to test and evaluate the scheme proposed in this article, we might as well take a garden community that has not been optimized as the object, and use the garden landscape space environment optimization design scheme based on interactive genetic algorithm proposed in this article to plan, and get the corresponding design effect. As shown in Figure 9, the comparison results of the effects before and after the optimization design of the garden landscape space environment are given.

In order to facilitate the objective and comprehensive evaluation of the optimized landscape design effect, it is necessary to establish the evaluation system of the landscape space environment. The evaluation system is composed of three levels of evaluation indicators: target level, system level, and index level, as shown in Table 1. According to Table 1, the target layer as the first level evaluation index is mainly the landscape space environment, while the system layer as the second level evaluation index mainly includes landscape elements, plant greening, landscape layout, landscape space, etc. Then, several corresponding observation points are set according to each second level evaluation index.

According to the established evaluation system, the evaluation value of the landscape design effect is obtained by issuing questionnaires and behavior observation to different groups in turn during the experiment. According to the survey results, each observation point in the index layer is assigned a value. Firstly, the evaluation value of the investigator on the observation point is calculated, and the assignment is multiplied by the weight of the corresponding observation point. Secondly, sum up the evaluation values of all indicators in the system layer to obtain the evaluation values of the system layer. Then, the evaluation value of the target layer can be calculated according to the evaluation value of the system layer and the corresponding weight, which is the comprehensive evaluation value of the design effect of the garden landscape space environment. As shown in Table 2, according to the evaluation value and corresponding weight of the system layer, the comprehensive evaluation value can be calculated as 3.0807.

In order to further show the superiority of the method proposed in this article in the design of garden landscape space and environment, the traditional garden landscape

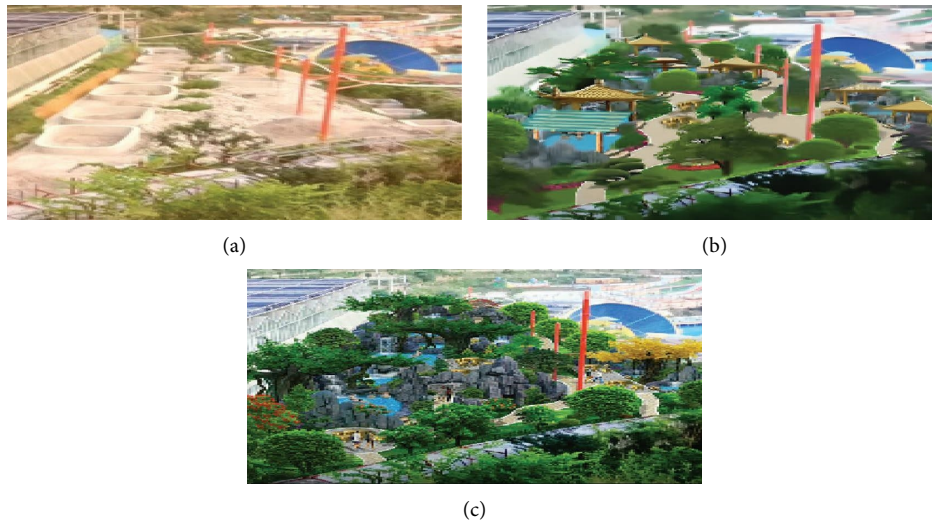


FIGURE 9: Comparative effect before and after optimization design of garden landscape space environment. (a) Original landscape state. (b) Effect of traditional landscape design methods. (c) The effect of this design method.

TABLE 1: Composition of evaluation index system of landscape spatial environment.

Evaluation target layer	Evaluation system level	Index observation layer
Garden landscape space environment	Landscape elements	Pieces of garden
		Garden architecture
	Plant greening	Waterscape design
		Number of plants
		Green conservation
	Landscape layout	Plant species
		Landscape zoning
		Landscape atmosphere
		Landscape function
	Landscape space	General layout
Space color		
Spatial scale		
Landscape facilities	Spatial organization	
	Entertainment facilities	
		Recreational facilities

TABLE 2: System level evaluation results.

Evaluation system level	Weight value	Evaluation assignment	Evaluation results
Landscape elements	0.132	3.6	0.4752
Plant greening	0.235	2.3	0.5405
Landscape layout	0.167	3.7	0.6179
Landscape space	0.319	3.2	1.0208
Landscape facilities	0.147	2.9	0.4263

design method was comprehensively compared with this method in terms of relevant evaluation indicators during the experiment, as shown in Figure 10. According to the comparison results reflected in Figure 10, the results of each

evaluation index of landscape obtained by using the method proposed in this article are better than the traditional landscape design methods, indicating that this method has obvious advantages.

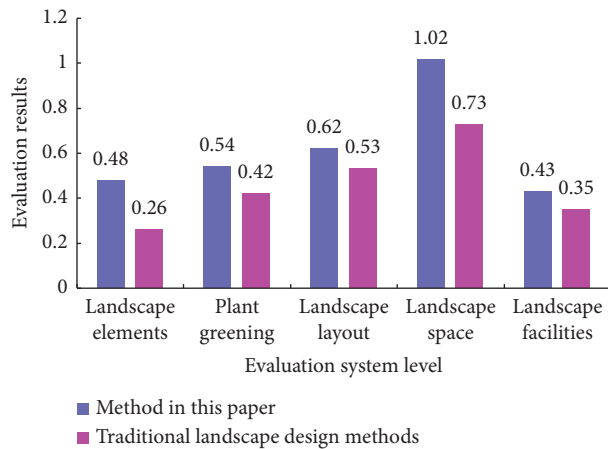


FIGURE 10: Comparison of evaluation results on relevant indicators between traditional landscape design methods and this method.

6. Conclusion

With the continuous development of economy and society, the traditional landscape design concept had been unable to meet the growing needs of people. There was a simple repetition in the design of modern garden landscape space environment, which was lack of certain innovation. Therefore, based on the innovative design theory of interactive genetic algorithm, this article proposed an optimization design method of garden landscape space environment. Based on the analysis of the relationship between garden landscape and buildings, the change in people's demand for garden landscape space environment and the relevant characteristics of garden landscape, this article expounded the basic principles and methods of garden landscape design, and expounded the common problems in garden landscape design. This article summarized the interactive genetic algorithm and its advantages in innovative design, and put forward the optimization design method of garden landscape space environment based on interactive genetic algorithm. Finally, taking a garden landscape design as an example, the evaluation index system of garden landscape space environment was constructed. Through experimental analysis and comparison, the results showed that compared with the traditional garden landscape design methods, the garden landscape space design scheme proposed in this article had achieved better evaluation results. The method proposed in this article not only has certain reference value for the in-depth study of the design of garden landscape space environment, but also has important guiding significance for urban garden planning and modern architectural design.

Data Availability

The labeled data set used to support the findings of this study can be obtained from the author upon request.

Conflicts of Interest

The author declares that there are no conflicts of interest.

Acknowledgments

This work was supported by the 2021 Shanxi Philosophy and Social Science Planning Project: Research on eco-cultural tourism development planning strategy in Shanxi old revolutionary base (project no. 2021YY109).

References

- [1] Y. J. Kim, J. G. Kim, Y. W. Kang, and J. J. Park, "Evaluation of pedestrian space sequences according to landscape elements: focus on large-scale residential complexes," *KSCE Journal of Civil Engineering*, vol. 25, no. 12, pp. 4834–4841, 2021.
- [2] S. J. Li and Z. Y. Fan, "Evaluation of urban green space landscape planning scheme based on PSO-BP neural network model," *Alexandria Engineering Journal*, vol. 61, no. 9, pp. 7141–7153, 2022.
- [3] Z. Jian and S. Hao, "Geo-spatial analysis and optimization strategy of park green space landscape pattern of Garden City-A case study of the central district of Mianyang City Sichuan Province," *European Journal of Remote Sensing*, vol. 53, no. 1, pp. 309–315, 2020.
- [4] L. W. An, "Spatial distribution of park landscape green space in ports: a study considering the constraints of ecological space," *Journal of Coastal Research*, vol. 106, no. sp1, pp. 351–354, 2020.
- [5] M. Y. Geng, L. Hong, K. X. Ma, and K. Wang, "Evolution of urban public space landscape in tianjin port city," *Journal of Coastal Research*, vol. 104, no. sp1, pp. 142–146, 2020.
- [6] D. D. Wang, X. D. Wang, Y. Li, and J. Xie, "Landscape environment design of urban public space based on visual enhancement technology," *Fresenius Environmental Bulletin*, vol. 29, no. 10, pp. 9005–9013, 2020.
- [7] D. Mao, Y. C. Zhang, D. Z. Kong, S. L. He, and X. Y. Li, "Evaluation of urban multi-scale landscape ecological pattern based on open space classification: a case study in xinxiang, China," *Applied Ecology and Environmental Research*, vol. 16, no. 5, pp. 6787–6799, 2018.
- [8] J. Wan and Z. B. Zhao, "Analysis of landscape pattern change and ecosystem service value of urban green space - taking beidaihe district as an example," *Fresenius Environmental Bulletin*, vol. 29, no. 7, pp. 5382–5389, 2020.
- [9] G. F. Han, Q. Wen, and S. L. Su, "Optimization analysis of environmental factors of public green space landscape pattern based on information interaction," *Fresenius Environmental Bulletin*, vol. 31, no. 3, pp. 2493–2500, 2022.
- [10] Q. F. Bu, P. D. Peng, and L. P. Sun, "Relevance of urban green space landscape features and PEOPLE'S physical health and mental health," *Journal of Environmental Protection and Ecology*, vol. 21, no. 4, pp. 1494–1500, 2020.
- [11] N. Stojanovic, N. Vasiljevic, B. Radic et al., "Visual quality assessment of roadside green spaces in the urban landscape - a case study of belgrade city roads," *Fresenius Environmental Bulletin*, vol. 27, no. 5A, pp. 3521–3529, 2018.
- [12] Z. J. Y. Liu and Y. Liu, "Reasonable allocation strategy of garden landscape space color based on decomposition and combination method," *Fresenius Environmental Bulletin*, vol. 30, no. 6, pp. 6137–6143, 2021.
- [13] A. Hami and B. Abdi, "Students' landscaping preferences for open spaces for their campus environment," *Indoor and Built Environment*, vol. 30, no. 1, pp. 87–98, 2021.
- [14] T. R. Etherington, F. J. Morgan, and D. O'Sullivan, "Binary space partitioning generates hierarchical and rectilinear neutral landscape models suitable for human-dominated

- landscapes,” *Landscape Ecology*, vol. 37, no. 7, pp. 1761–1769, 2022.
- [15] D. R. Grafius, R. Corstanje, and J. A. Harris, “Linking ecosystem services, urban form and green space configuration using multivariate landscape metric analysis,” *Landscape Ecology*, vol. 33, no. 4, pp. 557–573, 2018.
- [16] B. Senik and O. Uzun, “A process approach to the open green space system planning,” *Landscape and Ecological Engineering*, vol. 18, no. 2, pp. 203–219, 2022.
- [17] S. L. Bell, R. Foley, F. Houghton, A. Maddrell, and A. M. Williams, “From therapeutic landscapes to healthy spaces, places and practices: a scoping review,” *Social Science & Medicine*, vol. 196, pp. 123–130, 2018.
- [18] S. C. Lee, H. E. Tseng, C. C. Chang, and Y. M. Huang, “Applying interactive genetic algorithms to disassembly sequence planning,” *International Journal of Precision Engineering and Manufacturing*, vol. 21, no. 4, pp. 663–679, 2020.
- [19] H. Cong, W. N. Chen, and W. J. Yu, “A two-stage information retrieval system based on interactive multimodal genetic algorithm for query weight optimization,” *Complex & Intelligent Systems*, vol. 7, no. 5, pp. 2765–2781, 2021.
- [20] R. L. Dou, Y. B. Zhang, and G. F. Nan, “Application of combined Kano model and interactive genetic algorithm for product customization,” *Journal of Intelligent Manufacturing*, vol. 30, no. 7, pp. 2587–2602, 2019.
- [21] Z. Wei and J. H. Nie, “Research on interface design based on user’s mental model driven by interactive genetic algorithm,” *International Journal of Bio-Inspired Computation*, vol. 17, no. 1, pp. 42–51, 2021.
- [22] A. Kumar Chaudhary, L. A. Warner, and A. D. Ali, “Using perceived benefits to segment residential landscape irrigation users,” *Urban Forestry and Urban Greening*, vol. 38, pp. 318–329, 2019.
- [23] M. Gonzalez and T. Kania, “Grothendieck spaces: the landscape and perspectives,” *Japanese Journal of Mathematics*, vol. 16, no. 2, pp. 247–313, 2021.
- [24] Z. Li, Y. N. Cheng, S. Song, and Y. K. He, “Research on the space cognitive model of new Chinese style landscape based on the operator optimization genetic algorithm,” *Fresenius Environmental Bulletin*, vol. 28, no. 6, pp. 4483–4491, 2019.

Retraction

Retracted: Nontarget Suppression in Ball Sports Multitarget-Tracking Task

Mathematical Problems in Engineering

Received 26 September 2023; Accepted 26 September 2023; Published 27 September 2023

Copyright © 2023 Mathematical Problems in Engineering. This is an open access article distributed under the Creative Commons Attribution License, which permits unrestricted use, distribution, and reproduction in any medium, provided the original work is properly cited.

This article has been retracted by Hindawi following an investigation undertaken by the publisher [1]. This investigation has uncovered evidence of one or more of the following indicators of systematic manipulation of the publication process:

- (1) Discrepancies in scope
- (2) Discrepancies in the description of the research reported
- (3) Discrepancies between the availability of data and the research described
- (4) Inappropriate citations
- (5) Incoherent, meaningless and/or irrelevant content included in the article
- (6) Peer-review manipulation

The presence of these indicators undermines our confidence in the integrity of the article's content and we cannot, therefore, vouch for its reliability. Please note that this notice is intended solely to alert readers that the content of this article is unreliable. We have not investigated whether authors were aware of or involved in the systematic manipulation of the publication process.

In addition, our investigation has also shown that one or more of the following human-subject reporting requirements has not been met in this article: ethical approval by an Institutional Review Board (IRB) committee or equivalent, patient/participant consent to participate, and/or agreement to publish patient/participant details (where relevant).

Wiley and Hindawi regrets that the usual quality checks did not identify these issues before publication and have since put additional measures in place to safeguard research integrity.

We wish to credit our own Research Integrity and Research Publishing teams and anonymous and named external researchers and research integrity experts for contributing to this investigation.

The corresponding author, as the representative of all authors, has been given the opportunity to register their agreement or disagreement to this retraction. We have kept a record of any response received.

References

- [1] M. Li and L. Zhang, "Nontarget Suppression in Ball Sports Multitarget-Tracking Task," *Mathematical Problems in Engineering*, vol. 2022, Article ID 6848195, 8 pages, 2022.

Research Article

Nontarget Suppression in Ball Sports Multitarget-Tracking Task

Manchao Li and Liying Zhang 

College of International Culture, Kede College of Capital Normal University, Beijing 102602, China

Correspondence should be addressed to Liying Zhang; 2018010200040@jlxj.nju.edu.cn

Received 1 July 2022; Accepted 26 August 2022; Published 7 October 2022

Academic Editor: Hengchang Jing

Copyright © 2022 Manchao Li and Liying Zhang. This is an open access article distributed under the Creative Commons Attribution License, which permits unrestricted use, distribution, and reproduction in any medium, provided the original work is properly cited.

In order to solve the problem of large interference caused by nontarget tasks on the ball sports field, the author proposes a method for multitarget-tracking tasks. By changing the movement speed of the athletes in the expert group, the novice group, and the control group, we investigate the performance of visual attention tracking and neural oscillatory characteristics in ice hockey players. Experimental results show that the main effect of speed was significant ($F = 120.58$, $P < 0.01$, $\eta_p^2 = 0.81$), and post hoc comparison results showed that the faster the movement speed, the lower the tracking accuracy. The main effect of speed was significant ($F = 31.96$, $P < 0.01$, $\eta_p^2 = 0.53$). Post hoc comparison results showed that the faster the movement speed, the lower the ERSP value of the high-frequency alpha rhythm. It proves the influence of speed on the inhibitory effect of nontarget tasks, which is beneficial for athletes to suppress more interference information brought by opponents or the court in the game and plays an important role in improving sports performance and developing the scientific level of sports.

1. Introduction

In daily life, we often need to pay attention to multiple objects at the same time and track for a period of time to obtain information. For example, when we drive a car, we should not only pay attention to the vehicles passing by but also pay attention to the pedestrians at all times to avoid accidents. Multiobject tracking plays an important role in sports, especially ball games. For example, ice hockey players need to always pay attention to and track multiple moving objects on the field; when dribbling and passing the ball, the player with the ball will allocate resources to different key areas in the sports scene, and players need to always pay attention to the position of teammates who are sliding at high speed and flexibly change direction and also need to pay attention to the position and movement of the opponent's players; in other cases, other players should always pay attention to the position of the ball and the movement information of related players and track multiple moving objects for a period of time to collect information on the field [1]. The ability to notice and continuously track multiple moving objects in a sports scene is a prerequisite for an

athlete to make a reasonable tactical strategy. Therefore, the author proposes a related research on the multitarget-tracking task of ball sports and further studies its inhibitory effect on nontarget tasks. The multitarget-tracking task corresponds to the player's own ability to actively judge the ball, and the detection rate of detection stimuli in different regions corresponds to the athlete's ability to screen the opponent's true intention information, and the nontarget inhibition amount corresponds to the player's own ability to inhibit the court information, as shown in Figure 1. Athletes not only need their own subjective judgment and the ability to accept information but also more importantly, they need to know how to judge the opponent's intention, how to accept the opponent's information, how to screen a lot of information, and how to suppress interfering information [2]. Athletes suppress the interference information brought by their opponents or the stadium, such as the interference of the audience, the opponent's fake moves, and the opponent's tactics, and then can judge the opponent's true intentions, screen out the opponent's true intentions, and correct them; it plays an important role in improving sports performance and developing the scientific level of sports.

Multi-object tracking based on deep learning

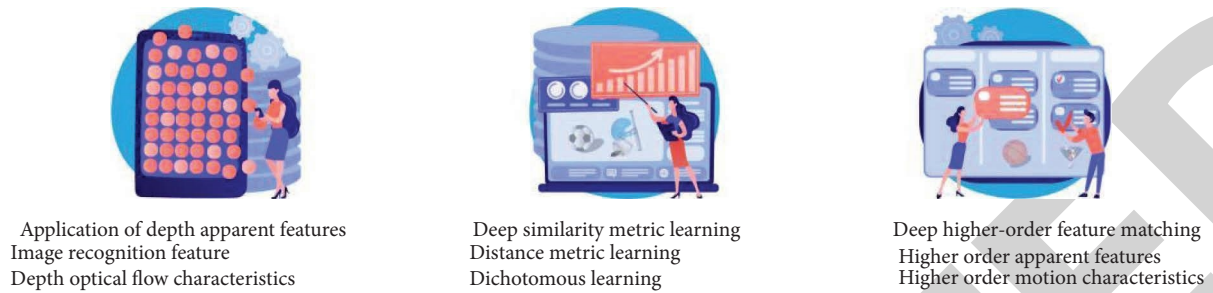


FIGURE 1: Multitarget-tracking tasks.

2. Literature Review

In response to this research problem, the multiobject tracking paradigm (“MOT” for short) proposed by Esghaei et al. is a common paradigm to study the visual attention processing mechanism in dynamic scenes [3]. This paradigm has become one of the main methods to explore the laws of dynamic visual attention and perceptual processing. The study by Suleimenova et al. found that compared with the novice group of the basketball team, the expert group performed better than the novice group in the multiobject tracking task, and there was a significant difference [4]. These studies show that athletes in collective ball sports such as basketball can receive a large amount of complex temporal and spatial information more frequently than ordinary people, so their dynamic visual attention has been developed. The resource sharing model theory also believes that the proficiency of cognitive operation tasks affects its operation effect, even in the same ball sports; due to the different division of labor on the court, long-term competition and training will lead to different cognitive characteristics of athletes [5]. A study of professional football players by Garcia-Fernandez and others found that the multitarget-tracking performance of defenders is better than that of forwards [6]. However, some studies have come to different conclusions; for example, Silva-Gago et al. used multitarget visual tracking to examine the visual attention of different groups of people and found that the performance of athletes and ordinary people in completing multitarget-tracking tasks was significantly different, see significant differences in Ref. [7]. He et al. took ice hockey players of different sports skill levels (expert group and novice group) as the research object and found that ice hockey players of different sports skill levels did not show significant differences in the multitarget-tracking task [8]. Sharma and Chaurasia studied the visual search features of ice hockey players of different levels and found that the gaze trajectories of the players were relatively concentrated, and in complex tasks, the way athletes get information is mainly based on the relationship between the opponent and the position of the field, while the novice group mainly observes the racket and the racket arm [9]. Similar experiments have also been confirmed in sports such as basketball, volleyball, tennis, table tennis, and short track speed skating. The reason for this result may be the difference in the multitarget-tracking task load or the difference in the sports skill level of the selected athletes.

According to the above research results, the author adopts a multitarget-tracking task by changing the movement speed of the athletes in the expert group, the novice group, and the control group and explores the performance of visual attention tracking and neural oscillation characteristics in ice hockey players [10]. Through experiments, it was observed that the movement speed increased, whether it can reduce the individual’s tracking performance and enhance the degree of neural oscillations, thereby reducing the inhibitory effect on nontarget tasks.

3. Research Methods

3.1. Research Objects and Methods

3.1.1. Research Objects. A total of 68 subjects (Table 1) were selected and divided into expert group, novice group, and control group according to their ice hockey training experience. The expert group had a national first-level athlete or above who should have been in sports for more than 4 years, and the training frequency is 6 times/week, about 3 hours each time; the athletes in the novice group had a sports level of the national second-level athlete and below, and the training period was not more than 3 years, and the training frequency was 6 times/week, about 2–3 hours each time; and the control group was ordinary college students who had not received team ball training. The subjects had normal vision or corrected vision, were right-handed, voluntarily participated in the experiment, and also signed the informed consent.

3.1.2. Test Design. A mixed design of three groups (expert group, novice group, and control group) \times 3 speed levels (slow, medium, and fast) was used. Group is the between-subject variable, and speed is the within-subject variable. The dependent variable is the tracking accuracy rate, and the EEG indicator is the ERSP value of the high-frequency alpha rhythm, as shown in Figure 2.

3.2. Test Equipment and Materials

3.2.1. Test Equipment. The experimental program was compiled in the Psych Toolbox toolbox in Matlab software, and a 23.8-inch DELL desktop computer (screen resolution

TABLE 1: Basic information of the subjects.

Category	Expert group	Novice group	Control group
Number of people	22	23	23
Gender: Male/female	10/12	11/10	10/13
Age	20.59 ± 2.55	19.5 ± 3.2	20.68 ± 1.97
Training years	5.56 ± 1123	1.75 ± 0.80	—
Training frequency/(times/week)	6	6	—
Training time/(h/time)	3	2 ~ 3	—
Sport class	7 national athletes	National level-2 athletes 10	No sports rating

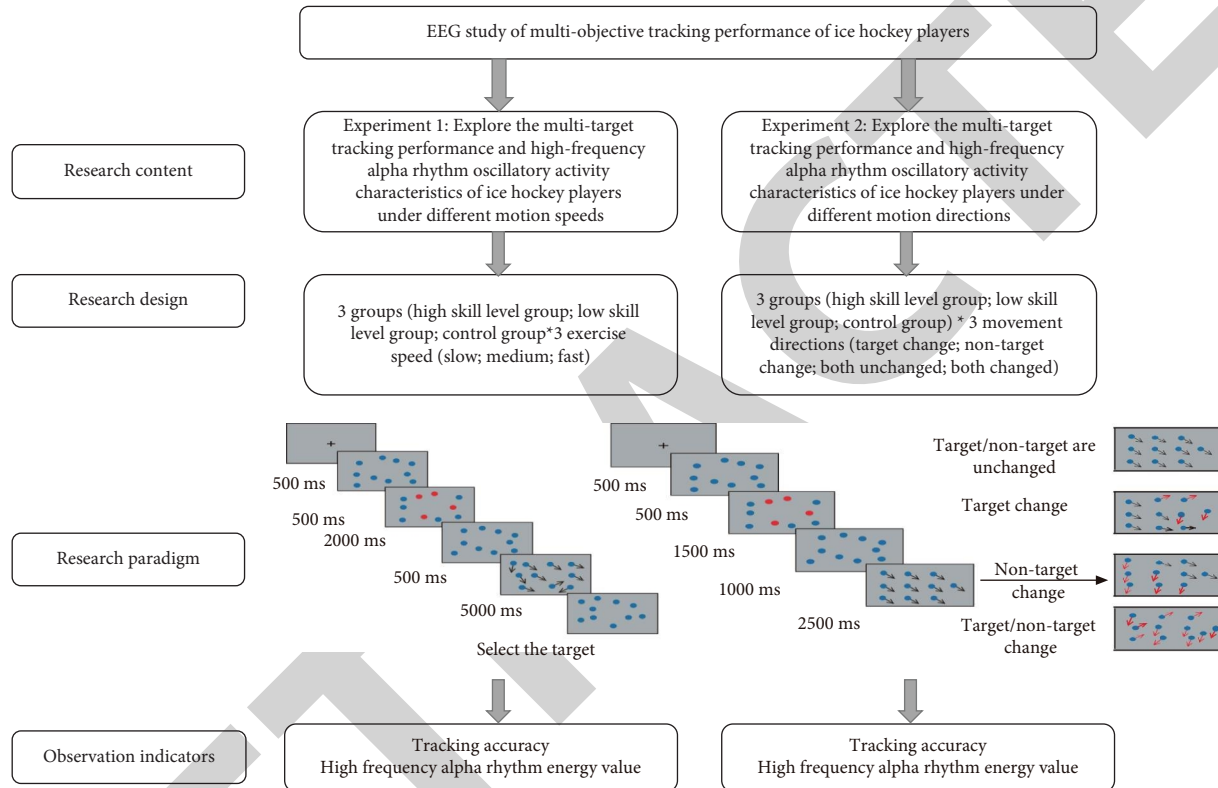


FIGURE 2: Technology roadmap.

of 1920 × 1080 pixels and refresh rate of 60 Hz) was used to present the stimuli in the experiment and record the behavioral data of the subjects.

3.2.2. *Stimulus Material.* The stimulus material is 10 blue balls with a size of 0.9 degree.

3.3. *Test Tasks.* The subject’s head was fixed with a bracket, and the distance between the subject’s eyes and the center of the screen was about 57 cm. The screen background is gray. A black fixation point “+” appeared in the center of the screen, and after 500 ms, 10 blue balls appeared. The initial positions of the 10 blue balls are randomly distributed, and the distance between each ball is greater than the diameter of the ball, and the distance between the initial position of the ball and the border of the tracking area is not less than 2 times the diameter of the ball [11]. After 500 ms, four blue balls turned red, the red balls were marked as target stimuli,

and the remaining six blue balls were interference stimuli, and the marking time was 2000 ms. After 2000 ms, four red balls turned blue, and after 500 ms, 10 blue balls moved randomly on the screen for 5000 ms. The movement speed of each trial is randomly presented, and during the movement, the balls do not block each other. When the ball collides with the edge of the tracking area, the ball will randomly change its movement direction. When the distance between the balls is smaller than the diameter, the balls randomly change the direction of movement. After 5000 ms, the movement of the ball stops, and the tested mouse selects the previously marked targets in turn; after selecting, press the space bar to enter the next trial. The specific test process is shown in Figure 3.

There are three speed conditions: the slow speed is 3(°)/s, the medium speed is 4(°)/s, and the fast speed is 5(°)/s. These three speed s were randomly presented, with 30 trials for each speed condition, for a total of 90 trials. After every 15 trials, the subjects rested for 1 min. Before entering the

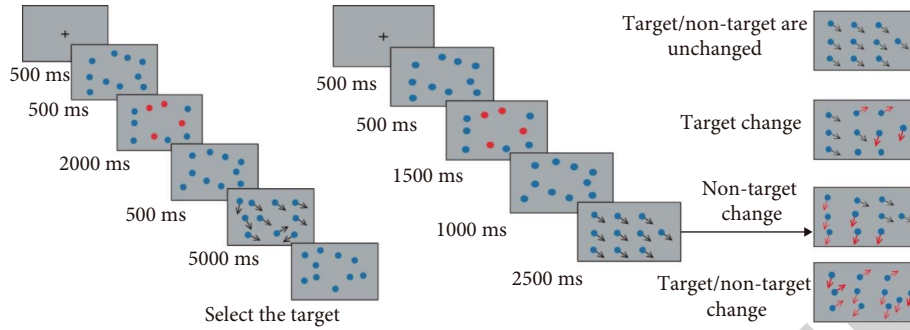


FIGURE 3: Test flow chart.

formal test, let the subjects practice six times to ensure that the subjects are familiar with the test process. The whole test process is about 50 min.

3.4. EEG Recording. EEG data were recorded using the ERP recording system produced by Brain Products, Germany, the 64-lead electrode cap (Brain Products GmbH, Munich, Germany) extended by the international 10–20 standard system was used, and the electrodes were Ag/AgCl electrodes. The reference electrode point was FCz, and the ground electrode point was AFz; horizontal electro-oculography was placed 1 cm lateral to the subject's right eye, and vertical electro-oculography was placed 1 cm below the subject's left orbit. The contact impedance between the scalp and the electrode was less than 5 k Ω , and the sampling frequency was set to 1000 Hz/conduction.

3.5. Data Processing

3.5.1. Behavioral Data. SPSS 25.0 software was used to perform arc sine function transformation (ARSIN) on the tracking accuracy rate, and then the arc sine transformation value of the tracking accuracy rate was three groups (expert group, novice group, and control group) \times 3 speed conditions (slow, moderate, and fast) repeated measures ANOVA.

3.5.2. EEG Data. The data were preprocessed with the BP analyzer. The average potential of both ear mastoids (TP9 and TP10) was used as the rereference electrode, and the FCz electrode was reduced. The rereferenced EEG data were filtered with a high pass of 1 Hz, a low pass of 30, and a slope of 24 dB/oct. Segmentation was performed according to three speed conditions, and the segmented data were baseline corrected, and the baseline time ranged from (–1000 ms) to (–500 ms). The electro-oculogram artifact was removed by the semiautomatic mode in principal component analysis, and the data with amplitude exceeding $\pm 80 \mu V$ were automatically removed. Finally, the preprocessed data were exported. The preprocessed data was subjected to time-frequency analysis in lets wave.7 software, and the data were subjected to wavelet transform in lets wave according to the gain model, and the transformed data were subjected to event-related spectral perturbation analysis (ERSP). The data were subjected to continuous wavelet transform to calculate

the event-related power spectrum for each trial. The mother wavelet short is set to $cmor1 \sim 1.5$, the low frequency is set to 1 Hz, the high frequency is set to 30 Hz, and the output format is set to the power value. Then for each frequency, the event-related spectral power for each time-frequency bin was divided by the average spectral power of the same frequency in the baseline period before stimulation. The percent ERS (ERSP%) is log-transformed, and by definition, the log-transformed unit is the decibel (dB) calculated as follows:

$$ERS(f, t) = \frac{1}{n} \sum_{k=1}^n |F_k(f, t)|^2. \quad (1)$$

Among them, F_k is the wavelet value of trial K at frequency f and time t , and n is the number of trials:

$$ERSP\% = \frac{ERS(f, t)}{\mu_B(f)}. \quad (2)$$

Among them, $\mu_B(f)$ is the average value of ERS in the baseline range at frequency f , and in order to make the distribution of ERS values tend to be more normal, logarithmic transformation of ERS is performed:

$$ERSP_{log}(f, t) = 10 \log_{10} [ERSP_{si}(f, t)]. \quad (3)$$

When completing the multitarget-tracking task, the brain activation areas of the subjects were concentrated in the occipital and parietal regions; according to the distribution of brain topographic maps and previous literature, the occipital (Oz), parietal (Pz), and parieto-occipital (POz) regions were selected. Of the electrode points, calculate the ERS average of the high-frequency alpha rhythm (10 ~ 13 Hz) of the three electrode points, and perform a 3×3 repeated measures ANOVA [12]. During the analysis, when the statistic did not satisfy the spherical test, the degrees of freedom and P values were corrected by Greenhouse Geisser's method, and Bonferroni's method was used for post hoc comparisons.

4. Analysis of Results

4.1. The Effect of Exercise Speed on the Tracking Performance of the Three Groups of Subjects. As shown in Figure 4, the main effect of speed was significant ($F = 120.58$, $P < 0.01$, $\eta_p^2 = 0.81$), and the post hoc comparison results showed that

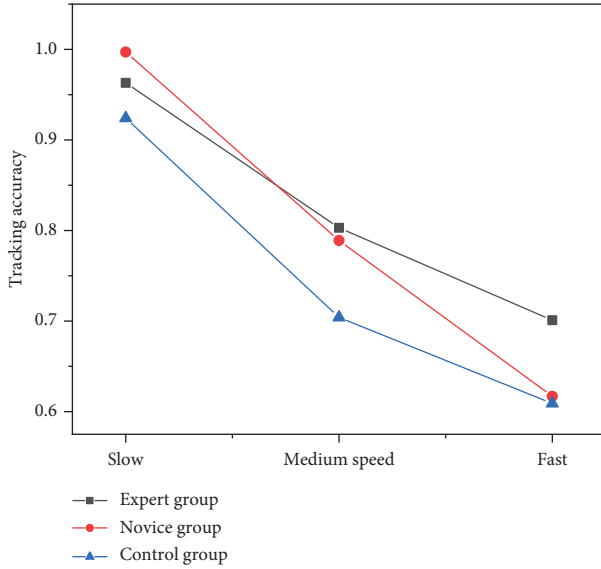


FIGURE 4: Differences in the tracking accuracy of the three groups of subjects under different speed conditions.

the faster the movement speed, the lower the tracking accuracy. The tracking accuracy rate under the slow speed condition was significantly higher than that of the medium speed condition ($P < 0.01$) and the fast condition ($P < 0.01$). The tracking accuracy rate under the medium speed condition was significantly higher than that of the fast condition ($P < 0.01$). The main effect of the group was significant ($F = 3.39$, $P < 0.05$, $\eta_p^2 = 0.10$), and post hoc comparison results showed that the tracking accuracy rate of the expert group was significantly higher than that of the control group ($P < 0.05$), and there was no significant difference between the expert group and the novice group ($P > 0.05$), and the tracking accuracy rate between the novice group and the control group was marginally significant ($P = 0.061$). The interaction between group and speed was significant ($F = 2.63$, $P < 0.05$, $\eta_p^2 = 0.082$). Further simple effect analysis found that under the slow speed condition, there was no significant difference in the tracking accuracy among the three groups ($P > 0.05$). Under the medium speed condition, the tracking accuracy of the control group was significantly lower than that of the expert group ($P < 0.01$) and the novice group ($P < 0.05$), and the tracking accuracy rate of the expert group under the fast condition was significantly higher than that of the control group ($P < 0.05$). Under the fast condition, there was no significant difference in the tracking accuracy between the novice group and the control group ($P > 0.05$), and the tracking accuracy of the expert group was higher than that of the novice group but did not reach a statistically significant level ($P > 0.05$). The above results show that with the increase of movement speed, the accuracy rate of multitarget-tracking of ice hockey players shows obvious advantages. Under medium speed conditions, the ice hockey player group (expert group and novice group) is significantly better than the control group. Under fast conditions, the multitarget-tracking performance of the expert group athletes still has an advantage.

TABLE 2: Statistical table related to high-frequency alpha precepts and behavioral performance.

		Variable	r	P
High skill level group	Slow	Tracking accuracy	-0.396	0.094
	Medium speed	Tracking accuracy	-0.536	0.018
	Fast	Tracking accuracy	-0.478	0.039
Low skill level group	Slow	Tracking accuracy	-0.427	0.053
	Medium speed	Tracking accuracy	-0.570	0.007
	Fast	Tracking accuracy	-0.547	0.010
Control group	Slow	Tracking accuracy	-0.397	0.092
	Medium speed	Tracking accuracy	-0.445	0.046
	Fast	Tracking accuracy	-0.516	0.024

4.2. *The Effect of Motion Speed on Neural Oscillations of High-Frequency Alpha Rhythms.* As shown in the statistics in Table 2, the main effect of speed was significant ($F = 31.96$, $P < 0.01$, $\eta_p^2 = 0.53$), and post hoc comparison results showed that the faster the movement speed, the lower the ERSP value of high-frequency alpha rhythm. Specifically, the ERSP values of high-frequency alpha rhythms under slow conditions were significantly higher than those in moderate ($P < 0.01$) and fast conditions ($P < 0.01$). The ERSP values of high-frequency alpha rhythms in the moderate speed condition were significantly greater than those in the fast condition ($P < 0.01$). The main effect of group was significant ($F = 5.1$, $P < 0.01$, $\eta_p^2 = 0.15$), and post hoc comparison results showed that the ERSP value of high-frequency alpha rhythm in the expert group was significantly higher than that in the control group ($P < 0.01$), and there was no significant difference in the ERSP values of high-frequency alpha rhythms between the expert group and the novice group ($P > 0.05$), and the ERSP values of high-frequency alpha rhythms in the novice group were slightly larger than those in the control group and marginally significant ($P = 0.061$). The interaction between group and speed was significant ($F = 3.01$, $P < 0.05$, $\eta_p^2 = 0.097$). Further simple effect analysis found that under the slow condition, there was no significant difference in the ERSP value of high-frequency alpha rhythm among the three groups ($P > 0.05$). Under the condition of moderate speed, the ERSP value of the high-frequency alpha rhythm of the control group was significantly lower than that of the expert group ($P < 0.01$) and the novice group ($P > 0.05$). Under the fast condition, the ERSP value of the high-frequency alpha rhythm of the expert group was significantly greater than that of the control group ($P < 0.01$), and the ERSP value of the high-frequency alpha rhythm of the expert group was greater than that of the novice group but did not reach a statistically significant level ($P > 0.05$). There was no significant difference in the ERSP values of high-frequency alpha rhythms between the novice group and the control

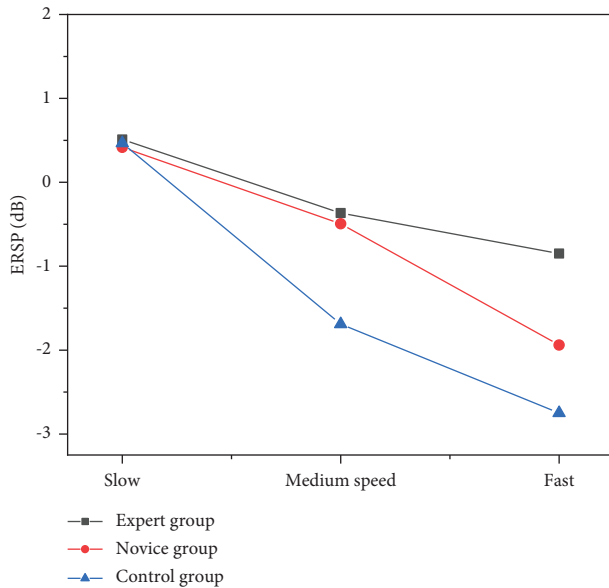


FIGURE 5: ERSP values of high-frequency alpha rhythms of the three groups of subjects at different speeds.

group ($P > 0.05$). The above results (Figure 5) show that as movement speed increased, hockey players had lower levels of oscillations in high-frequency alpha rhythms compared to controls. Under the moderate speed condition, the oscillation level of the high-frequency alpha rhythm of the ice hockey player group (expert group and novice group) was significantly lower than that of the control group. Under the fast condition, the oscillation level of the high-frequency alpha rhythm of the expert group players was significantly lower than that of the control group.

5. Discussion

The author adopted the multitarget-tracking paradigm combined with EEG technology and explored the visual attention tracking performance and neural oscillation characteristics of ice hockey players under different speed loads, and the results show that movement speed reduced the multitarget-tracking performance and enhanced the oscillation level of high-frequency alpha rhythm. The differences in multitarget-tracking performance and high-frequency alpha rhythm oscillation between the expert group hockey players, the novice group ice hockey players, and the control group were mediated by the movement speed.

5.1. Movement Speed Affects Multitarget Tracking Performance of Ice Hockey Players. With the acceleration of the exercise speed, the tracking performance of the expert group ice hockey players, the novice group ice hockey players, and the control group decreased significantly, which is consistent with the previous research results: Visual attention tracking performance degrades with faster motion [13]. The researchers proposed the flexible resource theory to explain the reasons for the impaired tracking performance, arguing

that there is a “resource pool” in the brain of the resources which needed to track the target, and the attentional resources required to track each target determines the number of targets that can be tracked simultaneously. When the object moves fast, tracking one target will consume most of the attention resources in the “resource pool,” and the subjects can only accurately track one target, lose or confuse other targets, resulting in impaired tracking performance [14]. Under moderate speed conditions, compared with the control group, the expert group hockey players and the novice group hockey players have superior visual tracking performance, which indicates that the multitarget-tracking ability of the hockey players is better than that of the nonathletes, which supports the results of some previous studies; that is, athletes have advantages in multitarget-tracking performance compared to nonathletes [15]. Under the fast condition, the expert group hockey players still had an advantage in visual tracking performance compared with the control group, and there was no significant difference in tracking performance between the novice group hockey players and the control group. This shows that as the speed of movement increases, the expert group hockey players still maintain the advantage of multitarget-tracking performance, while the tracking performance of the novice group hockey players and the control group is impaired. The authors verified from the behavioral level that the increase of exercise speed will reduce the tracking performance, which is in line with the flexible resource theory and found that with the increase of exercise speed, the multitarget-tracking performance of ice hockey players is better than that of the control group, and the higher the skill level, the better the tracking performance, the more obvious the advantage.

5.2. Movement Speed Affects the Level of Neural Oscillations in Ice Hockey Players. In order to effectively track multiple targets, certain attention resources need to be invested, so when completing multitarget-tracking tasks at different speeds, there may be differences in the degree of neural oscillations of the expert group ice hockey players, the novice group ice hockey players, and the control group. Oscillation levels of high-frequency alpha rhythms were assessed using the ERSP values of high-frequency alpha rhythms. Note that the more the focus on a certain task, the smaller the ERSP value of the alpha rhythm, and the higher the oscillation of the alpha rhythm [16]. Under the fast condition, the oscillation intensity of the high-frequency alpha rhythm of the expert hockey players was weaker than that of the control group, while the oscillation intensity of the high-frequency alpha rhythm of the novice group and the control group was not significantly different. This shows that under the fast task load, compared with the control group, the ice hockey players in the expert group can complete the tracking task with less attention resources, reflecting the characteristics of attention resource saving [17]. This revealed that under conditions of high task load, the expert group ice hockey players exhibited a lower degree of oscillation of high-frequency alpha rhythms and had more efficient use of attentional resources. This supports the ability to perform

specific tasks or cognitive tasks related to specific tasks and that athletes in the expert group have more obvious characteristics of resource consumption saving [18]. Research indicates that athletes may have higher neural efficiency and less attentional resource consumption during multiobject tracking tasks. When performing multitarget-tracking tasks, compared to nonathletes, ice hockey players showed lower alpha rhythm oscillation levels and more efficient attentional resource utilization, and the higher the skill level, the more obvious the advantage of saving attentional resources [19]. Combining the tracking accuracy and the high-frequency alpha rhythm oscillation, under moderate speed conditions, the tracking performance of the ice hockey players was better than that of the control group, and the high-frequency alpha rhythm oscillation level was lower than that of the control group. Under the fast condition, the expert group ice hockey players showed a tracking advantage and less attentional resource consumption, and the novice group ice hockey players and the control group showed no significant differences in tracking performance and the degree of high-frequency alpha rhythm oscillations [20].

6. Conclusion

The author proposed a multitarget-tracking task based on and by changing the movement speed of the athletes in the expert group, the novice group, and the control group, explored the visual attention tracking performance and neural oscillation characteristics of ice hockey players, and used the multiobject tracking paradigm combined with EEG technology to observe the performance of different exercise loads, differences in multitarget-tracking performance, and the degree of oscillation of high-frequency alpha rhythms between expert hockey players, novice hockey players, and control groups, revealing their inhibitory effect on nontarget tasks, and the specific performance is that as the movement speed increases, the multitarget-tracking performance of ice hockey players is better, the degree of neural oscillation is lower, and the higher the skill level, the more obvious the effect, and it has a strong inhibitory effect on nontarget tasks.

Data Availability

The data used to support the findings of this study are available from the corresponding author upon request.

Conflicts of Interest

The authors declare that there are no conflicts of interest.

References

- [1] A. Murata, T. Doi, K. Kageyama, and W. Karwowski, "Development of an eye-gaze input system with high speed and accuracy through target prediction based on homing eye movements," *IEEE Access*, vol. 9, no. 99, p. 1, 2021.
- [2] M. Marini, A. Ansani, and F. Paglieri, "Attraction comes from many sources: attentional and comparative processes in decoy effects," *Judgment and decision making*, vol. 15, no. 5, pp. 704–726, 2020.
- [3] M. Esghaei, S. Treue, and T. R. Vidyasagar, "Dynamic coupling of oscillatory neural activity and its roles in visual attention," *Trends in Neurosciences*, vol. 45, no. 4, pp. 323–335, 2022.
- [4] N. Suleimenova, D. Kalykov, B. Makhamedova, Z. Oshakbaieva, and Y. Abildayev, "A resource conservation technology for adapting argroecosystems to the new natural conditions of a warming climate in south-eastern Kazakhstan," *Online Journal of Biological Sciences*, vol. 21, no. 2, pp. 376–387, 2021.
- [5] S. Luo, Y. Zhao, Y. Xiao, R. Lin, and Y. Yan, "A temporal-spatial spectrum prediction using the concept of homotopy theory for uav communications," *IEEE Transactions on Vehicular Technology*, vol. 70, no. 4, pp. 3314–3324, 2021.
- [6] A. F. Garcia-Fernandez, J. Ralph, P. Horridge, and S. Maskell, "A Gaussian filtering method for multi-target tracking with nonlinear/non-Gaussian measurements," *IEEE Transactions on Aerospace and Electronic Systems*, vol. 57, p. 1, 2021.
- [7] M. Silva-Gago, F. Ioannidou, A. Fedato, T. Hodgson, and E. Bruner, "Visual attention and cognitive archaeology: an eye-tracking study of palaeolithic stone tools," *Perception*, vol. 51, no. 1, pp. 3–24, 2022.
- [8] Y. He, X. Lv, Z. Zhou, D. Sun, J. S. Baker, and Y. Gu, "Comparing the kinematic characteristics of the lower limbs in table tennis: differences between diagonal and straight shots using the forehand loop," *Journal of Sports Science and Medicine*, vol. 19, no. 3, pp. 522–528, 2020.
- [9] K. Sharma and B. K. Chaurasia, "Trust based location finding mechanism in VANET using DST," in *Proceedings of the Fifth International Conference on Communication Systems & Network Technologies*, pp. 763–766, IEEE, Gwalior, India, April, 2015.
- [10] K. Ogata, "Non-invasive brain stimulation and short-term cortical plasticity," *Neurology and Clinical Neuroscience*, vol. 9, no. 1, pp. 10–16, 2021.
- [11] J. Moysen and M. García Lozano, "Learning-based tracking area list management in 4g and 5g networks," *IEEE Transactions on Mobile Computing*, vol. 19, no. 8, pp. 1–1878, 2019.
- [12] E. Clausen, "Use of detailed topographic map evidence of the southeast Wyoming gangplank area to compare two fundamentally different geomorphology paradigms, USA," *Open Journal of Geology*, vol. 10, no. 04, pp. 261–279, 2020.
- [13] A. Rajendran, N. Balakrishnan, and P. Ajay, "Deep embedded median clustering for routing misbehaviour and attacks detection in ad-hoc networks," *Ad Hoc Networks*, vol. 126, Article ID 102757, 2022.
- [14] R. Ahmed and M. M. Doyley, "Parallel receive beamforming improves the performance of focused transmit-based single-track location shear wave elastography," *IEEE Transactions on Ultrasonics, Ferroelectrics, and Frequency Control*, vol. 67, no. 10, pp. 2057–2068, 2020.
- [15] A. Jc, B. Jl, L. B. Xin, A. Wg, Z. Jing, and C. Fza, "Degradation of Toluene in Surface Dielectric Barrier Discharge (SDBD) Reactor with Mesh Electrode: Synergistic Effect of UV and TiO₂ Deposited on Electrode," *Chemosphere*, vol. 288, 2021.
- [16] Y. Chen, C. Gong, Y. Tian et al., "Neuromodulation effects of deep brain stimulation on beta rhythm: a longitudinal local field potential study," *Brain Stimulation*, vol. 13, no. 6, pp. 1784–1792, 2020.
- [17] R. Huang, S. Zhang, W. Zhang, and X. Yang, "Progress of zinc oxide-based nanocomposites in the textile industry," *IET Collaborative Intelligent Manufacturing*, vol. 3, no. 3, pp. 281–289, 2021.

Retraction

Retracted: Parameter Optimization of Educational Network Ecosystem Based on BERT Deep Learning Model

Mathematical Problems in Engineering

Received 8 August 2023; Accepted 8 August 2023; Published 9 August 2023

Copyright © 2023 Mathematical Problems in Engineering. This is an open access article distributed under the Creative Commons Attribution License, which permits unrestricted use, distribution, and reproduction in any medium, provided the original work is properly cited.

This article has been retracted by Hindawi following an investigation undertaken by the publisher [1]. This investigation has uncovered evidence of one or more of the following indicators of systematic manipulation of the publication process:

- (1) Discrepancies in scope
- (2) Discrepancies in the description of the research reported
- (3) Discrepancies between the availability of data and the research described
- (4) Inappropriate citations
- (5) Incoherent, meaningless and/or irrelevant content included in the article
- (6) Peer-review manipulation

The presence of these indicators undermines our confidence in the integrity of the article's content and we cannot, therefore, vouch for its reliability. Please note that this notice is intended solely to alert readers that the content of this article is unreliable. We have not investigated whether authors were aware of or involved in the systematic manipulation of the publication process.

Wiley and Hindawi regrets that the usual quality checks did not identify these issues before publication and have since put additional measures in place to safeguard research integrity.

We wish to credit our own Research Integrity and Research Publishing teams and anonymous and named external researchers and research integrity experts for contributing to this investigation.

The corresponding author, as the representative of all authors, has been given the opportunity to register their agreement or disagreement to this retraction. We have kept a record of any response received.

References

- [1] S. Tao, "Parameter Optimization of Educational Network Ecosystem Based on BERT Deep Learning Model," *Mathematical Problems in Engineering*, vol. 2022, Article ID 3119014, 9 pages, 2022.

Research Article

Parameter Optimization of Educational Network Ecosystem Based on BERT Deep Learning Model

Sha Tao 

School of Marxism, Huaibei Normal University, Huaibei, Anhui 235000, China

Correspondence should be addressed to Sha Tao; 1821130039@e.gzhu.edu.cn

Received 17 August 2022; Accepted 19 September 2022; Published 30 September 2022

Academic Editor: Hengchang Jing

Copyright © 2022 Sha Tao. This is an open access article distributed under the Creative Commons Attribution License, which permits unrestricted use, distribution, and reproduction in any medium, provided the original work is properly cited.

The key sentimental words in the text cannot be paid attention to effectively, and language knowledge such as the text information and the sentimental resources are relied on. Therefore, it is necessary to make full use of this unique sentimental information to achieve the best performance of the model. In order to solve the problems, a method based on the fusion of the convolutional neural network and the bidirectional GRU network text sentiment analysis capsule model to analyze the ideological and political education of public opinion is put forward. In this model, each sentiment category is combined with the attention mechanism to generate feature vectors to construct sentiment capsules. Finally, the text sentiment categories are judged according to the attributes of the capsules. The model is tested on MR, IMDB, SST-5, and the data set of the ideological and political education review. Experimental results show that compared with MC-CNN-LSTM, the readiness rate of the proposed model is improved by 5.1%, 2.8%, 2.8%, and 1.6% on four public Chinese and English data sets, respectively. Compared with LR-Bi-LSTM, NSCL, and multi-Bi-LSTM models, the accuracy of the proposed MC-BiGRU-Capsule model on MR and SST-5 data are 3.2%, 2.4%, and 3.4% higher than that of the LR-Bi-LSTM, NSCL, and multi-Bi-LSTM models, respectively. It also shows a better classification effect on multiclassification data sets. It is concluded that compared with other baseline models, this method has a better classification effect.

1. Introduction

We all know that the new media represented by Weibo, WeChat, and QQ is a double-edged sword that shows the advantages of both pros and cons. New media technologies allow for “freedom and direct expression” and “everyone has a microphone.” All kinds of public opinion in the era of microphone floods, including educational public opinions, can be discussed and spread, which influences the social weather vane. Public perception of education refers to how ordinary people talk about education, including primary and secondary education, public opinion, good advice, anger, and rage. From the inclusion of education policy in the action plan to the formulation, implementation, evaluation, and even evaluation of it, public opinion has always been at the forefront. Today, we increasingly recognize the close connection between education, public opinion, and education policy [1].

In the era of “everyone has a microphone,” the wind begins to blow from the grass. Most people are overly concerned with the decision-making process in formulating, implementing, evaluating, and finalizing education policies, which is easy to cause neglect to other content. That is why some problems can be elevated to policy issues while others are excluded. How to detect and respond to the crisis of public opinion in a complex environment of public opinion is inextricably linked to the collection, study, evaluation, guidance, and intervention of public opinion in education. A multifaceted and systematic study of public opinion in education [2]. The Fourth Plenary Session of the 16th CPC National People’s Congress made it clear that China needs to gradually establish a comprehensive system for collecting and analyzing public opinion in order to ensure that it can further reflect public opinion. The Sixteenth Plenary Session of the 16th Central Committee reiterated its importance [3]. The Ministry of Education, in conducting a spiritual survey

of the 6th Plenary Session of the 17th Central Committee, called for the development of China's future education as a starting point, and the gradual establishment of a system that reflects scientific and standardized public opinion to provide timely and accurate public opinion.

Providing educational products and services is the main goal of developing educational informatization enterprises. From the perspective of the development of educational informatization enterprises as a whole, the sustainability of its products and services will be affected by the whole enterprise's ecological environment. Therefore, in order to achieve sustainable development of educational information products and services, it is first necessary to clarify the logical relationship between the elements of the educational information product and service system. Therefore, we need to start with the entire enterprise ecosystem in order to identify the key elements of the educational information product and service ecosystem and its interaction mechanisms. The service ecosystem model is shown in Figure 1.

2. Literature Review

Larson et al. proposed the application of the "survival of the fittest" principle to maintain the balance of the resource pool, establish a convenient feedback mechanism, promote the coevolution of the resource pool, promote the flow of information in the resource pool, and improve the utilization rate of resources [4]. From the perspective of basic knowledge of computer networks and ecology, Wu studied the network ecosystem, analyzed the structure, characteristics, and attributes of the ecosystem [5], and put forward some new concepts for a network system. Through the study of some network behavior of the network (including the competition between different network technologies or software), based on the model of population ecology, the competition model between network populations was constructed, and the software was used to simulate it, so as to provide a reference for the optimization and allocation of network resources. Deng studied the demands of administrators, users, and teaching supervisors for online educational resources by applying the EPSS concept to the educational resource management. The research tried to integrate the EPSS technology with educational resource management to construct an electronic performance support system for learning resource centers for the practical application of network teaching. Through the framework of the online education resource integration, the distributed education resource, database, and education resource integration service center were organically interconnected, forming a co-construction and sharing mode of online education resources with intensive management and distributed storage, thus achieving the best solution of resource construction, resource sharing, and resource application [6]. Lu proposed the integration of online education resources based on three kinds of social software: Blog, Wiki, and Model, and analyzed their respective integration methods, strategies, and characteristics [7]. Tang and T discussed the integration and integration modes of online education resources and put forward three integration modes, namely,

the education resource management database mode, the education resource center mode, and the distributed education resource network mode. There are three aspects of educational resource sharing in the network environment: self-sharing, sharing with others, and global educational resource sharing [8]. Aydn used a k-means clustering algorithm to cluster online public opinions as topics, so as to monitor public opinions [9]. In the context of the big data era, Guo and M. used the Mahout text algorithm to mine the online public opinion information [10]. Ferguson analyzed enterprise public opinions with the sentiment dictionary method and achieved good results [11]. On the application, data analytics companies were developing services that helped companies discover, attract, and assess industry influence by analyzing blogs on the Internet.

At present, there are still some issues that need to be addressed when using the in-depth learning model to address short text sensitivity analysis. The most important thing is not to focus effectively on the keywords of emotion in the text and not to rely on linguistic knowledge such as textual information and emotional sources. This unique emotional information must be fully utilized to achieve the best performance of the model. To address the above issues, a short text sensitivity analysis capsule model combining a circulatory neural network and a two-way GRU network is proposed to analyze public perceptions of ideological and political education. The model first focuses on the word vectors in the text in order to focus on emotionally important words in the short text. The advantages of CNN and BI-GRU are combined in the unpacking phase. Finally, according to each category of emotion, vectors are used to express emotional properties, and an emotional capsule is created, which improves the ability to express design features.

3. Methods

3.1. Fusion Convolutional Neural Network. The textual sensitivity analysis capsule design framework, combined with the circulatory neural network and the bidirectional GRU (MC-BiGRU-Capsule), consists of four parts: attention level, feature breakdown, character integration, and emotional capsule construction.

- (1) Layers: these systems contain multiple control systems that capture the ideas expressed in the text, encode the relationships between words, and create clear translations of the text.
- (2) Eigen decomposition provides text message vectors based on multiple norms for CNN and Bi-GRU, respectively. The CNN rotates with 3×300 , 4×300 , 5×300 , and 512 broken kernels in step 1, and then focuses on converting the N-gram energy of words into sentences and the structure's next level of structure. Therefore, the convolution function is only used to obtain the local product of the text. The Bi-GRU model makes the text temporarily pass through the GRU before and after the GRU, removing material from the Earth.

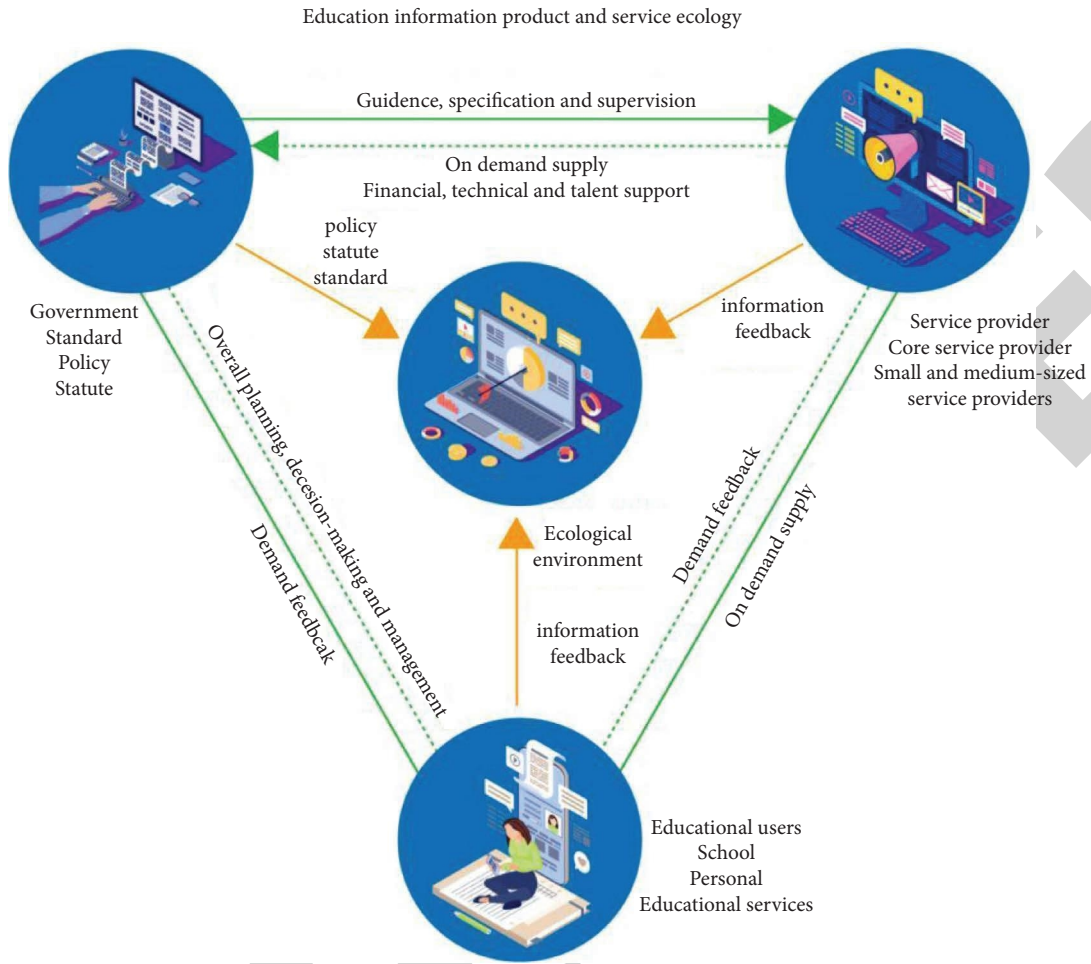


FIGURE 1: Educational informatization products and service ecosystem model.

- (3) Feature aggregation: feature vector H is decomposed by dialing the input of local features and global semantic properties, and the global averaging layer library vector H takes the representation of the text sample function and calculates the loss function [12].
- (4) Create thought capsules: the number of thought capsules corresponding to a set of thoughts. For example, two capsules correspond to positive and negative emotions, and each set of needs is called a "feature capsule." To get the probability of activating the capsule, enter the function vector H attached to the previous step in the emotional capsule P_i is calculated and the feature representation $r_{s,i}$ is reconstructed in combination with the attention mechanism. The probability of activating the capsule is considered active if it is the highest of all the capsules; otherwise, it will be inactive. A characteristic feature of the activation state capsule is the emotional classification of the input text, which is the model output.

3.2. Attention Layer. Attention mechanisms can focus on important information in the text. This study uses a variety of methods to obtain important information about sentences from multiple locations.

For the text $S = \{w_1, w_2, \dots, w_L\}$ with given length L , where w_i is the second word in the sentence, and each word is plotted on a D -dimensional vector, i.e., $S \in R^{L \times D}$.

First, convert the word vector S into a linear form and divide it into three matrices of the same size $Q \in R^{L \times D}$, $K \in R^{L \times D}$, $V \in R^{L \times D}$ and mapped to multiple different subspaces, as shown in the following formula:

$$\begin{aligned} [Q_1, \dots, Q_h] &= [QW^{Q_1}, \dots, QW^{Q_h}], \\ [K_1, \dots, K_h] &= [KW^{K_1}, \dots, KW^{K_h}], \\ [V_1, \dots, V_h] &= [VW^{V_1}, \dots, VW^{V_h}]. \end{aligned} \tag{1}$$

In Formula (1), Q_i, K_i, V_i is a query, key, and value matrix for each subspace. $W^{Q_i}, W^{K_i}, W^{V_i}$ is a conversion matrix, and h is the number of heads.

Then calculate the value of attention for each subspace in parallel, as shown in the following equation:

$$\mathbf{head}_i = \text{softmax}\left(\frac{\mathbf{Q}_i \mathbf{K}_i^T}{\sqrt{d}}\right) \mathbf{V}_i. \quad (2)$$

In Formula (2), \mathbf{head}_i is the attention value of the i th sub-space, and \sqrt{d} is to prevent the gradient from disappearing during the return distribution, the focus matrix is changed to a standard normal distribution.

Then, as shown in the following equation, the attention values of each subspace are connected and converted linearly.

$$\mathbf{Multi_head} = \text{concat}(\mathbf{head}_1, \dots, \mathbf{head}_h) \mathbf{W}^M. \quad (3)$$

In Formula (3), \mathbf{W}^M is the transformation matrix, $\mathbf{Multi_head}$ The meaning of all the sentences, the meaning of unification, is the act of unification. Finally, connect the residual connection between the $\mathbf{Multi_head}$ and \mathbf{S} is used to obtain the sentence matrix shown in the following formula:

$$\mathbf{X} = \text{residual_Connect}(\mathbf{S}, \mathbf{Multi_head}). \quad (4)$$

In Formula (4), $\mathbf{X} \in R^{L \times D}$ is the output of multiple attention, residual_Connect is the residual operation.

3.3. Fusion of CNN and Bidirectional GRU Text Feature Extraction. To provide a more detailed understanding of text-sensitivity features, this study combines the advantages of rotating neural networks and two-way GRU text characterization to model text sentimental features from the local level to the global level.

3.4. Text Feature Extraction Based on CNN. Inspired by visual arts research in bio-agriculture, the joint neural network's ability to learn and express energy resources has been widely used in the field of natural languages, such as the distribution of text and the distribution of hearing [13]. In the native function of CNN, the word vector formed by a sentence is used as a single input, and then the rotation function is performed by multiple rotation kernels matching the size of the word vector to obtain the attributes of several consecutive words.

During the study, a B-turn filter was selected to extract the local characteristics of the multifocus output matrix \mathbf{X} , and the feature matrix is $\mathbf{C}_i = [\mathbf{C}_{i,1}, \mathbf{C}_{i,2}, \dots, \mathbf{C}_{i,B}] \in R^{(L-k+1) \times B}$, where $\mathbf{C}_{i,B} = [c_1, c_2, \dots, c_{L-k+1}] \in R^{L-k+1}$ is the B column vector in \mathbf{C}_i . Element c_j . This vector can be obtained by the following formula:

$$c_j = f(\mathbf{W} \cdot \mathbf{x}_{j:j+k-1} + \mathbf{b}). \quad (5)$$

In Formula (5), f is the activation function ReLU, $\mathbf{W} \in R^{k \times D}$ is the convolution kernel, k is the window width, $\mathbf{x}_{j:j+k-1} \in R^{k \times D}$. \mathbf{K} represents the vectors of the word connecting the first and last two, and b is a biased term.

3.5. Text Feature Extraction Based on Bidirectional GRU. Machine learning techniques have traditionally been limited to preinformation based on material in semantic models, whereas repetitive neural networks (RNNs) can model all previous information in language [14]. However, the standard RNN has the problem of gradient disappearance or explosion. LSTM networks and GRU networks overcome this problem by selectively influencing the state of each moment in the model through some "gateway" structure. In the LSTM version, the GRU replaces the forget-me-not and entry-level update door in the LSTM. The structural definition of the GRU is shown in Figure 2, and the results of the relevant calculations are shown in formulas (6)–(9).

$$\mathbf{z}_t = \sigma(\mathbf{W}^z \mathbf{x}_t + \mathbf{U}^z \mathbf{h}_{t-1}), \quad (6)$$

$$\mathbf{r}_t = \sigma(\mathbf{W}^r \mathbf{x}_t + \mathbf{U}^r \mathbf{h}_{t-1}), \quad (7)$$

$$\tilde{\mathbf{h}}_t = \tanh(\mathbf{W}^h \mathbf{x}_t + \mathbf{U}^h (\mathbf{h}_{t-1} \odot \mathbf{r}_t)), \quad (8)$$

$$\mathbf{h}_t = (1 - \mathbf{z}_t) \odot \tilde{\mathbf{h}}_t + \mathbf{z}_t \odot \mathbf{h}_{t-1}. \quad (9)$$

In the Formulas, \mathbf{W}^z , \mathbf{W}^r , \mathbf{W}^h , \mathbf{U}^z , \mathbf{U}^r , \mathbf{U}^h are the weight matrix of GRU. σ is the sigmoid function. \odot is elements multiplication. \mathbf{z}_t is an update gate that controls the update level of the GRU unit activation value, which is determined by the current input state and the state of the top hidden layer. \mathbf{r}_t is a reset gateway that combines the new input information with the original information. \mathbf{h}_t is the hidden layer. $\tilde{\mathbf{h}}_t$ is the hidden layer of the candidate. To sum up, compared with the LSTM network, the GRU network reduces the design and complexity and reduces the test cost.

State changes in classical repetitive neural networks are one way. However, in some cases, the output of the current state is not only related to the previous state but also related to the next state [15]. For example, the prediction of missing words in a sentence must not only determine the preposition but also the meaning of the text that follows, and the emergence of bidirectional recurrent neural networks solves this problem.

A bidirectional repetitive neural network connects two unidirectional RNNs. Every time two RNNs enter a state in the same direction at the same time, the output is determined together, making it more accurate. Dual GRUs are created by transforming RNNs in bidirectional neural networks with standard GRUs.

The design uses a bidirectional GRU network to study semantic data globally through various agreed-upon matrices. H layers during training. The specific calculation process is shown in formulas (10)–(12).

$$\vec{\mathbf{h}}_t = \text{GRU}\left(\mathbf{X}, \vec{\mathbf{h}}_{t-1}\right), t \in [1, L]. \quad (10)$$

$$\overleftarrow{\mathbf{h}}_t = \text{GRU}\left(\mathbf{X}, \overleftarrow{\mathbf{h}}_{t+1}\right), t \in [L, 1], \quad (11)$$

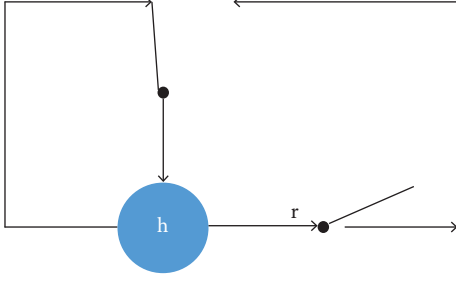


FIGURE 2: GRU unit structure diagram.

$$\begin{aligned} \tilde{h}_t &= \tanh(\mathbf{W}^h \mathbf{x}_t + \mathbf{U}^h (\mathbf{h}_{t-1} \odot \mathbf{r}_t)), \\ \mathbf{H}_t &= \begin{bmatrix} \vec{h}_t \\ \overleftarrow{h}_t \end{bmatrix}. \end{aligned} \quad (12)$$

In the formulas, \vec{h}_0 and \overleftarrow{h}_{t+1} are both initialized as zero vectors. $\vec{h}_t \in R^{L \times d}$. The vector matrix that combines the previous information is an expression of the sensory properties of the word X . $\overleftarrow{h}_t \in R^{L \times d}$ is the expression of the sentiment feature of the word vector matrix X integrating the later information. Moreover, d is the dimension of the GRU unit output vector. $\mathbf{H}_t \in R^{L \times 2d}$ combine the following information. Also, d is the size of the output vector of the GRU unit.

3.6. Feature Fusion. Neural network organization can reduce data loss by decomposing the internal components of the text. A bidirectional GRU network temporarily passes all text and provides global semantic storage [16]. This study combined the advantages of a collapsible neural network and a two-way GRU network and used a global average integration method to combine local properties and global semantic properties of text to obtain a typical representation of a text example V_s , this improves the design features.

During the experiment, the circulation vector B and the output vector dimension in the convolutional neural network were used $2d$. It connects the function vectors generated by the two networks by merging and connecting the two-way GRU network with the same meaning and as shown in the following formula:

$$\mathbf{H} = \text{concat}(\mathbf{C}, \mathbf{H}_t). \quad (13)$$

In Formula (13), $\mathbf{H} \in R^{(l+l) \times 2d}$ is the spliced vector, and $\mathbf{C} = [\mathbf{C}_1, \mathbf{C}_2, \dots, \mathbf{C}_n]$, $\mathbf{C} \in R^{l \times B}$ is the output vector of the convolutional neural network, $\mathbf{H}_t = [\mathbf{h}_1, \mathbf{h}_2, \dots, \mathbf{h}_l]$, $\mathbf{H}_t \in R^{L \times 2d}$. The output vector and concat of the two-way GRU is the connecting function.

To combine the mean values of the H vector to create the feature points, use the global mean aggregation layer and finally get the feature vector $\mathbf{V}_s \in R^{2d}$. To increase the robustness of the model and to avoid over-tuning, these function points have the characteristic of text-sensitive cases. The results of the calculations are shown in the following formula:

$$\mathbf{V}_s = \text{globalaveragepooling}(\mathbf{H}). \quad (14)$$

In Formula (14), global average pooling is the global average pooling operation.

3.7. Sentimental Capsule Construction. Surveillance module: the imaging module combines an H-vector device with a surveillance module to create realistic images in the capsule. The face-lobbing mechanism enables the demo module to measure the importance of words in different texts. For example, “wide” can provide recommendations for hotel reviews, but it does not matter in movie reviews [17]. The formula for calculating the attention mechanism is shown in formulas (15)–(17).

$$\mathbf{u}_{i,t} = \tanh(\mathbf{W}_w \mathbf{H} + \mathbf{b}_w), \quad (15)$$

$$\alpha_{i,t} = \frac{\exp(\mathbf{u}_{i,t}^T \mathbf{u}_w)}{\sum_t \exp(\mathbf{u}_{i,t}^T \mathbf{u}_w)}, \quad (16)$$

$$\mathbf{v}_{c,i} = \sum_t \alpha_{i,t} \mathbf{H}. \quad (17)$$

In the formula, H is the representation of the text after the attachment, and H is inserted into the fully connected layer to obtain the hidden representation of u_i and t . The similarity between u_i , t , and a randomly initiated context vector \mathbf{u}_w . Calculations are made to determine the significance of the words, and the weight of the words in the sentence is normalized using the softmax function to obtain $\alpha_{i,t}$. Weigh the vector H along the weight matrix to obtain the sum $\mathbf{v}_{c,i} \in R^{2d}$ of the attention mechanism. \mathbf{W}_w and \mathbf{u}_w are weight matrices, and \mathbf{b}_w is the bias value learned during training [18]. The attention-grabbing mechanism creates deeper properties at the top level of $\mathbf{v}_{c,i}$, and captures key information in semantic sensitivity.

The probability module calculates the probability of activating the capsule according to the $\mathbf{v}_{c,i}$ semantic properties combined with the following formula:

$$\mathbf{P}_i = \sigma(\mathbf{W}_{p,i} \mathbf{v}_{c,i} + \mathbf{b}_{p,i}). \quad (18)$$

In Formula (18), \mathbf{P}_i is the probability of activating the first capsule, $\mathbf{W}_{p,i}$ and $\mathbf{b}_{p,i}$ are the weight matrix and the bias matrix, and σ is a function of activating the sigmoid gland.

The recovery module multiplies the $\mathbf{v}_{c,i}$ semantic properties by a probability matrix \mathbf{P}_i obtain a description of the reconstructed semantic properties $\mathbf{r}_{s,i} \in R^{2d}$, as shown in the following formula:

$$\mathbf{r}_{s,i} = \mathbf{P}_i \mathbf{v}_{c,i}. \quad (19)$$

The three modules in the capsule complement each other. Each capsule has a characteristic (mental category) for entering text. Therefore, it is likely to be activated if the text sensitivity matches the capsule properties \mathbf{P}_i of the capsule should be maximum, and the reconstruction feature $\mathbf{r}_{s,i}$ of the capsule output should be most similar to the text instance feature \mathbf{V}_s .

Therefore, the spinal loss function is confirmed as shown in (20) and (21).

$$J(\theta) = \sum \max\left(0, 1 + \sum_{i=1}^N y_i \mathbf{P}_i\right), \quad (20)$$

$$U(\theta) = \sum \max\left(0, 1 + \sum_{i=1}^N y_i \mathbf{V}_s \mathbf{r}_{s,i}\right). \quad (21)$$

In Formula (20) and (21), y_i is the sensitivity class label corresponding to the text. The final loss function is the sum of (20) and (21).

$$L(\theta) = J(\theta) + U(\theta). \quad (22)$$

4. Results and Analysis

The experiments were performed on three English data sets: the Mr. (film review) data package, the IMDB data package, and the SST-5 data package, and the Chinese data package is an ideological and political education review package. The above data sets are widely used for sensitivity classification tasks, which makes the experimental results have a good evaluation effect. Mr.'s dataset is a collection of UK movie reviews. Each sentence is classified as positive or negative, with 5,331 positives and 5,331 negatives. The IMDB file contains 50,000 files from U.S. movie studios that are categorized into positive and negative categories in critical thinking analysis [19]. The SST-5 packet is a continuation of Mr. package files and provides separate training packages, available packages, and test packages, totaling 11,855 sentences. Text can be divided into five categories: "Excellent," "Good," "Neutral," "Poor," and "Poor". In this study, SST was trained at the sentence level. After distributing the data for the first time, 3,000 positive feedback and 3,000 negative feedback were obtained from this experiment. An overview of each data set is shown in Table 1.

The experiments in this study are based on PyTorch. English uses 300-dimensional glove word vectors to input words. For words not in the dictionary, start randomly using a similar distribution with a value of 0.05. To first train the Chinese word vectors, we use the fastHan tool to label the text, then train the SKPP-gram standard to use big data from Chinese Wikipedia, and resize the Chinese word vectors to 300 dimensions [20]. Headphones use 8 headphones ($h = 8$) and use the Adam optimizer during modeling with a learning rate of 0.001. Accuracy measures are used to measure the model, and specific areas of the hyper model are not included in Table 2.

In this study, 4 common data sets were compared with the 11 models mentioned above. The proposed MC-BiGRU-capsule model provides better class performance than the basic models on the four data sets. The model has an accuracy of 85.3% for the Mr data package, 50.0% for the SST-5 data package, 91.5% for the IMDB data package, and 91.8% for the Chinese data package [21, 22]. The accuracy of the optimal classification model in the 4 data sets is 1.5%, 0.5%, 2.2%, and 1.2% higher than the control tests, respectively.

First, for the traditional machine learning process, other groups do better than Mr. IMDB and NBSVM in terms of theoretical and cultural data analysis, which indicates that the neural network model has a better effect on sentiment classification tasks than the traditional method. At the same time, the performance of the capsule model is higher than that of deeply researched models such as CNN, BI-LSTM, and MC-CNN-LSTM, indicating that capsules are used to represent text sentiment features in the sentiment classification task, retaining more sentiment information and improving the model classification performance. In addition, the capsule method has a competitive advantage over model language integration experiments [23].

Second, among the in-depth learning methods, MC-CNN-LSTM is better than CNN and BI-LSTM in terms of test performance on all data sets, which verifies the necessity of integrating convolutional neural network local feature extraction and BI-GRU to capture the global text information. Han's public data shows that compared with MC-CNN-LSTM, our standard planning level is improved by 5.1%, 2.8%, 2.8%, and 1.6%, respectively, indicating that the vector neurons used by the capsule model have higher energy model thinking ability. In-depth studies, including an understanding of Mr.'s language and thinking skills and SST-5 show better classes compared to other base models. However, the MC-BiGRU-capsule model proposed in this study achieves 3.2%, 2.4%, and 3.4% higher accuracy than NSCL, NSCL, and multi-Bi-LSTM models, respectively and shows performance in multiple categories of class records [24]. Furthermore, the LR-Bi-LSTM and NSCL models rely heavily on linguistic knowledge such as sensory vocabulary and energy regulators. It is worth noting that constructing such language knowledge requires a great deal of human intervention. The multi-Bi-LSTM model is more detailed than the above two models but is also based on in-depth knowledge and concepts, which is very labor- and time-consuming. However, the research model does not require any linguistic or mental knowledge in the model, the capsule model of the textual mental model achieves more results than the sample instructions, and the depth of communication knowledge and information needs is good and easy [25].

This is because IMDB file sets are long file sets and Mr. file sets are short file sets. RNN-capsule uses a repetitive neural network to generate ad hoc text, average latent features along sentence length, and obtain behavioral representations of the final example. The longer the sentence, the fewer vector representations. It also does not better represent the categories of sensitive text that affect the final structure. Therefore, RNN capsules do not work properly in the IMDB file configuration. Capsule Network Capsule A and Capsule B use a dynamic routing mechanism, connecting to fully connected capsule layers to replace and sort-merge layers to form capsules. The length of the text has little effect on the capsule network. The classification accuracy of the MC-BiGRU-capsule model proposed in this study is higher than that of the RNN-capsule of the four datasets, and the classification accuracy of the MC-BiGRU-capsule model

TABLE 1: Experimental data set statistics.

Data set	The training set	Validation set	The test set	Number of categories
MR	8.64k	0.97k	1.15k	4
IMDB	25.11k	50.14k	25.21k	1
SST-5(Sentence-level)	8.54k	1.07k	2.24k	5
Tan Songbo hotel review	3.64k	1.29k	1.24k	2

TABLE 2: Experimental hyperparameter settings.

Parameter	MR	IMDB	SST-5(Sentence-level)	Tan Songbo hotel review
Convolution kernel width	2,1,4	3,2,5	1,4	2,3,5
Convolution kernel number	513	259	246	289
Number of hidden units	257	126	124	147
Batch size	59	38	61	31
Dropout	0.54	0.41	0.52	0.29

of the IMDB dataset is higher than that of the network capsule a and capsule b . The results show that the advantages of multi-listen-encoded word relations, integrated split neural network, and BI-GRU decomposition function RNN-capsule overcomes the limitations of scripted long vector representation and global media sharing layer representation to create Chinese text and English. Data package example features also demonstrate the strength and overall ability of the mc-BiGRU-capsule.

In this study, we introduce the concept of capsules into the model and use vector neurons to transform scalar neurons. This not only reduces data loss but also improves the ability to model emotions. Also, vector-based training differs from neural network architectures gentleman, a working model aimed at understanding how vector training affects a set of files. By changing the size of the Chinese sample vector and the size of the inverse vector of the sample capsule, the variation of the instrument sample size accuracy can be obtained. Experimental results show that the distribution model is more accurate when large vectors are used to represent the sensitivity of text. In this way, when the learning target is a vector, the ability of the text to express the target is improved, and the text can represent various objects. The results are shown in Figure 3.

To clarify that multiple listeners can capture thought words in texts and encode word relationships, this study shows the weights of words in sentences and reveals the meanings of words and important features of texts. Take the positive and negative patterns of the IMDB dataset as an example, which reminds us of the delicate material of the text.

Dynamic word vectors BERT works well in many languages. Compared to static languages such as Glove and Word2Vec, BERT can distinguish deep meanings from text and overcome racism by combining two encodings and different meanings to obtain word meanings. This study uses BERT dynamic word vectors from the IMDB database. Furthermore, the BERT was combined with the proposed MC-BiGRU-capsule model and compared with the

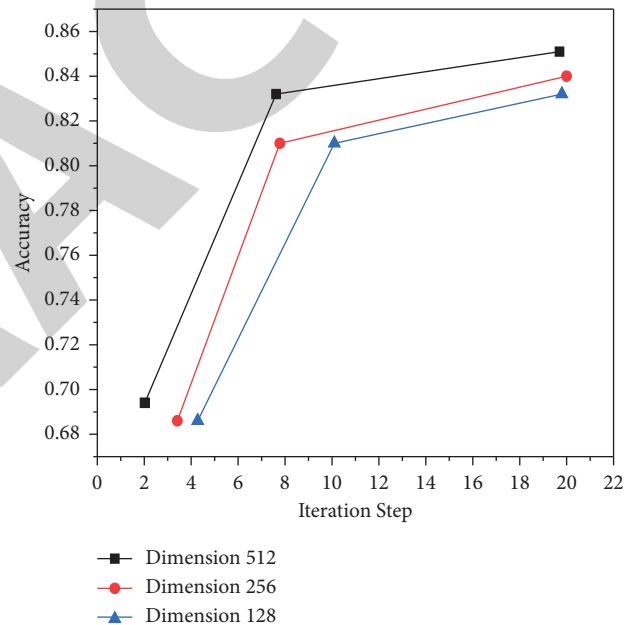


FIGURE 3: Variation of accuracy with vector dimensions.

precision-adjusted SentiBERT model, a pre-prepared sensitivity dictionary from BERT.

Since the BERT language is large and repeatable, many scholars use preplanned BERT models to refine the following activities. However, due to the limited space of the entries, many designs will cause problems such as quality and time. As shown in Table 3, the MC-BiGRU-capsule model in this study is not only designed for GloVe static word vectors but also has better class performance than the BERT model and ULMFIT (an LSTM-based preliminary scheme). The accuracy of the combined distribution of word dynamic vectors is improved by 1.2%, which is a 0.8% improvement over the SentiBERT model. Based on these models, Bert introduces a good vector design that enhances their performance and enhances the advantages of the mc-BiGRU model-capsule model.

TABLE 3: Comparison of experimental results combined with a dynamic word vector (unit: %).

Model	Accuracy
BERT	90.14
ULMFIT	91.21
SentiBERT	90.94
BERT + MC-BiGRU-capsule	91.89
MC-BiGRU-capsule	91.55

5. Conclusions

This study proposes a capsule model of sensitive literature connecting neural networks and two GRU methods. The model focuses on capturing words in the text and encoding word relationships; solving the problem that capsule networks cannot select; and focusing on keywords in text distribution. To eliminate multilevel, large-scale text-sensitive objects, CNN writes local features and uses a bidirectional GRU network to address global devices. The use of vector neurons (capsules) instead of scalar neurons to model text sensitivity is more classified as a method of integrating language knowledge and emotional resources, proving its ability to express capsule design features. Experiments on various data sets confirm the effectiveness of the model.

The next step may be to improve the internal mechanisms of the emotional capsule, such as optimizing the attention-grabbing mechanism. At the same time, the vector must better express the emotional properties and improve the ability to integrate functions to increase the stability and efficiency of the model.

Data Availability

The data used to support the findings of this study are available from the corresponding author upon request.

Conflicts of Interest

The author declares no conflicts of interest.

Acknowledgments

This work was supported by 2020 Provincial Quality Project of Anhui Province. (project no. 2020szjyxm123).

References

- [1] C. Yin and J. Han, "T pricing model of e-commerce platforms based on deep reinforcement learning," *Computer Modeling in Engineering and Sciences*, vol. 127, no. 1, pp. 1–24, 2021.
- [2] K. Obiero, T. Lawrence, J. Ives et al., "Advancing africa's great lakes research and academic potential: answering the call for harmonized, long-term, collaborative networks and partnerships," *Journal of Great Lakes Research*, vol. 46, no. 5, pp. 1240–1250, 2020.
- [3] C. I. Eke, A. A. Norman, and L. Shuib, "Context-based feature technique for sarcasm identification in benchmark datasets using deep learning and bert model," *IEEE Access*, vol. 9, no. 99, pp. 48501–48518, 2021.
- [4] J. Larson, S. S. Jordan, M. Lande, and S. Weiner, "Supporting self-directed learning in a project-based embedded systems design course," *IEEE Transactions on Education*, vol. 63, no. 2, pp. 88–97, 2020.
- [5] C. Wu, H. Jiang, P. Wang, and Z. Deng, "Education quality detection method based on the probabilistic neural network algorithm," *Diagnostyka*, vol. 21, no. 4, pp. 79–86, 2020.
- [6] M. Hammad, M. Al-Smadi, Q. B. Baker, and S. A. Al-Zboon, "Using deep learning models for learning semantic text similarity of Arabic questions," *International Journal of Electrical and Computer Engineering*, vol. 11, no. 4, pp. 3519–3528, 2021.
- [7] X. Lu and H. Zhang, "Sentiment analysis method of network text based on improved at-bigru model," *Scientific Programming*, vol. 2021, no. 12, pp. 1–11, 2021.
- [8] A. R. Abas, I. Elhenawy, H. Mohamed, and A. Abdel-Latef, "Deep Learning Model for fine-grained Aspect-Based Opinion Mining," *IEEE Access*, vol. 1, no. 99, 2020.
- [9] T. Zhang, C. Wu, Y. He, Y. Zou, and C. Liao, "Gain parameters optimization strategy of cross-coupled controller based on deep reinforcement learning," *Engineering Optimization*, vol. 54, no. 5, pp. 727–742, 2021.
- [10] M. Guo, Z. Yu, Y. Xu, Y. Huang, C. Li, and J. García-Haro, "Me-net: a deep convolutional neural network for extracting mangrove using sentinel-2a data," *Remote Sensing*, vol. 13, no. 7, pp. 1292–1324, 2021.
- [11] E. L. Ferguson, "Multitask convolutional neural network for acoustic localization of a transiting broadband source using a hydrophone array," *Journal of the Acoustical Society of America*, vol. 150, no. 1, pp. 248–256, 2021.
- [12] H. Pandowo, "Implementation of deep learning for slump optimization based on concrete quality using convolutional neural network in pt. selo progo sakti," *Jurnal AKSI (Akuntansi dan Sistem Informasi)*, vol. 5, no. 2, pp. 83–88, 2020.
- [13] A. Kliuev, R. Klestov, and V. Stolbov, "Neural network model for assessing the physical and mechanical properties of a metal material based on deep learning," *Journal of Digital Science*, no. 1, pp. 18–28, 2020.
- [14] T. Triwiyanto, I. P. A. Pawana, and M. H. Purnomo, "An improved performance of deep learning based on convolution neural network to classify the hand motion by evaluating hyper parameter," *IEEE Transactions on Neural Systems and Rehabilitation Engineering*, vol. 28, no. 7, pp. 1678–1688, 2020.
- [15] F. Bie, T. Du, F. Lyu, M. Pang, and Y. Guo, "An Integrated Approach Based on Improved Ceemdan and Lstm Deep Learning Neural Network for Fault Diagnosis of Reciprocating Pump," *IEEE Access*, vol. 9, no. 99, 2021.
- [16] Y. Zhao and D. Chen, "A facial expression recognition method using improved capsule network model," *Scientific Programming*, vol. 2020, no. 2, pp. 1–12, 2020.
- [17] X. Tian and J. Wang, "Retrieval of Scientific Documents Based on Hfs and Bert," *IEEE Access*, vol. 9, no. 99, 2021.
- [18] D. Jahanshahi, S. Chowdhury, S. B. Costello, and B. van Wee, "Review of key findings and future directions for assessing equitable cycling usage," *Transportation Research Record*, vol. 2675, no. 6, pp. 453–464, 2021.
- [19] T. Werder, R. Liebich, K. Neuhäuser, C. Behnsen, and R. King, "Active flow control utilizing an adaptive blade geometry and an extremum-seeking-algorithm at periodically-transient boundary conditions," *Journal of Turbomachinery*, vol. 143, no. 2, pp. 1–18, 2021.

Research Article

Application Analysis of Artificial Intelligence Algorithms in Image Processing

Lei Feng 

Yulin University, Yulin City, Shaanxi Province 719000, China

Correspondence should be addressed to Lei Feng; fenglei@yulinu.edu.cn

Received 27 July 2022; Revised 8 September 2022; Accepted 12 September 2022; Published 30 September 2022

Academic Editor: Kai Guo

Copyright © 2022 Lei Feng. This is an open access article distributed under the Creative Commons Attribution License, which permits unrestricted use, distribution, and reproduction in any medium, provided the original work is properly cited.

Due to the rapid development of information, the image recognition method based on the artificial intelligence algorithm has been applied to many application fields. As the product of modern information technology, the image recognition method based on the artificial intelligence algorithm is also a significant and pioneering research topic. With the development of digital image processing technology and the updating of computer electronic products, digital image processing technology has been applied to various fields and has made great contributions to the progress of science and technology and the development of productivity. Image processing methods cover a wide range of application fields, including image conversion, restoration, separation, enhancement and matching, and classification. In order to explore the application of the AI algorithm in image processing, on the basis of the latest BAS algorithm discovered recently, we have established a brand-new hybrid intelligent algorithm BAS based on C as computing, which is applied to multiple image processing fields and achieves good optimization results. Studying the problems and future development directions in the application is conducive to promoting such development of image recognition technology and is conducive to applying image recognition technology to more fields.

1. Introduction

1.1. Research Background. In the past, people could only repair ancient cultural relics and works of art by relying on their own experience and manual techniques [1]. These image processing methods are not only slow but also prone to deviation due to human subjective will and experience. Precious cultural relics are permanently damaged, resulting in the damage of national historical and cultural heritage [2]. Due to the development of science and technology, the US military developed the world's first electronic digital computer system "ENIAC" in 1946 and successfully applied it to ballistic research and large-scale military data statistics. At this time, electronic computers began to be used in all fields of scientific research and work, and it has been widely used [3]. Table 1 shows the subject fields and application fields of digital image processing.

In the middle of the last century, people began to apply computers to the field of image restoration, which greatly improved the efficiency and quality of image restoration and

effectively prevented the damage of human caused images [4]. Some researchers focus on the research in this field, resulting in the limited application of computer technology in the field of image processing [5]. For a long time, the use of computers for image processing is to improve the image quality. Therefore, the development of digital image processing technology is slow [6].

Due to the rapid development of modern science and technology and the increasing capability of computer technology, the main application fields of computer technology in the field of image processing and application are not only limited to image recovery but also involve image acquisition, image conversion, image enhancement, image separation, compression and decoding, boundary extraction, image preprocessing, image cutting, image feature analysis, image digital watermarking, and information identification. Digital image processing technology has gone through three processes of generation, improvement, and application. Its application scope is still expanding and extending. It has been applied to aerospace, land monitoring, urban planning,

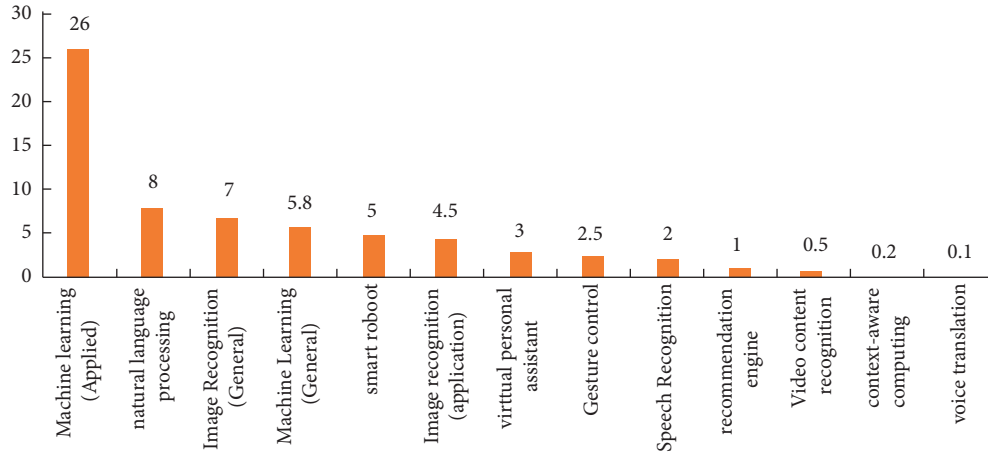


FIGURE 1: Application of artificial intelligence recognition technology.

TABLE 1: Application areas of digital image processing.

Academic area	Application field
Space exploration	Image processing of other stars
Communication	Image information transmission
Remote sensing	Address and terrain
Meteorological	Satellite cloud image analysis
Biomedical science	Cell analysis and chromosome analysis
Public security	Book of songs, live photos, and fingerprints
Archaeology	Spectrum analysis
Physics	Crystallization analysis
Chemical	Vegetation distribution check
Ocean	Robot
Forestry	Application field
Industry	Image processing of other stars

marine biomedical research and development, and other application industries.

Because of the high uncertainty of some image processing data and the difficulty of modeling, it is often difficult to obtain good results after analyzing the image processing data by using conventional methods (such as almanac, dynamic programming, and greedy algorithm) [7]. The service life is also relatively long, sometimes exceeding the unbearable limit [8]. In order to better manage such complex information data, many researchers have generated many intelligent algorithms with evolutionary and cognitive functions by simulating life activities and biological behavior laws in nature [9].

With the rapid development of science and technology, computer technology has been applied to various fields, providing many conveniences to the daily life of the public [10]. The artificial intelligence algorithm and its application in the current image processing field have attracted great attention [11]. The proper use of artificial intelligence methods in image processing can significantly improve the quality and efficiency of image processing [12]. Based on this, the concept of artificial intelligence algorithms and the connotation of processing work are described in this paper [13]. Such specific applications are explored, as shown in Figure 1 [14].

1.2. Research Purpose. In the current application field of computer technology, image recognition technology is still a major research and development content. However, with the development of new artificial intelligence computers, the progress of image recognition technology is also promoted. In terms of the current use of science and technology, image recognition technology has been applied to life and business. For example, the pattern recognition method was once used to swipe cards in the office, and the pattern recognition method was later used in face payment. However, with the further popularization of image recognition technology, it will also play an important role in more application fields.

In order to explore the wide application of artificial intelligence computing in image processing, this paper, based on the new BAS algorithm mentioned recently, integrates the CS algorithm and establishes a new hybrid intelligent algorithm BAS-CS, which has applications, so it has obtained good optimization benefits. In this way, human beings will be able to get rid of the tedious image processing and calculation, thus improving the work quality and efficiency and realizing the important foundation of image processing technology in the information age.

2. Related Concepts and Theoretical Basis

2.1. The Concept of Artificial Intelligence and Image Processing Work. In recent years, the computer has become a new science and technology, which has attracted the attention of all walks of life [15]. As machine intelligence, how does artificial intelligence help humans [16]? It can also develop intelligent technology according to human needs to improve the quality and efficiency of public work. Domestic water is the target [17]. Artificial intelligence is an antihuman way of thinking, but it lacks the same independent thinking ability as people and cannot calculate and solve problems [18]. Therefore, it is vital to serve human devices and tools. Table 2 shows the key technologies in the field of AI.

In recent years, due to the vigorous development of Internet information and computer science, people began to enter the information age [19]. While all kinds of information data have exploded, the workload and difficulty of

TABLE 2: Technical details in the artificial intelligence field.

Serial number	Technology categories	Hot technology
1	Machine learning algorithms and applications	Machine learning methods for predictive judgment research on regression algorithms research on clustering algorithms research on classification algorithms
2	Reinforcement learning algorithms	Reinforcement learning and policy networks reinforcement learning and time difference learning methods improvement and optimization of reinforcement learning algorithms
3	Approximation and optimization algorithms	Improvement and application of approximation algorithms research on estimation algorithms optimization theory and algorithms programming theory and answer set programming
4	Planning problem	Hash algorithm optimization and application planning problem research robot and multiagent system planning research search algorithm research

image processing are also increasing [20]. Needless to say, image processing is widely used in many industries, including industrial applications, military applications, and medical treatment. Image processing is to convert image data into digital information through various methods and programs and upload it to the computer. This paper analyzes the image of computer processor data and explains the main reasons for limiting image processing technology [21].

2.2. The Technical Principle of Image Recognition Technology.

In fact, the same as the algorithm principle of computer processing data, the whole principle of image recognition technology based on the artificial intelligence algorithm is not complicated, and simple image data information can be extracted by using the computer. However, when analyzing the principles of image recognition technology, in order to improve the quality and efficiency of image processing, relevant personnel should find more optimized methods to innovate. The principle of image recognition technology using artificial intelligence algorithm is image pattern recognition, which is a part of artificial intelligence technology and an important part of the composition principle of image recognition. Pattern recognition is to process different types of flat pictures in order to ensure the accuracy of pictures or actual things. Using artificial intelligence algorithms in image recognition technology can virtualize the recognized objects without analyzing the physical objects. For pictures, pattern recognition and artificial intelligence can be used for three-dimensionalization. For example, in the medical field, doctors can analyze the health status and three-dimensional structure of the human body by taking pictures. Therefore, some low-tech recognition techniques such as image processing are combined with artificial intelligence to do things that humans cannot.

2.3. Application of the Artificial Intelligence Algorithm in Image Processing

2.3.1. Artificial Neural Network. Artificial neural network, the so-called artificial neural network, is to establish a new intelligent algorithm mode by imitating the action characteristics of the neural network. Its characteristic is that the

simulated neural network can obtain more valuable information by identifying and managing information nodes. Screening can realize the rationalization of big data. The use of the artificial neural network intelligent algorithm can greatly improve the image storage space. At the same time, the use of network technology for high-speed data transmission can achieve the purpose of saving the space occupied by the data, thus improving the behavior quality in a certain sense and recovering the image accurately and efficiently. In addition, for the in-depth application of this technology, related scholars also put forward different opinions, such as using the multilayer BP network to implement image processing, or segmenting images, and in the selection of image classification methods, mainly using PCA to extract data features, which can also be done using neural networks in classifying chromosome images. In addition, neural networks have significant advantages in image resolution and can accurately recognize handwritten digits. See Figure 2 for details.

2.3.2. Genetic Algorithm. The transmission algorithm also comes from people's simulation of natural processes. It is a graphic processing algorithm derived from system design and optimization. Among them, Darwin's evolution theory is generally used as a reference for calculation. With the help of people's in-depth research and learning of biological processes, system design can quickly find optimal solutions. The important advantage of the genetic algorithm is that it is simple to operate, and it can directly process the image information so as to achieve the optimal solution effect, thus reducing various problems in image processing. However, in view of the comprehensive characteristics and complexity of the genetic algorithm, the establishment of its framework will be based on multiple scientific categories, including function optimization and combinatorial optimization. As a result, genetic algorithms have been widely used in image optimization segmentation and search optimization segmentation.

2.3.3. Ant Colony Algorithm. It adopts the natural animal model. It is mainly through certain principles to find the best probability calculation route. Its basic basis is ant man's foraging steps. In nature, the ant colony will generate a large

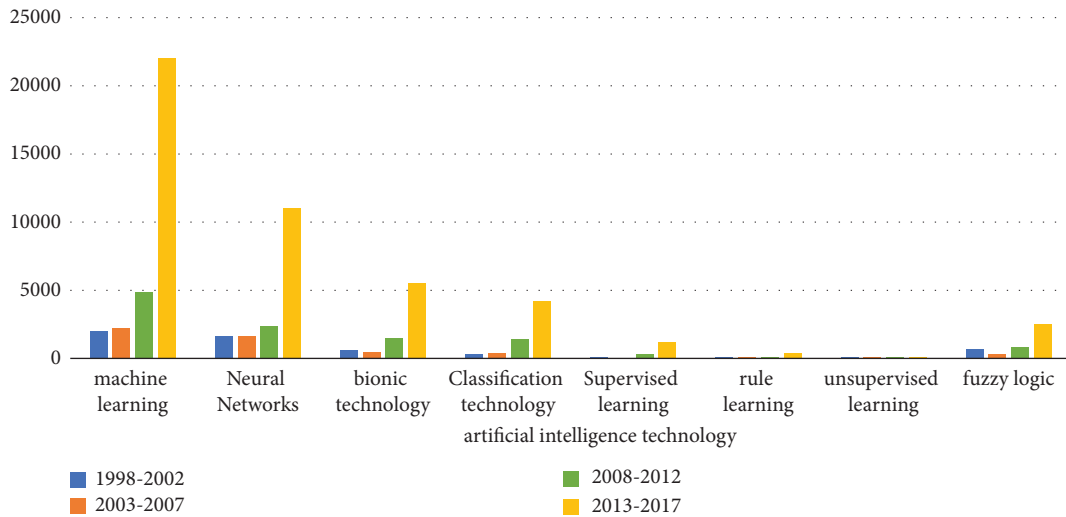


FIGURE 2: The development of the artificial neural network in artificial intelligence technology.

number of signals during the foraging process and guide its companions to find the foraging route correctly. It has the characteristics of large amount of information and large signal transmission capacity. Therefore, effective signal transmission has become an important cornerstone to ensure normal operation. Ant colony computing achieves the best value in image processing, thus achieving the most effective allocation of images, that is, it can find the best processing mode in the least time, thus greatly improving the efficiency of the new generation of artificial intelligence computing. Image matching is also an important image matching method using image structure modeling in the field of computer vision applications. However, the traditional help point optimization method is easy to fall into the shortage of local optimal solution, and the group algorithm can well optimize the objective function. Therefore, some scholars have proposed a high-order graph matching method based on previous algorithms. The algorithm provides bright knowledge by calculating the heuristic factor using the brightness value and then calculates the transition probability according to the heuristic factor and pheromone. Finally, the pheromone is updated locally and globally by using the searched solution. The algorithm can have high matching accuracy.

2.3.4. Annealing Algorithm. In this method, the best solution is obtained by the iterative method and the random method according to the physical solid annealing theory. In the process of heating the article, if the heated article exceeds the specified temperature value, it will be subject to rapid cooling treatment. In the process of warming up, the internal particles of the material will change due to the different ambient temperatures, thus presenting an irregular basic shape, and the movement ability in the material will also be strengthened. However, with the acceleration of the cooling process and the gradual decrease of the ambient temperature, the internal particles in the material will gradually change from an irregular state to an orderly state.

When the ambient temperature exceeds a certain threshold, the material state will remain relatively stable, and the internal value will also drop to the lowest point. Therefore, by applying this method to image processing, comprehensive processing can be realized theoretically, that is, the function and quality of image processing can be improved according to the nature and principle of the method; for example, the SA value can be edited; the image is segmented according to the application of the SA threshold, thereby improving the processing speed. The method can also be used to determine the Chinese character information contained in the picture so as to obtain the correct processing results. The organic fusion between the annealing algorithm and the genetic algorithm can achieve the goal of automatically coloring the map. Therefore, the practical application of image processing technology is completed by the combination of particle swarm optimization and different methods. The flow of the annealing algorithm is shown in Figure 3.

2.3.5. Particle Swarm Optimization Algorithm. This artificial intelligence calculation is based on the phenomenon that birds spread food. The particle swarm optimization algorithm selectively selects and modifies the individual information in the group. It is developed on the basis of iteration. However, there are differences between particle swarm optimization and genetic algorithms. The latter adopts the method of medium variation and crossover, but the former does not. The algorithm has to find the optimal particles on the object by searching for particles. This algorithm is relatively simplified. Because particle swarm optimization is helpful to fuzzy control and parameter optimization, it is also possible to use neural networks.

In this period, particle swarm optimization was mainly used to deal with image problems. As a cooperative random search method of a group, if this method is brought into image processing, it can be introduced into the multiagent optimization system to check the pixel boundary and deal

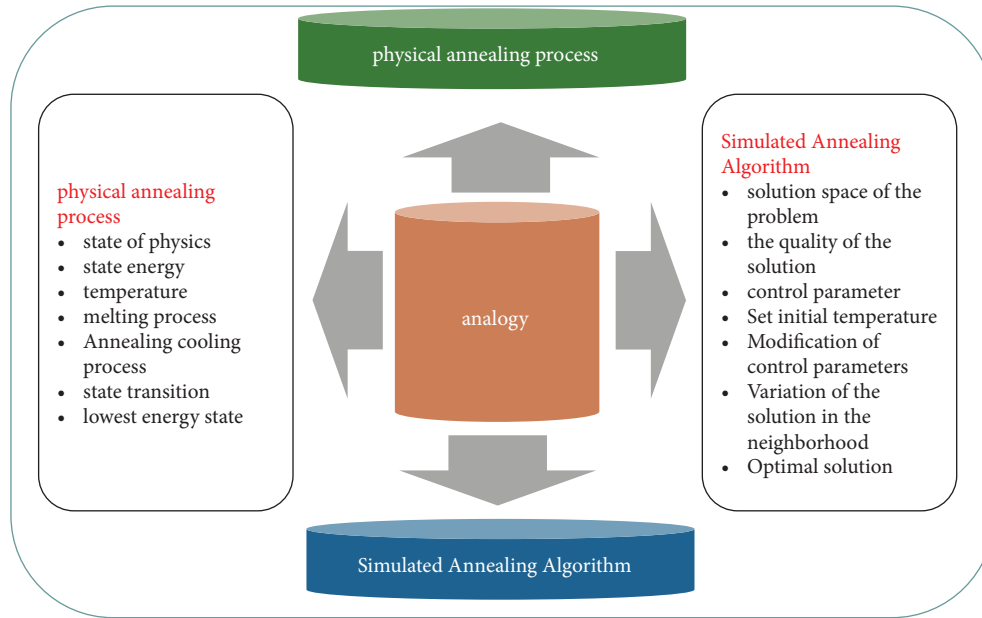


FIGURE 3: Schematic diagram of the annealing algorithm.

with the problem of pixel detail edge loss. It promotes the improvement of image accuracy and image segmentation effect on the whole.

2.3.6. 3D Otsu Algorithm. Otsu is a well-known pixel threshold division method. Pixel segmentation uses texture, gray histogram, edge, and other characteristics to divide pixels into parts with different characteristics. Generally speaking, it includes the target area and the background area, but the function difference is large. Gray threshold segmentation is one of the most common image segmentation algorithms. The image is divided into two parts, the main body and the background, by using the segmentation threshold of gray histogram; the basic principle of this method is simple, and the implementation is simple. It is applied to image segmentation. The algorithm makes use of the correlation between the gray value and the spatial position of the image to simplify the process and achieve the best separation effect. We invented a fast recursive 3D Otsu segmentation method. The calculation uses a large number of gray signals of pixels and integrates three-dimensional gray histograms, which not only increases the robustness of the calculation but also shortens the calculation time. The three-dimensional Otsu calculation not only examines the gray information of the image but also the spatial data of the image, including the neighborhood mean value and the neighborhood median value. Therefore, three-dimensional Otsu has certain antinoise performance, and its segmentation effect is better than one-dimensional Otsu and two-dimensional Otsu algorithms.

Then, aiming at the problems of large amount of computation and long operation time of the 3D Otsu algorithm, a 3D Otsu image segmentation algorithm based on cuckoo search optimization is proposed. The algorithm uses the cuckoo search algorithm to optimize 3D Otsu. Among

them, the three-dimensional interclass variance of pixel gray value domain mean domain median is used as the fitness function of the cuckoo search algorithm. By evaluating the fitness of pixels on Lévy flight path, the optimal segmentation threshold is obtained. The experimental results show that compared with the three-dimensional Otsu algorithm based on the mean gradient in the gray value domain, the algorithm has better stability and reliability for image segmentation with a low signal-to-noise ratio; at the same time, compared with the fast three-dimensional Otsu algorithm, the operation efficiency is improved by about 16.4%. Thus, the difficulty of calculation time is overcome, the speed of calculation is improved, the accuracy of segmentation is improved, the time loss of calculation is reduced, and it achieves better segmentation results.

In short, with the further development of the times, people have invested huge human and material resources to increase the research and development of artificial intelligence algorithms. The application of artificial intelligence algorithms in the field of image processing can improve the accuracy and quality of image processing on the one hand and promote the improvement of the quality of life of the public on the other hand. Due to the continuous improvement and optimization of artificial intelligence, people believe that artificial intelligence algorithms will be more perfect and developed in the future and will be applied to various fields to support the security, stability, and long-term development of human economy and society.

3. Related Technologies

3.1. Image Restoration Technology. Image restoration refers to the method of repairing and reconstructing the defective part of the image and removing the interference signal according to certain principles. It can recover the unknown area by special methods and technologies and through the

neighborhood information in the damaged area to be recovered. Its important purpose is to prevent the bystander from discovering that the picture has been damaged or repaired. Image restoration has been applied in digital image processing, computer graphics, data compression, computer animation creation, and virtual reality.

Assuming p is any point on the boundary Ω , the formula for calculating ones is as follows:

$$P(p) = C(p) \bullet D(p). \quad (1)$$

Among them: $C(p)$ is the confidence term, which represents the number of known points in the structural data.

$$C(p) = \frac{\sum_{q \in \psi_{p \cap \varphi}} C(q)}{|\psi_p|}, \quad (2)$$

$$D(p) = \frac{|\Delta I_p^+ \cdot n_p|}{|\psi_p|}.$$

Among them: φ represents the area; I_p represents the line; n_p is the patched p , so it will use the one of squared errors, which is calculated as follows:

$$\psi_p = \arg \min_{\psi_p \in \Phi} d(\psi_p, \psi_q), \quad (3)$$

where q_{pd} represents the squared error sum between the patch to be patched and the matching block, $p_a, q_b, R_a, R_b; G_a, G_b$ and B_a, B_b represent the R, G, B values of the corresponding pixels in p and $q\psi$, respectively.

The form looks like the following:

$$C(p)_{n+1} = C(p). \quad (4)$$

Next, conduct the research again till it is completed.

3.2. Image Segmentation Algorithm Based on BAS-CS. In many fields of image processing, people often need to analyze the target. In this way, in order to facilitate the classification of objects, the objects must be obtained in the image, and the image must be subdivided. In order to further improve the effect of image separation, many experts and scholars in China have introduced the genetic algorithm, ant colony algorithm, particle swarm algorithm, artificial fish swarm algorithm, bacterial foraging algorithm, artificial bee swarm algorithm, and chicken swarm algorithm to image segmentation in recent years. Therefore, many achievements have been generated, and the segmentation efficiency has been improved.

The expansion operation will expand the boundary of the object. If there are small gaps inside the object, these gaps can be well filled by the expansion operation, so the boundary will extend to the new area. If the object is eroded again at this time, the boundary will shrink back to its original position, and the gap inside the object will disappear forever.

$$f_1 = (A \oplus B) = \{x | \exists a \in A, b \in V: x = a + b\}. \quad (5)$$

Among them, A is the input image; B is the structural element, which has various shapes and sizes much smaller than A , such as square and disc. f_1 is the result of dilation operation on image A , and f_2 is the result of erosion operation on image A .

The erosion operation is usually used to remove boundary points of an image. Since the points included in one area will be regarded as edge points, they will be eliminated. If processing is repeated at this time, the retained large object will return to its original position, and the deleted small object will disappear permanently.

$$f_2 = (A \odot B) = \{x | \forall b \in V, \exists a \in V: x = a - b\}. \quad (6)$$

Mathematically, open operation is the result of thermal expansion after corrosion. It can also be used to remove the parts of the object that do not contain structural factors, smooth the outline of the object, break the narrow interface, and remove the large and small protrusions.

$$f_0 = f \oplus b \odot b. \quad (7)$$

The adaptability function of the BAS-CS algorithm is two-dimensional gray Otsu model, and the specific calculation formula is as follows:

$$t_r \sigma_B = w_0 \left[(u_{0i} - u_{Ti})^2 + (u_{0j} - u_{Tj})^2 \right] + w_1 \left[(u_{1i} - u_{Tj})^2 + (u_{1j} - u_{Tj})^2 \right]. \quad (8)$$

3.3. Image Matching Algorithm Based on BAS-CS. Image matching is also a very important image processing method. It can spatially correspond two or more images of the same scene obtained by one or more sensors at different times and environments and judge the translation between them. Image matching has great scientific research and application value in biomedical image processing, satellite navigation, biological fingerprint matching, and other application fields. It is an important cornerstone of image information fusion. With the progress of science and technology, new engineering application technology and more and more complex environments put forward higher requirements for matching calculation, and the research scope of matching calculation is more and more extensive.

Suppose the original picture is a and the size is $w \times H$. The template picture is B , and the size is $w \times H$, and set $w < W, h < H$.

The MAD algorithm is developed by Leese and is a well-known calculation method. The structure of this algorithm is simplified, but it is interfered by noise, and the matching efficiency decreases due to the increase of noise.

$$d(x, y) = \frac{1}{wh} \sum_{i=1}^w \sum_{j=1}^h |A(i+x, j+y) - B(i, j)|. \quad (9)$$

Among them, $d(x, y)$ is the similarity measure, when $d(x, y)$ gets the minimum value, (x, y) is the best matching position.

The SAD algorithm is similar to the MAD algorithm, and the difference is that the SAD algorithm does not take the average value of the error sum.

$$d(x, y) = \sum_{i=1}^w \sum_{j=1}^h |A(i+x, j+y) - B(i, j)|. \quad (10)$$

The sum of squares of errors is to square the errors obtained each time first and then to the sum of squares.

$$d(x, y) = \sum_{i=1}^w \sum_{j=1}^h [A(i+x, j+y) - B(i, j)]^2. \quad (11)$$

The MSD algorithm, also known as the mean square error algorithm, averages the SSDs.

$$d(x, y) = \frac{1}{wh} \sum_{i=1}^w \sum_{j=1}^h [A(i+x, j+y) - B(i, j)]^2. \quad (12)$$

The algorithm uses the normalized cross-correlation function as the similarity measure and has the advantages of strong antinoise ability and less influence by the scale factor error. The calculation formula of the normalized cross-correlation function is as follows:

$$\sum_{j=1}^h A(i+x, j+y) \cdot \frac{B(i, j)}{\sqrt{\sum_{i=1}^w \sum_{j=1}^h A(i+x, j+y)^2 \cdot \sum_{i=1}^w \sum_{j=1}^h B(i, j)^2}}. \quad (13)$$

Among them, $P(x, y)$ is the similarity measure, when $P(x, y)$ is the maximum; (x, y) is the best matching position found.

First, we select the normalized cross-correlation function (NCC) as the similarity measure and then judge whether the image contains noise. The NCC algorithm is used to design the fitness function of the BAS-CS algorithm. Finally, the BAS-CS algorithm is used as a search strategy to search for the optimal solution. Finally, the search method of BAS-CS is used so as to find the maximum matching between the template image and the original image.

4. Experimental Results and Analysis

The overall size of each calculation is $n = 40$, and the dimension of each function is $m = 2$. The maximum number of iterations is international thermonuclear fusion test reactor = 1500, and the maximum optimization accuracy is to $l = 1.0 \times 10^{-20}$, and when each calculation has completed the specified number of iterations, the final convergence accuracy will reach 1.0×10^{-20} , which is considered a successful optimization. The parameter settings of BAS-CS are step size $\text{step} = 10$, distance between two whiskers $d0 = 5$, discovery probability $a_p = 0.25$, step attenuation coefficient $\eta = 0.95$, and the acceleration factor of the PSO algorithm is set to $1C = 2C = 1.5$ (15).

Each algorithm operates independently for each test function about fifty times, the maximum fitness, average fitness, and minimum fitness in the 50 running results were counted, and the average running time and optimization success rate were recorded. The experimental results are shown in Figure 4.

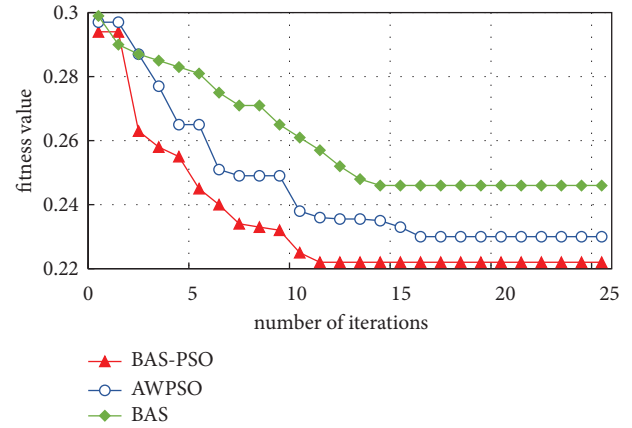


FIGURE 4: Convergence curves of algorithms at different latitudes.

As can be seen from Figure 4, under the same experimental environment and the same number of iterations, after 25 independent repeated experiments, in terms of fitness, the maximum fitness, average fitness, and minimum fitness of the BAS-CS algorithm are obviously better. For the PSO algorithm, BAS algorithm, and CS algorithm, it shows that BAS-CS has higher convergence accuracy than other algorithms; in terms of average optimization time, the running time of BAS-CS algorithm and CS algorithm is higher than that of PSO algorithm. The BAS algorithm is longer, but the convergence accuracy of the BAS-CS algorithm and the CS algorithm is much higher than that of the PSO algorithm and the BAS algorithm, so the overall performance is better than the PSO algorithm and the BAS algorithm. On the other hand, the BAS-CS algorithm has higher convergence accuracy than the CS algorithm. The average optimization time is shorter than the CS algorithm, and on the basis of high convergence accuracy and convergence speed, it still has a high optimization success rate, reaching 100% when testing each function, so it shows that the BAS-CS algorithm has strong stability.

Under the background of paying attention to economic benefits in the real engineering field, the method presented in this paper has good practical value. When the method used in this paper fixes three pictures, the population number is set to 100, they are 30, 50, and 100, respectively, and 50 experiments are here. The obtained PSNR values are shown in Figure 5.

This section discusses the influence of the dynamic adjustment parameters α and β in equation (6) on the image restoration quality when different weights are taken, and the results are shown in Figure 6.

In Figure 6, data α represents the weight of the confidence term, while the parameter β represents the weight of the data item. Because $\beta + \alpha = 1$, α values also follow β and changes with the change of β . For pictures with a complex texture structure, improved β value can make the repair process more sensitive to detail textures, while for images with a single texture structure, the β value can increase the accuracy of the priority algorithm and thus increase the recovery efficiency. As can be observed from Figure 6 $6\alpha = 0.6$,

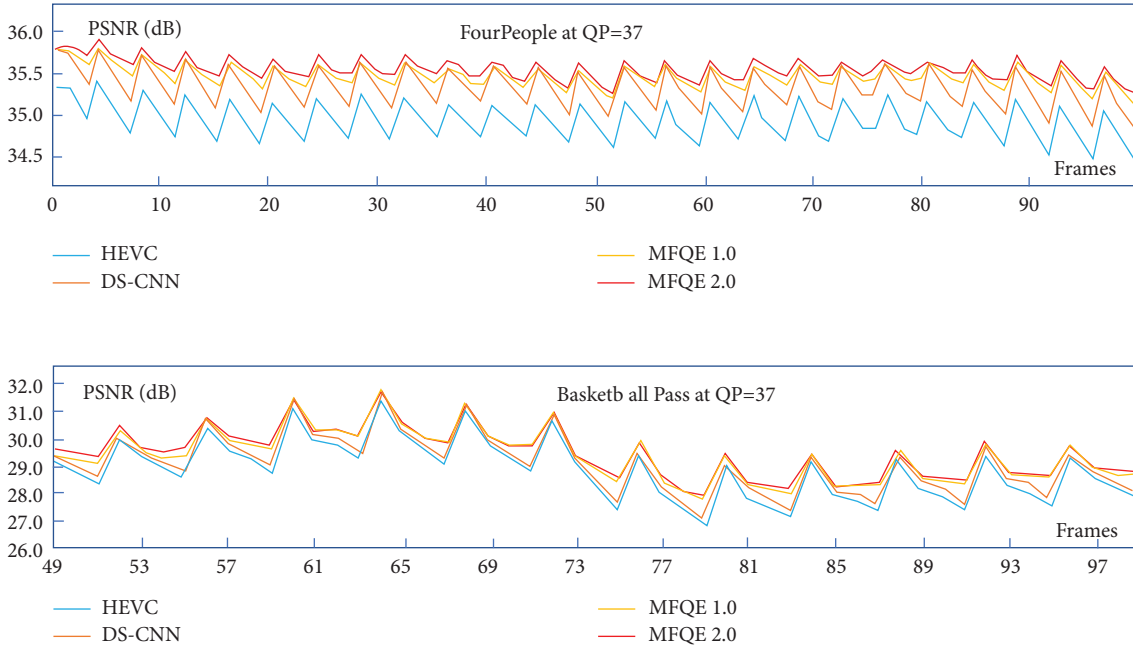


FIGURE 5: PSNR values obtained from each independent experiment.

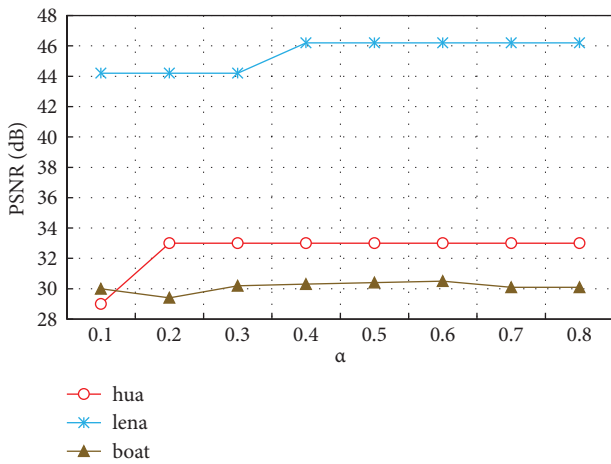


FIGURE 6: Influence of dynamic adjustment parameters on experimental results.

$\beta = 0.4$, the peak signal-to-noise ratio (PSNR) of the first three experimental pictures is the largest, so $\alpha = 0.6, \beta = 0.4$ is the optimal parameter selected for this test.

In order to further verify the convergence of the algorithm in this paper and the algorithm in the literature, this section gives the comparison of the convergence curves of the algorithm in this paper (BAS-CS) and the algorithm in the literature (GA) when segmenting the above three kinds of images. We take the fitness value as the optimal segmentation thresholds, as shown in Figure 7.

In order to test the effectiveness of this algorithm, the three-dimensional Otsu algorithm (CS-3Otsu algorithm), the two-dimensional Otsu algorithm, the M3Otsu algorithm, and the G3Otsu algorithm were based on the CS algorithm proposed by the algorithm in this paper and the

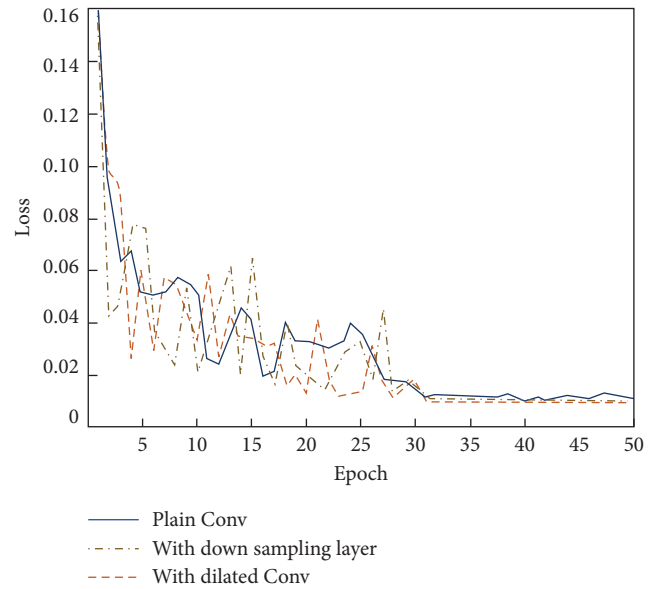


FIGURE 7: Convergence curve comparison between the algorithm in this paper and the algorithm in the literature.

literature. The truck image is cut, and the segmentation time of each algorithm is counted. In order to accurately calculate the segmentation of the two CS-3Otsu algorithms, the algorithms in this paper are set to a fixed value, the number of iterations is set at 100, and they are independently repeated 50 times. The specific experimental parameter settings and the searched optimal segmentation and the thresholds are shown in Figure 8.

As can be seen from Figure 8, after the Otsu threshold segmentation method is extended from two-dimensional to three-dimensional, the segmentation time increases

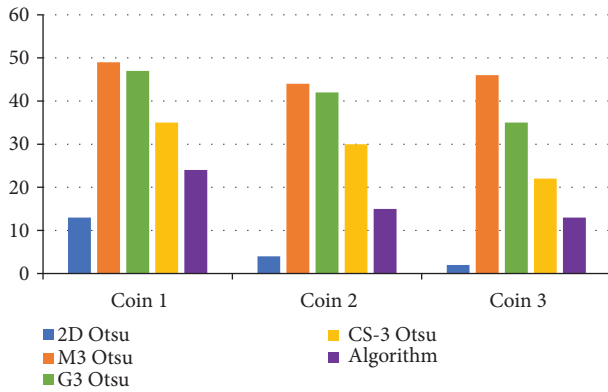


FIGURE 8: Comparison of segmentation time of different algorithms.

exponentially, but the CS-3Otsu algorithm uses the CS algorithm search strategy to quickly search for the best segmentation threshold, so it greatly reduces the time. The segmentation time is shortened, thereby improving the segmentation efficiency. The algorithm in this paper adopts the BAS-CS search strategy. When segmenting three different images, the segmentation time is shorter than that of the CS-3Otsu algorithm so as to maximize the improvement of the segmentation time and segmentation efficiency.

Pixel spatial separation is a major image processing technology, which can match one or more sensors with two or more images of the same background obtained at different times and conditions, and it can judge the translation and turnover between them. Image processing technology has great scientific research value and application significance in biomedical image processing, satellite navigation, and biometric fingerprint matching, and it is an important cornerstone of biological information application.

5. Conclusion

Because the combination of computer science and image processing technology can greatly improve the performance and efficiency of image processing, image processing technology has been widely used in military, remote sensing, medicine, industry, and other fields, providing a great deal for people's production and life. Convenience greatly promotes the development of social productive forces and also promotes the innovation and development of social enterprises. Therefore, as a field closely related to people's production and life, digital image processing technology has a lot of problems waiting for us to study and solve in both theoretical research and engineering application.

Based on the latest BAS algorithm discovered in recent years, this paper combines it with the CS algorithm to produce a new hybrid intelligent algorithm BAS-CS. This method has been widely used in many aspects of image processing and has obtained good optimization results. At present, as a new high-tech application technology, image recognition technology is attracting more attention and widely used, and it plays a key role in all aspects. With the rapid development of technology, image recognition

technology has been applied to many industries. With the rapid development of science and technology, it can also meet the different needs of the industry and family life. Image recognition technology can also be more effectively applied to the whole society, promote economic development, and ensure property safety. At present, the application of image recognition information technology based on artificial intelligence computing is more and more extensive, and more and more people pay attention to it. It is believed that in the future, with the needs of consumers and the innovation and reform of image identification products, the use efficiency of the market will be more prominent, and the application prospect and practical value will be greater.

Data Availability

The labeled data set used to support the findings of this study is available from the corresponding author upon request.

Conflicts of Interest

The author declares that there are no conflicts of interest.

Acknowledgments

This work was sponsored by The Key Research and Development Plan of Shanxi 2022 and research on the protection and dissemination of Ming and Qing ancient mural resources in Northern Shaanxi from the perspective of digital technology (No.: 2022GY-345).

References

- [1] K. Saikumar and V. Rajesh, "Coronary blockage of artery for heart diagnosis with DT artificial intelligence algorithm," *International Journal of Research in Pharmacy and Science*, vol. 11, no. 1, pp. 471–479, 2020.
- [2] S. Vaishnavi, R. Deepa, and P. Nanda Kumar, "A ophthalmology study on eye glaucoma and retina applied in AI and deep learning techniques," *Journal of Physics: Conference Series*, vol. 1947, no. 1, pp. 012053–012133, 2021.
- [3] S. K. Noh, "Recycled clothing classification system using intelligent IoT and deep learning with AlexNet," *Computational Intelligence and Neuroscience*, vol. 30, no. 2, pp. 353–358, 2021.
- [4] R. K. Mishra, G. Y. S. Reddy, and H. Pathak, "The understanding of deep learning: a comprehensive review," *Mathematical Problems in Engineering*, vol. 2021, no. 21, pp. 1–15, Article ID 5548884, 2021.
- [5] Y. R. Shrestha, V. Krishna, and G. V. Krogh, "Augmenting organizational decision-making with deep learning algorithms: principles, promises, and challenges (forthcoming at journal of business research)," *Journal of Business Research*, vol. 7, no. 03, pp. 27–31, 2020.
- [6] M. Emri, "Methods of artificial intelligence and their application in imaging diagnostics," *Magyar Onkológia*, vol. 64, no. 2, pp. 145–152, 2020.
- [7] D. Overhoff, P. Kohlmann, and A. Frydry chowicz, "The international radiomics platform - an initiative of the German and Austrian radiological societies - first application examples," *RöFo - Fortschritte auf dem Gebiet der R*, vol. 193, no. 3, pp. 13–22, 2021.

- [8] Y. . Zheng, S. Li, J. Huang, L. Fan, and Q. Shu, "Identification and characterization of γ -ray-induced mutations in rice cytoplasmic genomes by whole-genome sequencing," *Cytogenetic and Genome Research*, vol. 160, no. 2, pp. 100–109, 2020.
- [9] P. Sikka, A. R. Asati, and C. Shekhar, "High: speed and area efficient Sobel edge detector on field rogrammable gate array for artificial intelligence and machine learning applications," *Computational Intelligence*, vol. 35, no. 09, pp. 288–290, 2020.
- [10] M. Fradi, E. H. Zahzah, and M. Machhout, "Real-time application based CNN architecture for automatic USCT bone image segmentation," *Biomedical Signal Processing and Control*, vol. 71, pp. 103123–123, 2022.
- [11] D. Sotvoldiev, D. T. Muhamediyeva, and Z. Juraev, "Deep learning neural networks in fuzzy modeling," *Journal of Physics: Conference Series*, vol. 1441, no. 1, 13127 pages, Article ID 012171, 2020.
- [12] S. Bagheri, N. Wu, and S. Filizadeh, "Application of artificial intelligence and evolutionary algorithms in simulation-based optimal design of a piezoelectric energy harvester," *Smart Materials and Structures*, vol. 29, no. 10, pp. 309–312, 2020.
- [13] F. J. García-Pealvo, A. Vázquez-Ingelmo, and A. García-Holgado, "Application of artificial intelligence algorithms within the medical context for non-specialized users: the CARTIER-IA platform," *International Journal of Interactive Multimedia and Artificial Intelligence*, vol. 6, no. 6, pp. 77–86, 2021.
- [14] R. Malinidevi, S. Vinitha, and A. Sharma, "Application and analysis of asymptotic method of cholera dynamics model in Artificial Intelligence and Image Processing," *Materials Today Proceedings*, vol. 6, no. 2, pp. 184–195, 2021.
- [15] H. Khachnaoui, R. Mabrouk, and N. Khelifa, "Machine learning and deep learning for clinical data and PET/SPECT imaging in Parkinson's disease:a review Image Processing," *IET*, vol. 14, no. 1, pp. 536–540, 2020.
- [16] Z. Lutowski, "IoT application of transfer learning in hybrid artificial intelligence systems for acute lymphoblastic leukemia classification," *Sensors*, vol. 21, no. 3, pp. 309–312, 2021.
- [17] R. C. Ambagtsheer, N. Shafiabady, and E. Dent, "The application of artificial intelligence (AI) techniques to identify frailty within a residential aged care administrative data set," *International Journal of Medical Informatics*, vol. 136, no. 5, pp. 489–497, 2020.
- [18] J. Prim, T. Uhlemann, and N. Gumpfer, "A data-pipeline processing electrocardiogram recordings for use in artificial intelligence algorithms," *European Heart Journal*, vol. 39, no. 6, pp. 102–110, 2021.
- [19] J. Fitzgerald, D. Higgins, and C. M. Vargas, "Future of biomarker evaluation in the realm of artificial intelligence algorithms: application in improved therapeutic stratification of patients with breast and prostate cancer," *Journal of Clinical Pathology*, vol. 74, no. 7, pp. 717–725, 2021.
- [20] S. S. Tripathy, R. Poddar, and L. Satapathy, "Image processing-based artificial intelligence system for rapid detection of plant diseases," *Bioinformatics in Agriculture*, vol. 24, no. 1, pp. 619–624, 2022.
- [21] X. Zhang, "Application of artificial intelligence recognition technology in digital image processing," *Wireless Communications and Mobile Computing*, vol. 2022, Article ID 7442639, 10 pages, 2022.

Retraction

Retracted: The Influence of Brand Visual Communication on Consumer Psychology Based on Deep Learning

Mathematical Problems in Engineering

Received 8 August 2023; Accepted 8 August 2023; Published 9 August 2023

Copyright © 2023 Mathematical Problems in Engineering. This is an open access article distributed under the Creative Commons Attribution License, which permits unrestricted use, distribution, and reproduction in any medium, provided the original work is properly cited.

This article has been retracted by Hindawi following an investigation undertaken by the publisher [1]. This investigation has uncovered evidence of one or more of the following indicators of systematic manipulation of the publication process:

- (1) Discrepancies in scope
- (2) Discrepancies in the description of the research reported
- (3) Discrepancies between the availability of data and the research described
- (4) Inappropriate citations
- (5) Incoherent, meaningless and/or irrelevant content included in the article
- (6) Peer-review manipulation

The presence of these indicators undermines our confidence in the integrity of the article's content and we cannot, therefore, vouch for its reliability. Please note that this notice is intended solely to alert readers that the content of this article is unreliable. We have not investigated whether authors were aware of or involved in the systematic manipulation of the publication process.

Wiley and Hindawi regrets that the usual quality checks did not identify these issues before publication and have since put additional measures in place to safeguard research integrity.

We wish to credit our own Research Integrity and Research Publishing teams and anonymous and named external researchers and research integrity experts for contributing to this investigation.

The corresponding author, as the representative of all authors, has been given the opportunity to register their agreement or disagreement to this retraction. We have kept a record of any response received.

References

- [1] H. Wang, "The Influence of Brand Visual Communication on Consumer Psychology Based on Deep Learning," *Mathematical Problems in Engineering*, vol. 2022, Article ID 9599943, 8 pages, 2022.

Research Article

The Influence of Brand Visual Communication on Consumer Psychology Based on Deep Learning

Hui Wang 

Communication University of China, Nanjing, Jiangsu 211172, China

Correspondence should be addressed to Hui Wang; 1230442218@cjlu.edu.cn

Received 8 July 2022; Accepted 6 September 2022; Published 29 September 2022

Academic Editor: Hengchang Jing

Copyright © 2022 Hui Wang. This is an open access article distributed under the Creative Commons Attribution License, which permits unrestricted use, distribution, and reproduction in any medium, provided the original work is properly cited.

In order to solve the problem that there are few methods of users' consumption psychology, the author proposes a research on the influence of brand visual communication on consumer psychology based on deep learning. First, establish the mapping relationship between experience level-product features-aspect words and then use aspect word extraction technology, mining users' attention to different experience levels from user comments and dividing users into three types: instinctive preference, behavioral preference, and reflective preference; finally, the deep learning-based aspect sentiment analysis technology is used to calculate the user's preference for the product and further analyze the characteristics of different types of users. Experimental results show that based on the application analysis of more than 900,000 JD.com mobile phone review data, three types of consumer preference user groups were obtained, of which instinctive preference users accounted for 41.6%; it is higher than behavioral preference users (33.01%) and reflection preference users (25.39%), and the consumption characteristics of the three types of users are analyzed from the aspects of mobile phone brand and price. It is proved that the author's user portrait method can better express the consumption preferences of different types of users.

1. Introduction

In the process of developing the socialist market economy, it has become a major strategic decision and deployment to implement the brand strategy, pay full attention to the cultivation and protection of independent brands, and enhance the core competitiveness of enterprises. Since then, concepts such as "city brand," "national brand," and "cultural brand" have entered people's thinking field, and developing cultural industries and building cultural brands have become an important topic in China's medium and long-term cultural strategic planning [1]. In the process of development, the development of China's cultural industry has also encountered a series of problems; first, the total amount of cultural consumption is too low; there are three main reasons for this. First, the cultural consumption capacity of China's basic consumer groups is seriously insufficient, and the quality of cultural consumption subjects is not high, thus inhibiting the rapid growth of cultural consumption demand. Second, there is insufficient effective

demand for cultural brands, and there is a lack of high-quality, truly marketable cultural brands. The third is based on the drawbacks of the "one-size-fits-all" vacation system, which seriously restricts the maximization of the benefits of recreational cultural consumption resources. The second is that the cultural brand "has a license but no market," and the market adaptability is not strong. The third is that the market segmentation is not enough, and the homogenization competition of regional cultural brands is serious [2]. The fourth is the lack of strong policy support for the development of cultural brands. Finally, the theoretical research on cultural brand lags behind the practice. Therefore, in the modern business world where the types and numbers of cultural brands are increasing and the market competition is increasingly fierce, if you want to win consumers for your own cultural brand, you must be in the process of shaping the image of the cultural brand, fully consider the needs of consumers, especially the psychological needs of consumers, and provide consumers with more choices. Only in this way can cultural brands fully play the role of satisfying

consumers' psychological emotions. The author starts from this situation; it is proposed to analyze the related issues of cultural brand image building from the perspective of consumer psychology, in order to provide theoretical support for enterprises to build brand image, promote the effective building of Chinese cultural brands, and then promote the great development and prosperity of China's cultural industry [3].

2. Literature Review

Through the research on the related principles of the consumer behavior conditioning theory, it is proposed to strengthen the brand loyalty from the perspective of the classical conditioning principle. From the principle of operant conditioning, the behavioral loyalty to the brand is strengthened, and then, the brand loyalty of consumers is formed [4]. Lototsky et al. conducted an in-depth discussion on the mechanism of brand extension and further expounded consumers' trust and loyalty to the brand's original products from the aspects of learning theory, ratchet effect theory, risk theory, and demand hierarchy theory; through the low-cost transfer of brand extension to extended products, this almost recognized but lacking detailed analysis point of view has been analyzed, which has laid a theoretical foundation for the related research on brand extension [5]. Zhou et al. deeply analyzed the characteristics of consumer behavior, as shown in Figure 1, and studied the interaction and role between consumer behavior and brand image building. In addition, the research on brand image building based on consumer behavior provides new ideas for enterprises to carry out brand work from the perspective of consumer behavior, which is of strategic and tactical significance to enhance brand value [6]. The important point they made was that, in consumer perception of brands, build a long-term competitive brand by establishing effective mental differentiation and bringing consumers a pleasant effect [7]. Hu et al. segmented brand-sensitive consumers based on consumer psychology, analyzed the brand preferences of different types of consumers, and put forward marketing suggestions accordingly [8]. Lee and Ryu believe that the consumer brand relationship is a psychological contractual relationship built on the basis of mutual trust and mutual benefit between enterprises and consumers. The violation of consumers' psychological contract will lead to the change or even rupture of the brand relationship, which will eventually lead to the generation of brand crisis [9]. Sun et al. introduce knowledge from cognitive psychology, in-depth investigation, and analysis of consumers' internal cognition of brand choice. The author takes the construction of the consumer brand choice cognitive model as the main line, and the consumer's cognitive structure and cognitive process as the two branches, an in-depth investigation and analysis, was carried out [10].

Guided by the three-level experience theory, combined with aspect word extraction and sentiment analysis technology, the author proposes a user consumption mental portrait method based on aspect words.

3. Research Methods

3.1. Method Overview. The method can be divided into three stages:

(1) Consumer psychology (relationship analysis of aspect words): first of all, we must establish the relationship between consumer psychology and the words used in comments. According to the three-level experience theory, discuss with product experts and divide a number of product features into the instinct layer, behavior layer, and reflection layer, respectively; then, aspect words are extracted from reviews, and common aspect words are associated with product feature descriptions in combination with semantics, and a mapping table of experience level, product features, and aspect words is established [11].

(2) Attention analysis: on the basis of the above mapping vocabulary, the attention of product features and the attention of the experience level are obtained based on the frequency of the aspect words in the user comments being mentioned, and the users are divided into instinctive groups according to the user's attention to the experience level; there are three types of preference, behavioral preference, and reflective preference.

(3) Analysis of favorability: perform fine-grained aspect-level sentiment analysis on comments to obtain the user's emotional inclination for the aspect, and synthesize the emotional attitude of the aspect at different experience levels to obtain the user's favorability, and use the results of sentiment analysis to characterize different users and group's consumer psychology portrait [12].

3.2. Analysis of Consumer Psychology: Aspect Word Relationship. According to the three-level experience theory, the author firstly divides the product features into instinct level, behavior level, and reflection level.

Taking mobile phones as an example, the author analyzes the characteristics of products included in each level as follows.

The instinctive layer represents the initial impression of the product, which refers to the information and feelings that the user can obtain immediately before or when using the mobile phone, such as appearance, price, and parameters directly visible on the online shopping platform. The behavioral layer refers to the experience of using most complex functions of the mobile phone, such as performance, camera, and battery. The reflective layer refers to the user's perception of self-image and product image, such as brand, service, group using the phone, and abstract concepts such as domestic and technology.

Refer to the domain knowledge of mobile phone products, and map the three-level experience theory to specific mobile phone product characteristics:

- (1) Instinct layer: appearance, screen, sound, price, and parameters
- (2) Behavior layer: performance, battery, camera, communication, and auxiliary functions
- (3) Reflection layer: brand, service, user, overall feeling, and accessories

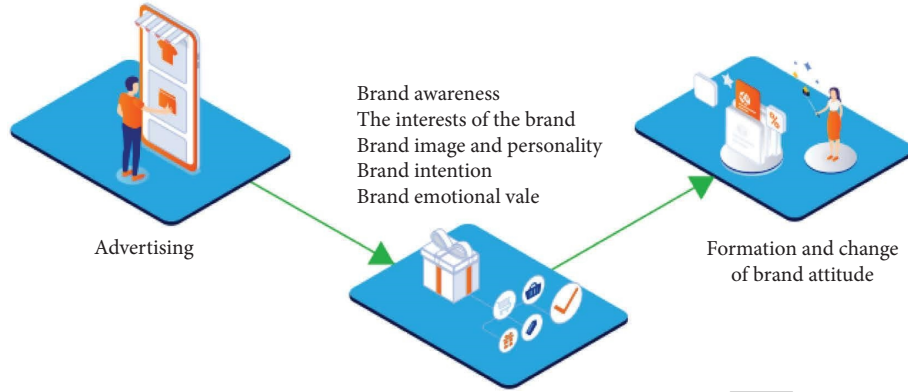


FIGURE 1: The impact of brand visual communication on consumer psychology.

Among them, “parameters” refer to parameters directly visible on the online shopping platform, “auxiliary functions” refer to functions such as fingerprints and Bluetooth, “user” refers to whether the mobile phone is suitable for a certain group of people, that is, the degree of matching between the user’s self-image and the product, and “overall feeling” refers to the experience of abstract concepts such as technology, humanization, and quality. In the comments related to “accessories,” most users do not pay attention to the quality of accessories, but only pay attention to whether the merchants have given away mobile phone accessories, so this is a concept similar to “service” and should be classified into the reflection layer.

Then, map the product features to its typical descriptive aspects. Considering that the current mainstream aspect word extraction algorithms are highly dependent on manual annotation, corpora, rule templates, or other forms of manual intervention and the problem of low portability of algorithm models in different fields, the author adopts the method of combining word segmentation and rules to obtain aspect words that describe product characteristics. Among them, aspect words are divided into explicit aspect words and implicit aspect words and explicit aspect words are mainly nouns, while implicit aspect words are extracted through the correspondence between adjectives and nouns.

3.3. Analysis of Attention. In the comments, the higher the frequency of a certain type of aspect word, the higher the user’s attention to the aspect. Therefore, attention is defined based on the frequency of appearance of aspect words.

Inspecting the set $P = \{p_k | k = 1, 2, \dots, K\}$ of K products, a total of J comment statements about product p_k are collected; then, the comment statement set of product p_k is $R_k = \{r_{jk} | j = 1, 2, \dots, J\}$, for a comment sentence r_{jk} , which contains L_{jk} aspect words; then, the sequence formed by all the aspect words in the comment sentence r_{jk} is $W_{jk} = \{w_{jkl} | l = 1, 2, \dots, L_{jk}\}$.

For an aspect word w_{jkl} , the instinct-level attention ii_{jkl} , the behavior-level attention ib_{jkl} , and the reflection-level attention ir_{jkl} of the aspect word can be given, as shown in the following formulas (1)–(3):

$$ii_{jkl} = \begin{cases} 1 & w_{jkl} \in \text{instinct layer} \\ 0 & w_{jkl} \notin \text{instinct layer} \end{cases}, \quad (1)$$

$$ib_{jkl} = \begin{cases} 1 & w_{jkl} \in \text{behavior layer} \\ 0 & w_{jkl} \notin \text{behavior layer} \end{cases}, \quad (2)$$

$$ir_{jkl} = \begin{cases} 1 & w_{jkl} \in \text{reflection layer} \\ 0 & w_{jkl} \notin \text{reflection layer} \end{cases}. \quad (3)$$

From this, the attention degree I_i of the user who gives the comment r_{jk} to the instinct layer design is obtained, as shown in the following formula:

$$I_i = \frac{1}{L_{jk}} \sum_{l=1}^{L_{jk}} ii_{jkl}. \quad (4)$$

In the same way, the users who give comment r_{jk} attention to the behavior layer and the design of the reflection layer I_b and I_r can be obtained, as shown in the following formulas:

$$I_b = \frac{1}{L_{jk}} \sum_{l=1}^{L_{jk}} ib_{jkl}, \quad (5)$$

$$I_r = \frac{1}{L_{jk}} \sum_{l=1}^{L_{jk}} ir_{jkl}. \quad (6)$$

According to the above calculation results, when the value of I_i is higher than the other two, it is considered that the user pays more attention to the design of the product instinct layer and belongs to the user with instinct preference; in the same way, when I_b or I_r is higher than the other two, it is considered that users pay more attention to the design of the product behavior layer or reflection layer, which belongs to users with behavior preference or reflection preference [13].

3.4. Likelihood Analysis. The user’s preference for a specific product is constituted by his emotional attitude towards various aspects of the product, so the user’s preference for

the product evaluated by the user is calculated by using the user's emotion for different aspects. In the sentiment analysis task of aspect words, the author adopts the DFAOA-BERT model [14]. The model combines the AOA (attention-over-attention) mechanism with the BERT pre-training model, comprehensively considers the correlation between aspect word information and context information, and combines global semantic features and local semantic features; judgmental aspect vocabulary expresses the sentiment in the comment sentence.

For the aspect word sequence W_{jk} in a comment statement r_{jk} of product p_k , the meaning of the context information \bar{r}_{jkl} corresponding to any aspect word w_{jkl} is the remaining content of the comment sentence r_{jk} after removing the aspect word w_{jkl} [15, 16]. Input the aspect word w_{jkl} and the context information \bar{r}_{jkl} into the network at the same time to obtain the emotional tendency s_{jkl} of the aspect word in the comment sentence r_{jk} ; the values of s_{jkl} are 0, 1, and 2, which represent negative, neutral, and positive emotions, respectively.

Then, user j 's preference E_{jk} for product p_k is expressed as the following formula:

$$E_{jk} = \frac{1}{L_{jk}} \sum_{l=1}^{L_{jk}} S_{jkl}. \quad (7)$$

Using c_{jk} to represent the user who gave the comment r_{jk} , from all the comments of the product p_k , the preference Ei_k for the product p_k from the instinctual preference user group Ci_k who purchased the product p_k can be comprehensively extracted, as shown in the following formula:

$$Ei_k = \frac{1}{|Ci_k|} \sum_{j=1}^{|Ci_k|} E_{jk} c_{jk} \in Ci_k. \quad (8)$$

Similarly, the favorability Eb_k of the behavioral preference user group Cb_k for the product p_k , and the favorability Er_k of the reflection preference user group Cr_k for the product p_k can be obtained, as shown in the following formulas:

$$Eb_k = \frac{1}{|Cb_k|} \sum_{j=1}^{|Cb_k|} E_{jk} c_{jk} \in Cb_k, \quad (9)$$

$$Er_k = \frac{1}{|Cr_k|} \sum_{j=1}^{|Cr_k|} E_{jk} c_{jk} \in Cr_k. \quad (10)$$

4. Analysis of Results

4.1. Data Collection and Mapping Table Construction. The author conducts experimental analysis based on JD.com mobile phone review data. Data crawlers are used to crawl relevant parameters and user reviews of mobile phones on sale from the Jingdong website, screen more than 3,000 mobile phones, and exclude products with unclear basic information such as product names or store names, reservations, and second-hand products, and each product is required to contain at least 5 positive reviews, 5 positive reviews, and 5 negative

reviews and finally got 904,232 reviews for a total of 1,171 mobile phone products; among them, 677,266 were positive, 73,443 were moderate, and 153,523 were negative. Since the website limits each mobile phone to display at most 1000 positive comments, 1000 moderate comments, and 1000 negative comments, the number of comments obtained for each mobile phone is between 32 and 3000 [17].

Use the stuttering word segmentation tool to segment the review text, and select the aspect words related to the product features from the words with a word frequency greater than 5/10,000, correct or complete words with inaccurate segmentation results, (for example, change "comprehensive" to "full screen"), add some words related to existing attribute words according to common sense (for example, add "double" to "price." 11), and then identify explicit and implicit aspect words respectively [18]. The meaning of the aspect words established on the JD mobile phone dataset is shown in Table 1.

4.2. Analysis of Consumer Psychology Preference Based on Attention. Based on the attention of comments, analyze the consumer psychology preferences of users. According to formulas (4)–(6), the instinct level attention, behavior level attention, and reflective level attention of each comment are calculated, respectively, and users are classified into three categories: instinctive preference, behavioral preference, or reflective preference [19].

Taking the overall mobile phone review data collected by the JD.com dataset as an example, the distribution of three types of users in the mobile phone purchase market can be obtained as shown in Figure 2.

It can be seen that, in the mobile phone purchase market, most users are instinctive preference users; that is, they pay attention to intuitive features such as the appearance and price of mobile phones. Behavioral preference users, that is, the number of users who pay attention to the experience of using various practical functions of mobile phones, are slightly smaller. The least number are reflective preference users.

The top nine most frequently mentioned aspect words in the process of extracting each type of user comments are shown in Table 2; from top to bottom, the mentioned frequency of aspect words decreases in turn, among the high-frequency aspect words mentioned by instinctual preference users; aspect words that belong to the instinctive layer are marked in black font; the same is true for the other two types of users.

Judging from the five specific features at each level, the instinctive preference users focus more on aspects that are more closely related to the actual hand experience, such as the appearance, screen, and sound of the instinctual layer, for features such as price and parameters that have little impact on the user experience, the attention is not as much as appearance, screen, and sound. It is worth noting that the instinctive preference users pay a high degree of attention to the words "speed," "photographing," and "standby time" in the behavioral layer.

Behavioral preference users focus more on performance, battery, and photography; for more traditional communication functions and more attention to auxiliary functions, it

TABLE 1: Experience level, product features, and aspect word mapping table established according to the three-level experience theory (example).

Three-level experience theory	Interpretation in the context of mobile phone design	Product features	Aspect word (example)	Number of explicit words	Number of implicit words
Instinct layer	Information and feelings that can be obtained before using a mobile phone or when using it lightly	Exterior	Color, border, and surface	53	27
		Screen	Display, quality, and clarity	29	3
		Sound	Sound quality, volume, and noise	19	0
		Price	Price	21	14
		Parameter	GB, memory, and chip	22	0
Behavioral layer	The experience of using most functions of the mobile phone	Performance	Black screen, game, and speed	26	9
		Battery	Battery, power, and battery life	20	0
		Photograph	Pixel, night scene, and beauty	26	0
		Communication	Internet speed, wireless, and signal	31	0
		Accessibility	Face recognition, fingerprint, and Bluetooth	41	3
Reflection layer	User perception of self-image and product image	Brand	Huawei, Xiaomi, and Apple	30	0
		Serve	Store, logistics, and after-sales	51	1
		User	Elderly, children, and girls	34	0
		Overall feeling	Technology, domestic production, and humanization	26	31
		Accessories	Headphones, data cables, and bracelets	18	0

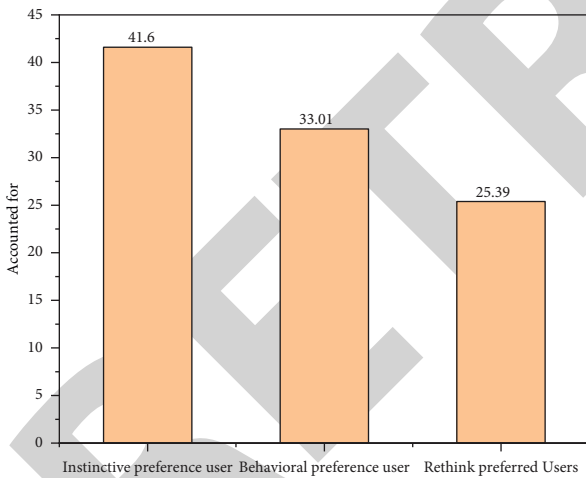


FIGURE 2: Distribution of three-tier user groups in the mobile phone market.

is not as good as performance, battery, photography, and other three aspects. For the three instinctive aspects of “screen,” “appearance,” and “sound effects,” behavior preference users pay a high degree of attention.

Reflection preference: the user’s concerns comprehensively cover all five characteristics of the reflection layer.

4.3. *User Analysis Based on Likeness.* The DFAOA-BERT model is used to analyze the favorability of the aspect words in the comment sentences, so as to obtain the favorability of

TABLE 2: Three-level user groups comment on high-frequency words.

Instinct preference user	Behavioral preference user	Reflect on preference users
Screen	Speed	JD.com
Appearance	Photograph	Elder
Speed	Standby time	Customer service
Photograph	Screen	Logistics
Sound effect	Appearance	Quality
Standby time	Sound effect	Huawei
Exterior	Card	Speed
Sound	Charge	Express delivery
Feel	Battery	Earphone

different types of users for their mobile phone purchases, and based on this, we analyze the consumption preferences of different types of users on brands and prices [20].

Taking eight mobile phone brands with a large number of users, such as Apple and Xiaomi, as examples, the user preference results of different preferences are shown in Table 3.

It can be obtained from Table 3; among the top seven types of mobile phone brands, instinctive preference users have higher preference for each brand of mobile phone than the other two types of users, while the other two types of users have little difference in their preference for the same brand.

Instinct preference users have the highest preference for Oppo, and behavior preference users have the highest preference for Huawei. Therefore, we can think that, among

these eight brands, Oppo and Huawei are the most suitable for user needs in the design of the instinct layer and the behavior layer, respectively. Reflection preference users have the highest preference for Philips because most users believe that Philips' design more accurately meets the needs of the target user group of the elderly, so its reflection layer design is optimal [21].

Then, according to the price distribution characteristics of mobile phones we obtained, the mobile phones are divided into the following five price levels, and the preference of each type of users for these five price mobile phones is compared; the results are shown in Table 4.

It can be seen from the table that users who prefer the instinctive and behavioral layers prefer midpriced phones, so we believe that the instinct-layer and behavior-layer designs of midpriced mobile phones are more able to meet users' expectations based on their price [22]. However, overall, instinct preference users are basically similar in their liking for each price point; while behavioral preference users have significantly lower evaluations of mobile phones below 1,000 yuan than other price points, which shows that the functions of mobile phones below 1,000 yuan are less and weaker; it cannot meet the needs of these users. In retrospect, the most popular mobile phone is the mobile phone below 1,000 yuan, which is related to the generally lower price of the old phone. At the same time, this score is significantly different from that of this type of users for higher-priced phones; it also shows that other price-point phones need to improve their own reflection layer design [23].

Judging from the preference of different types of users for mobile phones of the same price, at all price points, the instinctive preference users' preference for mobile phones at this price is higher than that of the other two types of users. At the four price points of more than 1,000 yuan, behavior preference users are more fond of mobile phones at this price than reflection preference users. Only in the mobile phones below 1,000 yuan, the preference of users with reflection preference is higher than that of users with behavior preference. Therefore, we believe that most mobile phones will pay more attention to the design of the instinct layer under the constraints of their pricing, followed by the design of the behavior layer; considering that users with instinct preferences account for the highest proportion in the market, the design bias is indeed more in line with the market status [24].

Furthermore, taking Xiaomi Mi 10 (the product id on the JD.com shopping website is 100011351676, 1095 instinctively prefer users, 1311 behavioral preference users, and 490 reflection preference users) as an example, the 15 features of the mobile phone are analyzed for different types of users, as shown in Table 5.

It can be seen from Table 5 that the three types of users have the highest preference for the feature of the phone's sound, so we believe that the phone's sound design is the best among the fifteen features.

For users with instinctive preference and users with reflective preference, the lowest preference is service, while for behavioral preference users, the lowest preference is

TABLE 3: The three-level user groups' ratings of their preference for different brands of mobile phones.

Brand	Favorite		
	Instinct preference user	Behavioral preference user	Reflect on preference users
Apple	1.570363	1.314607	1.326808
Millet	1.614227	1.317204	1.276268
Red rice	1.615018	1.284013	1.325327
Huawei	1.667817	1.493053	1.420238
Glory	1.619561	1.424737	1.35648
Oppo	1.756583	1.491	1.544588
Vivo	1.711509	1.488905	1.413475
Philips	1.556918	1.198661	1.596631

TABLE 4: Ratings of three-level user groups' preference for mobile phones at different price points.

Price	Favorite		
	Instinctive preference	User behavior preferences	User reflection preference
Below 1k	1.625137	1.212833	1.545395
1-2k	1.667669	1.427243	1.410421
2-3k	1.642409	1.431043	1.346138
3-5k	1.603784	1.387616	1.304926
Above 5k	1.614496	1.404115	1.323678

TABLE 5: Ratings of the three-level user groups' favorability of various features of Xiaomi Mi 10.

Feature	Favorite		
	Instinctive preference	User behavior preferences	User reflection preferences
Exterior	1.312435	1.16532	1.041837
Screen	1.297634	1.16561	1.005272
Sound	1.410963	1.198691	1.065646
Price	0.955867	1.007628	0.972449
Parameter	1.156625	1.048055	1.018367
Performance	1.338706	0.900032	1.029082
Battery	1.182451	1.015084	1.011395
Photograph	1.249389	1.030503	1.012517
Communication	0.98691	0.813709	0.959184
Accessibility	1.063318	0.953914	0.99966
Overall feeling	1.112557	1.04508	0.923129
Brand	1.168774	1.048695	0.960002
Serve	0.941993	0.928649	0.584262
Accessories	0.962731	0.979723	0.709796
User	1.019178	1.002288	0.986735

communication. We believe that if the Xiaomi Mi 10 mobile phone wants to attract the most instinctive preference users in the market or the reflective preference users who buy this mobile phone the least, it should improve its service level, including customer service level, store and platform cooperation, delivery logistics, and after-sales service quality. If you want to consolidate the base of the number of users who currently buy the most behavioral preference for this mobile phone, you should improve your communication quality,

including mobile phone communication and network signals [25].

5. Conclusion

According to the three-level experience theory, the author analyzes the consumer psychology of users and proposes a new user portrait analysis and calculation method. First, we constructed the mapping relationship between the experience level and the aspect words in the comment statement, corresponding the aspect words in the product reviews to the product features and then corresponding the fifteen product features to the three levels, thus establishing the experience level-product feature: aspect word mapping table. Based on this vocabulary, we can use aspect word extraction technology and deep learning-based aspect word sentiment analysis technology, obtain the attention and love of various types of users on different aspects and experience levels of the product, divide users into three types, instinctive preference, behavioral preference, and reflective preference, and further obtain the consumption characteristics of users with different preferences. From the merchant's point of view, when you understand the distribution characteristics and reasons of your product's user group, as well as various users' preferences for the product, you can combine the merchant's development goals to judge the direction of product improvement. Although the study only takes the mobile phone as an example for application analysis, as long as the product information and review content are combined, the product features are reasonably classified into three levels, and the method of the study is also applicable to the consumer psychology analysis of other product users. Mobile phones are search-type commodities in Nelson's product category; in the future, other commodities, such as experience-type products, can be selected for user portraits to further verify the universality and effectiveness of the author's method. In addition, there is still room for improvement in the construction of the experience level-product feature: aspect word mapping table. At present, we only take the mobile phone review dataset as an example. In the future, we can build a vocabulary across multiproduct and multiplatform review datasets, in order to conduct a more comprehensive analysis of user consumption characteristics. The current vocabulary is generated based on manual rules. In the future, a machine learning method for automatically generating vocabulary can be developed based on this, so as to improve the versatility and ease of use of user portraits based on the three-level experience theory in different fields.

Data Availability

The data used to support the findings of this study can be obtained from the corresponding author upon request.

Conflicts of Interest

The authors declare no conflicts of interest.

Acknowledgments

This study was funded by National Social Science Foundation project: "Research on the History of Image Communication in China," project no: 20BXW053.

References

- [1] A. K. Sangaiah, H. Lu, and Q. Hu, "Cognitive science and artificial intelligence for human cognition and communication," *IEEE Consumer Electronics Magazine*, vol. 9, no. 1, pp. 72-73, 2020.
- [2] B. Wang, E. Wang, Z. Zhu, Y. Sun, Y. Tao, and W. Wang, "An explainable sentiment prediction model based on the portraits of users sharing representative opinions in social sensors," *International Journal of Distributed Sensor Networks*, vol. 17, no. 10, pp. 3323-3330, 2021.
- [3] E. Xu, Z. Yu, B. Guo, and H. Cui, "Core interest network for click-through rate prediction," *ACM Transactions on Knowledge Discovery from Data*, vol. 15, no. 2, pp. 1-16, 2021.
- [4] Ö. Saritaş Nakip, Y. Yıldız, and A. Tokatlı, "Retrospective evaluation of 85 patients with urea cycle disorders: one center experience, three new mutations," *Journal of Pediatric Endocrinology & Metabolism*, vol. 33, no. 6, pp. 721-728, 2020.
- [5] M. Lototsky, M. W. Davids, D. Swanepoel et al., "Hydrogen refuelling station with integrated metal hydride compressor: layout features and experience of three-year operation," *International Journal of Hydrogen Energy*, vol. 45, no. 8, pp. 5415-5429, 2020.
- [6] Y. Zhou, Y. F. Lin, X. Meng et al., "Anal human papillomavirus among men who have sex with men in three metropolitan cities in southern China: implications for hpv vaccination," *Vaccine*, vol. 38, no. 13, pp. 2849-2858, 2020.
- [7] M. Cai, Y. Tan, B. Ge, Y. Dou, and Y. Du, "Pura: a product-and-user oriented approach for requirement analysis from online reviews," *IEEE Systems Journal*, vol. 16, pp. 1-12, 2021.
- [8] S. Hu, A. Kumar, F. Al-Turjman, S. Gupta, and S. Seth, "Reviewer credibility and sentiment analysis based user profile modelling for online product recommendation," *IEEE Access*, vol. 8, no. 1, pp. 26172-26189, 2020.
- [9] H. Lee and K. Ryu, "Product and design feature-based similar process retrieval and modeling for mold manufacturing," *International Journal of Advanced Manufacturing Technology*, vol. 115, no. 1, pp. 1-12, 2021.
- [10] C. Sun, L. Lv, G. Tian, Q. Wang, X. Zhang, and L. Guo, "Leverage label and word embedding for semantic sparse web service discovery," *Mathematical Problems in Engineering*, vol. 2020, no. 3-4, pp. 1-8, 2020.
- [11] S. Brand, T. Coopmans, and D. Elkouss, "Efficient computation of the waiting time and fidelity in quantum repeater chains," *IEEE Journal on Selected Areas in Communications*, vol. 38, no. 3, pp. 619-639, 2020.
- [12] C. Chai and V. V. Pachala, "Neural network-enhanced structural equation modeling of competitive communication levers in hospital services," *Solid State Technology*, vol. 63, no. 1s, pp. 320-331, 2020.
- [13] X. Yan and Y. Chang, "The influence of company microblog interaction tactics on consumer-brand relationship," *Journal of Contemporary Marketing Science*, vol. 2, no. 1, pp. 2-22, 2019.
- [14] H. Choi, J. M. Hahm, and L. N. Reid, "Do consumers trust healthy menu advertising from fast food brands? influence of brand and consumer-related factors," *Health Communication Research*, vol. 20, no. 1, pp. 75-113, 2021.

Retraction

Retracted: Analysis on Innovation Path of Business Administration Based on Artificial Intelligence

Mathematical Problems in Engineering

Received 8 August 2023; Accepted 8 August 2023; Published 9 August 2023

Copyright © 2023 Mathematical Problems in Engineering. This is an open access article distributed under the Creative Commons Attribution License, which permits unrestricted use, distribution, and reproduction in any medium, provided the original work is properly cited.

This article has been retracted by Hindawi following an investigation undertaken by the publisher [1]. This investigation has uncovered evidence of one or more of the following indicators of systematic manipulation of the publication process:

- (1) Discrepancies in scope
- (2) Discrepancies in the description of the research reported
- (3) Discrepancies between the availability of data and the research described
- (4) Inappropriate citations
- (5) Incoherent, meaningless and/or irrelevant content included in the article
- (6) Peer-review manipulation

The presence of these indicators undermines our confidence in the integrity of the article's content and we cannot, therefore, vouch for its reliability. Please note that this notice is intended solely to alert readers that the content of this article is unreliable. We have not investigated whether authors were aware of or involved in the systematic manipulation of the publication process.

Wiley and Hindawi regrets that the usual quality checks did not identify these issues before publication and have since put additional measures in place to safeguard research integrity.

We wish to credit our own Research Integrity and Research Publishing teams and anonymous and named external researchers and research integrity experts for contributing to this investigation.

The corresponding author, as the representative of all authors, has been given the opportunity to register their agreement or disagreement to this retraction. We have kept a record of any response received.

References

- [1] B. Lu, "Analysis on Innovation Path of Business Administration Based on Artificial Intelligence," *Mathematical Problems in Engineering*, vol. 2022, Article ID 6790836, 7 pages, 2022.

Research Article

Analysis on Innovation Path of Business Administration Based on Artificial Intelligence

Ben Lu 

Department of Business Administration and Economic Management, Shanghai PuTuo Sparetime University, Shanghai 200062, China

Correspondence should be addressed to Ben Lu; b20160505123@stu.ccsu.edu.cn

Received 3 July 2022; Accepted 19 September 2022; Published 28 September 2022

Academic Editor: Hengchang Jing

Copyright © 2022 Ben Lu. This is an open access article distributed under the Creative Commons Attribution License, which permits unrestricted use, distribution, and reproduction in any medium, provided the original work is properly cited.

In order to effectively promote the efficiency of retail enterprises, the innovation path of business administration based on artificial intelligence is studied. Through a questionnaire survey, collect the relevant data of retail enterprise value network, business model innovation, and enterprise benefits, and through regression analysis. The experimental results show that before the business model innovation, the coefficients of internal value network innovation and external value network innovation are 0.413 and 0.258, respectively. After the business model innovation is added, the coefficients of the two are reduced to 0.208 ($p = 0.012 < 0.05$) and 0.113 ($p = 0.005 < 0.01$). In addition, the coefficients of the two dimensions of business model innovation are significant at the 1% level. *Conclusion.* Both internal value network innovation and external value network innovation have a significant positive impact on the functional business model innovation and artificial intelligence business model innovation of retail enterprises. Functional business model innovation and artificial intelligence business model innovation have a significant positive impact on the financial and market benefits of retail enterprises. Internal value network innovation and external value network innovation have a significant positive impact on the financial and market benefits of retail enterprises. Business model innovation plays an intermediary role in the relationship between internal value network innovation, external value network innovation, and the financial and market benefits of retail enterprises.

1. Introduction

The new economic normal mainly emphasizes that China's economic development will grow at a medium speed rather than a high speed in the future. As the name suggests, business administration adopts some economic and management methods and is a method of managing enterprises under the current economic situation. When the new economic situation has just emerged, many enterprises are unable to adapt to this change, and their management is facing various problems. The reason for these problems is not only the impact of changes in the external market environment but also the lack of long-term vision for business administration and leadership, as well as the timely and optimal optimization of enterprises. In the process of project development, business administration is a very important content [1]. If enterprises can manage their business well

enough, they can better adapt to this rapidly changing society. In the new economic situation, enterprises need to strengthen business administration, improve business efficiency, enhance market competitiveness, and enable enterprises to obtain the power of sustainable development.

From the current management of most companies, there is a common problem, that is, there is no mature industrial and commercial management mechanism, and there is a lack of strong guidance. As a result, the development direction of the enterprise or the economic measures taken are very backward and even violate the laws of the entire market economy, which will affect the market competitiveness of the company. Imagine that if the enterprise can continue to innovate the path of business administration, keep pace with the pace of market development, and constantly improve the management mechanism and investment diversification strategy, it will run through the history of the company's

development and various departments (such as personnel department, scientific research and Technology Department, and sales department). So as to maximize the advantages of talents in each department, improve industrial and commercial management, and make the enterprise adapt to the trend of the times, continue to develop and expand, so as to give full play to its social value [2].

In the business innovation of enterprises, traditionally, they still tend to follow stereotypes, and the concept of innovation does not include new elements, but this method is not conducive to achieving long-term results in the long-term development of enterprises [3]. For the current situation, many companies are facing common problems, mainly because people do not have a good understanding of business innovation in business management. And, in practice, the guiding role of theory is very important as shown in Figure 1.

2. Literature Review

Raj and others proposed that for the comprehensive innovative design of the enterprise's business model, two different focuses should be taken into account. One is what value the enterprise can provide to customers; second, how to realize these values [4]. Innovation itself is a continuous process, constantly testing problems, and correcting errors, which specifically includes four stages: the analysis of the environment, and believes that strategic management theory, such as the analytical method, is an effective tool for analyzing environmental changes and trends; the status quo of dialysis organization is helpful to screen and determine the core competence and resources; promote the promotion of enterprise value, that is, redesign and improve the existing business model; implementation of innovation. Lindgren, P. and others believe that recognizing the basic elements of the business model framework is the starting point of the research on business model innovation and thus discussed the transformation of enterprise cost structure, the transformation of customer value, the transformation of vested profit protection mode and the application of relevant strategies [5]. Wang and Cao. and others proposed that the business model is a comprehensive description of three key factors for the production and operation of enterprises: value flow, revenue flow, and logistics [6]. Li et al. define a business model, which means that creating a profitable business activity will involve the overall structure of customers, processes, channels and suppliers, resources, and capabilities [7]. Bashir et al. put forward that the business model aims to effectively allocate all links of the enterprise to form a system in which all factors adapt to each other, and the purpose is to help customers create greater value. She believes that a complete business model should be composed of three subelements: accurate role description, correct motivation, and internal value creation plan [8].

Surkova and Mazhaiskii put forward the enterprise value network based on modularization and its competitive advantage; many scholars have studied the details of the value network [9]. Pan et al. made a literature summary and case analysis on the evolution path of the enterprise value

network and put forward how to maintain long-term advantages [10]. The purpose of a value network is to make all nodes in the network realize value creation. It mainly takes consumer value creation as the core. However, it is different from traditional organizations. The value network can not only realize self-organization, but also embed specific tasks or technologies into the value network to realize sharing, and assign value to nodes. Therefore, the value network is a multiple economic relationship network of different subjects, that is, different subjects present two-way or multi-directional economic relations. Lin believes that business models affect the value of online retail enterprises, and there is a significant two-way positive effect between model innovation and user resources; There is a significant two-way positive effect between configuration efficiency and functional complementarity. There are many breakthroughs and explorations in the practice and theory of business model innovation, but so far there are still many deficiencies [11]. This paper holds that: the enterprise resource allocation mode is determined by the business model, so its impact is determined by the enterprise benefit performance, and the resulting comprehensive present value determines the enterprise value; artificial intelligence value network is an innovation of this paper because artificial intelligence is the most economical and can best reflect the value network.

3. Research Methods

Based on the above-given concept explanation, this part will put forward the research hypothesis of the relationship among retail enterprise value network innovation, business model innovation, and enterprise benefit and reasonably select the research samples.

3.1. Research Assumptions. Value network innovation can be divided into internal value network innovation and external value network innovation. The innovation of an internal value network can make enterprises better understand the internal situation and reallocate internal resources in various ways to improve the value innovation ability [12]. Therefore, the internal value network innovation can provide a good internal foundation for the two types of business model innovation. The innovation of an external value network is to integrate external cooperation or competition relations, which can effectively achieve the acquisition and utilization of external resources, so as to provide external resources for business model innovation [13]. Therefore, this paper puts forward the following relevant assumptions:

H1a: the innovation of the internal value network has a significant positive impact on the functional business model innovation of retail enterprises

H1b: the innovation of internal value network has a significant positive impact on the artificial intelligence business model innovation of retail enterprises

H1c: the innovation of external value network has a significant positive impact on the functional business model innovation of retail enterprise

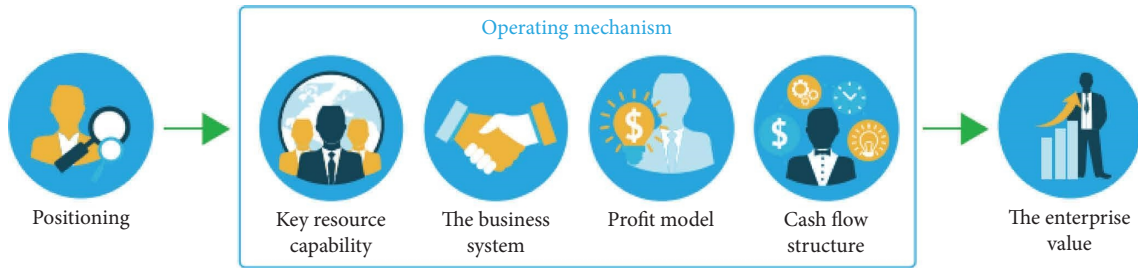


FIGURE 1: Operation diagram of business model elements of the theory.

H1d: the innovation of external value network has a significant positive impact on the innovation of the artificial intelligence business model of retail enterprises.

Both types of business model innovation aim at improving enterprise benefits, and functional innovation pays more attention to innovation from specific operations, such as technology and distribution relationship. [14]. The innovation of artificial intelligence is to replace the old model with a new model. At the same time, both internal and external value network innovation can enhance the value creation ability, so it can create more value for consumers and bring more benefits to enterprises. Therefore, this paper puts forward the following relevant assumptions:

H2a: functional business model innovation has a significant positive impact on the financial benefits of retail enterprises

H2b: functional business model innovation has a significant positive impact on the market efficiency of retail enterprises

H2c: artificial intelligence business model innovation has a significant positive impact on the financial benefits of retail enterprises

H2d: artificial intelligence business model innovation has a significant positive impact on the market efficiency of retail enterprises

H3a: the innovation of internal value network has a significant positive impact on the financial benefits of retail enterprises

H3b: the innovation of internal value network has a significant positive impact on the market efficiency of retail enterprises

H3c: the innovation of external value network has a significant positive impact on the financial benefits of retail enterprises

H3d: the innovation of external value network has a significant positive impact on the market efficiency of retail enterprises

Internal or external value network innovation is to realize value creation in a new way, so it indicates the value creation potential of enterprises, while business model innovation can stimulate the potential through specific reform measures [15]. Therefore, this paper puts forward the following relevant assumptions:

H4a: business model innovation plays an intermediary role in the relationship between the innovation of internal value network and the financial benefits of retail enterprises

H4b: business model innovation plays an intermediary role in the relationship between the innovation of internal value network and the market efficiency of retail enterprises

H4c: business model innovation plays an intermediary role in the relationship between external value network innovation and financial benefits of retail enterprises

H4d: business model innovation plays an intermediary role in the relationship between external value network innovation and retail enterprise market efficiency

3.2. Selection of Research Samples. In this paper, the corresponding questionnaire is prepared to obtain the data required for the research. In the process of preparing the questionnaire, it is necessary to formulate the items related to each variable and select the corresponding control variables [16]. The final questionnaire contains 22 items for value network, 16 items for business model innovation, 6 items for enterprise benefit, and control variables such as enterprise nature, scale, and establishment time. After completing the first draft, the questionnaire was reviewed and fed back by relevant scholars, and the final questionnaire was formed after careful modification. At the time of questionnaire distribution, 275 retail enterprises from many provinces and cities were selected. After that, I contacted the management personnel of each enterprise through e-mail or instant messaging, and they assisted in issuing the questionnaire. 328 questionnaires were received and 262 were valid, with an effective rate of 79.88%.

4. Result Analysis

Based on the research hypotheses proposed above and the selected research samples, this part will use the statistical software SPSS18.0 to conduct data correlation analysis and multiple linear regression analysis on the samples to test the research hypotheses and discuss and analyze the hypothesis test results [17].

The mathematical definition formula for factor correlation analysis by chi square test is as follows (1):

$$\chi^2 = \sum_{i=1}^r \sum_{j=1}^c \frac{(f_{ij}^0 - f_{ij}^e)^2}{f_{ij}^e}, \quad (1)$$

where r is the number of rows in the contingency table; c is the number of columns in the contingency table; f_{ij}^0 is the observation frequency; f_{ij}^e is the desired frequency.

The formula for calculating the expected frequency of f^e is as follows:

$$f^e = \frac{RT}{n} * \frac{CT}{n} * n = \frac{RT * CT}{n}, \quad (2)$$

where RT is the total of line observation frequencies; CT is the sum of the column observation frequencies.

From the chi square statistics obtained from the above formula, it can be seen that if the expected frequency and the observed frequency are the same, the least chi square statistics is 0, and it can be inferred that the two variables are completely independent without any correlation. The larger the difference between the expected frequency and the observed frequency, the larger the chi square statistics can be obtained, and the higher the degree of correlation [18].

4.1. Hypothesis Test. Based on the above-given research assumptions and data collected, this paper will explore the relationship between value network innovation, business model innovation, and enterprise benefits. In the data analysis, the dependency relationship between variables is first determined with the help of correlation analysis. The data results are shown in Table 1. It can be seen from Table 1 that in the correlation analysis results, the correlation coefficients of all variables are significant at the level of 5% or 10%, and the correlation coefficients are positive, indicating that there is a significant positive correlation between all variables. However, correlation analysis can only describe the degree of tightness but cannot determine the specific interaction between variables. Therefore, multiple linear regression analysis is required [19].

Regression analysis can infer another variable from one variable, so as to describe the interactive relationship between the changes of multiple variables. In the regression analysis, we first test the relationship between AI value network innovation and business model innovation. The results are shown in Table 2. According to Table 2, the coefficient of internal value network innovation and functional business model innovation is 0.584 ($p = 0.005 < 0.01$), the coefficient of internal value network innovation and artificial intelligence business model innovation is 0.415 ($p = 0.011 < 0.05$), the coefficient of external value network innovation and functional business model innovation is 0.305 ($p = 0.000 < 0.01$), and the coefficient of external value network innovation and artificial intelligence business model innovation is 0.337 ($p = 0.003 < 0.05$). It shows that each dimension of value network innovation can significantly and positively affect each dimension of business model innovation. Therefore, H1a, H1B, H1C, and h1d are established.

Next, we will test the impact of business model innovation and value network innovation on enterprise benefits. The results are shown in Table 3. It can be seen from Table 3 that the coefficient of functional business model innovation and financial benefit is 0.337 ($p = 0.003 < 0.01$), the coefficient of functional business model innovation and market benefit is 0.395 ($p = 0.003 < 0.01$), and the coefficient of artificial intelligence business model innovation and financial benefit is 0.413 ($p = 0.000 < 0.01$). The coefficient of AI business model innovation and market benefit is 0.299 ($p = 0.002 < 0.01$), the coefficient of internal value network innovation and financial benefit is 0.394 ($p = 0.005 < 0.01$), the coefficient of internal value network innovation and market benefit is 0.413 ($p = 0.005 < 0.01$), the coefficient of external value network innovation and financial benefit is 0.314 ($p = 0.022 < 0.05$), and the coefficient of external value network innovation and market benefit is 0.258 ($p = 0.003 < 0.01$). All dimensions of business model innovation and value network innovation can significantly and positively affect financial and market benefits. Therefore, H2A, H2B, H2C, H2D, h3a, H3B, H3C, and h3d are established.

Next, we will examine the intermediary role of business model innovation. The results are shown in Table 4. It can be seen from Table 4 that in the relationship between value network innovation and financial benefits, R^2 was 0.138 before the intermediary role of business model innovation was added and increased to 0.229 after it was added (see Figure 2), indicating that business model innovation has increased the explanatory power of financial benefits. At the same time, before the business model innovation, the coefficients of internal value network innovation and external value network innovation were 0.394 and 0.314, respectively. After the addition, the coefficients of the two decreased to 0.205 ($p = 0.007 < 0.01$) and 0.127 ($p = 0.004 < 0.01$). In addition, the coefficients of the two dimensions of business model innovation are significant at the 1% level. Therefore, it can be considered that business model innovation plays an intermediary role in the relationship between value network innovation and financial benefits. In the relationship between value network innovation and market benefits, R^2 was 0.124 before the intermediary role of business model innovation was added, and increased to 0.258 after the entry, indicating that business model innovation has increased the explanatory power of market benefits [20]. At the same time, before the business model innovation, the coefficients of internal value network innovation and external value network innovation were 0.413 and 0.258, respectively. After the addition, the coefficients of the two decreased to 0.208 ($p = 0.012 < 0.05$) and 0.113 ($p = 0.005 < 0.01$). In addition, the coefficients of the two dimensions of business model innovation are significant at the 1% level. Therefore, it can be considered that business model innovation plays an intermediary role in the relationship between value network innovation and market efficiency. Therefore, H4a, H4B, H4c, and H4d are established.

4.2. Result Discussion. This paper puts forward the hypotheses about value network, business model innovation, and enterprise benefit through theoretical analysis then

TABLE 1: Correlation analysis.

	1	2	3	4	5	6	7	8	9
1. Establishment time	1								
2. Enterprise scale	0.037**	1							
3. Nature of enterprise	0.595*	-0.171	1						
4. Innovation of internal value network	0.025*	0.400	0.612	1					
5. Innovation of external value network	0.402	-0.124	0.216	0.106**	1				
6. Functional business model innovation	0.664*	-0.071**	0.248	0.551**	0.389**	1			
7. Artificial intelligence business model innovation	0.272	0.488	0.488	0.290**	0.172**	0.045*	1		
8. Financial benefits	-0.036	0.356**	0.694	0.540**	0.468**	0.397**	0.026*	1	
9. Market benefit	0.121**	0.178	-0.098	0.310**	0.271*	0.335**	0.394*	0.555**	1

Note. **, *respectively represent significant levels above 5% and 10%.

TABLE 2: Value network innovation and business model innovation.

Variable	Functional business model innovation			Artificial intelligence business model innovation		
	Coefficient	T Value	P value	Coefficient	T Value	P value
Internal value network innovation	0.584	1.4835	0.005	0.415	0.2957	0.011
External value network innovation	0.305	2.483	0.000	0.337	1.394	0.003
Date of establishment	0.183	1.3042	0.094	0.039	0.324	0.134
Enterprise size	-0.024	-2.4421	0.022	-0.115	-1.393	0.131
Nature of enterprise	0.136	1.8641	0.112	0.038	0.9122	0.045
R ²		0.511			0.498	
F Value		38.284 (0.003)			39.153 (0.002)	

TABLE 3: Influencing factors of enterprise benefit.

	Financial benefits			Market benefit		
	Coefficient	T Value	P value	Coefficient	T Value	P Value
Functional business model innovation	0.337	2.333	0.003	0.395	0.217	0.003
Artificial intelligence business model innovation	0.413	1.581	0.000	0.299	1.423	0.002
Internal value network innovation	0.394	3.44	0.005	0.413	2.526	0.005
External value network innovation	0.314	0.2755	0.022	0.258	3.443	0.003
Date of establishment	0.175	2.5365	0.081	0.038	1.7430	0.158
Enterprise size	-0.011	-0.6702	0.225	0.052	-0.9466	0.116
Nature of enterprise	0.127	-0.9671	0.153	-0.106	-0.9889	0.004
R ²		0.115			0.153	
F Value		15.395 (0.003)			20.494 (0.000)	

TABLE 4: Intermediary role of business model innovation.

	Financial benefits		Market benefit	
	Coefficient	P value	Coefficient	P Value
Internal value network innovation	0.394 (0.005)	0.205 (0.007)	0.413 (0.005)	0.208 (0.012)
External value network innovation	0.314 (0.022)	0.127 (0.004)	0.258 (0.003)	0.113 (0.005)
Functional business model innovation		0.313 (0.001)		0.294 (0.007)
Artificial intelligence business model innovation		0.325 (0.006)		0.297 (0.000)
Date of establishment	0.175 (0.081)	0.118 (0.006)	0.038 (0.158)	0.049 (0.006)
Enterprise size	-0.011 (0.225)	-0.039 (0.003)	-0.052 (0.116)	-0.031 (0.006)
Nature of enterprise	0.127 (0.153)	0.154 (0.007)	-0.106 (0.004)	0.038 (0.010)
R ²		0.138 0.229		0.124 0.258
F Value		11.384 (0.003)		10.271 (0.005)
		22.439 (0.000)		25.893 (0.003)

Note. P value in brackets.

collects various variable data through questionnaire survey, and finally draws the following conclusions through correlation analysis and regression analysis: the internal

value network innovation and external value network innovation have a significant positive impact on the functional business model innovation of retail enterprises;

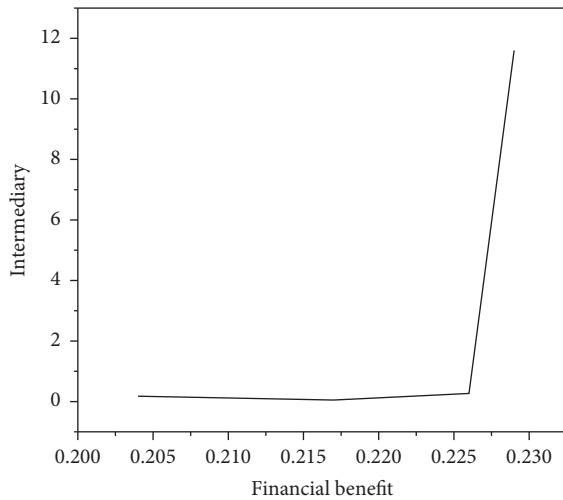


FIGURE 2: Comparison of financial benefits before and after joining the intermediary.

the innovation of internal value network and external value network has a significant positive impact on the artificial intelligence business model innovation of retail enterprises. This is mainly because the internal value network innovation can reallocate internal resources, optimize enterprise efficiency, and provide a better internal foundation for business model innovation. External value network innovation can help enterprises build a good relationship with suppliers and consumers and provide a complete value creation chain for business model innovation. Functional business model innovation and artificial intelligence business model innovation have a significant positive impact on the financial benefits of retail enterprises; Functional business model innovation and artificial intelligence business model innovation have a significant positive impact on the market efficiency of retail enterprises. Since the function is the pursuit of practicality, and artificial intelligence is the pursuit of uniqueness and progressiveness, it is obvious that the pursuit of practicality can improve efficiency. The pursuit of uniqueness is to obtain a competitive advantage through differentiated management with other enterprises. Therefore, both types of business model innovation can bring more benefits to enterprises. The innovation of internal value network and external value network has a significant positive impact on the financial benefits of retail enterprises; the innovation of internal value network and external value network have a significant positive impact on the market efficiency of retail enterprises. To some extent, enterprises are entities that allocate resources to achieve commodity production and value creation. Restructuring the value network from the outside can enable retail enterprises to better understand the needs of consumers, deepen the relationship with suppliers, and improve efficiency. Reforming the value network from the inside is to reasonably allocate the existing resources so that enterprises can better put into production or provide services and obtain higher profits, which can promote the

growth of benefits. Business model innovation plays an intermediary role in the relationship between internal value network innovation, external value network innovation, and the financial benefits of retail enterprises; business model innovation plays an intermediary role in the relationship between internal value network innovation, external value network innovation, and retail enterprise market efficiency. External or internal value network innovation is to better realize value creation by sorting out the resources owned by enterprises, while business model innovation is to directly change the business model and profit model of enterprises, so it can have a direct impact on enterprises. Therefore, external or internal value network innovation can not only directly affect enterprise benefits but also affect enterprise benefits through business model innovation.

5. Conclusion

To sum up, this paper summarizes the following management implications: first, retail enterprises urgently need to change the value network. In the era of the digital economy, the retail market is shifting to online, which brings new challenges to retail enterprises. In the past, retail enterprises needed to sell goods to consumers through physical stores, but now they can establish a purchase and sales relationship with consumers only by uploading commodity information on the shopping platform. Therefore, retail enterprises need to reprocess the relationship with consumers, suppliers, and logistics enterprises and reconstruct the value network to win more consumers. Second, retail enterprises should improve their business model innovation ability. Business model innovation means that retail enterprises obtain profits from a new perspective or allocate resources in a new way. Since the new business model refers to operating enterprises in an unprecedented way, it can generally bring strong competitive advantages to enterprises. However, when the new business model is imitated by most enterprises, the profitability of the new business model is averaged and no longer competitive. Therefore, retail enterprises must constantly carry out business model innovation to achieve sustainable development. Third, retail enterprises should focus on functional business model innovation, supplemented by artificial intelligence business model innovation. The direct goal of functional innovation is the enterprise benefit, which helps to improve the benefit as soon as possible. Although the artificial intelligence innovation takes the enterprise benefit as the goal, it pursues an unprecedented model, so it needs a long time to accumulate. Once the artificial intelligence innovation is realized, it may open an innovative retail era. Therefore, retail enterprises need to constantly look for parts that can be improved in their daily operations to promote functional innovation, and constantly accumulate experience to accumulate energy for artificial intelligence innovation. Fourth, retail enterprises should rely on digital technology for innovation. Digital technology is the main driving force of current economic development, and it has also changed the retail market. However, retail enterprises should not regard the transfer of an offline

Retraction

Retracted: Volunteer Service Participation Emergency Management Information Collection Platform Based on Big Data Technology

Mathematical Problems in Engineering

Received 8 August 2023; Accepted 8 August 2023; Published 9 August 2023

Copyright © 2023 Mathematical Problems in Engineering. This is an open access article distributed under the Creative Commons Attribution License, which permits unrestricted use, distribution, and reproduction in any medium, provided the original work is properly cited.

This article has been retracted by Hindawi following an investigation undertaken by the publisher [1]. This investigation has uncovered evidence of one or more of the following indicators of systematic manipulation of the publication process:

- (1) Discrepancies in scope
- (2) Discrepancies in the description of the research reported
- (3) Discrepancies between the availability of data and the research described
- (4) Inappropriate citations
- (5) Incoherent, meaningless and/or irrelevant content included in the article
- (6) Peer-review manipulation

The presence of these indicators undermines our confidence in the integrity of the article's content and we cannot, therefore, vouch for its reliability. Please note that this notice is intended solely to alert readers that the content of this article is unreliable. We have not investigated whether authors were aware of or involved in the systematic manipulation of the publication process.

Wiley and Hindawi regrets that the usual quality checks did not identify these issues before publication and have since put additional measures in place to safeguard research integrity.

We wish to credit our own Research Integrity and Research Publishing teams and anonymous and named external researchers and research integrity experts for contributing to this investigation.

The corresponding author, as the representative of all authors, has been given the opportunity to register their

agreement or disagreement to this retraction. We have kept a record of any response received.

References

- [1] D. Wang, "Volunteer Service Participation Emergency Management Information Collection Platform Based on Big Data Technology," *Mathematical Problems in Engineering*, vol. 2022, Article ID 6813463, 8 pages, 2022.

Research Article

Volunteer Service Participation Emergency Management Information Collection Platform Based on Big Data Technology

Daqing Wang ^{1,2}

¹Nanjing Tech University, Nanjing, Jiangsu 211816, China

²School of Marxism, Nanjing University of Aeronautics and Astronautics, Nanjing, Jiangsu 210016, China

Correspondence should be addressed to Daqing Wang; 201714040003@zknua.edu.cn

Received 8 July 2022; Accepted 31 August 2022; Published 22 September 2022

Academic Editor: B. Sivakumar

Copyright © 2022 Daqing Wang. This is an open access article distributed under the Creative Commons Attribution License, which permits unrestricted use, distribution, and reproduction in any medium, provided the original work is properly cited.

In order to fully integrate various emergency management information resources for volunteer service, the author proposes a volunteer service participation in emergency management information collection platform based on big data technology. Taking a municipal government as an example, the current situation of information integration in emergency management is investigated and studied, the needs of various departments are analyzed through interviews and questionnaires, and the problems existing in the government's information integration are studied. It tries to build a scientific, reasonable, and operational government information integration model based on theories of government information disclosure, government emergency management, and metadata technology. The survey results show the following observation: In the survey results of "the reasons that affect the integration of emergency linkage information of a city government," the first place is the poor information communication channels between departments, accounting for 22.7%; The second and the third are "administrative system restrictions" and "protection of the interests of the department," accounting for 21.4% and 19.4%, respectively. It is worth noting that the technical problem of information management is also one of the important factors affecting the government's emergency response management, accounting for 19.1%. *Conclusion.* This study analyzes the main shortcomings and reasons of the existing sharing models, so as to construct a reasonable information sharing work model.

1. Introduction

The history of human development is a history of coping with challenges, overcoming disasters, and making continuous progress. With the development of human society today, the economy, society, and culture have achieved unprecedented prosperity. The increasing generalization and deepening of globalization and modernization have not only brought countless opportunities to human society but also created countless risks. Natural disasters caused by human beings ignoring environmental damage and demanding from nature savagely, it has become more and more frequent, and the economy, society, and nature have entered a stage in which various emergencies have higher probability, greater destructive power, and stronger influence [1]. In recent years, a series of emergencies such as earthquakes, tsunamis, floods, freezing, high temperature, and the spread

of highly pathogenic infectious diseases have not only been much more than normal in the past but have also caused more and more serious harm to human life. From the general law of social development, when a country's economy develops to a certain stage, it will enter a stage of frequent disasters and accidents with prominent contradictions based on social resources and institutional constraints. At this stage, it often corresponds to the period when the bottleneck constraints of social contradictions such as population, resources, environment, efficiency, and fairness are the most serious, and it is also a critical period in which social and economic imbalances, national psychological imbalances, and social ethics anomie are prone to occur [2]. At present, China is in an accelerated period of economic transition and social transformation, with the continuous deepening of industrialization and urbanization, the pressure caused by the rapid growth of society and

economy is increasing, the deterioration of the natural ecological environment, and the cyclical changes in the activities of nature itself; this has led to the frequent occurrence of major natural disasters such as earthquakes, floods, droughts, hurricanes, and freezing of ice and snow in China in recent years, public health events such as SARS and highly pathogenic avian influenza frequently occur, and major criminal cases, foreign-related emergencies, mass violence, and political riots occur from time to time, accidents continue one after another [3].

2. Literature Review

Awajan et al. proposed the definition of “sustainable” community, based on the disaster reduction model, the reconstruction model, and the structural cognitive model and expounded on the connotation of “sustainability,” it is believed that the impact of sudden disaster events can be minimized through unified and coordinated organization and mobilization of the community public [4]. Lv and Li. proposed a community-based disaster reduction model, fully affirming the important role of the community in disaster reduction processing [5]. Guo studied the positive role of community participation in community disaster reduction work [6]. Tian, and others believe that the important role of volunteer organizations in urban community emergency management cannot be ignored, and the government departments should actively consider and provide an effective emergency participation mechanism [7]. Kaabar et al. Proposed a comprehensive urban community fire risk identification and assessment method, using a fire impact model to assess the risk factors affecting a given building fire [8]. Khan et al. studied the dynamic risk management model in the fast time-varying system, and constructed the framework of the emergency risk measurement model and risk decision model [9]. Ivanets et al. devised a simplified model for emergency risk management, and it is used to deal with the problem of too many treatment plans and risk sources in emergency risk analysis [10]. Yuan and Zhang studied the risk trust based on the total variation theory based on the trust research angle of emergency risk analysis [11]. Hannoun et al. used the accident risk assessment method in industry (ARAMIS) to analyze safety hazards, proposed an alternative protocol and method for risk reduction and reassessment, and used the odyssey marine accident to validate the proposed method’s effectiveness [12]. Huang et al. classified risk analysis, assessment methods, and techniques from the perspectives of qualitative, quantitative, and comprehensive (qualitative combined with quantitative, semi-quantitative), and finally achieved the effect of improving risk management capabilities [13]. Shamzhy et al. studied a diversification technique to analyze and predict the risk of regional maritime emergencies in the United States [14]. Hameed and Garcia-Zapirain proposed the uncertainty threat (RMS Probabilistic Terrorism) model of risk management schemes, which defined risk as a functional form; it is used for risk estimation under uncertainty of information [15]. The author mainly adopts the methods of theoretical research and questionnaire survey. In

the elaboration of related concepts, theoretical research methods are mainly used, and a simple and concise elaboration of big data technology, emergency management theory, information integration demand theory, etc. The information and data related to this thesis of a city government department are used in the form of questionnaires, and the integrated application of emergency management information in a city is taken as a research case, under the background of big data, the problems, and reasons existing in the integration of emergency linkage management information for volunteer services in a city government are comprehensively expounded, which are used as the basis for the practice of this topic.

3. Research Methods

3.1. Overview of Government Emergency Management Theory and Practice

3.1.1. Basic Theory of Emergency Management. Integrated emergency management system is a term commonly used in public safety management, or “Emergency Management Partnership” or called “All Agency Approach/All-agencies Approach” or “Integrated Approach”. When emergencies occur, representatives from different agencies, departments, and all levels of government are required to work together and cooperate with each other and decisions must be made quickly. If there is a lack of a set of planned, coordinated, and unified leadership, it will inevitably affect the government’s response speed and adaptability, and it will not be able to implement effective management, as shown in Figure 1 [16]. Therefore, it is required to establish a chain of command that enables all participants in the emergency management work to work together, called an integrated emergency management system. Emergency management is a dynamic process that includes disaster mitigation, preparedness, response, and recovery. Disaster mitigation includes two meanings: Through preliminary work, we avoid avoidable disasters as much as possible and reduce the impact of unavoidable disasters as much as possible. In China, it is also called disaster reduction and prevention. Disaster mitigation measures cannot prevent disasters from occurring nor can they completely eliminate the vulnerability of a community or area’s facilities to all hazards. Therefore, it is necessary to be fully prepared for all kinds of dangers that may occur. The purpose of preparation is to ensure the emergency response capability required for emergency rescue of major accidents, mainly focusing on the development of emergency operation plans and systems. The main contents of preparation for extremes are preparation of plans, the establishment of early warning systems, emergency training, and emergency drills. Response is “all actions to save lives and reduce losses in an incident”. Recovery is after the disaster event is over, the return of disaster-stricken communities and people to normal life and production order before the disaster.

3.1.2. The Importance of Information Integration in the Modern Emergency Management Theory. In accordance with the principles of “comprehensive coordination,

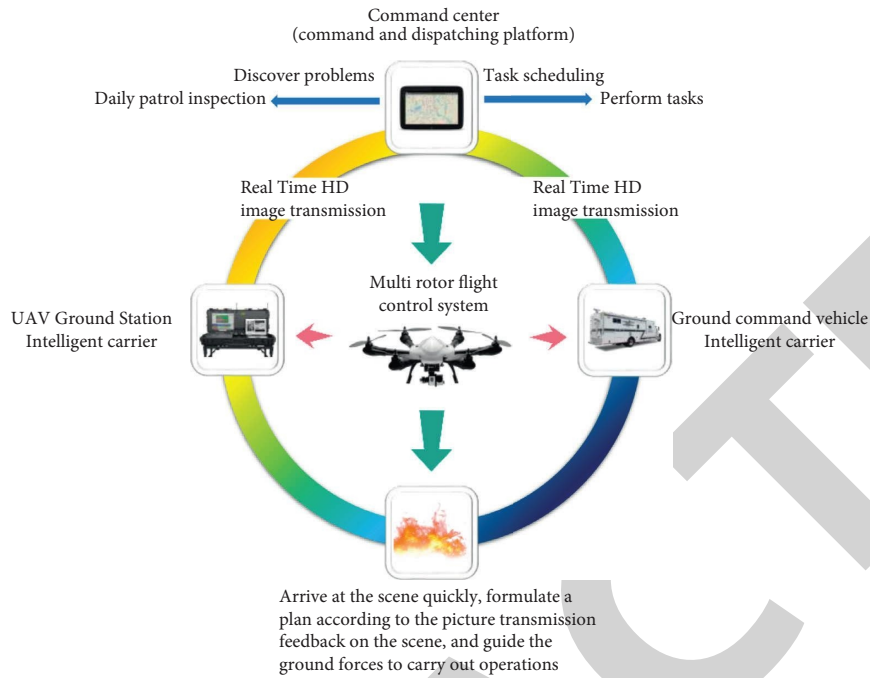


FIGURE 1: Emergency management.

professional disposal, territorial focus, and high authorization,” we scientifically define the relationship between the three levels of macrolevel strategic decision-making, meso-level campaign command, and microlevel tactical action. However, grasping all kinds of information for the first time is the premise of professional command. In the past, most of the information was obtained by manual submission. Basically, front-line personnel collect information manually and report it layer by layer. This is not inefficient and it costs a lot of manpower. In the era of big data, the way of information collection has changed from manual collection to information collection through scientific and technological means. Countries around the world have gradually changed the traditional “human sea tactics” characterized by huge numbers and huge consumption; instead, by optimizing and integrating various scientific and technological resources, strengthening the research and development of key technologies such as monitoring and early warning, command, and dispatch, and equipment support, as well as the development of complete sets of equipment, accelerated the application of remote sensing, geographic information system, global positioning system, network communication technology, cloud computing, Internet of Things and other technologies, as well as the comprehensive integration and transformation of high-tech achievements, and improved the ability to respond to emergencies in the first time, on the spot and at the first place. For example, through the development of advanced earthquake early warning and tsunami monitoring and early warning systems, millions of people can receive early warning information several seconds before the arrival of a strong earthquake and shear waves and thousands of minutes before the arrival of a tsunami, providing opportunities for self-rescue escape and refuge. In particular, the advanced subway early warning and

automatic shutdown system enabled 27 subway trains operating in the disaster area to stop safely, effectively preventing the occurrence of secondary disasters. Therefore, in emergency management, the premise for scientific decision-making is to quickly, accurately, and comprehensively collect information and present it to decision-makers [17].

3.1.3. Changes in Information Integration Work in the Era of Big Data Technology. Data are considered to be the basic means of life and market elements in the new era as important as material assets and human capital. The explosion of information has led to the explosion of the amount of information, and the data accumulated from the beginning of human history to the 1980s are not as good as our current data; the amount of data we generate is very huge, and now, there is a new trend in the era of the Internet of things. In the era of the Internet of things, we often see automatically formed interactions and automatically formed data processing; then, we will target ten times, hundred times, thousand times the equipment or the data generated all the time, this is the challenge of our data, in such a large amount of data, how much value can be really mined from it is actually very limited.

The explosive growth of information resources, among which the unstructured data information reaches about 85%, traditional information resource management technology has been unable to cope with the challenges of the big data era [18]. The emergence of big data technology and other big data tools and equipment, as well as the widespread use of cloud computing data processing and application models, provide an efficient, scalable, and low-cost solution for emergency management to deal with the growing mass of unstructured data, it makes up for the shortcomings of

traditional relational databases or data warehouses in processing unstructured data, deepens and expands the intelligence and knowledge service capabilities, forms a data-driven decision-making mechanism, and improves the level of decision making.

3.2. Overview of Big Data Integration Technology. In the local government's emergency management information integration work, the information and digital big data environment constitute its external macro environment. The government's internal integration technical means and information communication channels constitute its internal microenvironment; the two together constitute the local government's emergency management information integration environment.

3.2.1. Data Collection. In the era of big data, government information resources are all-encompassing; on the one hand, a large amount of data are generated when interacting with external customers and partners through text information, social networks, mobile applications, etc.. On the other hand, a large amount of information is generated by daily administrative management activities such as internal production, office work, and video surveillance of the government. These information resources are represented in the form of text, images, audio, video, etc., and are a mixture of multimedia, multilanguage, and multiplicity information. We determine which data sources to select as analysis targets based on project planning and mission objectives, as well as data analysis needs. These data include database design specification, E-R diagram, outline design, system requirement analysis report, and system operation report. The more complete the data collection, the better the understanding of the data and the accuracy of subsequent data integration operations.

3.2.2. Data Collation. The collected data may come from inside or outside the enterprise, and the platforms and formats of data sources are not necessarily the same. Different collection and processing methods are required for different data sources. The structure is complex and diverse and it is difficult to unify standards. In the era of big data, the organization of information resources is nonlinear, and hypertext and hypermedia information has gradually become the main way. Information resources on the same server may also differ in data structures, character sets, and processing methods. The complex and diverse structure of big data brings trouble to the establishment of unified standards and norms for information resources and makes the huge amount of structured and unstructured information resources in a disordered state. Standardization and standardization of enterprise information resources are one of the keys and difficult points of future enterprise informatization construction.

3.2.3. Data Analysis. Research shows that the amount of digital information captured and generated in China is

expected to increase to 8.5ZB between 2015 and 2020, achieving a 22-fold growth, or maintaining a compound annual growth rate of 50% [19]. Finding relevant information in petabytes or even exabytes of data is tantamount to looking for a needle in a haystack, and the cost and complexity of using the information to drive decision making is increasing day by day.

Generally, people who do data integration systems are not those who used to do operational databases for enterprises. Besides, there are many database systems in enterprises, which are generally completed by different personnel; therefore, it is very difficult to analyze data sources according to the found data, but this is an insurmountable work process and directly affects the quality of the new system. A very fundamental purpose of big data is to have very large storage and very large computing power, which can help us scale out the technologies we need to do.

3.2.4. Data Conversion. The process of data conversion is actually the process of data mapping. If the previous steps of data source analysis are done well, then this step is relatively easy. It can be mapped at the analysis topic level, data source entity level, and attribute level.

3.3. Investigation of the Existing Emergency Management Information Integration Model in a City. Splitting and combining ordered information applies a hierarchy pattern. The mode of emergency information application of a city government is a split-type if-type hierarchical system, which is innovative from a single traditional distributed mode and a centralized mode, which meets the information integration needs of a city's emergency linkage management. In this hierarchical structure model, there is a centralized and closed unified scheduler, which centralizes all the emergency information resources in the whole region and then hands them over to the main program, while the regional management information resources and organizational coordination information are passed through another independent is done by the scheduler, it supports the owners of remote information resources to implement specific individual preference schemes for specific external needs; at the same time, it is compatible with the independent maintenance functions of each subsystem; the central system only performs comprehensive overall scheduling for these subsystems, and matters within them retain their own management control. Obviously, a city's split and combined hierarchical information processing structure system has well absorbed the advantages of a single centralized unified scheduling and a single distributed independent processing, so the integration of emergency linkage management information is more hierarchical [20] as shown in Figures 2(a)–2(c):

In the process of local government emergency information integration, the main body of integration should extract the commonalities and individual characteristics in the information resource integration channels according to the current supply and demand of local actual information, human resources, and other resources, using the split-combined hierarchical model to interconnect the different

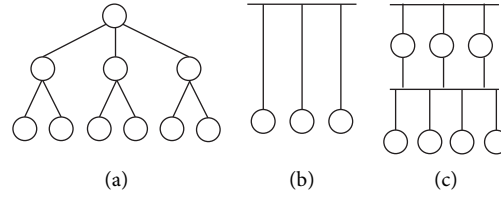


FIGURE 2: Information integration management mode diagram. (a) Centralized management model. (b) Distributed management model. (c) Hierarchical management model.

information integration channels, form an abstract model of emergency management information integration channels, and establish a concrete model according to the government affairs process, that is, the coexistence of multiple integration modes of component order integration, conditional selection integration, repeated integration, and parallel integration. The emergency information management platform of a city has constructed four routing relationships of parallel, condition, repetition, and sequence in accordance with the logical rules of the business processes of each department, so that the entire emergency information integration process has been interconnected, and significant results have been achieved in both the information update cycle and the information communication function. We form an ontology-based global mechanism. Before the establishment of the emergency linkage management office, various government organizations in a certain city used different information reporting and issuing methods to transmit the same information; due to too many transmission channels, it is easy to cause misinterpretation and low accuracy of the information in the process of information transmission; in the end, multiple versions of the same event information appeared, which undoubtedly had a huge negative impact on the feasibility and integrity of the information; in response to this thorny problem, the information management department of a city government, together with the public security, fire protection, and medical units, conducted an information communication reform attempts. All crisis cases, disposal information, etc., are incorporated into the government's unified split-level business flow model, and the goal of mapping and converting heterogeneous data sources to the global model has been preliminarily achieved. Based on the global mechanism of ontology, enhanced information integration, and sharing among departments across the region, the operation process of the emergency linkage center is shown in Figure 3.

It is obviously reasonable to look at the measures of a city government from a technical point of view, because even if the government manages the flow of information resources in emergency response [21]. Data sharing will involve organizations, departments, and information platforms with different permissions. However, after compatible processing through big data network technology, it has become a reality to transform the real "heterogeneous" environment into a virtual "homogeneous" environment, it can combine the same emergency management information with different description semantics; after the global integration mechanism based on the same ontology is transformed into the integration problem of

different modes, the information is finally transmitted accurately, and the effective optimization and integration of various information resources are finally realized for scientific scheduling and management.

4. Analysis of Results

4.1. Survey Objects and Process. This survey uses the questionnaire method and interview method to conduct field investigations on some government agencies in a city. The general object of the investigation is the current situation of emergency linkage information integration of a municipal government. A total of 350 questionnaires were distributed, 335 valid questionnaires were recovered, and the questionnaire recovery rate was 95.7%. Among them, 300 self-administered questionnaires were distributed to the staff of functional organizations; 50 interview questionnaires were distributed to leading cadres. The processing of the questionnaire data adopts Visual FoxPro, Excel, and other software for statistical verification.

The basic idea of the paired sample t test is to set the population X_1 to obey the normal distribution $N(\mu_1, \sigma_{12})$, and the population to obey the normal distribution $N(\mu_2, \sigma_{22})$, samples $(x_{11}, x_{12}, \dots, x_{1n})$, and $(x_{21}, x_{22}, \dots, x_{2n})$ are drawn from these two populations, respectively, and the two samples are paired with each other. It is required to test whether μ_1 and μ_2 are significantly different. Specific steps are as follows:

- (1) Introduce variables

Introduce a new random variable $Y = X_1 - X_2$, the corresponding sample value is (y_1, y_2, \dots, y_n) , where $y_i = x_{1i} - x_{2i}$ ($i = 1, 2, \dots, n$).

- (2) Establish the assumption as follows (1)

$$H_0: \mu_Y = 0. \quad (1)$$

- (3) Calculation formula and meaning

$$t = \frac{\bar{y}}{s_y / \sqrt{n}} \quad (2)$$

where $\bar{y} = \sum_{i=1}^n y_i / n$ is the mean of the paired sample differences; $S_y = \sqrt{\sum_{i=1}^n (y_i - \bar{y})^2 / (n - 1)}$ is the standard deviation of the paired sample differences; and n is the number of paired samples.

This statistic t follows a t -distribution with $n-1$ degrees of freedom under the condition that the null hypothesis ($\mu_Y = 0$) is true.

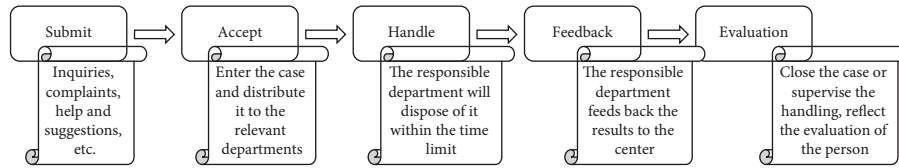


FIGURE 3: Operation process of emergency linkage center.

4.2. Questionnaire Design and Distribution. This questionnaire consists of 25 closed-ended questions and 5 semi-open-ended questions; the main contents include survey on the information communication platform of government departments, a survey on information sharing willingness of various departments and staff, a survey on the overall level of information sharing in a city including public security, finance, human resources, and education systems, and a survey on the influencing factors of information sharing by government functional departments.

4.3. Questionnaire Survey Results

4.3.1. Lack of the Information Integration Platform. Compared with the information sharing platforms owned by the administrative systems of the more developed cities in China (as shown in Table 1 and Figure 4), it can be seen that the number of information sharing platforms in the administrative system of a city is very lacking and can only basically meet the requirements of its jurisdiction. Information sharing needs. The data comparison shows that the public security system with the most information sharing platforms in a city differs by 21 units from the public security system in developed cities. The number of information sharing platforms for information management systems in a city is 30, while that in developed cities is 78, a difference of 48 units. The education system has the least number of platforms in a city's administrative system, with only 9 platforms, the administrative system with the least number of platforms in a developed city is the civil affairs system, with 37 platforms, 28 more than a city. These numerical gaps basically reflect the gap between a city's information sharing hardware and other developed regions in China.

4.3.2. Not Willing to Share Information. Regarding the disclosure and sharing of daily common information of government departments, more than 50% of units or individuals believe that cross-departmental information sharing is necessary and feasible; However, when it comes to the core interests of the department, such as the property of officials and the specific procedures of the disaster relief plan, the vast majority of departments are still opposed.

It shows that despite the background of big data, there are still many departments in the consideration of departmental interests, and reluctance to provide the department's data. In fact, the data are not only the appearance of information gaps between departments but also reveal some hidden reasons behind the reluctance of various departments to share their own departments with

other departments. Based on their own short-term interests, many departments usually treat information sharing in a conservative manner and are unwilling to share their own information and data, which directly leads to the fragmentation and isolation of emergency management information. There are also department leaders or managers who have a relatively shallow understanding of the application of big data technology and are overly worried about the risk of leakage of departmental confidential information caused by information sharing. The deep-seated reason why some departments are reluctant to share information across departments is that the business of this department is completely different from that of other departments, and its powers and responsibilities are irrelevant; therefore, there is a bystander attitude of "everyone sweeps the snow in front of the door, and does not care about the frost on other people's tiles". In addition, based on privacy protection considerations, many government departments are reluctant to take the risk of information leakage due to information sharing and would rather sacrifice convenience than share information [22]. Therefore, in actual operation, the level of information sharing between departments is extremely low; it can be said that the information communication channels between horizontal government departments are not smooth.

4.3.3. The Reasons That Affect the Integration of Emergency Linkage Information Are Complex. According to the survey results of "the reasons that affect the integration of emergency linkage information of a city government" (see Figure 5), the first is the poor information communication channels between departments, accounting for 22.7%. The second and third are "administrative system restrictions" and "protection of the interests of the department," accounting for 21.4% and 19.4% respectively. It is worth noting that the technical problem of information management is also one of the important factors affecting the government's emergency response management, accounting for 19.1%. Obviously, the factors affecting the integration of emergency linkage information of a city government are both objective and subjective, both internal and external. It can be said that the influencing factors are complicated and summed up as follows: China's current government organizations are slightly bloated, with too many management levels and confusing powers and responsibilities, which will inevitably increase the number of information transmission links, which is quite unfavorable for the dissemination of work information; otherwise, the accuracy of many critical emergency information will be affected to varying degrees,

TABLE 1: Number of government information management platforms in some developed cities.

Department name	Number of emergency management platforms (unit: units)	Network equipment	Degree of information sharing
Public security system	63	High quality	General
Financial system	43	High quality	High
Civil affairs system	37	Generally	High
Education system	38	High quality	High
Information management system	78	Premium	High

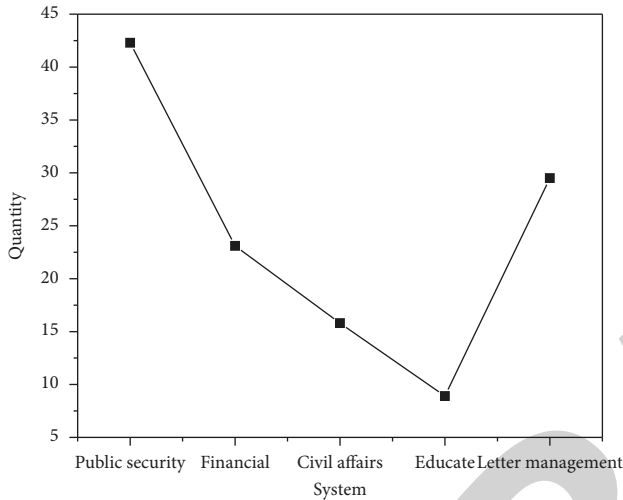


FIGURE 4: The number of some government information management platforms in a city.

which will inevitably affect the management of emergency linkage information and the progress of crisis disposal. There are information gaps between various departments and lack of crisis management mechanism, as a result, the existing emergency linkage management information system faces greater difficulties and challenges, and the theoretical collaborative combat effectiveness has not been fully reflected in practical operations. Furthermore, the top-down one-way one-line communication method is too simple, if all emergency linkage information is top-down one-line communication, the speed of information dissemination will be slow and the feedback information will be less. In addition, in the reporting of crisis accident information, in order to maintain the performance and interests of the department, local government departments usually report lightly or delay reporting, resulting in the dilemma of unbalanced emergency information. Under the management system of the existing traditional government departments, various units and departments of local governments still have difficulties such as lack of unity, information occlusion, and poor management communication and coordination in the public crisis, after forming a pattern of police and civilians, participation in multiple subjects, and multisector linkage; however, in terms of actual operation, it is far from exerting emergency linkage management.

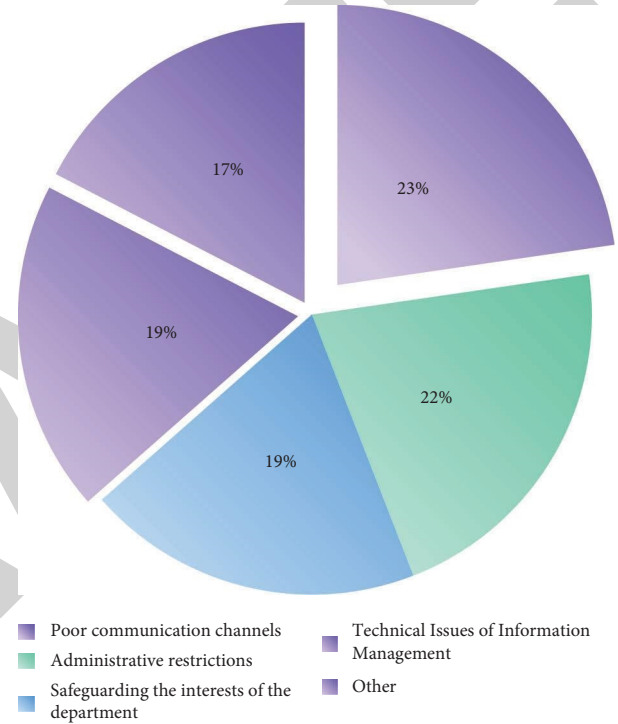


FIGURE 5: A survey of the reasons that affect the integration of emergency linkage information in a municipal government.

5. Conclusion

The use of information technology can promote the unified “big linkage” reform of information flow, workflow, and responsibility flow; there are still some problems in practice, especially in the field of social management difficulties with relatively lagging law and system construction, and cross-responsibilities; some line departments have the responsibility of drilling legal vulnerabilities and “inaction in accordance with the law,” which leads to “connect” in form, but it cannot be “moved” in the solution mechanism of the problem. Second, the integration of human resources is very difficult to be restricted by the interests of the department. We analyze the main disadvantages and reasons of existing sharing models. At the same time, in combination with the application methods of big data in other industries, we analyze the needs of data sharing in the field of emergency management, so as to build a reasonable information sharing work model.

Retraction

Retracted: Construction of Hotel Resource Information Platform Based on the Internet of Things Technology

Mathematical Problems in Engineering

Received 8 August 2023; Accepted 8 August 2023; Published 9 August 2023

Copyright © 2023 Mathematical Problems in Engineering. This is an open access article distributed under the Creative Commons Attribution License, which permits unrestricted use, distribution, and reproduction in any medium, provided the original work is properly cited.

This article has been retracted by Hindawi following an investigation undertaken by the publisher [1]. This investigation has uncovered evidence of one or more of the following indicators of systematic manipulation of the publication process:

- (1) Discrepancies in scope
- (2) Discrepancies in the description of the research reported
- (3) Discrepancies between the availability of data and the research described
- (4) Inappropriate citations
- (5) Incoherent, meaningless and/or irrelevant content included in the article
- (6) Peer-review manipulation

The presence of these indicators undermines our confidence in the integrity of the article's content and we cannot, therefore, vouch for its reliability. Please note that this notice is intended solely to alert readers that the content of this article is unreliable. We have not investigated whether authors were aware of or involved in the systematic manipulation of the publication process.

Wiley and Hindawi regrets that the usual quality checks did not identify these issues before publication and have since put additional measures in place to safeguard research integrity.

We wish to credit our own Research Integrity and Research Publishing teams and anonymous and named external researchers and research integrity experts for contributing to this investigation.

The corresponding author, as the representative of all authors, has been given the opportunity to register their agreement or disagreement to this retraction. We have kept a record of any response received.

References

- [1] Y. Meng, "Construction of Hotel Resource Information Platform Based on the Internet of Things Technology," *Mathematical Problems in Engineering*, vol. 2022, Article ID 4898550, 8 pages, 2022.

Research Article

Construction of Hotel Resource Information Platform Based on the Internet of Things Technology

Yi Meng 

Business School, Lingnan Normal University, Zhanjiang, Guangdong 524048, China

Correspondence should be addressed to Yi Meng; 14518095@xzyz.edu.cn

Received 16 June 2022; Accepted 26 July 2022; Published 22 September 2022

Academic Editor: Hengchang Jing

Copyright © 2022 Yi Meng. This is an open access article distributed under the Creative Commons Attribution License, which permits unrestricted use, distribution, and reproduction in any medium, provided the original work is properly cited.

In order to meet the expectations and needs of hotel managers and hotel occupants, the author proposes a smart hotel system based on the six-domain model of the Internet of things. The system has designed the intelligent hotel guest control unified management cloud platform in detail, including hotel management, guest room management, equipment management, scene management, authority management, system management, Tmall wizard docking, WeChat applet interface, and MQTT client; we design a smart hotel room controller (RCU) hardware system based on Espressif ESP32 (WiFi Soc) and realize centralized management and control of curtains, lamps, air conditioners, and other equipment in hotel rooms; RCU connects to the MQTT server through WiFi and exchanges and controls data with the cloud intelligent platform by means of message subscription and publishing. At the same time, the equipment set of RCU can be arbitrarily cut and added according to the actual hotel scene, and the logic control function can be reconstructed and designed according to the user's personalized requirements. In addition, considering the edge-cloud computing processing scheme, the framework of the system is designed and the software to simulate the edge-cloud computing system is finally used; the system simulation results show that the total failure rate of the edge-cloud computing structure is less than 5%, and the processing time of the task is relatively short. *Conclusion.* It can meet the needs of diversified application scenarios of smart hotels.

1. Introduction

With the rapid development of Internet technology, various industries all over the world have changed due to the Internet; for example, in the tourism and travel industries, many Internet companies have emerged, for example, Huazhu Group, Ctrip.com, eLong.com, and other well-known companies; the Internet has changed the tourism and travel industries. On the basis of that, the Internet has also affected the traditional hotel industry; it can be said that from the 1990s to the present, the hotel industry has seen the biggest changes in millennia and has also expanded rapidly in size. Due to the rapid expansion of the hotel industry in recent years, there is currently a very fierce competition in the industry; as a result, a large number of budget hotels were born in the country, which further stimulated the competition in the industry; therefore, there is a saying that “running a hotel is the least profitable business”. Indeed, the

hotel has very little profit after removing operating costs, rent, shop assistants, etc. In addition, the hotel density is too high and the passenger flow is limited; hence, the situation of the industry needs to be changed urgently [1].

Major group companies have also seen the situation in the industry, so they have launched their own high-end hotels to change the fate of traditional economy hotels. The most typical domestic hotel is the Orange Crystal Hotel, which is a design hotel, where the intelligent control system of the guest rooms is unique, so the hotel can be quickly promoted in China [2]. In recent years, due to the continuous development of the Internet of things technology, many intelligent control systems have appeared, such as the Internet of things remote control technology and smart home control systems in recent years [3]. At present, this type of technology has been applied maturely, and it is applied in many industries, such as high-end apartments, high-end hotels, and villas, as shown in Figure 1.

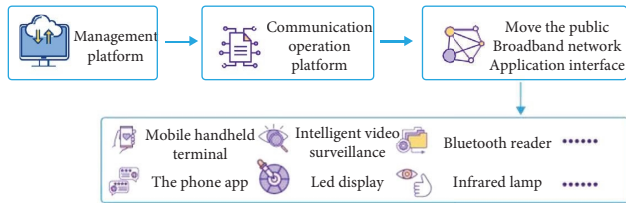


FIGURE 1: Hotel resource information platform based on the Internet of things technology.

2. Literature Review

The Internet of Things technology has gradually improved the hotel service level, which provides technical conditions for effective integration of tourism resources. The application of Internet of Things technology in the construction of smart hotels mainly includes online booking, passenger check-in, and check-out. In addition, it also includes hotel registration, intelligent guidance, room application, electronic restaurant, online landscape, leisure and entertainment, one click check-out, and online evaluation. Din and Paul defined the connotation of intelligent hotel: through a complete intelligent system, the hotel will digitalize, intelligentize and network the operation, management and service, so as to achieve personalized, humanized service, and efficient management of the hotel [2]. Through research, it is believed that the era of big data promotes the transformation and upgrading of the hotel industry; with the development and application of smart hotels, hotel management will adopt a new model suitable for it [4]. Xie et al. believe that the construction of smart hotels is a new idea for the development of contemporary hotels under the Internet thinking [5]. Shi and Zhou studied a smart hotel system based on ZigBee wireless sensor technology, through which the hotel's smart control can be realized [6]. Barnawi et al. believes that smart hotels should be promoted in three following areas: smart management, smart service, and smart control; the three levels form a cross-dimensional smart space with each other, covering not only the application of new technologies such as the Internet of things, data analysis, and control engineering but also new business models [7].

With the development of the Internet of things technology, a multifunctional smart hotel control system is created more and more in line with the expectations and needs of hotel managers and hotel occupants. In view of this, this paper refers to the design idea of the top-level architecture of the six-domain model of the Internet of things and builds a smart hotel system based on the six-domain model of the Internet of things.

3. Research Methods

3.1. The Six-Domain Model of the Internet of Things. In 2018, the international standard "Internet of Things Reference Architecture" (ISO/IEC30141 : 2018) led by my country was officially released [8]. The reference architecture is shown in Figure 2, which includes the user domain, the resource

exchange domain, the service provision domain, the operation and maintenance management domain, the perception control domain, and the target object domain [9].

The user domain identifies users of different IoT types, through which the perception and manipulation tasks of actual physical objects can be completed. From the overall classification of users, it can include government users, enterprise users, and public users.

The resource exchange domain realizes the exchange and sharing of information resources between the IoT system and other systems. According to the function, it can be divided into the information resource exchange system and the market resource exchange system.

The service provider domain is based on a large amount of data information on the hardware device side, carries out in-depth data processing and processing, such as cloud computing and artificial intelligence algorithms, and provides various service interfaces for different users in the user domain.

The operation and maintenance control domain manages and ensures the reliability and safe operation of the IoT system and ensures that the corresponding application system complies with legal norms and industry norms.

The perception control domain uses certain technical means to realize the perception and control of the target object; through different perception and execution functional units, the control operation and information collection of the target object are realized. In the prior art, the perception control domain includes sensor network systems, label identification systems, location information systems, audio and video acquisition systems, and intelligent equipment interface systems [10]. Among them, the intelligent equipment interface system has the functions of communication, protocol conversion, data processing, etc.; in practical applications, the intelligent equipment interface system can be integrated into the target object.

The target object domain, that is, the "object" of the Internet of things that the Internet of things users are concerned about; it is the source of constructing a new value that is different from traditional products and services, the source of information resources in the perception and control domain, and the entity collection of information acquisition and control objects (including perception objects and control objects). The sensing object and the control object can adopt the way of communication interface or noncommunication interface, associated with the perception control domain, implementing the interface binding between the physical reality and the virtual world.

3.2. Design of Smart Hotel Systems Based on the Six-Domain Model. Based on the above design principles of the six-domain model of the Internet of things, a smart hotel system based on the Internet of things technology is constructed according to the standard structure of the system. Compared with the traditional hotel management system, the smart hotel includes the basic functions of the traditional hotel PMS (hotel management system) system, it has also added functions that allow passengers to go through a series of

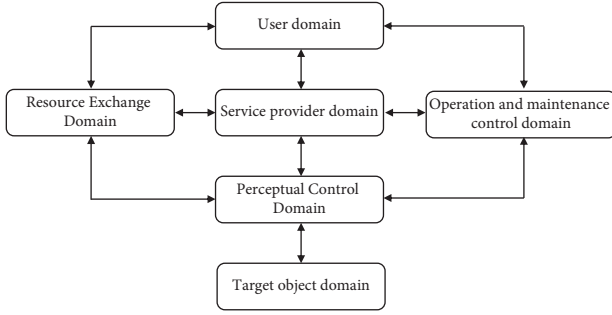


FIGURE 2: Internet of things system reference architecture.

procedures such as self-check-in, room selection, and check-out through WeChat, APP, official account, and other means. Providing the intelligent guest control system for diversified scene setting and user habit setting, customers can control room lights, curtains, air conditioners, etc., through the AI voice recognition, APP operation, and other means, providing customers with tailor-made personalized service, greatly improving the check-in experience. Since the customer needs to monitor the equipment in the room in real time, the power consumption of the room equipment is detected and intelligently controlled through the intelligent algorithm, so as to achieve the effect of energy saving, emission reduction, and operation cost reduction. The intelligent hotel system can connect data with third-party food, entertainment and transportation systems, and conduct targeted marketing through big data to expand hotel marketing channels and reduce marketing costs while increasing hotel operating revenue [2].

3.3. The Edge Cloud Computing Solution. Compared with the cloud computing structure, the edge computing layer is introduced between the cloud center computing layer and the terminal node layer. The process of data uploading first passes through the edge layer and then transmits to the cloud center. For the top layer, it can be seen as decentralizing computing power [11]. We extend the original central infrastructure into a star, as shown in Figure 3.

Channels vary from layer to layer. Between the cloud center computing layer and the edge nodes, the wired WAN connection is usually used, and between the edge computing layer and the terminal node layer, there are various short-distance wireless connection methods, for example, WiFi, ZigBee, Bluetooth, and other connection methods, because the physical location is relatively close, usually an edge node, and its lower terminal nodes form a local network.

Each part of the execution process of edge computing can be modularized. The entire edge computing process is abstracted into a core computing module, a task output module, an edge coordination module, and a network transmission module; the 4 modules together constitute the edge computing model. The relationship between modules is shown in Figure 4. Among them, the core computing module includes edge nodes and cloud centers, which are mainly responsible for performing cloud tasks, and the core module includes edge computing modules and core

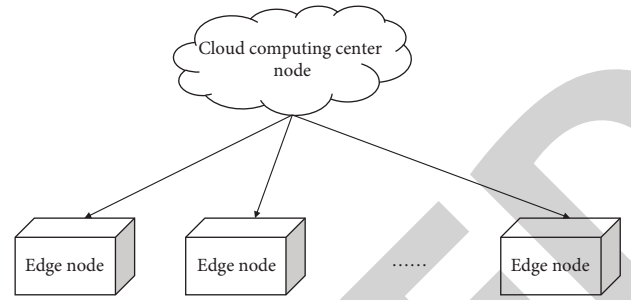


FIGURE 3: Star diagram of the edge computing node structure.

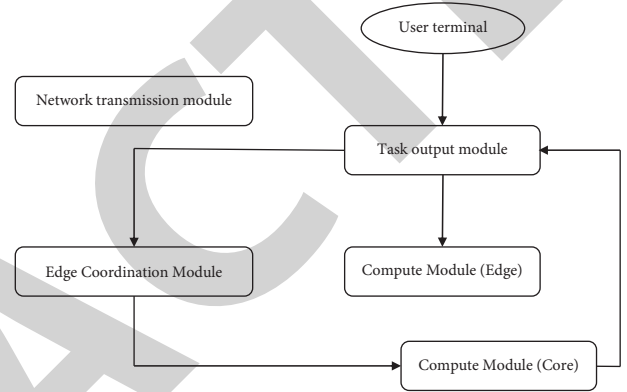


FIGURE 4: Flowchart of processing between modules.

computing modules. The task generation module is responsible for randomly generating tasks to be executed. The edge coordination module is responsible for decision-making; this layer decides how edge tasks are allocated and which host performs the tasks; although the computing power of edge devices is not comparable to that of central cloud devices, they can still undertake a small number of cloud tasks within the framework. The network transmission module is responsible for the process of network transmission, including the upload and download of processing tasks, and the WAN network has high latency and limited bandwidth, while the LAN network has low latency and high bandwidth [12].

The author introduces a long short-term memory network (LSTM), which can effectively use the characteristics of the data information before and after, the variable composition sequence is fed into the LSTM for training. The LSTM realizes the protection and control of information through 3 gates. These three gates are input gate, forget gate, and output gate. The update of each gate is as follows [13]:

$$f_i = \sigma(W_f \cdot [h_{t-1}, x_t] + b_f), \quad (1)$$

$$i_i = \sigma(W_i \cdot [h_{t-1}, x_t] + b_i), \quad (2)$$

$$o_i = \sigma(W_o \cdot [h_{t-1}, x_t] + b_o). \quad (3)$$

In the formula, f_i is the input gate; i_i is the forgetting gate; o_i is the output gate; W and b are the weights and offsets

of the corresponding threshold layers, respectively; and σ is the sigmoid activation function.

3.4. Design of Guest Control Systems for Smart Hotels

3.4.1. Cloud Intelligent Platform Design. We build a cloud-based intelligent platform to realize intelligent, automated, and unified management of hotel room guest control systems, including hotel management, room management, equipment management, scene management, authority management, system management, Tmall wizard docking, WeChat applet interface, and MQTT client. The RCU controller connects to the MQTT server through WiFi, so that the RCU and the cloud intelligent platform can subscribe and publish messages through, realize interaction, and control functions. The cloud intelligent platform follows the third-party docking protocol standard, connect third-party smart products to the system platform, and can bind and control the RCU system in each room, realizing the free expansion of third-party intelligent products, such as docking with Tmall Genie to realize the AI voice control of various devices in hotel rooms. The user management module is designed to implement hierarchical authority management for hotel personnel, system administrators, and hotel check-in users. The API extension interface provides user APP, WeChat applet, and docking PMS [14].

The business process of the cloud intelligent platform system [15, 16] (as shown in Figure 5) is as follows:

- (1) Log in to the system administrator account, create a hotel, for example, create a Hanting Hotel, save, and exit.
- (2) Log in to the hotel management system account, select the Hanting Hotel created in the previous step, and log in to the hotel management account.
- (3) Create room types, for example, the hotel contains double room, standard room, etc. The RCU devices corresponding to different room types contain different sets of devices, and the RCU logic modules need to be reconstructed and configured, generate matching RCU device sets, and control logic.
- (4) The user connects the Tmall Genie and the hotel guest control system RCU to the Internet through the WiFi network and open the Tmall Genie APP to bind the corresponding AI speaker. Then, open the background of the smart hotel guest control system, log in to the hotel administrator account, and click on the hotel guest control management interface. Create a room based on the previously saved room type, enter the room number, and bind the room number to the RCU scanned in the system; at the same time, bind the Tmall Genie to the RCU device, configure speech recognition entries and user execution scenarios, and associate with the RCU command; after the configuration is completed, the room is released and saved to the database. The RCU configuration topic is published through the MQTT server, and the RCU receives configuration data by

subscribing to the topic, reconstructs and upgrades local devices and logical devices, and restarts to take effect [17].

- (5) At this point, users who stay in the hotel can control the equipment in the room, such as lamps, curtains, and scenes, through the voice of the Tmall Genie. Hotel users can also log in to the WeChat applet and control the equipment in the room through the mobile terminal interface. Hotel managers can also use the intelligent cloud system background and control and detect the logical state of each device in the room RCU [18].

3.4.2. Smart Room Controller (RCU) Design. In order to meet the personalized customization of smart hotels, as well as diversified scene configurations and applications, it is required that the RCU can also be configured and logically reconfigurable according to customized requirements. In the design, the equipment used in the hotel occasion should be exhausted as much as possible, and each equipment should be atomized according to the equipment attributes and functional events; this atomic equipment will be added and deleted according to the actual needs of the equipment, achieving free expansion. Each atomic device directly constructs the function event dynamic cross table, configures the cross table, and realize the local control logic reconstruction function.

(1) *Hardware Design.* The RCU main control adopts the super cost-effective ESP32 WiFi SOC designed by Espressif. The chip integrates a dual-mode SOC chip for 2.4 GHz WiFi and Bluetooth, and an Ethernet MAC controller for dedicated DMA. Integrated Xtensa® 32 bit LX6 single/dual-core processor, with a computing power up to 600 MIPS and the highest CPU frequency up to 240 MHz, with rich peripheral resources, integrates a maximum of 448 KB ROM and 520 KB SRAM on-chip and support external expansion of a maximum of 16 MB FLASH memory. And software resources support rich routines, such as Modbus routines, and MQTT routines, and can speed up product development cycle. The hardware structure of RCU is shown in Figure 6 [19]. For various hotel room equipment, such as weak current switch panels, light relay panels, door magnets, curtains, house numbers, music panels, through Modbus access, and wireless RF technology, users can access devices in the 2.4 GHz frequency band such as ZigBee and Bluetooth. This design also takes into account the reasons such as wall penetration and signal interference, and uses Sub1G to access wireless devices.

(2) *Software Logic Design.* The RCU software layer consists of Free-RTOS system software package, the WiFi network configuration management process (Smart-Config), the abnormal daemon process, the MQTT client service process, the device management configuration process, the device logic control process, the device table, the device scene table, and the device binding table; it consists of Modbus adapter interface, wireless device adapter interface, and drivers for each

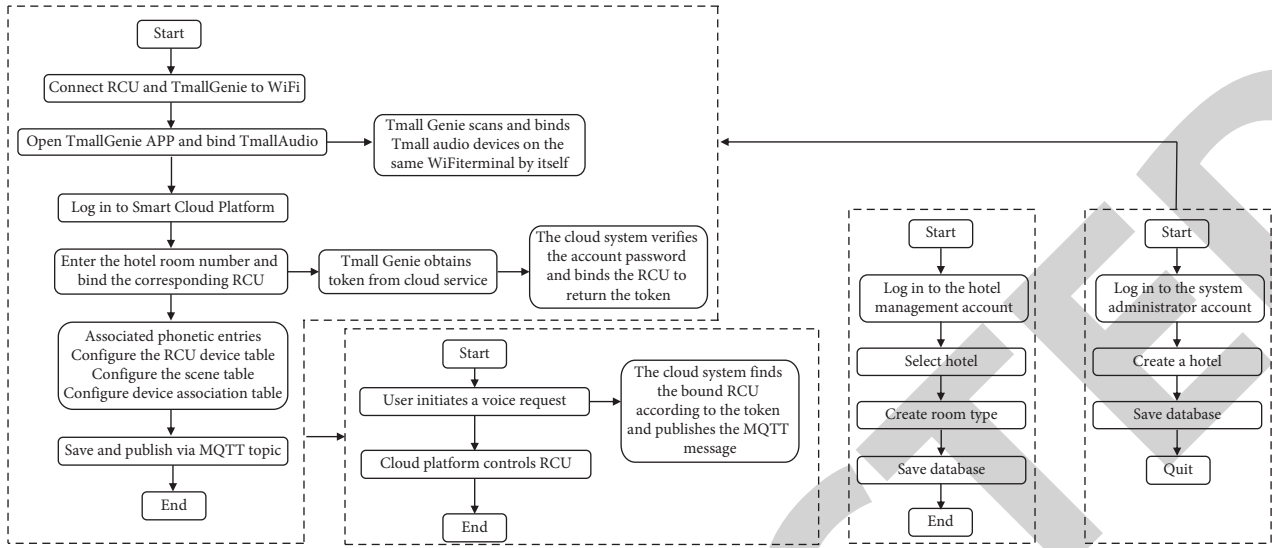


FIGURE 5: The business process of the terminal intelligent platform system.

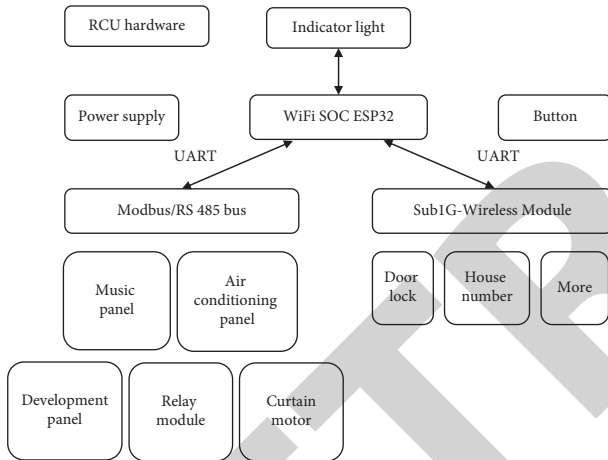


FIGURE 6: RCU hardware structure.

peripheral module (WiFi, KEY, LED, serial port). The MQTT client service process implements the communication between the RCU and the cloud MQTT server, receives control and configuration instructions from the cloud intelligent platform through message subscription and publishing, and performs corresponding device control and device status reporting; the software running process is shown in Figure 7. The device logic control process periodically scans the devices in the system and reads the hardware device status, when the state of a device changes, the process generates corresponding control logic according to the logic of the device table and the device binding table, and publish the upstream message queue of the device status update to the MQTT client service process. At the same time, the process needs to process the downlink message queue from the MQTT client service process, if the received downlink message is a device control command, it will directly control the hardware device, if the received message queue is the device configuration, the device configuration management process will be started to modify and logically reconstruct the local device. The abnormal daemon will monitor and control the

above processes, and once an abnormal error occurs, the corresponding error handling mechanism will be triggered to ensure the stability of the system.

(3) *Main Controller Module Circuit Design.* In the PCB of electronic products, the lower layer is the reference plane, and the upper layer is a circuit board model of a transmission line type called a microstrip line. The copper thickness, linearity and green oil thickness of the transmission line, the dielectric thickness between the bottom surfaces, and the dielectric parameters of the circuit board uniformly determine the value of the characteristic impedance of the microstrip line. The bottom copper layer is the reference plane of the transmission line, which can be a ground plane or a power plane. The recommended calculation formula of microstrip line parameters is shown in

$$Z_0 = \left\{ \frac{87}{[\text{sqrt}(Er + 1.41)]} \right\} * 1n \left[\frac{5.98H}{(0.8W + T)} \right]. \quad (4)$$

Among them, W is the line width, T is the copper thickness of the trace, H is the distance from the trace to the reference plane, and Er is the dielectric constant of the PCB board material. The formula for calculating the total current flowing through the previous loop is shown in

$$I_1 = \frac{((VISO1+) - Vf)}{(3.3K) = 6.9ma}. \quad (5)$$

Therefore, the passing current of the front-end loop is 6.9 ma, and the transmission ratio of the front-end stage is 6.9 ma.

4. Analysis of Results

4.1. *Simulation Description.* EdgeCloudSim is a simulation environment simulation software for edge scenarios based on CloudSim, which can effectively simulate actual scenarios, building multiple data centers, virtual machines, and simulating users and user tasks can also modularize workflows.

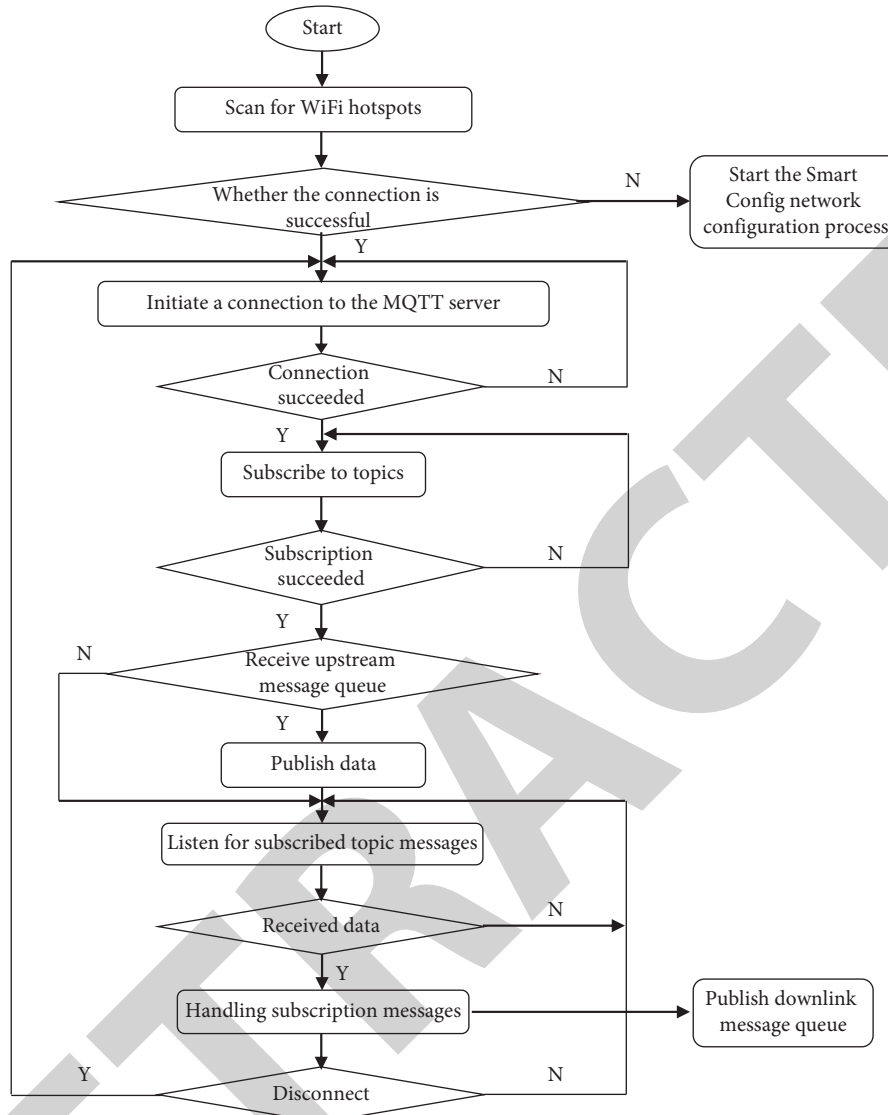


FIGURE 7: RCU software design process.

In EdgeCloudSim, there are 3 transport structures for internal structure settings, denoted as single-layer, multi-layer, and multilayer structures with edge arranger [20]. Among them, the single-layer structure means that the information cloud task only runs in the area of the edge server; The multilayer structure means that cloud tasks can be uploaded to the common cloud platform; the multilayer structure with edge orchestrator can also offload single-layer tasks to adjacent edge nodes. For the first task, simulating the face recognition task. In the actual situation, the camera terminal at the door of the room collects images, stores and initiates a request for face recognition, and can perform operations such as opening the door and alarming according to the recognition result. The computing tasks under the three structures are simulated respectively, and the results are statistically processed. It is set that the task needs to upload the face image to be recognized, the image size is 1 500 kB, and the task recognition result needs to be returned at the same time, where the data size is 15 kB. The

second task is the information task, the upload data is 25 kB, and the download data is 20 kB.

4.2. Simulation Result Analysis of Face Recognition Task.

After the simulation of EdgeCloudSim, the simulation results are shown in Figure 8. Experimental results The X -axis represents the number of devices, the Y -axis represents the feedback results of the tasks performed, and the two curves represent two different transmission structures. By analyzing the simulation results, the characteristics of the edge-cloud computing system are given. It should be noted that under the single-layer structure, tasks will only be submitted to edge nodes, and will not be uploaded to cloud computing via WAN network [21].

Figure 8 shows the task failure rates in face recognition applications under different architectures. It can be seen that with the increase of the number of devices, especially after more than 200 devices, the task failure rate of the single-layer

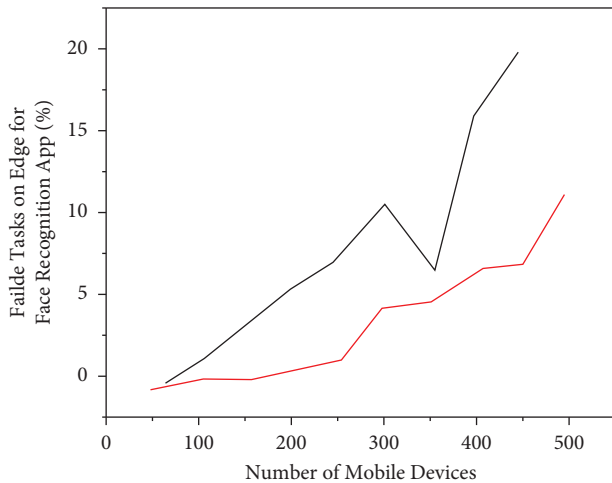


FIGURE 8: Failure rate of face recognition cloud tasks.

and double-layer structure will increase significantly. The analysis shows that the high probability of task failure occurs on the LAN side, which is due to the limited performance of edge devices, the virtual machine used to process the task was unable to process the received task, causing the task to fail. From this, it can be seen that, the processing power of the virtual machine is a key factor in determining the probability of mission failure. Correspondingly, in a structure with an edge orchestrator, since it is possible to decide how to allocate tasks according to the utilization of the virtual machine of the local edge node, that is, whether to allocate it to an idle edge node or upload it to the cloud. Under this structure, if the number of devices increases, the failure rate of the task can still be maintained at a very low level, and the total failure rate is less than 5% [22, 23].

In terms of processing time, since the virtual machine performance of the central node is better than that of the edge, the processing time of the task is also relatively short. For the single-layer structure, the processing delay is all concentrated in the edge nodes. It can also be noticed that with the increase of the number of devices, the processing time of the single-layer structure and the two-layer structure increases rapidly, and there are certain difficulties in dealing with multiple tasks, this is also in line with the increase in processing equipment, reasons for the increase in task failure rate in single- and two-layer structures. Comparing the task processing time of the two-layer structure and the two-layer structure with edge orchestrator, it can be seen that the structure with edge orchestrator can offload tasks to other edge nodes, the overall processing latency is better than the two-layer structure [24–26].

5. Conclusion

The smart hotel system based on the six-domain model of the Internet of Things realizes the intelligent and unified management of the hotel system through the cloud intelligent platform, including hotel management, guest room management, equipment management, scene management, authority management, system management, Tmall Genie

docking, WeChat applet interface, and MQTT client. The emergence of edge computing has broadened the application scenarios for cloud computing, and the edge side allows some cloud tasks to be processed locally, the transmission delay is shortened, the processing time of the task is reduced, and a good running environment can be provided for delay-sensitive applications. Hotel users can control room lights, curtains, air conditioners, etc. through WeChat applet, cloud background, AI voice recognition, and other means, and provide customers with tailor-made personalized scene services, greatly improving the check-in experience; In addition, the unified management platform can also help hotel managers to complete the management of the daily operation of the hotel more conveniently, saving human and financial costs.

Data Availability

The data used to support the findings of this study are available from the author upon request.

Conflicts of Interest

The author declares no conflicts of interest.

References

- [1] B. Prakash and V. Viswanathan, "Distributed cat modeling based agile framework for software development," *International Journal of Engineering Education*, vol. 2, no. 1, pp. 20–32, 2020.
- [2] S. Din and A. Paul, "RETRACTED: erratum to "Smart health monitoring and management system: toward autonomous wearable sensing for Internet of Things using big data analytics [Future Gener. Comput. Syst. 91 (2019) 611–619]"", *Future Generation Computer Systems*, vol. 108, pp. 1350–1359, 2020.
- [3] C. Chellaswamy, R. Ganesh Babu, and A. Vanathi, "A framework for building energy management system with residence mounted photovoltaic," *Building Simulation*, vol. 14, no. 4, pp. 1031–1046, 2021.
- [4] W. Kang, Y. Zhao, X. Jia, L. Hao, L. Dang, and H. Wei, "Paraffin/sic as a novel composite phase-change material for a lithium-ion battery thermal management system," *Transactions of Tianjin University*, vol. 27, no. 1, pp. 55–63, 2021.
- [5] P. Xie, J. M. Guerrero, S. Tan, N. Bazmohammadi, and Y. Al-Turki, "Optimization-based power and energy management system in shipboard microgrid: a review," *IEEE Systems Journal*, vol. 16, no. 99, pp. 1–13, 2021.
- [6] Y. Shi and Y. Zhou, "Gene extraction of leizhou kiln porcelain patterns based on safety internet of things and its application in modern design," *IETE Journal of Research*, vol. 2021, no. 3, pp. 1–8, 2021.
- [7] A. Barnawi, P. Chhikara, R. Tekchandani, N. Kumar, and B. Alzahrani, "Artificial intelligence-enabled internet of things-based system for covid-19 screening using aerial thermal imaging," *Future Generation Computer Systems*, vol. 124, pp. 119–132, 2021.
- [8] P. Zinn-Justin, "Six-vertex model with domain wall boundary conditions and one-matrix model," *Physical Review A*, vol. 62, no. 3, pp. 3411–3418, 2000.

Retraction

Retracted: Distributed 3D Environment Design System Based on Color Image Model

Mathematical Problems in Engineering

Received 8 August 2023; Accepted 8 August 2023; Published 9 August 2023

Copyright © 2023 Mathematical Problems in Engineering. This is an open access article distributed under the Creative Commons Attribution License, which permits unrestricted use, distribution, and reproduction in any medium, provided the original work is properly cited.

This article has been retracted by Hindawi following an investigation undertaken by the publisher [1]. This investigation has uncovered evidence of one or more of the following indicators of systematic manipulation of the publication process:

- (1) Discrepancies in scope
- (2) Discrepancies in the description of the research reported
- (3) Discrepancies between the availability of data and the research described
- (4) Inappropriate citations
- (5) Incoherent, meaningless and/or irrelevant content included in the article
- (6) Peer-review manipulation

The presence of these indicators undermines our confidence in the integrity of the article's content and we cannot, therefore, vouch for its reliability. Please note that this notice is intended solely to alert readers that the content of this article is unreliable. We have not investigated whether authors were aware of or involved in the systematic manipulation of the publication process.

Wiley and Hindawi regrets that the usual quality checks did not identify these issues before publication and have since put additional measures in place to safeguard research integrity.

We wish to credit our own Research Integrity and Research Publishing teams and anonymous and named external researchers and research integrity experts for contributing to this investigation.

The corresponding author, as the representative of all authors, has been given the opportunity to register their agreement or disagreement to this retraction. We have kept a record of any response received.

References

- [1] K. Huai, L. Ni, M. Zhu, and H. Zhou, "Distributed 3D Environment Design System Based on Color Image Model," *Mathematical Problems in Engineering*, vol. 2022, Article ID 9268632, 6 pages, 2022.

Research Article

Distributed 3D Environment Design System Based on Color Image Model

Kang Huai ^{1,2,3}, Longjiao Ni,¹ Miaomiao Zhu,¹ and Huihui Zhou¹

¹College of Art and Design, Huainan Normal University, Huainan 232038, Anhui, China

²School of Arts, Southeast University, Nanjing 211189, Jiangsu, China

³School of Arts, Shandong University of Technology, Zibo 250000, Shandong, China

Correspondence should be addressed to Kang Huai; 1700210516@stu.sqxy.edu.cn

Received 27 July 2022; Accepted 8 September 2022; Published 22 September 2022

Academic Editor: Hengchang Jing

Copyright © 2022 Kang Huai et al. This is an open access article distributed under the Creative Commons Attribution License, which permits unrestricted use, distribution, and reproduction in any medium, provided the original work is properly cited.

In order to improve the effect of distributed 3D interior design, a distributed 3D interior design method based on color image model is proposed in this paper. In this paper, the author uses the distributed feature information fusion method to construct the color image model of the distributed 3D interior design, and carries out edge contour detection and feature extraction for the distributed 3D interior spatial distribution image. The RGB color decomposition method is used to decompose the color pixel features of the three-dimensional indoor spatial distribution image. Combined with the three-dimensional point cloud feature reorganization method, the color space reconstruction of the distributed three-dimensional interior design is realized, and the optimal combination of color features of the distributed three-dimensional interior design is realized. Based on the design of image and color processing algorithm, the development and design of distributed 3D interior design system is carried out based on virtual reality and visual simulation technology. The 3D modeling of distributed 3D interior design is carried out using 3ds max, and the indoor hierarchical structure design is realized using the modeling software Multigen Creator. The experimental results show that, according to the color information fusion results, the distributed 3D interior design optimization is realized. Compared with the traditional manual design method, the root mean square error of this method is greatly reduced from 0.232 to 0.023, and the time cost is 82.8% faster. This method has a better visual effect and strong feature expression ability. *Conclusion.* The visual effect of distributed 3D interior design with this method is good, the error is small, and the visual expression ability is strong.

1. Introduction

With the continuous development of computer science and technology, it has a certain impact on people's normal lives. In addition, computer science and technology have changed the methods of traditional architectural design, especially with virtual reality technology (VR), which has become the most likely technology to change the world in the 21st century. Virtual reality technology integrates computer graphics and artificial intelligence to provide users with realistic images, sounds, and virtual environment simulation, so that users can truly feel integrated into the physical environment [1]. Generally, a realistic and real three-dimensional simulation environment is created through interactive software and hardware, and then the user can touch the environment like the real environment by using body

movement. Virtual technology also has good real-time immersion and interaction, providing people with the same virtual world as in the real world. In architectural design, architectural engineers can show their works through 3D virtual world. Virtual reality technology can not only fully show the new expression, but also change the methods and concepts of architectural design. At present, virtual reality technology is widely used in the field of architecture, especially in the fields of interior design and decoration [2, 3]. Designers and customers can feel the indoor layout through indoor reality technology, decorate the virtual room with their own ideas, and change their position in the virtual room to observe the design effect.

Mohammadi et al. and others, the organic combination of architectural landscape design and virtual reality technology is analyzed, the key technology for the use of real

technology is separated and written, the process of integration of virtual reality technology into architectural landscape design is learning and discussion, and ultimately the landscape design. A discovery is created. This technology will be used and designed in future architectural landscape designs [4, 5]. Jung and Lee can make full use of the visual method of building design, especially the visual method of building design for different indoor and outdoor environments, which can help them develop the visual method of building design in real-time [6]. A voice-based communication system has been successfully developed in the virtual home environment by Jung and others. Ren et al. and others mentioned that VR technology is no longer a patent in professional fields and laboratories, and VR technology is gradually moving towards people's lives. He analyzed the specific impact of VR technology on future interior design, making the design scheme diversified and comprehensive [7]. Liu and Pan and others discussed the practical application of VR technology in architectural interior design according to the concept and composition characteristics of VR technology [8]. Wang and Liu and others expounded on the advantages of VR technology from the experience of interior design space, the analysis of external environment, and the dynamic comparison of elements [9]. Lammler et al. and others believe that satisfying users' sensory experience is the main role of virtual reality technology in the application of residential interior design. The popularization of this technology has a positive role in promoting the rapid development of the field of architectural interior design [10].

This project provides a color scheme and color décor of an interior space to create a 3D interior design based on virtual machines and decorate the interior with 3D graphics. The distributed 3D visual reconstruction method is used for the 3D design of indoor environment, and the system design is carried out under the virtual reality and visual simulation environment. Using MAYA, 3DS MAX, SoftImage, Light-Wave3D, and other 3D simulation software, the optimal design of a distributed 3D interior design system is realized, and the effectiveness conclusion is obtained through experimental analysis.

2. Research Methods

2.1. Visual Communication Information Collection and Analysis of Distributed 3D Interior Design

2.1.1. Distributed 3D Interior Design Image Sampling. Image segmentation is an important part of image processing and computer vision. In recent years, it has not only been a hot topic in the field of computer vision but has also been widely used in real life. For example, in terms of communication, the contour structure and regional content of the target can be extracted in advance to ensure that the useful information is not lost, and the image can be compressed in a targeted manner to improve the efficiency of network transmission. In the field of transportation, it can be used to extract the contour of vehicles, recognition or tracking, pedestrian detection, etc. In general, all content

related to the detection, extraction, and recognition of objects needs to use image segmentation technology. In order to improve the visual communication information of 3D interior design, the snake algorithm is used to decompose the contour energy of the edges of 3D interior design visualization and processing layers, contents, and modifies data according to product decomposition [11, 12]. The corner distribution Jacobian matrix $J(x, y, \sigma)$ of interior design can be expressed as the following formula:

$$J(x, y, \sigma) = \begin{bmatrix} \frac{\partial P}{\partial x} \\ \frac{\partial P}{\partial y} \end{bmatrix} = \begin{bmatrix} 1 \ 0 \ L_x(x, y, \sigma) \\ 0 \ 1 \ L_y(x, y, \sigma) \end{bmatrix}, \quad (1)$$

where $L(x, y, \sigma) = G(x, y, \sigma) * I(x, y, \sigma)$, $G(x, y, \sigma)$ is the seed point of 3D interior design visual image, and $I(x, y, \sigma)$ is the gray feature of 3D interior design visual image area fusion. According to the histogram decomposition method, the template matching matrix is obtained, which is expressed as the following formula:

$$\mathbf{M} = \begin{bmatrix} \frac{\partial^2 P}{\partial x^2} \vec{N} & \frac{\partial^2 P}{\partial x \partial y} \vec{N} \\ \frac{\partial^2 P}{\partial x \partial y} \vec{N} & \frac{\partial^2 P}{\partial y^2} \vec{N} \end{bmatrix} = \begin{bmatrix} L_{xx}(x, y, \sigma) & L_{xy}(x, y, \sigma) \\ L_{xy}(x, y, \sigma) & L_{yy}(x, y, \sigma) \end{bmatrix}. \quad (2)$$

The continuous 3D reconstruction method is used to detect the edge contour and extract the feature of the distributed 3D indoor spatial distribution image.

2.1.2. Visual Feature Reconstruction. The LBG vector quantization method of the point-to-line model is used to mark the maximum gray value of the image, and the distributed three-dimensional contour feature is extracted to obtain the fusion center of the image as $d(x, y)$. Adjust the numerical value of the broken 3D interior design vector image, subtract the gray pheromone from the image, and obtain the model of the front image of the split image of the 3D interior design, which is described from the following structure:

$$P(\phi) = \int \frac{1}{2} (|\nabla \phi| - 1)^2 dx. \quad (3)$$

Define E^{LBF} as the local template matching item of the image; E_{RGB} is the sampling component of edge pixels. Using the sparse linear segmentation method, the regional fusion template function of 3D interior design visual image is obtained as follows:

$$\text{Data}(x, y, d(x, y)) = |u(x - d(x, y), y) - \tilde{u}(x, y)|^2, \quad (4)$$

where: \tilde{u} represents the reference template image; u represents the image to be reconstructed. Thus, the 3D visual feature reconstruction of interior design is realized [13–15].

2.2. Distributed 3D Interior Vision Optimization

2.2.1. Information Fusion. The network design system creates 3D internal image data to improve the distribution of the necessary. The component data of the measurement of the relationship between the images seen in the 3D interior design division are shown by the following model:

$$\frac{\tau_d u', \tilde{u}}{\tau_d u_{\varphi_{x_0}} \tilde{u}_{\varphi_{x_0}}} - \frac{\tau_d u', \tilde{u}_{\varphi_{x_0}} \tau_d u', \tau_d u_{\varphi_{x_0}}}{\tau_d u_{\varphi_{x_0}}^3 \tilde{u}_{\varphi_{x_0}}}. \quad (5)$$

Introduce the technology of extracting high-quality pixel-by-pixel materials together to enhance the visual image of 3D interior design through the creation of similar effects, the benefits of which are as follows:

$$\frac{\partial}{\partial d} \left(\frac{\tau_d u', \tilde{u}_{\varphi_{x_0}}}{\tau_d u_{\varphi_{x_0}} \|\tilde{u}\|_{\varphi_{x_0}}} \right) = \frac{\tau_d u', \tilde{u}_{\varphi_{x_0}}}{\tau_d u_{\varphi_{x_0}} \|\tilde{u}\|_{\varphi_{x_0}}} - \frac{\tau_d u', \tilde{u}_{\varphi_{x_0}} \tau_d u', \tau_d u_{\varphi_{x_0}}}{\left(\left(\tau_d u_{\varphi_{x_0}} \right)^3 \|\tilde{u}\|_{\varphi_{x_0}} \right)}, \quad (6)$$

where $\tau_d u_{\varphi_{x_0}}$ represents the combination of texture pixel sets, and gradient processing techniques are used to present features using the local space and redesign the broken 3D interior design visuals [16, 17].

2.3. Optimized Color Combination Features. Using the pixel edge conversion method, the segmentation process of the image seen on the 3D internal design division of the pixels is as follows:

$$G = \sum_{r=1}^t \sum_{q=1}^{k_2} W_i^T x_{ir} - W_i^T x_{ir}^2 B_{ir} = \text{tr}(W_i^T H_2 W_i), \quad (7)$$

where

$$H_2 = \sum_{r=1}^t \sum_{q=1}^{k_2} (x_{ir} - x_{ir}^2) (x_{ir} - x_{ir}^2)^T B_{ir}. \quad (8)$$

It represents the grid region eigenvalues reconstructed in different three-dimensional vision. Combined with pixel area segmentation and adaptive function switching method, it uses integrated color combination and three-dimensional interior design optimization.

2.4. System Development and Design

2.4.1. Overall Design. The information transmission model of the distributed 3D interior design system is constructed by using PCI bus technology, the basic entity object of the distributed 3D interior design system is constructed, the local information processing of the distributed 3D interior design system is carried out by using a multi-threaded scheduling method, the virtual reality visual application support layer is constructed by using client/server model, and the research and development of the distributed 3D interior design system is carried out under CCS 2.20 development platform [18]. The overall design structure of the system is shown in Figure 1.

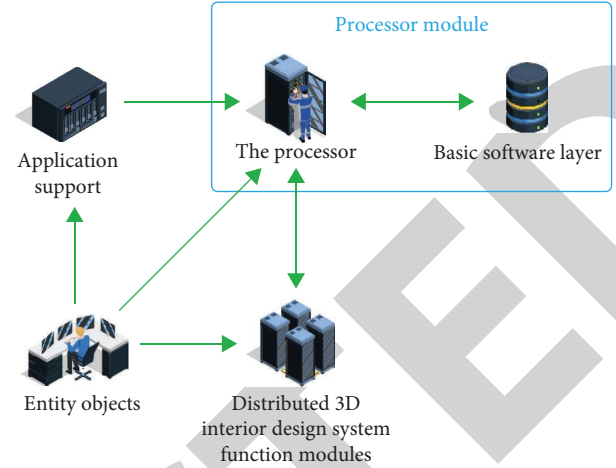


FIGURE 1: Overall design framework of the system.

According to the overall design framework of Figure 1, carry out the modular development design and bus design of the system, and provide executable real-time 3D application files for rendering distributed 3D interior design through the surface hierarchical rendering method. Use Vega Prime API to dynamically change the application loading mode in the process of rendering distributed 3D interior design, use PCI9054 local bus to control program loading, and output 8-way D/a conversion signals at the output terminal to realize the bus adjustment and communication protocol development of the distributed 3D interior design system. The parallel peripheral interface (PPI) is used for man-machine communication, the embedded scheduling of the distributed 3D interior design system is realized in the ARM Cortex-M3 core, the creator interactive design method is used for the cross compilation control and program online reading and writing of the distributed 3D interior design system, and the hierarchical compilation software is constructed. The bus transmission control of the system is carried out in the application layer of the distributed 3D interior design system, and the adaptive forwarding control and link loading control of the distributed 3D interior design system are carried out in the Simulink modeling environment, so as to improve the information sending and receiving and intelligent information processing ability of the distributed 3D interior design system. In the internal bus design of the distributed 3D interior design system, the OpenFlight modeling environment is used for the virtual reality design of the distributed 3D interior design system, and a 3D graphics observer is provided in the compilation software to observe the design effect of the distributed 3D interior design system [19]. To sum up, the development and implementation process of the distributed 3D interior design system designed in this paper is shown in Figure 2.

2.4.2. Design of Indoor Model. Indoor modeling mainly refers to the house type structure model and the models of household appliances and installations. 3ds Max is used as the modeling tool. The created model should meet the following technical requirements:

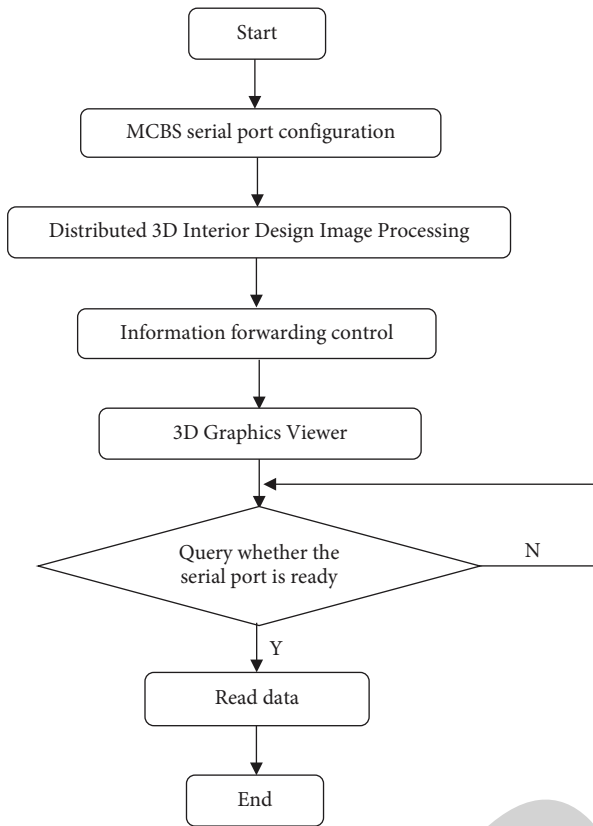


FIGURE 2: Development and implementation process of the system.

- (1) In 3ds max, the setting of 1 unit equal to 1 cm is realized, and the unit is displayed as M. The model is made according to the ratio of 1 : 1, so as to ensure that the experienced personnel can observe the indoor scene in the VR equipment to meet the normal visual ratio. After the model is exported, the data interaction format with unity3d is set to FBX, and the export unit is set to cm, so that FBX can be imported into the model in unity3d, and the scale is set to 1 : 1, so there is no need to realize scaling and matching.
- (2) Using polygons to realize modeling, avoid too many model faces, otherwise the real-time rendering speed will be reduced. After completing the model, check whether it is quadrilateral or trilateral, and also check the normal direction of the model, false solder joints, isolated points, etc. After completion, sort out the historical records.
- (3) In order to display the scene model map, it is generally necessary to realize the UV of the model and make the map with correct UV. The commonly used map types include: diffuse map is mainly reflected in the reflection and color of the object surface, concave convex map can increase the three-dimensional feeling of the model, but will not change the shape of the model; the normal map can define the inclination of the model surface; the height map is a black-and-white map, which defines the height of the model surface; the specular map can show the

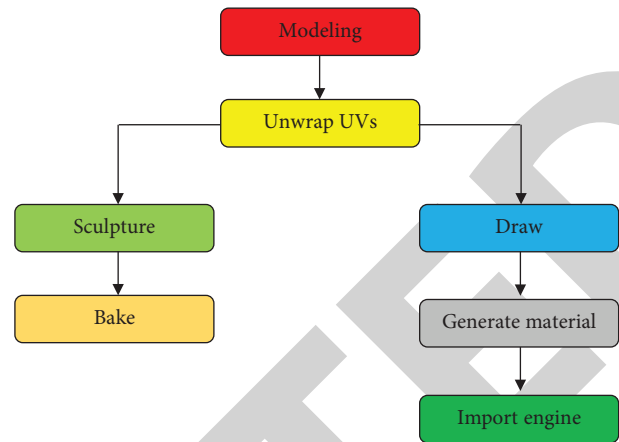


FIGURE 3: PBR material generation process.

surface attribute texture of the model in the light irradiation; and AO map can simulate the distance of each face of the model and realize the generation of ambient occlusion map. This different type of mapping depends on the actual situation. Not all models need mapping [20].

- (4) The map width and length are set to $2n$ pixels, which is convenient for optimization in unity3d.

2.4.3. Use of PBR Technology. In order to improve the authenticity of the model, after the model is imported into unity3D, the light, environment, and materials are processed through physical dynamic rendering technology. Based on the physical rendering to shading and rendering (PBR) method, the current PBR algorithm can directly and indirectly illuminate [21, 22]. The rendering technology of the PBR-based real world lighting physical model simulates the light in a way that meets the laws of physics, improves the authenticity of the rendering effect, directly adjusts the physical parameters, generates a new PBR map, and transmits it to the shader, so as to improve the application scope and work efficiency of the map. Figure 3 shows the generation process of PBR material.

Realize the production of low-precision model in 3ds Max, then unfold the model UV, and input the low-precision model in ZBrush to realize engraving, so as to generate high-precision model. In substance painter, the low-precision model and high-precision model are imported in baked normal map and AO map. The above maps are made in combination with PBR material to realize the generation of SBSAR file. The generation of PBR map can be realized by importing SBSAR file in unity3D.

2.4.4. Interaction Design of Indoor Scene. Virtual reality should be able to provide users with multiple scenes to meet the aesthetic needs of different users in interior design. In order to realize more interactive functions of scenes, scene design is required to have strong selectivity. For example, if the room is not closed and the windows and doors are opened, users can go to the room and look around. By

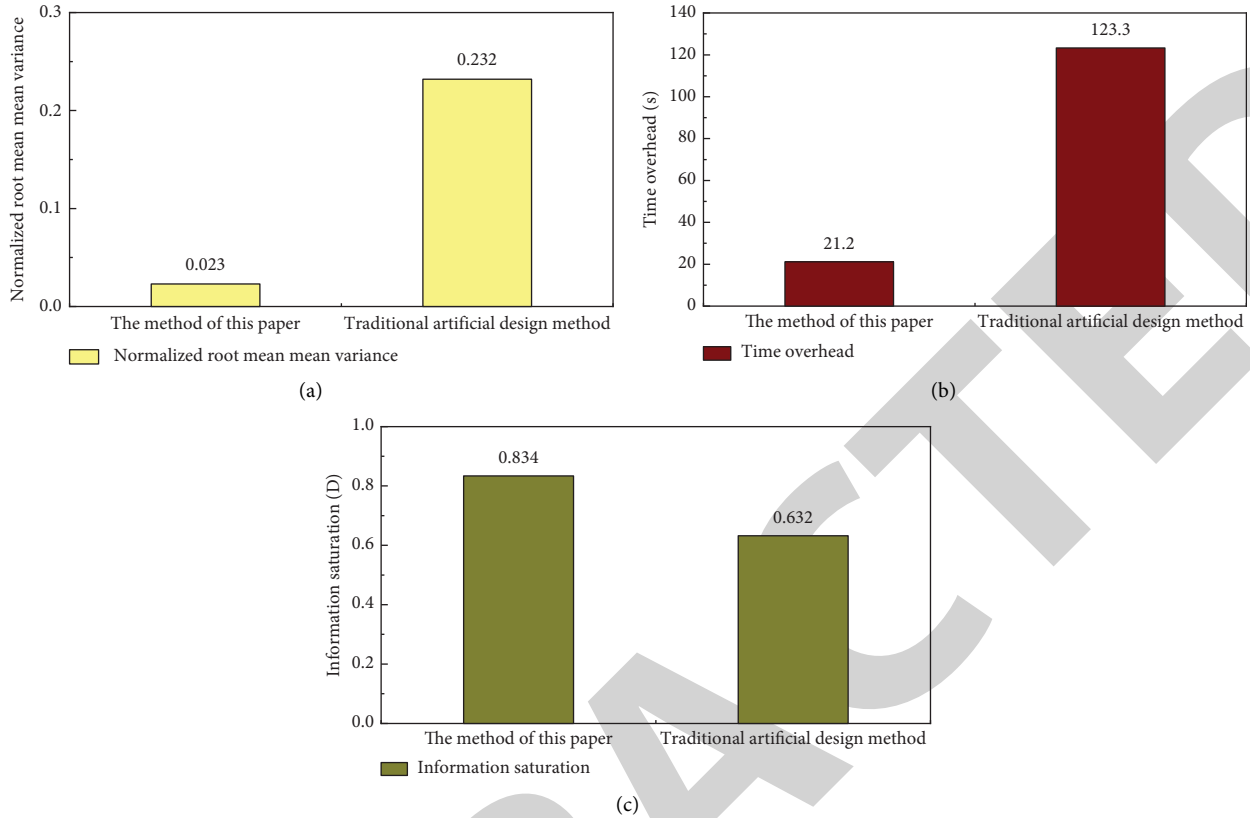


FIGURE 4: Performance comparison test. (a) Normalized root mean square error. (b) Time cost. (c) Information saturation.

changing the wall pattern, users can decide which wall to use according to their preferences. Change the wall pattern and turn on the wall lamp of the room, so that users can fully feel the light and dark of the indoor lamp. Moving the glass of the cabinet in the room can also change the interior decoration and tables and chairs. In order to improve the authenticity of the scene and the infiltration of the virtual environment, the collision detection of three-dimensional scene is realized. Import the model in UDK, and this axis is automatically positioned at the origin of 3ds Max. Therefore, in order to align the position in a short time, the same coordinate is set for all model axis positions in UDK. If there is no collision model in 3D image, automatic collision should be realized in UDK. Automatic roaming mainly includes system default path roaming and crossfield animation. The system automatic roaming is realized through UDK camera animation. The event trigger components in UDK mainly include multi-type automatic trigger and interactive trigger, and the interactive function is realized by using the setting of event trigger [23].

3. Result Analysis

The size of the partition of the 3D interior design visual model is 1200, the area of the 3D visual block area is $256 \times 256 \times 224$, and the coefficient corresponds to the specific design of the interior 3D design is 0.15. Virtual vision simulation software is used in 3D interior design.

TABLE 1: Performance comparison test.

Method	Normalized root mean square error	Time cost/s	Information saturation
Paper method	0.023	21.2	0.834
Traditional manual design method	0.232	123.3	0.632

Combined with the 3D point cloud feature reconstruction method, the color space reconstruction of the distributed 3D interior design is realized, and the optimal combination of color features of the distributed 3D interior design is realized.

The results of the integration of color data show that partition 3D interior design optimizations were achieved, and the square root process error and design time were tested. The results of the comparison are shown in Figure 4. According to the analysis, the square root error decreases from 0.232 to 0.023, and the time value is 82.8% faster. The 3D visualization of the interior design using this method is effective and has the ability to present strong features as shown in Table 1.

4. Conclusion

In order to improve the interior, combine the choice of home appliances and the time of zoning of the interior, improve the interior space and improve the results of

Retraction

Retracted: Application of Wireless Sensor Network Data Fusion Technology in Mechanical Fault Diagnosis

Mathematical Problems in Engineering

Received 8 August 2023; Accepted 8 August 2023; Published 9 August 2023

Copyright © 2023 Mathematical Problems in Engineering. This is an open access article distributed under the Creative Commons Attribution License, which permits unrestricted use, distribution, and reproduction in any medium, provided the original work is properly cited.

This article has been retracted by Hindawi following an investigation undertaken by the publisher [1]. This investigation has uncovered evidence of one or more of the following indicators of systematic manipulation of the publication process:

- (1) Discrepancies in scope
- (2) Discrepancies in the description of the research reported
- (3) Discrepancies between the availability of data and the research described
- (4) Inappropriate citations
- (5) Incoherent, meaningless and/or irrelevant content included in the article
- (6) Peer-review manipulation

The presence of these indicators undermines our confidence in the integrity of the article's content and we cannot, therefore, vouch for its reliability. Please note that this notice is intended solely to alert readers that the content of this article is unreliable. We have not investigated whether authors were aware of or involved in the systematic manipulation of the publication process.

Wiley and Hindawi regrets that the usual quality checks did not identify these issues before publication and have since put additional measures in place to safeguard research integrity.

We wish to credit our own Research Integrity and Research Publishing teams and anonymous and named external researchers and research integrity experts for contributing to this investigation.

The corresponding author, as the representative of all authors, has been given the opportunity to register their agreement or disagreement to this retraction. We have kept a record of any response received.

References

- [1] X. Zhao, Z. Shen, and Z. Jing, "Application of Wireless Sensor Network Data Fusion Technology in Mechanical Fault Diagnosis," *Mathematical Problems in Engineering*, vol. 2022, Article ID 5707210, 8 pages, 2022.

Research Article

Application of Wireless Sensor Network Data Fusion Technology in Mechanical Fault Diagnosis

Xinle Zhao , **Zuhui Shen**, and **Zhisheng Jing**

Xinxiang Vocational and Technical College, Xinxiang, Henan 453000, China

Correspondence should be addressed to Xinle Zhao; 1810300512@mail.sit.edu.cn

Received 10 July 2022; Accepted 6 September 2022; Published 22 September 2022

Academic Editor: Hengchang Jing

Copyright © 2022 Xinle Zhao et al. This is an open access article distributed under the Creative Commons Attribution License, which permits unrestricted use, distribution, and reproduction in any medium, provided the original work is properly cited.

In order to solve the problem that a large number of vibration signals cannot be transmitted in real time in the application of wireless sensor networks (WSNs) in mechanical fault diagnosis, a mechanical fault diagnosis method based on multilevel and hierarchical information fusion of WSNs was proposed. In this method, the cluster tree network structure is used to expand the coverage of network monitoring, and WSNs information fusion is divided into three levels: data-level fusion, feature-level fusion, and decision-level fusion. The terminal node performs data-level fusion on the original vibration information to extract feature information; the cluster-head node performs feature-level fusion on the feature information to obtain pattern recognition results; and the gateway node performs decision-level fusion on the recognition results to evaluate the running status of mechanical equipment. The results show that the slight damage fault of the bearing inner ring can be accurately diagnosed by decision-level fusion based on four groups of probability distribution functions. According to the statistics of 30 test results, the fault recognition rate is 83.3%. The method can be applied to mechanical fault diagnosis effectively.

1. Introduction

Construction machinery plays a very important role in China's manufacturing of equipment. It plays a vital role in infrastructure, mining machinery, transportation engineering, industrial production, and other industries. In the production and operation of construction machinery, it often works for a long time at full load. Traditional construction machinery is generally checked and maintained by engineers and technicians after failure. When the problem is serious, the production of enterprises is often delayed, and there are large hidden dangers to safe operation [1].

The Internet of Things (IoT) is the latest development of the Internet. It is called the Internet of Things, or IOT for short. It means the Internet of everything, and it is based on RFID technology, video recognition technology, infrared sensing, global positioning technology, and laser scanner technology to install all kinds of information sensors on the device and deploy ZigBee wireless sensor network 4G or 5G network internally or externally, according to the standard agreed application protocol to achieve multiple entities for

intelligent identification information exchange and measurement control [2]. An Expert System, whose full English name is Expert System, is the latest technology in contemporary artificial intelligence technology and computer technology integration development. It can focus on the knowledge and experience of domain experts, search their built-in knowledge base according to the questions raised by users, carry out artificial intelligence logic reasoning of various complex algorithms, and finally give reasonable judgement conclusions or relatively correct solutions [3]. Therefore, an expert system has incomparable advantages in the fault diagnosis of construction machinery equipment.

Therefore, combining the Internet of Things technology and expert system technology, an intelligent fault diagnosis expert system for construction machinery equipment has been designed and developed. It can realize the operation of engineering machinery equipment before the failure of early and rapid warning to improve the efficiency of engineering operations, so as to ensure the maximum extent of enterprise safety production, which has very important practical significance.

2. Literature Review

In the field of mechanical equipment fault diagnosis in wireless sensor networks, some researchers have studied this problem. Xueyi studies online remote induction motor energy monitoring and performs intelligent data processing in WSNs instead of direct transmission of original data. Only relevant and necessary information is transmitted to upper computer users, which reduces network communication load. However, the performance and storage capacity of the sensor nodes used are limited [4]. Cao et al. [5] applied a wireless sensor network to vibration monitoring of rotating machinery equipment in a power plant, judged the similarity of vibration data in time series by a data-level fusion algorithm, and decided on the data sending strategy by a task-level fusion algorithm. To reduce the total bandwidth and energy demand, this method is only applicable to redundant data from similar sources and has great limitations [5]. Zhao et al. [6] adopt the star wireless sensor network topology, obtain monitoring signals based on Jennic JN5139 sensor nodes, carry out signal feature extraction and fault pattern recognition on terminal nodes, and only transmit recognition results to gateway nodes. The recognition results are fused on the gateway node to solve the data transmission problem to a certain extent. However, the coverage of star topology is limited, and multitasks such as signal acquisition, feature extraction, and pattern recognition on terminal nodes will lead to a heavy load on terminal nodes. All nodes used are collected independently, and the network and data transmission protocol stack adopted do not support the synchronous acquisition of vibration signals from multiple sensor nodes [6]. Wang et al. [7] adopt a tree-like network topology to obtain vibration signals based on Imote2 wireless sensor network nodes and extract quality parameters and frequency components exceeding the amplitude threshold from sensor nodes. Data fusion is performed on the data fusion node based on quality parameters, and the quality evaluation and fusion results are output. This method promotes the transmission of uncertain information about measured values between the source sensor node and the gateway node, reduces the potential attenuation of acquired or transmitted diagnostic information, and does not consider the synchronous acquisition of vibration signals [7].

In order to increase the coverage of network monitoring and balance the load of sensor nodes, the author adopts a cluster tree network structure to perform hierarchical information fusion for nodes at all levels in WSNs and to evaluate the overall operating status of mechanical equipment by transmitting a small amount of characteristic information instead of a large number of original vibration signals.

3. Research Method

3.1. WSNs's Multilevel Hierarchical Information Fusion Fault Diagnosis Architecture. The mechanical fault diagnosis architecture of WSNs multilevel and hierarchical information fusion is shown in Figure 1, which consists of a gateway node, multiple cluster-head nodes, and terminal nodes to

form a cluster tree network [8]. WSN information fusion can be divided into three levels: data fusion, feature fusion, and decision fusion. The terminal node is responsible for collecting vibration signals and performing a data-level fusion of vibration information to extract feature information. The cluster-head node is responsible for performing a feature-level fusion of feature information of terminal nodes in the cluster to obtain pattern recognition results. The gateway node is responsible for the establishment, management, and maintenance of the whole WSNs, and integrates the d-S evidence theory to express the uncertainty of the identification results at the decision level. It has advantages in measurement and combination, and the artificial neural network has nonlinear processing ability, which can solve the problem of the difficult assignment of basic probability in the D-S evidence theory. At the same time, it has many similarities with WSNs in structure and function and can be well combined with WSNs [9]. Therefore, the cluster head nodes in this architecture are trained to generate the radical Basis Function (RBF) neural network classifier and perform feature-level fusion on the feature set of the terminal node hybrid domain to obtain the pattern recognition results describing the running state of mechanical equipment. Based on d-S evidence theory, the gateway node makes fusion decisions for independent diagnosis results of the cluster-head node and evaluates the overall running status of mechanical equipment.

3.2. Dual-Core WSNs Node Design. WSNs' multilevel hierarchical information fusion requires strong signal processing capability and large enough sample storage space for all sensor nodes in the fusion [10]. The author designs a dual-core sensor node, which uses two independent processing and control cores to control the signal processing unit and the wireless module, respectively, and has a large capacity SD card as the main storage medium to meet the requirements of information fusion.

The dual-core WSNs node design scheme is shown in Figure 2. Core 1 is a low-power STM32f103 microcontroller based on the ARM cortex-m3 kernel running at 72 MHz, utilizing the processor's excellent computing performance and excellent system response to events. It is capable of performing thumb-2 instruction sets including hardware division single-period multiplication and bit-field operations for optimal performance and code size, with 256 kB Flash space and 64 kB internal RAM, allowing the node to easily run more complex algorithms. Transplant μ C/OS-II real time operating system to improve processor utilization, design real time task dynamic priority configuration to ensure real time response and efficient processing of tasks [11]. The Core 2 is an enhanced 8051 microprocessor integrated with the RADIO frequency chip TI CC2430, which supports the IEEE802.15.4 wireless communication protocol and is responsible for completing tasks such as time synchronization and data receiving and receiving in WSNs ad hoc networks.

The dual-core design divides a complex task into multiple subtasks and maps them to a heterogeneous dual-core

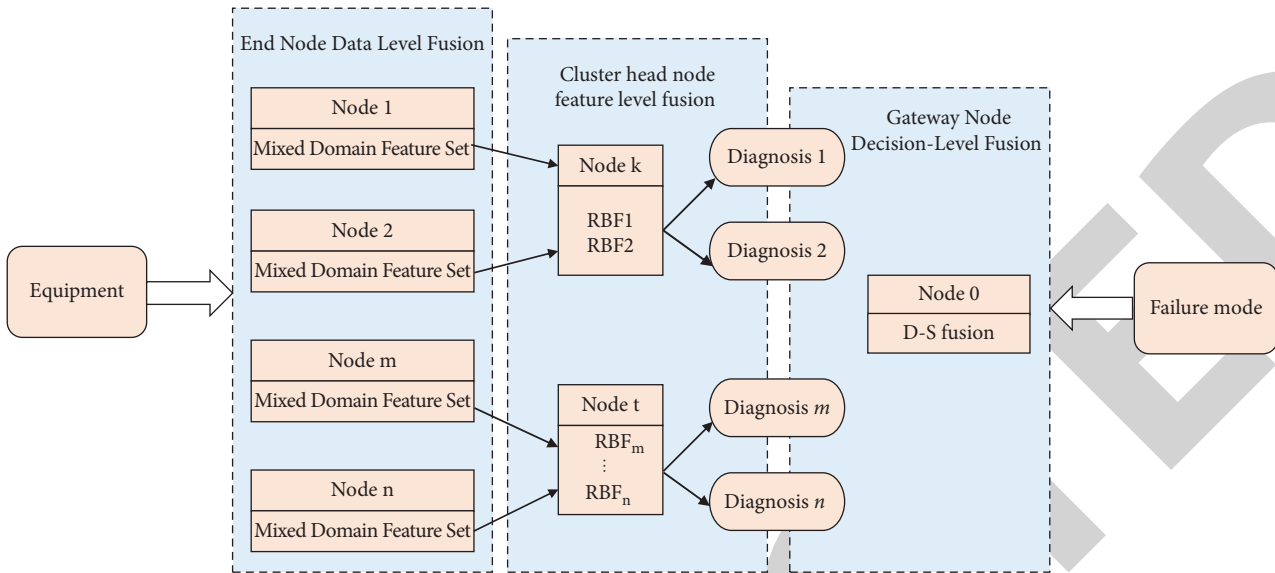


FIGURE 1: WSNs's multilevel hierarchical information fusion fault diagnosis architecture.

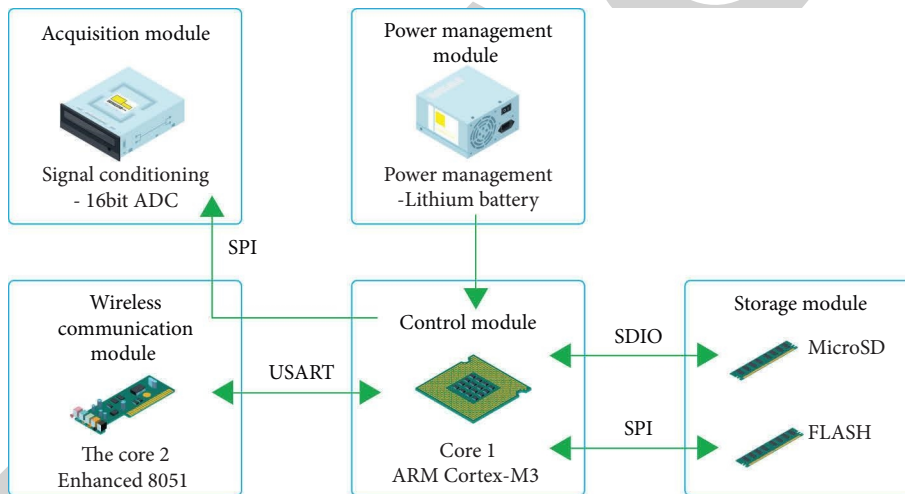


FIGURE 2: Dual core WSNs node.

processor for coordination. It can not only enhance the overall performance of sensor nodes but also reduce the coupling between software and hardware modules, so as to meet the real time processing of node vibration signals and multitask scheduling, such as network communication, without mutual interference [12]. The two cores interact with each other in the form of command packets. When receiving a command packet or a response packet, they first go through the eight-order CRC check. If the check is correct, they perform the corresponding tasks to enhance system stability. The nodes are powered by large-capacity rechargeable lithium batteries with protective circuits.

The WSNs node storage module uses an 8 GB microSD memory card as the main storage medium, and the FAT32 file system is established on the card. A large number of original vibration data and important calculation parameters are stored on the card in the form of files, which is convenient for data retrieval and management. The node with

the method of dynamically allocated memory pool allocation effectively nodes to run efficiently during the execution of a more complex algorithm. A long array can be temporarily stored in the form of a file on an SD card, setting up the dynamic variables in memory space can be used to store other data needed to be immediately operation, effectively easing the node load calculation [13]. The SDIO interface of the cortex-M3 microprocessor is used to read and write microSD memory cards in 4-bit Direct Memory Access (DMA) mode, and the maximum speed can reach 1.5 MB per second, fully meeting the requirements of real-time signal processing on the storage system.

An independent signal processing unit is designed on WSNs nodes to avoid the problems of high cost and high node energy consumption caused by using high-performance microprocessors. Design and develop the real-time preprocessing and common analysis functions for mechanical vibration signal analysis and optimize the algorithm

to form a relatively complete set of high-efficiency and low-complexity embedded function library [14]. The structural block diagram of the embedded function library is shown in Figure 3, which includes 8 modules, including a basic mathematical function module, a statistics function module, a transformation function module, an interpolation operation function module, and a filtering function module, and the corresponding function functions of each module [15].

3.3. Realization of WSNs Information Fusion Fault Diagnosis Method. Due to the limited computing resources and energy of WSNs nodes, the complexity of algorithms needs to be considered in information fusion processing. Time complexity and space complexity are two important characteristics of algorithm complexity as well as two important characteristics for measuring software power consumption, so the author uses these two characteristics to measure the complexity of the node fusion algorithm at all levels. Time complexity is mainly measured by O_s in terms of algorithm average time complexity. The measurement of spatial complexity S_s mainly includes three aspects: the space used by the problem itself, the space used by the program itself, and the space used by dynamic variables [16]. The space used by the problem itself has nothing to do with the algorithm, and the space occupied by the program code has little influence on the spatial complexity of the algorithm, so it is not discussed here, but the memory occupied by the dynamic variables of the measurement algorithm.

3.3.1. WSNs Data-Level Fusion of Terminal Nodes. When mechanical equipment fails, the amplitude and probability distribution of vibration signals will change, and the corresponding spectral components and the amplitude of different spectral peaks will also change. By constructing some quantitative characteristic statistical indexes of mechanical equipment vibration signals in the time domain or frequency domain, the characteristic statistical indexes of various fault modes of mechanical equipment can be represented in the data-level fusion of WSNs nodes and finally selected according to the following criteria: calculate requirements, classification performance, feature domains (time domain, frequency domain, etc.), and the optimal number of features [17]. D feature statistical indexes were selected to form feature sets and used to construct a d -dimensional feature space $x \in R^d$.

Taking the feature extraction of data with a len of 2048 points as an example, the time complexity of node extraction of the statistical index of each time domain feature is $O(1)$, and the memory space occupied by the data involved in the operation is $4 \times \text{len}$ bytes. During the fast Fourier transform, the original vibration signals and characteristic information obtained by the 24 kB node are stored in the SD card in the form of files to save the memory space dynamically opened for the sample input array and transform output array.

3.3.2. WSNs Cluster-Head Node Feature-level Fusion. The cluster-head node receives the feature information sent by the terminal node in the cluster and performs feature-level

fusion as a sample [18]. The algorithm flow is shown in Figure 4.

During the neural network training, h training samples are randomly selected as the clustering center c_i ($i = 1, 2, \dots, h$), and the Euclidean distance between the input training samples x_p and the center c_i . Assign x_p to each cluster set of input samples Ω_p ($p = 1, 2, \dots, P$), calculate the average value of training samples in each cluster set Ω_p , and get the new cluster center c_i . If the new cluster center c_i does not change, get the final base function center c_i of the RBF neural network; otherwise, regroup according to the nearest neighbour rule to get the new cluster center c_i . The Gaussian function was selected as the basis function to solve the variance σ_i . The calculation formula is shown in formula (1) [19]. The weights w between the hidden layer and the output layer are modified by the supervised learning algorithm. The clustering center c_i , variance σ_i and weights w of the trained neural network are saved in file form on the SD card of the cluster-head node.

$$\sigma_i = \frac{c_{\max}}{\sqrt{2h}} \quad (1)$$

c_{\max} is the maximum distance between the selected centers.

The cluster-head node receives the test samples of the terminal nodes in the cluster and determines whether the neural network classifier is generated first. If not, the training sample set on its SD card is read for training to generate the neural network classifier. Otherwise, the neural network parameters in the corresponding files of the SD card are directly read and the test samples are fused at the feature level, and the basic probability assignment (BPA) of each pattern to be identified is obtained by using the neural network generalization ability. Since D-S theory requires the sum of probability distribution functions of each evidence body to be 1, the probability distribution function is normalized by the output results of the neural network, and the following formula (2) is obtained [20]:

$$m(B_i) = \frac{y(B_i)}{\sum_{i=1}^N y(B_i)} \quad (2)$$

$y(B_i)$ is the output result of the neural network classifier; B_i ($i, 2, \dots, N$) indicates the fault of i type. N is the number of fault types to be identified; the probability distribution function $my(B_i)$ is used to further the decision-level fusion.

The time complexity of each function is $O(1)$ in the process of generating a neural network classifier for cluster head node training, and the size of the memory space dynamically allocated to it is determined by the specific size of the network classifier. The training samples and test samples obtained by nodes are stored on SD cards in the form of files. The neural network is used to manage the data in the test stage through the file system, and the memory call strategy is designed to reduce the memory pressure of nodes. The embedded function library is loaded when the node application is written to realize the neural network learning and testing better so that the cluster-head node can realize the feature-level fusion [21].

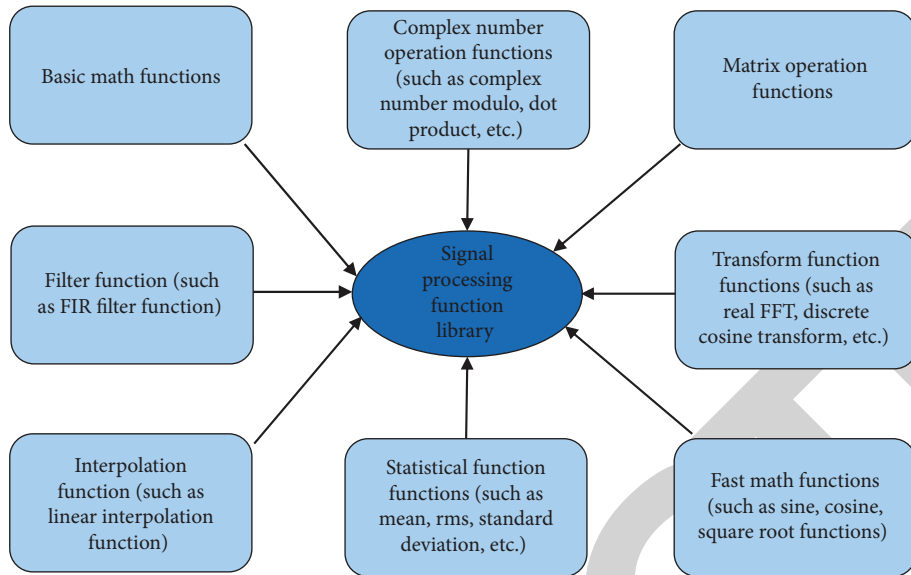


FIGURE 3: Embedded function library structure block diagram.



FIGURE 4: Cluster-head node feature-level fusion algorithm flow.

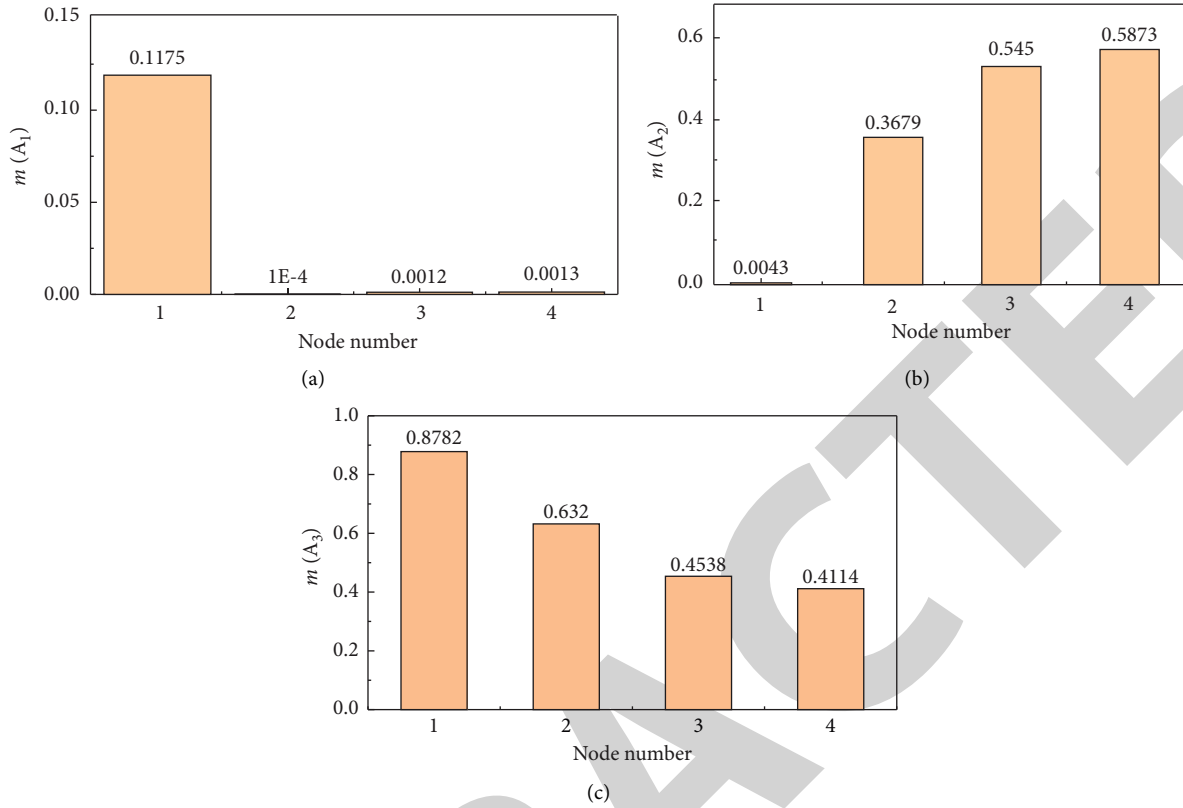


FIGURE 5: Probability distribution and fusion decision result of unknown state of gearbox. (a) $m(A_1)$. (b) $m(A_2)$. (c) $m(A_3)$.

3.3.3. Decision-Level Fusion of WSNs Gateway Nodes. The cluster-head node uses an RBF neural network classifier to recognize the characteristic information of terminal nodes in the cluster, and the probability distribution function of each pattern is obtained as an evidence body. The gateway node uses D-S theory synthesis rules to fuse the probability distribution functions of multiple evidence bodies at the decision level, and the principle is as follows [22]. Θ is set as the recognition frame, a defined function $m: 2^\Theta \rightarrow [0, 1]$, called the mass function, satisfies $m(\varphi) = 0$ (φ is the empty set), $\sum m(A) = 1 (A \in 2^\Theta)$ and $m(A)$ of 2^Θ is called the probability distribution function of, $m(A)$ is the basic probability number of proposition 2^Θ , so $m(A)$ is called Dempster's synthesis rule of finite A . The Dempster composition rule of a limited number of Θ , and m_1, m_2, \dots, m_n on the identification framework is:

$$(m_1 \oplus m_2 \oplus \dots \oplus m_n)(A) = \frac{\sum_{A_1 \cap A_2 \cap \dots \cap A_n = A} m_1(A_1) m_2(A_2) \dots m_n(A_n)}{(1 - k)}, \quad (3)$$

k is the uncertainty of evidence.

$$k = \sum_{A_1 \cap A_2 \cap \dots \cap A_n = \varphi} m_1(A_1) m_2(A_2) \dots m_n(A_n). \quad (4)$$

The gateway node fused the probability distribution functions of multiple evidence bodies into a new set of probability distribution functions, and the fused functions

were used as the decision-making basis to obtain the overall running state of mechanical equipment.

4. Interpretation of Result

The gearbox fault simulation test bench consists of a monopole reduced gearbox speed regulating motor, magnetic powder brake WSNs node, and MEMS acceleration sensor ADXL001, etc. The motor drive speed is 1.2 kr per minute and the sampling frequency is 10 kHz. Two fault types of simulated gearbox: a. Gear root damage of drive input end; b. Damage to the inner ring of the bearing at the driving input end. Where: number of teeth of the gearbox, $z_1 = 55$, $z_2 = 75$, modulus $m = 5$, bearing model N205.

Four terminal nodes (numbered 1, 2, 3, 4), two cluster-head nodes (numbered 5, 6), and one gateway node are arranged near the driver input terminal bearing seat and output terminal bearing seat to form a cluster tree network. In order to reduce the computation complexity of nodes, the time domain characteristic statistical indexes such as the amplitude of root variance and root-mean-square value and the frequency domain characteristic statistical indexes such as the mean frequency standard deviation frequency were used to characterize the gearbox operation state. For the vibration signals in normal state and two fault states, the terminal node constructs 40 groups of characteristic information samples with 2048 consecutive sampling values as one unit in time order, and the total number of samples is

120 groups. Cluster-head nodes receive 120 groups of samples from terminal nodes and input RBF neural network for network learning to generate a fault diagnosis classifier in order to reduce the network learning pressure of cluster head nodes [23], the training target error was set to 0.05. The number of neurons in the neural network input layer is determined by the characteristic dimension of 5. Set the number of neurons in the hidden layer as 3 and 1 bias neuron to consider the three operating states of the gearbox, and set the number of neurons in the design output layer as 3, namely the normal state of tooth root damage and bearing inner ring damage. The corresponding outputs are denoted as [1, 0, 0], and [0, 0], [0, 0, 1] respectively.

The damaged running state of the inner ring of the bearing at the driving input end was selected as the unknown state for the neural network test. Meanwhile, the terminal nodes in the cluster constructed a group of characteristic information samples for the running state of the gearbox. The cluster head node reads the corresponding neural network classifier parameters from the SD card and inputs the feature information samples into the classifier to obtain the probability distribution function for the recognition pattern. Gateway nodes use the D-S fusion decision theory to make integrated decisions on the bodies of evidence. The fused function is used as a decision basis to identify the fault type. 30 groups of tests were conducted respectively, and the results of probability allocation and fusion decision of one group of tests are shown in Figure 5. (a) A_1 , (b) A_2 , (c) A_3 respectively represent the normal state of bearing root damage and bearing inner ring damage [24]. m represents the probability distribution function (D-S fusion: $m(A_1) = 0.0000$, $m(A_2) = 0.0049$, $m(A_3) = 0.9951$).

It can be seen that no. 3 and no. 4 nodes do not support mild damage to the bearing of the inner ring obviously, so no. 3 or No. 4 nodes can only be used to identify the operating state of the gearbox. Because the fault characteristics of slight damage to the bearing inner ring are very weak, and the sensor measuring points of no. 3 and No. 4 nodes are far away from the fault source due to the signal propagation path and other reasons, no. 3 and No. 4 nodes have not completely touched the corresponding fault characteristic signals. Based on the probability distribution function of the four groups, the decision-level fusion was carried out, and the slight damage fault of the bearing inner ring was accurately diagnosed. The results of 30 groups were statistically analyzed, and the fault recognition rate was 83.3%.

5. Conclusion

A mechanical fault diagnosis method based on multilevel hierarchical information fusion in wireless sensor networks is proposed. Compared with the star network structure, the network monitoring coverage of the adopted cluster tree network structure is larger. The dual-core WSNs nodes are designed to meet the requirements of the fault diagnosis architecture of WSNs with multilevel and hierarchical information fusion. Multilevel hierarchical information fusion is used to distribute computing tasks to nodes at all levels and effectively balance the computing load of sensor nodes.

By transmitting a small amount of characteristic information to replace a large number of original vibration signals, the total amount of network data transmission is reduced, network bandwidth is saved, and network energy consumption is reduced, which provides a new idea for WSNs application in mechanical equipment fault diagnosis.

Data Availability

The data used to support the findings of this study are available from the corresponding author upon request.

Conflicts of Interest

The authors declare that they have no conflicts of interest.

References

- [1] A. Zz, A. Hc, B. Sl, and B. Za, "Sparse filtering based domain adaptation for mechanical fault diagnosis - sciencedirect," *Neurocomputing*, vol. 393, pp. 101–111, 2020.
- [2] E. Hosseini and A. Mirzaei, "An improved method for diagnosis of induction motor load mechanical unbalance fault using current signal analysis," *Russian Electrical Engineering*, vol. 91, no. 3, pp. 217–224, 2020.
- [3] K. Zhang, J. Chen, T. Zhang, S. He, T. Pan, and Z. Zhou, "Intelligent fault diagnosis of mechanical equipment under varying working condition via iterative matching network augmented with selective signal reuse strategy," *Journal of Manufacturing Systems*, vol. 57, pp. 400–415, 2020.
- [4] X. Li, J. Li, Y. Qu, D. He, and & Qu, "Semi-supervised gear fault diagnosis using raw vibration signal based on deep learning," *Chinese Journal of Aeronautics*, vol. 33, no. 2, pp. 418–426, 2020.
- [5] C. Cao, M. Liu, B. Li, and Y. Wang, "Mechanical fault diagnosis of high voltage circuit breakers utilizing vmd based on improved time segment energy entropy and a new hybrid classifier," *IEEE Access*, vol. 8, pp. 177767–177781, 2020.
- [6] X. Zhao, M. Jia, and Z. Liu, "Semisupervised graph convolution deep belief network for fault diagnosis of electromechanical system with limited labeled data," *IEEE Transactions on Industrial Informatics*, vol. 17, pp. 1551–3203, 2020.
- [7] R. Wang, F. Liu, X. Hu, and J. Chen, "Unsupervised mechanical fault feature learning based on consistency inference-constrained sparse filtering," *IEEE Access*, vol. 8, pp. 172021–172033, 2020.
- [8] B. Zhao, C. Cheng, G. Tu, Z. Peng, Q. He, and G. Meng, "An interpretable denoising layer for neural networks based on reproducing kernel hilbert space and its application in machine fault diagnosis," *Chinese Journal of Mechanical Engineering*, vol. 34, no. 1, pp. 44–11, 2021.
- [9] M. Nain and N. Goyal, "Energy efficient localization through node mobility and propagation delay prediction in underwater wireless sensor network," *Wireless Personal Communications*, vol. 122, no. 3, pp. 2667–2685, 2021.
- [10] E. B. Priyanka, T. K. Devi, P. Sakthivel, and A. S. Sagayaraj, "Gate diffusion input (gdi) codes involved viterbi decoders in wireless sensor network for enhancing qos service," *Analog Integrated Circuits and Signal Processing*, vol. 111, no. 2, pp. 287–298, 2022.
- [11] S. Fu, W. Lou, J. Wang, T. Ji, and W. Liu, "Multi-barycenter nodes localization method in wireless sensor network based

Retraction

Retracted: Design of the Violin Performance Evaluation System Based on Mobile Terminal Technology

Mathematical Problems in Engineering

Received 8 August 2023; Accepted 8 August 2023; Published 9 August 2023

Copyright © 2023 Mathematical Problems in Engineering. This is an open access article distributed under the Creative Commons Attribution License, which permits unrestricted use, distribution, and reproduction in any medium, provided the original work is properly cited.

This article has been retracted by Hindawi following an investigation undertaken by the publisher [1]. This investigation has uncovered evidence of one or more of the following indicators of systematic manipulation of the publication process:

- (1) Discrepancies in scope
- (2) Discrepancies in the description of the research reported
- (3) Discrepancies between the availability of data and the research described
- (4) Inappropriate citations
- (5) Incoherent, meaningless and/or irrelevant content included in the article
- (6) Peer-review manipulation

The presence of these indicators undermines our confidence in the integrity of the article's content and we cannot, therefore, vouch for its reliability. Please note that this notice is intended solely to alert readers that the content of this article is unreliable. We have not investigated whether authors were aware of or involved in the systematic manipulation of the publication process.

Wiley and Hindawi regrets that the usual quality checks did not identify these issues before publication and have since put additional measures in place to safeguard research integrity.

We wish to credit our own Research Integrity and Research Publishing teams and anonymous and named external researchers and research integrity experts for contributing to this investigation.

The corresponding author, as the representative of all authors, has been given the opportunity to register their agreement or disagreement to this retraction. We have kept a record of any response received.

References

- [1] Y. Lin, "Design of the Violin Performance Evaluation System Based on Mobile Terminal Technology," *Mathematical Problems in Engineering*, vol. 2022, Article ID 8269007, 7 pages, 2022.

Research Article

Design of the Violin Performance Evaluation System Based on Mobile Terminal Technology

Yixuan Lin 

Academy of Music, Putian University, Putian, Fujian 351100, China

Correspondence should be addressed to Yixuan Lin; 201904020933@stu.zjsru.edu.cn

Received 3 August 2022; Accepted 8 September 2022; Published 20 September 2022

Academic Editor: Hengchang Jing

Copyright © 2022 Yixuan Lin. This is an open access article distributed under the Creative Commons Attribution License, which permits unrestricted use, distribution, and reproduction in any medium, provided the original work is properly cited.

In order to solve the problem that violin performance evaluation is too subjective, this paper proposes a violin performance evaluation system based on mobile terminal technology. Violin sound evaluation mainly includes two indicators such as pronunciation quality and distance transmission ability. LabVIEW 8.2 is used to collect data, and fast Fourier transform (FFT) is used to analyze the time-domain signal in frequency domain, and the pronunciation process of violin is discussed in depth. Using statistical methods to process the test data of pronunciation distance transmission, a parameter model representing the pronunciation distance transmission ability is proposed, and finally the WeChat applet is used to control the recording and display. The results show that the process of violin sound production is accompanied by the weakening of octave peaks and the development of overtone peaks. The stable stage is marked by the stability of each octave peak and overtone peak. The sound head initially presents a simple excitation response, with only one near octave overtone and three cycles. Its maximum overtone peak/dominant frequency peak ratio coefficient is $k = 0.36$; the back entry complex excitation response has about nine cycles, with $k = 0.735$. Then enter the quasi-stable excitation response, whose waveform is similar to the typical A-string empty string pull waveform in the later stage, with $k = 0.36$; the maximum overtone peak/main frequency peak proportional coefficient is $k = 0.39$ in the rising section of the start, $k = 0.2$ in the loudest section, and $k = 0.26$ in the stable section. *Conclusion.* The system has initially established a new instrumented evaluation method, which provides a way of thinking for improving the quantifiable evaluation system in the future.

1. Introduction

With the development of the Internet, the transmission cost of information has dropped sharply. Because the education industry can be highly informationized due to its knowledge attribute, online education has developed rapidly. In the first half of 2020, due to the impact of the epidemic, all primary and secondary schools and colleges and universities could not start school normally, and online education became an important basis for nonstop classes because of its noncontact characteristics [1]. With so many advantages, online education has developed rapidly in China, and many excellent products have emerged in the field of music education. Traditional education needs space and small class teaching. The Internet attribute of online education can greatly reduce the cost of education, reduce the cost of education, and even

provide free online classes. The wide audience of Internet products has led to a rapid increase in the concentration of the industry. Excellent textbooks and teachers can be quickly and widely disseminated. The quality of education people receive is also higher than the traditional education model [2]. With the development of artificial intelligence technology, various intelligent functions are also embedded in music education software, such as practice music recommendation and intelligent music level rating, and some intelligent software are connected with the electronic piano, realizing the combination of software and hardware. It can intelligently correct errors and intelligently follow music according to the players' piano keys, greatly improving the learners' learning enthusiasm and efficiency.

With the popularity of smart phones, a large number of music education mobile software has entered our vision.

Through market research, we found that most of the musical instrument education software in the market focuses on providing learners with musical instrument teaching videos, or through the video function of mobile phones, real-time transmission of the fingering, and instrument pronunciation of the practitioners to the musical instrument teachers, so as to realize the accompaniment and remote guidance of musical instrument learning [3].

2. Literature Review

Gliga proposed a multitone detection system, in which two notes are input, and the system can detect the original note from the audio superimposed by two notes [4]. Waltham adopted the heuristic signal processing method, and his system can recognize polyphonic music played by eight organ ensembles. However, the problem of multitone detection has not been solved. Although the system proposed by them can recognize more notes, in fact, the effect it achieves is the recognized notes which are consistent with the sensory effect of the input audio instead of pursuing the accuracy of note results [5]. At the same time, if the fundamental frequencies of polyphonic music with multinote superposition overlap each other, they will affect each other in time-domain and frequency domain, which will bring greater difficulties to recognition. Elmezayen proposed a piano multinote estimation algorithm based on spectral envelope non-negative matrix decomposition, and its performance has been greatly improved on the international universal dataset maps in MIREX (Music Information Retrieval Evaluation eXchange) [6]. Mastellone used a new spectrum analysis method to realize the non-negative matrix decomposition system, which currently performs well on maps datasets [7]. Chen proposed the hidden Markov/semiMarkov model to solve the location problem. However, the HMM algorithm needs careful design and training, and the DTW algorithm only needs simple model without training to obtain good results. In recent years, the characteristic value selected by dynamic time warping algorithm is the pitch information of audio. The recorded audio information is serialized into numbers for fuzzy string matching. The music score following system based on DTW has the characteristics of high efficiency, accuracy, and simple model. It can occupy a small amount of resources to get accurate results. It is very suitable for a lightweight piano performance evaluation system [8]. In the system proposed by Zhang, the system based on non-negative matrix decomposition is used in piano teaching [9]. Otomański and others implemented a piano transcription interface device based on non-negative matrix decomposition [10]. In the system proposed by Rajpar, the system based on non-negative matrix decomposition is used in piano teaching [11].

In the international violin-making competition in Mittenwald, Germany, all musical instruments are evaluated by the judges in terms of timbre and technology. The scoring system of the judges is based on the following characteristics: (a) the quality of the process; (b) dimensions and specifications; (c) paint and paint treatment; (d) general impression, including material selection; (e) pronunciation; (f)

sound transmission capacity; (g) performance feeling; and (h) overall impression of sound quality. Almost all evaluation means are based on people's subjective feelings and require music experts with considerable professional knowledge, and the evaluation means are not easy to popularize. On the other hand, because people have different feelings and cannot form specific data to save, this evaluation method has certain subjectivity, and there are some deficiencies in inheritance, which is not convenient for further development and improvement. Based on LabVIEW 8.2, this paper proposes a new instrumented evaluation method and displays the results through WeChat applet, aiming to establish a quantifiable data evaluation system, which is of great significance to the quantitative evaluation of violin sound.

3. Research Methods

3.1. Pronunciation Quality Evaluation System. Pronunciation quality is an important indicator of system evaluation. The violin sound is transmitted to the computer through the microphone and analog-to-digital converter by the manual playing method, and then the time-domain diagram of playing waveform is given through the analysis and calculation of relevant programs, and then the frequency domain analysis diagram is obtained through FFT processing of waveform, as shown in Figure 1.

3.2. Evaluation System of Pronunciation and Telepathy Ability. The ability to pronounce far is another important index in the systematic evaluation. The system uses computer as the core and LabVIEW 8.2 as the working platform to establish the secondary application program. Through the audio sampling card of Dell core dual core computer, the dual channel synchronous sampling at the distance of 1 m and 10 m is realized. At the same time, a number of general-purpose software are combined to establish the analysis program block for sampling data, forming the prototype system of "quantitative analysis of violin pronunciation transmission performance" [12].

3.3. Evaluation Software System. The virtual sampling instrument system for violin sound is designed by LabVIEW 8.2. This system, together with the Dell dual channel sampling card, can achieve those as follows:

- (1) 11/22 kps sampling rate
- (2) 12 bit sampling accuracy
- (3) Sampling time not less than 20 seconds
- (4) Synchronous storage capacity of not less than 60000 data in each channel
- (5) The sampling results are displayed in real time and can also be played back or postprocessed by other software [13]

Due to the particularity of the data structure of LabVIEW 8.2, effective data text, curve group diagram, and analysis curve group diagram can be formed through the

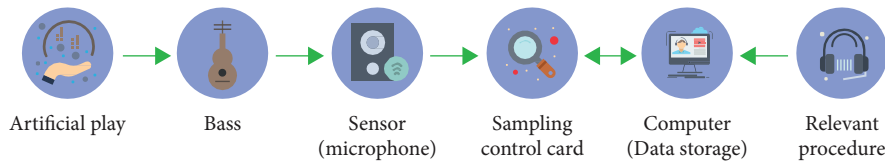


FIGURE 1: Pronunciation quality hardware system.

connection of Microsoft office software and origin data processing software.

3.4. Implementation of the WeChat Applet Module. The WeChat applet module is the main part of interaction with users. The system uses the function of applet front-end module to meet the needs of users in the actual use process. The WeChat applet module in this system is mainly divided into four functions, namely, displaying music score content, adding/deleting music score, uploading recording, and displaying evaluation results [14]. The two functions of displaying music score content and adding/deleting music score are relatively simple, which can be completed through image size adaptation display and database related operations. Here, we will focus on the recording upload function and the evaluation result display function.

The recording upload module mainly completes the function of recording the user's performance content and uploading it to the background server. The recording module directly calls the relevant interfaces of WeChat applet to realize. After the "recording" button is pressed, the applet calls the recording manager `wx.getrecordmanager()` to start recording [15].

The recording and uploading module of the applet mainly controls the transformation of different states by two buttons. When the system is initialized, the status of the two buttons are "record" and "upload." At this time, the "upload" button is disabled, and audio cannot be uploaded without recording files. When the user clicks the recording button, the recording starts, and the state of the first button is switched to "stop." After the user finishes recording, click the "stop" button to end recording. Then the WeChat applet will record the user's performance content during this period and store it as an MP3 format audio file. At this time, the "upload" button can be used. The user clicks the "upload" button to upload the audio file to the background server. At this time, the status of button 2 changes from "upload" to "evaluation." After clicking button 2 to obtain the evaluation, this button is disabled. The status in button 2 can only be enabled after recording and ending recording in button 1, and the recording in button 1 can start and end recording at any time. In the actual use, users may record repeatedly until they are satisfied, so the state change design meets the actual use needs of users.

The superposition and display of performance evaluation results in this system are realized in the WeChat applet front-end module. In order to intuitively present the performance evaluation results to users, the system displays errors by directly superimposing error information on the

music score pictures. The wrong note played by the user will be directly marked in the corresponding position in the music score picture, and the bar rhythm that may be too fast or too slow will also be displayed in the corresponding position. Drawing in the WeChat applet is similar to other programming languages, and corresponding data drawing operations need to be performed on canvas [16]. In this system, some preset data are first required for small program drawing, and these data are encapsulated into render property objects in small programs.

4. Result Analysis

4.1. Sound Quality Evaluation Test Equipment. Computer, Dell dual channel sound card (12 bits, 22050 cps), LabVIEW 8.2 secondary development software, Origin 7.51 Stradivarius Guqin in 741 and Stradivarius Guqin in 1692, and short-range and remote microphones are the equipment used for the sound quality evaluation test.

4.2. Analysis of the Violin Sounding Process. In 1741, the waveform of Stradivarius Guqin was obtained after LabVIEW 8.2 data acquisition. The sampling time was 3 seconds. Analyze the sound head and intercept the waveform between 0.3 s and 0.33 s of representative time nodes. Due to the fact that the effect of the bow on the string cannot be stabilized instantaneously, and the resonant cavity lags behind the vibration of the string, there will be a transition period before the resonant cavity stabilizes the vibration, that is, the sound head. It is not difficult to see from the waveform that the waveform of the sound head can be divided into four stages: starting, simple excitation response, complex excitation response, and quasi-stable excitation response [17].

After the start, the sound head initially presents a simple excitation response, with only one near octave overtone and three cycles. Its maximum overtone peak/dominant frequency peak ratio coefficient $k=0.36$, and then enters the complex excitation response, about nine cycles, with $k=0.735$, and then enters the quasi-stable excitation response. Its waveform is similar to the later typical A-string empty string playing waveform, with $k=0.36$.

4.3. FFT Analysis and Comparison of Each Stage of Violin Sound Production. By comparing and analyzing Figures 2 to 5, the first dominant frequency is around 438 Hz, which is related to the natural frequency of the violin. At the beginning of the start, as shown in Figure 2, the dominant frequency is not very obvious, and there is a phenomenon of

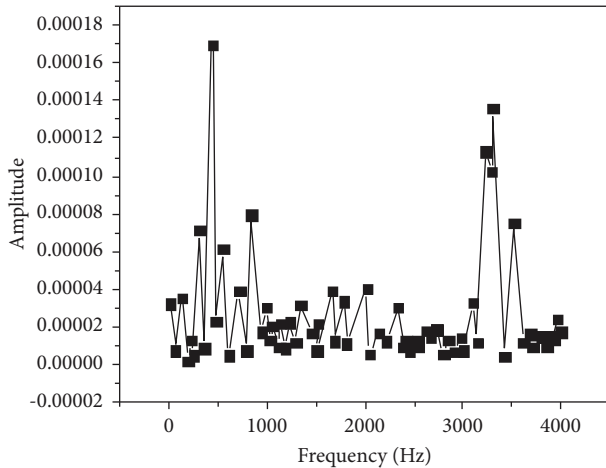


FIGURE 2: Amplitude frequency curve of sound head start (0.3 ~ 0.33 s).

multiple frequencies and the peak value is not much different from the dominant frequency. This is related to the asynchronous vibration of the resonant cavity and the string, that is, the so-called “uncoordinated period.” At this time, the sound generated is very irregular, and the start time should be shortened as far as possible. Then enter the quasi-stable excitation response, the first dominant frequency peak of the curve is sharpened and strengthened, the maximum overtone peak/dominant frequency peak ratio coefficient $k=0.36$, while other octaves are gradually reduced and weakened, and there is overtone peak development between octaves [18, 19]. As shown in Figure 3, in the rising stage of the start, in addition to the main frequency, there are seven octave peaks, and there are three overtone peaks between the two adjacent octave peaks. In the loudest stage of the start, as shown in Figure 4, the main frequency peak is further sharpened and strengthened, $k=0.2$, the frequency doubling peak is further reduced, and only five frequency doubling peaks are left. At the same time, the overtone peaks between frequency doubling are further developed and the number becomes more. In the stable playing stage, $k=0.26$, and the peak value of each octave peak has little difference, and the development of overtone peak tends to be stable; that is, it enters the stable pronunciation stage [20].

To sum up, the following conclusions can be drawn:

- (1) The process of violin sound production is accompanied by the weakening of octave peak and the development of overtone peak. The stable stage is marked by the stability of each octave peak and overtone peak.
- (2) Excitation response: The sound head initially presents a simple excitation response, with only one near octave overtone and three cycles [21]. Its maximum overtone peak/dominant frequency peak ratio coefficient is $k=0.36$; the back entry complex excitation response has about nine cycles, with $k=0.735$. Then enter the quasi-stable excitation response, whose waveform is similar to the typical A-string empty string pull waveform in the later stage, with $k=0.36$.

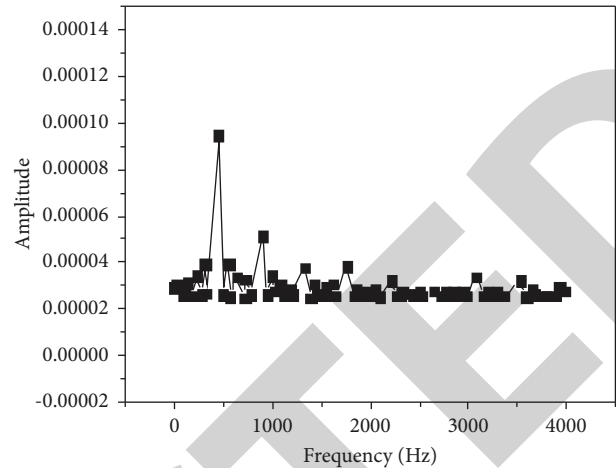


FIGURE 3: Rising amplitude frequency curve of starting (0.632 ~ 0.646 s).

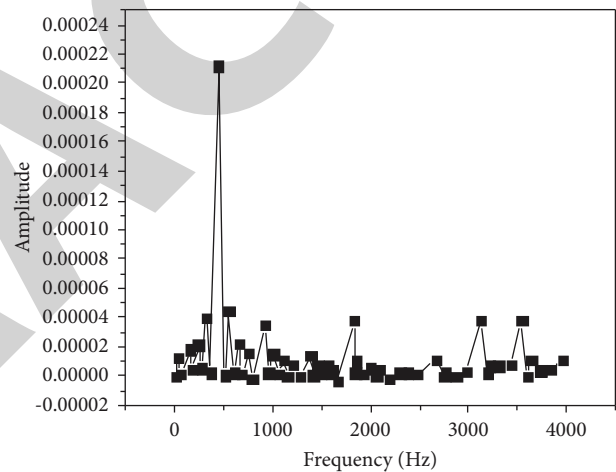


FIGURE 4: The loudest amplitude frequency curve of starting (0.830 ~ 0.844).

- (3) maximum overtone peak/main frequency peak proportional coefficient is $k=0.39$ in the rising section of the start, $k=0.2$ in the loudest section, and $k=0.26$ in the stable section;
- (4) Generally speaking, the violin pronunciation can pass through the complex excitation response stage within 0.02 seconds, and the shorter the transition time, the better. The maximum overtone peak/dominant frequency peak proportional coefficient k is controlled at the level of 0.26, which can be used as a professional piano.

4.4. Performance Analysis of Violin Articulation with Time Amplitude Curve. Obviously, the amplitude of a short-range microphone is much larger than that of a remote microphone. Although it is required to play each string smoothly, it can be seen from the curve of the short-range microphone that the vibration development behavior of different strings is different, and it generally presents the phenomenon of

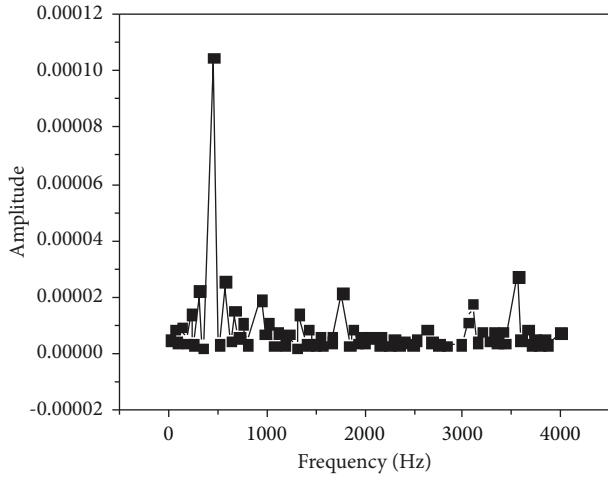


FIGURE 5: Amplitude frequency curve of stable playing (2.504 ~ 2.518 s).

“high low higher,” in which a and e strings have more obvious characteristics. However, the waveform of the remote microphone is not a simple linear attenuation of the curve of the short-range microphone. Its waveform is obviously different from that of the short-range microphone, and the difference in the pronunciation of the four strings can be observed from its “macro” distribution.

The amplitude ratio of time amplitude curve of two microphones can be used to characterize the sound transmission performance of violin. Because the vibration signal is positive and negative distribution, it is necessary to carry out absolute value processing before the next step of statistical processing. Figure 6 is a comparison curve of the average of absolute values of 100 subsamples (the average of 100 data) for two microphones. Figure 7 is a comparison curve of the peak values (the maximum value of 100 data) of the absolute values of 100 subsamples adopted by the two microphones.

Kc value is a parameter that uses absolute value average value to characterize the sound transmission performance of violin, which is defined as follows:

$$Kc = \frac{\sum_{i=n}^i V_{1,i}}{\sum_{i=n}^i V_{2,i}}, \quad (1)$$

where i is the subsample serial number that changes with the sampling time; n is the number of statistical subsamples, $n = 20$ and $n = 100$; $V_{1,i}$ is the transient value of the remote microphone; and $V_{2,i}$ is the transient value of the remote microphone [22].

Kp value is a parameter that represents the sound transmission performance of the violin by using absolute value peak value, which is defined as follows:

$$Kp = \frac{V_{1p,i}}{V_{21p,i}}; (i - n \sim i), \quad (2)$$

where i is the subsample serial number that changes with the sampling time; n is the number of peak statistical

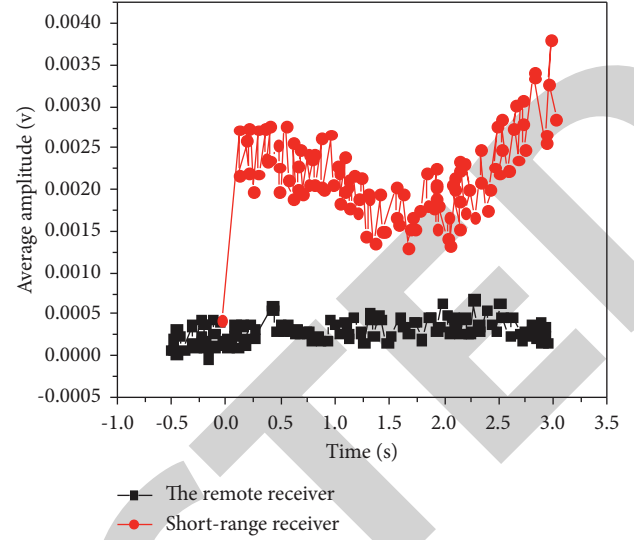


FIGURE 6: Comparison curve of average absolute values of 100 subsamples.

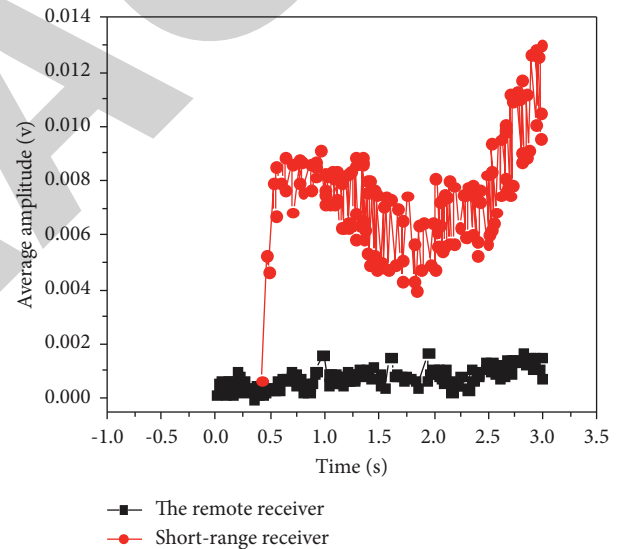


FIGURE 7: Peak value comparison curve of absolute values of 100 subsamples.

subsamples, $n = 100$; $V_{1p,i}$ is the transient peak of the remote microphone; and $V_{21p,i}$ is the transient peak of the remote microphone [23].

It is preliminarily believed those as follows:

- (1) The KC value using the absolute value average method has high sensitivity, but the dispersion is also large.
- (2) The absolute value peak method can obtain higher data amplitude (three times larger than the average value).
- (3) Details of the loss waveform: The sensitivity of KP is slightly lower, but the dispersion is also relatively small.

- (4) Increasing the number of statistical subsamples can reduce the dispersion: The statistical results of the 0.5 second time period for the teletransmission performance of Stradivarius 1692 show that string a is the best, string e is the second best, string D is also the second best, and string G is the worst. These results were obtained through five groups of 11000 data in each group, including $Kc(G) = 0.1192$, $Kc(D) = 0.1320$, $Kc(A) = 0.2669$, and $Kc(E) = 0.1561$ & 0.1262 .

To sum up, the following conclusions can be drawn:

- (1) This paper studies the basic methods of evaluating the performance of violin pronunciation and telepathy and forms an experimental analysis scheme of Kc , Kp parameter evaluation, and instantaneous FFT analysis [24].
- (2) Based on the measured data of Stradivarius 1692 violin playing with four empty strings, the performance evaluation of violin pronunciation is carried out.
- (3) Kc and Kp parameters can be easily obtained by software. Experiments show that they can accurately express the pronunciation and telepathy performance of each string. It further shows that it can be used for the comparison of pronunciation and telepathy performance of different violins [25];

5. Conclusion

On the basis of traditional violin evaluation methods, the concept of instrumented evaluation is proposed, and a relatively simple hardware system is established. Through sound acquisition and FFT analysis of violin pronunciation process, some characteristics and parameters representing violin sound quality are preliminarily obtained, which lays a good foundation for further discussion of violin sound evaluation methods. This paper puts forward a quantifiable evaluation method; that is, using the combination of software and hardware, through the data collection of LabVIEW 8.2 and the supporting use of Excel and Origin 7.5, the data and curves of violin pronunciation process and transmission ability are obtained, as well as the subsequent analysis conclusions.

Data Availability

The data used to support the findings of this study are available from the corresponding author upon request.

Conflicts of Interest

The authors declare that they have no conflicts of interest.

References

- [1] Y. Ran, D. Hu, Z. Xu et al., "Vertical-fluid-array induced optical microfiber long period grating (violin) refractometer,"

Journal of Lightwave Technology, vol. 38, no. 8, pp. 2434–2440, 2020.

- [2] S. Gonzalez, D. Salvi, F. Antonacci, and A. Sarti, "Eigenfrequency optimisation of free violin plates," *Journal of the Acoustical Society of America*, vol. 149, no. 3, pp. 1400–1410, 2021.
- [3] S. L. Lämmlein, B. Van Damme, D. Mannes, F. W. M. R. Schwarze, and I. Burgert, "Violin varnish induced changes in the vibro-mechanical properties of spruce and maple wood," *Holzforschung*, vol. 74, no. 8, pp. 765–776, 2020.
- [4] V. G. Gliga, M. D. Stanciu, S. M. Nastac, and M. Campean, "Modal analysis of violin bodies with back plates made of different wood species," *Bioresources*, vol. 15, no. 4, pp. 7687–7713, 2020.
- [5] C. Waltham, "The violin: a social history of the world's most versatile instrument," *Journal of the Acoustical Society of America*, vol. 147, no. 1, pp. 381–382, 2020.
- [6] A. Elmezayen and A. El-Rabbany, "Performance evaluation of real-time tightly-coupled gnss ppp/mems-based inertial integration using an improved robust adaptive kalman filter," *Journal of Applied Geodesy*, vol. 14, no. 4, pp. 413–430, 2020.
- [7] M. L. Mastellone, "Technical description and performance evaluation of different packaging plastic waste management's systems in a circular economy perspective," *The Science of the Total Environment*, vol. 718, Article ID 137233, 2020.
- [8] H. Chen, S. Ye, T. Wang, X. Zheng, and T. Li, "Extraction of common-mode impedance of an induction motor by using all-phase fft with intermediate-frequency filtering," *IEEE Transactions on Electromagnetic Compatibility*, vol. 63, no. 5, pp. 1593–1598, 2021.
- [9] Z. Zhang, F. Wang, G. Xu, J. Jia, X. Liu, and Y. Cao, "Improved carrier frequency-shifting algorithm based on 2-fft for phase wrap reduction," *Mathematical Problems in Engineering*, vol. 2021, pp. 1–10, Article ID 6664841, 2021.
- [10] P. Otomański, E. Pawłowski, and A. Szlachta, "The evaluation of expanded uncertainty of dc voltages in the presence of electromagnetic interferences using the labview environment," *Measurement Science Review*, vol. 21, no. 5, pp. 136–141, 2021.
- [11] A. H. Rajpar, A. E. Eladwi, I. Ali, and M. B. Ali Bashir, "Reconfigurable articulated robot using android mobile device," *Journal of Robotics*, vol. 2021, no. 3, pp. 1–8, Article ID 6695198, 2021.
- [12] Y. Duan, Z. Yang, W. Ge, and Y. Sun, "Explosive thermal analysis monitoring system based on virtual instrument," *Journal of Beijing Institute of Technology (Social Sciences Edition)*, vol. 30, pp. 218–224, 2021.
- [13] J. Meng, M. Singh, M. Sharma, D. Singh, P. Kaur, and R. Kumar, "Online monitoring technology of power transformer based on vibration analysis," *Journal of Intelligent Systems*, vol. 30, no. 1, pp. 554–563, 2021.
- [14] M. Irfan, G. Cascante, D. Basu, and Z. Khan, "Novel evaluation of bender element transmitter response in transparent soil," *Géotechnique*, vol. 70, no. 3, pp. 187–198, 2020.
- [15] Y. Deng, G. Zhang, and X. Zhang, "A method to depress the transmitting voltage response fluctuation of a double excitation piezoelectric transducer," *Applied Acoustics*, vol. 158, Article ID 107066, 2020.
- [16] X. Zhang, L. Ma, G. Zhang, and G. S. Wang, "An integrated model of the antecedents and consequences of perceived information overload using wechat as an example," *International Journal of Mobile Communications*, vol. 18, no. 1, pp. 19–40, 2020.

Retraction

Retracted: Layout Simulation of Prefabricated Building Construction Based on the Markov Model

Mathematical Problems in Engineering

Received 26 September 2023; Accepted 26 September 2023; Published 27 September 2023

Copyright © 2023 Mathematical Problems in Engineering. This is an open access article distributed under the Creative Commons Attribution License, which permits unrestricted use, distribution, and reproduction in any medium, provided the original work is properly cited.

This article has been retracted by Hindawi following an investigation undertaken by the publisher [1]. This investigation has uncovered evidence of one or more of the following indicators of systematic manipulation of the publication process:

- (1) Discrepancies in scope
- (2) Discrepancies in the description of the research reported
- (3) Discrepancies between the availability of data and the research described
- (4) Inappropriate citations
- (5) Incoherent, meaningless and/or irrelevant content included in the article
- (6) Peer-review manipulation

The presence of these indicators undermines our confidence in the integrity of the article's content and we cannot, therefore, vouch for its reliability. Please note that this notice is intended solely to alert readers that the content of this article is unreliable. We have not investigated whether authors were aware of or involved in the systematic manipulation of the publication process.

Wiley and Hindawi regrets that the usual quality checks did not identify these issues before publication and have since put additional measures in place to safeguard research integrity.

We wish to credit our own Research Integrity and Research Publishing teams and anonymous and named external researchers and research integrity experts for contributing to this investigation.

The corresponding author, as the representative of all authors, has been given the opportunity to register their agreement or disagreement to this retraction. We have kept a record of any response received.

References

- [1] X. Jiao, "Layout Simulation of Prefabricated Building Construction Based on the Markov Model," *Mathematical Problems in Engineering*, vol. 2022, Article ID 6882522, 7 pages, 2022.

Research Article

Layout Simulation of Prefabricated Building Construction Based on the Markov Model

Xin Jiao 

Shenyang Institute of University, Shenyang, Liaoning 110000, China

Correspondence should be addressed to Xin Jiao; 15221020896@stu.cpu.edu.cn

Received 19 July 2022; Accepted 8 September 2022; Published 20 September 2022

Academic Editor: Hengchang Jing

Copyright © 2022 Xin Jiao. This is an open access article distributed under the Creative Commons Attribution License, which permits unrestricted use, distribution, and reproduction in any medium, provided the original work is properly cited.

In order to meet the needs of the simulation function of prefabricated building construction layout, the author proposes a technology based on the Markov model. The main content of this technology is based on Markov model technology and takes Jinzhong Zhaimen as an example to conduct spatial scale research, according to the sensitivity of spatial scale, and finally through analysis, a systematic research method is constructed. Experimental results show that in the cell size range used, 80 m and 400 m can be regarded as the cell size threshold and limit value affecting the simulation accuracy, and when the cell size is below 80 m, the simulation result coefficient values are all more accurate. *Conclusion.* A technical study demonstrates that the Markov model can meet the needs of prefabricated building construction layout simulation functions.

1. Introduction

The prefabricated type adopts standardized design, factory production, prefabricated construction, information management, and intelligent application, and a large number of on-site operations in traditional construction methods are transferred to modern industrial production methods in factories, and it is an important measure to promote the transformation and upgrading of China's construction industry, realize the development of new urbanization, and implement the strategy of energy conservation and emission reduction [1]. The development of prefabricated buildings is not only a fundamental way to solve a series of major problems such as quality, performance, safety, efficiency, energy saving, environmental protection, and low carbon in the process of traditional housing construction but also an effective means to solve the problems of disconnection between architectural design, parts production, construction, maintenance and management, and backward production methods, and it is an inevitable choice to solve the current rising cost of China's construction industry and the shortage of labor and skilled workers and to improve the production and living conditions of construction workers. Prefabricated buildings refer to buildings assembled on-site

with prefabricated parts, mainly including prefabricated concrete structures, steel structures, and modern wood structures, as shown in Figure 1. At present, China is actively promoting the development of prefabricated buildings, but the development of prefabricated buildings is still in its infancy and still faces many difficulties and challenges. In the future, we will learn from the development experience of foreign prefabricated buildings and explore and improve the technology and management system suitable for national conditions. Prefabricated buildings are the key to the transformation and upgrading of the construction industry and the future development direction of the construction industry; through continuous research and development, prefabricated buildings will gradually become mature and help the transformation and upgrading of the construction industry. Simulation of the indoor space layout plays a huge role in improving people's quality of life because people spend 87% to 90% of their time indoors [2]. The simulation of indoor space feature layout has always been the focus of related scholars' research. The indoor spatial feature layout can be completed by 3D laser scanners or sensors, but due to its poor clustering effect, the overall deviation does not meet the ideal requirements, resulting in low data accuracy. The assembly type adopts standardized design, factory

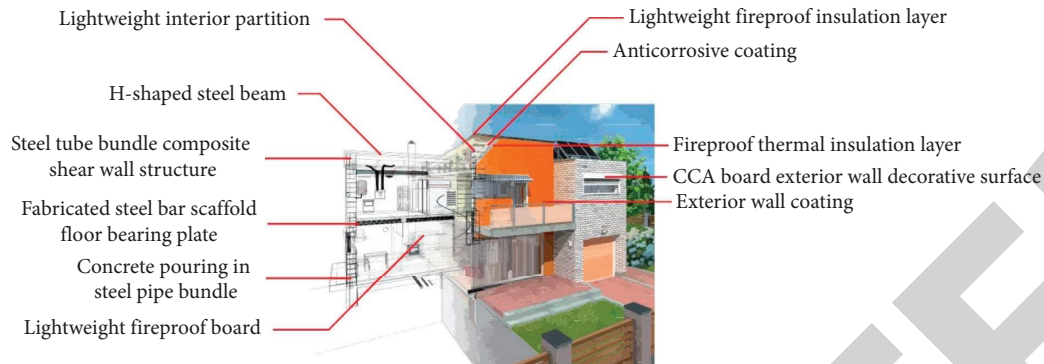


FIGURE 1: Prefabricated building.

production, assembly construction, information management, and intelligent application and transfers a large number of on-site operations in the traditional construction method to the factory, and it is a modern industrial production method. Architecture is a form of artistic expression; in the spatial layout of the interior environment of the building, the safety of the building should be ensured, and the integration of practicality and artistry should be realized. The layout results obtained by the current building indoor environment space layout method have problems of high energy consumption and low rationality, and it is necessary to study the building indoor environment space layout method [3].

2. Literature Review

In the current society, prefabricated buildings have not yet formed a large enough market scale, and the upstream and downstream supporting industries are not yet mature. The design, production, construction, and supporting materials enterprises in the industrial chain cannot keep up with the pace of market expansion, and the electromechanical parts, decoration parts, and accessories have also not formed modular, general and collaborative design standards, production standards, and installation standards; design, production, and assembly are disconnected from each other, and the industrial chain needs to be improved and integrated [4]. The relevant supporting policies for the exhibition of prefabricated buildings are not perfect enough, and there are many policies in various regions that set development goals and development directions, and the specific industrial support measures need to be further improved. The supervision system of prefabricated buildings is not synergistic enough, and the promotion of management innovation of prefabricated buildings is still lagging behind, and the implementation of the general contracting management model of prefabricated construction projects is not powerful enough. Due to the lack of independent research and development capabilities of enterprises, there are still relatively few enterprises that can fully open up the technology system of the whole industry chain; the research and development focuses of enterprises

in different links of the industry chain are different, and the research and development lacks synergy. The R & D focus of each enterprise is still focusing on individual technologies such as connection, waterproofing, and earthquake resistance, and the research and development of the full decoration technology of prefabricated buildings is not enough, and there is a lack of systematic research on the integration of the whole industry chain. In domestic and foreign research, the multilevel layout simulation method of indoor space features is yet to improve the convergence and efficiency, but the accuracy is insufficient [5]. The main purpose of the layout design of the interior environment of modern buildings is to consider the harmonious relationship between people and interior design within the scope of living space to the greatest extent. Construct a living environment space that meets the psychological and physiological needs of contemporary human beings through modern technology. The layout design of architectural indoor environment space refers to the use of structural language to describe what professional engineers and architects want to express and to provide high-quality architectural indoor environment space for human beings. Interior textiles, family structure, furniture, lifestyle, electrical safety requirements, hobbies, and interests should be considered when arranging the indoor environmental space of the building. In addition, the floor, ceiling material, wall, and lighting of the building interior should also meet the customer's requirements. Aiming at the above problems, the author proposes a simulation study of prefabricated and building construction layout based on the Markov model [6]. The main content of this technology is based on the Markov model technology and takes Jinzhong Zhaimen as an example to conduct spatial scale research, according to the sensitivity of spatial scale, and finally through analysis, a systematic research method is constructed. Combined with the current application status of the Markov model in simulation and the needs of the simulation research and development of prefabricated and building construction layout, the research on basic theory and model should be continuously strengthened in future research, combining cellular and Markov models into practice, providing more scientific and effective methods for future research.

3. Research Methods

3.1. Research on the Markov Model

3.1.1. Markov Model. The Markov model is a method for predicting the probability of events based on the Markov process theory, through the study of the initial probability of different states and the frequency of transitions between states, and the changing trend of the state is determined so as to achieve the purpose of predicting the future [7]. In the study of land use change, the process of land use change can be regarded as a Markov process, and the land use type at a certain moment corresponds to the possible state in the Markov process, which is only related to the land use type at the previous moment, and the number or proportion of the area of mutual conversion between utilization types is the state transition probability [8]. Markov models are widely used in land use change prediction research. Since the 1960s, it has been used in hydrology and meteorological prediction research, and in the 1970s, it has been used in earthquake prediction and research. In recent years, it has been widely used in land use change prediction and other aspects. In the study, due to the complex factors and driving forces affecting the future land use status, the future trend of land use change cannot be completely predicted based on the data in the early stage of the forecast period. Therefore, only by continuously adjusting and improving the Markov model and calculation method, it is possible to have a better and more accurate prediction on the changing trend of land use in the future. At this stage, the research of Markov model in land use change is more combined with other models, such as GIS, spatial logistic model, and cellular automata model [9]. Only when the Markov model and other models are combined and applied to the simulation of land use, can the characteristics of the Markov model be brought into full play and complement each other.

3.1.2. CA-Markov Model. A cellular automaton (CA) is a dynamical system that is discrete in time and space. The study area is divided into several units (rasters), and these units are called cells, and each cell corresponds to a certain land use type. The land suitability, related policies, and socio-economic factors of land use change constitute rules, and the rules determine the possibility of land use type conversion in each cell, and when the possibility exceeds the control threshold, the land use type will be converted [10]. Using the local transformation rules of cells, the complex evolution of land use can be simulated. Its formula (1) is given as

$$S_{(t+1)} = f(S_t, N). \quad (1)$$

In the formula, t and $t + 1$ are the time before and after the cell; S is the state set of the cell; f is the cell transformation rule; and N is the cell neighborhood.

The Markov model is a classic method for land use change simulation. Based on the assumption of no after-effects, the state of land use types at time $t + 1$ only depends

on the state of land use types at time t , and the land use change process can be represented by

$$S_{(t+1)} = P_{ij} \cdot S_t. \quad (2)$$

In the formula, P_{ij} is the state transition probability matrix, which represents the probability of land type i transitioning to land type j .

3.2. Shanxi Jinzhong House Gate

3.2.1. The Location and Shape Characteristics of the Ancient City of Pingyao. The ancient city of Pingyao, located in Pingyao County, south of Jinzhong city, was built during the period of King Xuan of the Western Zhou Dynasty, and it is an outstanding representative of Han culture in the Ming and Qing dynasties of China. The ancient city of Pingyao is one of the only two cases in China that successfully declared the world cultural heritage with the entire ancient city, and it has a high historical and cultural value, as well as a theoretical reference for the protection and activation of traditional dwellings, and the typical demonstration role is self-evident. The ancient city of Pingyao is located on the eastern edge of the Loess Plateau, with a square shape, sitting north facing south. According to the factors of terrain and sunshine, it is 15° eastward. There is one gate on the north and south walls of Pingyao, and two gates on each of the east and west walls. Due to its geographical advantage, agriculture and commerce in Jinzhong area are highly developed. During the period of Ming and Qing dynasties, Jinzhong merchants accumulated a lot of wealth, and the houses were large in scale and beautifully decorated, and the buildings they lived in all showed their status and wealth, and at the same time, they also showed the cultural concept and value orientation of Jin merchants. In addition, the residents of Jinzhong follow Confucianism, the folk customs are simple, and they abide etiquette and law, and in architecture also, they reflect the strict principles of etiquette and norms [11].

3.2.2. Features of Jinzhong House Gate. In terms of architectural form, Jin merchants respect Confucianism, and the houses they live in strictly abide by the norms of ancient etiquette and laws, and the courtyard space is square and neat, with a compact layout and a clear longitudinal axis. Jinzhong residential buildings break through the traditional single and second courtyard and develop into a horizontal and vertical multigroup. The traditional houses in the ancient city of Pingyao have several types of courtyards. One is a one-entry triplex or one-entry quadrangle where ordinary people live, and the other is a commodity shop opened along the street, and there is also an escort ticket type for business in the front room, vertical multientry serial courtyards for sleeping in the back room, horizontal multispans parallel courtyards, and horizontal and vertical multientry multispans group courtyards [12]. Residential color and shape decoration art also had certain norms. Although the use of colors in Shanxi dwellings is strictly restricted, the colors of their appearance are simple, natural, and varied, showing their natural colors. The blue-gray bricks, tan wood, yellow-

brown clay, green-yellow stone, and black-gray tiles constitute the harmonious tone of the local dwellings.

3.3. Study on the Spatial Scale Taking Jinzhong Zhaimen as an Example

3.3.1. Landscape Space. All planning is inseparable from solid data support; therefore, technology should be used to dynamically monitor the current situation of the landscape pattern in the study area in real time, obtain time-sensitive landscape pattern data, and control the evolution process and direction of the landscape pattern so as to take relevant measures, adapted planning programs, or related policies, and timely guidance and regulation for unreasonable places [13]. The landscape structure of the study area changed obviously in the early stage of the study section and gradually tended to be balanced in the later stage. The areas of urban residential landscapes, urban green space landscapes, road landscapes, and other construction landscapes show an increasing trend, while the areas of residential landscapes, agricultural landscapes, and woodland landscapes show a decreasing trend, all of which will be balanced and stable in 2025. The water landscape area fluctuates greatly every year, which is related to the water level, and the area change trend is not obvious [14].

3.3.2. Spatial Scale Sensitivity. Based on the type map, the sampling function of the software was used to obtain data of different resolutions in 2010, 2015, and 2020, and the sampling algorithm was the nearest neighbor pixel method. The resampling resolution was set to 100, 150, 200, 300, 400, 500, and 800 m, trying to cover cell size commonly used in research. Obtain the transition area and transition probability data from 2015 to 2020 through the Markov module in the software. Based on this data, the 2020 land use classification was simulated using the Markov model. Neighborhood types are set to 5×5 mole neighborhood, 3×3 mole neighborhood, and 3×3 von Neumann neighborhood [15]. The accuracy evaluation of the simulation results uses the validate module to obtain the quantitative Kappa coefficient (K), the location Kappa coefficient (Klocation), and the standard Kappa coefficient (Kstandard). The landscape pattern analysis of the simulation results is carried out by software, and the number of patches (NP), patch density (PD), landscape shape index (LSI), average patch shape index (SHAPE_MN), average patch fractal dimension index (FRAC_MN), and other indicators are selected for analysis [16].

As can be seen from Figures 2–4, regardless of the use of any of the three neighborhoods, the Kappa coefficient values of the simulation results show very similar trends. When the cell size is increased from 30 m to 80 m, K , Klocation, and Kstandard all remain almost unchanged. When the cell size increased to 90 m, the Kappa coefficient values of the simulation results decreased rapidly, K decreased from 0.74 to below 0.7, Klocation decreased from 0.73 to about 0.64, and K also decreased from 0.65 to about 0.58 [17].

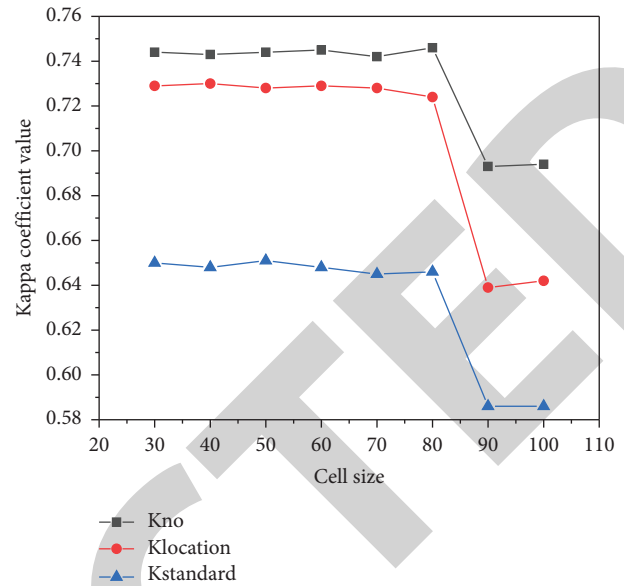


FIGURE 2: 5×5 molar neighborhood.

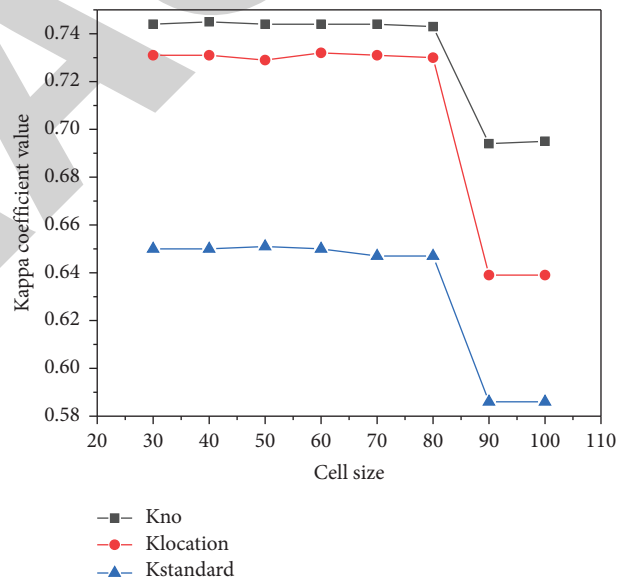


FIGURE 3: 3×3 molar neighborhood.

4. Analysis of Results

It can be seen from Table 1 that for the three selected neighborhood types, as the cell size increases from 30 m to 400 m, the Kappa coefficient value of the simulation results decreases continuously. When the cell size continues to increase to 500 m, the Kappa coefficient of the simulation results increases, which is significantly higher than the value at 400 m [18]. When it continues to increase to 800 m, the Kappa coefficient value of the simulation results decreases again, but it is still higher than the value at 400 m. By comparing the simulation results and the actual classification results at 400, 500, and 800 m by visual observation, it is found that the accuracy of the simulation results at the

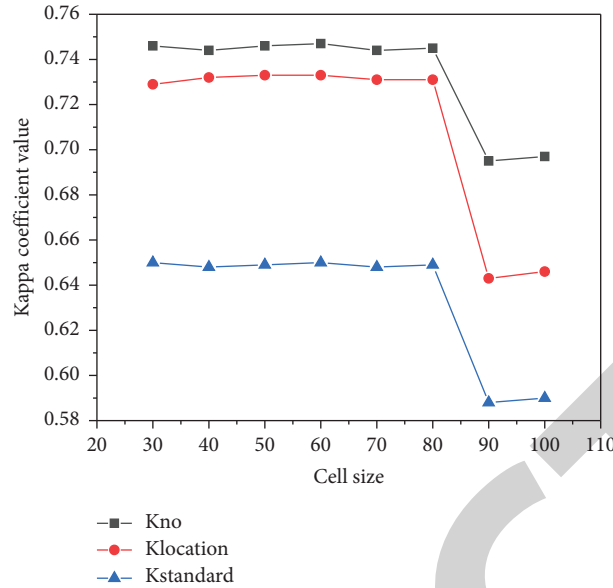


FIGURE 4: 3 × 3 von Neumann.

TABLE 1: Kappa coefficient of simulation results.

Neighborhood type Size (m)	5 × 5 moles			3 × 3 moles			3 × 3 von Neumann		
	K	Klocation	Kstandard	K	Klocation	Kstandard	K	Klocation	Kstandard
30	0.7384	0.7307	0.6490	0.7438	0.7306	0.6490	0.7431	0.7295	0.6481
100	0.6935	0.6399	0.5856	0.6941	0.6408	0.5864	0.6952	0.6424	0.5879
150	0.6916	0.6368	0.5826	0.6922	0.6376	0.5833	0.6918	0.6371	0.5829
200	0.6664	0.5979	0.5527	0.6683	0.6006	0.5552	0.6673	0.5992	0.5539
300	0.6632	0.5955	0.5500	0.6635	0.5960	0.5505	0.6657	0.5991	0.5534
400	0.6481	0.5699	0.5365	0.6497	0.5721	0.5386	0.6512	0.5743	0.5406
500	0.7355	0.7105	0.6382	0.7391	0.7160	0.6431	0.7376	0.7137	0.6410
800	0.7211	0.6972	0.6217	0.7234	0.7008	0.6248	0.7194	0.6947	0.6195

resolutions of 500 and 800 m is much lower than that of the 400 m. It can be seen that the Kappa coefficient cannot simply be used as a standard for evaluating the quality of the simulation results. When the cell size exceeds a certain limit value, the Kappa coefficient value of the simulation result may be relatively large, but the accuracy of the actual simulation result is very low. Therefore, we believe that when using the Markov model to simulate the evolution of land use, we should pay attention to the limit value of the cell size in the simulation. When this limit is exceeded, the Kappa coefficient cannot simply be used as a criterion for evaluating the simulation results. From the perspective of neighborhood types and the simulation results generated by the three neighborhoods, there is no significant difference in the Kappa coefficient values, which to a certain extent indicates that when using the CA-Markov model to simulate the evolution of land use, the use of these three neighborhoods may have little effect on the Kappa coefficient of the simulation results [19]. In addition, the Kappa coefficient value of the simulation results generated by the 3 × 3 molar neighborhood is slightly higher than that of the simulation results of the 5 × 5 molar neighborhood, which also indicates

that with the increase of the neighborhood size, the Kappa coefficient value of the simulation results also decreased accordingly.

From the analysis of the landscape pattern index of the simulation results (Table 2), the fine-scale simulation results are very similar to the coarse-scale results. The reason may be that due to the increase of the neighborhood size, more neighboring cells are included in the cell transformation rule, and the number of isolated cells is reduced so that more cells can aggregate to form patches, and this results in a decrease in plaque number and plaque density. However, since the author only selects three kinds of neighborhoods for comparison, it is not easy to think that the von Neumann neighborhood must form a larger number of patches and a higher density of patches than the Moore neighborhood [20].

Combined with the previous analysis, it can be seen that in the range of cell size used for sitting, 80 m and 400 m can be regarded as the cell size threshold and limit value that affect the simulation accuracy; when the cell size is less than 80 m, the Kappa coefficient values of the simulation results all have high accuracy. Therefore, when performing CA-

TABLE 2: Simulation results of the fine-scale range.

Neighborhood type	Size (m)	NP	PD	LSI	SHAPE_MN	FRAC_MN
5 × 5 moles	30	6581	3.0191	44.6095	1.6289	1.0732
	40	3960	1.8163	33.9649	1.6612	1.0751
	50	2882	1.3223	28.8474	1.6615	1.0749
	60	2543	1.1658	25.9303	1.5935	1.0682
	70	2215	1.0169	23.7211	1.5699	1.0660
	80	2057	0.9427	22.4598	1.5309	1.0611
	90	6216	2.8496	28.0617	1.2219	1.0344
	100	5824	2.6722	26.8870	1.2124	1.0322
3 × 3 moles	30	11803	5.4148	45.2261	1.3724	1.0506
	40	6781	3.1101	36.1719	1.4151	1.0540
	50	4347	1.9945	32.6571	1.4771	1.0588
	60	3322	1.5229	27.9316	1.4996	1.0604
	70	2841	1.3043	25.4798	1.4826	1.0581
	80	2460	1.1274	23.6687	1.4766	1.0564
	90	7474	3.4263	30.7606	1.2105	1.0341
	100	6744	3.0943	29.1633	1.2066	1.0329
3 × 3 von Neumann	30	13914	6.3832	57.5943	1.5766	1.0794
	40	7216	3.3096	45.8206	1.6742	1.0837
	50	5171	2.3726	40.6488	1.6516	1.0767
	60	3364	1.5422	27.9550	1.4920	1.0599
	70	3453	1.5853	31.4966	1.6060	1.0698
	80	2907	1.3323	28.8998	1.6025	1.0676
	90	8783	4.0264	35.4682	1.2340	1.0372
	100	8127	3.7289	33.7463	1.2130	1.0337

Markov simulation, for cell size selection, we must pay attention to the existence of cell size thresholds and limit values.

5. Conclusion

The research study is based on the simulation of prefabricated building construction based on the Markov model, and the main content is based on Markov model technology, taking Jinzhong Zhaimen as an example to study the spatial scale, according to the sensitivity of the spatial scale, and finally through analysis, a systematic research method is constructed. Combined with the current application status of the Markov model in simulation and the needs of the research and development of prefabricated building layout simulation research, the research on basic theories and models should be continuously strengthened in future research, and the combination of cell and Markov model should be applied in practice in order to provide more scientific and effective methods for future research.

Data Availability

The data used to support the findings of this study are available from the corresponding author upon request.

Conflicts of Interest

The authors declare that they have no conflicts of interest.

References

- [1] M. Ma, K. Zhang, L. Chen, and S. Tang, "Analysis of the impact of a novel cool roof on cooling performance for a low-rise prefabricated building in China," *Building Service Engineering Research and Technology*, vol. 42, no. 1, pp. 26–44, 2021.
- [2] Y. Zhang, J. Chen, S. Guo, X. Yang, and G. Cui, "Building layout tomographic reconstruction via commercial wifi signals," *IEEE Internet of Things Journal*, vol. 8, no. 20, pp. 15500–15511, 2021.
- [3] H. D. Islam, I. W. Y. A. Putra, and N. W. A. Utami, "Redesain interior pasar ngentak desa dayu di kabupaten blitar," *Jurnal Patra*, vol. 2, no. 1, pp. 27–36, 2020.
- [4] U. D. S. Perera, U. Kulatunga, F. N. Abdeen, S. M. E. Sepasgozar, and M. Tennakoon, "Application of building information modelling for fire hazard management in high-rise buildings: an investigation in Sri Lanka," *Intelligent Buildings International*, vol. 14, no. 2, pp. 207–221, 2021.
- [5] Q. Zhang, "Relay vibration protection simulation experimental platform based on signal reconstruction of MATLAB software," *Nonlinear Engineering*, vol. 10, no. 1, pp. 461–468, 2021.
- [6] S. Ritter, G. Giardina, A. Franza, and M. J. Dejong, "Building deformation caused by tunneling: centrifuge modeling," *Journal of Geotechnical and Geoenvironmental Engineering*, vol. 146, no. 5, pp. 1–17, 2020.
- [7] B. Nowogońska, "Consequences of improper renovation decisions in a 17th century half-timbered building," *Scientific Review Engineering and Environmental Studies (SREES)*, vol. 29, no. 4, pp. 557–566, 2020.
- [8] R. Huang, P. Yan, and X. Yang, "Knowledge map visualization of technology hotspots and development trends in China's

Research Article

Gearbox Fault Diagnosis Based on a Sparse Principal Component-Generalized Regression Neural Network

Yimo Wang  and Yajun Han

Department of Automotive and Transportation Engineering, Jiangsu University of Technology, Changzhou 213001, Jiangsu, China

Correspondence should be addressed to Yimo Wang; wangym0617@163.com

Received 12 July 2022; Revised 25 August 2022; Accepted 5 September 2022; Published 20 September 2022

Academic Editor: Kai Guo

Copyright © 2022 Yimo Wang and Yajun Han. This is an open access article distributed under the Creative Commons Attribution License, which permits unrestricted use, distribution, and reproduction in any medium, provided the original work is properly cited.

The fault diagnosis of urban rail transit gearboxes has the characteristics of complex vibration signals and large amounts of data. The daily scheduled maintenance cannot meet the needs of gearbox maintenance, so it is necessary to predict the fault types in advance. In this paper, a method of gearbox fault prediction based on sparse principal component analysis and a generalized regression neural network is presented, and the result of fault prediction can provide a reference for making maintenance plans. Based on principal component analysis (PCA), a sparse principal component is obtained by adding the LASSO penalty term, which reduces the risk of overfitting of PCA while obtaining a sparse solution. Then, the sparse reduced dimension principal component is input into the generalized regression neural network model for fault diagnosis. The results show that the fault diagnosis method based on the sparse principal component-generalized regression neural network model has high accuracy and is time-consuming.

1. Introduction

The gearbox is a key component of the urban rail transit walking arrangement, and its failure can threaten the normal operation of the train and bring safety problems. Fault diagnosis allows the maintainer to predict the gearbox fault types to be repaired, organize the maintenance strategy in advance, determine the maintenance time, and reduce the maintenance cost and the loss caused by the fault event.

The progress of artificial intelligence technology makes the application of neural network models in device diagnosis research common. The literature [1] applied the short-term memory (LSTM) recurrent neural network to aircraft fault prediction. Reference [2] used a CNN-GRU neural network model to predict short-term transformer faults. Reference [3] predicted the possible faults of power systems using a deep convolutional neural network model. The literature [4] used the convolutional neural network method for fault determination of characteristic turnout characteristic pattern. Reference [5] used the PCA-NARA neural network

model for the degradation trend assessment and prediction of wind turbine gearboxes. Reference [6] constructed a GRU recurrent neural network-based fault prediction model for cloud data center applications. When performing data-centric fault diagnosis and prediction, data noise and redundancy can affect the accuracy of fault type determination. Based on this, this paper adopts sparse principal component analysis for sparse processing of fault vibration data on the basis of traditional principal component analysis and combines a generalized regression neural network algorithm to establish a fault diagnosis model, which can be used for gearbox fault diagnosis and provide guidance on the development of maintenance plans for urban rail transit vehicles.

2. Sparse Principal Component Analysis

Principal component analysis (PCA), which can reduce the dimensionality of multicharacteristic indicator data, is a commonly used dimensionality reduction technique [7].

This method simplifies the data structure by constructing a new set of variables and uses fewer eigenvectors to approximate the information of the original data [8]. The calculation process is as follows:

- (1) After normalizing the original data set with i observations and j process variables with different dimensions, the matrix X is obtained, $X \in R^{i \times j}$.
- (2) The eigenvalue decomposition of X is performed; that is, the covariance solution is performed, and the score matrix T is calculated. That is,

$$\begin{aligned} \text{cov}(X) &= \frac{X^T X}{n-1} = V \Lambda V^T, \\ T &= X P, \end{aligned} \quad (1)$$

where Λ is the diagonal matrix of eigenvalues, $\Lambda \in R^{j \times j}$. V is the matrix [9], and $V \in R^{j \times j}$. P is the load matrix, constructed from the top n columns of V , $V \in R^{j \times k}$

- (3) By projecting T back into the $j \times i$ -dimensional space, the new matrix \hat{X} after dimensionality reduction can be obtained, and the cumulative contribution rate v_t can be calculated. Usually, the top n principal components corresponding to indicators with a v_t value greater than 85% are selected [10] which is

$$\begin{aligned} \hat{X} &= T P^T, \\ v_t &= \frac{\sum_{n=1}^k \Lambda_n}{\sum_{n=1}^j \Lambda_n} \times 100\%. \end{aligned} \quad (2)$$

PCA has an obvious effect on the dimensionality reduction of fault data, but it also has disadvantages; that is, it is difficult to use for nonlinear faults, and it is difficult to explain the characteristics of the principal component load of nonzero vectors [11] characteristic. Sparse dynamic principal component analysis (SDPCA) can be used to compensate for the shortcomings of the PCA method. Based on PCA, SPCA obtains the sparse principal components of data by adding LASSO penalty items [12]. This paper takes Zou [13]'s sparse method as an example to introduce the solution process of the sparse principal component.

- (4) Based on the principal component analysis method, the residual vector E is calculated, and the residual vector is the difference between the original matrix X and the new matrix after dimensionality reduction.

$$\begin{aligned} E &= X - T P^T \\ &= X - X P P^T. \end{aligned} \quad (3)$$

The principal component solution is to make the residual vector as small as possible and retain as much information as possible about the principal component in the original data, so the principal component solution can be performed using the

following equation, where Q is the solution of the principal component matrix P ; that is,

$$Q = \arg \min \sum_{n=1}^i \|x_n - P_n^T P_n x_n^2\|. \quad (4)$$

- (5) Adding the LASSO penalty term to sparse the obtained principal component reduces the risk of overfitting of the PCA solution while obtaining a sparse solution [13]. That is,

$$\begin{aligned} A_s, B_s &= \arg \min \sum_{n=1}^i \|x_n - A B^T x_n^2\| \\ &+ \lambda \sum_{m=1}^k \|\beta_m^2 + \lambda_{1,m}\| \sum_{m=1}^k \|\beta_{m1}\|, \end{aligned} \quad (5)$$

where A and B are the load matrix and sparse load matrix, respectively. A_s, B_s is the solution of A, B when the right side of the equation takes the minimum value. β is the load vector after sparsity. $\lambda, \lambda_{1,m}$ is the coefficient of the penalty terms, $\lambda > 0$.

- (6) The solution is the cumulative contribution rate v_s the SPCA model.

$$v_s = \frac{\sum_{n=1}^k S \Lambda_n}{\sum_{n=1}^k \Lambda_n} \times 100\%, \quad (6)$$

$$S \Lambda = \left[\frac{\text{diag}(qr(X P_s))}{i} \right]^2,$$

$S \Lambda$ is the diagonal array of explained variance after sparsity. P_s is the load vector matrix after sparsity.

3. GRNN Fault Prediction Model

A generalized regression neural network (GRNN) consists of an input layer, a pattern layer, a summation layer, and an output layer [14]. GRNN has a good fitting effect on nonlinear data when the data accuracy is poor or the amount of data is small. The structure of the GRNN network is shown in Figure 1.

The vector $X = [x_1, x_2, \dots, x_n]^T$ is input from the input layer, and the number of original characteristic parameters is n . The pattern layer accepts the data output from the input layer, which is transformed into $P = [p_1, p_2, \dots, p_n]^T$ by the neuron transfer function and passed to the summation layer. σ in the GRNN model represents the smoothing factor, and the ideal σ value can usually be calculated according to the distribution probability of the sample. That is,

$$P_i = \exp \left[-\frac{(X - X_i)^T (X - X_i)}{2\sigma^2} \right]. \quad (7)$$

There are two types of neurons in the summation layer, the denominator unit and numerator unit [15], and the S_D and S_{Nj} ($j = 1, 2, \dots, k$, where k is the dimension of the output vector) are obtained after the output of the hidden layer is multiplied by the corresponding weight and then added and summed, and the output vector is $Y = [y_1, y_2, \dots, y_n]^T$; that is,

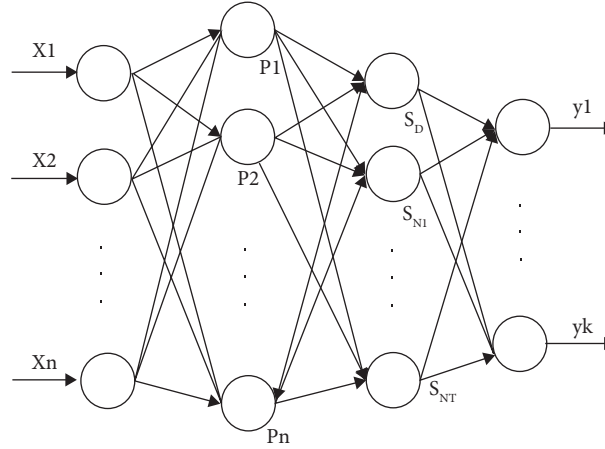


FIGURE 1: GRNN structure.

$$\begin{aligned}
 S_D &= \sum_{i=1}^n P_i \\
 S_{Nj} &= \sum_{i=1}^n y_{ij} P_i, \\
 Y &= \frac{S_{Nj}}{S_D}.
 \end{aligned} \quad (8)$$

Suppose x and y are two random variables. The joint probability density is $f(x, y)$, in which x_0 is the observed value of x , and the regression relationship between y and x is

$$E(y|x_0) = \frac{\int_{-\infty}^0 y f(x_0, y) dy}{\int_{-\infty}^0 f(x_0, y) dy}. \quad (9)$$

Applying the Parzen nonparametric estimation, the probability density function $f(x_0, y)$ can be estimated from the sample data set. That is,

$$\begin{aligned}
 f(x_0, y) &= \frac{1}{n(2\pi)^{p+1/2} \sigma^{p+1}} \sum_{i=1}^n \exp \left[-\frac{(X-X_i)^T (X-X_i)}{2\sigma^2} \right] \\
 &\cdot \exp \left[-\frac{(Y-Y_i)^2}{2\sigma^2} \right].
 \end{aligned} \quad (10)$$

In Equation (10), n is the sample size, and p is the dimensionality of the random variable x . Substituting this into Equation (9), exchange the order of integration and summation and simplify it to obtain:

$$y(x_0) = \frac{\sum_{i=1}^n y \exp \left[-\frac{(X-X_i)^T (X-X_i)}{2\sigma^2} \right]}{\sum_{i=1}^n \exp \left[-\frac{(X-X_i)^T (X-X_i)}{2\sigma^2} \right]}. \quad (11)$$

4. Gearbox Fault Prediction and Analysis

4.1. Data Preprocessing. The gearbox contains mechanical parts, such as gears, shafts, rolling bearings, and boxes, which are common power transmission devices in urban rail

vehicles. Its working principle is that the rotating shaft drives the sector gears in the gearbox and transmits torque vertically to the other shaft. According to the data [16], gearbox faults occur more often in the gears and rolling bearings, 59% and 20%, respectively. This paper takes the transmission system diagnostic simulator (DDS) as the data acquisition object, the speed is 2000 r/min, and the sampling frequency is 5120 Hz. Four typical faults of the gearbox were selected for fault prediction, including bearing ball error, bearing inner and outer ring fault, gear missing teeth, and gear surface cracks. The gearbox parameters are shown in Table 1.

The collected vibration signals were taken as a sample set every 1024 points, and 30 sample sets were extracted under five working conditions: normal, bearing ball misalignment, bearing inner and outer ring fault, gear missing teeth, and gear surface cracks. A total of 29 indicators in the time domain and frequency domain were extracted from each sample set, which can comprehensively describe the faults of gears and bearings in the gearbox. However, characteristics in the frequency domain were obtained through a Fourier transform on the basis of the time domain, so there is information redundancy. In addition, some indicators are sensitive to faults, and some indicators are not sensitive to faults, so if not processed, it will cause inaccurate prediction results. This paper uses PCA and SPCA to reduce the dimensionality of 29 characteristic indicators, eliminate the indicators with low fault sensitivity, eliminate data redundancy, and improve the fault prediction accuracy.

The 150 gearbox vibration data sets under five working conditions are used as input for PCA and SPCA analysis, and the dimensionality reduction results obtained are shown in Table 2.

In Table 2, PC1~PC6 are the first six principal components after dimensionality reduction. It can be seen from the dimensionality reduction results that although the cumulative contribution rate of SPCA is 85.2% lower than that of PCA, 88.3%, there are zero elements in the principal component load extracted by the SPCA dimensionality reduction method, and the number of the corresponding zero elements are 2, 4, 8, 7, 8, and 10, which reduces the complexity of variable dimensionality reduction. The first six

TABLE 1: Gearbox parameters.

Component	Parameter	Value
Gear	Teeth number of driven gear	88
	Teeth number of the master gear	44
	Spiral angle	9°22'
	Pressure angle	20°
	Modulus	1.5
	Engage frequency	959.39 Hz
Rolling bearings	Rolling body diameter	8 mm
	Number of rolling elements	17↑
	Contact angle	15°
	Pitch radius of high-speed shaft	62 mm
	Pitch radius of low-speed shaft	72 mm
	Rotational frequency of high-speed shaft	10.902 Hz
	Rotational frequency of low-speed shaft frequency	21.804 Hz

TABLE 2: The dimensionality reduction results of PCA and SPCA.

Methods	Variables	PC1 (%)	PC2 (%)	PC3 (%)	PC4 (%)	PC5 (%)	PC6 (%)
SPCA	Contribution rate	57.6	16.3	4.7	3.3	2.1	1.2
	Cumulative contribution rate	57.6	73.9	78.6	81.9	84	85.2
PCA	Contribution rate	54.5	22	5.5	3.1	1.8	1.4
	Cumulative contribution rate	54.5	76.5	82	85.1	86.9	88.3

TABLE 3: SPCA principal component partial load matrix.

Variables	PC1	PC2	PC3	PC4	PC5	PC6
Mean value	-0.199	0	0	0	0	0
Peak value	-0.183	0.148	0.024	0	0	0
Peak value	-0.136	0.041	0	0	0	0
Square root amplitude	-0.224	0	0	0	0	0
Absolute mean value	-0.113	0.119	0.065	0.140	0.557	0.005
...
Frequency root mean square value	-0.173	0.124	-0.084	0.118	0.009	0
Frequency standard deviation	0.159	0.366	0	-0.120	-0.003	-0.106
Frequency dispersion	-0.192	-0.075	-0.020	-0.065	-0.243	0.268
Frequency skewness	0.187	0.003	0	0	0	-0.127
Normalized spectral mean	0.163	0.106	0.231	0.0726	-0.038	0
Main frequency band position	0	0	0.038	0.060	0.090	0

principal components of SPCA can represent 85.2% of the original information, the first six principal components of PCA represent 88.3% of the original information, all greater than 85%, and the first six principal components can be used as input to represent the original information. The partial load matrix of the first six principal components of SPCA is shown in Table 3.

4.2. Comparison of Fault Prediction Results. The 150 groups of fault characteristic sets composed of five working conditions and 29 characteristic indicator values were transformed into a fault characteristic set composed of 6 characteristic indicators through PCA and SPCA, and 24 groups and 6 sets of fault characteristics of each working condition were randomly selected. The set consists of 120 training sets and 30 testing sets. To compare the fault prediction effects of the GRNN, PCA-GRNN, and SPCA-GRNN models, 29 time-domain and frequency-domain

fault characteristic sets were used as the input of the GRNN model, and the fault characteristic sets transformed by the PCA and SPCA analysis were used as input to the PCA-GRNN and SPCA-GRNN models. The value of the smoothing factor in the GRNN model determines the prediction result. In this paper, the smoothing factor corresponding to the highest accuracy rate is determined by inputting the training samples and the changed smoothing factor value. The interval of the smoothing factor value is [0.1, 1]. When this value is 0.7, the maximum accuracy is 96%. The main parameters of the models were determined based on the input indicator characteristics of the three models and the type of faults predicted, as shown in Table 4.

By inputting the training set for model training and inputting the test set to test the performance of the model, the fault prediction results of the gearbox are obtained, as shown in Figures 2–4, and the comparison of the fault prediction results of the three models is shown in Table 5.

TABLE 4: Main parameters.

Parameters	GRNN	PCA-GRNN	SPCA-GRNN
Input layer	29	6	6
Output layer	5	5	5
Smoothing factor	0.7	0.7	0.7

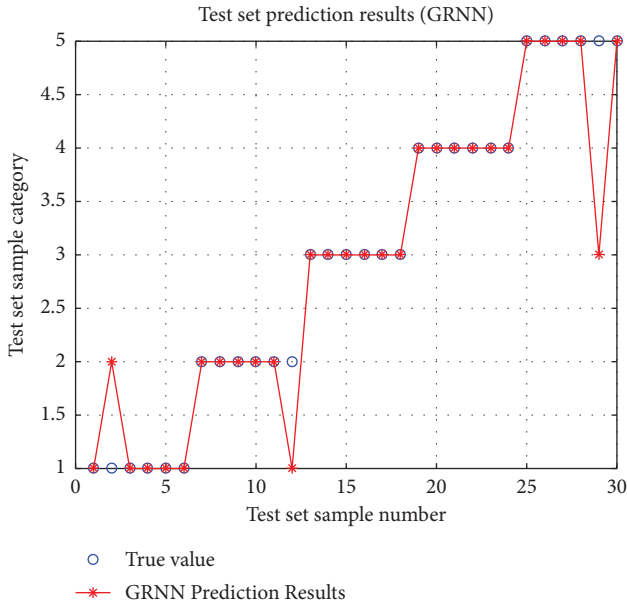


FIGURE 2: GRNN prediction results.

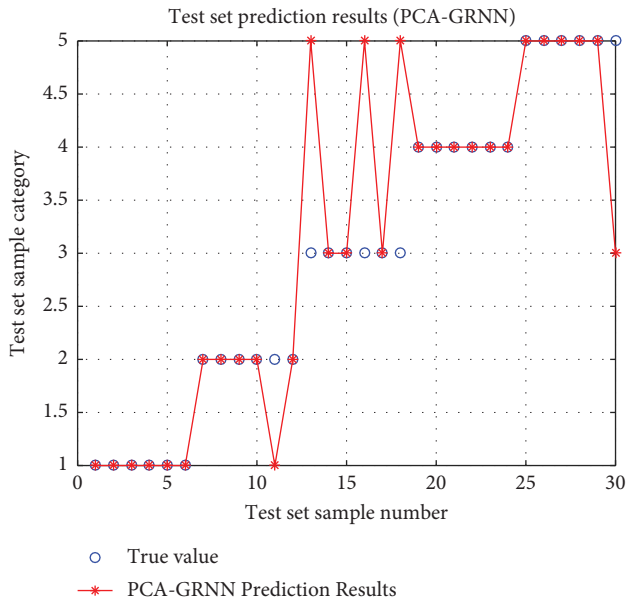


FIGURE 3: PCA-GRNN prediction results.

When the original data before dimension reduction are used as input for fault prediction, the accuracy rate is 43.3%, and the prediction time is 10.23 s. The fault prediction accuracy of the generalized regression neural network based on principal component analysis can reach 90%, and the

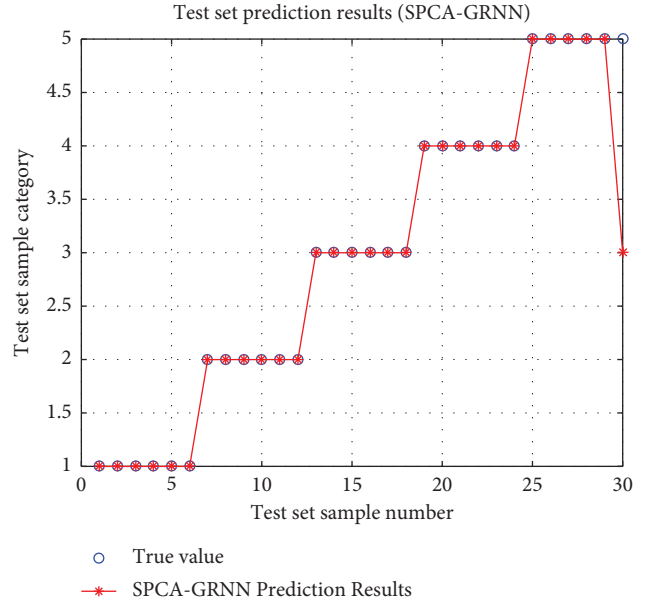


FIGURE 4: SPCA-GRNN prediction results.

TABLE 5: Comparison of results.

Model	Cumulative contribution rate (%)	Prediction accuracy (%)	Prediction time (s)
GRNN	100	43.30	10.23
PCA-GRNN	88.30	83.3	2.63

prediction time is 2.63 s. Although the SPCA-GRNN model, which extracted six sparse principal elements for generalized regression neural network prediction, had the lowest cumulative contribution of the three models, the prediction accuracy reached 96.6%, and the prediction time was 82% shorter than the GRNN model. Compared with the PCA-GRNN model, it was 30% shorter and the model predicted the best results.

5. Conclusion

- (1) SPCA reduces the dimension of sample data on the basis of PCA by adding the LASSO penalty item, and the six sparse principal components obtained contain more than 85% of the information of the original data, which improves the interpretability of the principal component while reducing the computational complexity.
- (2) Aiming at the gearbox fault prediction problem, this paper adopts the prediction method combining sparse principal component analysis and a generalized regression neural network. After comparing the fault prediction results of the three models of GRNN, PCA-GRNN, and SPCA-GRNN, it is concluded that the prediction ability is SPCA-GRNN > PCA-GRNN > GRNN.

- (3) In this paper, sparse principal component analysis is introduced into the research of fault vibration data processing, and combined with GRNN, it is used for gearbox fault prediction. Future research will consider the feasibility of integrating kernel principal component analysis with other machine learning and fault prediction effects.

Data Availability

The labeled dataset used to support the findings of this study is available from the corresponding author upon request.

Conflicts of Interest

The author declares no conflicts of interest.

Acknowledgments

This research was supported by the Jiangsu University Basic Science (Natural Science) Research Project--Research on Coordination Optimization of Driverless Vehicle Tracking System in Narrow Area (No. 22KJB120002).

References

- [1] X. Wang, J. Wu, C. Liu, H. Yang, Y. Du, and W. Niu, "Fault time series prediction based on LSTM recurrent neural network," *Journal of Beihang University*, vol. 44, no. 4, pp. 772–784, 2018.
- [2] W. Yang, C. X. Pu, K. Yang, A. A. Zhang, and G. L. Qu, "Transformer short-term fault prediction method based on CNN-GRU combined neural network," *Power System Protection and Control*, vol. 50, no. 6, pp. 107–116, 2022.
- [3] H. Ren, Z. J. Hou, B. Vyakaranam, H. Wang, and P. Etingov, "Power system event classification and localization using a convolutional neural network," *Frontiers in Energy Research*, vol. 8, no. 1, p. 607826, 2020.
- [4] M. Sun, *Research on Fault Diagnosis Method of Switch Machine Based on Neural Network*, University of Electronic Science and Technology of China, Chengdu, China, 2020.
- [5] Y. Xing, *Evaluation and Prediction of Wind Turbine Gearbox Deterioration Trend Based on PCA-NAR Neural Network*, Southwest Jiaotong University, Chengdu, China, 2019.
- [6] X. Hu, "Application fault prediction method of cloud data center based on GRU recurrent neural network," *Railway Computer Application*, vol. 31, no. 2, pp. 7–11, 2022.
- [7] C. Hui and Y. Zhou, "Research on equipment failure prediction based on PCA-BP neural network," *Logistics Engineering and Management*, vol. 43, no. 6, pp. 150–153, 2021.
- [8] Y. Wang and R. Liu, "Vehicle pantograph fault diagnosis based on principal component analysis-probabilistic neural network," *Urban Rail Transit Research*, vol. 24, no. 1, pp. 88–92, 2021.
- [9] Y. Duan, P. Wu, and J. Gao, "Fault detection method based on sparse dynamic principal component analysis," *Computer Measurement & Control*, vol. 27, no. 4, pp. 46–50, 2019.
- [10] K. Zhang, K. Zhang, and L. Kun, "Principal component analysis-neural network rockburst grade prediction model," *Chinese Journal of Safety Science*, vol. 31, no. 3, pp. 96–104, 2021.
- [11] A. K. Seghouane, N. Shokouhi, and I. Koch, "Sparse principal component analysis with preserved sparsity pattern," *IEEE Transactions on Image Processing*, vol. 28, no. 7, pp. 3274–3285, 2019.
- [12] Y. Duan, *Research on Fault Detection Based on Sparse Principal Component Analysis [D]*, Zhejiang Sci-Tech University, Hangzhou, China, 2019.
- [13] T. Hastie, H. Zou, and R. Tibshirani, "Sparse principal component analysis," *Journal of Computational & Graphical Statistics*, vol. 15, no. 2, pp. 265–286, 2006.
- [14] L. Gu, *Research and Application of Greenhouse Tomato Fertilization Regulation Based on Generalized Regression Neural Network*, Heilongjiang University, Harbin, China, 2021.
- [15] G. Cheng, *Rolling Force Prediction Based on Generalized Regression Neural Network*, Metallurgical Automation Research and Design Institute, Beijing, China, 2021.
- [16] B. Liang, *Research on State Modelling and Remaining Life Prediction of Wind Turbine Gearbox*, North China Electric Power University, Beijing, China, 2019.

Retraction

Retracted: E-Commerce Data Access Control and Encrypted Storage Based on Internet of Things

Mathematical Problems in Engineering

Received 8 August 2023; Accepted 8 August 2023; Published 9 August 2023

Copyright © 2023 Mathematical Problems in Engineering. This is an open access article distributed under the Creative Commons Attribution License, which permits unrestricted use, distribution, and reproduction in any medium, provided the original work is properly cited.

This article has been retracted by Hindawi following an investigation undertaken by the publisher [1]. This investigation has uncovered evidence of one or more of the following indicators of systematic manipulation of the publication process:

- (1) Discrepancies in scope
- (2) Discrepancies in the description of the research reported
- (3) Discrepancies between the availability of data and the research described
- (4) Inappropriate citations
- (5) Incoherent, meaningless and/or irrelevant content included in the article
- (6) Peer-review manipulation

The presence of these indicators undermines our confidence in the integrity of the article's content and we cannot, therefore, vouch for its reliability. Please note that this notice is intended solely to alert readers that the content of this article is unreliable. We have not investigated whether authors were aware of or involved in the systematic manipulation of the publication process.

Wiley and Hindawi regrets that the usual quality checks did not identify these issues before publication and have since put additional measures in place to safeguard research integrity.

We wish to credit our own Research Integrity and Research Publishing teams and anonymous and named external researchers and research integrity experts for contributing to this investigation.

The corresponding author, as the representative of all authors, has been given the opportunity to register their agreement or disagreement to this retraction. We have kept a record of any response received.

References

- [1] Y. He and W. Hu, "E-Commerce Data Access Control and Encrypted Storage Based on Internet of Things," *Mathematical Problems in Engineering*, vol. 2022, Article ID 4547002, 7 pages, 2022.

Research Article

E-Commerce Data Access Control and Encrypted Storage Based on Internet of Things

Yue He  and Wanda Hu 

Chongqing Open University (Chongqing Technology and Business Institute), Chongqing 400000, China

Correspondence should be addressed to Yue He; yuehe5@126.com and Wanda Hu; 1440140109@xs.hn.it.edu.cn

Received 15 June 2022; Accepted 26 July 2022; Published 19 September 2022

Academic Editor: Hengchang Jing

Copyright © 2022 Yue He and Wanda Hu. This is an open access article distributed under the Creative Commons Attribution License, which permits unrestricted use, distribution, and reproduction in any medium, provided the original work is properly cited.

In order to discuss the access control and encrypted storage of Internet of Things data for e-commerce data, a method of Internet of Things data access control and encrypted storage based on optical fiber network communication is proposed. Build an IoT application model based on optical fiber network communication, which consists of a perception layer, a network layer, and an application layer. The network layer is through the optical fiber communication network. The information collected by the optical fiber sensor in the perception layer is transmitted to the application layer for processing. And the model-aware layer adopts the dynamic transformation encryption method for attribute decomposition, and the Internet of Things data access control strategy based on key management and implement IoT data access control and encrypted storage based on the IoT application model of optical fiber network communication. The experimental results show that when this method implements access control and encrypted storage of IoT data, it has the advantages of high efficiency, low storage space overhead, and low computational cost of fiber network nodes, and the security of the processed IoT data is as high as 97.77%. *Conclusion.* This method can effectively deal with the limited computing performance and storage performance of the perception layer nodes of the application model; larger and larger application requirements with a large number of nodes.

1. Introduction

With the emergence and development of new computing technologies such as cloud computing, Internet of Things, and big data, the informatization of the world has led to a deep reform of information transmission technology on a global scale, at every level of national upgrading, and social development. The demand for information technology has also reached a height that has never been reached [1]. Build a global information sharing mechanism. It is of key significance to improve international economic, technological, educational cooperation, and cultural exchanges. Information security issues cover every corner of society such as finance, medical care, and electricity. There are non-singularity of attack forms, diversity of threats, large scope of influence, and strong suddenness. Security issues in information networks have become an explosive drawback in the development of informatization in various countries around

the world [2]. In the big data environment, information security has become a key issue in the field of information security. With the development of Internet technology, e-commerce has gradually become popular in daily life, which not only reduces the cost of business, but also drives the rapid development of the logistics industry. In the process of e-commerce transactions, some user privacy data is easily leaked, posing a threat to user privacy security. Therefore, it is necessary to use access control and encrypted storage technology and privacy protection of e-commerce data to ensure that users' privacy is not leaked as shown in Figure 1 [3]. By adopting the method of joint network feature analysis, the feature extraction and statistical analysis of e-commerce group user access data in the era of big data is realized, and the level of information management and e-commerce information access is improved. However, in the process of statistical analysis of user access to e-commerce groups, there is no in-depth analysis of user data

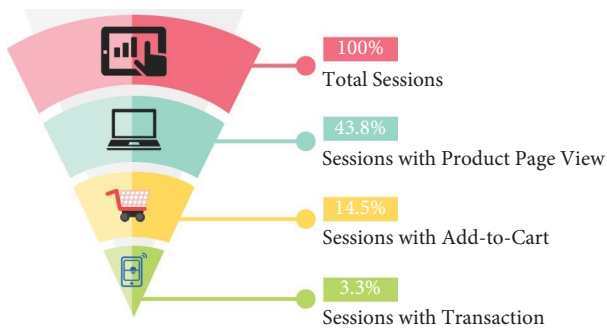


FIGURE 1: E-commerce data access control.

access and encrypted storage. It is very easy to have information leakage problems.

2. Literature Review

In the early stage of the development of the Internet of Things, some researches put forward the data processing scheme of the Internet of Things based on cloud computing. Cloud-centric IoT usually consists of three layers, namely, cloud server layer, IoT device layer, and application layer [4]. The device layer and the application layer are separated, the device is the edge component of the IoT network, and all devices are identified, authenticated, and connected through the cloud server, abstract IoT edge components into virtualized resources, take the system from a device-centric single device transaction, and shift to IoT services and applications that simultaneously provide a large number of device transactions. Shi et al. proposed a data storage framework based on cloud computing, the framework combines and extends multiple existing databases in order to store and manage various types of IoT data, the disadvantage of this framework is the long waiting time, which is also an inherent property of cloud storage schemes [5]. Dhiman et al. proposed a three-tier IoT data storage framework with front-end-middleware-backend, which can be seamlessly integrated into existing enterprise information systems, however, this scheme has low storage efficiency for heterogeneous data [6]. In order to store large amounts of heterogeneous data, Bradha et al. propose a hybrid structure- and object-oriented approach to optimize data storage and retrieval [7]. Sun et al. proposed a method to realize data communication from cloud to IoT devices based on buffer and communication link-state, in order to improve the overall performance [8]. Nie et al. solved the problem of uncontrolled malicious modification under cloud platform that may destroy the availability of shared data, a public audit solution is proposed and the identity privacy and identity traceability of group members can be protected at the same time [9]. However, cloud computing does not support the processing and storage of low-latency sensitive data, and because cloud data allows multiple authorized users to access, it cannot provide sufficient evidence for the whereabouts of data information and the operation history of subjects at all levels. Therefore, some special fields cannot be satisfied (such as industrial control systems and

traceability systems) the need to audit the access process of system dynamic data. Once a problem occurs, it is difficult to determine the responsibility. The Internet of Things technology can establish a collection between users and permissions and monitor access requests in the process of data use in real-time, which is conducive to dynamic access and access control. Therefore, the authors introduce IoT technology into e-commerce data access control and encrypted storage with the advantage of IoT real-time monitoring of data access requests. The authors study e-commerce data access control and encrypted storage technology based on IoT in order to further protect the privacy of e-commerce data.

3. Research Methods

3.1. Building an E-Commerce Data Sharing Model. In order to realize the access control and encrypted storage of e-commerce data based on the Internet of Things, first of all, establish an e-commerce data security sharing model, preset data attribute collection, and verify that user access meets the requirements. This ensures data sharing security. After the data is encrypted, the key may be lost and leaked during the key management process. In order to solve this problem, a sharing model is established based on user attributes. Different attribute set users obtain different private keys [10]. Therefore, each private key will not reveal the core information, reducing the risk of leakage. The restored complete e-commerce data is obtained by combining multiple authorized user sets. If only some of the user attribute keys are known, the original e-commerce data cannot be restored, which improves the security of data sharing to a certain extent.

Because IoT applications based on optical fiber network communication are mostly developed around a certain industry problem, an IoT application model based on optical fiber network communication is constructed. The details of the IoT application model based on optical fiber network communication are shown in Figure 2. In Figure 2, the perception layer is based on the data collected by optical fiber sensors. The network layer is based on the optical fiber communication network to transmit the information obtained by the perception layer to the application layer for processing. The difference between this method and the broadband transmission method is that the former can complete long-distance transmission of information [11, 12]. There are several common application support sub-layer technologies and application platforms in the application layer and complete the high integration of network technology.

3.2. Dynamic Transformation Encryption Based on Attribute Decomposition. Because the number of cloud data storage in the IoT application model based on optical fiber network communication is very large, if the IoT data attributes are decomposed and encrypted for each data relationship, different keys will appear. If each key is saved, it will increase the storage space, use dynamic encryption methods, and

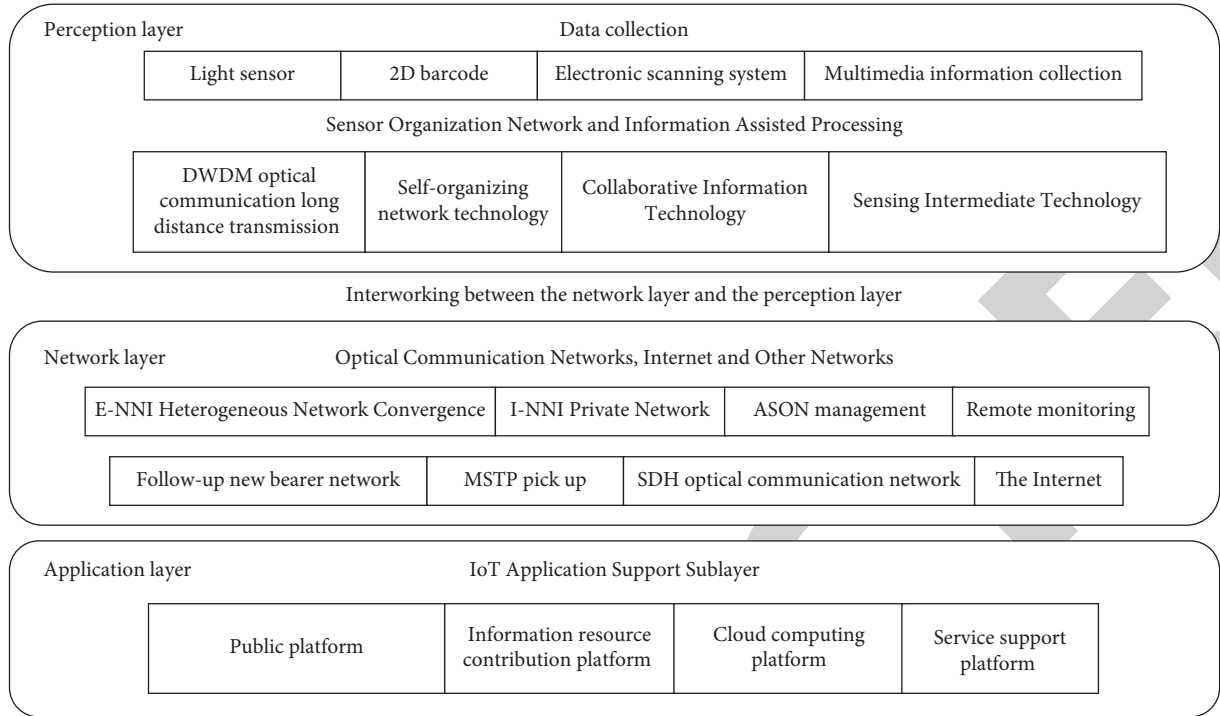


FIGURE 2: IoT application model based on optical fiber network communication.

dynamically generate keys. It is used to reduce the storage space of cloud data and improve data security [13]. When generating keys dynamically, the probability of duplicate keys must be close to 0, even if the elements have shared plaintext, the difference in position will generate differential ciphertext, and the dynamic generation of ciphertext is difficult. For element $b_{ji} \in O$, if $x_1 > x_2$, then $x_2 = \text{mod}(x_1)$, conversely, $x_1 < x_2$, then set $x_j = x_1$, then stop at $x_1 = x_2$, where x represents a single attribute. If b_{ji1} and b_{ji2} correspond, take whichever is used for encryption calculation.

Assuming that the IoT data attribute record code j in b_{ji} is known, then its key $H = \sum_{i=1}^m (b_i \otimes O_j)$, this is the first dynamic transformation, representing XOR calculation, and O_j describes the balance coefficient [14]. Again the dynamic transformation key is H_{ij} , then

$$H_{ij} = g(b_{ij}) = \sum_{j=1}^z H(\text{mod}i) \otimes O_i = \sum_{j=1}^m \left(\sum_{i=1}^m (b_i \otimes O_j) \otimes O_i \right). \quad (1)$$

Among them, $g(b_{ij})$ represents the positive attribute decomposition of element b_{ij} . For a random data relationship set O , through the minimum encryption strength attribute decomposition, the Internet of Things data attribute set $T = \{T_1, T_2\}$ that conforms to the privacy constraint rules is generated, for the finite element group $K = \{k_1, k_2, \dots, k_n\}$ decomposed by positive attribute T_1 , its element is $O = \{b_1, b_2, \dots, b_m\}$. Assuming that M_{ij} is numerical data, the value range is $[-b, b]$, then $H'_{ij} = H_{ij}(\text{mod}|b|)$. Here, the original value and non-regular transformation are used. It can realize dynamic encrypted storage [15].

3.3. IoT Data Access Control Strategy Based on Key Management. Because in the IoT application model based on optical fiber network communication, the types of data collected by optical fiber sensors in the perception layer are generally only allowed to access or deny access to users. Therefore, previous access control methods are not suitable for IoT environments. However, different types of information have different access levels, so that users can use the keys set in section 3.2 to access data at different levels according to the model, high-level users can not only access data at their own level, but also access data at different levels, it is also possible to obtain access rights for low-level users based on key derivation to access more resources [16]. Hierarchical access control mechanisms can be accomplished using key management methods.

3.4. Scheme Description. After the IoT application model based on optical fiber network communication is initialized, each level node u_j ($j = 1, 2, \dots, m$) corresponds to a unique identifier LA_j and a key h_j , h_j is used to protect this layer of resources, then $u_j \rightarrow 2^{z_j}$ and LA_j identify public information release, and set the topological structure of the directed acyclic graph B as public information release, then release $C = \{c_1, c_2, \dots, c_h\}$. In order to obtain the information resources corresponding to u_j , the user must obtain the valid key h_j issued by the authorization center, and then perform the decryption operation to realize the access to the corresponding resources of the hierarchical nodes [17].

Based on theoretical analysis, the user must obtain a h_j when accessing an $u_j \rightarrow 2^{z_j}$, and perform decryption processing, with the increase of the access level, when the user extracts the key multiple times, not only does it cause

communication burdens and threats to the perceptual layer network accessed, but also users will suffer from insufficient storage performance and long-distance communication performance, the problem of being attacked by an adversary. Evaluate the partial order relationship between neighboring nodes in the directed acyclic graph, so that the user can obtain the corresponding key of the upper node u_j , the lower-level key can be obtained by designing a suitable algorithm, and according to this principle, the keys of all nodes in the directed tree with u_j as the root can be obtained.

Based on the access control strategy proposed by the authors, taking into account the security status of the user and the hierarchical node u_j , only the key material zh_j that can obtain u_j is stored. In this way, the non-public information corresponding to the network node u_j is the key material zh_j , and the corresponding public information is LA_j ; zh_j becomes two keys (h_j, q_j) after operation, the key h_j is used to ensure the security of the self-layer resource Z_j , and the keys q_j and $d_{ji} \rightarrow (d_j, d_i)$ obtain the lower-layer key material zh_j by the designed key acquisition method. In this way, the key h_j for accessing the resources of this layer is obtained. If there are still lower-level nodes that need to be accessed, this method is used cyclically to obtain the corresponding key material, where the numbers of LA_j and d_{ji} indicate the release of public information; zh_j represents private information and saves it; the purpose of the strategy is to use upper layers zh_j and d_{ji} , according to the key acquisition method, the lower-layer zh_j can be obtained safely and quickly.

3.5. Strategy Building

- (1) Initialize. Set the directed acyclic graph $B = (X, Y)$ and security parameters β ; among them, X represents the node set of B , and Y represents the set of directed edges. The initialization process of the access control policy is as follows:
 - (i) Step 1: Select each node $u_j \in X$ in graph B , assign a unique identifier $LA_j \in \{0, 1\}^\beta$, at the same time, the corresponding key material $zh_j \in \{0, 1\}^\beta$ is arbitrarily selected. Use zh_j and LA_j to operate $q_j = g_{zh_j}(LA_j, Z dp_1)$ and operate $h_j = g_{zh_j}(LA_j, Z dp_2)$, where $Z dp_1, Z dp_2 \in \{0, 1\}^\beta$, both represent random values [18, 19].
 - (ii) Step 2: Select each directed edge $d_{ji} \in Y$, $d_{ji} \leftarrow (u_j, u_i)$, and operate $d_{ji} = Y_d^j(zh_j \| LA_j)$ in graph B .
 - (iii) Step 3: Set the acquired LA_j as public information release by operation, zh_j as private information for storage, and stop after initialization.
- (2) Key acquisition method. If a user accesses the network resources of the perceptual layer, it must obtain the key material of the corresponding layer. Set graph B , hierarchical nodes u, \bar{w} , among which $\bar{w} \leq u$, the user has obtained the key material zh_j of the corresponding u and the public information in graph B [20]. The purpose of the user is to use the designed

key acquisition method based on the mastered key material and public information, in order to obtain the key material of the hierarchical node u and to operate the key material of access \bar{w} in turn, so as to calculate the key to access \bar{w} . This key acquisition method does not need to analyze the detailed hierarchical structure of the perception network, the user only controls the $zh_{\bar{w}}$ of the source layer node, and the intermediate result obtained does not have the key h_j for each layer of protection resources, which can reduce the security risk of the method. Furthermore, this method is not limited to tree-like hierarchies. Assuming that the user has obtained the u_1 -related key material zh_1 , and the object is to access the hierarchical node u_7 resource, then obtain the h_7 , then the user can obtain the h_7 by using the 2-round key acquisition method to achieve access.

4. Analysis of Results

In the experiment, the efficiency of the three programs of encryption, key acquisition, and decryption is tested by increasing the number of IoT data attributes in the IoT application model based on optical fiber network communication and expanding the scale of the access structure and comparing the performance of the method in this paper, the cloud storage data access control method based on CP-ABE algorithm, and the multi-privilege secure cloud storage access control method based on CP-ABE and XACML. The processor used in the experiment is set to Inter 2. 3 GHz CPU, the memory is 9 GB, the virtual machine is VMware Workstation 6. 5. 2, and the performance test software is Ubuntu 10. 11. In the experiment, the number of IoT data attributes of the IoT application model based on optical fiber network communication was increased from 0 to 8 000, the test results of the three programs are shown in Figure 3. Figure 3(a) shows the time consumption result of encryption, Figure 3(b) shows the time consumption result of decryption, and Figure 3(c) shows the time consumption result of key acquisition. According to Figure 3, the proposed method takes time in the whole process with the IoT application model based on optical fiber network communication, and the number of IoT data attributes increases, the time-consuming access control methods of cloud storage data based on the CP-ABE algorithm and multiauthority secure cloud storage based on CP-ABE and XACML also significantly increase with the increase of the number of IOT data attributes in the IOT application model. However, among the three methods, the method proposed in this paper is always the least time-consuming when applied to the encrypted storage of IOT data [21].

Figure 4 shows the test results of cloud data storage space under the control of three methods. According to Figure 4, it can be seen that, 3 ways to save space, with the increase in the number of users of the Internet of Things application model based on optical fiber network communication. Among them, the increase rate in the former stage is slower, and the increase rate in the latter stage is faster [22]. When the number of users is as high as 800, when the three methods

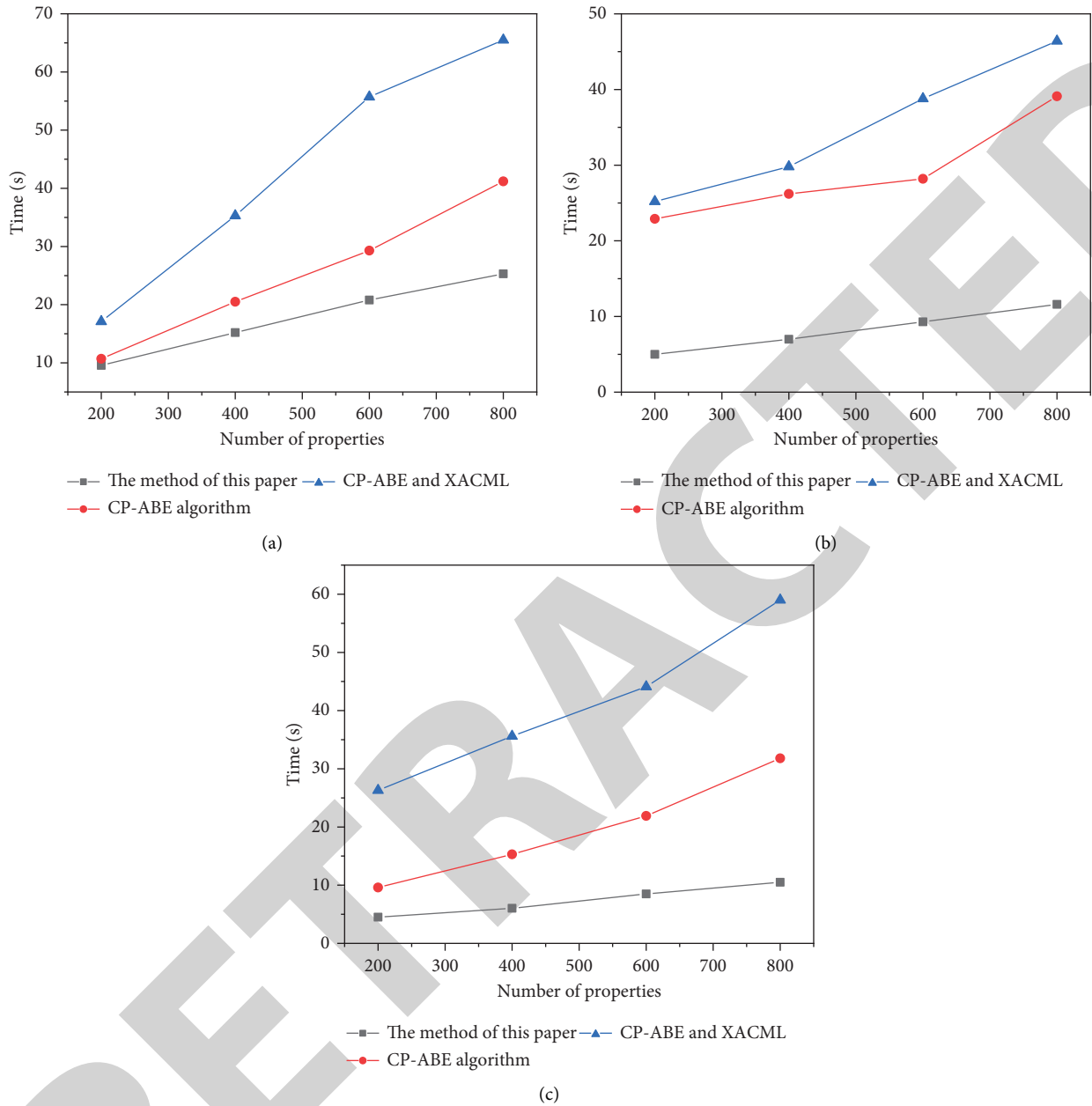


FIGURE 3: Test results of the three methods. (a) Encryption time consumption results, (b) decryption time consumption result, (c) and time consumption result of key acquisition.

deal with the problems of IoT data access control and encrypted storage, the storage space occupied is 16 MB, 33 MB, and 61 MB, compared with the other two methods, the proposed method has obvious advantages and can store the key information corresponding to the data more closely, so there is a small storage space overhead.

The data security test results of the IOT application model show that the data security is as high as 97.77% after being processed by the method proposed in this paper, while the maximum data security of the IOT application model processed by the cloud storage data access control method using the CP-ABE algorithm and the cloud storage access control method using CP-ABE and XACML multiauthority security are 85.01% and 77.98%, respectively. Under the proposed

method, the IoT application model based on optical fiber network communication has the highest IoT data security.

For the three methods of statistical data of the IOT application model, the calculation amount of optical network nodes when they implement access control and encrypted storage is compared, and the comparison results are shown in Table 1. In Table 1, the proposed method for the Internet of Things application model based on optical fiber network communication, when the Internet of Things data implements access control and encrypted storage, the maximum amount of network node calculation is 10.24 MB, 10.45 MB, and 10.45 MB, and less than the other two methods; the proposed method can reduce the calculation amount of fiber network nodes when implementing access control and encrypted storage of IoT data.

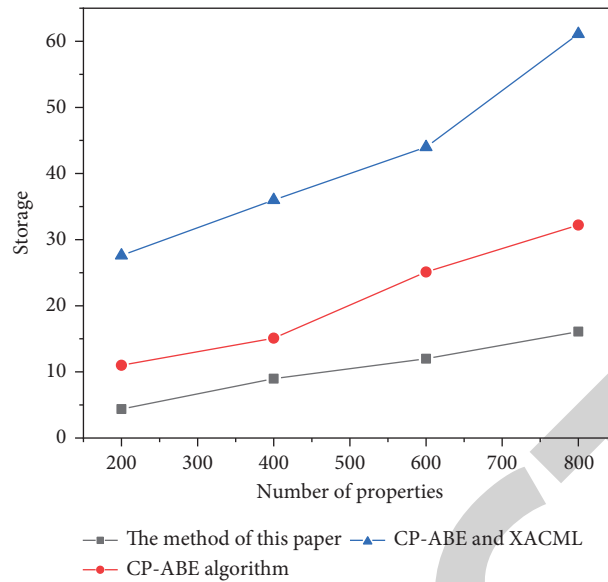


FIGURE 4: Cloud data storage space test results.

TABLE 1: The amount of computation in the IoT data network stage (unit/MB).

Processing times	The proposed method		CP-ABE algorithm		CP-ABE and XACML methods	
	Access control	Encrypted storage	Access control	Encrypted storage	Access control	Encrypted storage
1	10.23	10.44	50.79	50.89	110.23	110.89
2	10.24	10.45	50.77	50.89	110.24	110.89
3	10.23	10.43	50.79	50.88	110.25	110.34
4	10.23	10.43	50.78	50.89	110.43	110.99
5	10.23	10.43	50.76	50.88	110.25	110.56

5. Conclusion

The computing performance and storage performance of the sensing layer nodes of the IoT application model based on optical fiber network communication are limited, and the number of nodes is large, which increases with the increase of application requirements, a method of IoT data access control and encrypted storage based on optical fiber network communication is proposed, this problem is dealt with and its effectiveness is verified in experiments. The conclusions obtained from the experiments are as follows:

- (1) The proposed method is always the least time-consuming in the three procedures of encryption, key acquisition, and decryption and can complete the encrypted storage of IoT data in the shortest time.
- (2) When the number of users is as high as 800 and when the three methods deal with the problems of IoT data access control and encrypted storage, the storage space occupied is 16 MB, 33 MB, and 61 MB, and the storage space overhead of the proposed method is the smallest.
- (3) The security of IoT data after the proposed method is as high as 97.77%.
- (4) When the proposed method implements access control and encrypted storage of IoT data, the maximum amount of network node computation is 10.24 MB, 10.45 MB, and 10.45 MB, compared with

other methods, when the proposed method implements access control and encrypted storage of IoT data, it can reduce the computational load of fiber network nodes.

Data Availability

The data used to support the findings of this study are available from the corresponding author upon request.

Conflicts of Interest

The authors declare no conflicts of interest.

References

- [1] M. Dabbagh, B. Hamdaoui, and A. Rayes, "Peak power shaving for reduced electricity costs in cloud data centers: opportunities and challenges," *IEEE Network*, vol. 34, no. 3, pp. 148–153, 2020.
- [2] Y. Wu, Y. Liu, S. H. Ahmed, J. Peng, and A. Abd El-Latif, "Dominant data set selection algorithms for electricity consumption time-series data analysis based on affine transformation," *IEEE Internet of Things Journal*, vol. 7, no. 5, pp. 4347–4360, 2020.
- [3] C. T. Yang, T. Y. Chen, E. Kristiani, and S. F. Wu, "The implementation of data storage and analytics platform for big data lake of electricity usage with spark," *The Journal of Supercomputing*, vol. 77, no. 6, pp. 5934–5959, 2021.

Retraction

Retracted: Analysis of the Influencing Factors of Urban Sports Brand Sales Volume Based on AHP

Mathematical Problems in Engineering

Received 8 August 2023; Accepted 8 August 2023; Published 9 August 2023

Copyright © 2023 Mathematical Problems in Engineering. This is an open access article distributed under the Creative Commons Attribution License, which permits unrestricted use, distribution, and reproduction in any medium, provided the original work is properly cited.

This article has been retracted by Hindawi following an investigation undertaken by the publisher [1]. This investigation has uncovered evidence of one or more of the following indicators of systematic manipulation of the publication process:

- (1) Discrepancies in scope
- (2) Discrepancies in the description of the research reported
- (3) Discrepancies between the availability of data and the research described
- (4) Inappropriate citations
- (5) Incoherent, meaningless and/or irrelevant content included in the article
- (6) Peer-review manipulation

The presence of these indicators undermines our confidence in the integrity of the article's content and we cannot, therefore, vouch for its reliability. Please note that this notice is intended solely to alert readers that the content of this article is unreliable. We have not investigated whether authors were aware of or involved in the systematic manipulation of the publication process.

Wiley and Hindawi regrets that the usual quality checks did not identify these issues before publication and have since put additional measures in place to safeguard research integrity.

We wish to credit our own Research Integrity and Research Publishing teams and anonymous and named external researchers and research integrity experts for contributing to this investigation.


The corresponding author, as the representative of all authors, has been given the opportunity to register their agreement or disagreement to this retraction. We have kept a record of any response received.

References

- [1] M. Zhang, Y. Wu, and X. Zhou, "Analysis of the Influencing Factors of Urban Sports Brand Sales Volume Based on AHP," *Mathematical Problems in Engineering*, vol. 2022, Article ID 9625049, 7 pages, 2022.

Research Article

Analysis of the Influencing Factors of Urban Sports Brand Sales Volume Based on AHP

Mingyue Zhang,¹ Yuxin Wu,^{2,3} and Xiaolong Zhou ^{2,3}

¹School of East Asia, Pai Chai University, Daejeon 35345, Republic of Korea

²Zhengzhou Vocational College of Finance and Taxation, Zhengzhou 450000, Henan, China

³Department of Leisure Services and Sports, Pai Chai University, Daejeon 35345, Republic of Korea

Correspondence should be addressed to Xiaolong Zhou; 2111818011@e.gzhu.edu.cn

Received 1 July 2022; Accepted 5 August 2022; Published 15 September 2022

Academic Editor: Hengchang Jing

Copyright © 2022 Mingyue Zhang et al. This is an open access article distributed under the Creative Commons Attribution License, which permits unrestricted use, distribution, and reproduction in any medium, provided the original work is properly cited.

In order to evaluate the brand image and help enterprises to build an ideal brand image, the influence factors of urban sports brand sales volume based on AHP are studied. The article takes the A sports brand as the research object, selects six dimensions including product dimension, enterprise dimension, and service image dimension, establishes a brand image evaluation model, and uses the AHP to study the A sports brand image. The experimental results show that: it is found that the overall evaluation value of A sports brand image is 81.153 points, which is rated as very satisfactory, it is proven that the research gives relevant recommendations for maintaining and developing brand image.

1. Introduction

Archetypes are ubiquitous in many sports brand images, they more or less contain the shadow of some archetypes, and marketers may not realize this, but as soon as a brand enters the world of meaning, it will touch the archetype. In the image advertising of world-renowned sports brands, the image of the prototype generally exists. Although the research on consumer brand cognition based on the “cognition-attribute” research paradigm has achieved fruitful results, it still lacks a deep understanding of consumer brand cognition [1]. In the field of brand research, there are several special concepts, such as brand spirit, brand essential, brand soul, and brand resonance. From the perspective of analytical psychology, these concepts point to something similar at the bottom of the consumer psyche, which is related to the archetypes deep within us.

Brands, like where we work, study or the environment around us, have become an important part of our daily lives. In today’s age of brands, some super brands have become a symbol, and some brands are trying to become international brands recognized by consumers [2]. The

prototype paradigm based on Jung’s prototype theory has received more and more attention from foreign brand marketing scholars. The rationale for incorporating archetype theory into global brand marketing is that brand archetypes reflect the way humans interpret their relationship to their lifestyle, combined with the bottom layer of consumer psychology, providing consumers with cross-cultural symbolism for identity construct. Therefore, brand marketers try to discover the “soul” of the brand, combine the basic psychological tendencies of consumers, and express it in a way that connects universal archetypes to create a truly global icon. Logo brands acquire symbolic meaning through association with archetypes, and consumers buy logo brands to acquire the symbolic meaning of mythological archetypes to construct the self, social, and cultural identities. Unique stories and myths infused or crafted around a product create consumer beliefs about the brand [3]. By associating the brand with the positive characteristics of an archetypal image, marketers integrate and disseminate the advertising marketing information chain with a specific archetypal trait, bringing a mysterious experience to consumers.

2. Literature Review

Seyyedamiri and Khosravani proposed the five-star model of brand equity, that is, “five-star” consists of brand awareness, recognition, association, loyalty, and other unique assets, the theory believes that the purpose of brand communication is to accumulate brand equity [4]. Liu et al. put forward the theory of integrated marketing communication, which has far-reaching influence on communication and marketing so far. Its core idea is that when an enterprise conducts communication activities, all communication means should be unified and reorganized, but at the same time, consumers will get the same information no matter which channel they choose [5]. Cai and Wei proposed “global brand strategy” and many other theories have promoted the development of brand communication theory [6]. Yang et al. put forward the concept of brand ecology, thinking that the brand has the characteristics of life and exists in a complex environment, and its survival and development conform to the characteristics of ecological behavior [7]. Sui et al. put forward some innovative viewpoints, such as the choice of advertising communication is not the chaotic media, but the precise advertising carrier [8]. Lopez et al. believes that “brand communication is an activity to communicate with consumers through advertising, marketing activities, sales communication and other channels [9]. Yadav, proposed that the process of brand communication is the process of transmitting brand information to consumers. The concept of brand communication is defined as follows: the so-called brand communication, also known as brand image communication, is the process of transmitting the information contained in brand elements to consumers and the public through various communication channels or means of communication, only when consumers recognize, accept, consume and experience can a brand become a real brand. It will analyze the various elements of brand communication, and provide the basis for the shaping and communication of brand image [10]. Song et al. proposed that brand is a two-way value relationship, that is, there is a two-way value relationship between consumers, enterprises, and brands. In the book, he thought about the development of brand communication in the Internet era and also constructed a theoretical system of integrated brand communication from the perspective of value integration and proposed related models [11].

As a well-known local sporting goods company in China, A-Sports brand integrates honors such as “China Famous Brand,” “China Famous Brand Product,” “China Quality Inspection Free Product,” “China Top 500 Brand,” and its sales performance ranks among the top in the country, the comprehensive market share of sports shoes has ranked first among similar products in the country for many consecutive years and has a good reputation among. The author takes the sports brand of A sports brand as the research object and establishes a brand image evaluation model. By determining the six dimensions of the brand image, including product dimension, enterprise dimension, service image dimension, publicity image dimension, enterprise-customer relationship dimension, and brand symbol dimension, the brand

image of A sports brand is evaluated, and relevant conclusions are drawn and the future brand is given, advice on image development.

3. Research Methods

3.1. Analysis of the Current Situation of a Sports Brand Sports Brand. The growth of A sports brand has gone through three stages: start-up, rapid growth, and brand promotion. The initial stage has completed the original accumulation, and the rapid growth stage mainly relies on advanced channel construction and advertising strategies. At present, the A sports brand is mainly in the stage of brand promotion. Under the attack of many sports brands at home and abroad, how to cultivate the brand of A sports brand and stand out is undoubtedly the primary task of the company [12]. According to the difference in market position and product substitution degree, the competitors of A Sports brand can be divided into direct competitors and industry competitors, direct competitors are competitors with similar positioning to A sports brand and strong product substitution; Industry competitors refer to competitors whose brand positioning is very different from that of A Sports and whose products are less substitutable. An analysis of the advantages and disadvantages of A sports brand and its main competitors is shown in Table 1.

3.2. Determination of A Sports Brand Brand Image Evaluation Index. In the evaluation of the brand image, the factors that affect brand image are complicated, based on the Fan Xiucheng model and the characteristics of the sporting goods industry, the author proposes six evaluation dimensions: product dimension, enterprise dimension, service image dimension, publicity image dimension, enterprise-customer relationship dimension and symbol dimension [13]. On the basis of these six dimensions, it is subdivided into 30 factors such as product quality, style, and price (see Table 2). And, the Analytic Hierarchy Process (AHP method) is used to determine the weight of each element at each level and form the A sports brand image evaluation index system. Figure 1 is a tree structure diagram of the A sports brand image evaluation factor index system.

According to the brand image evaluation factor index system, it is determined that the target layer X layer is the comprehensive evaluation value of A sports brand image, $X_1, X_2, X_3, \dots, X_6$ is the product dimension, enterprise dimension, service image dimension and other six dimensions, $X_{11}, X_{12}, X_{13}, \dots, X_{63}$ are 30 evaluation factors such as product quality.

3.3. Determination of the Weight of Factors in the Brand Image Evaluation of a Sports Brands. In order to make the weight of the brand image evaluation factors better reflect the importance of each factor to the brand image, the author interviewed 2 scholars in brand management and 5 representative sales managers, marketing managers, and employees with at least 3 years of work experience in the sports product industry, on the importance of brand image evaluation factors at all levels to grade the degree, the scores are

TABLE 1: Analysis of the advantages and disadvantages of A sports brand and its main competitors.

Type	Brand	Advantage	Disadvantage
Direct competitor	B	(1) Early start, mature management and operation level (2) large market share and high brand awareness (3) production has been outsourced, focusing on R&D and branding	(1) The product is not very professional, the positioning is not clear, it is both leisure and sports (2) The product name is easy to be regarded as gymnastics, and the consumer's cognition is poor. (3) The product concept "anything is possible" is similar to "impossible is nothing" of the D brand, but lacks features
Industry competitor	C, D, etc.	(1) industry leader, leading market share, high brand loyalty and reputation (2) production outsourcing, strong R&D and marketing capabilities, strong financial strength, and advanced management level (3) Clear market and product positioning, pyramid-shaped scientific brand planning (4) strong star endorsement lineup	(1) The disease of large enterprises, low management efficiency, lack of innovation and vitality (2) due to outsourced production of products, there are supply chain and product quality risks (3) In the Chinese market, it is not acclimatized, and the channel strategy of its sales agents is an obstacle to its development
Research object	A	(1) strong learning ability, independent research, and development ability is better than direct competitors (2) Strong supply chain integration ability and R&D ability make the product cost lower and the quality better (3) perfect production and sales system: with integrated construction from product design, production to terminal sales	(1) in the low-end market, the bargaining power of products is low (2) core competencies to be cultivated and developed (3) The brand lacks overall planning, and the brand awareness, loyalty, and reputation need to be further improved

TABLE 2: Hierarchy structure of factors for brand image evaluation of A sports.

A comprehensive evaluation value of sports brand image X	Product dimension X1	X11	Product quality	
		X12	Product style	
		X13	Product material	
		X14	Product price	
		X15	Product color	
	Enterprise dimension X2	X16	Additional services (such as promotions, additional gifts, etc.)	
		X21	The company's position in the market	
		X22	Knowledge of the business	
		X23	The stability of enterprise product quality	
		X24	Enterprise innovation	
		X25	The reliability of the products produced by the enterprise	
		Service image dimension X3	X31	Store location
	X32		Store environment	
	X33		The quality of service personnel	
	X34		Number of service staff	
	X35		Service staff clothing	
	X36		After-sales service	
	X37		Ease of purchasing the product	
	X41		Discounts, giveaway promotions	
	Publicity image dimension X4		X42	Membership card and VIP card system
			X43	Impressed by the ad
		X44	Advertising spokesperson image	
		X45	Advertising slogan	
		X51	The role of brands in life	
		Enterprise-customer relationship dimension X5	X52	The degree of impact after the brand is discontinued
	X53		Brand irreplaceability	
	X54		The degree of conformity with the consumer's personality and taste	
	Brand symbol dimension X6	X61	Brand name	
		X62	Branded	
		X63	Logo	

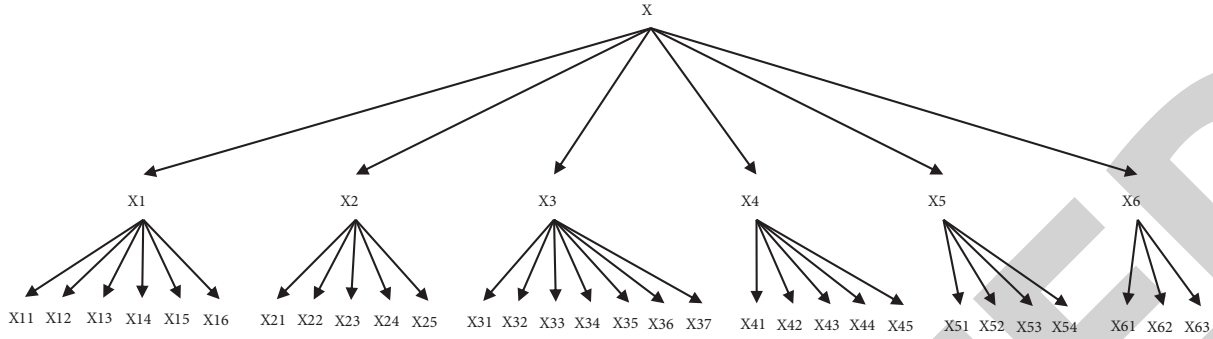


FIGURE 1: A tree structure diagram of sports brand image evaluation factor index system.

weighted and averaged to obtain a judgment matrix, and the yaahp software is further used to calculate the priority weights of factors at each level [14]. After calculation, the maximum eigenvectors of A, A1, A2, A3, A4, A5, and A6 are 6.5446, 6.3079, 5.4273, 7.5475, 5.2587, 4.1384, and 3.0385, respectively. Random consistency ratio C. R. They are 0.0878, 0.0496, 0.0954, 0.0692, 0.0578, 0.0512, and 0.0333, respectively, which passed the consistency test.

Table 3 shows the weights of all factors at the three levels. Among them, among the secondary factors, the product dimension X1 has the largest weight, which is 0.4586, indicating that the product has the greatest impact on the brand image of the A sports brand; The second is the dimension of publicity image, and the dimension of the enterprise-customer relationship, with weights of 0.2411 and 0.1295, respectively; compared with the other five dimensions, the symbol dimension is the smallest at 0.0291, indicating that the impact of symbols on the brand image of A sports brand is relatively small [15]. For the third-level factor, in the product dimension, the weight of product quality X11 is the highest, which is 0.4121, followed by the price of the product; in the enterprise dimension, the position of the enterprise in the market contributes the most to it, with a contribution rate of 0.5183, followed by the reliability of the enterprise’s products and the stability of the enterprise’s product quality; in terms of service image, the largest weight of store environment is 0.3579, followed by the convenience of purchasing products and the location of the store; in the dimension of publicity image, the impression of advertisement has the largest weight, which is 0.5242, followed by membership card, VIP card system and advertising image spokesperson; in the dimension of enterprise-customer relationship, the largest contribution rate is 0.4937, followed by the role of the brand in life; in the dimension of brand symbol, the contribution rate is the brand name, brand packaging and brand logo [16].

3.4. Calculation of Fuzzy Evaluation of Brand Image of a Sports Brand. In the fuzzy evaluation calculation, the qualitative description of the quality of the evaluation object, the author uses four levels of evaluation to establish the evaluation vocabulary V: V1 (very satisfied) V2 (satisfied) V3 (general) V4 (dissatisfied).

TABLE 3: A sports brand image evaluation index weight table.

Index	Weight set
X	A = {0.4586, 0.0882, 0.0535, 0.2411, 0.1295, 0.0291}
X1	A1 = {0.4121, 0.1279, 0.0485, 0.2863, 0.0321, 0.0931}
X2	A2 = {0.5183, 0.0761, 0.1238, 0.0438, 0.2380}
X3	A3 = {0.1613, 0.3579, 0.0964, 0.0228, 0.0296, 0.0560, 0.2760}
X4	A4 = {0.0672, 0.2475, 0.5242, 0.1224, 0.0387}
X5	A5 = {0.3072, 0.0887, 0.1104, 0.4937}
X6	A6 = {0.6370, 0.2583, 0.1047}

The prior standard of satisfaction is P: [100–90] (excellent), (90–80] (good), (80–70] (good), (70–60] (pass), (60–0] (no pass).

A matrix R is established to perform single-factor evaluation on the subfactor layer. On this basis, according to the multiplication rule of fuzzy evaluation, the fuzzy evaluation matrix E of the first-level index can be obtained as follows:

$$E = \begin{bmatrix} A_1 \times R_1 \\ \dots \\ A_i \times R_i \end{bmatrix} = \begin{bmatrix} 0.5195, 0.0388, 0.0326, 0.2991 \\ 0.5182, 0.0808, 0.3748, 0.0263 \\ 0.5031, 0.3202, 0.1461, 0.0306 \\ 0.5560, 0.3911, 0.0393, 0.0136 \\ 0.3316, 0.4000, 0.1657, 0.1027 \\ 0.5404, 0.0326, 0.4261, 0.0009 \end{bmatrix} \quad (1)$$

Among them, R_i is the fuzzy matrix of the secondary index, A_i is the weight of the secondary index, and $i = 1, 2, 3, 4, 5, 6$.

Calculate the variance of the subindex layer and determine the weight of the index layer: $A = [0.4586, 0.0882, 0.0535, 0.2411, 0.1295, 0.0291]$, then there are the following formulas (2) and (3):

$$X = A \times E = [0.5035, 0.2527, 0.0994, 0.1444], \quad (2)$$

$$X' = [0.5035, 0.2527, 0.0994, 0.1444], \quad (3)$$

Then, the comprehensive evaluation result is the following formula (4):

$$Q = X' \times P = [0.5035, 0.2527, 0.0994, 0.1444] \times \begin{bmatrix} 90 \\ 80 \\ 70 \\ 60 \end{bmatrix} = 81.153. \quad (4)$$

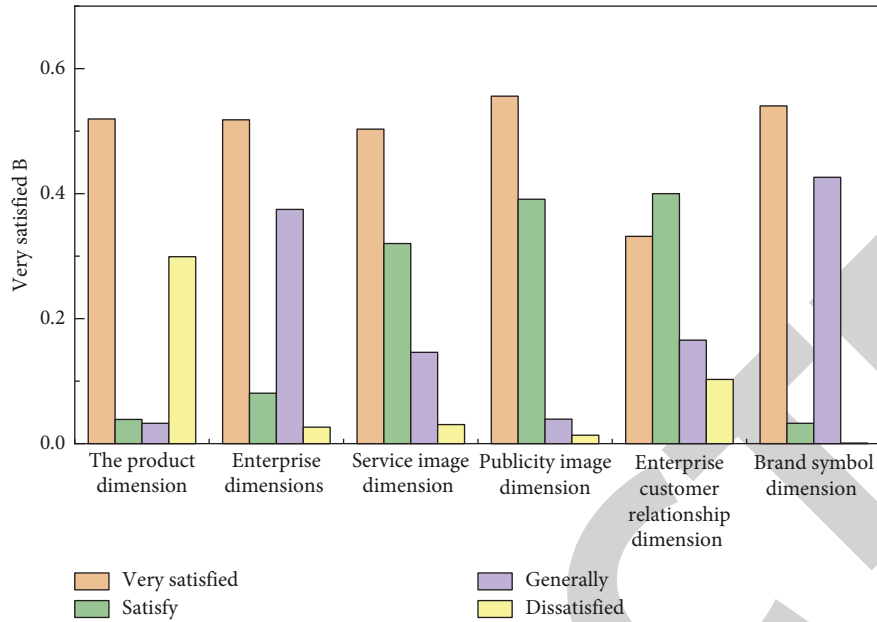


FIGURE 2: The overall situation of the evaluation of each dimension of A sports brand image.

TABLE 4: Evaluation of various dimensions of A sports brand image.

	Very satisfied	Satisfy	Generally	Dissatisfied
Sort from high to low	Publicity image dimension	Enterprise-customer relationship dimension	Dimension brand symbol dimension	Product dimension
	Brand symbol dimensions	Publicity image dimension	Enterprise dimension	Enterprise-customer relationship dimension
	Product dimension	Service image dimension	Enterprise-customer relationship dimension	Service image dimension
	Enterprise dimension	Enterprise dimension	Publicity image	Enterprise dimension
	Service image dimension	Product dimension	Product dimension	Brand symbol dimensions
	Enterprise-customer relationship dimension	Brand symbol dimensions	Service image dimension	Publicity image dimension

The application of the evaluation model and the feedback on the evaluation results can be seen, A sports brand sports brand image evaluation index and actual evaluation results have a good consistency in connotation and extension, and each index is measurable, which basically reflects the scientificity and operability of brand image evaluation. The overall situation of A sports brand sports brand image evaluation is shown in Figure 2.

4. Analysis of Results

Through 30 factors of six dimensions, including product dimension, enterprise dimension, service image dimension, publicity image dimension, enterprise-customer relationship dimension, and brand symbol dimension, the brand image evaluation model of A sports brand is constructed, and the result of A sports brand sports is obtained, the evaluation results of the overall brand image and the evaluation results of the six dimensions [17].

From the overall results of the evaluation model, it can be seen that the total value of the sports brand image evaluation

of A sports brand is 81.153 points, and the weight distribution of the comment grades is: very satisfied 0.5035, satisfied 0.2527, generally 0.0994, dissatisfied 0.1444, indicating that the A sports brand image is in the between excellent and good, the rating is very satisfied.

The weights of the six evaluation dimensions are product dimension (0.4586), publicity image dimension (0.2411), enterprise-customer relationship dimension (0.1295), enterprise dimension (0.0882), service image dimension (0.0535), brand symbol dimension (0.0291), the evaluation of each dimension is shown in Table 4. Except for the enterprise-customer relationship dimension, which is at the satisfaction level, the other five dimensions are at the very satisfactory level, indicating that the role of the enterprise in life and the degree of influence after production suspension are low, reflecting the high risk of brand replacement. In the dissatisfaction level, the product dimension ranks first, but the product dimension has the largest weight among all factors, it shows that consumers still hope that the A sports brand can guarantee the quality of products, further reduce prices and provide more complete additional services [18–24].

5. Conclusion

Compared with the international strong sports brand, the sports brand has a big gap in terms of the marketing concept, capital strength, technical ability, and management level. In order to adapt to the changing market competition environment, A sports brand still needs to practice internal strength, study consumer psychology and behavioral characteristics, cultivate its own long-term competitive advantage, especially establish a brand concept, and create a positive, clear, and unique in the minds of customers, brand image, maintain customer satisfaction and loyalty. The specific measures are as follows:

Establish a Scientific Brand Concept. A sports brand decision makers must have scientific brand awareness and attach great importance to the construction of their own brands; in the process of brand building, we must adhere to scientific decision-making and tactful choices, starting from the actual situation of the enterprise, while fully excavating the essence of national culture, we must absorb the design experience of Nike, Adidas, and other brands, carefully build brand image, reasonably choose brand promotion channels, and actively participate in international brand competition.

Refine and Promote the Core Value of the Brand. The core value of the brand is the foundation of the A sports brand, the A sports brand is based on the middle and low-end market, the core value is "grass-roots culture," which is different from Nike's elite culture and Li Ning's national culture and represents the value of the broadest class, culture is a kind of perseverance in the face of failure, hope to win respect and glory through unremitting struggle. Therefore, a series of activities such as VI design, celebrity endorsement, sponsorship, and public relations of A sports brand sports brand must focus on this core value and realize the concept of "keep moving."

Increase Brand Recognition, Loyalty, and Reputation. High brand recognition requires A sports brand to fulfill basic commitments such as product quality, price, and appearance based on its high-quality and low-cost product positioning. Increase awareness through word-of-mouth communication and enhance the positive image of the A sports brand. High brand loyalty requires A sports brand to provide better products and services on the basis of fulfilling its basic commitments, and to maintain and manage the relationship with new and old customers. It can increase sales, reduce costs, and form competition barriers. High brand reputation, on the one hand, A sports brand should rely on marketing to provide customers with more transfer value and improve customer satisfaction.

Data Availability

The data used to support the findings of this study are available from the corresponding author upon request.

Conflicts of Interest

The authors declare that there are no conflicts of interest.

References

- [1] H. K. Leng, I. M. Rozmand, Y. H. Low, and Y. X. P. Phua, "Effect of social environment on brand recall in sports video games," *International Journal of Gaming and Computer-Mediated Simulations*, vol. 13, no. 1, pp. 1–11, 2021.
- [2] E. Mayes, J. P. Lineberger, M. Mayer, A. Sanborn, H. Smith, and E. Walker, "Automated brand color accuracy for realtime video," *SMPTE Motion Imaging Journal*, vol. 130, no. 3, pp. 45–49, 2021.
- [3] Y. N. Fan, W. Y. Wang, C. W. Kan et al., "Q-max test analysis of men's quick-dry sportswear," *Materials Science Forum*, vol. 1033, pp. 136–140, 2021.
- [4] N. Seyyedamiri and A. Khosravani, "Identification of the effective e-promotional tools on improving destination brand image," *Journal of Global Information Management*, vol. 28, no. 3, pp. 169–183, 2020.
- [5] K. Liu, X. Li, Z. Zhu, L. Brand, and H. Wang, "Factor-bounded nonnegative matrix factorization," *ACM Transactions on Knowledge Discovery from Data*, vol. 15, no. 6, pp. 1–18, 2021.
- [6] W. Cai and Z. Wei, "Piigan: generative adversarial networks for pluralistic image inpainting," *IEEE Access*, vol. 8, no. 1, pp. 48451–48463, 2020.
- [7] L. Yang, B. Li, W. Li, H. Brand, B. Jiang, and J. Xiao, "Concrete defects inspection and 3d mapping using cityflyer quadrotor robot," *IEEE/CAA Journal of Automatica Sinica*, vol. 7, no. 4, pp. 991–1002, 2020.
- [8] Y. Sui, G. Li, and J. Ge, "Sales associations between brand stores based on spatial interaction effects," *Mathematical Problems in Engineering*, vol. 2021, no. 2-3, pp. 1–10, Article ID 9990947, 2021.
- [9] R. Lopez, S. Larsson, and J. Silfwerbrand, "Discrete element modelling of rockfill railway embankments," *Granular Matter*, vol. 23, no. 3, pp. 1–14, 2021.
- [10] R. Yadav, "Analytic hierarchy process-technique for order preference by similarity to ideal solution: a multi criteria decision-making technique to select the best dental restorative composite materials," *Polymer Composites*, vol. 42, no. 12, pp. 6867–6877, 2021.
- [11] Z. Song, H. Gao, W. Liu, L. Li, W. Zhang, and D. Wang, "Systematic assessment of dredged sludge dewaterability improvement with different organic polymers based on analytic hierarchy process," *Journal of Environmental Sciences*, vol. 103, pp. 311–321, 2021.
- [12] J. Shin, I. You, and J. T. Seo, "Investment priority analysis of ics information security resources in smart mobile iot network environment using the analytic hierarchy process," *Mobile Information Systems*, vol. 2020, no. 3, pp. 1–11, 2020.
- [13] C. Wu, Y. Guo, and L. Su, "Risk assessment of geological disasters in nyingchi, tibet," *Open Geosciences*, vol. 13, no. 1, pp. 219–232, 2021.
- [14] E. S. Ari and C. Gencer, "The use and comparison of a deterministic, a stochastic, and a hybrid multiple-criteria decision-making method for site selection of wind power plants: an application in Turkey," *Wind Engineering*, vol. 44, no. 1, pp. 60–74, 2020.
- [15] J. J. Zhao, R. N. Chen, J. H. Wang, and X. Y. You, "Multiple indicators and analytic hierarchy process (ahp) for comprehensive performance evaluation of exhaust hood," *Building Simulation*, vol. 15, no. 6, pp. 1097–1110, 2022.

Retraction

Retracted: Research on the Financial Support Performance Evaluation of Big Data Industry Development

Mathematical Problems in Engineering

Received 5 December 2023; Accepted 5 December 2023; Published 6 December 2023

Copyright © 2023 Mathematical Problems in Engineering. This is an open access article distributed under the Creative Commons Attribution License, which permits unrestricted use, distribution, and reproduction in any medium, provided the original work is properly cited.

This article has been retracted by Hindawi, as publisher, following an investigation undertaken by the publisher [1]. This investigation has uncovered evidence of systematic manipulation of the publication and peer-review process. We cannot, therefore, vouch for the reliability or integrity of this article.

Please note that this notice is intended solely to alert readers that the peer-review process of this article has been compromised.

Wiley and Hindawi regret that the usual quality checks did not identify these issues before publication and have since put additional measures in place to safeguard research integrity.

We wish to credit our Research Integrity and Research Publishing teams and anonymous and named external researchers and research integrity experts for contributing to this investigation.

The corresponding author, as the representative of all authors, has been given the opportunity to register their agreement or disagreement to this retraction. We have kept a record of any response received.

References

- [1] W. Fu, J. Zhao, C. Wang, and X. Zhou, "Research on the Financial Support Performance Evaluation of Big Data Industry Development," *Mathematical Problems in Engineering*, vol. 2022, Article ID 1972726, 9 pages, 2022.

Research Article

Research on the Financial Support Performance Evaluation of Big Data Industry Development

Wenyu Fu,¹ Jingfeng Zhao ,² Changming Wang,¹ and Xiaobin Zhou¹

¹School of Economics & Management, Northwest University, Xi'an 710127, Shaanxi, China

²Research Center of Western China's Economic Development, Northwest University, Xi'an 710127, Shaanxi, China

Correspondence should be addressed to Jingfeng Zhao; 17055101210023@hainanu.edu.cn

Received 10 July 2022; Accepted 10 August 2022; Published 15 September 2022

Academic Editor: Hengchang Jing

Copyright © 2022 Wenyu Fu et al. This is an open access article distributed under the Creative Commons Attribution License, which permits unrestricted use, distribution, and reproduction in any medium, provided the original work is properly cited.

In order to solve the problem that the traditional information systems have such as slow running responses and cannot meet the expected requirements of users, a performance evaluation method of financial support for the development of the big data industry is proposed. According to the characteristics of financial support, this paper uses the analytic hierarchy process (AHP) and the fuzzy comprehensive evaluation principle to establish a specific evaluation index system for the performance evaluation of financial support in the big data industry and select a suitable index group. In order to reflect the financial support performance, the analytic hierarchy process (AHP) is used to calculate the weight of various performance evaluation indicators, and the fuzzy comprehensive evaluation is used to combine qualitative analysis and quantitative analysis to evaluate and calculate the big data industry scientifically, objectively, fairly, and accurately. In financial support performance, experiments show that the proposed method not only has a fast response time but also can ensure that the actual results after the system runs are in line with the expectations of the system users.

1. Introduction

The big data industry is an economic set related to all links of data, such as its production, storage, analysis, processing, and application, and it is becoming a new growth point of the future economy and an important factor to promote economic structure transformation and industrial upgrading, leading to a new pattern of economic and social development. Adhering to the innovation-driven development, accelerating the deployment of big data and deepening the big data applications have become the intrinsic need and inevitable choice of stabilizing the growth, promoting the reform, adjusting the structure, benefiting the people, and driving the modernization of government governance ability. In order to keep up with the development pace of the world's big data, in recent years, the Chinese government has begun to pay attention to the research and development of the big data industry, with an investment exceeding 50% in the big data industry. The State Council of the People's Republic of China, the National

Development and Reform Commission of the People's Republic of China, the Ministry of Industry and Information Technology of the People's Republic of China, and so on are steadily promoting the development of the big data industry by means of targeted support, project support, and so on[1].

In the era of big data, by building a financial sharing center, the accounting processing efficiency can be improved. After the financial sharing center is established, an effective performance evaluation system can enable the management and employees of the financial sharing center to clarify their responsibilities and goals to ensure financial sharing. The center provides high-quality services for customers and at the same time promotes the continuous optimization of the process and improves the overall performance level. The article proposes a method to improve financial support from the aspects of clarifying performance evaluation goals, establishing performance evaluation indicators in the big data environment, improving information integration capabilities, and implementing performance evaluation work. The performance evaluation system

promotes the healthy and orderly development of the financial sharing center. Big data is an interdisciplinary field, and the big data industry stretches across education, transportation, consumption, electricity, energy, health, finance, and other fields, and as an emerging industry with huge strategic significance, it should be supported and helped by finance in the early stages of development. Therefore, it is necessary for us to increase our financial investment in the big data industry, improve the infrastructure of the industry, and promote the healthy and rapid development of the big data industry [2–4].

2. Literature Review

There are few research studies on the financial support of the big data industry by scholars at home and abroad, but since the big data industry belongs to the emerging high-tech industry, the research on financial support for the high-tech industry's development can also be applied to the big data industry. This paper summarizes and sorts out the existing domestic and foreign literature mainly on two aspects: the influence of financial support and the performance evaluation of financial expenditure.

Some scholars have found through research studies that the effect of financial subsidies and preferential tax policies is obvious, and these research studies mainly focus on the incentive effect on enterprise R&D activities. Bloom et al. carried out comparative analysis on the economic data of eight countries in the OECD and believed that the preferential tax policies had a promoting effect on the improvement of enterprise R&D investment [5–7]. The economists, Rosa, Hanel, and Czarnitzki et al., researched Canadian companies and believed that the tax credit policy for enterprise R&D activities not only stimulates enterprises to increase R&D investments but also improves the output and profit of enterprise R&D activities. Kohler et al. believed that tax preferences or financial subsidies can promote the research and development of enterprises. Through researching the financial policies that play a major role at different stages, Deng Ziji found that the financial subsidy policy had a certain incentive effect at all stages of technological innovation, including the research and development stage and the achievement transformation stage. However, by researching, other scholars believed that financial subsidies and preferential tax policies had no effect or even had negative effects. Jaffe believed that financial subsidies or preferential tax policies had an inhibitory effect on the research and development of enterprises. Guellec and van Pottelsberghe analyzed the panel data of 17 countries in the OECD and found that the price elasticity of tax preference to enterprise R&D expenditure was negative. Tzelepis and Skuras researched and found that financial subsidies implemented for enterprise investment cannot improve the operation efficiency and profitability [8–10].

In terms of financial expenditure performance evaluation, Drongelen and Cook pointed out that the performance evaluation system of government financial investment in science and technology should take the dynamic change characteristic of the requirements of stakeholders into

consideration, and the key points of the performance evaluation at all stages should be different to some extent. Sohn, YongGyuJoo, and HongKyuHan used the SEM model to study the Science and Technology Promotion Fund of South Korea from three aspects, and Toshiyuki Sueyoshi et al. used the method of data envelopment analysis (DEA) to evaluate and compare the importance of R&D expenditures on Japan's IT enterprises and other manufacturing enterprises. Luo and Chen et al. used the DEA method to establish the financial investment performance evaluation index system and its main index. The science and technology output, which included scientific and technological achievements, economic benefits, and social effects, and the system were verified by taking the performance of local financial investment in science and technology as an example. Qin combined the AHP method and the variation coefficient weighting method, used manpower and financial investment as investment indexes, and used the output of scientific and technological achievements, output of economic benefits, and output of social benefits as the output indexes to build the science and technology performance evaluation model to analyze the financial expenditure performance [11, 12]. Liu built a specific framework for financial data management that accelerates the innovation process of modern enterprises' financial management models and focusses on the advantages of using the financial sharing center for enterprises and five specific processes for cost control, hoping to update people's perception of enterprises and traditional concepts of financial management [13].

3. Establishment of the Fuzzy Hierarchy Model

It is a complicated and systematic engineering to fully, accurately, objectively, and fairly carry out the comprehensive evaluation of financial expenditure performance, and it is necessary to establish the advanced, optimized, simple, and practical data model and rely on scientific decision method [14]. Guided by the theory of performance evaluation, this paper starts from the construction of the financial support performance evaluation index system of the big data industry, establishes a proper performance evaluation index system, discusses the basis and method for the determination of evaluation index standard value, and puts forward the comprehensive application of the analytic hierarchy process (AHP) method and fuzzy comprehensive evaluation method to make the empirical evaluation in order to solve the problem of fuzzy evaluation of qualitative indexes.

Using the FAHP method to carry out the quantitative evaluation is not only beneficial for making a comprehensive and objective evaluation of the efficiency of financial expenditure, reflecting the influence of various factors on the performance from different perspectives but also convenient for guiding and standardizing the management of financial expenditure in China. In view of the characteristics of nonlinearity and fuzziness in the process of the financial support performance evaluation of big data industries, this paper intends to construct several evaluation indexes, use

TABLE 1: Financial support performance evaluation index system of big data industry.

Target hierarchy	Criterion hierarchy	Index hierarchy	Concrete meaning
Financial support performance index evaluation system of the big data industry A	Financial investment A_1	The proportion of financial investment in the total financial amount	The proportion of big data industry investment in the total financial investment
		The total number of invested personnel	The number of the personnel engaging in big data industry
		The structure of invested personnel	The situation of the education background and professional titles of the personnel engaging in big data industry
		Invested material resources	The amount, category, and so on of material resources invested in big data industry
		The completion rate of financial investment fund plan	The ratio of the actual amount of funds invested to the amount of funds planned
	Financial implementation A_2	Financial capital management system	Whether the use of management system of financial investment funds is perfect
		Completion status of the technical indexes	Whether the technical indexes meet the expected goals
		Profit-tax rate of financial investment	The ratio of newly increased taxes to total financial investment
		Output rate of financial investment	The ratio of financial investment to the output of big data industry
		Application conversion rate of big data achievements	The ratio of the achievements of the transformed application to the successful application achievements
	Financial profit A_3	Per-capita number of published articles of the invested personnel	The ratio of the number of published articles to the total number of invested personnel
		Per-capita number of obtained patents of the invested personnel	The ratio of the number of obtained patents to the total number of invested personnel

FAHP (fuzzy analytic hierarchy process) to determine the index weight, calculate the composite score of the financial support performance, and finally obtain the quantitative and specific evaluation.

3.1. Evaluation Index. The diversity of big data output performance determines the multiobjective feature of its evaluation, so the financial support performance evaluation system of the big data industry should be a multiobjective evaluation system. The evaluation system can be constructed according to the idea of an analytic hierarchy process, reasonably choosing and setting the index system by hierarchy, attribute, quantity, and quality, and using the performance evaluation as the core. The evaluation index system is divided into the target hierarchy (financial investment performance), the criterion hierarchy (describing main aspects of the performance), and the index hierarchy (that can reflect the quantitative and qualitative indexes of the elements' characteristics).

According to the characteristics of financial support in the big data industry, this paper chooses three major categories of indexes, namely, financial investment, financial implementation, and financial profit, to reflect the financial support performance of the big data industry.

The financial investment mainly reflects the government's degree of emphasis on the investment in the big data

industry. This paper selects four indexes to describe it from the perspective of investment, and the four indexes are the proportion of financial investments in the total financial amount, the total number of invested personnel, the structure of invested personnel, and the invested material resources.

The financial implementation mainly reflects the execution status in actual implementation of the government's financial support for the big data industry. There are four secondary indexes, and they are, respectively, the completion rate of a financial investment fund plan, the financial capital management system, the completion status of the technical indexes, and the profit-tax rate of financial investment.

The financial profit mainly reflects the economic and social benefits brought by the development of the financially supported big data industry. This paper chooses four secondary indexes to measure it, and they are the output rate of financial investment; the application conversion rate of big data achievements; the per-capita number of published articles of the invested personnel; and the per-capita number of obtained patents of the invested personnel.

3.2. Construction of Fuzzy Hierarchy Model. The fuzzy hierarchy model is constructed according to the evaluation index system, in which the criterion hierarchy of financial support performance evaluation index system of the big data

industry has three elements, and the index hierarchy has 12 indexes. The evaluation content and scope of each level are shown in Table 1:

4. Empirical Analysis

4.1. Determination of Index Weight

4.1.1. Construction of Judgment Matrix. Before calculating the weight of each index, the relative importance of each index should be judged, and these judgments are expressed numerically to generate the judgment matrix, as shown in Table 2. The judgment matrix represents the comparison of the relative importance between the relevant indexes of this hierarchy aiming at the target of the previous hierarchy. Based on the idea of analytic hierarchy process and on the basis of the above hierarchical structure of financial support evaluation index system, let us suppose that the judgment matrix to be constructed is $A = (a_{ij})$, in which the value of a_{ij} is the relative importance of the indexes and is determined by the following method.

In this paper, the relative importance of the indexes is obtained through pairwise comparison according to the specific situation, and then the judgment matrices of the primary and secondary indexes are obtained, as shown in Table 3.

Judgment matrix of the first-order indexes is as follows:

$$A = \begin{bmatrix} 1 & \frac{1}{3} & \frac{1}{7} \\ 3 & 1 & \frac{1}{2} \\ 7 & 2 & 1 \end{bmatrix}. \tag{1}$$

$$A = \begin{bmatrix} 1 & \frac{1}{3} & \frac{1}{7} \\ 3 & 1 & \frac{1}{2} \\ 7 & 2 & 1 \end{bmatrix} \xrightarrow{\text{normalization}} \begin{bmatrix} 0.09 & 0.10 & 0.09 \\ 0.27 & 0.30 & 0.30 \\ 0.64 & 0.60 & 0.61 \end{bmatrix} \xrightarrow{\text{summation according to rows}} \begin{bmatrix} 0.28 \\ 0.87 \\ 1.85 \end{bmatrix} \xrightarrow{\text{normalization}} \begin{bmatrix} 0.09 \\ 0.29 \\ 0.62 \end{bmatrix}. \tag{3}$$

Similarly, the weight vectors of each element of each hierarchy of the judgment matrices of A_1 , A_2 , and A_3 can be calculated.

Thus, we can obtain the weights of the index in Table 1, and the results are shown in Table 4.

4.1.3. Matrix Consistency Check. The pairwise comparison matrix constructed above constitutes the foundation of decision analysis, and when comparing and judging the relative importance of the indexes because it is a man-made

Similarly, judgment matrix of the second-order indexes can be obtained as shown in the following formula:

$$A_1 = \begin{bmatrix} 1 & 3 & 3 & 1 \\ \frac{1}{3} & 1 & 1 & \frac{1}{3} \\ \frac{1}{3} & 1 & 1 & \frac{1}{3} \\ 1 & 3 & 3 & 1 \end{bmatrix}, \quad A_2 = \begin{bmatrix} 1 & \frac{1}{3} & 3 & 5 \\ 3 & 1 & 5 & 6 \\ \frac{1}{3} & \frac{1}{5} & 1 & 3 \\ \frac{1}{5} & \frac{1}{6} & \frac{1}{3} & 1 \end{bmatrix}, \quad A_3 = \begin{bmatrix} 3 & \frac{1}{3} & 1 & 3 \\ 4 & 1 & 3 & 4 \\ 1 & \frac{1}{4} & \frac{1}{3} & 1 \\ 1 & \frac{1}{4} & \frac{1}{3} & 1 \end{bmatrix}. \tag{2}$$

4.1.2. Normalization Processing. The methods of calculating weight include the weighted least square method, the eigenvalue method, the square root method, the sum-product method, and so on. In the calculation of the financial support performance index evaluation system of the big data industry discussed in this article, the sum-product method is adopted to calculate the weight for the judgment matrix: normalize each column of the judgment matrix first, then sum the matrix after the normalization of columns according to rows, and normalize the vectors after the summation as the weight of each index factor. Take the judgment matrix A, for example,

comparison and judgment, there are often inconsistent judgments. Therefore, the consistency must be checked to find out whether the weight vector values calculated are scientific and reasonable. The specific checking steps are as follows.

Firstly, calculate the eigenvalue of the maximum of the judgment matrix λ_{\max} : $\lambda_{\max} = 1/n \sum_{i=1}^n \sum_{j=1}^n a_{ij} w_j / w_i$.

Calculate by taking the judgment matrix A as an example, $w = (0.09, 0.29, 0.62)^T$.

$$Aw = (0.28, 0.87, 1.83)^T \tag{4}$$

TABLE 2: Judgment matrix scale table.

Scale X_{ij}	Meaning
1	Factor i is as important as factor j
3	Factor i is slightly more important than factor j
5	Factor i is more important than factor j
7	Factor i is very important compared with factor j
9	Factor i is absolutely important compared with factor j
2, 4, 6, 8	Med-value of the above two adjacent judgments
Reciprocal 1, 1/2, ... 1/9	The judgment value obtained by the comparison of factor j and factor i is the reciprocal of X_{ij} $X_{ji} = 1/a_{ij}X_{ii} = 1.$

TABLE 3: Primary indexes judgment matrix A.

Financial support performance A	Financial investment A_1	Financial implementation A_2	Financial profit A_3
Financial investment A_1	1	1/3	1/7
Financial implementation A_2	3	1	1/2
Financial profit A_3	7	2	1

TABLE 4: Weights of the indexes.

Target hierarchy	Criterion hierarchy	Weight	Index hierarchy	Weight
Financial support performance index evaluation system of the big data industry A	Financial investment A_1	0.09	The proportion of financial investment in the total financial amount	0.35
			The total number of invested personnel	0.15
			The structure of invested personnel	0.15
	Financial implementation A_2	0.29	Invested material resources	0.35
			The completion rate of financial investment fund plan	0.27
			Financial capital management system	0.55
			Completion status of the technical indexes	0.12
	Financial profit A_3	0.62	Profit-tax rate of financial investment	0.06
			Output rate of financial investment	0.27
			Application conversion rate of big data achievements	0.52
			Per-capita number of published articles of the invested personnel	0.10
			Per-capita number of obtained patents of the invested personnel	0.11

So, the judgment matrix A's $\lambda_{max} = 1/3(0.28/0.09 + 0.87/0.29 + 1.83/0.62) = 3.02$.

Secondly, calculate the deviation index from the consistency, the CI value $CI = (\lambda_{max} - n)/(n - 1)$, and n is the number of indexes in the matrix. The CI value of A is calculated according to the above formula: $CI = (3.02 - 3)/(3 - 1) = 0.01$.

Thirdly, find the average random consistency index, the RI value, as shown in Table 5.

Fourthly, calculate the random consistency ratio CR, $CR = CI/RI$. If $CR \geq 0.1$, the judgment matrix constructed fails in the consistency check and it needs to be adjusted; and if $CR < 0.1$, it can be considered that the judgment matrix has satisfactory consistency and the index weights obtained by the judgment matrix can be applied to the comprehensive measurement model. As CR is obtained by the above calculation: $CR = CI/RI = 0.01/0.5149 = 0.019 < 0.1$, which indicates that A has passed the consistency check.

Similarly, through processing and checking the judgment matrix of the index hierarchy, it is found that the judgment matrices of A_1 , A_2 , and A_3 pass the consistency check.

4.2. Fuzzy Comprehensive Evaluation. The fuzzy mathematics comprehensive judgment is a method that makes comprehensive judgment of the subordinate hierarchy status of the evaluation object from multiple factors (or indexes) based on the composition principle of fuzzy relations. The following is a comprehensive judgment of fuzzy mathematics based on the above analytic hierarchy process.

4.2.1. Determine the Set of Evaluation Factors. The financial support for the big data industry is a complicated process, and the factors that constitute it are complex, changeable, and uncertain, so these factors constitute a fuzzy set. How to

TABLE 5: RI value.

<i>n</i>	2	3	4	5	6	7	8	9	10
RI	0	0.5149	0.8931	1.1185	1.2494	1.3450	1.4200	1.4616	1.4874

TABLE 6: Judgment set of the factors.

Factor	Level 1	Level 2	Level 3	Level 4	Level 5
The proportion of financial investment in the total financial amount	Very high	High	General	Low	Very low
The total number of invested personnel	A great many	Many	General	A few	Few
The structure of invested personnel	Very good	Good	General	Poor	Very poor
Invested material resources	A great many	Many	General	A few	Few
The completion rate of financial investment fund plan	Very good	Good	General	Poor	Very poor
Financial capital management system	Very good	Good	General	Poor	Very poor
Completion status of the technical indexes	Very good	Good	General	Poor	Very poor
Profit-tax rate of financial investment	Very high	High	General	Low	Very low
Output rate of financial investment	Very high	High	General	Low	Very low
Application conversion rate of big data achievements	Very high	High	General	Low	Very low
Per-capita number of published articles of the invested personnel	A great many	Many	General	A few	Few
Per-capita number of obtained patents of the invested personnel	A great many	Many	General	A few	Few

TABLE 7: 0.1–0.9 scale table.

Definition	Scale	Meaning
Equally important	0.5	Two factors are equally important by comparison
Slightly more important	0.6	Factor A is slightly more important than factor B by comparison
Obviously more important	0.7	Factor A is obviously more important than factor B by comparison
Much more important	0.8	Factor A is much more important than factor B by comparison
Extremely more important	0.9	Factor A is extremely more important than factor B by comparison
Reverse comparison	0.1–0.4	$a_{ij} = 1 - a_{ji}$

select the main factors reflecting the financial support performance from this fuzzy set is the key in establishing the comprehensive evaluation model of financial support performance for the big data industry. According to the setting of the index system of the above analytic hierarchy process, the financial support performance evaluation system of the big data industry contains 12 secondary evaluation indexes. Thus, the fuzzy factor vector of the financial support performance evaluation system of the big data industry is obtained:

$$U = (u_1, u_2, u_3, \dots, u_{12}). \tag{5}$$

4.2.2. *Establish a Set of Judgment Vectors.* Since there are three main factors of $A_1, A_2,$ and A_3 and 12 secondary factors that affect the “financial support performance,” the weights of the factors can be given according to the hierarchical analysis, as shown in Table 4. The judgment set consisting of five elements can be given for each of the secondary factors, for example (very good, good, general, poor, and very poor), (very high, high, general, low, and very low), and (a great many, many, general, a few, and few), as shown in Table 6.

4.2.3. *Acquire Fuzzy Evaluation Information.* Although using the method designated by experts is of a certain significance, its scientificity is questionable. Studies show that people can give more accurate judgment only at pairwise comparison, and when the number of factors is greater than 4, the fuzziness of determining the weight is more obvious, and the processing by the method of constructing a fuzzy consistent judgment matrix can eliminate the influence of man-made factors.

The fuzzy consistent judgment matrix R represents the comparison of the relative importance between a certain factor in the previous hierarchy and its related factors in this hierarchy. Suppose the factor C in the previous hierarchy is related to the factors $a_1, a_2, a_3, \dots, a_n$ in the next hierarchy, then the fuzzy consistent judgment matrix F can be expressed as

$$F = \begin{bmatrix} r_{11} & r_{21} & \cdots & r_{1n} \\ r_{21} & r_{22} & \cdots & r_{2n} \\ \cdots & \cdots & \cdots & \cdots \\ r_{n1} & r_{n1} & \cdots & r_{nn} \end{bmatrix}. \tag{6}$$

Thereinto, r_{ij} indicates that factor a_i has a subordinate degree of the fuzzy relation of “ a_i is more important than a_j ” with factor a_j . It can be described in Table 7.

Experts are asked to give a fuzzy judgment of the pairwise comparison of the above 12 factors, and the following fuzzy complementary judgment matrix is obtained after the integration and adjustment:

$$A_1 = (r_{ij}) = \begin{bmatrix} 0.5 & 0.6 & 0.8 & 0.6 \\ 0.4 & 0.5 & 0.7 & 0.5 \\ 0.2 & 0.3 & 0.5 & 0.3 \\ 0.4 & 0.5 & 0.7 & 0.5 \\ 0.4 & 0.5 & 0.7 & 0.5 \end{bmatrix} \quad A_2 = \begin{bmatrix} 0.6 & 0.6 & 0.8 & 0.6 \\ 0.5 & 0.5 & 0.7 & 0.5 \\ 0.3 & 0.3 & 0.5 & 0.3 \\ 0.5 & 0.5 & 0.7 & 0.5 \\ 0.5 & 0.5 & 0.7 & 0.5 \end{bmatrix}$$

$$A_3 = \begin{bmatrix} 0.7 & 0.6 & 0.6 & 0.4 \\ 0.6 & 0.5 & 0.5 & 0.3 \\ 0.4 & 0.3 & 0.3 & 0.1 \\ 0.6 & 0.5 & 0.5 & 0.3 \\ 0.6 & 0.5 & 0.5 & 0.3 \end{bmatrix}.$$

(7)

4.2.4. Determine the Fuzzy Weight Vector. The weight of each factor in the single-factor set is determined by analytic hierarchy process, and thus the fuzzy weight vector is obtained $\Omega = (w_1, w_2, w_3, w_4)$. The weight vector is obtained according to Table 4.

$$\begin{aligned} \Omega_1 &= (0.35 \ 0.15 \ 0.15 \ 0.35)^T \\ \Omega_2 &= (0.27 \ 0.55 \ 0.12 \ 0.06)^T \\ \Omega_3 &= (0.27 \ 0.52 \ 0.10 \ 0.11)^T. \end{aligned} \quad (8)$$

4.2.5. Comprehensive Judgment. The comprehensive judgment models adopted by the fuzzy relation matrix F with respect to weight Ω , include the main factor determining model, the main factor highlighting model, the weighted average model, and so on. The weighted average model $M(\bullet, +)$ can be used if all factors are considered to have an impact on the financial support performance.

$$A_1\Omega_1 = \begin{bmatrix} 0.342 \\ 0.210 \\ 0.404 \\ 0.210 \\ 0.210 \end{bmatrix} \quad A_2\Omega_2 = \begin{bmatrix} 0.407 \\ 0.210 \\ 0.133 \\ 0.210 \\ 0.210 \end{bmatrix} \quad A_3\Omega_3 = \begin{bmatrix} 0.364 \\ 0.210 \\ 0.126 \\ 0.210 \\ 0.210 \end{bmatrix}. \quad (9)$$

4.2.6. Assign Values to the Judgment Set. The components of the comprehensive evaluation level vector obtained above are generally a group of decimals, and a group of percentages can be obtained through multiplying 100%, respectively, by each of the elements of the vector, the meaning of which can

be considered to be the percentage of people favoring the evaluation levels of “Very satisfied, Satisfied, Basically satisfied, Dissatisfied, and Very dissatisfied.” In practical applications, each level of the evaluation set is usually represented by a corresponding specific number. For this reason, we use the median method to assign values to the evaluation set and determine the centesimal system scores from high to low for each evaluation level. v_1 means the score interval of “Very satisfied” is [90, 100]; v_2 means the score interval of “Satisfied” is [80, 89]; v_3 means the score interval of “Basically satisfied” is [60, 79]; v_4 means the score interval of “Dissatisfied” is [50, 59]; v_5 means the score interval of “Very dissatisfied” is [30, 49]. Let us use the medians of the corresponding score sections of 95, 85, 70, 55, and 40 to assign values to the evaluation levels and assume that the valuation vectors of the judgment set, $V = \{v_1, v_2, v_3, v_4, v_5\}$, are (95, 80, 70, 55, and 40), so the comprehensive evaluation valuation of A_1 is (95, 80, 70, 55, 40), $[0.342, 0.210, 0.404, 0.210, 0.210]^T = 97.485$. Similarly, we can obtain the comprehensive evaluation valuations of A_2 and A_3 , and they are 84.702 and 80.091, respectively.

5. Analysis of Results

According to the characteristics of the financial support performance evaluation of the big data industry, we evaluate from three aspects of financial investment, financial implementation, and financial profit. By consulting relevant experts and scholars and according to the analytic hierarchy process, the respective weights of the three evaluation subjects are obtained, and thus the weight matrix is known as $w = (0.09, 0.29, 0.62)^T$. Suppose the centesimal system scores of the comprehensive evaluation results of the three aspects are H_1, H_2 , and H_3 , respectively so, the final evaluation of the financial support performance of the big data industry is as follows:

$$H_{\text{totalscore}} = w \begin{bmatrix} H_1 \\ H_2 \\ H_3 \end{bmatrix} = 0.09 * H_1 + 0.29 * H_2 + 0.62 * H_3. \quad (10)$$

It can be known from the evaluation set valuation content that $H_1 = 97.485$, $H_2 = 84.702$, and $H_3 = 80.091$ and combining with the above formula, the final score of the financial support performance evaluation of the big data industry is obtained.

$$\begin{aligned} H_{\text{totalscore}} &= 0.09 * 97.485 + 0.29 * 84.702 \\ &\quad + 0.62 * 80.091 = 83.001. \end{aligned} \quad (11)$$

So, the final score of the financial support performance evaluation of the big data industry is 83.001.

Among the three primary evaluation indexes selected in this paper, it can be seen from the weight vectors that the weight or proportion of financial profit is the largest, which shows that improving the economic and social benefits of the big data industry is the most important way to financially

support the development of big data industry. Therefore, it is necessary to strengthen the social contribution performance of enterprises, enhance the sense of social responsibility of enterprises, endeavor to improve the research and innovation ability of enterprises, and create the core competitiveness of enterprises at the same time.

6. Conclusion and Recommendation

This paper aims to evaluate the financial support of the big data industry in China. According to the evaluation process, by identifying the factors affecting the performance evaluation of financial support, choosing different evaluation methods, establishing a suitable evaluation, and in conjunction with the results of the evaluation of 3, a detailed analysis of financial support performance for large business data is carried out. Based on the understanding of each influencing factor, highlight the main and secondary effects. Pay special attention to the formulation and implementation of some financial rules, and provide better development suggestions and support for the big data industry.

In terms of the financial investment, the most important thing is the proportion of financial investment in the total financial amount and the invested material resources, which shows that the healthy and rapid development of the big data industry needs heavy financial investment from our country, including the investment of material resources, such as capital, research and development personnel, and infrastructure. This requires the country to integrate existing policy measures, perfect the financial policy system of the big data industry, and clarify the key areas and scope of the financial support.

In terms of the financial implementation, the weight of the financial fund management system is the largest, which indicates that fund management plays an important role in the development of the big data industry. In order to guarantee the reasonable and sound development of the big data industry, it is necessary for the country to introduce the big data industry standard as soon as possible and establish a systematic and thorough fund management system for the big data industry. The development of the big data industry will have a leapfrog change on the future development. First, big data technology will enhance the national governance capacity. Through the integration, analysis, summary, and application of historical data between different departments, it will have a positive prediction and prevention effect on public health, national defense security, education and medical care, public transportation, and other aspects. Second, the big data industry will bring about business model innovation. Third, the big data industry will change the way people think. One of the characteristics of the big data industry is that you

know what, but not why. That is, we only need to know the final result of the data analysis, and we do not need to know its specific calculation process.

Data Availability

The data used to support the findings of this study are available from the corresponding author upon request.

Conflicts of Interest

The authors declare that there are no conflicts of interest.

Acknowledgments

This study was funded by Social Science Foundation of Research Base Project of Ministry of Education, China (15JJD790025).

References

- [1] P. Hanel, D. Czarnitzki, and J. M. Rosa, *Evaluating the impact of R&D tax credits on innovation: a microeconomic study on Canadian firms*, EIB Papers, no. 1, pp. 144–169, Washington, DC, USA, 2009.
- [2] S. G. Cecchetti and M. Kohler, *When Capital Adequacy and Interest Rate Policy Are Substitutes (And when They Are Not)*, BIS Working Paper, Switzerland, 2012.
- [3] Z. Deng and Z. Yang, “The theoretical and empirical analysis of fiscal and taxation policies encouraging the enterprise technology innovation,” *Finance & Trade Economics*, vol. 2011, no. 5, pp. 5–136, 2011.
- [4] A. B. Jaffe, R. G. Newell, and R. N. Stavins, “Environmental policy and technological change,” *Environmental and Resource Economics*, vol. 22, no. 1/2, pp. 41–70, 2002.
- [5] D. Guellec and B. V. P. D. Potterie, “The internationalisation of technology analysed with patent data,” *Research Policy*, vol. 30, no. 8, pp. 1253–1266, 2001.
- [6] D. Tzelepis and D. Skuras, “The effects of regional capital subsidies on firm performance: an empirical study,” *Journal of Small Business and Enterprise Development*, vol. 11, no. 1, pp. 121–129, 2004.
- [7] I. C. Kerssens-van Drongelen and A. Cooke, “Design principles for the development of measurement systems for research and development processes,” *R & D Management*, vol. 27, no. 4, pp. 345–357, 1997.
- [8] S. Y. Sohn, Y. Gyu Joo, and H. Kyu Han, “Structural equation model for the evaluation of national funding on R&D project of SMEs in consideration with MBNQA criteria,” *Evaluation and Program Planning*, vol. 30, no. 1, pp. 10–20, 2007.
- [9] T. Sueyoshi and M. Goto, “A use of DEA-DA to measure importance of R&D expenditure in Japanese information technology industry,” *Decision Support Systems*, vol. 54, no. 2, pp. 941–952, 2013.

Retraction

Retracted: Simulation of Video Image Fault Tolerant Coding Transmission in Digital Multimedia

Mathematical Problems in Engineering

Received 8 August 2023; Accepted 8 August 2023; Published 9 August 2023

Copyright © 2023 Mathematical Problems in Engineering. This is an open access article distributed under the Creative Commons Attribution License, which permits unrestricted use, distribution, and reproduction in any medium, provided the original work is properly cited.

This article has been retracted by Hindawi following an investigation undertaken by the publisher [1]. This investigation has uncovered evidence of one or more of the following indicators of systematic manipulation of the publication process:

- (1) Discrepancies in scope
- (2) Discrepancies in the description of the research reported
- (3) Discrepancies between the availability of data and the research described
- (4) Inappropriate citations
- (5) Incoherent, meaningless and/or irrelevant content included in the article
- (6) Peer-review manipulation

The presence of these indicators undermines our confidence in the integrity of the article's content and we cannot, therefore, vouch for its reliability. Please note that this notice is intended solely to alert readers that the content of this article is unreliable. We have not investigated whether authors were aware of or involved in the systematic manipulation of the publication process.

Wiley and Hindawi regrets that the usual quality checks did not identify these issues before publication and have since put additional measures in place to safeguard research integrity.

We wish to credit our own Research Integrity and Research Publishing teams and anonymous and named external researchers and research integrity experts for contributing to this investigation.

The corresponding author, as the representative of all authors, has been given the opportunity to register their agreement or disagreement to this retraction. We have kept a record of any response received.

References

- [1] F. Li, "Simulation of Video Image Fault Tolerant Coding Transmission in Digital Multimedia," *Mathematical Problems in Engineering*, vol. 2022, Article ID 4657091, 7 pages, 2022.

Research Article

Simulation of Video Image Fault Tolerant Coding Transmission in Digital Multimedia

Feng Li 

School of Humanities and Arts, Nanchang Institute of Technology, Nanchang, Jiangxi 330099, China

Correspondence should be addressed to Feng Li; 20148579@stu.sicau.edu.cn

Received 16 June 2022; Accepted 25 July 2022; Published 13 September 2022

Academic Editor: Hengchang Jing

Copyright © 2022 Feng Li. This is an open access article distributed under the Creative Commons Attribution License, which permits unrestricted use, distribution, and reproduction in any medium, provided the original work is properly cited.

In order to effectively improve the quality of video image transmission, this paper proposes a method of digital multimedia video image coding. The transmission of digital multimedia video image fault-tolerant coding requires sparse decomposition of a digital multimedia video image to obtain the linear form of the image and complete the transmission of video image fault-tolerant coding. The traditional method of fault-tolerant coding is based on human visual characteristics but ignores the linear form of the digital multimedia video image, which leads to the unsatisfactory effect of coding and transmission. In this paper, a fault-tolerant coding method based on wavelet transform and vector quantization is proposed to decompose and reconstruct digital multimedia video images. The smoothness of wavelet transform can remove visual redundancy; the decomposed image is vector quantized. The mean square deviation method and the similar scalar optimal quantization method are used to select and calculate the image vector, construct the over complete database of a digital multimedia video image, and normalize it; the digital multimedia video image is thinly decomposed by asymmetric atoms, and a linear representation of the image is obtained. According to the above-given operations, we can master the distribution range and law of pixels and realize fault-tolerant coding. The experimental results show that when the number of iterations is 15, the CR index is the same, PSNR increases by 8.7%, coding is 23.7% faster and decoding is 15% faster. *Conclusion.* The proposed method can not only improve the speed of fault-tolerant coding but also improve the quality of video image transmission.

1. Introduction

At present, video images have greatly affected people's life. People obtain visual perception through video and also use images to serve themselves. With the development of image recognition technology, this technology has been widely used in video images. Through image recognition, people can get more concerned objects from video. An intelligent video surveillance system is a carrier of image recognition technology. The normal operation of this system is coordinated by image recognition, automatic control, and other technical means [1]. The core application of the video surveillance system is the detection of moving targets. The purpose is to automatically process the collected video information through the monitoring equipment, obtain the moving objects in the video, and then carry out a series of deeper analysis, such as anomaly detection, target tracking, and behavior recognition. Corresponding to these moving

objects in the video are static objects, which constitute the static background image of the video. However, people often pay more attention to the dynamic objects, and conduct a lot of research on the subsequent analysis of dynamic targets [2] but ignore the complete extraction of the static background image. To separate dynamic objects from these static backgrounds, background subtraction [3] is the most commonly used method. The moving foreground target can be obtained by subtracting the background image from the current frame image. Among them, the extraction of the video background image is the most critical step. Whether the background image in the video can be obtained accurately will directly affect the result of foreground target detection. Therefore, the extraction of the video background image is very important for foreground target detection and is a meaningful research direction. Figure 1 shows the video image coding transmission framework.

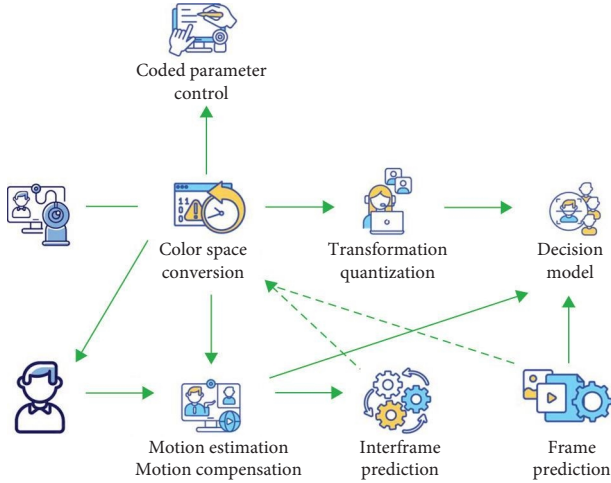


FIGURE 1: Video image coding transmission framework.

2. Literature Review

Pretto and others proposed an image reconstruction algorithm based on image data set. The algorithm attempts to find similar image blocks from the image data set by using feature matching and reconstruct the original image by using similar image blocks. Although the reconstruction effect obtained by this algorithm is not ideal, the method of using local features to find the correlation between image blocks is worthy of reference [4]. Cao and others proposed a cloud based distributed coding algorithm. The algorithm uses the thumbnail of the image to be coded to search for similar images in the cloud dataset and uses the super-resolution reconstruction method similar to the cloud dataset to obtain the preliminary reconstructed image as the edge information of the distributed source coding and then iteratively optimizes between the final reconstruction and the edge information through the bit plane based checker coding to improve the reconstruction quality. This algorithm can obtain good color reconstruction and geometric reconstruction, but the iterative reconstruction process using edge information has high complexity [5]. Wang and others proposed a region prediction coding algorithm based on cloud storage image. Firstly, the reference image is divided into multiple planar regions according to the superpixel and local feature matching results; then, the geometric and illumination differences are compensated in the matching area between the reference image and the target image; finally, multiple references are generated from the estimated compensation model and organized into pseudosequences, so that the pseudosequences containing the input image can be differentially encoded by classical video coding tools to improve the rate distortion performance of the encoded input image [6]. In the process of coarse quantization of the original image based on the a priori quantization of the fine-grained image stored in the JPEG bin. Bin and others proposed a priori quantization of the image based on the a priori quantization of the sparse image. This algorithm can realize high-quality image reconstruction while saving the upload code stream [7].

The application of the fault-tolerant coding method of digital multimedia video image has been widely concerned by the industry. Xc and others proposed a fault-tolerant coding method based on human visual characteristics. This method ignores that the original digital multimedia video image contains more visual redundancy, which seriously affects the coding/decoding speed and reconstruction quality of digital multimedia video image [8]. The histogram based fault-tolerant coding method studied by Wang and others makes the energy concentration effect worse when quantizing and coding the digital multimedia video image and finally leads to the obvious decline of the reconstructed image quality [9].

Aiming at the defects and shortcomings of these methods, a fault-tolerant coding method based on wavelet transform and sparse decomposition is proposed. The experimental results fully prove that the proposed method can improve the quality of digital multimedia video image reconstruction and ensure the speed of image coding and decoding.

3. Research Methods

3.1. Fault Tolerant Digital Video Transmission System. The three parameters of spatial contrast sensitivity function, brightness adaptive factor, and contrast masking factor of the digital multimedia video image are calculated, respectively. According to the product of the three parameters, the transform domain JND model of the digital multimedia video image is established, and the model is used for the quantization and coding of multimedia video multi-resolution image [10, 11].

The JND model of digital multimedia video image based on the DCT transform domain can be described as the product of digital multimedia video image spatial contrast sensitivity function, image brightness adaptive factor, and image contrast masking factor. Its calculation formula is as follows:

$$J_{\text{DCT}}(i, j) = J_{\text{CSF}}(i, j) \times A_{\text{lum}} \times F_{\text{contrast}}(i, j), \quad (1)$$

where A_{lum} represents the brightness adaptive weighting factor of the image; $F_{\text{contrast}}(i, j)$ represents the contrast masking weighting factor of the image; $J_{\text{CSF}}(i, j)$ represents the spatial contrast sensitivity function of a digital multimedia video image, which reflects the basic minimum detection error (JND) threshold of DCT transform domain coefficient with index number (i, j) , (i, j) in the image, and its expression is as follows [12]:

$$J_{\text{CSF}}(i, j) = \frac{s}{\vartheta_i \vartheta_j} \times \frac{\exp(c\omega_{ij}) / (a + b\omega_{ij})}{\tau + (1 - \tau \cos \vartheta_{ij})}. \quad (2)$$

Here, s represents the collective effect of digital multimedia video images; ϑ_i and ϑ_j represent the normalization coefficient of DCT change domain, respectively; ω_{ij} represents the spatial frequency of the coefficient of image DCT variation domain; $\tau + (1 - \tau \cos \vartheta_{ij})$ represents the tilt effect of human vision; ϑ_{ij} represents the direction angle of the corresponding DCT coefficient of the digital multimedia video image; a and b represent the translation factor and expansion factor of the image spatial transformation domain, respectively.

A_{lum} in equation (1) shows that the brightness adaptive masking effect makes the sensitivity of human vision to different brightness areas in digital multimedia video images different. The value of A_{lum} is related to the average brightness value \bar{I} of the local area of the image. The specific expression is as follows [13]:

$$A_{lum} = \begin{cases} 1 + \frac{60 - \bar{I}}{150}, & \bar{I} \leq 60, \\ 1, & 60 < \bar{I} < 170, \\ 1 + \frac{\bar{I} - 170}{425}, & \bar{I} \geq 170. \end{cases} \quad (3)$$

$$F_{contrast}(i, j) = \begin{cases} \psi, & (i^2 + j^2) \leq 16 \text{ and in the smooth area or edge area,} \\ \psi \times \min\left(4, \max\left(1, \left(\frac{C(i, j)}{J_{CSF}(i, j) \times A_{lum}}\right)^{0.36}\right)\right), & \text{others,} \end{cases} \quad (4)$$

where ψ represents the weighting of digital multimedia video image; $C(i, j)$ represents the texture region masking effect of a digital multimedia video image.

When calculating the contrast masking weighting factor of the digital multimedia video image, first divide the digital multimedia video image into three regions, namely, smooth region, texture region, and edge region. Weight different regions of the image according to formula (4).

According to the above-given steps, the transform domain JND model of the digital multimedia video image can be established [14].

The digital multimedia video image is divided into several subimages, and the digital multimedia video image is quantized and encoded by the following formula (5). The specific expression is as follows:

$$M(\mu, \kappa) = J_{DCT}(i, j) \left[\frac{C(\mu, \kappa)}{Z(\mu, \kappa)} \right], \quad (5)$$

where $C(\mu, \kappa)$ represents the coefficient matrix of multimedia video image; $Z(\mu, \kappa)$ represents the transformation matrix of d-coefficient selection and quantization of multimedia video image.

To sum up, it is the fault-tolerant coding principle of a multimedia video image. According to this principle, the coding and transmission of the digital video image is completed [15].

3.2. Fault Tolerant Coding Transmission Method of Digital Multimedia Video Image

3.2.1. Wavelet Transform and Vector Quantization of Multi-Resolution Image. The speed of fault-tolerant coding of digital multimedia video image and the quality of

reconstructed image seriously restrict the effect of fault-tolerant coding of the multimedia video image. The method of wavelet transform is used to decompose and reconstruct the digital multimedia video image; vector quantization is carried out on the video image after wavelet decomposition. The mean square deviation method and similar scalar optimal quantization method are used to select and calculate the multimedia video image vector, respectively, and each reconstruction vector is deduced to realize the preliminary image coding and overcome the block effect [16, 17].

The wavelet transform of digital multimedia video image solves the disadvantage that the DCT transform used in the current compression method is limited by the network bandwidth. The multiresolution transformation characteristics of wavelet transform enable the digital multimedia video image to make full use of the visual characteristics of human eyes and retain the detail information of the original image under various resolutions. Suppose that h and g , respectively, represent the low-pass filter and high pass filter of the same wavelet base corresponding to the multimedia video image; C_{j-1} represents the original digital multimedia video image; C_j represents the brightness value of the digital multimedia video image after wavelet transform; d_j^1, d_j^2 , and d_j^3 represent the edge subimage of digital multimedia video image after wavelet transform [18]. Then, the wavelet decomposition calculation formula of a digital multimedia video image is as follows (6)~(9):

$$C_j(n, m) = \frac{1}{2} \sum_{k, l \in Z} C_{j-1}(k, l) h_{k-2n} h_{l-2m}, \quad (6)$$

$$d_j^1(n, m) = \frac{1}{2} \sum_{k, l \in Z} C_{j-1}(k, l) g_{k-2n} h_{l-2m}, \quad (7)$$

$$d_j^2(n, m) = \frac{1}{2} \sum_{k, l \in \mathbb{Z}} C_{j-1}(k, l) h_{k-2n} g_{l-2m}, \quad (8)$$

$$d_j^3(n, m) = \frac{1}{2} \sum_{k, l \in \mathbb{Z}} C_{j-1}(k, l) g_{k-2n} g_{l-2m}, \quad (9)$$

$$\begin{aligned} C_{k-1}(n, m) &= \frac{1}{2} \left\{ \sum_{k, l \in \mathbb{Z}} C_{j-1}(k, l) h_{k-2n} h_{l-2m} + \sum_{k, l \in \mathbb{Z}} C_{j-1}(k, l) h_{k-2n} g_{l-2m} + \sum_{k, l \in \mathbb{Z}} C_{j-1}(k, l) g_{k-2n} h_{l-2m} + d_j^3(n, m) \right\} \\ &= \frac{1}{2} \sum_{k, l \in \mathbb{Z}} C_{j-1}(k, l) g_{k-2n} g_{l-2m}. \end{aligned} \quad (10)$$

According to the above-given calculation, the wavelet decomposition of a digital multimedia video image is realized, and the original signal of a multiresolution image is decomposed into four subbands, including an approximation signal represented as *LL* (the low-frequency component of a multiresolution image, including the main energy of image) and three detail signals represented as *LH*, *HL*, and *HH* (the high-frequency component of a multiresolution image, including the detail information of image) [19].

The original digital multimedia video image is divided into several subgraphs of $m \times n$ each subgraph of the multiresolution image can be rewritten into $k = m \times n$ -dimensional vector form and its expression is as follows:

$$f_i(f_{i1}, f_{i2}, \dots, f_{ik})'. \quad (11)$$

The k dimensional space of digital multimedia video image is decomposed into subspaces, that is, $D_l (l = 0, 1, \dots, L-1)$. Assuming $f_i \in D_l$, a known and determined vector γ_l in D_l is used to replace f_i , that is, any image vector in D_l is quantized. The mean square deviation method is used to select the digital multimedia video image vector γ_l , and the expression is as follows:

$$e^2 = \sum_{l=0}^{L-1} \int_{D_l} (f_i - \gamma_l)' (f_i - \gamma_l) p(f_i) = \min, \quad (12)$$

where $p(f_i)$ is the probability density function of f_i .

Using the scalar like optimal quantization method to calculate the digital multimedia video image vector γ_l can be obtained.

$$\gamma_l = \frac{\int_{D_l} f_i p(f_i)}{\int_{D_l} p(f_i)}. \quad (13)$$

For any digital multimedia video image, each reconstruction vector γ_l can be deduced according to formula (13), and all γ_l obtained can be calculated to generate a table a [20]. The completion of vector quantization of digital multimedia video image can overcome the block effect of other coding methods and enable the digital multimedia video image to obtain high image quality at a low bit rate,

where k represents the dimension of digital multimedia video image; n represents the number of vectors of multimedia video images; l represents the wavelet coefficient of multimedia video image; m represents the continuous wavelet generating function of a multimedia video image.

Then, the wavelet reconstruction calculation expression of the digital multimedia video image is as follows:

realize the preliminary image coding, and lay a good data foundation for the subsequent implementation of image fault-tolerant coding.

3.2.2. Multiresolution Image Coding Based on Wavelet Transform and Vector Quantization. Wavelet transform can well remove the correlation between pixels and has the characteristics of multiresolution analysis. Many researchers have studied the image coding algorithm in the wavelet transform domain and achieved a good compression effect. The image coding and decoding framework based on wavelet transform is shown in Figure 2.

Based on the preliminary coding of digital multimedia video images, the over complete database of digital multimedia video images is constructed and normalized. The digital multimedia video image is thinly decomposed by asymmetric atoms to obtain a linear representation of the image; using a few base atoms as the main components of the image, the asymmetric atoms of the image are transformed by rotation, translation, and expansion, and the type parameters are introduced to construct the atom library [21]. According to the above operations, we can understand and master the distribution range and distribution law of digital multimedia video image pixels and realize image fault-tolerant coding.

Suppose that the digital multimedia video image is represented as X and the image size is represented as $M1 \times M2$, where $M1$ and $M2$ represent the length and width of the digital multimedia video image, respectively. If the multiresolution image can be decomposed on a set of complete orthogonal bases, then $M1 \times M2$ is the number of these bases, and the over a complete library of the multiresolution image is the set composed of these bases.

Suppose $D = \{g_r\}$, $r \in \Gamma$ represents the sparse decomposition over a complete library of digital multimedia video images, and g_r represents the base atom defined by the parameter group r of the over a complete library. After normalization, the following formula can be obtained:

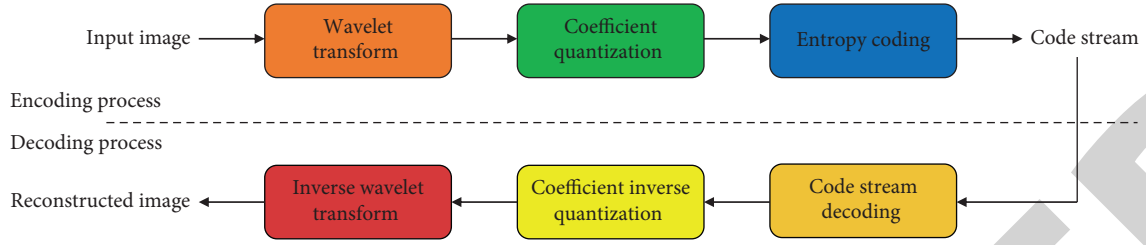


FIGURE 2: Image CODEC framework based on wavelet transform.

$$\|g_r\| = 1. \quad (14)$$

Assuming that the image sparse decomposition exceeds the number of base atoms in the complete library D , then

$$P \gg M_1 \times M_2. \quad (15)$$

According to the sparse decomposition of the multimedia video multiresolution image, a linear representation of the multiresolution image is obtained as follows:

$$X = \sum_{k=0}^{\infty} \langle R_k X, g_{rk} \rangle g_{rk}, \quad (16)$$

where $R_k X, g_{rk}$ represents the component of base atom g_{rk} corresponding to a digital multimedia video image. A few base atoms are used to represent the main components of a digital multimedia video image, and the calculation expression is as follows:

$$X \approx \sum_{k=0}^{n-1} \langle R_k X, g_{rk} \rangle g_{rk}. \quad (17)$$

Fault tolerant coding of a digital multimedia video image, that is, quantization and coding of the data of equation (17). The asymmetric atom is used for sparse decomposition of a digital multimedia video image, and its basic expression is as follows:

$$g(x, y) = \frac{1}{\sqrt{\pi}} e^{-(x^2+y^2)} + \frac{2}{\sqrt{3\pi}} (4x^2 - 2) e^{-(x^2+y^2)}, \quad (18)$$

where in, the first item of equation (18) represents that the low-frequency component of the digital multimedia video image is smooth in all directions; the second item represents the smoothing of the low-frequency component of the image in the same direction [22]. Which is mainly used to capture the edge information and contour information of multimedia video multiresolution image.

The asymmetric atoms of the image are rotated, translated, and expanded, and the type parameters are introduced to construct the atomic Library of multimedia multiresolution images. The calculation expression is as follows:

$$D = \{g_r\}, r \in \Gamma$$

$$= \left(\frac{1}{\sqrt{s_x s_y}} g_{\varphi} \left(\frac{x-u}{s_x}, \frac{y-u}{s_y} \right) \right), \quad (19)$$

TABLE 1: Performance test results of other methods.

Number	CR	PSNR/dB	Coding	Decoding
5	8.1	41.20	16.49	15.24
10	7.66	38.15	59.88	57.66
15	7.15	46.72	118.24	103.87

where $r = (\varphi, u, v, s_x, s_y)$; φ represents the rotation of multimedia video multiresolution image; u and v represent the translation of the image in the x direction and y direction, respectively; s_x and s_y represent the scale of the multiresolution image in x direction and y direction, respectively [23].

According to equations (14)–(19), the final data obtained by sparse decomposition of a digital multimedia video image is as follows:

$$(\langle R_k X, g_{rk} \rangle, \varphi_k, u, v, s_x, s_y). \quad (20)$$

Analyze the data calculated by formula (20), understand, and master the distribution range and distribution law of digital multimedia video image pixels, so as to realize fault-tolerant coding [24].

4. Result Analysis

Simulation test environment: the CPU processor is Intel Pentium E2200 3.2 GHz, the running memory is 1024 MB, and the operating system is Windows7. The simulation test tool uses MATLAB 7.11.0 to simulate a random digital multimedia video image with the size of 512×512 . Peak signal-to-noise ratio (PSNR) and fault-tolerant coding speed are used as the coding performance metrics of this method and other methods. The test results are shown in Table 1 and Figure 3.

As can be seen from Table 1 and Figure 3, Number represents the number of iterations of digital multimedia video image fault-tolerant coding; CR represents the compression ratio of digital multimedia video image; Coding represents the encoding time of digital multimedia video image; Decoding represents the decoding time of digital multimedia video image.

By analyzing the simulation test data in Table 1 and Figure 3 above, it can be seen that compared with other methods, the method proposed in this paper not only improves the reconstruction quality of digital multimedia video image but also greatly shortens the encoding and decoding time of digital multimedia video image. When the number of

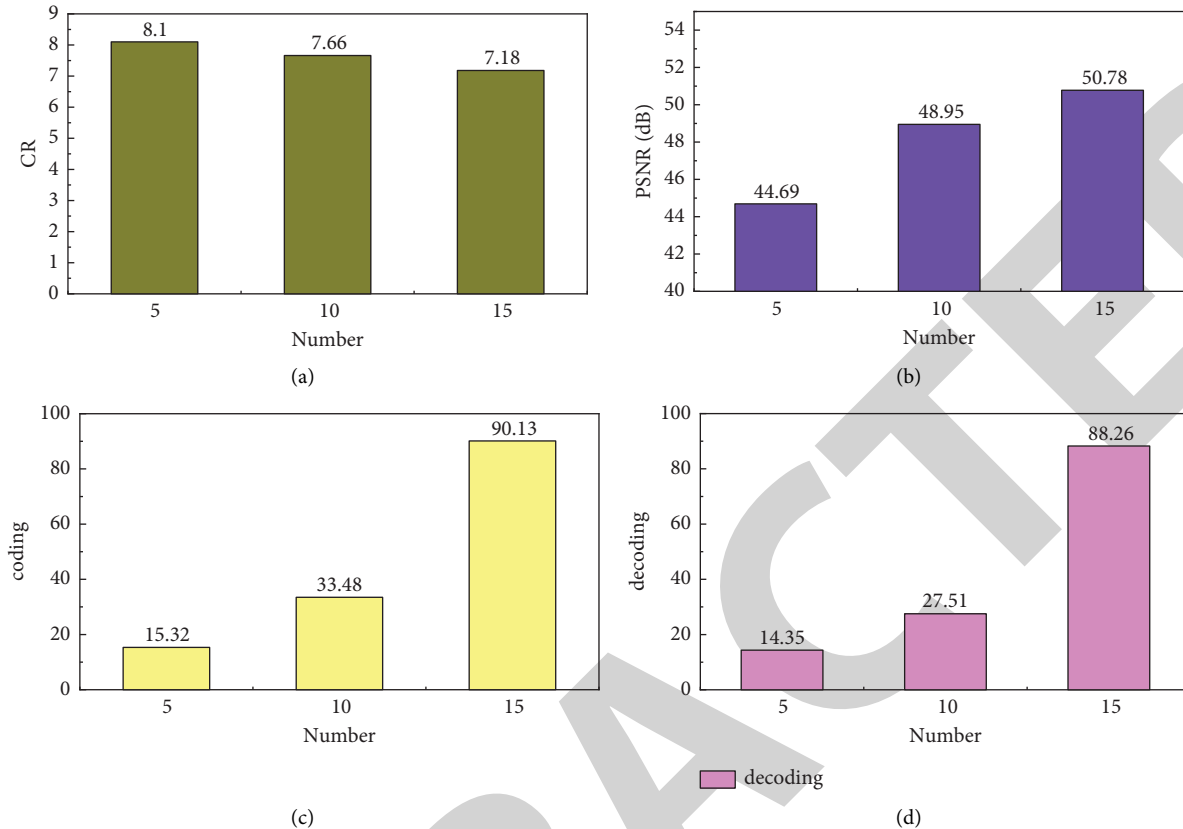


FIGURE 3: Performance test results of this method. (a) CR. (b) PSNR/dB. (c) Coding. (d) Decoding.

iterations is 15, the CR index is the same, PSNR increases by 8.7%, coding is 23.7% faster and decoding is 15% faster.

5. Conclusion

At present, most of the widely used fault-tolerant coding methods realize fault-tolerant coding at the expense of image quality or seriously restrict the coding speed even if it does not affect the image quality. The fault-tolerant coding method based on wavelet transform and sparse decomposition proposed in this paper not only improves the fault-tolerant coding speed of digital multimedia video image but also significantly improves the quality of image reconstruction. The simulation results show that compared with other methods, the performance of the proposed method has obvious advantages and broad application prospects. Based on the research of this paper, we can try to combine more different methods, so as to further strengthen and improve the transmission quality of digital multimedia video images.

Data Availability

The data used to support the findings of this study are available from the author upon request.

Conflicts of Interest

The author declares that there are no conflicts of interest.

References

- [1] Z. Zhou, Z. Qingshan, L. Dongyi, and T. Weihong, "Three-dimensional reconstruction of huizhou landscape combined with multimedia technology and geographic information system," *Mobile Information Systems*, vol. 2021, no. 5, pp. 1–13, 2021.
- [2] P. Zhu, W. Tao, X. Lu, F. Mo, F. Guo, and H. Zhang, "Optimisation design and verification of the acoustic environment for multimedia classrooms in universities based on simulation," *Building Simulation*, vol. 15, no. 8, pp. 1419–1436, 2021.
- [3] T. Li and C. Zhang, "Research on the application of multimedia entropy method in data mining of retail business," *Scientific Programming*, vol. 2022, no. 2, Article ID 2520087, 13 pages, 2022.
- [4] N. Pretto, E. Micheloni, A. Chmiel et al., "Multimedia archives: new digital filters to correct equalization errors on digitized audio Tapes," *Advances in Multimedia*, vol. 2021, no. 2, Article ID 5410218, 11 pages, 2021.
- [5] W. Cao, "Applying image registration algorithm combined with cnn model to video image stitching," *The Journal of Supercomputing*, vol. 77, no. 12, Article ID 13879, 2021.
- [6] H. Wang, Y. Zhang, and X. Fan, "Rapid early fire smoke detection system using slope fitting in video image histogram," *Fire Technology*, vol. 56, no. 2, pp. 695–714, 2020.
- [7] S. Zebhi, S. Almodarresi, and V. Abootalebi, "Converting video classification problem to image classification with global descriptors and pre-trained network," *IET Computer Vision*, vol. 14, no. 8, pp. 614–624, 2020.

Retraction

Retracted: Financial Accounting Information Data Analysis System Based on Internet of Things

Mathematical Problems in Engineering

Received 8 August 2023; Accepted 8 August 2023; Published 9 August 2023

Copyright © 2023 Mathematical Problems in Engineering. This is an open access article distributed under the Creative Commons Attribution License, which permits unrestricted use, distribution, and reproduction in any medium, provided the original work is properly cited.

This article has been retracted by Hindawi following an investigation undertaken by the publisher [1]. This investigation has uncovered evidence of one or more of the following indicators of systematic manipulation of the publication process:

- (1) Discrepancies in scope
- (2) Discrepancies in the description of the research reported
- (3) Discrepancies between the availability of data and the research described
- (4) Inappropriate citations
- (5) Incoherent, meaningless and/or irrelevant content included in the article
- (6) Peer-review manipulation

The presence of these indicators undermines our confidence in the integrity of the article's content and we cannot, therefore, vouch for its reliability. Please note that this notice is intended solely to alert readers that the content of this article is unreliable. We have not investigated whether authors were aware of or involved in the systematic manipulation of the publication process.

Wiley and Hindawi regrets that the usual quality checks did not identify these issues before publication and have since put additional measures in place to safeguard research integrity.

We wish to credit our own Research Integrity and Research Publishing teams and anonymous and named external researchers and research integrity experts for contributing to this investigation.

The corresponding author, as the representative of all authors, has been given the opportunity to register their agreement or disagreement to this retraction. We have kept a record of any response received.

References

- [1] Y. Bi, "Financial Accounting Information Data Analysis System Based on Internet of Things," *Mathematical Problems in Engineering*, vol. 2022, Article ID 6162504, 6 pages, 2022.

Research Article

Financial Accounting Information Data Analysis System Based on Internet of Things

Yulin Bi 

Catholic University, Daegu 42708, Republic of Korea

Correspondence should be addressed to Yulin Bi; 2020020541@stu.cdut.edu.cn

Received 15 July 2022; Accepted 25 August 2022; Published 12 September 2022

Academic Editor: Hengchang Jing

Copyright © 2022 Yulin Bi. This is an open access article distributed under the Creative Commons Attribution License, which permits unrestricted use, distribution, and reproduction in any medium, provided the original work is properly cited.

In order to meet the intelligent demand of modern financial data analysis, this paper proposes a financial accounting information data analysis system based on the Internet of things. Based on the central reinforcement learning architecture, the model uses multiple execution modules to enhance the computing and generalization ability of the single-agent reinforcement learning algorithm. In the selection of reinforcement learning algorithm, the instantaneous time difference algorithm is introduced. The algorithm can synchronize the experience of the previous iteration state in the learning process and does not depend on the final prediction value, which greatly saves the storage cost. In the establishment of the financial data analysis index system, the paper comprehensively considers the enterprise's operation, development, debt repayment, and other capabilities, ensuring the integrity and rationality of the index system. In order to evaluate the performance of the algorithm, this paper takes the real financial data as the sample and uses BP neural network to conduct a comparative experiment. The experimental results show that the recognition accuracy of the model is better than that of the BP neural network in each experimental scenario, and the recognition accuracy of Experiment 3 is improved by 4.6%. *Conclusion.* The performance of the distributed reinforcement learning algorithm is better than that of the common back-propagation neural network in the real data set scenario.

1. Introduction

With the increasing competition, many enterprises begin to pay more and more attention to the fine management reform based on "accurate decision-making, accurate planning, accurate control, and accurate assessment." How to transform massive data into valuable information in a timely and effective manner, how to give full play to the maximum value of enterprise information, so that managers can have an insight into the huge economic benefits brought by data management solutions and effectively help enterprises realize information strategies have become the most concerned issues of many enterprise managers [1, 2]. Business intelligence is another important application in the field of enterprise management software after ERP (enterprise resource planning). After years of development, business intelligence covers a wider range of contents, including financial intelligence, sales intelligence, procurement intelligence, and production intelligence. We need to think

deeply and study the new intelligent three-dimensional dynamic accounting information platform [3]. Through this system, we can realize various functions including shortening the response time of complex problems, tentatively sending out new views and insights, trying the effects of different strategies, enhancing management control, reducing costs, and making objective decisions, so as to meet the needs of accounting data mining [4]. Under the guidance of this trend, the intelligent three-dimensional dynamic accounting information platform will constitute the main content of accounting informatization in the twenty-first century.

2. Literature Review

The accounting information of an enterprise is mainly used to analyze the operation of a certain period of time. It is an important way for the outside world to understand the operation of an enterprise. Therefore, the research on accounting information has always been the focus of the economic

industry. Zheng and others put forward through the investigation of the actual situation that the quality of accounting information is relatively low when managers hold low shares in the company. With the continuous increase of their shares, the quality of accounting information is also increasing. However, when the shareholding level of managers is high, the relationship between the two is opposite [5]. Ah and others also conducted research on the quality of accounting information. Through a large number of studies, they believe that the quality of accounting information of an enterprise has a great relationship with the company shares held by the managers. The lower the shareholding ratio, the higher the quality of accounting information [6]. Lin and others have the same research results on accounting information and corporate governance. They believe that there are many determinants of the quality of accounting information, of which corporate governance behavior is a very important aspect [7]. Through empirical research, Zhang and others proposed that the higher the ownership concentration of an enterprise, the lower the quality of accounting information of the enterprise, and the two are negatively correlated [8]. Modalavalasa and others put forward through a large number of investigations that with the increase of the number of external directors, the probability of fraud in the enterprise will be lower [9]. Zhou and others studied from the perspective of the size of corporate directors and believed that there was a negative correlation between earnings management and the size of corporate directors [10]. Dominic and others believe that if the enterprise's earnings management fails to achieve the corresponding objectives, the company's directors will take certain measures to curb earnings management [11].

At present, with the development of artificial intelligence technology, building an intelligent financial data analysis model with the help of computer technology to realize the identification and alarm of abnormal financial data is one of the important manifestations of the "Finance + computer" integration trend. However, the existing analysis algorithms have the disadvantages of low efficiency and poor accuracy. In order to overcome these shortcomings, this paper studies the distributed reinforcement learning algorithm. By establishing a reasonable financial data analysis index system, the identification of abnormal financial data is realized.

3. Research Methods

3.1. Distributed Reinforcement Learning. The inspiration of reinforcement learning comes from human observation of animal learning behavior. Reinforcement learning is a typical artificial intelligence system [12, 13]. The system takes exploratory actions by sensing changes in the environment. At the same time, the system perceives the feedback result of this action to judge the fitness of the state. The system repeats this feedback process continuously to obtain the optimal response behavior in this environment. The traditional reinforcement learning method usually has only one learning carrier. In recent years, with the enhancement of computer computing ability, the distributed reinforcement learning system with multiple learning units has become one of the research hotspots. The distributed reinforcement learning

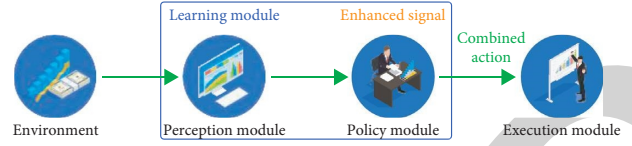


FIGURE 1: Central reinforcement learning system structure.

system includes central reinforcement learning, independent reinforcement learning, and group reinforcement learning. The central reinforcement learning system is used in this paper.

Figure 1 shows the architecture of central reinforcement learning. The central reinforcement learning method can be expressed in mathematical form as the following formula:

$$RLC = (L, E, W), \quad (1)$$

where W represents the set of RLC system environment variables, L is the set of learning units, and E is the set of execution units. W, E is defined in the following formula:

$$\begin{aligned} E &= \{A_1, A_2, \dots, A_n\}, \\ W &= \{S, \Delta, T, R\}. \end{aligned} \quad (2)$$

In the definition of environment variable set W , S is all possible different states in this environment; Δ is composed of several transition vectors, representing the transition probabilities of different states in S ; T is the transition mapping set of state environment. According to the definition of variables in W , the relationship shown in formula (3) can be obtained:

$$T: S \times \hat{A} \rightarrow \Delta, \quad (3)$$

where \hat{A} is the set of all possible actions of the execution unit in E , as shown in the following formula (4):

$$\hat{A} = A^n. \quad (4)$$

W contains the environment enhancement module R . The module maps the real number excitation as shown in the following equation (5) through the instruction pair of < environment, action >:

$$R: S \times \hat{A} \rightarrow \Gamma. \quad (5)$$

In RLC system, L is the learning unit of the system, and its definition is shown in the following formula:

$$L = \{X, I, \hat{A}, P\}, \quad (6)$$

where $X = \{x_1, x_2, \dots, x_n\}$ is the set of learning unit inputs, I is the mapping from the environment state S to the learning unit, and P is the learning rate of L . According to these definitions, (7) can be obtained:

$$\begin{aligned} I: S &\rightarrow X, \\ P: X \times \hat{A} \times \Gamma &\rightarrow \hat{A}. \end{aligned} \quad (7)$$

For RLC system, its learning module does not have the ability of active learning, so it can passively perform the

obtained tasks and optimize the parameters of the strategy module through relevant learning algorithms.

3.2. Instantaneous Time Difference Algorithm. For the strengthened system, there is a delay in a certain excitation to the system, so a certain response of the system may be caused by a very early action [14]. In order to solve this delay problem, the paper introduces the temporary difference algorithm, which can synchronize the previous state experience in learning. For the specific TD algorithm, the state s_i at $m + 1$ different times, the observed data \bar{x}_i , and the predicted value V_i of each state are defined, as follows:

$$\begin{aligned} s_i &= \{s_1, s_2, \dots, s_m, s_{m+1}\}, \\ \bar{x}_i &= \{x_1, x_2, \dots, x_m\}, \\ V_i &= \{V(s_1), V(s_2), \dots, V(s_m), V(s_{m+1})\}. \end{aligned} \quad (8)$$

In the learning process of TD algorithm, for time t , it is not necessary to wait until the final predicted value y is obtained to correct the state, but it can be updated at time $t + 1$, that is, the following formula:

$$V(s_t) < -V(s_t) + \alpha[r_{t+1} + \gamma V(s_{t+1}) - V(s_t)]. \quad (9)$$

When implementing TD algorithm, it is necessary to introduce a neural network structure to record $V(s_t)$. At this time, the learning process in the TD algorithm can use the \bar{w} rule, as shown in the following formula:

$$\bar{w}, \bar{w} + m \sum_{t=1}^m \Delta \bar{w}_t. \quad (10)$$

The correction of \bar{w} needs to be based on the back propagation of the “predicted value actual value” error. First, define the error function, as shown in the following formula:

$$E_t = \frac{1}{2} [y - V(s_t)]^2. \quad (11)$$

Calculate the partial derivative of $\Delta \bar{w}_t$ as follows:

$$\Delta \bar{w}_t = -\eta \frac{\partial E_t}{\partial \Delta \bar{w}_t} = \eta [y - V(s_t)] \nabla_w V(s_t). \quad (12)$$

Usually, $V(s_t)$ is linear with \bar{x}_t and \bar{w} . In this case, the above equation can be written as

$$\Delta \bar{w}_t = \eta \left(y - \bar{w}^T \bar{x}_t \right) \bar{x}_t. \quad (13)$$

According to equation (5), equation (12) can be written as follows:

$$\Delta \bar{w}_t = \eta [V(s_{t+1}) - V(s_t)] \sum_{k=1}^t \nabla_w V(s_k). \quad (14)$$

The advantage of (14) is that the value of $\Delta \bar{w}_t$ is only determined by the sum of the prediction difference and $\nabla_w V(s_k)$. In the implementation, there is no need to store the value of $\nabla_w V(s_t)$ at each time in the past, which greatly saves the storage overhead.

3.3. Intelligent Accounting Information Platform. In order to realize the new accounting function, the accounting information system must be reconstructed, but how to reconstruct it is a topic worth pondering. The traditional accounting information system has the characteristics of integration, integrity, uniqueness, and personalization. Integration is the restriction of practical conditions, which reflects the integration of accounting and business. Integrity is the high-level requirement of information users for information. Uniqueness is the requirement of the accounting business and the significance of accounting information system. Personalization is the preference of information users and the vitality of accounting information system. However, in the new accounting functions, information resource integration requires the provision of multidimensional accounting information, value creation management requires the provision of intelligent decision-making support, process supervision and control require the provision of intelligent, three-dimensional, and dynamic control, and three-dimensional dynamic reflection directly emphasizes the two characteristics of three-dimensional and dynamic. It can be seen that the principles of accounting information system reconstruction are intellectualization, three-dimensional, and dynamic.

4. Result Analysis

4.1. Establishment of Index System. It is one of the demands of the capital market to conduct real-time analysis of the enterprise’s finance, timely find abnormal financial data, and give an early warning [15]. Therefore, it is necessary to follow the principles of authenticity, systematization, scientificity, and feasibility when constructing the financial index system. Therefore, the selection of indicators needs to comprehensively reflect the company’s debt repayment, operation, profitability, growth, and other aspects. In addition, the operating data of an enterprise do not only include financial indicators, and nonfinancial indicators can also reflect the financial status of the company. Therefore, it can be properly introduced when establishing the index system.

The indicator system includes financial and nonfinancial indicators [16]. Financial indicators can not only reflect the solvency, operation, profitability, development, and other capabilities of enterprises but also reflect the cash flow of enterprises. In addition, financial indicators also introduce the per share index of listed enterprises. Nonfinancial indicators mainly reflect the corporate governance structure, equity structure, and financial audit opinions and can reflect the financial status of the company from the side [17].

In the process of data testing and analysis, on the data collection of the algorithm, the paper screened the real financial data of 300 companies from 2018 to 2021. In these data, there are 150 ST companies and 150 non-ST companies in 2021, and the ratio of ST to non-ST is 1 : 1. For each enterprise, these data include its $T, T - 1, T - 2, T - 3$ years.

TABLE 1: Simulation data structure.

Particular year	Number of ST companies
2018	32
2019	78
2020	130
2021	150

TABLE 2: Experiment I.

Enter data year	Year of output data
$T - 3$	$T - 2$
$T - 2$	$T - 1$
$T - 1$	T

As shown in Table 1, since each company became an ST company in different years due to abnormal financial data, the data attributes of each company in this data set are also different. If a company does not become an ST company until 2021, there will be sufficient data to analyze its T , $T - 1$, $T - 2$, $T - 3$ change status. According to Table 1, 20 companies can analyze the data changes in 3 years.

4.2. Financial Data Analysis and Early Warning Simulation.

In the data analysis, $T - 1$, $T - 2$, and $T - 3$ data are used to simulate the algorithm model designed above. In order to better evaluate the impact of changes in time, financial data, and other dimensions on the performance of the algorithm, this paper designs several groups of experiments, each of which uses financial data in different years. The design of the experiment is shown in Tables 2–4.

The software and hardware environment for the simulation experiment in this paper is shown in Table 5.

Based on the index system, build an RLC system based on TD algorithm [18, 19]. Before the simulation of the algorithm, the number of execution modules in the RLC system should be determined. In the mode of Experiment 1, the algorithm accuracy and running time under different number of execution modules are calculated by traversal, as shown in Figures 2(a) and 2(b), respectively.

As can be seen from Figure 2(a), when the number of modules is less than 8, the accuracy of the algorithm increases rapidly, from about 45% to nearly 80%. When the number of execution modules is greater than 8, the correct rate of the algorithm increases slowly and remains at about 80% [20]. As can be seen from Figure 2(b), when the execution module is less than 7, the running time of the algorithm increases slowly and remains at about 1.8×10^5 s. When the number of execution modules is greater than 7, the operation time increases rapidly. Considering Figures 2(a) and 2(b), the number of execution modules used is finally determined to be 8.

TABLE 3: Experiment II.

Enter data year	Year of output data
$T - 3, T - 2$	$T - 1$
$T - 2, T - 1$	T

TABLE 4: Experiment III.

Enter data year	Year of output data
$T - 3, T - 2, T - 1$	T

TABLE 5: Algorithm simulation environment.

Name	Parameter
Operating system	Centos 6.0
Programming environment	Python2.3
CPU	Intel Corei7-10700K
Graphics card	GIGABYTE GTX 1660

Table 6 shows different experimental results under distributed reinforcement learning [21]. For comparison, BP neural network is also introduced, as shown in Table 7. From the calculation results, it can be seen that for the analysis of abnormal financial data, the recognition accuracy of a distributed reinforcement learning algorithm for ST company is better than BP neural network in each experimental scenario. The calculation accuracy of Experiment 3 is improved by 4.6%. From the perspective of the algorithm itself, the accuracy of Experiment 3 is better than that of Experiment 2, and the accuracy of Experiment 2 is better than that of Experiment 1 [22, 23]. This result shows that the financial status of an enterprise can be better analyzed through the accumulation of financial data in multiple different years.

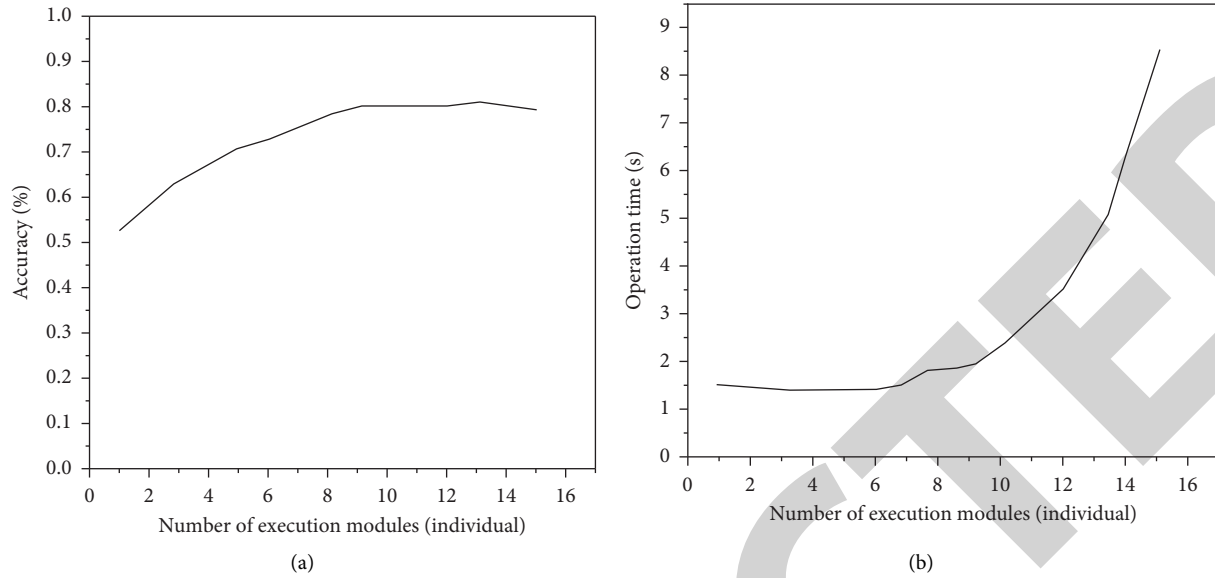


FIGURE 2: Effect of the number of execution modules on algorithm accuracy and operation time. (a) The influence of the number of execution modules on the accuracy of the algorithm. (b) The influence of the number of execution modules on the algorithm operation time.

TABLE 6: Experimental results based on distributed reinforcement learning.

Category	Experiment 1 (%)	Experiment 2 (%)	Experiment 3 (%)
Is ST	79.1	93.0	95.3
Non-ST	79.1	86.0	93.0
Population	79.1	89.5	94.2

TABLE 7: Experimental results based on neural network.

Category	Experiment 1 (%)	Experiment 2 (%)	Experiment 3 (%)
Is ST	70.4	84.7	89.2
Non-ST	73.1	82.1	90.0
Population	72.5	83.3	89.6

5. Conclusion

The financial data analysis of an enterprise is a complex system engineering. In this paper, the distributed reinforcement learning method is introduced into the enterprise's financial data analysis, and the accurate evaluation of the enterprise's operating status is achieved by constructing a reasonable financial evaluation index system. The data test and simulation results using real data sets show that the performance of distributed reinforcement learning algorithm is better than that of an ordinary back-propagation neural network in this scenario.

Data Availability

The data used to support the findings of this study are available from the corresponding author upon request.

Conflicts of Interest

The authors declare that they have no conflicts of interest.

References

- [1] M. E. Morochocayamcela and W. Lim, "Lateral confinement of high-impedance surface-waves through reinforcement learning," *Electronics Letters*, vol. 56, no. 23, pp. 1262–1264, 2020.
- [2] T. Ziemke, L. N. Alegre, and A. Bazzan, "Reinforcement learning vs. rule-based adaptive traffic signal control: a fourier basis linear function approximation for traffic signal control," *Ai Communications*, vol. 34, no. 2, pp. 1–15, 2021.
- [3] P. Chen, Y. Xia, and C. Yu, "A novel reinforcement-learning-based approach to workflow scheduling upon infrastructure-as-a-service clouds," *International Journal of Web Services Research*, vol. 18, no. 1, pp. 21–33, 2021.
- [4] Y. Zhao, I. G. Niemegeers, and S. M. H. De Groot, "Dynamic power allocation for cell-free massive mimo: deep reinforcement learning methods," *IEEE Access*, vol. 9, pp. 102953–102965, 2021.
- [5] Y. Zheng, Z. Yan, K. Chen, J. Sun, Y. Xu, and Y. Liu, "Vulnerability assessment of deep reinforcement learning models for power system topology optimization," *IEEE Transactions on Smart Grid*, vol. 12, no. 4, pp. 3613–3623, 2021.
- [6] A. Heiberg, T. N. Larsen, E. Meyer, A. Rasheed, O. San, and D. Varagnolo, "Risk-based implementation of colregs for autonomous surface vehicles using deep reinforcement learning," *Neural Networks*, vol. 152, pp. 17–33, 2022.
- [7] K. Lin, C. Li, Y. Li, C. Savaglio, and G. Fortino, "Distributed learning for vehicle routing decision in software defined internet of vehicles," *IEEE Transactions on Intelligent Transportation Systems*, vol. 22, no. 6, pp. 3730–3741, 2021.
- [8] J. Zhang, B. Cui, X. Dai, and Z. Jiang, "Iterative learning control for distributed parameter systems based on non-collocated sensors and actuators," *IEEE/CAA Journal of Automatica Sinica*, vol. 7, no. 3, pp. 865–871, 2020.
- [9] S. Modalavalasa, U. K. Sahoo, and A. K. Sahoo, "Sparse distributed learning based on diffusion minimum generalised rank norm," *IET Signal Processing*, vol. 14, no. 9, pp. 683–692, 2020.

Retraction

Retracted: Application of Multi-Measurement Vector Based on the Wireless Sensor Network in Mechanical Fault Diagnosis

Mathematical Problems in Engineering

Received 26 September 2023; Accepted 26 September 2023; Published 27 September 2023

Copyright © 2023 Mathematical Problems in Engineering. This is an open access article distributed under the Creative Commons Attribution License, which permits unrestricted use, distribution, and reproduction in any medium, provided the original work is properly cited.

This article has been retracted by Hindawi following an investigation undertaken by the publisher [1]. This investigation has uncovered evidence of one or more of the following indicators of systematic manipulation of the publication process:

- (1) Discrepancies in scope
- (2) Discrepancies in the description of the research reported
- (3) Discrepancies between the availability of data and the research described
- (4) Inappropriate citations
- (5) Incoherent, meaningless and/or irrelevant content included in the article
- (6) Peer-review manipulation

The presence of these indicators undermines our confidence in the integrity of the article's content and we cannot, therefore, vouch for its reliability. Please note that this notice is intended solely to alert readers that the content of this article is unreliable. We have not investigated whether authors were aware of or involved in the systematic manipulation of the publication process.

Wiley and Hindawi regrets that the usual quality checks did not identify these issues before publication and have since put additional measures in place to safeguard research integrity.

We wish to credit our own Research Integrity and Research Publishing teams and anonymous and named external researchers and research integrity experts for contributing to this investigation.

The corresponding author, as the representative of all authors, has been given the opportunity to register their agreement or disagreement to this retraction. We have kept a record of any response received.

References

- [1] W. Kang, "Application of Multi-Measurement Vector Based on the Wireless Sensor Network in Mechanical Fault Diagnosis," *Mathematical Problems in Engineering*, vol. 2022, Article ID 2390119, 7 pages, 2022.

Research Article

Application of Multi-Measurement Vector Based on the Wireless Sensor Network in Mechanical Fault Diagnosis

Wei Kang 

Anshan Normal University Liaoning China, Anshan 114007, Liaoning, China

Correspondence should be addressed to Wei Kang; 1117410434@st.usst.edu.cn

Received 26 June 2022; Accepted 20 August 2022; Published 7 September 2022

Academic Editor: Hengchang Jing

Copyright © 2022 Wei Kang. This is an open access article distributed under the Creative Commons Attribution License, which permits unrestricted use, distribution, and reproduction in any medium, provided the original work is properly cited.

In order to solve the problem of low positioning accuracy of mechanical fault diagnosis, a polarization GPR imaging reconstruction algorithm based on the MMV model was proposed. The algorithm was mainly based on the joint processing of the measured data of multiple polarization channels to achieve the reconstruction of the reflectance of the detection scene corresponding to each polarization channel. The simulation data processing results based on FDTD showed that compared with the traditional SMV model polarization imaging algorithm, the proposed imaging algorithm could improve the accuracy of target location reconstruction and the ability of background clutter suppression significantly. Compared with the SMV model, TCR obtained by the MMV model increased by 30%. As for the imaging results at different noise ratios, TCR obtained by the MMV model was 10% higher than that obtained by the SMV model. And when the ratio of available real data samples decreased to 25%, the sample data generation based on the adversarial generation network could greatly improve the classification accuracy of the fault diagnosis model. It could realize the detection of the target better, so as to locate faults accurately.

1. Introduction

In the increasingly intelligent society, the application of mechanical equipment is more and more widely in industrial production and daily life. From aerospace, industrial production, and national defense to the travel means of transportation, such as aircraft, cars, and high-speed train which are closely related to people's lives, rotating machinery plays an important role. With the continuous development of modern science and technology, all kinds of mechanical systems are developing towards the large-scale, complex, and high-speed direction, which also increases the uncertainty of mechanical system safety. Once the rotating machinery equipment breaks down, it will not only cause the stagnation of industrial production but also cause serious safety problems. In addition to affecting the production efficiency and economic loss of the enterprise, it may also bring irreversible casualties [1]. Mechanical equipment fault diagnosis is a scientific technology to monitor, diagnose, and predict the state of continuous running equipment and ensure the safe operation of mechanical equipment. Its

outstanding characteristic is the close combination of theoretical research and engineering practical application. It is a kind of advanced technology that uses various measurement and monitoring methods to record and analyze the equipment state and identify and alarm the abnormal state (see Figure 1). Using this technology, the failure state of mechanical equipment can be found in time to avoid the occurrence of catastrophic events. It can also avoid the economic loss caused by insufficient or excessive maintenance and has greater economic benefits. As the most important part of the mechanical system, rotating machinery, such as induction motor, is the main device to drive all kinds of mechanical equipment, widely used in all kinds of mechanical equipment. The reliability and security of its operation should be higher. Generally, mechanical equipment is divided into three basic parts, gear, bearing, and rotating shafting. While rotating parts, such as bearings and gears, are also widely used in all kinds of mechanical systems. According to the survey, bearing damage and gear failure account for about 40% of the faults of rotating machinery, and 10.3% of the faults caused by gear failure [2]. Therefore,

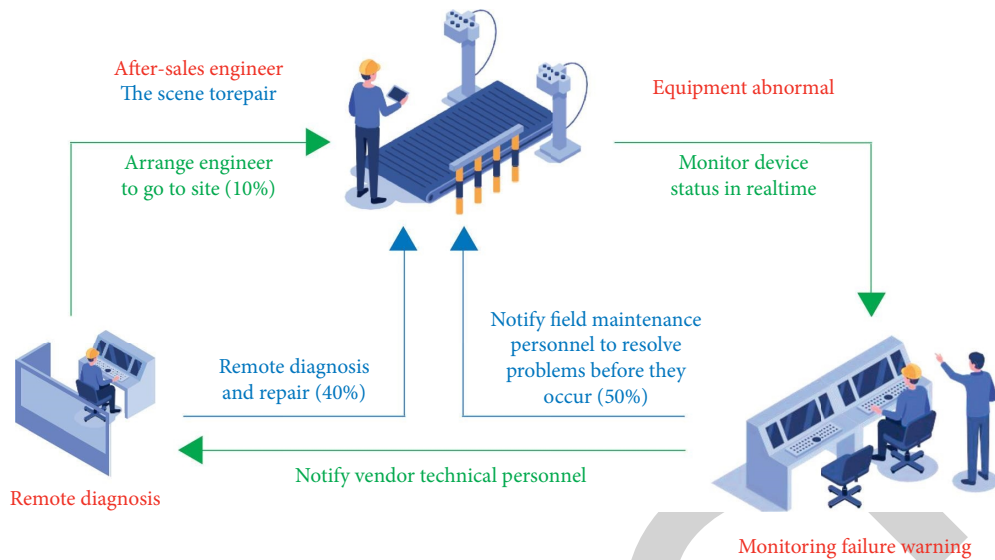


FIGURE 1: Mechanical fault diagnosis.

it is of great significance to find out the fault status of the rotating machinery in time and to make accurate fault diagnosis and maintenance for the rotating machinery so as to ensure the safe and stable operation of the production system and reduce the probability of catastrophic accidents.

2. Literature Review

With the development of network technology, multi-measurement vector machine fault diagnosis technology has been paid more attention. In the aspect of signal processing and feature extraction, vibration signals of rotating machinery parts are complicated when faults occur, and the signals obtained by sensors are nonlinear, non-stationary, and noisy. Therefore, it is difficult to extract useful fault features directly from original signals. Feature extraction based on signal processing is widely used in fault diagnosis. The traditional signal processing technology mainly consists of three aspects: time-domain analysis, frequency domain analysis, and time-frequency domain analysis. Time domain processing is mainly based on statistical feature analysis. The frequency domain processing method mainly analyzes the signal frequency domain components. Fourier transform is the classical frequency domain processing method, in addition to envelope analysis, thinning spectrum, cepstrum, high order spectrum, holographic spectrum analysis, and other methods. A more widely used method is the time-frequency domain analysis method, which can capture the fault-related transient components in non-stationary signals and provide the joint distribution of time domain and frequency domain, such as short-time Fourier transform, Winger-Ville distribution, empirical mode decomposition, and wavelet transform theory. Gonzalez-Arango et al. proposed the deep learning model, which got rid of the inevitable uncertainty of artificial feature extraction and enhanced the structural depth of the network model [3]. Hriez et al. proposed a software measurement method to

scientifically organize the whole process of software and also proposed a method that can be used for many times in this process [4]. Shahid et al. proposed the rationality of assumptions required by the MMV model combined with sparse reconstruction, that is, when multiple observation signals share a sparse structure, the MMV model is superior to the SMV model [5]. Qi et al. proposed a feature extraction method for mechanical faults based on category-independent component analysis and the correlation coefficient. Firstly, the independent component analysis of mechanical fault signals in different working conditions were carried out to obtain the independent components of various working conditions, which contained some inherent characteristics of the working conditions. Then, the absolute sum of the correlation coefficients between the sample and the independent components extracted from signals under different working conditions was used as the characteristics of the sample [6]. Sharma et al. used the Morlet wavelet and the particle swarm optimization algorithm to de-noise bearing vibration signals [7]. Kim et al. proposed empirical mode decomposition based on adaptive variable-scale frequency-shift band-pass stochastic resonance denoising, a denoising method of a vibration signal with an interval threshold of empirical mode decomposition [8]. Gong et al. proposed a rolling bearing fault feature extraction method based on the improved envelope spectrum based on EMD and spectrum kurtosis, namely, the holographic spectrum technique for mechanical fault diagnosis [9]. Shriram et al. proposed the method of the multi-scale envelope order spectrum to evaluate the health status of the mechanical system under variable speed conditions and used the instantaneous frequency obtained by the empirical mode decomposition method to detect the state degradation of bearings [10]. Ma et al. used wavelet packet decomposition to decompose the original signal into a series of time-domain waveforms and reduced them into one-dimensional signals by local tangent space arrangement, so as to achieve denoising of the original

signal [11]. Bashar et al. combined continuous wavelet transform and local tangent space arrangement for non-linear noise reduction [12]. Based on the characteristics of mixed time-frequency domain, Ping et al. carried out fault diagnosis of the wind turbine transmission system [13]. Chen et al. introduced an iterative algorithm for matching demodulation transformation to generate time-frequency distribution images of energy concentration. It was beneficial to weak fault feature extraction. Good results were achieved in the simulation signal and real data [14].

To solve the above problems, a sparse imaging reconstruction algorithm of polarization GPR based on the MMV model for mechanical diagnostic echo signals was proposed, which equivalently transformed the measured data of each polarization channel into multiple measurement vectors. The multi-task Bayesian compressed sensing (MT-BCS) algorithm was used to process the measurement data of different polarization channels, and then the sparse high-resolution imaging reconstruction of the mechanical fault detection region was realized. Compared with the traditional SMV reconstruction algorithm, the proposed algorithm could reduce the background clutter and improve the quality of image reconstruction, so as to achieve the accurate judgment of mechanical failure.

3. Research Methods

3.1. Traditional SRC Model. If multi-measurement vectors can share the sparse structure, the prior information can be used to constrain the selection of representation atoms to improve the performance of joint sparse reconstruction. However, in practical application, it is difficult to obtain measurement vectors with exactly the same sparse structure. Few signal sources meet the assumption conditions of the shared sparse structure. And these measurement vectors may not share the sparse structure even if they observe the same thing. The possible reasons are as follows: first, the sparsity structure of actual signals is time-varying. Second, the high dimension of the signal makes the feature space of the same type of the signal may have a large gap. For example, the photos taken by the same person under different circumstances may have a large gap. Third, the limitation of feature description space makes the measurement matrix lack feature description atoms, resulting in incomplete feature description. It can be seen that measurement vectors with identical sparse structures are difficult to obtain. In the MMV model, the general sparsity hypothesis is only valid for a small number of measurement vectors. In practical application, multi-measurement vectors with the non-shared sparse structure are often encountered [15]. The measurement vector of the traditional SRC model is single. However, intuitively, the information provided by multiple observation signals obtained from the same object is significantly more than that provided by a single observation signal. Even if these multiple observation signals do not share the sparse structure, they should still provide more effective information. If the increased information can be effectively utilized, the performance of

sparse classification can be improved. In the data dictionary of the SRC model, similar training sample sets are arranged. If multiple measurement vectors are observations of the same object, then their representation atoms should be concentrated in a certain region of the measurement matrix. The corresponding representation coefficient is non-0, but the non-0 elements are not necessarily in the same line, that is, the sparse structure is not shared [16]. The non-zero terms of the coefficient matrix are concentrated in a certain category, but the sparse structure is not shared among the columns of the coefficient matrix. This prior structural information can be used to improve the accuracy of diagnosis [17].

3.2. Polarization Signal Model. The schematic diagram of polarization GPR system detection is shown in Figure 2. The polarization GPR antenna system has four polarization measurement channels, which are XX , XY , YX , and YY polarization, among which the first represents the polarization direction of the transmitting antenna and the second represents the polarization direction of the receiving antenna. The direction of the measuring line is parallel to the Y direction. Assuming that the system adopts the working mode of single station stepping frequency, for the l th ($l = 1, 2, 3, 4$) polarization channel, the system at the m ($m = 0, 1, \dots, M - 1$) antenna positions and the n th ($n = 0, 1, \dots, N - 1$) measurement data $r_l(m, n)$ of frequency points are expressed as the following formula:

$$r_l(m, n) = \sum_{p=1}^P \delta_{p,l} \exp(-j2\pi f_n \tau_{p,m}). \quad (1)$$

In the formula, $\delta_{p,l}$ is the complex reflection coefficient of the p th target. $f_n = f_0 + n\Delta f$ is the n th working frequency point. f_0 is the starting frequency of the working bandwidth. Δf is the step interval of frequency in the working bandwidth. $\tau_{p,m}$ is the round-trip delay between the p th target and the m th antenna position.

The detection area is divided into $N_y \times N_z$ uniform spatial grids, where N_y and N_z represent the number of discrete grids in horizontal direction and depth direction, respectively. The reconstructed image can be transformed into $N_y N_z \times 1$ -dimensional scene reflectance vector δ_l by column stacking operation. Then the received signal r_l of the system in the l th polarization channel can be expressed as the following formula:

$$r_l = \psi \delta_l. \quad (2)$$

In the formula, $r_l = [r_l(0, 0), \dots, r_l(0, N - 1), r_l(M - 1, N - 1)]^T$. δ_l represents the scene reflectance vector corresponding to the l th polarization measurement channel. ψ is the $MN \times N_y N_z$ -dimensional lexicographical matrix, and the elements in the r th row and q th column can be expressed as the following formula:

$$[\psi]_{r,q} = \exp(-j2\pi f_n \tau_{p,m}). \quad (3)$$

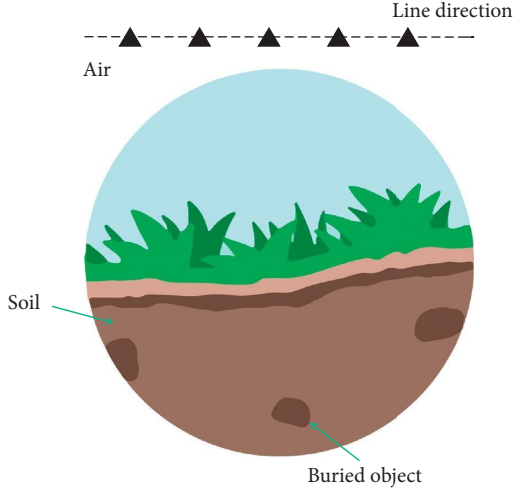


FIGURE 2: Schematic diagram of system detection.

In the formula, $r = 0, 1, MN - 1$; $q = 0, 1, N_y N_z - 1$; $n = r \bmod N$; $m = \lceil r/N \rceil$. $\tau_{p,m}$ represents the round-trip delay between q imaging grid and m_{th} antenna location.

Because the target of interest only occupies a few space positions in the detection scene, δ_l is a sparse vector. A random measurement matrix ϕ_l can be constructed to achieve the reduction sampling and obtain the measurement vector, as shown in the following formula:

$$y_l = \phi_l r_l = \phi_l \psi \delta_l = A_l \delta_l + n_l. \quad (4)$$

In the formula, $A_l = \phi_l \psi$ is a $J \times MN$ dimensional matrix, which can be constructed by randomly selecting J rows from the $MN \times MN$ dimensional identity matrix. The dictionary matrix A_l may be the same or different for different polarization measurement channels. The additive White Gaussian noise vector n_l is added into the formula. And n_l represents the measurement noise of the l th polarization channel.

3.3. Polarization GPR Imaging Based on the SMV Model. By the polarization GPR imaging method based on the SMV model, the measurement data of a single polarization channel were processed, respectively, so as to reconstruct the reflectivity of the corresponding detection scene of each polarization channel [18]. The scene reflectance vector δ_l corresponding to the l th polarization measurement channel can be reconstructed by l_1 norm minimization method, as shown in the following formula:

$$\begin{aligned} \hat{\delta}_l &= \arg \min \|\delta_l\|_1 \\ \text{s.t. } &\|y_l - A_l \delta_l\|_2 < \varepsilon. \end{aligned} \quad (5)$$

In the formula, $\|\cdot\|_1$ and $\|\cdot\|_2$ represent the l_1 and l_2 norm, respectively. ε is a regularization parameter. The reconstructed δ_l is expanded according to the N_y column and the N_z row to obtain the reconstructed target image. The imaging reconstruction process represented by formula (5) only utilizes the measured data of a single polarization channel, without considering the correlation of the

measured data of each polarization channel, so the imaging reconstruction effect achieved is very limited.

3.4. Polarization GPR Imaging Based on the MMV Model. In the detection process of GPR, for different polarization measurement channels, the detection area and the working frequency band of the system are the same, but the difference is only the reflectivity of the detection scene [19]. Therefore, for XX , XY , YX , and YY polarization channels, δ_l has a common sparse support set, namely, the positions of the non-zero elements of δ_l remain unchanged in the measurement, while the positions of the non-zero elements of δ_l correspond to different element values [20]. The polarization GPR imaging model based on MMV can be constructed, and the measurement data of multiple polarization channels can be processed jointly by using the multi-task Bayesian compressive sensing ($MT - BCS$) framework, so as to realize the joint reconstruction of the reflectance of the detection scene corresponding to each polarization channel. Since ($MT - BCS$) framework is based on the real-value signal model, formula (5) is converted into the real-value signal model, as shown in the following formula:

$$\hat{y}_l = \hat{A}_l \hat{\delta}_l + \hat{n}_l, \quad l = [1, 2, 3, 4]. \quad (6)$$

In the formula, $\hat{y}_l = [\text{Re}(y_l)^T, \text{Im}(y_l)^T]^T$, $\hat{\delta}_l = [\text{Re}(\delta_l)^T, \text{Im}(\delta_l)^T]^T$, $\hat{n}_l = [\text{Re}(n_l)^T, \text{Im}(n_l)^T]^T$.

The dictionary matrix is shown in the following formula:

$$\hat{A}_l = \begin{bmatrix} \text{Re}(A_l) & -\text{Im}(A_l) \\ \text{Im}(A_l) & \text{Re}(A_l) \end{bmatrix}. \quad (7)$$

In formula (6), each process of $\hat{\delta}_l$ reconstruction from \hat{y}_l is called the l th reconstruction task, thus realizing the multi-task signal reconstruction. Given a Gaussian prior distribution with zero mean for each element of \hat{n}_l in formula (6), the Gaussian likelihood model of the measurement vector can be expressed as follows:

$$p(\hat{y}_l | \hat{n}_l, \beta) = \left(\frac{2\pi}{\beta}\right)^{-J} \exp\left(-\frac{\beta}{2} \|\hat{y}_l - \hat{A}_l \hat{\delta}_l\|^2\right). \quad (8)$$

In the formula, β is the accuracy of the Gaussian density function (reciprocal of the noise variance). For each element in $\hat{\delta}_l$, it is assumed that the Gaussian prior distribution of zero mean is satisfied, as shown in the following formula:

$$p(\hat{\delta}_l | \alpha, \beta) = \prod_{i=1}^{2N_x N_y} N(\delta_l(i) | 0, \beta^{-1} \alpha_i^{-1}). \quad (9)$$

The hyperparameter $\alpha = \{\alpha_i\}_{i=1}^{2N_x N_y}$ is common to all four polarization channels. Therefore, the measurement vector \hat{y}_l in each task will contribute to the estimation of the hyperparameter, so as to realize the sharing of information. It is assumed that both super-parameter α and β obey gamma distribution. According to Bayes criterion, the posterior probability density function of δ_l satisfies multi-variable Student-1 distribution. Its mean value is shown as follows:

$$u_1 = \left((\hat{A}_l)^T \hat{A}_l + D \right)^{-1} (\hat{A}_l)^T \hat{y}_l. \quad (10)$$

In the formula, $D = \text{diag}[\alpha_1, \alpha_1, \dots, \alpha_{2N_x N_y}]$. The hyperparameter α is solved by the fast correlation vector machine. When the hyperparameter α is obtained, the scene reflectance vector δ_l corresponding to each polarization channel can be obtained from the following formula:

3.5. Experimental Simulation. In order to simulate the effectiveness of the mechanical fault diagnosis method of multi-measurement vectors in the line sensor network, the induction motor experimental platform was used for experimental verification, and the model performance was evaluated by statistical indicators [21]. The experimental platform used in this experiment was the induction motor experimental platform. What experimental platform collected was the vibration signals of the sensor. Here, a direction of the vibration signal was picked as the input signal of the experiment. At the data preprocessing stage, 4096 consecutive sampling data points would be contained as a sample. 300 independent samples were collected in each working condition. Therefore, as for corresponding six different induction motor running states, the entire data set consisted of 1,800 samples. At the same time, the data set was divided into the training data and the testing data in a ratio of 2:1, namely, for each working condition, there were 200 vibration signal samples for training adversarial generation network, and 100 samples for model testing. The improved model was trained with the training data set and the corresponding generated samples were obtained. In the testing process, only test data (real sample data) were used to test the trained ACGAN model. At the same time, the sample quality of the generated data were evaluated. In this case, the test data were the real sample data. In the process of training, in order to prevent the generation of over-learning, a test was set up after the end of each training round. The model was used to predict the test data that did not participate in the model training, and the results were compared with the training results. If the difference was large, it indicated the existence of over-learning. The generator generated samples from the potential variable space to explore simulated learning of the distribution of input data. During the training, the Epoch of the training cycle was set to 100.1000 pseudo samples would be generated for each induction motor running state. The performance of the model is shown in Figure 3.

In the initial stage of model training, the model errors of both generator and discriminator advanced towards Nash equilibrium, but the final classification accuracy was not improved, indicating that model updating was not carried out towards the optimal solution. After 15 Epochs, the classification accuracy of the model improved significantly. The error curves of generator and discriminator were approaching Nash equilibrium and the performance of the model tended to be stable. After 60 Epochs, the error curve gradually tended to the Nash equilibrium point and the

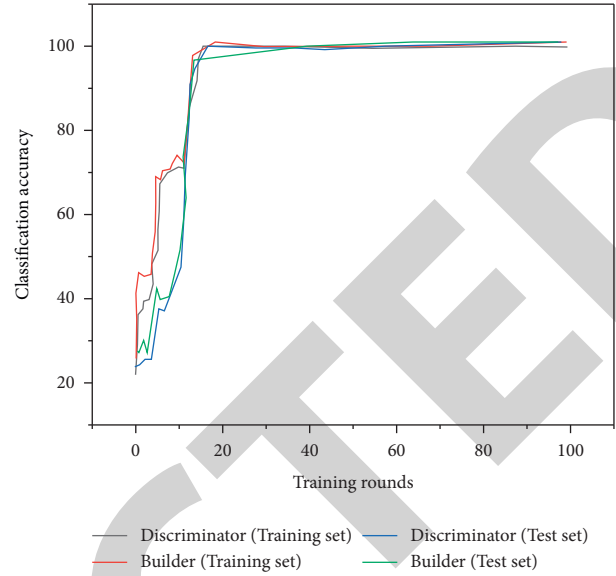


FIGURE 3: Diagnostic performance.

classification accuracy of the model was stable at the highest point, at which time the model had been well trained.

4. Result Analysis

In order to further verify the effectiveness and accuracy of the image extraction algorithm, firstly, the finite-difference time-domain (FDTD) method based on GprMax software was used to construct the detection scene and obtain the polarization GPR full-wave simulation data. Then the imaging algorithm was used to process the simulation data to obtain the imaging results. The simulation model was set as follows: The detection scene was composed of two layers of media. The first layer was air; the second layer was soil; the relative dielectric constant and conductivity of soil were $\epsilon_r = 6$ and $\delta = 1$ mS/m, respectively. Four steel bars with a radius of 0.01 m were buried in the soil, evenly arranged along the horizontal direction. The buried depth of steel bars was 0.2 m. The excitation source was a Laker wave with a center frequency of 1000 MHz and the height of the antenna from the ground was 5 cm. The transmitting antenna and the receiving antenna were in the same position and moved evenly along the horizontal direction with a moving step of 5 cm. The number of data acquisition channels was 21 and the sampling time was 20 ns. The time-domain scattering echo at each measurement aperture was obtained by FDTD calculation. Since the image acquisition algorithm was carried out in the frequency domain, the background elimination technology was first used to remove the strong reflected echo at the interface between air and soil, and then the time-domain echo data were obtained by Fourier transform to obtain the target frequency domain back-scattering signal with 21 frequency points within the working bandwidth of 500–1500 MHz. The frequency step interval was 50 MHz. Thus, each polarization channel had a total of $21 \times 21 = 441$ measurement data. Additive White Gaussian noise was added to the scattering field data in

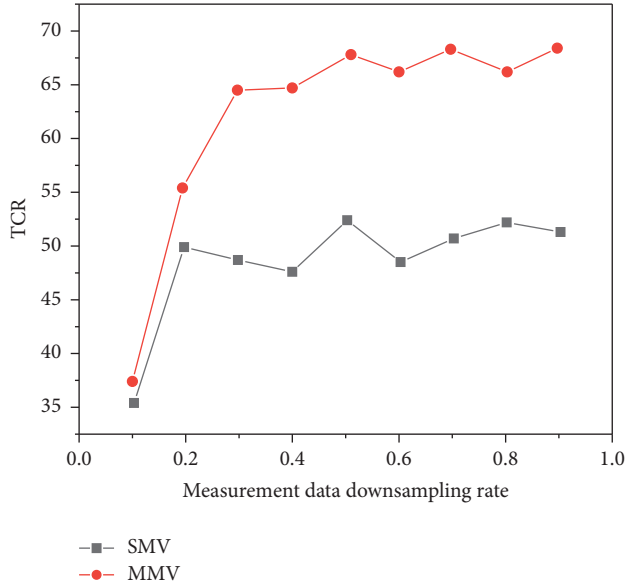


FIGURE 4: Imaging results at different down-sampling rates.

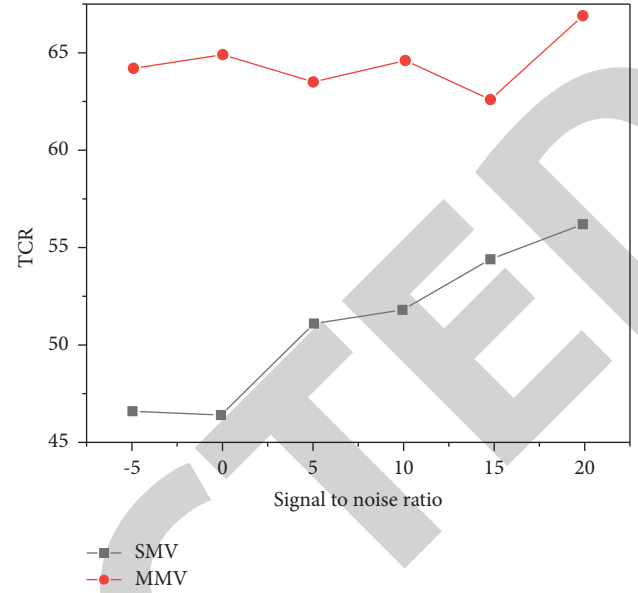


FIGURE 5: Imaging results at different noise ratios.

frequency domain of each polarization channel and the signal-to-noise ratio was 10 dB. The imaging area was set to 1.2 m in both horizontal direction and depth direction. The imaging region was divided into 61×61 spatial grids in the horizontal direction and depth direction [22]. In order to quantitatively compare the reconstruction performance of the two imaging algorithms under the different sampling rate reduction of measured data, the signal-to-noise ratio of the measured data was fixed at 10 dB at first, and then 100 independent experiments were conducted corresponding to the sampling rate reduction of each measured data. The average TCR of the obtained imaging results was shown in Figure 4. It could be seen from Figure 4 that under the condition of the same sampling rate reduction of measurement data, the imaging algorithm based on the MMV model had a larger TCR than the SMV model, which was more conducive to target detection and recognition.

In order to compare the imaging reconstruction performance of the two imaging algorithms under different SNRS, the reduction sampling rate of the measured data was first fixed at 0.5 and then 100 independent experiments were conducted for each SNR. The average TCR of the obtained imaging results was shown in Figure 5. It could be seen from Figure 5 that under the same SNR condition, the imaging algorithm based on the MMV model could obtain a larger TCR, and the background clutter interference energy in the imaging results was less.

At the same time, the class imbalance of training data was simulated by changing the proportion of available training data. At the same time, different numbers of generated data samples were used for experimental comparison, and the method model without data enhancement strategy was also adopted. The final classification results of fault diagnosis models under different settings were shown in Table 1. The results showed that when the training data was sufficient, the data enhancement strategy based on the

TABLE 1: Fault diagnosis and recognition accuracy of different training datasets.

Sample number of generated data	Percentage of real data samples (%)		
	25	50 (%)	100%
0	95	91	99%
50	97	98	99%
100	98	99	99%
200	98	99	99%
300	98	100	100%

adversarial generative network did not improve the classification accuracy greatly. When the proportion of available real data samples decreased to 25%, the adversarial generation network was used to generate sample data for data enhancement, so that the classification accuracy of the fault diagnosis model improved greatly. It also showed that the adversarial generative network was helpful for accurate classification of fault diagnosis models when the number of samples was limited.

5. Conclusion

In the research, based on the sparsity of the detection scene, a polarization GPR imaging reconstruction algorithm based on the MMV model was proposed. The measurement data of multiple polarization channels were processed jointly to achieve the reconstruction of the reflectance of the detection scene corresponding to each polarization channel. The simulation data processing results based on FDTD showed that compared with the polarization GPR imaging algorithm based on the traditional SMV model, the proposed algorithm improved the accuracy of target location reconstruction and the ability of background clutter suppression significantly, which could realize the detection of buried

Retraction

Retracted: Automatic Scoring Model of Japanese Interpretation Based on Semantic Scoring

Mathematical Problems in Engineering

Received 8 August 2023; Accepted 8 August 2023; Published 9 August 2023

Copyright © 2023 Mathematical Problems in Engineering. This is an open access article distributed under the Creative Commons Attribution License, which permits unrestricted use, distribution, and reproduction in any medium, provided the original work is properly cited.

This article has been retracted by Hindawi following an investigation undertaken by the publisher [1]. This investigation has uncovered evidence of one or more of the following indicators of systematic manipulation of the publication process:

- (1) Discrepancies in scope
- (2) Discrepancies in the description of the research reported
- (3) Discrepancies between the availability of data and the research described
- (4) Inappropriate citations
- (5) Incoherent, meaningless and/or irrelevant content included in the article
- (6) Peer-review manipulation

The presence of these indicators undermines our confidence in the integrity of the article's content and we cannot, therefore, vouch for its reliability. Please note that this notice is intended solely to alert readers that the content of this article is unreliable. We have not investigated whether authors were aware of or involved in the systematic manipulation of the publication process.

Wiley and Hindawi regrets that the usual quality checks did not identify these issues before publication and have since put additional measures in place to safeguard research integrity.

We wish to credit our own Research Integrity and Research Publishing teams and anonymous and named external researchers and research integrity experts for contributing to this investigation.

The corresponding author, as the representative of all authors, has been given the opportunity to register their agreement or disagreement to this retraction. We have kept a record of any response received.

References

- [1] Q. Wang, "Automatic Scoring Model of Japanese Interpretation Based on Semantic Scoring," *Mathematical Problems in Engineering*, vol. 2022, Article ID 3299549, 7 pages, 2022.

Research Article

Automatic Scoring Model of Japanese Interpretation Based on Semantic Scoring

Qin Wang 

School of Foreign Languages, Yan'an University, Shaanxi 716000, Yan'an, China

Correspondence should be addressed to Qin Wang; lugd@zjnu.edu.cn

Received 16 July 2022; Accepted 8 August 2022; Published 6 September 2022

Academic Editor: Hengchang Jing

Copyright © 2022 Qin Wang. This is an open access article distributed under the Creative Commons Attribution License, which permits unrestricted use, distribution, and reproduction in any medium, provided the original work is properly cited.

In order to improve the current level of Japanese teaching and the difficulty of non-standard Japanese spoken language, the author proposes a method for the study of the automatic scoring model of Japanese tests for scoring. The author introduces a semantic scoring model that integrates the long short-term memory neural network and self-attention mechanism, which can be applied to keyword scoring and sentence semantic scoring. The scoring principle of the model is as follows: firstly, extract the word and sentence features and represent them in a vectorized form, then use a bidirectional long short-term memory neural network to optimize the feature vector, and then use the self-attention mechanism to obtain the semantic features of the word or sentence. Finally, the semantic score is calculated by a simple neural network. Experiments show that compared with the semantic scoring model based on a stretchable recursive autoencoder that performs better in semantic scoring, the average correlation between this model and the original score is 0.444; the lowest rate of agreement with the original score is 95%; and the highest rate of agreement with adjacent ones is 74%. The automatic scoring model for Japanese interpreting with semantic scoring is proved to be practical and has excellent results.

1. Introduction

In the traditional oral teaching classroom, a teacher faces dozens of students, and it is difficult for students to get one-on-one targeted guidance. Students get a lot of listening, reading, and writing-related training in traditional classrooms, but little training in speaking. Due to the lack of environment and atmosphere for students to practice oral English, although students can complete the tasks of listening, reading, and writing well, it is difficult for them to pass the oral examination. This social status quo has led researchers to think about how to improve learners' oral English. Education management departments and teaching departments have also paid more and more attention to the development of relevant oral language teaching work, adding the oral language test to the large-scale foreign language test. They try to arouse students' attention to oral language learning by means of examinations. However, at present, most of oral examinations use generalized scoring standards, and the scoring standards are not quantified,

resulting in unclear scoring points. Such a scoring standard is not conducive to the scorer's grasp of the scoring details [1]. The scoring method of the speaking test is mainly based on the manual overall scoring method. This traditional scoring method is easily affected by the subjective factors of the rater, such as the rater's grading status, educational background, and teaching experience. In order to reduce the influence of the subjective factors of the raters on the scoring, scholars began to refine the generalized scoring criteria and develop a spoken automatic scoring system suitable for scoring large-scale speech samples [2].

In 2017, the Central People's Government will use intelligent technology to build a new education system and incorporate it into the artificial intelligence development plan. Among them, the new education system includes intelligent learning and interactive learning. The smart education innovation and development action is one of the eight implementation actions of the "Education Informatization 2.0 Action Plan" issued by the Ministry of Education in 2018. This development action includes the construction of an intelligent

education platform, the intelligentization of the education process, the mining of education big data, and the construction of an education knowledge map [3]. The development plans and action plans successively issued by the government fully demonstrate that smart education is the general trend of education development in the Internet era.

Automatic scoring is an important part of the intelligentization of the educational process, which can be used for both teaching assistance and teaching quality assessment.

Using an automatic grading system in the teaching process, in terms of learning, it can not only provide students with a platform for after-school practice but also allow students to receive timely feedback and guidance. From the examination, it can not only reduce the workload of the graders but also avoid the inconsistency of the grades caused by the subjective factors of the graders and improve the objectivity and fairness of the grades.

2. Literature Review

Hayden's survey pointed out that in order to cultivate applied and compound Japanese talents, many domestic colleges and universities have opened Japanese interpretation courses. For undergraduate students, because the learners' Japanese listening and speaking abilities are low and they are still in a stage of ability development, interpretation has also become a difficult subject [4]. Sichkoriz. pointed out that in the teaching of interpretation at the postgraduate level, we should actively explore and focus on interpreting skills training, the special training teaching mode is supplemented by language ability improvement [5]. Han, T. discussed the current situation of college students participating in the national translation professional qualification (level) examination and analyzed some problems existing in the examination preparation process, as well as the experience and lessons in the examination process [6]. Farooque Research pointed out that candidates mainly have problems such as low listening ability, high data translation error rate, prominent information translation omission, and insufficient background knowledge reserve [7]. A. Patterson pointed out that interpretation is an information processing process with multitask parallel processing and high cognitive load. And in this process, working memory plays an important role. As an important cognitive ability of learners, working memory is closely related to second language listening and reading, which are processed in parallel with multiple tasks and is an important support for learners to give full play to their language ability [8]. Ansarin pointed out through empirical research that the capacity of working memory affects the content comprehension in the process of Japanese listening, and learners with high working memory capacity can improve the efficiency of information processing in the listening process [9]. In addition, in the process of second language listening learning, it is also an important cognitive ability for learners to quickly and accurately understand the information they hear. Ji pointed out that the learners can process the phonetic and semantic information of auditory cue words quickly and accurately, that is, the processing speed of auditory vocabulary is also

closely related to the content comprehension in the listening process [10].

On the basis of the current research, the author proposes a method to study the automatic scoring model of Japanese interpretation based on semantic scoring. The author focuses on the semantic scoring of spoken Chinese-to-English questions and introduces a semantic scoring model that integrates the long-term memory neural network and self-attention mechanism, which can be applied to keyword scoring and sentence semantic scoring. The scoring principle of the model is as follows: firstly, extract word and sentence features and represent them in vectorized form, then use a bidirectional long-term and short-term memory neural network to optimize the feature vector and then use the self-attention mechanism to obtain the semantic features of words or sentences. Finally, the semantic score is calculated by a simple neural network. Based on the research on semantic scoring, the author proposes a multi-parameter automatic scoring model for Japanese sentence-level interpretation based on semantic scoring. The automatic scoring model calculates the candidate's Japanese sentence interpretation score by fusing the feature parameters at the two levels of speech and content. At the voice level, fluency is selected as the feature scoring parameter, and the automatic scoring model directly scores the fluency feature on the candidates' recordings. At the content level, two feature scoring parameters, keyword and sentence semantics, are selected, and the content features are scored after the candidates' recordings are converted into texts by manual conversion. Specifically, the zero-energy product method is used to extract speech features to calculate the fluency feature score. Use the semantic scoring model introduced by the author to calculate the keyword and sentence semantic feature scores. Finally, the random forest algorithm is used to fuse the above three feature scoring parameters to obtain the total score of Japanese interpretation quality. The performance of the automatic scoring model is tested by real test data, the scoring results of the automatic scoring model for Japanese interpretation proposed by the author have a high average consistency rate with the original score, which verifies the validity of the feature scoring parameters selected by the author and proves that the author's research is effective, and the automatic scoring method of Japanese interpretation based on semantic scoring proposed by him is feasible [11].

3. Methods

3.1. Eigenvector Representation

3.1.1. Discrete Representation. The discrete representation directly uses the combination of the number 0 and the number 1 to represent all words. One-hot encoding removes the repeated words in the corpus and arranges the words into a vocabulary list in a certain order. Assuming that the total number of words in the vocabulary is N , the length of the word vectors in the vocabulary is N . The position of each word corresponds to a value of 1, and all other positions are 0. Although the discrete representation program is simple to

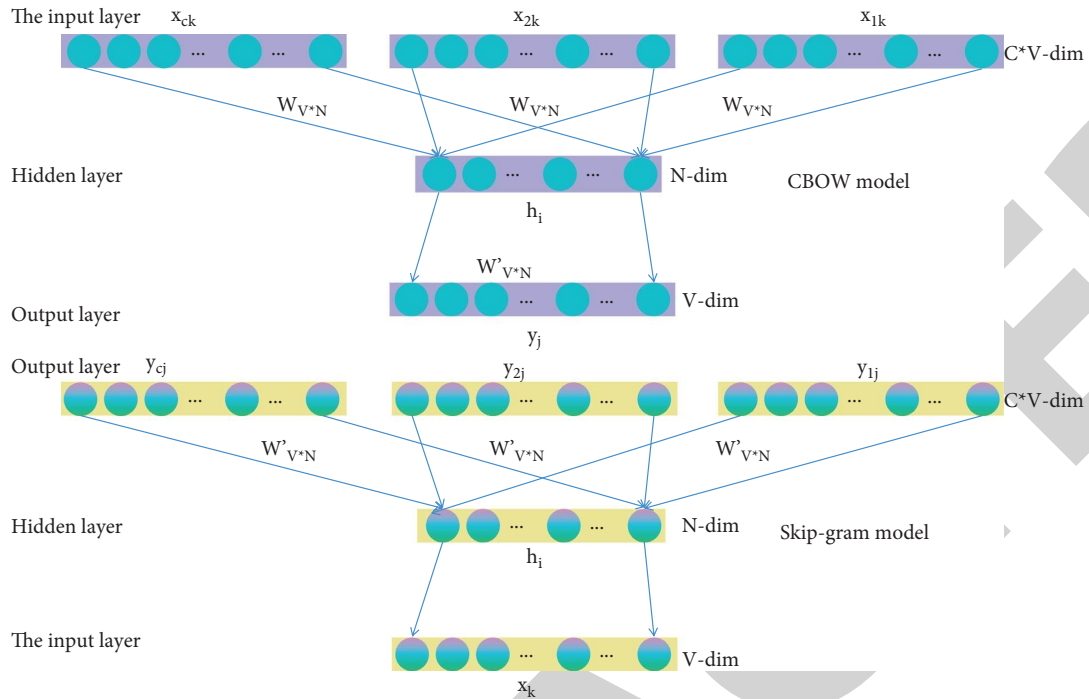


FIGURE 1: Two model structures of Word2Vec.

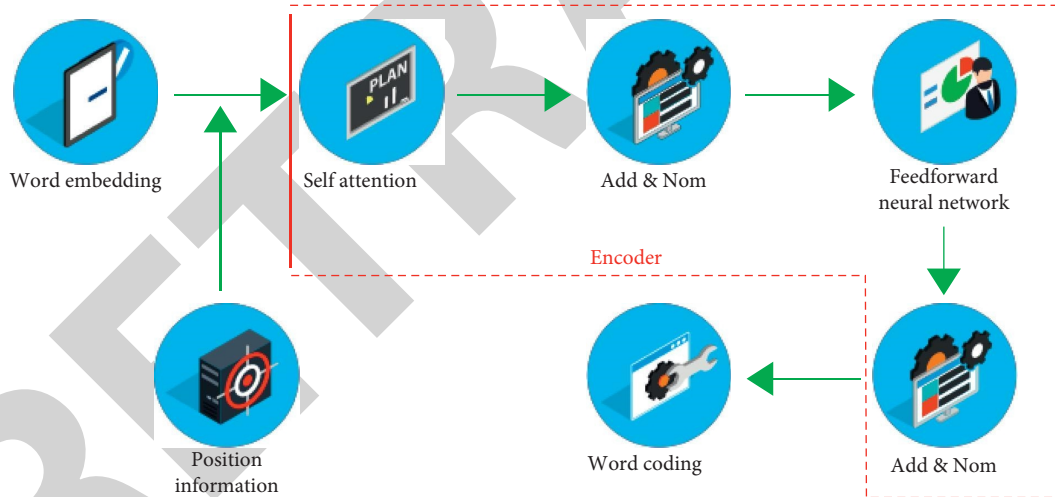


FIGURE 2: Structure diagram of the encoder part of the transformer.

implement, this sparsely stored encoding representation method. When the number of words in the vocabulary increases, the problem of dimension explosion is prone to occur. Furthermore, with this vector representation, all words are discrete symbols, and we cannot understand the similarity between words through vectors. In real life, people use language and words, and there are semantic associations between words. Distributed representations were born to address these shortcomings of discrete representations [12].

3.1.2. *Distributed Representation.* The idea of distributed representation stems from the distribution hypothesis. The hypothesis states that the context of the word determines the meaning of the word. If two words are in a similar context, their semantics are also similar. Therefore, the distributed representation of the vector is different from the discrete representation, which is a vector representation that uses a neural network to convert words into continuous values [13]. Researchers can represent the semantic similarity between

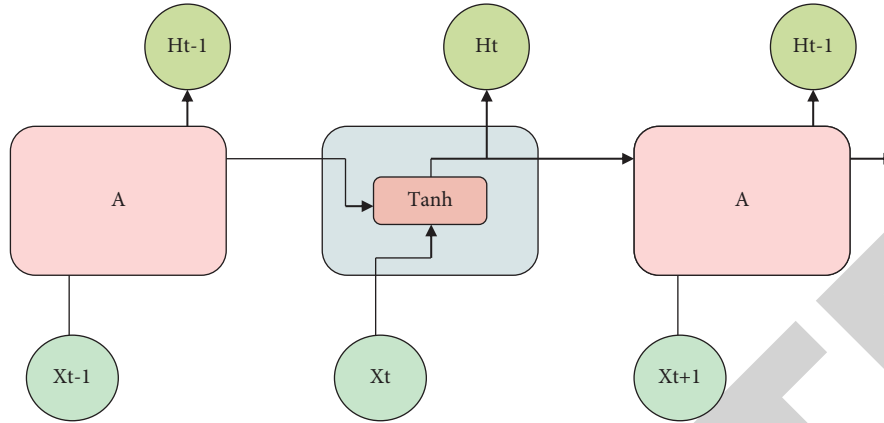


FIGURE 3: RNN unit structure diagram.

different words by calculating the spatial distance between distributed vectors. Euclidean distance and cosine similarity are commonly used spatial distance calculation methods. As shown in Figure 1, the Word2Vec model is an important model for generating distributed vectors based on contextual information.

3.1.3. BERT Model. As shown in Figure 2, feature extraction (Features Extract) and fine-tuning (Fine-Tuning) are currently the main applications of BERT. The BERT model is a model trained through massive text and can directly generate word vectors. Feature extraction is to use the trained model to convert new words or new texts into vector representations as input to the network model. Fine-tuning means that the BERT model can be adapted to the needs of the applied model, and appropriate adjustments are made to the internal parameters of the BERT model to get a better text vector representation.

3.2. Recurrent Neural Network. The specific structure of the RNN unit, shown in Figure 3, represents the processing of data at a time. In addition to X , the hidden layer input at time t also includes the output H_{t-1} of the hidden layer at time $t-1$. Therefore, the RNN model can use the previous information to process the t -th target word, which can better solve the problem of sequence prediction. The researchers use RNNs to process long text sequences, successively learn the texts divided into single word sequences and then save the learned text features into a fixed-size hidden layer. RNN can memorize historical information, so it has been widely used in time series modeling.

3.2.1. Long-Term Memory Model. The LSTM storage unit is mainly composed of four parts: memory cells, forgetting gates, input gates, and output gates. The forget gate is used to filter out old cell information and update the current memory cell according to the memory cell candidate information generated by the input gate. The sigmoid activation function in the forget gate processes the input information and outputs a value between $[0, 1]$. The output value represents the state in which the old memory cell

information is retained, the output value of 0 means that all the old memory cell information is forgotten, and the output value of 1 means that all the old memory cell information is retained. The information state calculation formula of the forget gate is shown in formula (1) and the update formula is shown in formula (2).

$$f_t = \sigma(W_f \cdot [H_{t-1}, X_t] + b_f), \quad (1)$$

$$C_t = f_t * C_{t-1} + i_t * \tilde{C}_t. \quad (2)$$

3.2.2. Bidirectional Long Short-Term Memory Model. Although the LSTM model can obtain historical information, it can only predict the output at the next moment based on the historical information, and the current output can only be combined with the previous sequence information. In practical tasks, the output at the current moment is not only related to historical information but may also be related to subsequent information at the current moment. For example, in order to predict the semantics of words in a sentence, not only need to judge according to the previous text but also need to consider the information behind the words. Only the joint context information can accurately judge the semantics of words, which is the meaning of the existence of the bidirectional long and short-term memory model [14]. The model saves the information before and after the text, which effectively solves the problem that LSTM can only save the previous information. The BiLSTM model is composed of a forward LSTM model and a backward LSTM model, and the unit outputs of the two LSTM models are spliced to generate a unit output with historical information and future information.

3.2.3. Activation and Loss Functions in Neural Networks. Activation function is a nonlinear functional relationship between the upper and lower layers of nodes in a multilayer neural network. The existence of the activation function enables the neural network to have the ability to model nonlinear expressions. Activation function is the key to deep learning to obtain strong learning ability [15].

3.3. Application of the Semantic Scoring Model. In essence, the attention mechanism can be regarded as the mapping from query to key-value, and its calculation is mainly divided into three stages. The first stage is to obtain the weight by calculating the similarity between the query value and the key value, the calculation formula is shown in formula (3) [16]. Formula (3) is a commonly used function method, they are dot product (Dot), concatenation (Concatenation), and perceptron (Perceptron). The second stage uses the softmax function to normalize the weights obtained in the first stage processing, the calculation formula is shown in formula (4). In the third stage, the weight and the corresponding value are weighted and summed to obtain the final calculation result of attention, the calculation formula is shown in formula (5). In most natural language processing tasks key and value are the same, i.e., Key = Value. In the formula, Q represents the query, K represents the key, V represents the key value, and W and U are the parameter matrices during the training process.

$$f(Qk_i) = \begin{cases} Q^t k_i & \text{dot} \\ W_\alpha [Q; k_i] & \text{concat} \\ v_\alpha^t \tanh(W_\alpha Q + U_\alpha k_i) & \text{perceptron} \end{cases}, \quad (3)$$

$$\alpha_i = \text{soft max}(f(Q, k_i)) = \frac{\exp(f(Q, k_i))}{\sum_j \exp(f(Q, k_j))}, \quad (4)$$

$$\text{Attention}(Q, K, V) = \sum_i \alpha_i V_i. \quad (5)$$

3.3.1. Keyword-Based Semantic Scoring. Japanese interpreters pay more attention to the key information points of answering questions. A good scoring model should consider not only the scores of keywords that are consistent with the reference answer but also the scores of synonyms related to the keywords [17].

Word2vec can mine the semantics of keywords and their synonyms and express them in the form of vectors and can also be used to calculate the semantic similarity of words. In the application of word vector representation, the main difference between the Word2Vec model and the BERT model is that the Word2Vec model generates a static word vector, and each word has only a unique word vector representation. The BERT model can dynamic word vectors according to the context, and each word may have different representations in different contexts, which is conducive to the representation of polysemy. In order to compare the performance of the two models applied to keyword semantic scoring, when other layers of the semantic scoring model are unchanged, replace the BERT model in the word embedding layer with the Word2Vec model for control experiments. In the experiment, the word vector dimension of the Word2Vec model is set to 128. We will analyze the performance of the two models in keyword scoring from two evaluation

TABLE 1: Comparison of BERT model, Word2vec model, and original score correlation.

Topic	BERT-BLSTM-ATT	Word2Vec-BiLSTM-ATT
A_1	0.57	0.56
A_2	0.35	0.25
A_3	0.57	0.48
A_4	0.46	0.32
A_5	0.59	0.47
B_1	0.61	0.47
B_2	0.47	0.39
B_3	0.32	0.21
B_4	0.5	0.34
B_5	0.45	0.35

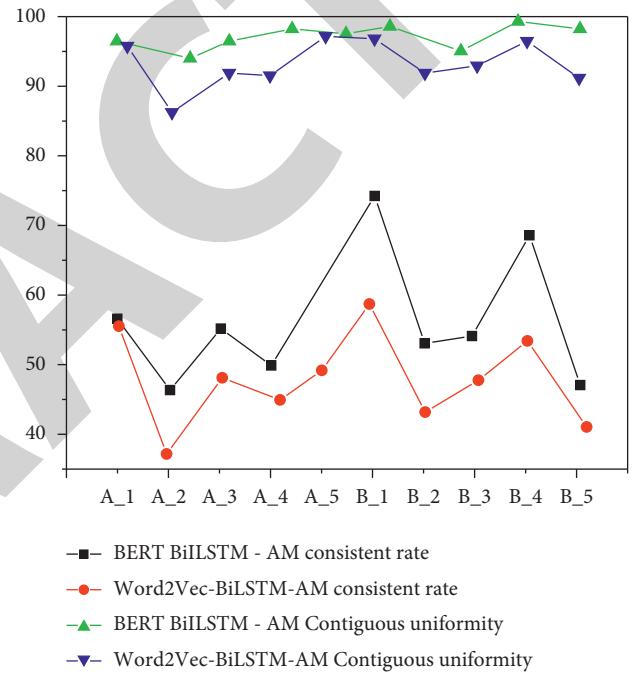


FIGURE 4: The consistency rate between the keyword semantic scoring model and the original score.

indicators, the correlation between the model scoring results and the original scores, and the consistency between the model scoring results and the original scores [18].

3.3.2. Sentence-Based Semantic Scoring. Sentence semantic scoring is not only a test of the overall understanding of the candidate's sentence but also a reflection of the candidate's ability to express the sentence. In the manual scoring, there is no specific item of sentence semantics, but the scorer will score the overall situation of the candidate's translation. The rater can tell directly by listening to the recording, and the examinee uttered a complete sentence or a string of key words. However, computers cannot easily make such judgments. From the semantic level, sentences usually consist of key words and general words. Key words are words that can affect the meaning of a sentence, and are generally composed of words with specific meanings such as

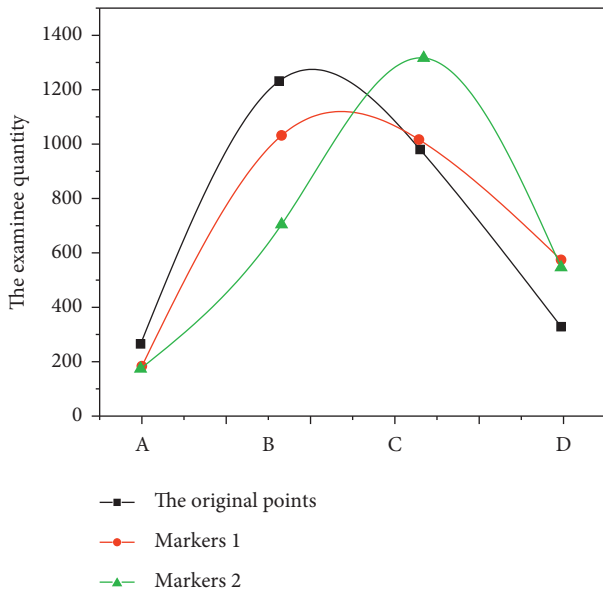


FIGURE 5: Distribution of manual scoring levels.

nouns, verbs, and adjectives. While general words do not have a decisive influence on understanding the meaning of the whole sentence, they are also an indispensable part of the sentence, such as prepositions, conjunctions, articles, and so on. In this section, we will use the sentence semantic scoring model based on the stretchable recurrent autoencoder neural network and the BiLSTM-AM-based semantic scoring model proposed by the author to conduct an experimental comparison and analyze the advantages and disadvantages of the two models in sentence semantic analysis [19].

4. Results and Discussion

The results of the correlation analysis between the BERT model, the Word2Vec model, and the original score are shown in Table 1 and Figure 4, it can be seen that the average correlation between the BERT model and the original score is 0.444, which is higher than the Word2Vec model of 0.349. In terms of the consistency rate with the original score, the lowest is 95% for the BERT model, and the lowest for the Word2Vec model is 86%. In terms of the adjacent consistency rate, the highest for the BERT model is 74%, and the highest for the Word2Vec model is 59%. It can be seen that the performance of the BERT model is due to the Word2Vec model in all aspects.

In order to reduce the impact of artificial subjectivity on the scoring results, the recorded answer sheet data used in this experiment were independently scored by two raters, taking the average of the two teachers' scores as the raw score. In order to ensure the authority of the original score and the validity of the experimental data, we eliminate the speech data with two scorers scoring more than 0.5 points and verify the validity of the machine scoring model by comparing the differences between the scores of the two scorers [20]. Figure 5 shows the distribution of manual scoring levels. Marker 1, Marker 2, and the original point all

conform to the normal distribution law. Studies have shown that in general, the distribution of students' grades obeys a normal distribution, which reflects the rationality of the two graders' grades and the reliability of the original grades [21]. The scoring results of the automatic scoring model for Chinese-English interpretation based on semantic scoring are compared with the manual scoring, and the overall average similarity between the scoring results of this model and the original scores is 0.93% [22–25].

5. Conclusion

The author proposes a method of automatic scoring model research for Japanese interpretation based on semantic scoring, which introduces a semantic scoring model based on BiLSTM-AM. The model extracts local and global features of sentence information by using the semantic representation ability and local feature extraction ability of the BERT model and uses the BiLSTM model to simplify the vector representation. A self-attention mechanism is introduced to obtain the relationship between words and appropriate weights are assigned to each word. Finally, a fully connected layer is used to obtain a semantic score. Through multiple sets of experiments, the effectiveness and advancement of the model in keyword scoring and sentence semantic scoring are effectively verified.

Data Availability

The data used to support the findings of this study are available from the corresponding author upon request.

Conflicts of Interest

The author declares that there are no conflicts of interest.

References

- [1] Z. Li, B. Zeng, P. Lei et al., "Differentiating pneumonia with and without COVID-19 using chest ct images: from qualitative to quantitative," *Journal of X-Ray Science and Technology*, vol. 28, no. 3, pp. 583–589, 2020.
- [2] Y. Zhang, "Interactive intelligent teaching and automatic composition scoring system based on linear regression machine learning algorithm," *Journal of Intelligent and Fuzzy Systems*, vol. 40, no. 2, pp. 2069–2081, 2021.
- [3] S. Schmeelk and L. Tao, "Mobile software assurance informed through knowledge graph construction," *The Owasp Threat of Insecure Data Storage*, vol. 2, no. 2, p. 13, 2020.
- [4] L. B. Hayden, C. Yonezawa, and S. Shang, "Nasa hyperwall and remote sensing outreach in Japan [education]," *IEEE Geoscience and Remote Sensing Magazine*, vol. 8, no. 2, pp. 142–143, 2020.
- [5] O. E. Sichkoriz, "Results of survey of doctors who have undergone thematic advanced training with the help of multidisciplinary cycles," *Bulletin of Problems Biology and Medicine*, vol. 1, no. 1, p. 342, 2020.
- [6] T. Han and Y. Zhang, "Comment and analysis on the major national strategies of cyberspace," *World Scientific Research Journal*, vol. 6, no. 5, pp. 275–281, 2020.
- [7] M. Farooque, "A comparative analysis of translation software using data science approach to Arabic statements,"

Retraction

Retracted: Data Analysis and Optimization of English Reading Corpus Based on Feature Extraction

Mathematical Problems in Engineering

Received 1 August 2023; Accepted 1 August 2023; Published 2 August 2023

Copyright © 2023 Mathematical Problems in Engineering. This is an open access article distributed under the Creative Commons Attribution License, which permits unrestricted use, distribution, and reproduction in any medium, provided the original work is properly cited.

This article has been retracted by Hindawi following an investigation undertaken by the publisher [1]. This investigation has uncovered evidence of one or more of the following indicators of systematic manipulation of the publication process:

- (1) Discrepancies in scope
- (2) Discrepancies in the description of the research reported
- (3) Discrepancies between the availability of data and the research described
- (4) Inappropriate citations
- (5) Incoherent, meaningless and/or irrelevant content included in the article
- (6) Peer-review manipulation

The presence of these indicators undermines our confidence in the integrity of the article's content and we cannot, therefore, vouch for its reliability. Please note that this notice is intended solely to alert readers that the content of this article is unreliable. We have not investigated whether authors were aware of or involved in the systematic manipulation of the publication process.

Wiley and Hindawi regrets that the usual quality checks did not identify these issues before publication and have since put additional measures in place to safeguard research integrity.

We wish to credit our own Research Integrity and Research Publishing teams and anonymous and named external researchers and research integrity experts for contributing to this investigation.

The corresponding author, as the representative of all authors, has been given the opportunity to register their agreement or disagreement to this retraction. We have kept a record of any response received.

References

- [1] N. Fan, "Data Analysis and Optimization of English Reading Corpus Based on Feature Extraction," *Mathematical Problems in Engineering*, vol. 2022, Article ID 1746329, 7 pages, 2022.

Research Article

Data Analysis and Optimization of English Reading Corpus Based on Feature Extraction

Nengwei Fan 

School of Foreign Languages, Yancheng Normal University, Yancheng, Jiangsu 224002, China

Correspondence should be addressed to Nengwei Fan; 0107009@yzpc.edu.cn

Received 18 July 2022; Accepted 10 August 2022; Published 31 August 2022

Academic Editor: Hengchang Jing

Copyright © 2022 Nengwei Fan. This is an open access article distributed under the Creative Commons Attribution License, which permits unrestricted use, distribution, and reproduction in any medium, provided the original work is properly cited.

In order to solve the difficulties faced by English reading teaching, this paper proposes a feature extraction-oriented method for data analysis and optimization of English reading corpus. This method specifically includes the evaluation of vocabulary coverage, comparing the value and vocabulary distribution evaluation of the two sets of textbooks in helping students master English core vocabulary and adapt to the English reading environment as soon as possible, testing whether the teaching of the three sets of textbooks can enable learners to reach the level of free reading corresponding English materials, and testing whether the gradient of the textbooks can be in line with the average language level required for reading corresponding English materials. The experimental results show that, compared with the blog-1565 based on the four authoritative core word lists, the English core word coverage of the two tutorials has reached 91.8% and 93.7%, respectively, and can be improved to 96% and 97.4%, respectively, after optimization. *Conclusion.* It is proved that the data analysis and optimization of English reading corpus based on feature extraction can play a directional role in the current English reading-related textbooks.

1. Introduction

With the development of the times, information technology changes with each passing day and penetrates into all aspects of social life. Information technology has a revolutionary impact on the development of education, which must be of great importance. We must “strengthen the development and application of high-quality educational resources” [1]. Reading is an important means for people to obtain information and improve their literacy. As far as foreign language learning is concerned, reading is not only the main goal of foreign language learning, but also an effective way to learn a foreign language. In non-English-speaking countries, reading has always been the main goal of English teaching. English reading can effectively promote the development of comprehensive language skills including listening and speaking ability, improve language level, enrich cultural knowledge, and promote the development of learners’ autonomous learning ability so as to achieve the goal of college English teaching [2]. Therefore, the integration and utilization of information resources and technical means to

explore the construction of reasonable college English reading resources based on corpus has been paid more and more attention. Nowadays, English reading teaching is facing many difficulties, and the teaching effect is unsatisfactory, which restricts the development and improvement of learners’ comprehensive language skills. First of all, reading ability, as a language skill, needs a lot of effective practice, and it is difficult to improve significantly in a short time.

The development of reading ability is influenced not only by learners’ vocabulary, sentences, chapters, and other language knowledge, reading skills, and strategies, but also by learners’ personal experience, background knowledge, psychological cognition, and many other factors. Therefore, its development and improvement cannot be achieved overnight. In this environment, the data analysis and optimization of English reading corpus based on feature extraction will point out the path for the content of language learning. A large number of facts have proved that corpus research can present the most common language expressions and show the focus of language teaching [3].

Curriculum designers and teachers need to better reflect this information in the teaching materials and syllabus. Especially in the process of second language teaching, the distribution of information on these language factors can affect the selection of teaching materials, the teaching process, and the teaching focus, which is conducive to improving the effectiveness and efficiency of foreign language teaching and achieving the objectives of English teaching. Figure 1 shows the method of making an English reading corpus analysis system based on feature extraction.

2. Literature Review

A corpus is a collection of real language samples. After scientific collection, classification, and annotation, a corpus of appropriate size can reflect and record the actual use of language and help people analyze and study the laws of the language system. Busby and others have established an academic English spoken corpus and designed academic English vocabulary and reading and writing textbooks using the corpus [4]; Lange and others explored ESP teaching and literature research by using the method of corpus linguistics [5]; Komolafe and others applied the corpus-driven approach to ESP teaching practice [6]. Looking at the current situation of ESP research in the last ten years, it is found that there is still room for the development of ESP corpus research in both theory and practice. Alotaibi and others used sketch engine system to discuss the specific application of corpus technology in ESP vocabulary data teaching from two aspects: corpus construction and teaching activity design [7]. Secondly, most studies focus on static or dynamic corpora, and there are few studies using corpus technology to serve ESP teaching. Xu and others tried to use the new senior high school English (NSEC) textbook corpus and corpus retrieval software to design senior high school English reading teaching. Through pre-reading, prediction, context guessing, and fast reading plot, they deeply discussed the teaching of reading micro skills [8]. Lesnevsky and others analyzed the pragmatic methods and teaching significance of corpus in assisting in understanding the main content of the text, retelling the text, learning anaphora, extracting the main line of story development, and guessing words in the context in combination with the case of corpus-assisted high school English reading teaching [9]. In order to obtain first-hand language data and explore the combination of corpus theory and textbook evaluation theory, in addition to the ready-made BNC corpus, the author has created two corpora [10, 11]. One is a 1 million word English annotation corpus of American and English newspapers and periodicals, and the other is a corpus of English reading textbooks. The corpus of the PCRC comes from three sets of reading materials used by English majors, namely, the American and English newspapers and periodicals reading course (universal, intermediate, and advanced) and the selected English newspapers and periodicals (volume 1–4) published by Peking University Press and the extensive reading course (volume 1–4) published by Shanghai Foreign Language Education Press. The course of reading American and British newspapers and periodicals (hereinafter referred to as

American and British newspapers and periodicals) and selected readings of English newspapers and periodicals (hereinafter referred to as English newspapers and periodicals) are the only two sets of self-contained textbooks among all published textbooks for reading newspapers and periodicals, and they are for English majors. At present, some high-quality newspaper reading textbooks are also published, but they are not systematic. In the teaching of reading for English majors in colleges and universities across the country, extensive reading course is very popular and representative. Therefore, the source of the corpus of the PCRC is obtained from these three sets of reading materials [12]. All teaching materials and articles are scanned, identified, corrected, and marked into electronic text storage. Each corpus is attached with detailed annotation, including the source of the corpus, subject matter, genre, author, publication time, and other information. See Tables 1 and 2 for the composition of NEC (newspaper corpus) and PCRC (textbook corpus) corpora built in this research institute.

3. Method

3.1. Vocabulary Coverage Assessment. The vocabulary coverage assessment aims to test the ratio of a certain type of vocabulary that students should master as presented in the textbook. It is an important basis for assessing the value of the textbook in language learning. The teaching objects of “American and English newspapers” and “English newspapers” cover English majors in the upper and lower grades of undergraduate courses, so the two sets of textbooks are comparable [13]. It can be seen from Table 2 that the “extensive reading course” is only for junior English majors. It is not comparable in this assessment, so it is not used for the time being.

3.1.1. Evaluation Objectives and Investigation Contents. This evaluation has two objectives:

- (1) By means of corpus, this paper tests the extent to which the two sets of textbooks “American and English newspapers” and “English newspapers” are consistent with the vocabulary learning requirements stipulated in the “Syllabus for English Majors in Colleges and universities (2000 EDITION)” (hereinafter referred to as the “Syllabus”).
- (2) Compare the value of the two sets of textbooks in helping students master English core vocabulary and adapt to English reading environment as soon as possible.

3.1.2. Investigation Process

- (1) The vocabulary requirements of the syllabus are most directly reflected in the vocabulary of CET-4 and CET-8. First, import the preprocessed vocabulary into wordsmith to obtain the reference vocabulary LEM-8. Then, the sublibraries of “American and English newspapers” and “English newspapers” are extracted from the PCRC, and the generated word

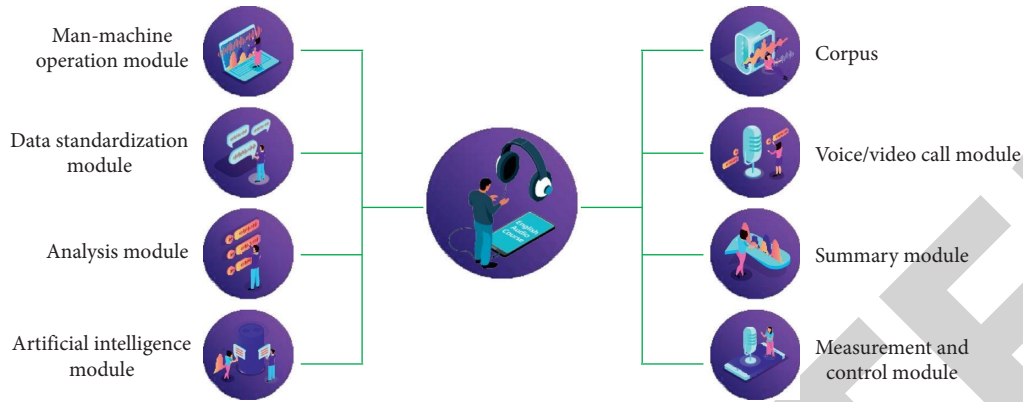


FIGURE 1: The method of making an English reading corpus analysis system based on feature extraction.

TABLE 1: Structure and distribution of NEC (newspaper library) (unit: word order).

NEC		
English sublibrary of British newspapers	British straight news report (BSNR)	112 995
	British opinion writing (BOPW)	389 584
	Subtotal	502 579
American newspaper English sublibrary	American straight news report (ASNR)	143644
	American opinion writing (AOPW)	360 125
	Subtotal	503769
Total		1006 348

TABLE 2: Structure and distribution of PCRC (textbook library) (unit: word order).

PCRC		Primary	Intermediate	Token
American and British newspapers	Shape symbol	22 211	122 811	145 022
	Classifier	4 751	13 560	14747
English newspapers and periodicals	Shape symbol	59 211	102 017	161 228
	Classifier	9 434	12412	16 379
Extensive reading tutorial	Shape symbol	174 866		174 866
	Classifier	14 742		14 742
Total				481 116

lists are truncated to obtain the respective word lists of the two sets of textbooks. Finally, using word-smith’s word list comparison function, check the degree to which the word lists of the two teaching materials are consistent with LEM-8 reference word lists. The higher the degree of coincidence, the closer the teaching materials are to the vocabulary requirements specified in the syllabus.

- (2) The survey of coverage assessment is to compare the two textbooks’ vocabulary generated in the above survey with the English core vocabulary to see the extent to which they are consistent with the English core vocabulary. The higher the degree of coincidence, the greater the help of the textbooks for students to master the English core vocabulary, and the higher the value of enabling students to adapt to English reading activities as soon as possible. The study of core vocabulary should be the focus of vocabulary teaching and the focus of teaching materials. This survey involves the selection and

definition of English core vocabulary. It is found that 87% of the vocabulary in English is concentrated on 2000 high-frequency words. These core high-frequency words should be the focus of English vocabulary teaching. On the basis of these results, this study extracted the intersection 1565 words of the four lists (the shared words of the four core lists), and the integrated English core list (blog-1565) is more scientific and representative. NHPP Software Reliability Modeling Framework considering the test workload shown in formula (1) is very helpful for calculating coverage.

$$\frac{dm(t)}{dt} \times \frac{1}{w(t)} = r(t)[N - m(t)]. \quad (1)$$

Here $m(t)$ represents the expected mean function of the number of detected defects within the time interval $[0, t]$; $w(t)$ represents the test workload consumption rate function, which is the test

workload function (recorded as the derivative of $w(t)$ to the test time t , $w(t) = dW(t)/dt$. When the boundary condition is $m(0) = 0, W(0) = 0$, different forms of test workload function $w(t)$ are substituted into the above differential equation and solved to obtain various NHPP Software reliability models.

3.2. Vocabulary Distribution Assessment

3.2.1. Research Purpose and Tools. In this study, three sets of teaching materials from the whole PCRC library are selected, because these three sets of teaching materials are systematic and constitute a language level gradient in reading content. This study has two purposes:

- (1) Using real data to verify whether the vocabulary distribution among the three sets of textbooks is scientific, whether there is a level of gap in language level, and whether it meets the requirements of textbook compilation step-by-step.
- (2) To test whether the teaching of these three sets of textbooks can enable learners to freely read the corresponding English materials, that is, to test whether the gradient of the textbooks can be in line with the average language level required for reading the corresponding English materials. This study analyzes the samples from the three sets of textbooks one by one with the help of range analysis software. The basic function of range is to calculate the word frequency range and relevant statistical data of the input text with reference to the three-level benchmark vocabulary [14]. Based on this characteristic, the range analysis software can be combined with the reference corpus to conduct quantitative research on the whole set of teaching materials. The analysis results can provide a scientific basis for the compilation of teaching materials and the selection of teaching materials in teaching. In order to ensure the objectivity and scientificity of the study, the author sampled the three sets of textbooks by layers according to the three standards of volume, subject matter, and genre, and took random sampling among the layers. After preprocessing, the three sets of textbook samples become range recognizable texts, and then the 440 word frequency breadth data calculated by the range and the 360 data calculated from the reference corpus samples are input into SPSS to test one by one [15]. With the help of SPSS, it is necessary to call an independent sample t -test to calculate whether texts from two different sources have the same difficulty level distribution. This test can compare the difficulty between each textbook and the reference corpus [16]. Since the independent sample t -test can detect whether the two independent samples come from the same population and whether the data distribution of the two samples is the same, that is, it can test whether there is no difference between the textbook text and the reference corpus text because they both come from the

same text population with the same difficulty level. Therefore, we can compare the difficulty of the textbook with the average language level required for reading English materials. Since all the texts of the “American and English newspapers” and “English newspapers” subdatabases of PCRC are from English newspapers, the evaluation of these two sets of textbooks is based on the NEC corpus (newspaper library).

4. Results and Discussion

As can be seen from Figure 2, there is no substantive difference in the vocabulary coverage of the two sets of textbooks, reaching 41.3% and 44.8%, respectively. The coverage of level 8 vocabulary is low, and the number of exclusive words exceeds the number of shared words. Exclusive words are supersyllabic words, which are not included in the learning requirements of LEM-8. From the perspective of material sources, the newspaper articles included in the two sets of textbooks are articles read by the British and American public every day, and most of the vocabulary in the textbooks is daily commonly used words. Through word by word analysis, it is found that another reason why the number of exclusive words in the vocabulary of the two sets of teaching materials exceeds the number of shared words is that there are a large number of proper nouns such as people’s names, place names, and abbreviations of institutions and companies such as NRA and Boeing [17]. The “Outline” has no high requirements for mastering proper nouns and abbreviations. After retrieving LEM-8, it is found that there are only 29 proper nouns and 3 abbreviations. In the language practice of students after graduation, a large number of working vocabulary involve these two categories of words. The above analysis shows that LEM-8 deviates from the modern vocabulary actually used by Britain and the United States to a certain extent. The reason lies in the timeliness of language [18].

The calculation results show that, compared with the blog-1565 generated based on the four authoritative core word lists, the English core word coverage of the two tutorials is quite high, reaching 91.8% and 93.7%, respectively, and there is no qualitative difference between the two. Through further analysis of the missing words, it is found that although the prototypes of these word families are missing in the vocabulary of the two sets of textbooks, many of their derivatives have been reflected in the textbooks. If these derivatives are also included in the category of shared words, the vocabulary coverage will be increased to 96% and 97.4%, respectively. This shows that the two sets of textbooks are of great help in mastering English core words [19]. The comparison of the above two findings shows a contradiction. The two sets of textbooks have a high coverage of English core vocabulary but a low coverage of vocabulary in the syllabus. This just shows that when the syllabus contains the vocabulary that students need to master, the frequency of vocabulary is not the only selection standard [20].

From the data in Table 3, we draw the following conclusions through analysis.

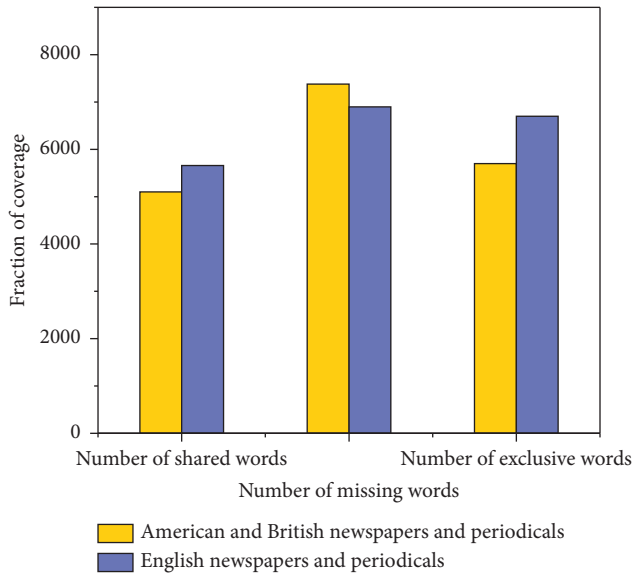


FIGURE 2: Survey results of coverage assessment.

- (1) There is a significant difference between the first-class vocabulary and rare vocabulary of the “universal edition” and the average level of British and American newspaper English at 95% confidence. Since the “popularization book” sets the minimum language level for learners to start reading British and American newspapers, the most commonly used words that learners have mastered will appear in the articles as much as possible, so that the vocabulary of level 1 is more than the average level, and rare words are used as little as possible, resulting in the vocabulary beyond level 3 being less than the average level.
- (2) There is no significant difference between the vocabulary at all levels of the “intermediate edition” and the average English level of British and American newspapers and periodicals. It can be seen that the “intermediate edition” has improved the language level of readers to the level of being able to read most British and American newspapers and periodicals normally.
- (3) Compared with the average language level of British and American newspaper English, the first-class words and rare words in the advanced edition have significant differences within the 95% confidence interval. As the compiling principle of “Advanced Edition” is the highest level of British and American newspaper English, its difficulty is higher than that of ordinary British and American newspapers.
- (4) Level 2 and level 3 vocabulary belong to secondary and unusual words. Each volume in the course has the same level as the average vocabulary level of British and American newspapers and periodicals on these two levels of vocabulary, and there is no significant difference in the test, which reflects the good combination between the course and the actual

TABLE 3: SPSS test results of “American and British newspapers”.

Group	<i>t</i> value	<i>p</i> value
Elementary level range 1 vs. NEC range 1	2.393	0.22*
Elementary level range 2 vs. NEC range 2	-1.151	0.257
Elementary level range 3 vs. NEC range 3	0.082	0.935
Elementary level outsiders vs. NEC range outsiders	-2.33	0.25*
Intermediate level range 1 vs. NEC range 1	1.107	0.275
Intermediate level range 2 vs. NEC range 2	-0.348	0.73
Intermediate level range 3 vs. NEC range 3	-0.179	0.859
Intermediate level outsiders vs. NEC outsiders	-960	0.343
Advanced level range 1 vs. NEC range 1	-2.636	0.12*
Advanced level range 2 vs. NEC range 2	1.776	0.084
Advanced level range 3 vs. NEC range 3	-0.411	0.683
Advanced level outsiders vs. NEC outsiders	2.591	0.14*

language application of British and American newspapers and periodicals.

In this study, the results of Mann–whitney *U* test in the nonparametric test are consistent with the results of *t*-test for independent samples. This study confirms that the vocabulary distribution among the “American and British newspapers” has a level gap in language level. The compilation of the whole set of textbooks meets the requirements of step-by-step, and its gradient is in line with the average language level required for reading British and American newspapers. In an ideal state, learners who can complete the whole set of textbooks will likely exceed the average level required by the British and American newspapers, and their language literacy will reach a new level as shown in Table 4:

The SPSS test results of “English newspapers” show that there is no significant difference between the four levels of vocabulary in each volume and the average level of English in British and American newspapers. It can be seen that the full set of “English newspapers” sets the language level of potential readers at the level that they can normally read in most British and American newspapers. This shows that the language level of “English newspapers and periodicals” has been in line with the average level required for reading British and American newspapers and periodicals, but there is no gradient in the distribution of vocabulary among the subvolumes, there is no level gap in the language level, and the compilation of the whole set of textbooks does not reflect the requirements of step-by-step as shown in Table 5:

In general, the reading content of the fourth volume of the “extensive reading course” prepared for the second semester of grade 2 basically reached the reading level of Britain and the United States, while the first three volumes reduced the vocabulary difficulty of the reading materials in order to adapt to the level of lower grade students. Since the fourth volume of the “extensive reading course” is still used by junior English majors, there has not been a significant decrease in the number of first-class words and a significant increase in the number of rare words in the highest volume of the “American and British newspapers.”

TABLE 4: SPSS test results of “English newspapers”.

Group	<i>t</i> value	<i>p</i> value
Volume 1 range 1 vs. NEC range 1	-0.865	0.393
Volume 1 range 2 vs. NEC range 2	0.216	0.83
Volume 1 range 3 vs. NEC range 3	-0.615	0.543
Volume 1 outsiders vs. NEC range outsiders	1.285	0.207
Volume 2 range 1 vs. NEC range 1	0.671	0.506
Volume 2 range 2 vs. NEC range 2	0.313	0.752
Volume 2 range 3 vs. NEC range 3	0.596	0.562
Volume 2 outsiders vs. NEC outsiders	-1.611	0.116
Volume 3 range 1 vs. NEC range 1	-0.219	0.828
Volume 3 range 2 vs. NEC range 2	-0.005	0.996
Volume 3 range 3 vs. NEC range 3	-1.853	0.72
Volume 3 outsiders vs. NEC outsiders	1.27	0.212
Volume 4 range 1 vs. NEC range 1	-0.714	0.48
Volume 4 range 2 vs. NEC range 2	-0.837	0.408
Volume 4 range 3 vs. NEC range 3	0.402	0.69
Volume 4 outsiders vs. NEC outsiders	0.993	0.327

TABLE 5: SPSS test results of “extensive reading tutorial”.

Group	<i>t</i> value	<i>p</i> value
Volume 1 range 1 vs. BNC range 1	3.730	0.003*
Volume 1 range 2 vs. BNC range 2	-0.572	0.571
Volume 1 range 3 vs. BNC range 3	-0.27	0.788
Volume 1 outsiders vs. BNC range outsiders	-4.961	000*
Volume 2 range 1 vs. BNC range 1	7.616	000*
Volume 2 range 2 vs. BNC range 2	-1.488	0.145
Volume 2 range 3 vs. BNC range 3	-1.596	0.119
Volume 2 outsiders vs. BNC outsiders	-5.145	000*
Volume 3 range 1 vs. BNC range 1	4.064	000*
Volume 3 range 2 vs. BNC range 2	-0.110	0.913
Volume 3 range 3 vs. BNC range 3	-0.23	0.819
Volume 3 outsiders vs. BNC outsiders	-4.052	000*
Volume 4 range 1 vs. BNC range 1	0.959	0.344
Volume 4 range 2 vs. BNC range 2	-2.373	0.023
Volume 4 range 3 vs. BNC range 3	1.28	0.208
Volume 4 outsiders vs. BNC outsiders	-0.983	0.332

5. Conclusion

This paper presents a method for data analysis and optimization of English reading corpus based on feature extraction and systematically evaluates three sets of textbooks collected in the PCCC corpus with the real language data of the corpus. By observing the theme of textbook selection, the popularity of language, language rhetoric, latent semantics, pragmatics, and other aspects, this paper proves that this method plays an important role in realizing the scientization and effectiveness of English textbooks. Specifically, compared with BLOG-1565 based on the four authoritative core word lists, the coverage of English core words in the two tutorials is quite high, reaching 91.8% and 93.7%, respectively. There is no qualitative difference between the two. The language level of “English newspapers and periodicals” is equal to the average level required for reading British and American newspapers and periodicals. However, there is no gradient in the distribution of vocabulary among the sub-volumes, and there is no level gap in the language level. The

compilation of the whole set of textbooks does not reflect the requirements of gradual progress.

Data Availability

The data used to support the findings of this study are available from the corresponding author upon request.

Conflicts of Interest

The authors declare no conflicts of interest.

References

- [1] N. A. Khan and S. M. Shafi, “Open educational resources repositories: current status and emerging trends,” *International Journal of Digital Literacy and Digital Competence*, vol. 12, no. 1, pp. 30–44, 2021.
- [2] X. Gu and Y. Zhao, “Integration of teaching and assessing intercultural communicative competence,” *Chinese Journal of Applied Linguistics*, vol. 44, no. 2, pp. 241–258, 2021.
- [3] E. Baik and H. Joo, “The effect of dramatic play using multimedia on physical expression, language expression and peer play behavior of young children,” *Journal of Children’s Media & Education*, vol. 20, no. 1, pp. 1–26, 2021.
- [4] N. L. Busby and A. Dahl, “Reading rate of academic English texts: comparing l1 and advanced l2 users in different language environments,” *Nordic Journal of English Studies*, vol. 20, no. 1, pp. 36–61, 2021.
- [5] C. Lange, “Review of esimaje, gut & antia (2019): corpus linguistics and african englishes,” *English World-Wide*, vol. 42, no. 1, pp. 111–115, 2019.
- [6] B. F. Komolafe, M. O. Ogunniran, F. Y. Zhang, and X. S. Qian, “A comparative perspective of teaching skill acquisition in pre-service physics teacher (pspt) training program in China and Nigeria,” *Journal of Baltic Science Education*, vol. 19, no. 3, pp. 356–373, 2020.
- [7] S. S. Alotaibi, T. Kumar, and A. Benyo, “Significance and teaching strategies of mathematics and its skills to the students of other departments at prince sattam bin Abdulaziz university, ksa,” *International Journal of Advanced Science and Technology*, vol. 29, no. 7, pp. 13768–13783, 2020.
- [8] J. Xu and T. Li, “The application of artificial intelligence and virtual reality in the auxiliary teaching of American science fiction literature,” *Journal of Intelligent and Fuzzy Systems*, vol. 1, no. 6, pp. 1–10, 2021.
- [9] Y. Y. Lesnevsky, “Assistive technologies as a search tool for the demanded profile of special library,” *Bibliotekovedenie [Russian Journal of Library Science]*, vol. 70, no. 2, pp. 135–147, 2021.
- [10] D. Selva, B. Nagaraj, D. Pelusi, R. Arunkumar, and A. Nair, “Intelligent network intrusion prevention feature collection and classification algorithms,” *Algorithms*, vol. 14, no. 8, p. 224, 2021.
- [11] G. Pujadas and C. Muñoz, “Examining adolescent efl learners’ tv viewing comprehension through captions and subtitles,” *Studies in Second Language Acquisition*, vol. 42, no. 3, pp. 551–575, 2020.
- [12] K. JuusoEsko, “Intelligent temporal analysis of coronavirus statistical data,” *Open Engineering*, vol. 11, no. 1, pp. 1223–1232, 2021.
- [13] S. Zhu, Y. Han, X. Yang, and Yang, “An automatic analysis approach toward indistinguishability of sampling on the lwe

Research Article

A Genetic Algorithm Model for Human Resource Management Optimization in the Internet Marketing Era

Yi Li¹ and Wang Linna ^{1,2}

¹Jeonju University, 303, Cheonjam-ro, Wansan-Gu, Jeollabuk-Do 55069, Republic of Korea

²Langfang Normal University, No. 100 Aiminxiadao, Langfang City, Hebei Province 065000, China

Correspondence should be addressed to Wang Linna; linnawang1220@jj.ac.kr

Received 21 June 2022; Accepted 19 July 2022; Published 31 August 2022

Academic Editor: Kai Guo

Copyright © 2022 Yi Li and Wang Linna. This is an open access article distributed under the Creative Commons Attribution License, which permits unrestricted use, distribution, and reproduction in any medium, provided the original work is properly cited.

In the context of the Internet marketing era, rational use of big data for quantitative analysis of human resource management can effectively help each unit better understand the industry talent and analyze the development trend of the industry. Personnel competency is the key factor affecting job performance. The renewable resources in the resource constrained project scheduling problem are transformed into human resources with competency differences through a series of scientific and reasonable methods. A human resource constrained project scheduling problem model emphasizing competency differences is constructed. The most prominent advantage of this model lies in the selection of indicators that can objectively and reasonably evaluate the competency of personnel, and the rigorous and scientific relationship is provided. The complex multiproject double-objective minimization problem of the total construction period and total cost is transformed into a comprehensive index single-objective maximization problem. Then, a mathematical optimization model is established and solved by a genetic algorithm. Finally, the effectiveness of the algorithm is shown by comparing numerical experiments with other algorithms.

1. Introduction

Human resource refers to the sum of all the human brain and physical strength to provide products and services or achieve established goals [1]. As an important resource, it has an extremely important impact on the development of social undertakings and the economy. Such resources usually have strong initiative and are characterized by reproducibility and sociality [2].

Human resources can not only improve the social adaptability of the unit but also contribute to the sustainable development of talents [3]. Only in this way, the unit can more adapt to social changes and strengthen its competitiveness. From the perspective of value creation and evaluation as well as value distribution and cultural construction, optimizing management measures can achieve great development effectiveness.

Under the promotion of the stable development of the network marketing era, in order to achieve the orderly progress of all work, we must strengthen the attention to the development of the era. In the context of the market

economy, enterprise competition is increasingly intensified, and it is of great significance to do a good job in internal human resource management [4]. Influenced by history, culture, system, and other factors, the human resource management mode of most enterprises has always remained unchanged [5]. Obviously, this model is not suitable for the current needs of enterprise development. Under the background of the gradual in-depth development of marketization, enterprises must further improve performance and combine employee performance with working years and seniority, thus providing a strong guarantee for human resources training and management. At present, although the efficiency of human resource management in many enterprises has been significantly improved, there is a big gap between the leadership and the grassroots, which affects the interaction between the two.

Resource Investment Problem (RIP) is a classic project scheduling problem, whose goal is to optimize human resource investment and minimize its cost [6]. RIP is derived from the classical Resource Constrained Project scheduling problem

(RCPSp), which aims to solve the minimum resource input under a given construction period. In reference [7], some scholars first put forward the problem of RIP and proved that the problem is NP hard. The duality of RIP and the single mode resource constrained project scheduling problem (S-MRCPSp) is proved. Literature [8] transformed RIP into multiple S-MRCPSp and proposed the precise algorithm of MBA (Minimum bounding Algorithm). Literature [9] proposed a branch and bound algorithm, which further improved the solving efficiency of the algorithm. Due to the limitations of accurate algorithms in solving large-scale problems, many scholars have designed different heuristic algorithms to solve this problem. Literature [10] transformed RIP into an RCPSp problem, which was solved by the metaheuristic algorithm based on Scatter Search. Literature [11] uses a genetic algorithm to solve the resource input problem with delay penalty and codes the job priority and resource capacity respectively. Literature [12] solved the RIP problem by path reconnection and genetic algorithm for the first time without transforming the RIP problem into RCPSp. However, its algorithm may produce a list of jobs with infeasible priorities and also cause problems of algorithm efficiency. Moreover, when scheduling jobs, the influence of current selection on global resource investment is not taken into account. Literature [13] proposed a multistart iterative search method based on the iterative search algorithm. This algorithm improves the RIP solution quality effectively. In view of the problem of resource input, many scholars also carried out extensive research on this basis.

However, with the continuous improvement of the depth and breadth of research, some scholars say that the skill level of employees does not have a great impact on their performance, and the main factor affecting performance is the competency of employees. In view of the level of employee, competency will not only have a significant impact on the work completion cycle but also directly related to the amount of material input. This paper selects the indicators that can reasonably and objectively evaluate the competency of employees and creates a rigorous, perfect, and simple mathematical optimization model. A large number of studies have proved that for this kind of problems, both mathematical optimization model considering competency difference and genetic algorithm, which is highly respected by industry insiders, show strong applicability.

The innovations of this paper are as follows:

- (1) This model lies in the selection of indicators that can objectively and reasonably evaluate the competency of personnel, and a rigorous and scientific relationship is provided
- (2) The complex multiproject double-objective minimization problem of the total construction period and the total cost is transformed into a comprehensive index single-objective maximization problem
- (3) A mathematical optimization model is established and solved by a genetic algorithm

This paper consists of four main parts: Section 1 is the Introduction, Section 2 is Methodology, Section 3 is Result Analysis and Discussion, and Section 4 is the Conclusion.

2. Methodology

2.1. Problem Definition. The research content of this paper is on how to develop a rigorous and reasonable project schedule with good feasibility, and how to achieve multiobjective human resource management optimization reasonably and clearly and synchronously. To put it simply, the company currently has a cluster of parallel R&D projects, and internal employees are assigned to work accordingly. The relationship between the work of each project has been clarified, the working hour quota of each work has been clarified, and the number of personnel arrangement and the amount of capital investment of each work has been clarified. The problem to be solved is how to put forward a rigorous, reasonable, and feasible mode of multi-project work and how to select the appropriate starting time, so as to achieve the goal of completing several collaborative projects with the minimum economic input and the shortest time with high quality. In this paper, the variable of man-hour coefficient is selected, hoping to objectively and reasonably evaluate the competency level of employees through this index.

2.2. Problem Modelling

2.2.1. Original Problem Model. In order to solve this problem efficiently, this section creates a scientific, reasonable, rigorous, and perfect mixed integer programming model based on previous research results. The symbol definitions are shown in Table 1.

$$\sum_{x=1}^{TR} \sum_{w=1, x \in w} d_{yzw} Z_{xyz} \geq T_{yz} N_{yz}, \quad (1)$$

$$\forall y = 1, \dots, TU, \quad z = 1, \dots, Ty,$$

$$d_{yzw} \Phi_{yzwk} \leq L_{yzk}, \quad \forall y, z, w = 1, \dots, W, k = 1, \dots, K. \quad (2)$$

(1) Objective function

$$\min \sum_{n=0}^N n j_{1, T_1+1, 1, n} \quad (3)$$

$$\min \sum_{k=1}^K \sum_{n=0}^N \sum_{y=1}^{TU} \sum_{z=1}^{Ty} \sum_{w \in B(y, z)} d_{yzw} j_{yzwn} \phi_{yzwk} u_k. \quad (4)$$

(2) Constraints

$$\sum_{y=1}^{TU} \sum_{z=1}^{Ty} \sum_{w \in B(y, z)} \sum_{n=n-d_{yzw}+1} \quad (5)$$

$$j_{yzwn} \leq 1,$$

$$\forall n = 0, \dots, N, \quad x = 1, \dots, TR,$$

$$\sum_{n=0}^N \sum_{w \in B(y, z)} j_{yzwn} = 1, \quad \forall y = 1, \dots, TU, \quad z = 1, \dots, Ty, \quad (6)$$

TABLE 1: Symbol definitions.

Problem parameters	Symbolic meaning
g_{yz}	Activity z of project y
U_{yz}	Immediately preceding activity set of activity z of item y .
TU	Total number of projects
T_y	Total number of activities for project y
TR	Total number of employees x
N	Upper limit of multiproject construction period
N_{yz}	Work quota for activity z of project y
T_{yz}	Set the number of employees assigned to activity z in project y .
T_x	Set the maximum number of employees that can be allocated in each period.
Z_{xyz}	Man hour factor for employee x to complete activity z of project y .
$x \in w$	Employee x is in the personnel combination of mode w .
$B(y, z)$	Set of feasible execution modes for activity z of project y . $B(y, z)$ is composed of execution modes that simultaneously satisfy formulas (1), (2) and (8).
K	Number of types of material K
U_k	Unit price of material K
L_{yzk}	Limit of material k for activity z of project y
Φ_{xk}	Employee x 's material k consumption rate
J_{yzwn}	The activity z of project y adopts mode w and starts at time n . The value is 1. Otherwise, the value is 0.
I_{xyzn}	When employee x is assigned to activity z of project y in time period, the value is 1. Otherwise, the value is 0.
Φ_{yzwk}	The sum of the consumption rate of material k under the employee combination of mode w for activity z of project y , $\Phi_{yzwk} = \sum_{x \in w} \Phi_{xk}$
d_{yzw}	Construction period of activity z of project y when mode w is adopted. The value of d_{yzw} is the smallest integer satisfying formulas (1) and (2) below.

$$\sum_{y=1}^{TU} \sum_{z=1}^{T_y} \sum_{x=1}^{TR} i_{xyzn} \leq T_x, \quad (7)$$

$$\sum_{x=1}^{TR} i_{xyzn} = T_{yz}, \quad (8)$$

$$\sum_{n=0}^N \sum_{w \in B(y,z)} n j_{yzwn} \geq \sum_{n'=0}^N \sum_{w \in B(y,z)} N \quad (9)$$

$$j_{y'z'wn'} \left(n + d_{y'z'w} \right),$$

$$\forall g_{y'z'} \in U_{yz},$$

$$j_{yzwn} \in \{0, 1\},$$

$$\forall y = 1, \dots, TU, z = 1, \dots, T_y,$$

$$n = 0, \dots, N, w \in B(y, z). \quad (10)$$

According to formula (1), it can be known that the total amount of work actually completed by the combination of active employees is at least greater than the rated workload of the activity. The work completion period is usually determined by rounding up. According to formula (2), it can be known that the materials used by employees in the process of work should be less than the work limit, which is usually determined by rounding down. According to formula (3), the core goal is to minimize the total construction period of multiple projects. According to formula (4), it can be learned that the secondary goal is to achieve the most economical multiproject and complete the project quickly and with the least economic input. According to formula (5), all

employees can only carry out one job at a certain time. According to formula (6), all activities can only choose one mode and only start at a certain period. Formula (7) specifies the upper limit of the number of employees that can be allocated at the same time. Formula (8) specifies the number of employees assigned to project J activity K . According to formula (9), it can be understood that there is a certain logical order relationship among various jobs. According to formula (10), the decision variable of the model has its specific value range, which is 0~1 decision variable.

2.2.2. Comprehensive Index Model. The evaluation function method is a scientific and reasonable real function which is constructed by combining all kinds of information and data provided by decision-makers. Then, the multiobjective optimization problem is transformed into a single-objective optimization problem which is easy to understand and analyze. In simple terms, it is a way to solve multiobjective optimization problems by combining people's preferences and provided data. It can deduce the optimization result satisfying the decision condition efficiently and conveniently according to the decision data and materials provided by people.

In this paper, the linear weighted synthesis method is used to transform the two-objective optimization of the project construction period and cost into a single-objective optimization problem. Specifically, the original problem model is transformed into a comprehensive indicator model through the following steps.

Firstly, expert investigation and fuzzy comprehensive evaluation are used to assign weights to the indexes. For software projects, the actual requirements of the project construction period are more stringent than the

requirements of project cost, so the weight of the project construction period should be greater than the weight of cost.

Secondly, since both construction period and cost are cost indicators, a smaller value of the indicator means a better solution, but a larger value of the fitness function means a better individual. At the same time, considering the construction period and cost of the unit is not unified, must be dimensionless processing.

The dimensionless formula of total project construction period N is

$$N_s = \frac{(\{\max N\} - N + 1)}{(\{\max N\} - \{\min N\} + 1)}. \quad (11)$$

The dimensionless formula of total project cost C is

$$C_s = \frac{(\{\max C\} - C + 1)}{(\{\max C\} - \{\min C\} + 1)}. \quad (12)$$

where N_s and C_s represent the dimensionless index values of the project construction period and project cost, respectively.

Finally, the objective function formula of the comprehensive index model is as follows:

$$\max CX = \omega \times N_s + (1 - \omega) \times C_s, \quad (13)$$

where ω represents the weight of the construction period. CX is the comprehensive index value. The constraint conditions of the comprehensive index model are the same as those of formulas (5)~(10) in the original model.

In this study, the time of work is not fixed, in other words, the work involves “many different working modes,” and so one might classify the problem in this paper as traditional. In fact, the main differences between S-MRCPSP and MRCPSP are as follows.

First, in MRCPSP, the amount of resources allocated in each work development cycle is generally unified and basically fixed. The “multiple different working mode” is reasonable and clear under the premise of the workload of each project, input cost, and other relevant factors.

Second, there are differences in the number of modes. In terms of working modes, the number of the former may significantly exceed the latter. The number of working modes of MRCPSP is usually not very large.

Third, in the S-MRCPSP problem, only after the formulation of a rigorous and reasonable human resources allocation plan, can accurately determine the work cycle, which is obviously different from MRCPSP. For example, in project A, the MRCPSP method calculated the construction period to be 7 units of time, but it could be reduced to 4 units of time if competent employees were arranged.

Many analysis methods, including the MRCPSP scheduling method, will inevitably misjudge the start time of activities in the process of use, resulting in unsatisfactory decoding quality. Therefore, for S-MRCPSP, this paper should explore an efficient and reasonable method for calculation.

2.3. Design of Genetic Algorithm

2.3.1. *Coding.* This paper studies the special multimode resource constrained project scheduling problem (S-

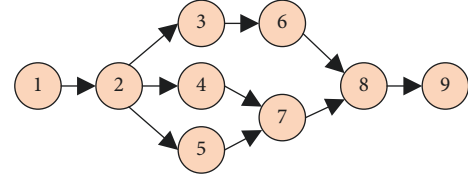


FIGURE 1: Project single code network diagram with 9 tasks.

1	2	3	4	5	6	7	8	9
0	1	0	0	0	0	0	0	0
0	0	1	1	1	0	0	0	0
0	0	0	0	0	1	0	0	0
0	0	0	0	0	0	1	0	0
0	0	0	0	0	0	0	1	0
0	0	0	0	0	0	0	0	1
0	0	0	0	0	0	0	0	0
0	0	0	0	0	0	0	0	0

FIGURE 2: Adjacency matrix.

MRCPSP). The research object is human resources considering the difference in competency level, which will not only further increase the scale of decision factors of traditional MRCPSP but also greatly increase the number of constraints. As a result, the problem model is more complex than before and the difficulty of solving the problem is further increased. In this paper, the coding method of double-linked list structure is adopted. Two linked lists represent the task linked list and execution mode linked list, respectively. If X is a double-linked chromosome.

$$X = \begin{bmatrix} L \\ W \end{bmatrix} = \begin{bmatrix} y_1 & y_2 & \cdots & y_Y \\ w_1 & w_2 & \cdots & w_{y_Y} \end{bmatrix}. \quad (14)$$

Among them, $L = (y_1, y_2, \dots, y_Y)$ is a task linked list, which is a permutation of all tasks satisfying the constraint of task compact-relation. $W = (w_1, w_2, \dots, w_{y_Y})$ is a pattern linked list, and represents the corresponding execution pattern vector of each task in the task linked list.

(1) *Generation of Task Linked List L.* There is always an established sequential priority relationship among various tasks. Unfeasible solutions may occur when tasks are organized randomly. In the algorithm, it is very important to scientifically and reasonably define the task coding method of priority relationship, which can be determined through the following process:

According to Figure 3, it can be seen clearly and intuitively that the most important step is to accurately lock qualified tasks, which refers to the tasks that have been completed for each immediate task.

Take the example described in Figure 3 as an example. The main function of vector $A[\cdot]$ is to safely and reliably preserve the formed encoding sort. In the beginning, $A[1] = 1$, there are very few qualified tasks, only one is task 2, at

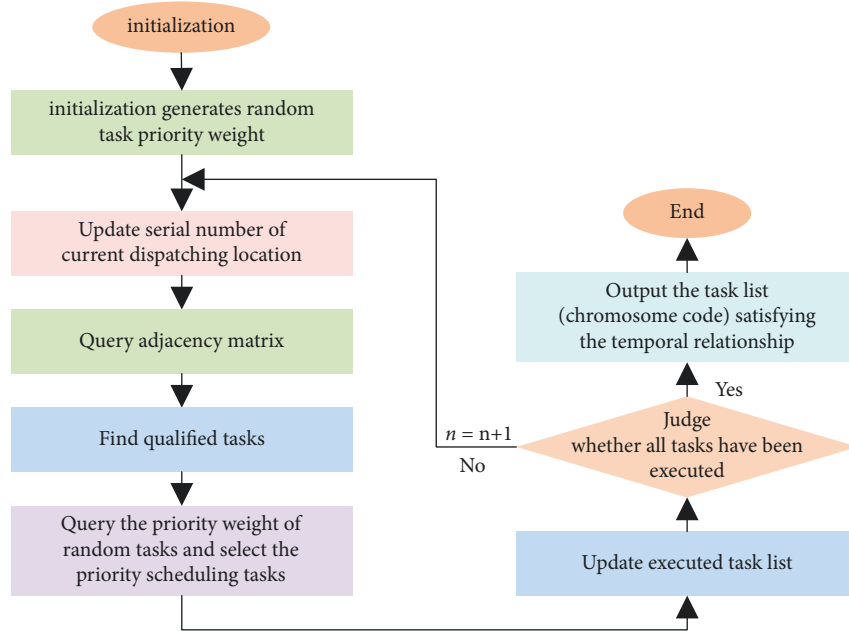


FIGURE 3: Task code generation process satisfying timing relation.

TABLE 2: List of randomly generated task priority values.

Task number	1	2	3	4	5	6	7	8	9
Priority value of the task	9	3	7	1	6	4	5	2	8

TABLE 3: Task coding satisfying timing relation.

Scheduling sequence number	1	2	3	4	5	6	7	8	9
Scheduled task number	1	2	3	5	6	4	7	8	9

which $A[2] = 2$. After combing and analyzing the adjacency matrix, it is found that qualified tasks are 3, 4, and 5, respectively, and all three of them are likely to become $A[3]$. As can be seen from Table 2, their priority values are 7, 1, and 6 in sequence. Of the above-given tasks, 3 has the highest priority, so $A[3] = 3$. Next, tasks 4, 5, and 6 compete for $A[4]$. Task 5 wins and gets $A[4] = 5$. Then, the following two procedures are followed:

- (a) The qualified task set is obtained by combining adjacency matrix b . Determine the task with the highest priority according to the random priority value and fix its position until each task is properly executed. The coding of tasks corresponding to Table 1 can be referred to as Table 3. If the priority value changes, the task coding scheme will definitely change, so the coding can reflect the potential encoding of the network graph.

It should be noted that the generated task linked list only satisfies the sequential priority relationship, without considering the resource constraints.

(2) *Generation of Schema Linked List W .* Pattern linked list W represents the feasible pattern vector corresponding to

each task in the task linked list. Pattern linked list W corresponds to each gene in the two linked lists of the task linked list L . The feasible mode corresponding to y_1 activity is w_1 , and w_1 can be any mode in the feasible mode set corresponding to y_1 activity. The generated schema linked list not only considers the number of people specified by the activity in the renewable resource constraint, and also considers the nonrenewable resource constraint.

2.3.2. Decoding. Schedule Generation Scheme (SGS) is required for all priority-based heuristics. SGS has a serial schedule generation mechanism (SSGS) and parallel schedule generation mechanism (PSGS). Scheduling plans for single-pattern resource-constrained item. Scheduling problems (SRCPSP) generated by PSGS based on any priority rules are nondelayed scheduling plans. The scheduling plan based on any priority rule and using SRCPSP generated by SSGS is an active scheduling plan, which not only reduces the search scope but also does not miss the optimal solution. When the execution mode of each activity is specified and the specified mode satisfies the nonupdatable resource constraint, MRCPSP degenerates into SRCPSP. Therefore, MRCPSP also satisfies the properties and theorems of SRCPSP. In view of this, this paper adopts the serial scheduling generation mechanism. When the task scheduling sequence and corresponding feasible mode are given, a feasible solution can be obtained by considering all renewable resource constraints when the serial scheduling generation mechanism is used for decoding.

2.3.3. Fitness Function. Both construction period and cost are cost indexes. The smaller the index value is, the better the solution is. However, the fitness function should be that the larger the fitness value is, the better the individual is.

Considering the disunity of the construction period and cost units, dimensionless processing should be carried out, so that the dimensionless index values are within the range of 0~1. Therefore, the fitness function designed is as follows:

$$CX = \omega \times N_S + (1 - \omega) \times C_S. \quad (15)$$

Here, ω is the weight coefficient of the construction period. T_S and C_S are the dimensionless index values of the total project construction period and total cost of individual projects, respectively. For dimensionless treatment, see formulas (11) and (12).

2.3.4. Select Operations. The selection operation is to select some individuals from the parent population and transfer them to the next generation population through a scientific and reasonable algorithm based on the evaluation of individual fitness. After comprehensive consideration of all aspects of the factors, this paper finally selected the current widely used roulette favoured by the industry. The mechanism is that there is a significant positive correlation between the possibility of individual selection and its fitness. If the population size is represented by t and the fitness of individual x is F_x , the probability of x being selected successfully can be calculated by the following formula:

$$U_x = \frac{F_x}{\sum_{x=1}^t F_x}. \quad (16)$$

2.3.5. Cross Operations. The single-point crossover operator introduced in literature [14] is intended to complete the crossover operation of chromosome task genes, where the possibility of crossover changes of mode genes is represented by U_c . Suppose the parent and the parent perform a series of crossovers to form two children, a son and a daughter. When an integer t is randomly formed between 1 and T , the task genes at the first t positions of the son inherit from the father, but the task genes at the last $t - t$ positions of $t + 1 \sim T$ inherit from the mother. For the existing tasks, this paper does not analyze them and ensures that the distribution of each task is consistent with that of the mother. The same is true for daughter genes. Literature [15] shows that the order of jobs in offspring individuals obtained based on crossover operator still conforms to the tight front tight back relationship. The crossover process is shown in Figure 4.

2.3.6. Mutation Operation. The mutation operator will carry out a series of standard and reasonable mutation operations on the model genes of chromosomes through scientific and reasonable methods. In this process, the task genes will not have any change. In this paper, the allelic mutation gene value at the mutation point is determined by a uniform mutation operator; that is, the model locus in each individual coding string is the possible mutation point. Loci for mutation operation were selected according to mutation probability U_w . Then, for each variant loci, a feasible pattern matching the uniform probability distribution was randomly selected from the feasible pattern set corresponding

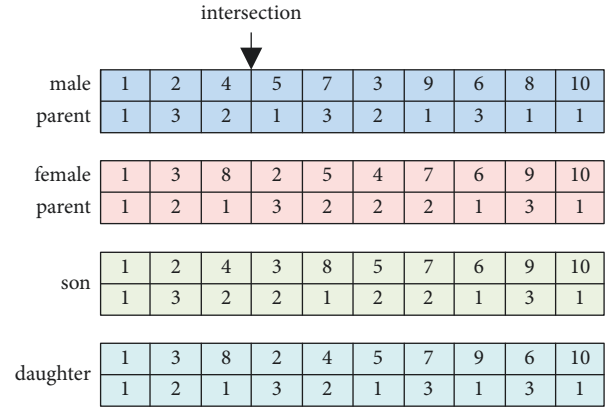


FIGURE 4: Point crossing.

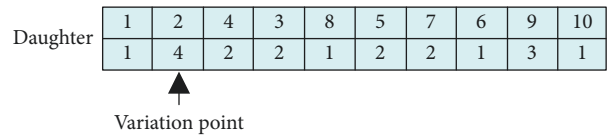


FIGURE 5: Mutation process.

to the loci to replace the original feasible mode. The mutation process is shown in Figure 5.

3. Experiment and Analysis

In order to verify the effectiveness of the algorithm in this paper, 10 jobs, 14 jobs, 18 Jobs, 30 Jobs, and 60 Jobs were selected to carry out numerical experiments, and compared with literature [16]. The numerical experiment was programmed in C# (Visual Studio 2017) language environment, and the test platform was Intel Core i5 4th processor, 2.40 GHz main frequency, and 4G memory. The results are shown in Tables 4 to 6. Here, AD, AF, and AC are the average objective function values obtained by this group of examples in this paper, literature [16] and literature [17], respectively. TD, TF, and TC are the average operation time, respectively. G1 and G2 are the differences between the objective function value obtained by the proposed algorithm and the algorithm in literature [16] and the optimal solution in literature [17], respectively. G is the gap between the algorithm in this paper and the algorithm in literature [16].

Tables 4 to 5, Table 6 show the results of small-scale calculation examples, with the size of 10 Jobs, 14 jobs, and 18 jobs, respectively, and each group contains 10 cases. As can be seen from the tables, when the number of jobs is 10 jobs and 14 jobs, the optimal solution obtained by the algorithm designed in this paper is basically equal to the optimal solution obtained in literature [17], while the results of the comparison algorithm are significantly different from the optimal solution, and the three algorithms are all in the same order of magnitude range in terms of solving time. When the number of jobs is 18, the optimal solution of the algorithm designed in this paper is only 1.5% compared with that obtained in literature [17], but the deviation of the comparison algorithm reaches 9.5%. However, the solution time

TABLE 4: 10 jobs experimental results.

Cases	AC	TC/s	AD	TD/s	G1/%	AF	TF/s	G2/%
1	134	0.306	135	0.663	0.87	137.0	0.297	2.51
2	116	0.645	116	0.89	0.05	117.2	0.395	1.20
3	155	0.731	155	0.603	0.05	155.0	0.292	0.16
4	130	0.362	130	0.394	0.05	130.8	0.215	0.73
5	178	0.651	178	0.917	0.05	185.1	0.395	4.33
6	143	0.779	143	0.901	0.05	143.0	0.368	0.05
7	121	0.474	121	0.612	0.05	123.0	0.231	1.88
8	170	0.664	170	0.769	0.05	170.0	0.321	0.05
9	166	1.034	166	0.995	0.05	176.2	0.431	6.67
10	118	0.542	118	0.58	0.11	125.3	0.236	5.05
Average						0.14		2.26

TABLE 5: 14 jobs experimental results.

Cases	AC	TC/s	AD	TD/s	G1/%	AF	TF/s	G2/%
1	152	0.571	152.0	0.443	0.05	152.5	0.105	0.26
2	141	0.266	142.0	0.605	0.05	146.5	0.152	3.35
3	143	3.714	148.2	1.408	0.77	146.8	0.558	2.18
4	207	1.175	207.3	0.348	0.14	214.1	0.085	3.03
5	110	2.231	110.9	1.876	0.73	116.7	0.65	0.35
6	157	0.742	157.1	0.402	0.05	165.8	0.108	1.12
7	115	0.376	115.1	0.402	0.05	119.5	0.103	3.18
8	169	2.485	169.6	0.625	0.33	171.5	0.127	1.06
9	167	1.012	167.2	0.486	0.11	168.9	0.109	0.05
10	174	0.725	174.1	0.415	0.05	175.3	0.058	0.02
Average						0.23		1.46

TABLE 6: 18 jobs experimental results.

Cases	AC	TC/s	AD	TD/s	G1/%	AF	TF/s	G2/%
1	181	26.655	191.8	1.401	0.59	205.0	0.272	11.40
2	138	90.517	150.3	1.895	1.68	170.6	0.526	14.14
3	167	4.852	171.8	3.569	2.22	191.1	1.243	6.89
4	151	4.212	161.5	1.208	4.69	184.4	0.273	13.75
5	244	4.128	253.5	0.688	0.05	277.5	0.138	8.14
6	116	4.342	129.2	2.476	2.12	135.8	1.206	7.68
7	175	4.019	176.6	0.583	0.73	203.2	0.127	8.66
8	172	45.201	175.7	1.275	2.13	201.4	0.453	9.48
9	115	40.417	135.4	2.405	0.69	141.3	0.937	12.61
10	110	56.062	142.8	2.217	0.10	144.4	0.665	2.25
Average						1.5		9.5

of the proposed algorithm is in the same order of magnitude as that of the comparison algorithm, which is far shorter than that of the literature [17]. Therefore, the following conclusions can be drawn: the genetic algorithm proposed in this paper can solve better results within a certain error range in small-scale examples.

In order to compare the advantages and disadvantages of the six algorithms, the solution results of algorithm 6 at different iterations were compared under the same setting of other parameters. In 2 different scales, 10 cases were taken, and the average value of each case under different iterations was recorded, and then the average value of 10 cases was taken. Figures 6 and 7 show the comparison of 6 different algorithms when the number of jobs is 30 jobs and 60 jobs.

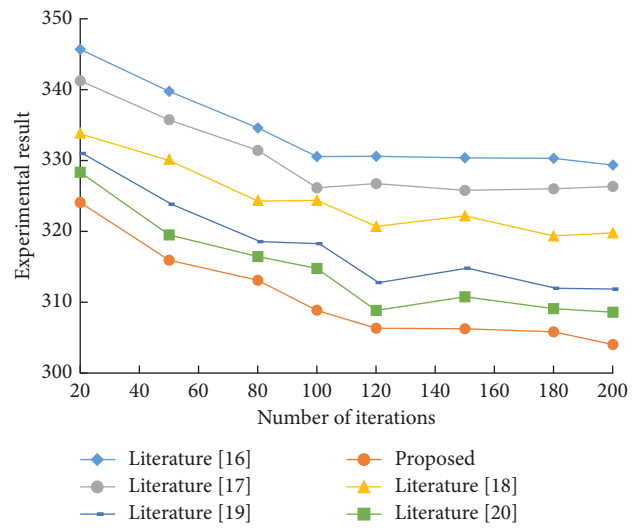


FIGURE 6: Comparison of experimental data of 30 Jobs.

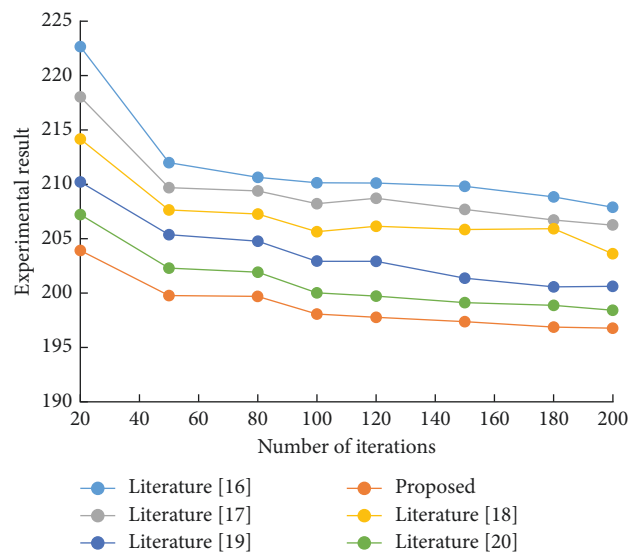


FIGURE 7: Comparison of experimental data of 60 jobs.

The abscissa is the number of iterations, and the ordinate is the average value of 10 calculation examples. As can be seen from the figure, with the increase of iteration times, the values of the six algorithms gradually decrease, and under

different iteration times, the algorithm designed in this paper is obviously superior to the other five comparison algorithms (literature [16], literature [17], literature [18], literature [19], and literature [20]).

4. Conclusion

In recent years, China's network information technology has developed rapidly. In the era of network marketing, in order to achieve sustainable development, the company not only needs to objectively consider its own actual development but also needs to build an efficient and orderly human resource management system. Only in this way, can the company comprehensively manage human resources and then achieve sustainable development. The latest research shows that the level of employee competency will have a profound impact on job performance. Based on MRCPS, the human resource scheduling problem of special "multimode" projects is discussed and analyzed comprehensively and deeply. In order to objectively and accurately evaluate the competency level of employees, this paper selects the index of employee time coefficient. The total project cost only emphasizes the material consumption generated during the development of R&D work, and the optimization target is the maximum comprehensive index value weighted by the total construction period and total cost. Because the original method is not perfect and rigorous, this paper decided to use a genetic algorithm to carry out single-objective optimization of the comprehensive index. The experimental results show that both small-scale model splitting and large-scale algorithm building have achieved good results. However, when using the model, portfolio model number increased obviously, both increased analysis difficulty, also prone to NP-hard phenomenon. Therefore, the genetic algorithm is used to analyze and deal with this problem still has its imperfections, the late should intensify their efforts to research and optimize the algorithm, or to find a more reasonable, more rigorous, more efficient algorithm.

Data Availability

The labeled data set used to support the findings of this study is available from the corresponding author upon request.

Conflicts of Interest

The authors declare that there are no conflicts of interest.

Acknowledgments

This work was supported by the Langfang Normal University.

References

- [1] C. Pellegrini, F. Rizzi, and M. Frey, "The role of sustainable human resource practices in influencing employee behavior for corporate sustainability," *Business Strategy and the Environment*, vol. 27, no. 8, pp. 1221–1232, 2018.
- [2] G. K. Stahl, C. J. Brewster, D. G. Collings, and A. Hajro, "Enhancing the role of human resource management in corporate sustainability and social responsibility: a multi-stakeholder, multidimensional approach to HRM," *Human Resource Management Review*, vol. 30, no. 3, Article ID 100708, 2020.
- [3] D. Vrontis, M. Christofi, V. Pereira, S. Tarba, A. Makrides, and E. Trichina, "Artificial intelligence, robotics, advanced technologies and human resource management: a systematic review," *International Journal of Human Resource Management*, vol. 33, no. 6, pp. 1237–1266, 2022.
- [4] E. Farndale, S. Horak, J. Phillips, and M. Beamond, "Facing complexity, crisis, and risk: o," *Thunderbird International Business Review*, vol. 61, no. 3, pp. 465–470, 2019.
- [5] B. E. Kaufman, "The real problem: the deadly combination of psychologisation, scientism, and normative promotionism takes strategic human resource management down a 30-year dead end," *Human Resource Management Journal*, vol. 30, no. 1, pp. 49–72, 2020.
- [6] A. A. Najafi, E. Merrikhi, and A. Shahsavari, "Project resource investment problem under progress payment model[J]," *Journal of Industrial and Systems Engineering*, vol. 11, no. 3, pp. 84–101, 2018.
- [7] Z. Zuo, Y. Li, J. Fu, and J. Wu, "Human resource scheduling model and algorithm with time windows and multi-skill constraints," *Mathematics*, vol. 7, no. 7, p. 598, 2019.
- [8] X. Zhu, R. Ruiz, S. Li, and X. Li, "An effective heuristic for project scheduling with resource availability cost," *European Journal of Operational Research*, vol. 257, no. 3, pp. 746–762, 2017.
- [9] S. Tanaka and K. Tierney, "Solving real-world sized container pre-marshalling problems with an iterative deepening branch-and-bound algorithm," *European Journal of Operational Research*, vol. 264, no. 1, pp. 165–180, 2018.
- [10] J. Behnamian, S. Memar Dezfooli, and H. Asgari, "A scatter search algorithm with a novel solution representation for flexible open shop scheduling: a multi-objective optimization," *The Journal of Supercomputing*, vol. 77, no. 11, Article ID 13138, 2021.
- [11] A. Delgoshaei, S. Esmaeili Hanjani, and A. Hossein Nasiri, "A genetic algorithm for scheduling multimode resource-constrained project problem in the presence of preemptive resources," *Journal of Project Management*, vol. 4, no. 3, pp. 195–212, 2019.
- [12] A. A. K. Taher and S. M. Kadhim, "Hybrid between genetic algorithm and artificial bee colony for key generation purpose," *Journal of Al-Qadisiyah for computer science and mathematics*, vol. 11, no. 4, pp. 37–46, 2019.
- [13] L. Garcia-Romero, J. Paredes-Arquiola, A. Solera, and E. Belda, "Optimization of the multi-start strategy of a direct-search algorithm for the calibration of rainfall-runoff models for water-resource assessment," *Water*, vol. 11, no. 9, p. 1876, 2019.
- [14] W. Zhu, L. I. U. Li, and L. Teng, "Multi-UAV reconnaissance task allocation for heterogeneous targets using an opposition-based genetic algorithm with double-chromosome encoding," *Chinese Journal of Aeronautics*, vol. 31, no. 2, pp. 339–350, 2018.
- [15] S. G. Varun Kumar and R. Panneerselvam, "A study of crossover operators for genetic algorithms to solve VRP and its variants and new sinusoidal motion crossover operator," *International Journal of Computational Intelligence Research*, vol. 13, no. 7, pp. 1717–1733, 2017.

- [16] A. C. Lossada, G. D. Hoke, L. B. Giambiagi et al., “Detrital thermochronology reveals major middle miocene exhumation of the eastern flank of the andes that predates the Pampean Flat slab (33°–33.5°S),” *Tectonics*, vol. 39, no. 4, Article ID e2019TC005764, 2020.
- [17] A. R. Pitombeira-Neto and B. D. A. Prata, “A metaheuristic algorithm for the one-dimensional cutting stock and scheduling problem with heterogeneous orders,” *Journal of Topology*, vol. 28, no. 1, pp. 178–192, 2020.
- [18] J. Sorribes, D. Celma, and E. Martínez-García, “Sustainable human resources management in crisis contexts: interaction of socially responsible labour practices for the wellbeing of employees,” *Corporate Social Responsibility and Environmental Management*, vol. 28, no. 2, pp. 936–952, 2021.
- [19] S. Berhil, H. Benlahmar, and N. Labani, “A review paper on artificial intelligence at the service of human resources management,” *Indonesian Journal of Electrical Engineering and Computer Science*, vol. 18, no. 1, p. 32, 2020.
- [20] P. Tambe, P. Cappelli, and V. Yakubovich, “Artificial intelligence in human resources management: challenges and a path forward,” *California Management Review*, vol. 61, no. 4, pp. 15–42, 2019.

Research Article

An Enhanced Triadic Color Scheme for Content-Based Image Retrieval

S. K. B. Sangeetha ¹, Sandeep Kumar Mathivanan,² Thanapal Pandi,² K. Arivu selvan,² Prabhu Jayopal,² and Gemmachis Teshite Dalu ³

¹Department of Computer Science and Engineering, SRM Institute of Science and Technology, Chennai, Tamilnadu, India

²School of Information Technology and Engineering, Vellore Institute of Technology, Vellore, Tamil Nadu, India

³Department of Software Engineering, College of Computing and Informatics, Haramaya University, POB 138, Dire Dawa, Ethiopia

Correspondence should be addressed to S. K. B. Sangeetha; skbsangeetha@gmail.com and Gemmachis Teshite Dalu; gemmachis.teshite@haramaya.edu.et

Received 19 June 2022; Revised 18 July 2022; Accepted 6 August 2022; Published 29 August 2022

Academic Editor: B. Sivakumar

Copyright © 2022 S. K. B. Sangeetha et al. This is an open access article distributed under the Creative Commons Attribution License, which permits unrestricted use, distribution, and reproduction in any medium, provided the original work is properly cited.

The complexity of multimedia content, particularly images, has risen dramatically in recent years, and millions of images are shared on social media every day. Finding or retrieving an appropriate image is becoming more difficult due to the increase in the volume of shared and archived multimedia data. Any image retrieval model must, at a bare minimum, locate and classify images that are visually related to the user's query. The vast majority of Internet search engines employ text algorithms that fetch images using captions as input. Even though there is a lot of study being done to increase the effectiveness of automatic image annotation, retrieval errors can occur due to differences in visual perception. Content-based image retrieval (CBIR) addresses the aforementioned issue because visual analysis of the content is included in the query image. On the other hand, feature extraction is significantly challenging because of semantic gap. This work proposes a strategy for effective retrieval in similarity images using the triadic color scheme RGB, YCbCr, and $L^*a^*b^*$ based on reranking. We want to increase image similarity and encourage more relevant reranking. As a result of the findings, it can be concluded that a triadic color scheme improves precision by 5% more dramatically than existing schemes and also efficiently improves retrieved results while reducing user effort.

1. Introduction

Recent developments in big data technology have produced a sizable number of image databases. A capable visual search tool is required for all of these image libraries. There are two methods for conducting a search. Keywords are used to annotate images in text-based image retrieval [1].

This approach has a number of drawbacks:

- (1) It is impossible to manually annotate large databases
- (2) The technique must be annotated by the end user, making it sensitive to human perception
- (3) Only one language is covered by these annotations

To address the above challenges with multimedia research, CBIR analyses large-scale images employing local and global features in digital image processing [2]. There are several ways in which this method differs from text-based image retrieval systems. The CBIR system's most crucial element is feature extraction [3]. Because color extraction is usually straightforward and retrieval performance is quite high, it is frequently used in CBIR systems [4]. There are yet to be published complete and accurate definition of form features. The Fourier descriptor, aspect ratio, and circularity are all common ways for acquiring geometric form information. Furthermore, three texture-description approaches are used: statistical, structural, and spectral methods [5, 6].

TABLE 1: Conventional methods comparison.

Reference	CBIR classifier	Method	Accuracy (%)
[17]	Random forest	Multikey image hashing	72
[18]	Support vector machine	Two-step strategy	81
[19]	Naive bayes	Statistical approach	65
[20]	K nearest neighbor	Discrete wavelet transform	68.7
[21]	Fuzzy rule	Discrete wavelet transform	84

Image processing applications including image compression, edge detection, and picture retrieval have all exploited wavelet features, a sort of texture. A technique for locating and eliminating pointless and unnecessary feature components is feature selection [7, 8]. Low temporal complexity and excellent system accuracy could be attained as a result. For a variety of applications, including face identification, data mining and pattern recognition, automatic speaker verification systems, and image processing applications [9], a number of feature selection algorithms have been developed. Finding similar images using visual cues including shape, color, texture, and edge detection is the primary objective of CBIR [10, 11]. The primary flaw is that images with low-level attributes may differ from the queried image in the user's perception of semantic locations. The major purpose of this research is to integrate color features in order to obtain images that are more similar. Color images can be represented as RGB or indexed images. The RGB information of an image is found using color moments. RGB, YCbCr, and $L^*a^*b^*$ are some of the color methods utilized for a color histogram. Color approaches employed in image processing are quite sensitive to these strategies [12].

The fundamental color scheme is YCbCr, which is expressed as one color brightness and two different colors in photos and movies. Brightness (luma), minus luma (B-Y), and red minus luma (R-Y) are all represented by the letters Y, Cb, and Cr, respectively [13]. Cb and Cr, two color-difference components, are used to hold color data. Differences between the blue and reference values are denoted by the letters Cb, while the differences between the red and reference values are denoted by the letters Cr [14]. The $L^*a^*b^*$ method for color space translation separates gray-scale data from color data like red, green, and blue [15, 16]. Table 1 shows the various conventional methods along with its performance metric.

$L^*a^*b^*$ has two main processes as follows:

- (1) The color channel's gray-scale information is more clearly separated. The character L^* denotes more gray-scale information. The characters a^* and b^* provide color information.
- (2) The $L^*a^*b^*$ generated by the Euclidean distance difference between colors is perceptually consistent.

The main contributions of the study are as follows:

- (1) To construct a triadic color scheme, and this is a mixture of low-level elements such as RGB, YCbCr, and $L^*a^*b^*$ and are defined as visual information content

- (2) We proposed a new framework that can be utilized with a variety of primary color approaches to capture and classify integrated heterogeneous image data.

2. System Model

The proposed method is hybrid features extracted from an individual RGB, YCbCr, and $L^*a^*b^*$. To decrease the significant feature vector length of a recommended descriptor, the hybrid features were extracted from color and use gray level and color information from a color map to compute numerous color properties. A color histogram is made using RGB, YCbCr, and $L^*a^*b^*$, among other digital color approaches. These tactics have a very high sensitivity of color recognition cells in human visual information. RGB to YCbCr and RGB to $L^*a^*b^*$ conversions are used in digital picture processing. For RGB images of type unit 8 and unit 16, the range of values is [0, 255] and [0, 65535]. We present a set of integrated color attributes in this paper that can be used to generate more relevant images. Feature extraction methods identify the most important features and simplify image retrieval computations. The combined color channel includes RGB, YCbCr, and $L^*a^*b^*$ features, which are based on K-means classification and then reranking features. Certain images have greater color traits, while others have more sensitive image features. The RGB, YCbCr, $L^*a^*b^*$, and optimal color attributes are integrated to make image retrieval easier.

In order to increase image retrieval rate and simplify computation of image retrieval methods, we conducted a number of analyses and comparisons on integrated color information. By deriving ideal combination features from original features, the retrieval rate is enhanced. RGB, YCbCr, and $L^*a^*b^*$ are triadic color schemes that use gray level and color information from a color map to compute numerous color properties. Our goal is to make reranking picture results more relevant by maximizing image retrieval of mixed color features. The proposed color algorithms can be applied to medical imaging, face recognition, and form matching, to name a few. Figure 1 depicts the framework for combined color approaches.

2.1. Feature Extraction. Extraction of visual features to a considerable extent in order to improve categorization is known as feature extraction. The CBIR uses a number of different feature extraction approaches. Our analysis is based on a mix of color and frequency prominent properties extracted from the input images.

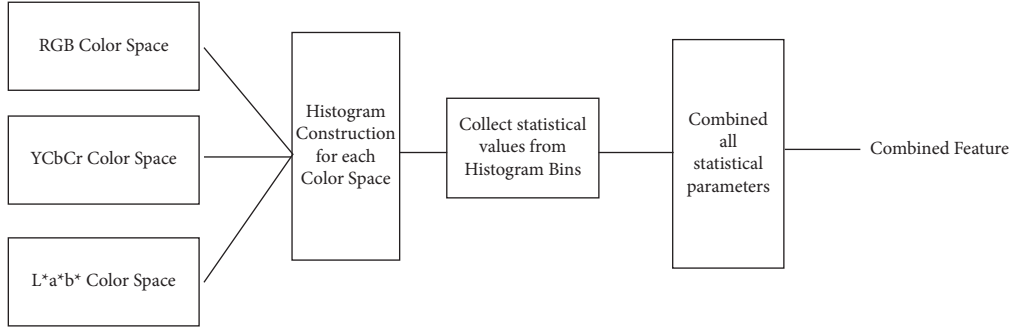


FIGURE 1: Triadic combined color framework.

2.2. Procedure

2.2.1. *RGB Color Space.* The RGB color model is additive; therefore, the following can be used:

- (1) Magenta = red + blue
- (2) Red plus green = yellow
- (3) Cyan is made up of two colors: blue and green

Color auto-correlogram features are the likelihood of color Q_i pixels in a query image, and they are calculated in various sections of the image. It locates spatial information, which is then utilized to include color and histogram data. The auto-correlogram of image I with distance d for color Q_i is defined as

$$\gamma_{Q_i}^d(I) = X_r[|X_1 - X_2| = d, |X_2 \in IQ_i, X_1 \in IQ_i|]. \quad (1)$$

Equation (1) shows the autocorrelation of color adjusted fluctuation with distance space information. In the auto-correlogram, color information and spatial information are integrated. In the same way, each pixel in the image might travel through all of its neighbors. The computation complexity is calculated as

$$O(d^* n^2), \quad (2)$$

where n is the number of neighbor pixels, and d is defined as pixel distance.

2.3. *YCbCr Color Space.* The basic color approach is YCbCr, which is included in images and videos and is expressed as one color luminance and two color-difference signals. The letters Y, Cb, and Cr stand for brightness (luma), minus luma (B-Y), and red minus luma (R-Y). Two color components, Cb and Cr, are used to store color information. Cb indicates the difference between the blue and the reference value, while Cr indicates the difference between the red and the reference value.

$$Y = 16 + 65.74R/256 + 129.06G/256 + 25.06B/256,$$

$$Cb = 128 + \frac{37.95R}{256} - \frac{74.49G}{256} + \frac{112.44B}{256}, \quad (3)$$

$$Cr = 128 + \frac{112.44R}{256} - \frac{94.15G}{256} + \frac{18.29B}{256}.$$

2.4. *L*a*b* Color Space.* Gray-scale information is represented using the $L^*a^*b^*$ approach. More gray-scale information is indicated by the letter L^* . Both a^* and b^* are used to indicate color information. The $L^*a^*b^*$ formula is dubbed perceptually uniform since it is designed by the Euclidean distance difference between colors:

$$\begin{aligned} L^* &= 116 \left(\frac{R}{R_n} \right)^{1/3} - 16, \text{ for } \frac{R}{R_n} > 0.009, \\ L^* &= 903.3 \left(\frac{R}{R_n} \right)^{1/3}, \text{ for } \frac{R}{R_n} > 0009, \\ a^* &= 500 \left(f \left(\frac{S}{S_n} \right) - f \left(\frac{R}{R_n} \right) \right), \\ b^* &= 200 \left(f \left(\frac{S}{S_n} \right) - f \left(\frac{T}{T_n} \right) \right). \end{aligned} \quad (4)$$

Color feature extraction and concatenation were conducted on each of the original color image channels, such as the R, G, and B channels. RGB, YCbCr, and $L^*a^*b^*$ are applied to the color image channels. Each channel's distance is calculated separately, and the best values are used. To match a completely RGB, YCbCr, and $L^*a^*b^*$ image, the Euclidean distance is employed. This method is applied to all color-characteristics channels. Single feature extraction does not provide optimal performance, which is one of the main reasons for missing the proper feature values. The combined RGB, YCbCr, and $L^*a^*b^*$ three channel characteristics are a great compromise for long-range tasks because they are exceptionally fast to retrieve.

3. Ranking Procedure and Metrics

3.1. *Distance Metrics.* There are two points, q and t , in the Euclidean distance. The database images are identified by the letters t and q , respectively. At points $t = (t_1, t_2, t_3, t_4, t_n)$, $q = (q_1, q_2, q_3, q_4, \dots, q_n)$, measure the Euclidean distance. The reranking algorithm is used after the Euclidean distance.

4. Experimental Evaluation and Analysis

CBIR image datasets include the Corel Collection, Wang Collection, ZuBuD, Coil-100, UW, INRIA Holiday, DP challenge, and Google Flickr, to name a few. Corel databases

- (1) Choose the most important inquiry images
- (2) The input image is in RGB color space
- (3) Detection of important objects
- (4) Utilize the segmentation methods
- (5) Look for the detected object (R , G , and B)
- (6) Calculate the correlogram for each RGB-based color feature extraction frame using (1)
- (7) Apply YCbCr techniques. For each YCbCr-based color feature extraction image channel, calculate the mean and standard deviation
- (8) Use the $L^*a^*b^*$ methods
- (9) Construct the final feature vector (auto-correlogram, $L^*a^*b^*$ for color moments and YCbCr for color moments) that will be used to represent the image with numerical values
- (10) Utilize the C-means algorithm to group the database's image content
- (11) Using Euclidean Distance, calculate the distance between the input image and each cluster's centroid, and then apply reranking methods to find the shortest distance
- (12) Returns the top n images

ALGORITHM 1: Triadic color procedure.



FIGURE 2: Top most images retrieved.

were used in most of the input. The experimental databases used are listed in Table 2 and are taken from Kaggle website. The performance of the proposed technique is measured in terms of precision, recall, and accuracy. When compared to other similar color approaches that are already in use, our combined color feature approach outperforms them.

Color images are used to populate entire databases. Humans, animals, flowers, food, and other objects are included in the database. WANG Datasets, Holidays Datasets, and other CBIR approaches rely heavily on them. When compared to several database images, the retrieval result was high. Over 50 image query tests are put to the test using the approaches we have proposed. These tests assist us in determining the outcome and level of achievement. Finally, we used 80% datasets for training and 20% datasets for testing in our Corel database experiment.

4.1. Performance Analysis. Three important metrics are analyzed for performance evaluation. The measure values where its efficiency and accuracy are evaluated over the Corel Database using precision (Pr), recall (Re), and F -score (Fs) using equations (5) to (7):

$$\text{Precision} = \frac{\text{Relevant images count}}{\text{Total images count}}, \quad (5)$$

$$\text{Recall} = \frac{\text{Relevant images fetched}}{\text{Total relevant images}}, \quad (6)$$

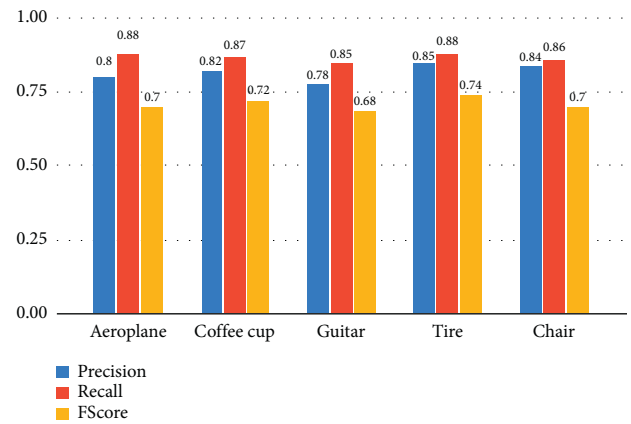


FIGURE 3: Image-comparison analysis.

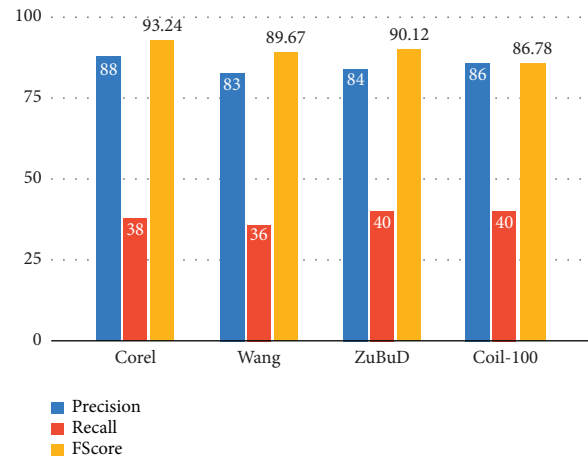


FIGURE 4: Dataset-comparison analysis.

$$F = \frac{2PR}{P + R} = \frac{2}{(1/R) + (1/P)}, \quad (7)$$

The proposed method's overall performance evaluation has shown to be satisfactory. Figure 2 displays the outcomes of finding the top images. The triadic color method, also

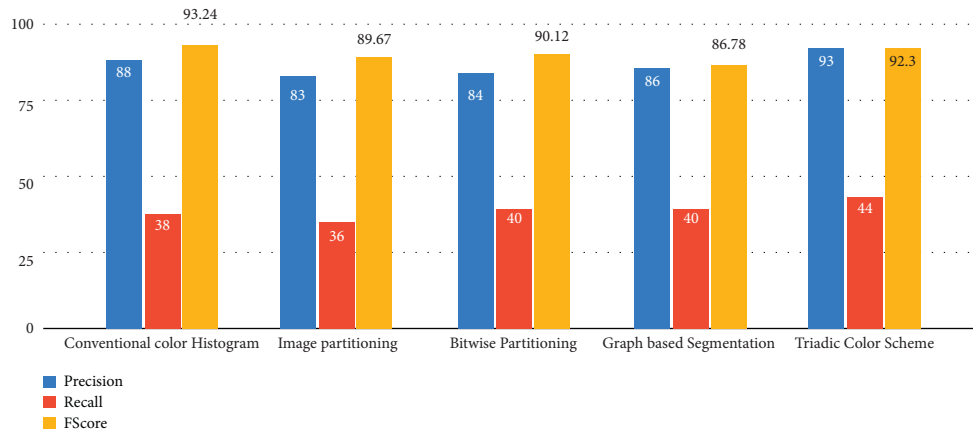


FIGURE 5: Existing schemes vs proposed scheme-comparison analysis.

TABLE 2: Datasets.

Database	No of Images	Test Image size
Corel	10000	200 * 140
Wang	1000	256 * 256
ZuBuD	1000	400 * 400
Coil-100	500	192 * 192
Holiday	1200	640 * 480

known as the hybrid method, explains how to get an upgraded top comparable image in the right order. Figure 3 depicts an image performance metric comparison, whereas Figure 4 depicts a dataset performance metric comparison. When compared to a current method, the suggested method significantly increases the average value of the performance metrics, as shown in Figure 5.

From Figure 3, it can be observed that the tire image is recognized with 85% accuracy which is higher than other images. Guitar is the least identified image with 78% accuracy. Chair and tire recognizing accuracy is almost the maximum difference by 1%. *F*-score for airplane and chair equals 70%. The comparison analysis for various datasets is depicted in Figure 4. The accuracy of the Corel Dataset is 88% in comparison with other datasets. Coil-100 dataset gives the lowest *F*-score 86% which is 7–8% lower than the Corel dataset. From Figure 5, it is shown that image partitioning has the lowest accuracy of 83% and highest accuracy of 93% in comparison with other methods.

5. Conclusion

In this study, a novel model of combined color features is presented that computes distinct color features from color information with a limited number of chosen pixels, making it computationally appealing. The suggested method performed better than earlier detectors and was also compared to other color-characteristics techniques, such as RGB, YCbCr, and $L^*a^*b^*$, which are less noise-sensitive and result in more comparable images. The Corel Dataset was used to test this method, and the results showed that most of the images had issues. The results of the evaluation revealed that

the suggested triadic color features method outperforms the existing method in terms of accuracy.

Data Availability

The article contains the data that were utilized to support the study's findings.

Conflicts of Interest

The authors declare that they have no conflicts of interest.

References

- [1] O. I. Khalaf, K. A. Ogudo, and S. K. B. Sangeetha, "Design of Graph-Based Layered Learning-Driven Model for Anomaly Detection in Distributed Cloud IoT Network," *Mobile Information Systems*, 2022.
- [2] P. Srivastava and A. Khare, "Integration of wavelet transform, Local Binary Patterns and moments for content-based image retrieval," *Journal of Visual Communication and Image Representation*, vol. 42, pp. 78–103, 2017.
- [3] C.-H. Lin, R.-T. Chen, and Y.-K. Chan, "A smart content-based image retrieval system based on color and texture feature," *Image and Vision Computing*, vol. 27, no. 6, pp. 658–665, 2009.
- [4] K. T. Ahmed, S. Ummesafi, and A. Iqbal, "Content based image retrieval using image features information fusion," *Information Fusion*, vol. 51, pp. 76–99, 2019.
- [5] A. K. Tiwari, V. Kanhangad, and R. B. Pachori, "Histogram refinement for texture descriptor based image retrieval," *Signal Processing: Image Communication*, vol. 53, pp. 73–85, 2017.
- [6] L. K. Pavithra and T. S. Sharmila, "An efficient framework for image retrieval using color, texture and edge features," *Computers & Electrical Engineering*, vol. 70, pp. 580–593, 2018.
- [7] C. Singh, E. Walia, and K. P. Kaur, "Color texture description with novel local binary patterns for effective image retrieval," *Pattern Recognition*, vol. 76, pp. 50–68, 2018.
- [8] D. Giveki, M. A. Soltanshahi, and G. A. Montazer, "A new image feature descriptor for content based image retrieval using scale invariant feature transform and local derivative pattern," *Optik*, vol. 131, pp. 242–254, 2017.

- [9] M. I. Thusnavis Bella and A. Vasuki, "An efficient image retrieval framework using fused information feature," *Computers & Electrical Engineering*, vol. 75, pp. 46–60, 2019.
- [10] G.-H. Liu and J.-Y. Yang, "Content-based image retrieval using color difference histogram," *Pattern Recognition*, vol. 46, no. 1, pp. 188–198, 2013.
- [11] C. Singh and K. Preet Kaur, "A fast and efficient image retrieval system based on color and texture features," *Journal of Visual Communication and Image Representation*, vol. 41, pp. 225–238, 2016.
- [12] J. Pradhan, S. Kumar, A. K. Pal, and H. Banka, "A hierarchical CBIR framework using adaptive tetrolet transform and novel histograms from color and shape features," *Digital Signal Processing*, vol. 82, pp. 258–281, 2018.
- [13] S. K. B. Sangeetha, R. Dhaya, D. T. Shah, R. Dharanidharan, and K. P. S. Reddy, "An empirical analysis of machine learning frameworks for digital pathology in medical science Journal of Physics: Conference," *Journal of Physics: Conference Series*, vol. 1767, no. 1, Article ID 012031, 2021, February.
- [14] J. Yue, Z. Li, L. Liu, and Z. Fu, "Content-based image retrieval using color and texture fused features," *Mathematical and Computer Modelling*, vol. 54, no. 3-4, pp. 1121–1127, 2011.
- [15] N. Shrivastava and V. Tyagi, "An efficient technique for retrieval of color images in large databases," *Computers & Electrical Engineering*, vol. 46, pp. 314–327, 2015.
- [16] Z. Tang, L. Huang, X. Zhang, and H. Lao, "Robust image hashing based on color vector angle and Canny operator," *AEU - International Journal of Electronics and Communications*, vol. 70, no. 6, pp. 833–841, 2016.
- [17] F. Sabahi, M. Omair Ahmad, and M. N. S. Swamy, "Perceptual image hashing using random forest for content-based image retrieval," in *Proceedings of the 2018 16th IEEE International New Circuits and Systems Conference*, pp. 348–351, Montreal, QC, Canada, June 2018.
- [18] K. Sugamya, S. Pabboju, and A. V. Babu, "A CBIR classification using support vector machines," in *Proceedings of the 2016 International Conference on Advances in Human Machine Interaction*, pp. 1–6, Doddaallapur Bangalore India, March 2016.
- [19] M. Kaur and S. Dhingra, "Comparative analysis of image classification techniques using statistical features in CBIR systems," in *Proceedings of the 2017 International Conference on I-SMAC (IoT in Social, Mobile, Analytics and Cloud) (I-SMAC)*, pp. 265–270, Palladam, India, February 2017.
- [20] K. S. Mardi, V. C. Mawardi, and N. J. Perdana, "KNN classification for CBIR with color moments, connected regions, discrete wavelet transform," in *Proceedings of the 2019 International Conference on Electrical Electronics and Information Engineering (ICEEIE)*, pp. 238–243, Denpasar, Indonesia, October 2019.
- [21] D. Yuvaraj, M. Sivaram, B. Karthikeyan, and J. Abdulazeez, "Shape, color and texture based cbir system using fuzzy logic classifier," *Computers, Materials & Continua*, vol. 59, no. 3, pp. 729–739, 2019.

Retraction

Retracted: Analysis of Financial Management Target Architecture Based on ISM Model

Mathematical Problems in Engineering

Received 8 August 2023; Accepted 8 August 2023; Published 9 August 2023

Copyright © 2023 Mathematical Problems in Engineering. This is an open access article distributed under the Creative Commons Attribution License, which permits unrestricted use, distribution, and reproduction in any medium, provided the original work is properly cited.

This article has been retracted by Hindawi following an investigation undertaken by the publisher [1]. This investigation has uncovered evidence of one or more of the following indicators of systematic manipulation of the publication process:

- (1) Discrepancies in scope
- (2) Discrepancies in the description of the research reported
- (3) Discrepancies between the availability of data and the research described
- (4) Inappropriate citations
- (5) Incoherent, meaningless and/or irrelevant content included in the article
- (6) Peer-review manipulation

The presence of these indicators undermines our confidence in the integrity of the article's content and we cannot, therefore, vouch for its reliability. Please note that this notice is intended solely to alert readers that the content of this article is unreliable. We have not investigated whether authors were aware of or involved in the systematic manipulation of the publication process.

Wiley and Hindawi regrets that the usual quality checks did not identify these issues before publication and have since put additional measures in place to safeguard research integrity.

We wish to credit our own Research Integrity and Research Publishing teams and anonymous and named external researchers and research integrity experts for contributing to this investigation.

The corresponding author, as the representative of all authors, has been given the opportunity to register their agreement or disagreement to this retraction. We have kept a record of any response received.

References

- [1] Y. Bi, "Analysis of Financial Management Target Architecture Based on ISM Model," *Mathematical Problems in Engineering*, vol. 2022, Article ID 3416671, 8 pages, 2022.

Research Article

Analysis of Financial Management Target Architecture Based on ISM Model

Yulin Bi 

Catholic University, Daegu 42708, Republic of Korea

Correspondence should be addressed to Yulin Bi; 2020020541@stu.cdut.edu.cn

Received 15 July 2022; Accepted 5 August 2022; Published 29 August 2022

Academic Editor: Hengchang Jing

Copyright © 2022 Yulin Bi. This is an open access article distributed under the Creative Commons Attribution License, which permits unrestricted use, distribution, and reproduction in any medium, provided the original work is properly cited.

In order to better construct the financial management standard distribution architecture, this paper proposes a financial management target architecture based on the ISM model. By discussing the stability, periodicity, and hierarchy of enterprise financial management objectives, this paper describes the system structure of enterprise financial management objectives by using the ISM model method of system engineering and establishes a five-level hierarchical structure model of financial management objective system. In this paper, the ISM algorithm is improved, two algorithms are proposed and their root mean square error is compared and analyzed. The experimental results show that the root mean square error of the EWISM algorithm and ETISM algorithm is significantly smaller than that of the traditional ism algorithm when the signal-to-noise ratio is 5–20db. *Conclusion.* By analyzing the architecture of financial management objectives based on the ISM model and improving the ISM algorithm, it can provide a better reference for enterprises to determine financial management objectives.

1. Introduction

Financial management is a part of enterprise management, and it is the management work related to the acquisition and effective use of funds; its goal is the desired result of the system. Different goals can be determined according to the problems to be solved and studied by different systems [1]. Financial management objectives are the desired results of financial management activities of enterprises and the basic standard to evaluate whether the financial management work of enterprises is reasonable. The construction of an enterprise financial management objective system is directly related to the survival and development of enterprises [2]. Establishing reasonable financial management objectives is of great significance both in theory and practice. From the perspective of major countries in the world, there are obvious differences in financial management objectives. In Japan, shareholders, creditors, employees, and the government all play an important role in enterprise financial decision-making. Financial decision-making must take into account the interests of all parties [3]. This makes the pursuit of maximizing enterprise value a reasonable goal of financial

management. The maximization of enterprise value means to maximize the total value of the enterprise on the basis of ensuring the long-term and stable development of the enterprise by adopting the optimal financial policies and taking full account of the time value of funds and the relationship between risk and reward.

In 1973, a conceptual interpretive structure model, namely, the ISM model, was developed to analyze the problems related to complex socio-economic systems [4]. The first task is to collect the relevant factors that affect the problem in as much detail as possible, number them and assign the influence degree to the value. Secondly, the numerical values are processed with the help of mathematical calculation tools. According to the calculation results, these influencing factors are divided into primary, secondary, tertiary, and other categories, and then the reachability matrix is established. On the basis of the reachability matrix, a multilevel structure model is constructed. This structure model can more intuitively see what factors have a greater impact on the cost from a quantitative point of view, so as to facilitate the project management to implement management more effectively.

Therefore, by discussing the stability, phased and hierarchical characteristics of financial management objectives, the ISM model method of system engineering is used to describe the system structure of enterprise financial management objectives, and a five-level hierarchical structure model of financial management objective system is established [5]. It aims to provide a reference for enterprises to determine financial management objectives.

2. Literature Review

Article 5 of China's "company law" stipulates that the goal of the company is to maintain and increase the value of the enterprise. From the day when the enterprise was born, it was destined to be an organization for the purpose of the operation. The financial management objective is the starting point of enterprise financial management activities, and financial management must meet the company's business objectives. From the perspective of different business objectives of the company, there are two major financial management models in the world, namely, the financial management model based on the developed market represented by the United States and the financial management model based on the developed banking industry represented by Japan [6]. Some people have made a special comparison between the two financial management modes, and the comparison results are shown in Table 1.

It can be seen from Table 1 that the roles of stakeholders in the United States and Japan in corporate financial management are not exactly the same. In the United States, shareholders play a leading role in financial decision-making, while employees, creditors, and the government play a very small role, which makes American financial managers attach great importance to the interests of shareholders and take maximizing shareholders' wealth as the goal of financial management. The shareholders' wealth is mainly reflected in the rise of stock price. Therefore, the goal of financial management is transformed into the highest stock price. The financial decisions of American enterprises are all based on the stock price. In Japan, shareholders, creditors, employees, and the government all play an important role in the financial decision-making of enterprises. Financial decision-making must take into account the interests of all parties. This makes the pursuit of maximizing enterprise value a reasonable goal of financial management. The maximization of enterprise value means to maximize the total value of the enterprise on the basis of ensuring the long-term and stable development of the enterprise by adopting the optimal financial policy, fully considering the time value of the capital and the relationship between risk and reward [7].

The goal of financial management is to require the financial management activities of enterprises to fully consider the needs of long-term development in the future, that is, the sustainable development of finance, on the premise of meeting the current stable production and operation of enterprises. The author believes that the general goal of modern enterprise financial management should be the sustainable development of enterprise finance, and the

comprehensive development of enterprise financial status, enterprise financial achievement, and enterprise capital accumulation [8]. These three aspects are progressive and guided by the general goal of sustainable development. According to the requirements of this general goal, enterprises should not only have a good financial situation, the basis for enterprise survival but also obtain satisfactory financial results, the source of enterprise survival and development but also maintain an appropriate level of accumulation. The guarantee for the sustainable development of enterprises is only by maintaining the unity and coordination of the three can enterprises obtain the realistic conditions for survival and development.

The first task of the ISM model is to collect the relevant factors affecting the problem in detail as much as possible, number and assign the influence degree to the value and then deal with the value with the help of mathematical calculation tools. According to the calculation results, these influencing factors are divided into primary, secondary, and tertiary categories, and then the reachability matrix is established. On the basis of the reachability matrix, a multilevel structure model is constructed. This structure model can more intuitively see the factors that have a greater impact on the cost from a quantitative point of view, so as to facilitate the project management to implement management more effectively [9].

Based on the above-given research, this paper analyzes the financial management objective system structure based on the ISM model, discusses the stability, phased and hierarchical characteristics of enterprise financial management objectives, describes the enterprise financial management objective system structure by using the ISM model method of system engineering, and establishes a five-level hierarchical structure model of the financial management objective system, in order to provide a reference for enterprises to determine the financial management objectives.

3. Research Methods

3.1. Introduction to Ism Method. ISM (interpretative structural modeling) is the abbreviation of an interpretative structural model. It was developed by Warfield in the United States in 1973 as a method to analyze problems related to complex socio-economic systems [10]. Its characteristic is that the complex system is decomposed into several sub-systems (elements). With the help of people's practical experience and knowledge and computer, the system is finally constructed into a multilevel hierarchical structure model.

A large number of application practices show that the ism method is not only applicable to the analysis of social and economic problems but also applicable to the study and understanding of various problems with complex relationships and has a wide range of applications.

Typical steps of the ISM method are as follows:

- (1) Organize the Team to Implement ISM. The number of team members is generally about 10. They have a

TABLE 1: Comparison of financial management modes between the United States and Japan.

	U.S.A	Japan
Owner	More individual shareholders	Most shareholders are legal persons, with relatively concentrated equity
Workers	Unstable relationship between employees and enterprises	Stable relationship between employees and enterprises
Creditor	Creditor and enterprise are contractual relations	Firm relationship between enterprises and banks
Government	Less government intervention	More government intervention

good understanding of the problems to be solved and can express their mature views.

- (2) Select the Elements that Make Up the System. The team members wrote down the relevant issues they thought of on paper and then discussed, studied, and proposed the scheme of system elements based on it. After repeated discussion, a more reasonable scheme of system elements was formed and based on this, a detailed list of elements was prepared for future use.
- (3) According to the list of elements, the conceptual model is made, and the adjacency matrix and reachability matrix are established.
- (4) After analyzing the reachability matrix, the structure model is established.
- (5) According to the structural model, the interpretive structural model is established.

3.2. Specific Implementation of ISM Method. An interpretive structure model of financial management objectives is established by the ISM method [11].

We selected 9 representative financial management objectives from the relevant literature from 1988 to 2002, as follows.

S1-profit maximization; S2-maximization of shareholders' wealth; S3-maximization of enterprise value; S4-maximization of stakeholders' interests; S5-maximization of cash flow; S6-capital cost minimization; S7-capital structure optimization; S8-maximization of earnings per share; S9-maximize the profit margin of equity capital. We have invited professionals who are familiar with financial management and ISM to conduct a logical analysis on the above-given system elements and reach an agreement. The results can be expressed in a square diagram, as shown in Figure 1.

∨: the upper elements have an influence on the lower elements; ∧: inferior elements have an influence on superior elements;

× : The upper and lower elements influence each other.

The elements are arranged in the box in order according to the level division and then find out the relationship between the elements at all levels in order to obtain the financial management objective system structure model shown in Figure 2 [12]. Fill in Figure 2 with the names of system elements to obtain the explanatory structure model of the enterprise financial management objective system, as shown in Figure 3.

∨	∨	∧	∧	∨			∨	S1
	∧				∨	∨		S2
					∨			S3
∧	∧	∧	∧	∧				S4
								S5
∨	∨	×						S6
∨	∨							S7
								S8
								S9

FIGURE 1: System element grid.

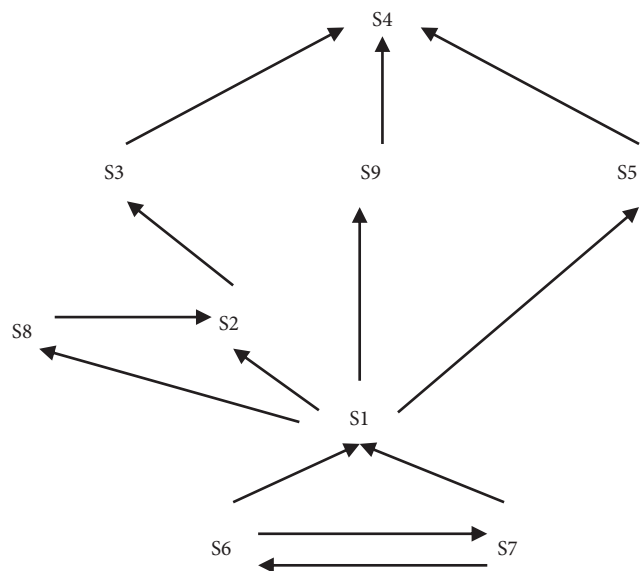


FIGURE 2: Financial management objective system structure model.

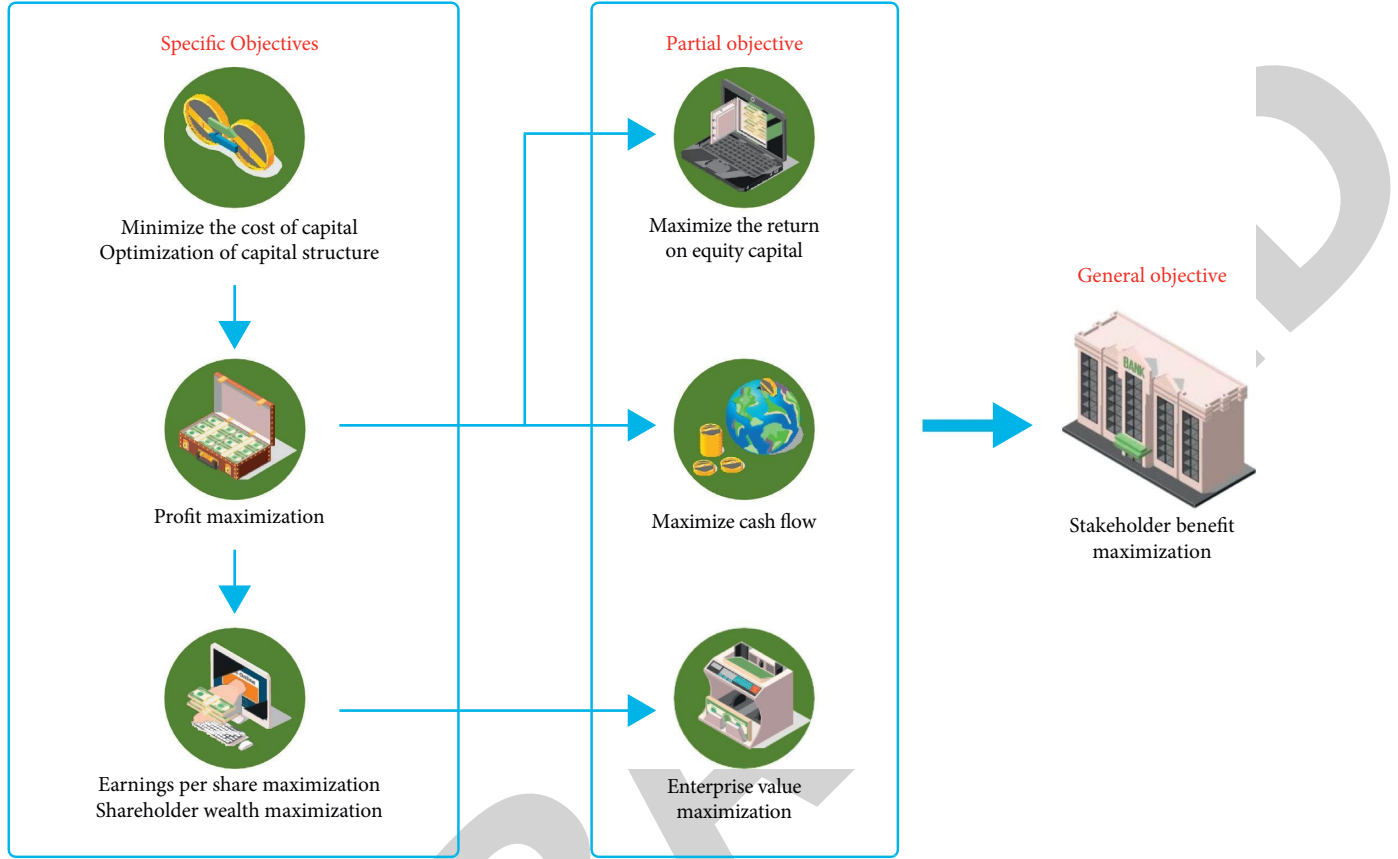


FIGURE 3: Explanatory structure model of enterprise financial management objective system.

3.3. ISM Model Algorithm Analysis

3.3.1. ISM Traditional Algorithm. The traditional ism algorithm decomposes the broadband signal into J narrow-band components in the frequency domain, directly decomposes the array output covariance matrix of each sub-band to obtain the orthogonal signal subspace and noise subspace, and then uses the music algorithm for spectrum estimation [13–15]. In order to estimate the covariance matrix on each narrow band, it is necessary to convert the time domain observation signal to the frequency-domain [16]. Firstly, the signals collected in the observation time are divided into k segments, then the time length of each segment is $T_d = T_0/K$, and then each segment is DFT to obtain K groups of uncorrelated narrow-band frequency-domain components. In broadband processing, K is called frequency-domain snapshots, so K snapshots can be obtained, which is recorded as $X_k(f_j), k = 1, 2, \dots, K, f = 1, 2, \dots, J$. The aim of the ISM algorithm is to estimate the azimuth of multiple targets from these K frequency-domain snapshots. For space ideal white noise, and the noise power is σ^2 , the corresponding covariance matrix at frequency f_j can be expressed as follows:

$$\begin{aligned} R_x(f_j) &= E[XX^H] = AE[SS^H]A^H + E[NN^H] \\ &= AR_sH^H + R_N = AR_sA^H + \sigma^2I, \end{aligned} \quad (1)$$

where: R_s and R_N are signal covariance matrix and noise covariance matrix, respectively. Perform feature decomposition for them, including

$$R_x(f_j) = U \Sigma U^H, \quad (2)$$

where U is the eigenvector matrix, and the diagonal matrix Σ composed of eigenvalues is as follows:

$$\Sigma = \begin{bmatrix} \lambda_1 & & & \\ & \lambda_2 & & \\ & & \ddots & \\ & & & \lambda_M \end{bmatrix}. \quad (3)$$

The eigenvalues in the above formula satisfy the following relationship:

$$\lambda_1 \geq \lambda_2 \geq \lambda_p > \lambda_{p+1} = \dots = \lambda_M = \sigma^2. \quad (4)$$

3.3.2. ISM Improved Algorithm. Energy weighted algorithm (EWISM).

The traditional ism algorithm is to process the equal weight average method of DOA estimates of J frequency points, that is,

$$P = \frac{1}{J} \sum_{j=1}^J P_j. \quad (5)$$

This method ignores the difference of signal energy of each sub-band and considers that the signal-to-noise ratio of each sub-band is consistent, resulting in poor DOA estimation performance [17]. EWISM algorithm is based on the maximum ratio combining the technology of diversity combining technology to weight the spectral value of the spatial estimated value of each sub-band. The sub-band with large energy is given a larger weight, and the sub-band with small energy is given a smaller weight.

$$P = \sum_{j=1}^J \lambda_j P_j = \sum_{j=1}^J \frac{W_j}{W_1 + W_2 + \dots + W_J} P_j. \quad (6)$$

Formula (6) shows that the greater the proportion of the energy in a sub-band to the total energy, the greater the proportion of the estimated spatial spectrum in the final estimated value. That is to say, the greater the signal energy, the higher the reliability of the spatial spectrum estimation of the sub-band; on the contrary, the smaller the signal energy, the lower the reliability of the spatial spectrum estimation of the sub-band.

Energy threshold algorithm (ETISM).

The traditional ism algorithm needs to process each sub-band, and each processing involves feature decomposition and spectral peak search, which requires a lot of computation. ETISM algorithm first calculates the energy value of each sub-band and then sets an appropriate energy threshold [18]. If the energy of a certain sub-band is greater than the threshold, the narrow-band spatial spectrum is processed, otherwise, it is not considered. For example, take the mean of all sub-band energies as the threshold, that is,

$$T_W = \frac{1}{J} \sum_{j=1}^J W_j, \quad (7)$$

where W_j is the energy of the j sub-band, and T_W is the average energy of each sub-band. Taking T_W as the threshold value, if the energy of a certain sub-band is greater than T_W , the narrow-band spatial spectrum processing will be performed. If the energy of a certain sub-band is less than T_W , the sub-band will not be considered. For different thresholds, the computation and root mean square error of the algorithm are also different.

Figure 4 shows the root mean square error diagram corresponding to the ETISM algorithm under three different threshold conditions. T_1 represents the intermediate case, T_2 represents the low threshold case, and T_3 represents the high threshold case. It can be seen from Figure 4 that the root mean square error of the high threshold case is less than that of the middle case, and the root mean square error of the middle case is less than that of the low threshold Case [19]. The algorithm sets an energy threshold, discards the sub-bands whose energy is less than the threshold, and then narrow-band processes the subbands whose energy is greater than the threshold, which not only reduces the root mean

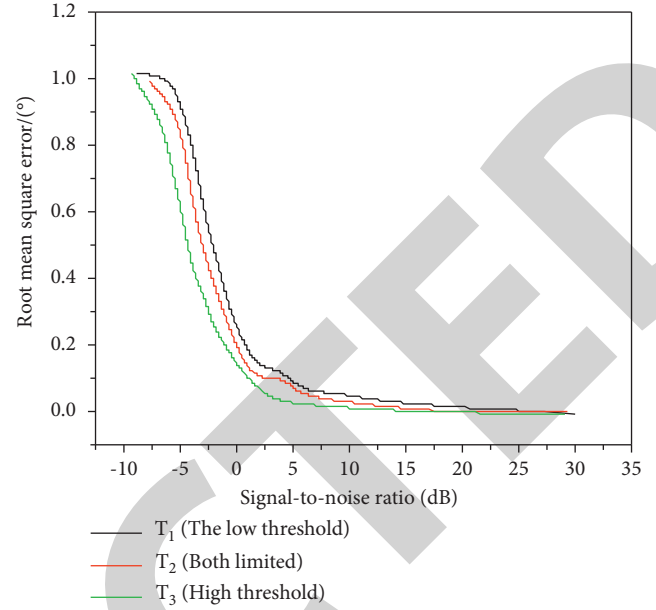


FIGURE 4: Comparison of root mean square error under three different thresholds.

square error, improves the resolution probability but also reduces the amount of computation [20].

4. Results and Analysis

4.1. Analysis of Enterprise Financial Management Objective Architecture Based on ISM Model

- (1) The highest level in Figure 3 is “maximizing the interests of stakeholders,” which shows that maximizing the interests of stakeholders is the ultimate goal of enterprise financial management. The “stakeholders” here refers to the main stakeholders represented by shareholders and creditors and should also include customers, enterprise employees, community organizations, governments, and other secondary stakeholders. Enterprise financial management should not only take into account the interests of shareholders and creditors but also improve the welfare of employees, improve or be conducive to the surrounding environment of the enterprise, be enthusiastic about social welfare undertakings, and create a good corporate image [21].
- (2) The second level of Figure 3 has three subobjectives, namely, “maximizing enterprise value,” “maximizing profit margin of equity capital,” and “maximizing cash flow,” which constitute the segment objective level of the entire financial management objective system. These three subgoals explain the maximization of the interests of the main stakeholders from different aspects. “Enterprise value maximization” represents the absolute value interests of shareholders and creditors at the same time; “Maximizing the profit margin of equity capital” mainly emphasizes the relative interests of shareholders; “Cash flow

maximization” emphasizes the balance between shareholders’ and creditors’ interests in terms of risk and reward [22].

- (3) The third layer in Figure 3 has two subgoals, namely, “maximizing earnings per share” and “maximizing shareholder wealth.” Among them, the maximization of shareholder wealth is the core element. The maximization of earnings per share emphasizes the relative profitability of equity capital. The realization of this subgoal will help to achieve the subgoal of “maximizing shareholder wealth.” The subgoal of “maximizing shareholders’ wealth” mainly emphasizes the maximization of shareholders’ interests.
- (4) The fourth layer in Figure 3 has a subgoal “profit maximization.” This subobjective is also the core element of the whole financial management objective system. The subgoal of “profit maximization” is the basis for realizing the hierarchical subgoals of “maximization of shareholder wealth,” “maximization of earnings per share,” “maximization of enterprise value,” “maximization of profit margin of equity capital,” “maximization of cash flow,” and the ultimate goal of “maximization of stakeholders’ interests.”
- (5) The last layer of Figure 3 has two subgoals, namely, “capital cost minimization” and “capital structure optimization”. There is a loop relationship between the two subtargets. Both explain the efficiency of financing behavior from different angles, and both are conducive to the realization of the subgoal of “profit maximization” [23].

The third level, the fourth level, and the fifth level subobjectives constitute the specific objective level of the entire financial management objective system.

From the above-given analysis, it can be seen that the enterprise financial management objective system mainly includes five levels. Among them, “maximization of shareholders’ wealth” and “maximization of profits” are the two core elements of the entire objective system, and they are also the two objectives that have been most agreed by the financial management theory circle for a long time; “Maximizing the interests of stakeholders” is the overall goal of the target system. After layer by layer decomposition, it can be gradually decomposed into divisional goals and specific goals. This objective system can provide a reference for enterprises to determine their own financial management objectives. Enterprises can timely revise their financial management objectives according to changes in the macro- and microenvironment, their own development stages, and their management objectives, so as to better guide the enterprise’s investment management, financing management, income distribution management, and other financial management work [24].

4.2. Simulation Effect and Analysis of EWISM Algorithm. Simulation conditions: a uniform linear array with 8 array elements. The array element spacing is the half wavelength of

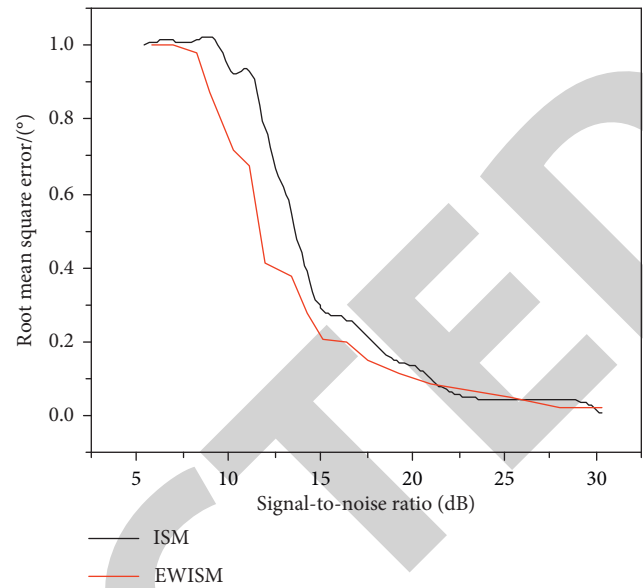


FIGURE 5: Comparison of root mean square error between EWISM algorithm and original algorithm.

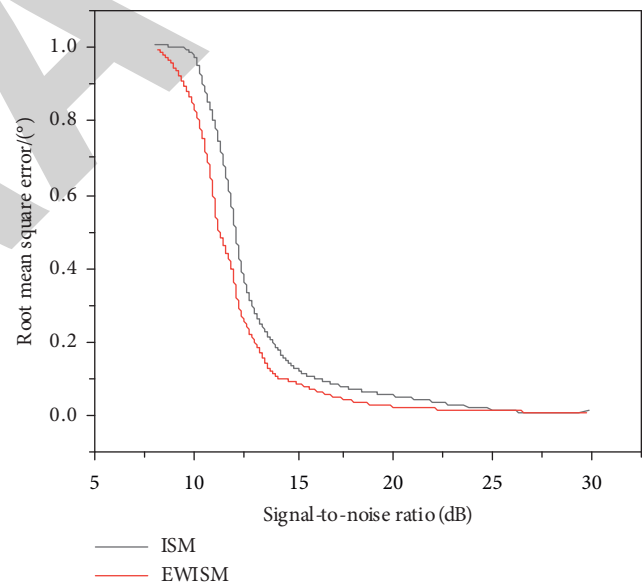


FIGURE 6: Comparison of root mean square error between ETISM algorithm and original algorithm.

the highest frequency. The highest frequency is 200 kHz and the lowest frequency is 20 kHz. The incident angles of two independent broadband signals are 10° and 14.3° . The signal bandwidth is divided into $j=64$ frequency points. The central frequency point is taken as the reference frequency point, and the number of snapshots at each frequency point is 50. Figure 5 is a Monte Carlo simulation conducted for 200 times at each point, comparing the root mean square error of the two algorithms. As can be seen from Figure 5, when the signal-to-noise ratio is 5–20 dB, the root mean square error of the EWISM algorithm is significantly smaller than that of the traditional ism algorithm.

4.3. Simulation Effect and Analysis of Energy Threshold Algorithm. Simulation conditions: a uniform linear array with 8 array elements. The array element spacing is the half wavelength of the highest frequency, the highest frequency is 110hz, and the lowest frequency is 90hz. The incident angles of two independent broadband signals are 5° and $\text{minus } 5^\circ$. The signal bandwidth is divided into $j = 64$ frequency points, the number of snapshots is 2048, and the central frequency point is taken as the reference frequency point. Figure 6 shows the Monte Carlo simulation conducted for 200 times at each point, comparing the root mean square error of the two algorithms [25].

5. Conclusion

This paper analyzes the architecture of financial management objectives based on the ISM model, discusses the stability, periodicity, and hierarchy of enterprise financial management objectives, describes the architecture of enterprise financial management objectives by using the ISM model method of system engineering, and establishes a five-level hierarchical structure model of financial management objective system. In this paper, the ISM algorithm is improved, two algorithms are proposed and their root mean square error is compared and analyzed. The experimental results show that the objective system can provide a reference for enterprises to determine their own financial management objectives. Enterprises can timely revise their financial management objectives according to the changes of macro- and microenvironment, their own development stages, and their management objectives, so as to better guide the financial management of enterprises, such as investment management, financing management, and income distribution management; through the comparison and analysis of algorithms, it is found that the root mean square error of the EWISM algorithm and ETISM algorithm is significantly smaller than that of traditional ism algorithm when the signal-to-noise ratio is 5–20 dB. It can be seen that by analyzing the architecture of financial management objectives based on the ISM model and improving the ISM algorithm, it can better provide a reference for enterprises to determine financial management objectives.

Data Availability

The data used to support the findings of this study are available from the author upon request.

Conflicts of Interest

The author declares that there are no conflicts of interest.

References

- [1] D. Graziano and D. Magni, “Unpacking the sustainability of sovereign wealth funds. the effect of financial performances on sustainability disclosure,” *International Journal of Managerial and Financial Accounting*, vol. 14, no. 2, p. 157, 2022.
- [2] O. O. Nesterenko, “The place of reporting in the management of financial results of the enterprise,” *Problems of Theory and Methodology of Accounting Control and Analysis*, vol. 1, pp. 26–32, 2021.
- [3] N. Sivasankaran, A. Kanagaraj, D. Israel, and R. Prasad, “The hungry energised allergic disease-ridden matrix for financial decision dilemmas of entrepreneurs,” *International Journal of Electronic Finance*, vol. 11, no. 2, p. 101, 2022.
- [4] R. Barzegarkhoo, S. A. Khan, Y. P. Siwakoti, R. P. Aguilera, S. S. Lee, and M. N. H Khan, “Implementation and analysis of a novel switched-boost common-ground five-level inverter modulated with model predictive control strategy,” *IEEE Journal of Emerging and Selected Topics in Power Electronics*, vol. 10, pp. 731–744, 2022.
- [5] I. R. Chuy, T. Y. Andreikiv, and I. Y. Mutyan, “The financial sustainability of consumer cooperation enterprises of Ukraine in the system of management of its financial resources,” *Business Inform*, vol. 3, no. 518, pp. 162–170, 2021.
- [6] A. T. Emmanuel and J. E. Ekpenyong, “Impact of crude oil volatility on stock market performance in Nigeria, over two decades,” *International Journal of Econometrics and Financial Management*, vol. 9, no. 1, pp. 23–33, 2021.
- [7] B. Yang and L. Gan, “Contingent capital Tobin’s q and corporate capital structure,” *The North American Journal of Economics and Finance*, vol. 55, no. 3, Article ID 101305, 2021.
- [8] L. Y. Zhang, X. Yin, J. Yang, A. Li, and G. K. Xu, “Multilevel structural defects-induced elastic wave tunability and localization of a tensegrity metamaterial,” *Composites Science and Technology*, vol. 207, no. 12, Article ID 108740, 2021.
- [9] W. Xin and Y. Wang, “Research on influencing factors of reservoir construction risk based on interpretative structural modeling,” *World Journal of Engineering and Technology*, vol. 09, no. 04, pp. 727–736, 2021.
- [10] I. Mirsayapov and G. Apkhadze, “Modified trilinear stress-strain diagram of concrete designed for calculation of beams with fiberglass rebar,” *IOP Conference Series: Materials Science and Engineering*, vol. 890, no. 1, Article ID 012079, 2020.
- [11] M. Hucumenoglu and P. Pal, “Effect of sparse array geometry on estimation of co-array signal subspace,” *Applied Computational Electromagnetics Society*, vol. 35, no. 11, pp. 1435–1436, 2021.
- [12] J. Chen, H. Mao, Z. Wang, and X. Zhang, “Low-rank representation with adaptive dictionary learning for subspace clustering,” *Knowledge-Based Systems*, vol. 223, no. 13, Article ID 107053, 2021.
- [13] Q. Zheng, L. Luo, H. Song, G. Sheng, and X. Jiang, “A rssi-aoa based uhf partial discharge localization method using music algorithm,” *IEEE Transactions on Instrumentation and Measurement*, vol. 70, pp. 1–9, 2021.
- [14] J. O. Ajadi, A. Wong, T. Mahmood, and K. Hung, “A new multivariate cusum chart for monitoring of covariance matrix with individual observations under estimated parameter,” *Quality and Reliability Engineering International*, vol. 38, no. 2, pp. 834–847, 2022.
- [15] X. Lin, X. Zhang, L. He, and W. Zheng, “Multiple emitters localization by uav with nested linear array: system scheme and 2d-doa estimation algorithm,” *China Communications*, vol. 17, no. 3, pp. 117–130, 2020.
- [16] R. B. A. Kardono, N. S. P. Jaya, and N. Rochaeti, “Hukuman kebiri terhadap kejahatan seksual anak,” *Kanun Jurnal Ilmu Hukum*, vol. 22, no. 3, pp. 567–582, 2020.
- [17] F. Watanabe, “Wireless sensor network localization using aoa measurements with two-step error variance-weighted least squares,” *IEEE Access*, vol. 9, pp. 10820–10828, 2021.
- [18] Y. Sun, P. Feng, H. Zhou et al., “Optimization of self-consistent approach for quantum cascade laser using shooting

Retraction

Retracted: Remote Human-Computer Interaction and STEM Teacher Online Training Based on Embedded Internet of Things

Mathematical Problems in Engineering

Received 8 August 2023; Accepted 8 August 2023; Published 9 August 2023

Copyright © 2023 Mathematical Problems in Engineering. This is an open access article distributed under the Creative Commons Attribution License, which permits unrestricted use, distribution, and reproduction in any medium, provided the original work is properly cited.

This article has been retracted by Hindawi following an investigation undertaken by the publisher [1]. This investigation has uncovered evidence of one or more of the following indicators of systematic manipulation of the publication process:

- (1) Discrepancies in scope
- (2) Discrepancies in the description of the research reported
- (3) Discrepancies between the availability of data and the research described
- (4) Inappropriate citations
- (5) Incoherent, meaningless and/or irrelevant content included in the article
- (6) Peer-review manipulation

The presence of these indicators undermines our confidence in the integrity of the article's content and we cannot, therefore, vouch for its reliability. Please note that this notice is intended solely to alert readers that the content of this article is unreliable. We have not investigated whether authors were aware of or involved in the systematic manipulation of the publication process.

In addition, our investigation has also shown that one or more of the following human-subject reporting requirements has not been met in this article: ethical approval by an Institutional Review Board (IRB) committee or equivalent, patient/participant consent to participate, and/or agreement to publish patient/participant details (where relevant).

Wiley and Hindawi regrets that the usual quality checks did not identify these issues before publication and have since put additional measures in place to safeguard research integrity.

We wish to credit our own Research Integrity and Research Publishing teams and anonymous and named external

researchers and research integrity experts for contributing to this investigation.

The corresponding author, as the representative of all authors, has been given the opportunity to register their agreement or disagreement to this retraction. We have kept a record of any response received.

References

- [1] X. Wu and Q. Zhang, "Remote Human-Computer Interaction and STEM Teacher Online Training Based on Embedded Internet of Things," *Mathematical Problems in Engineering*, vol. 2022, Article ID 2896481, 8 pages, 2022.

Research Article

Remote Human-Computer Interaction and STEM Teacher Online Training Based on Embedded Internet of Things

Xinning Wu  and Qian Zhang

Hunan University of Science and Technology, Xiangtan 411201, Hunan, China

Correspondence should be addressed to Xinning Wu; 201730704175@stu.swun.edu.cn

Received 9 July 2022; Accepted 10 August 2022; Published 29 August 2022

Academic Editor: Hengchang Jing

Copyright © 2022 Xinning Wu and Qian Zhang. This is an open access article distributed under the Creative Commons Attribution License, which permits unrestricted use, distribution, and reproduction in any medium, provided the original work is properly cited.

In order to expand the concept and form of teacher training, a remote human-computer interaction and STEM teacher online training platform based on the embedded Internet of Things is proposed. Based on the content analysis method, this article sorts out the development status of the current online teacher training platform and points out the shortcomings of the platform in information aggregation, resource construction, content setting, presentation, learning support services, and other aspects. Based on the combination of new concepts and new technologies, an online training platform for STEM teachers is proposed for the construction of the platform from four perspectives: innovative design concepts, enriching platform promotion ideas, developing educational makers, and improving support services, and the results of the use are investigated. The results show that the subjects believe that the STEM teacher online training system has clarified the STEM curriculum design steps, standardized STEM design methods, improved their cooperative learning ability, and cultivated design thinking. Among them, 13 people think that the training system has made STEM design steps clearer, “the design process is clearer,” “it makes me clearer about the whole design process,” and “the course design and development process is clearer.” *Conclusion.* This platform can provide a reference for online training and professional development of Chinese teachers.

1. Introduction

In recent years, 'China's education level has been greatly improved, and the quality of people has been constantly improved. The concept of lifelong learning has been more and more accepted by people. Online education is conducive to overcoming the problem of uneven distribution of educational resources and realizing professional training. At present, some enterprises and public institutions have established online learning platforms for employees, as shown in Figure 1. Through the online learning platform to provide targeted teaching, staff work level has been improved, work efficiency has been improved. Online learning platform utilizes Internet technology to implement network teaching and can assist in providing online examinations and online q&a functions, which is an important means of on-the-job education at present [1]. Teachers are an important factor in the development of education, and their

knowledge renewal determines the level and quality of education. Therefore, it is necessary to provide better resources and methods for 'teachers' lifelong learning. Teachers can better improve teaching effects through continuous learning [2]. At present, 'teachers' later learning is mainly carried out by inviting in and going out. On the one hand, experts will be invited to relevant units for special training. On the other hand, some teachers are sent to universities or training institutions for further study and promotion. While these methods improve 'teachers' personal ability, they also have disadvantages such as high learning cost, and limited by time and space. Online learning can break through these limitations. Teachers can learn independently through online training and learning platforms so that they can obtain more learning opportunities, learning resources, and teachers [3]. At the same time, through the online training and learning platform, teachers can freely choose learning content, develop personalized



FIGURE 1: Online teacher training.

learning plans, and enhance their interest in learning with the help of multimedia teaching methods.

2. Literature Review

By analyzing successful STEM classroom practices, Rodrigues and Tomasi proposed the idea of reverse learning design, that is, taking clear STEM course learning objectives as the starting point, STEM learning evaluation design takes priority over STEM teaching activity design, so as to promote the achievement of STEM course learning objectives. At the same time, it is pointed out that interdisciplinary STEM courses designed and integrated should be based on real problems and integrate scientific inquiry, technical literacy, mathematical thinking, and engineering design into the process of problem exploration, analysis, and solution through close cooperation between teachers of different disciplines [4]. Morell and Ksenia Nickolaevna proposed the use of the Universal Learning Design Approach (ULD) in STEM courses. That is, to achieve a deep understanding and innovative application of interdisciplinary concepts and STEM core concepts by designing flexible and diverse ways of information acquisition, activity participation and information expression [5]. Oliveira and Silva believe that teaching skills can be improved by providing new teachers with “simulated practice” teaching practice experience. Similar to the idea of a flight simulator for training pilots, they designed simSchool. Based on the learning theory, the computational models of students’ personality, teachers’ behavior, students’ classroom behavior, and academic performance were established, and the classroom teaching environment was simulated by a simulation engine. Preservice teachers need to analyze the learning needs of different types of virtual students in the virtual classroom, make teaching decisions and evaluate the impact of teaching behavior on student performance [6]. In addition, the researchers also explored the design of social media, Internet technology, and multimedia technology applied to the online teacher practice community. The Video paper designed by Li et al. integrate classroom video and forum functions, allowing teachers to observe classroom teaching, students’ homework

samples and lecturers’ teaching plans online, as well as the relevant questions raised by lecturers for the research teachers to discuss and reflect on teaching [7]. Chen et al., from the perspective of social constructivism and learning community, use the famous multiplayer online virtual reality game platform Second Life to create a teaching practice learning environment, in which normal university students play the roles of teachers and students and carry out teaching practice activities such as collaborative teaching design, simulation teaching and lesson evaluation [8]. Sharma et al. point out that an open online learning environment can track learning behaviors. Their nBrowser online platform is based on the architecture of the Intelligent Learning Guidance System (ITS), including domain model, learner model, teaching method model, and user interface model, providing teachers with the task of independently completing curriculum plan design. At the same time, self-planning learning guidance and support in the process of interaction with teachers can be realized through teaching agent [9]. To meet the requirements of the development of national education informatization, a lot of work has been carried out in improving teachers’ information technology application ability, especially in teachers’ information training. Compared with traditional centralized training, online training is characterized by trans-temporal, large-scale, easy implementation, good communication, and low cost and has obvious advantages in knowledge transfer, regional coverage, resource acquisition, cost effectiveness, collaboration, and exchange [10]. Relying on the Internet, advanced educational concepts, high-quality training resources, and innovative teaching technologies can be shared within a short period of time, which has made an important contribution to improving the overall quality of Chinese teachers and narrowing the digital divide between regions. In recent years, online training institutions such as the National network for continuing education of primary and secondary school teachers and the China Teacher Research and Training Network have been set up. Many universities and local government departments have also set up online training platforms. Teacher distance training has gradually moved from the edge to the center, becoming one of the “three carriages” of Teacher

training for primary and secondary schools in China, parallel with centralized training and school-based training [11].

3. Research Methods

3.1. Content Analysis Based on Online Teacher Training Platform

3.1.1. Selection of Research Objects. First of all, “teacher training and Research platform” and “teacher education network” were used as keywords to search for research objects in search engines. After excluding for-profit learning websites, 59 relatively open online teacher training platforms in China were investigated [12]. Public welfare, professionalism, and service are the common characteristics of the platform, which reflect the development status of Online teacher training in China. After that, a comparative analysis is made on 59 platforms one by one. Six influential national online training platforms and four local online training platforms are selected as specific research objects in view of the host and management organization, service scope, service objects, registered users, and results obtained, and their practicability and influence are considered comprehensively. They are supervised by the Department of Teacher Work of the Ministry of Education, colleges and universities, education and training institutions, local education departments, and other units, respectively. They are representative of the platform in terms of organizational structure, technology application, content design, etc., [13].

The survey shows that the current online teacher training platform can be divided into two types: portal website and training management. The first-level portal mainly integrates the latest national education news, policies, and trends and gathers famous teachers and high-quality education resources, with rich contents. The second-level portal provides specific training information, training program, training assessment, training results display, and training data statistics according to the needs of specific regional training programs. After logging in, teachers can enter the personal learning space, manage personal information and learn [14]. The training management platforms are generally only for local teachers, and most of them are set up by local education institutions, providing relatively single services and resources.

3.1.2. Establishment of Research Dimension. Through literature analysis, theoretical research, and online training platform investigation, the analysis dimension was established [15]. The research mainly adopts the content analysis method and takes an online training platform as the analysis unit. Based on the functional modules within the platform, a comparative analysis is made: the interface content design and personal learning space design of the platform are taken as the dimension of horizontal analysis, and the development status of the online teacher training platform is analyzed from the aspects of content, communication, management, and service (see Figure 2).

3.2. Analysis on the Construction of Online Training Platform for Teachers. With the further integration of information technology and learning, online learning continues to surpass the technology itself as a means to develop into an important media that integrates people, technology, and culture. The development of teachers’ online learning cannot be separated from the support of platforms, which often determine the implementation mode and management mode of teachers’ online training and even affect the enthusiasm of teachers in participating in the training and the final training effect [16]. At present, the design and construction of an online training platform for teachers mainly have the following problems.

3.2.1. It Focuses on Gathering Information and Resources and Lacks Effective Classification and Push. “We are submerged in the ocean of network data, but we are suffering from the thirst for knowledge.” The disordered information and its disordered transmission increase the difficulty for users to extract it effectively [17]. Today, with the increasingly close combination of network technology and teacher education, online training gradually shows the absolute advantages of information technology in information transmission, resource sharing, remote interaction, and other aspects. However, with the improvement of teachers’ information literacy, the traditional single divergent information transmission can no longer meet the needs of teachers’ personalized development. Online training means that teachers can easily access effective information and selective learning resources. However, the actual construction display platform has shortcomings in the convergence and presentation of information resources. Although the Settings of information modules are slightly different on different platforms, their types and functions are basically the same (see Table 1), mainly about education news, project dynamics, policy documents, and expert team. The resource module includes training project briefs, teachers’ training logs, excellent works of participating teachers, and other expansion resources [18]. It can be found that (1) the homepage of the national online training platform is rich in content and covers a wide range of areas, while the regional platform only releases news bulletins and other information, without project achievements display and relevant introduction of the training expert team; (2) although the homepage of the platform presents a large amount of content, it lacks in-depth analysis and cannot effectively classify and push resources purposefully according to the learning needs of participating teachers; (3) the search function is not complete, 1/3 of the platforms lack the search function, which causes some troubles for the participating teachers to search information and resources [19].

3.2.2. The Content Is Presented in a Single way and Lacks Multiterminal Adaptive Design. With the rapid development of information technology and communication technology, ubiquitous learning has become the norm. Smart phones, tablets, and other mobile devices have become a necessity in People’s Daily life, not only changing the

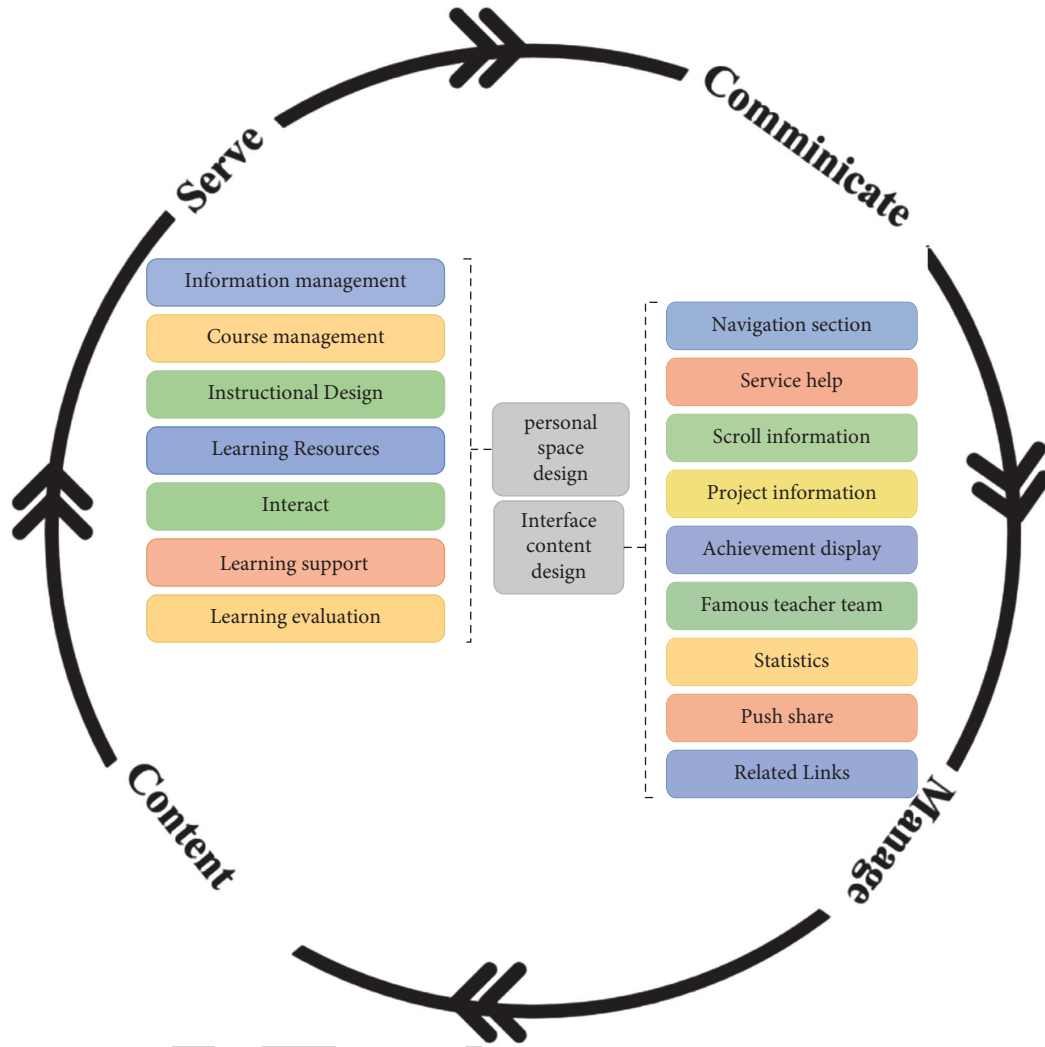


FIGURE 2: Platform analysis dimensions.

TABLE 1: Function module Settings of the homepage of online teacher training platform.

	Module	Number of national platforms	Number of local platforms
Information	Dynamic	6	4
	News	2	3
	Policy	2	3
	Announcement	2	4
	Experts	5	1
	Search	3	3
Resources	Brief	6	1
	Post	3	0
	Show	2	0
	Activity	4	0
	Homework	3	0
	Resources	3	0

way of interpersonal communication but also affecting people’s way of learning. In addition to the time at home and teaching, teachers’ learning time is relatively fragmented. Therefore, network learning resources should be presented on different mobile terminals in appropriate forms to break through the barriers between different devices, and to realize

the fragmentation and ubiquitination of learning, to reduce the interference of resource presentation on teachers’ online learning, and to meet the needs of scattered learning, which is the inevitable trend of the development of online teacher training platforms in the future [20]. At present, online training platforms for teachers are still dominated by

traditional web page presentation (see Table 2), lacking adaptive display support for portable device screens, and only a few platforms provide users with mobile clients [21]. It can be seen that although studies on mobile learning and ubiquitous learning continue to deepen, there are few learning platforms that can meet the needs of new training methods, and there is a lack of design and development for mobile terminals. That is, the adaptive display design, the display of web content does not match the screen of mobile devices, which brings inconvenience to teachers in acquiring knowledge and greatly reduces the user adhesion of the platform.

3.2.3. The Training Content Is Mainly Prearranged, And Not Strongly Targeted. With the development of new learning theories, such as socialized learning theory and situational learning theory, as well as the transformation of learning methods, people have a new understanding of the nature of learning. Teacher online training platform should not only realize technological innovation and build adaptive seamless learning space but also make breakthroughs in the organization of learning content. Currently, the training content in the online training platform for teachers is basically preset and solidified, created and modified by experts, and presented to the participating teachers, which is a typical one-way information transmission mode of expert production and user consumption and has a poor response to the dynamic and complexity of the real situation [22]. Under this mode of information transmission, the update of training content is too slow, which is not coordinated with the pace of knowledge update and the change of teachers' needs. Teachers passively receive information, and valuable information generated in the training process can not be fully reflected, let alone shared with other participating teachers. In addition, the content of primary and secondary school teacher training is mainly based on education and teaching theories, teaching methods, and teaching strategies integrated with technology, focusing on how teachers teach, less on how students learn and ignoring the guidance of students' mental health. The training content is single, lack of cross-disciplinary learning, the content is abstract, disjointed from daily teaching work, poor timeliness, weak pertinence, and other problems always exist. Teachers' learning needs in the information age are becoming more and more personalized and diversified. The preset training content cannot be flexibly adjusted according to actual teaching and cannot meet the personalized and numerous learning needs of participating teachers.

3.2.4. Limited Resource Expansion and Slow Replenishment. Nowadays, knowledge is updated faster and faster, and learning is no longer about mastering existing knowledge. Through social networks, learners can not only get the resources they need but also discover other relevant content, and then learn knowledge and wisdom from other channels or learners. In addition to providing teachers with basic knowledge, online teacher training is necessary to develop resources such as recommendation of excellent cases,

TABLE 2: Content presentation of an online training platform for teachers.

	T1	T2	T3	T4	T5	T6	T7	T8	T9	T10
Traditional web edition	√	√	√	√	√	√	√	√	√	√
Mobile terminal edition	—	—	—	√	—	—	—	—	—	—
Client APP	—	—	√	—	—	—	—	—	—	—

presentation of famous teachers, and introduction of learning software and links of relevant content, as well as the construction of extended content other than training classes [23]. However, the current online training platforms for teachers are not enough to provide resources for expansion (as shown in Figure 3). The platforms with expansion resource modules account for only half of the total number of the survey. The content is mainly about the display and sharing of excellent homework, lacking the support of learning tools. The analysis shows that the development resource module construction of the national platform is relatively complete, while the local platform is very short, with only 1 case, and these resources are mainly from students' sharing and uploading. Therefore, in terms of resource development, national platforms have been gradually improved, while local platforms are still in the stage of starting from scratch. Although each region has established its own teacher training institutions in order to improve the professional ability of teachers, the updating and supplementing of resources is still in its infancy.

3.2.5. Insufficient Learning Support and Personalized Service. In addition to rich learning resources, learning support is also one of the important factors to ensure the quality of online teacher training. The purpose of providing learning support is to help, guide, and promote learners' autonomous learning and improve the quality and effectiveness of online training. As an important part of online learning, learning support is divided into academic support and nonacademic support, including content support, technical support, resource support, process support, activity support, communication support, evaluation support, management support, and so on. In addition to the content and resource support discussed above, the function construction of the online teacher training platform in terms of communication, service, evaluation, and management is not satisfactory (see Table 3).

In a word, due to the characteristics of openness, high efficiency, and interactivity, the network training platform shows absolute advantages in teacher training. However, with the development of online training, the disadvantages of the platform become more and more prominent and gradually hinder the use of teachers. For example, its ease-of-use, compatibility, and interactive functions are increasingly unable to meet the needs of participating teachers. In addition, the injection training method, unreasonable organizational structure, and single evaluation management mode are the current online teacher training platform to solve the problems.

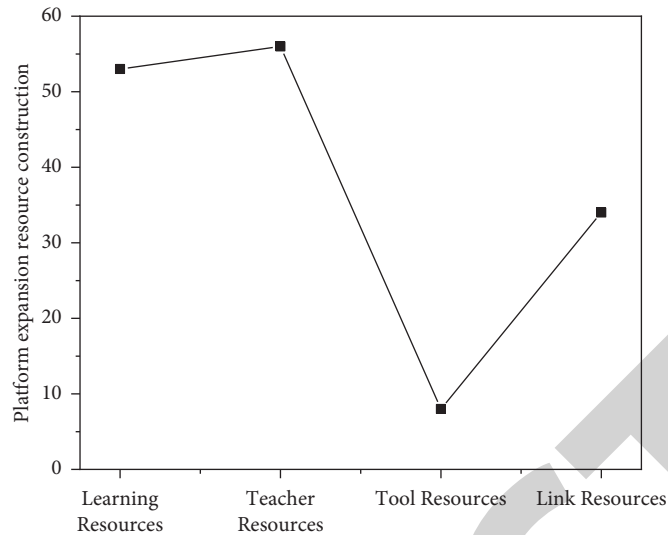


FIGURE 3: Resources construction of online training platform for teachers.

TABLE 3: Status quo of learning support service construction of online teacher training platform.

Service type	Support functions	Lack of functionality
Communication support	Forums, reviews, online seminars	Synchronous interaction, collaborative learning, maker space
Service support	Study guide, statistical inquiry, consultation, and q&A	Intelligent search, learning tools, learning analysis
Evaluation support	Exams, assignments, work, attendance	Learning monitoring, process evaluation, incentive mechanism
Management support	Personal information, course information	Independent course selection, personal customization, dynamic adjustment

4. Result Analysis

Based on the results of the first round of teaching practice, the research improved the online training system for STEM teachers and replaced the original text-based STEM learning design method with a visual learning design tool, aiming to further improve the learning design ability of normal university students and their understanding of STEM teaching method. The research will carry out the teaching practice of the second round of online training for STEM teachers, and investigate the influence of the improved online training system for STEM teachers on the teaching design ability and design thinking level of preservice teachers through questionnaires before and after the issuance. The questionnaire was used to understand the usability, ease of use, behavioral intention of using the STEM teacher online training system, and the views and suggestions of preservice teachers on the training system. This study was conducted on 40 students in their second year who majored in educational technology in a university. Students participate in STEM teacher training programs as preservice teachers by using the STEM teacher online training platform that has been developed. The second round of practice was conducted from October 2019 to January 2020 and lasted for ten weeks. The questionnaire of the second round of the experiment was sent online through the system task mail. Thirty-eight questionnaires were collected, of which 34 were valid, with an effective rate

of 89.47%. Thirty-four questionnaires were collected after the experiment, and 34 were valid, with an effective rate of 100%. Among them, a total of 34 normal university students completed the pre - and post-test two questionnaires. 40 questionnaires were collected for technical acceptance, and 39 were valid, with an effective rate of 97.5%. The questionnaire data will be statistically analyzed by SPSS Statistics software. Paired sample statistics and paired sample test will be used to describe the changes of TPACK level and design thinking level of 34 normal university students before and after training. The technology acceptance questionnaire data will conduct a descriptive statistical analysis of the core variables of the technology acceptance model and summarize and analyze the answers to open questions.

The basic idea of paired sample t test is to assume that population X_1 follows a normal distribution $N(\mu_1, \sigma_{12})$, and population X_2 follows a normal distribution $N(\mu_2, \sigma_{22})$. Samples $(x_{11}, x_{12}, \dots, x_{1n})$ and $(x_{21}, x_{22}, \dots, x_{2n})$ are extracted from these two populations, respectively, and the two samples are paired with each other. It is required to test whether μ_1 and μ_2 are significantly different. The specific steps are as follows:

4.1. Introduce Variables. A new random variable $Y = X_1 - X_2$ is introduced, and the corresponding sample value is (y_1, y_2, \dots, y_n) , where $y_i = x_{1i} - x_{2i}$ ($i = 1, 2, \dots, n$).

4.2. *Establish Hypotheses.* As shown in the following formula:

$$H_0: \mu_Y = 0. \quad (1)$$

4.3. *Calculation Formula and Significance*

$$t = \frac{\bar{y}}{S_y/\sqrt{n}} \quad (2)$$

Here, $\bar{y} = \sum_{i=1}^n y_i/n$ is the average of the difference values of paired samples; $S_y = \sqrt{\sum_{i=1}^n (y_i - \bar{y})^2/n - 1}$ is the standard deviation of the difference of paired samples; n is the number of paired samples.

The statistic t obeys the t -distribution with $n - 1$ degree of freedom under the true null hypothesis ($\mu_Y = 0$).

The analysis results of the influence of the system on the design course of the subjects are shown in Figure 3. According to the statistics, the subjects believe that the online TRAINING system for STEM teachers has clarified the steps of STEM curriculum design, standardized STEM design methods, improved their cooperative learning ability, and cultivated design thinking. Among them, 13 people think that the training system has made STEM design steps clear, “the design process is clearer,” “it makes me more clear about the whole design process,” and “the course design and development process is clearer.” Nine people think that the training system can cultivate the design thinking. They mentioned that “problems will be considered from more angles when designing courses,” “the design course will go deep into the subject knowledge,” “focus on student-centered design course,” “design is a coherent process, and the previous design content will be modified in the subsequent design,” and “cultivate the overall thinking of course design.” Six people thought that the training system could standardize STEM design methods, “master the standardized design template,” “have a certain understanding of the standardized requirements of STEM design,” and “standardize the STEM design process.” Three people think that the training system can improve cooperative learning ability, “group communication enables me to learn cooperative learning,” and “I learn a lot from team members in the process of sharing communication”.

5. Conclusion

With the development and application of information technology, online training has gradually replaced traditional centralized training and become the main way of professional improvement of teachers. The design and construction of an online teacher training platform is an important factor that affects the effect of teacher training. In fact, the essence of an online training platform is “content + service.” Quality content is the foundation, personalized service is the guarantee, content, and service is the core of online training platform construction. Under the background of education informationization, online teacher training in China is developing rapidly. But the construction of platforms has not kept pace with actual demand. Online

training platform for the construction of the future teachers, therefore, should be the fusion of advanced education idea and information technology, to create a network, digital, mobile, and personalized teachers online training environment, breakthrough time and space limit, break from online, really change the traditional training pattern of indoctrination, implementation of teacher training of generalization, socialization, mobile, and service. After two rounds of training, we found that the online STEM teacher training system can effectively improve the TPACK level and design thinking level of preservice teachers. After the improvement of the training program and system, the online STEM teacher system can significantly improve the seven dimensions of TPACK of preservice teachers and thus promote the improvement of their STEM teaching design ability at the TPACK level. At the level of design thinking, the system can effectively promote the level of design practice and design tendency.

Data Availability

The data used to support the findings of this study are available from the corresponding author upon request.

Conflicts of Interest

The authors declare that there are no conflicts of interest.

Acknowledgments

This study was funded by Educational Science Planning Project of Hunan Province, under Project no. XJK19QXX003.

References

- [1] C. Zambrano, “A study on lexical availability in the area of self regulated learning in the initial teacher training,” *Linguística Y Literatura*, vol. 42, no. 79, pp. 11–33, 2021.
- [2] G. G. Santos, J. d. L. Nascimento, and P. C. M. d. A. Santos, “Educação de jovens e adultos x formação de professores: reflexões e insurgências/youth and adult education x teacher training: reflections and insurgencies,” *Brazilian Journal of Development*, vol. 7, no. 1, pp. 3029–3041, 2021.
- [3] J. J. d. Souza and E. C. Moraes, “A formação do professor e a legislação pertinente à educação inclusiva/teacher training and legislation relevant to inclusive education,” *Brazilian Journal of Development*, vol. 7, no. 1, pp. 10530–10541, 2021.
- [4] R. V. L. Rodrigues and Á. R. G. Tomasi, “A formação de professores na perspectiva da inovação social/the teacher training in the perspective of social innovation,” *Brazilian Journal of Development*, vol. 7, no. 1, pp. 10196–10215, 2021.
- [5] T. Morell and V. Ksenia Nickolaevna, “Introduction,” *Revista Alicantina de Estudios Ingleses*, vol. 34, no. 34, pp. 7–13, 2021.
- [6] S. M. S. d. Oliveira and C. D. M. d. Silva, “Formao de professores em tempos de retrocesso: o que dizem os documentos oficiais?/teacher training in times of setback: what do the official documents say?” *Brazilian Journal of Development*, vol. 7, no. 1, pp. 141–152, 2021.
- [7] B. Li, J. Wang, Z. Gao, and N. Gao, “Light source layout optimization strategy based on improved artificial bee colony

Retraction

Retracted: Recommendation Model of Tourist Attractions Based on Deep Learning

Mathematical Problems in Engineering

Received 8 August 2023; Accepted 8 August 2023; Published 9 August 2023

Copyright © 2023 Mathematical Problems in Engineering. This is an open access article distributed under the Creative Commons Attribution License, which permits unrestricted use, distribution, and reproduction in any medium, provided the original work is properly cited.

This article has been retracted by Hindawi following an investigation undertaken by the publisher [1]. This investigation has uncovered evidence of one or more of the following indicators of systematic manipulation of the publication process:

- (1) Discrepancies in scope
- (2) Discrepancies in the description of the research reported
- (3) Discrepancies between the availability of data and the research described
- (4) Inappropriate citations
- (5) Incoherent, meaningless and/or irrelevant content included in the article
- (6) Peer-review manipulation

The presence of these indicators undermines our confidence in the integrity of the article's content and we cannot, therefore, vouch for its reliability. Please note that this notice is intended solely to alert readers that the content of this article is unreliable. We have not investigated whether authors were aware of or involved in the systematic manipulation of the publication process.

Wiley and Hindawi regrets that the usual quality checks did not identify these issues before publication and have since put additional measures in place to safeguard research integrity.

We wish to credit our own Research Integrity and Research Publishing teams and anonymous and named external researchers and research integrity experts for contributing to this investigation.

The corresponding author, as the representative of all authors, has been given the opportunity to register their agreement or disagreement to this retraction. We have kept a record of any response received.

References

- [1] X. Cheng and W. Su, "Recommendation Model of Tourist Attractions Based on Deep Learning," *Mathematical Problems in Engineering*, vol. 2022, Article ID 9080818, 7 pages, 2022.

Research Article

Recommendation Model of Tourist Attractions Based on Deep Learning

Xinquan Cheng  and Wenlong Su

Department of Tourism Management, PaiChai University, Daejeon 35345, Republic of Korea

Correspondence should be addressed to Xinquan Cheng; 1706300107@xy.dlpu.edu.cn

Received 12 July 2022; Accepted 10 August 2022; Published 28 August 2022

Academic Editor: Hengchang Jing

Copyright © 2022 Xinquan Cheng and Wenlong Su. This is an open access article distributed under the Creative Commons Attribution License, which permits unrestricted use, distribution, and reproduction in any medium, provided the original work is properly cited.

In order to solve the problem of tourism information overload caused by the rapid development of tourism and the Internet era, the author proposes a tourist attraction recommendation model based on deep learning. Convolutional Neural Network (CNN) is used to extract the sentiment of text comments, the Pearson similarity formula is used to calculate similar user groups, and the mean absolute error (MAE) is used to evaluate the resulting error. Compare with traditional collaborative filtering methods. Experimental results show that: the MAE value is smaller than the MAE value of the collaborative filtering method, indicating that considering tourists' behavioral information, contextual information, and emotional factors in comments can effectively improve the accuracy of recommendation, as the data volume of the test set increased from 250 to 2000; although there was an increase in the MAE value, the overall trend showed a downward trend, indicating that the quality of the model can be more fully verified when the data volume is large. The model proposed by the author can effectively reduce the prediction error and improve the efficiency of tourist attractions recommendation.

1. Introduction

With the rapid growth of information technology, the need for deepening of the information technology industry and information technology has become increasingly strong [1]. In the data age, which is overloaded with data, users can not quickly find the data they are interested in [2]. Therefore, the tourism consulting industry has been designed to meet the needs of consumers and provide customer satisfaction. One-person travel advertising has been widely used because it integrates referrals into the tourism industry, allowing consumers to make informed personal decisions, and provide their favorite and most accurate products. Research costs.

The design recommendations are effective based on an analysis of user data behavior and provide users with the quality of the model as they see fit [3]. Recommendations can be divided by data: user behavior data, data usage data, content data, and social network data. In recent years, many scientists have proposed hybrid technology-approved and restricted-based technology to improve the technology performance of feedback and to ensure the use of multiple restrictions.

As personal tourism referral technology has become a hotspot for research and industry research, the author evaluates referral technology, including information on the behavior of consumers, consumer information, content, and social network information years [4]. At the same time, the latest advances in related activities have been studied, highlighting the use of technology that can improve performance and limitations-based approval high-performance technology that meets various options [5]. Currently, the most widely used training models in the field of communication include multilayer sensors, automatic encoders, repeat neural networks, circulatory neural networks, and interactive interactions alk different versions [6]. The framework for the approval by in-depth research is shown in Figure 1.

2. Literature Review

In recent years, with the rapid development of information technology such as the Internet, big data, and cloud computing, people have expanded to big data in the environment around [7]. Big data contains a lot of information and

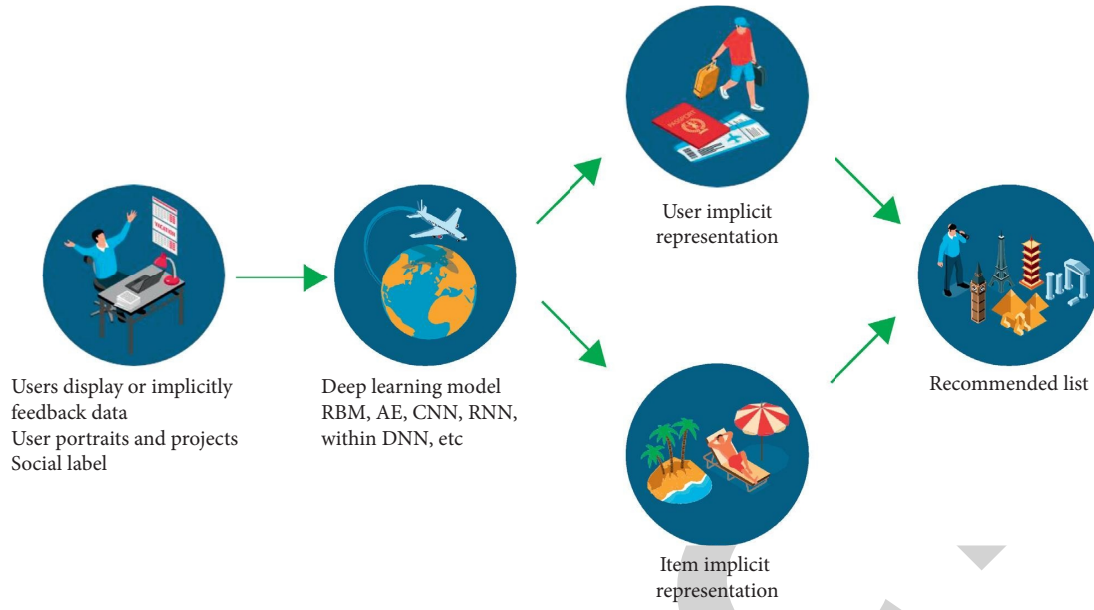


FIGURE 1: Framework of a recommender system based on deep learning.

knowledge, which allows people to access big data in a short amount of time [8]. At the same time, however, the negative impact of cracked data is that “broadcast data” is problematic because it is difficult for users to get still content. Importance of hard data when encountering large data. In terms of data filtering technology, the conventional system solution of data overload by providing users with personal quality content has become an important technology in various areas of application and is focused on research.

Technically, there are two consensus points: a combination filter based on consensus and a consensus based concept. The first is based on the relationship of user impact, and the latter focuses on the appropriate ranking by the characteristics of the content. In recent years, through in-depth research, the system has become increasingly important to many scientists’ ability to study and represent the negative effects of consumer products and provide essential products of consumers and products [9]. Although in-depth training works very well to facilitate the study of the secrets of users and products, and to advance the level of research and application of recommendations, it is difficult to obtain get enough information of users to choose from in a variety of different, low starting cold and Other problems, the problem still exists. At the same time, model approval determines everything on its own in determining consumer preferences, and it is not possible to model product relationships in chronological order. because he could not determine the status of his system.

Learning-improvement strategies have led to advances in game and robotics management, new breakthroughs in science in the age of intelligence, and new ways to explore research in a commentary. Reinforcement learning combined with deep learning methods has the ability to process large-scale data and discover and extract low-level features, so as to achieve specific goals more accurately. As an Interactive Recommendation (IR) method, the recommendation model

based on reinforcement learning can update the recommendation strategy by interacting with users in real time and obtaining real feedback from users, compared with traditional static methods, it is more in line with realistic recommendation scenarios [10]. At the same time, since reinforcement learning problems are usually normalized as Markov Decision Process (MDP), such models have the natural characteristics of modeling user behavior sequences, which can fully characterize the sequence features and capture users’ dynamic preferences [11]. In addition, the setting of the exploration mechanism can enable the agent to fully explore the state and action space, which improves the diversity of recommendation results to a certain extent; finally, since this type of model often maximizes the cumulative revenue of the recommendation system, that is, the long-term feedback of users, updating the recommendation strategy as an optimization goal can improve the long-term satisfaction of users to a certain extent [12].

From the current point of view, the research application of reinforcement learning in recommender systems has become one of the research focuses in recent years. However, there is still a lack of corresponding review summaries. The applications of deep reinforcement learning in search, recommender systems, and advertising are reviewed, but the review is relatively small in terms of recommendation system related research. In addition, as far as we know, there is no Chinese literature that systematically recommends the system as the research object, and comprehensively and systematically summarizes and analyzes the implementation method based on reinforcement learning [13].

The recommendation, based on the DRL value function, uses a deep neural network to estimate the Q-value function, and the purpose of the optimization is to modify the neural network regularly from gradient to complete all the gifts and find good ideas. The DRL framework based on the agreed function values is shown in Figure 2.

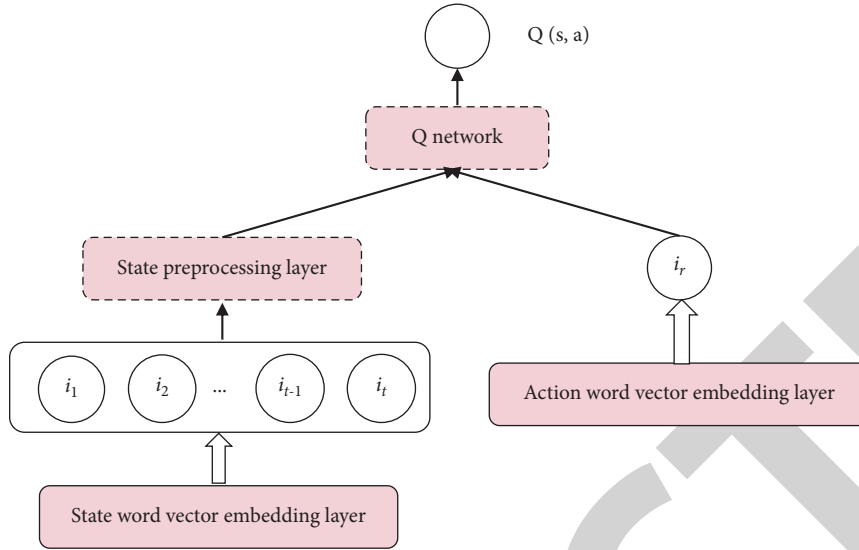


FIGURE 2: Recommendation framework based on value iterative DRL.

Since reinforcement learning can dynamically obtain user behavior information, incorporating the latest preference information in real time, more and more reinforcement learning is currently being used in news, e-commerce, medical and other fields. Among them, tourism is one of the entertainment items involved in people's life, and there are few research studies on the recommendation of tourist attractions [14]. The inverse reinforcement learning is applied to the recommendation of tourist attractions, using the user's past selection order of attractions and the current scene context to understand the user's preferences and establishes a preference learning model that takes into account the timing of commodity consumption, then further use the inverse reinforcement learning method for tourist attraction recommendation.

The classification of recommendation models based on reinforcement learning is shown in Table 1.

Recommendations for tourism always ignore information about tourists, characteristics of tourists, and tourists, and make predictions based on a survey of tourists and tourist destinations. The advantages of tour recommendations can be improved by identifying features and descriptive information only using a collapsible neural network. In order to differentiate between different features in the video, the author proposes an approved multimodal algorithm based on a multimodal in-depth study to obtain a wide range of data added by video. A combination of neural frequencies is used to provide users and video recordings, and long-term and short-term memory is used to generate historical data to provide users movies correctly. The battery and finally improve the accuracy of the instructions. The author has developed models of travel recommendations as the rupture of the neural network interferes with excessive travel information [15].

3. Methods

3.1. Related Work. In the past, recommendations for tourists were rarely considered in the recommendations for tourists,

but these recommendations contain the notion of tourism, which is the basis of reason important for others to measure. The authors combine the connections of neural networks and cofiltering methods to obtain and distribute features through the connections of neural networks and estimate user rating using the coax filtering method-filtering. Among them, decomposing the role in the agreement would be to alleviate the problem of data thinning of the disrupted neural network sharing method, which can preserve the shared knowledge and personal experience advantage of the shared filter method.

3.1.1. Cotest approval algorithm. For the most commonly used recommendations, the key concept of integrated filters is to calculate the compatibility of users or products to complete the agreement [4]. A consumer sharing algorithm filter algorithm counts the similarities of users, creates proximity user groups, and then provides product satisfaction to the user group close to each other; the product-based cofilter approval algorithm takes into account the similarity of the products; the standard-based cofilter approval algorithm combines some smart models, train, and test data so that the user can get the desired information better when making the recommendations.

Considering the consistency is important for finding potential customers or products nearby. The most common methods for calculating consistency are the Pearson method and the cosine method. Among them, Pearson's similarity is necessary for computing data and determining different users in more detail, so model (1) is shown as follows:

$$\text{sim}(a, b) = \frac{\sum_{i \in I_{a,b}} (R_{a,i} - \bar{R}_a)(R_{b,i} - \bar{R}_b)}{\sqrt{\sum_{i \in I_{a,b}} (R_{a,i} - \bar{R}_a)^2 \sum_{i \in I_{a,b}} (R_{b,i} - \bar{R}_b)^2}} \quad (1)$$

In formula (1), $\text{sim}(a, b)$ represents the similarity between users a and b ; $I_{a,b}$ are the common user characteristics of users a and b ; $R_{a,i}$ is the i th eigenvalue of user a , $R_{b,i}$ is the

TABLE 1: Classification of recommendation models based on reinforcement learning.

Type	Traditional reinforcement learning recommendation		Deep reinforcement learning recommendation	
	MAB-based recommendation	MDP-based recommendation	Recommendation based on value function DRL	Recommendation based on policy gradient DRL
Enter	Actions/States and actions	State and action/State	State and action/State	State and action/State
Output	Reward value	Q value	Q value	Probability of taking an action
Feature	Maximize step reward MusicCN-Bandit DCdrift CoLin	Maximize total reward Constrained PSRL Multi_With Bic-RL	Maximize total reward DRN Robust DEERS	Maximize total reward LEAP CRS Top-k Corrected RCR
Literature model	Corr-Bandit MF-Bandit e-TSbandit DMCB POMDP-Rec Web-bandit	Bayes-UCB-CN ϵ -SVR-C DPG-FBE DJ-MC APG IRL-based	FeedRec GAUM SLATEQ Pseudo Dyna-Q Value-aware UDQN GCQN	REINFORCE MARDPG LSIC VL-Rec TPGR MaHRL HRL-Rec KERL LIRD KGRL NRRS

ith eigenvalue of user b ; \bar{R}_a and \bar{R}_b are the average feature scores of users a and b , respectively.

The author divides users and objects into K groups and adopts the new dynamic evolution group algorithm for similar groups. Integrated filter systems are used to estimate each group of K , and it is recommended that the target user be estimated according to the level of demand from the group. The use of offline experiments using an integrated integration filter algorithm improves the authenticity of group websites.

3.1.2. Metabolic neural network. The Convolutional Neural Network (CNN) is one of the current sources of in-depth research, and its use in image processing has evolved and has been widely used in text interpretation [16]. In the case of the anterior neural network, the basic structure of CNN is similar to that of other neural networks, with the entry process, the bottom layer, and the release process as the data source. The CNN secret code includes 3 layers of rotation, integration, and integration. Among these, the convolution process is the most important, resulting in the calculation of the rotation of the convolution core, which contains the signal input and extractor characteristics, and the data processing in the deep case; the pool consolidation layer filters the extracted material by aggregating, reducing the residual material, and preserving the data of the core material [17]; a single layer combines all the function data completed in the top layer and sent to the output process. The CNN model can be seen in Figure 3.

Use the nonlinear features of the convolutional layer and the pooling layer in the convolutional neural network to filter the microblog text content, ensuring the security of search information. Combining the outputs of deep convolutional neural networks and weighted feature extraction, implement correlation extraction between user data and music.

3.2. Construction of Travel Recommendation Model

3.2.1. Problem description. The goal of the author's study is to develop travel recommendations based on a user-friendly integration algorithm, which is used to deepen the experience deep neural network because it is difficult to solve the inadequacy of deep data separate and interpret tourism information. Visitors commenting on the tourism industry have different views on the tourism process, which is divided into pros and cons. Integrating important data of travel users, behavioral data, and data points to solve the problem of data alone. The specific categories of consumer data are as follows:

- (1) The basic information P_i of the user includes: name (ID), age (age), gender (sex), location (place), and other attributes, of which the name (ID) plays a unique role in identifying and does not participate in the analysis of the data, that is, $P_i = \{\text{name}_i, \text{age}_i, \text{sex}_i, \text{place}_i\}$
- (2) Behavior information S_i is divided into demand (demand), interest preference (prefer), and consumption situation (consume), namely, $S_i = \{\text{demand}_i, \text{prefer}_i, \text{sex}_i, \text{consume}_i\}$
 - (a) Demand information refers to the user's food, housing, transportation, and travel methods. Travel methods include family travel, close friend travel, solo travel, couple/couple travel, local travel, surrounding travel, and off-site travel (referring to far away from the city where you are located)
 - (b) Interest preferences include what kind of environment, what style of attractions, and what activities do you like
 - (c) Consumption situation refers to the user's price preference, such as travel mode, ticket price, and accommodation price

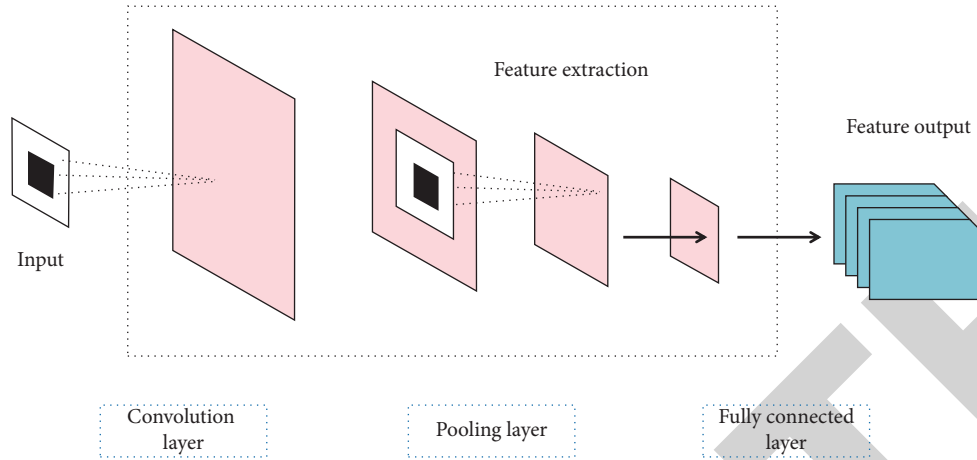


FIGURE 3: Convolutional neural network structure.

(3) Contextual information Q_i includes the time (time), the user's location (location), the user's session and interaction information (interact) on the network platform, and the session and interaction information refers to the user's visit time and the number of visits to the scenic spot, favorite records, etc., $Q_i = \{\text{time}_i, \text{location}_i, \text{interact}_i\}$.

3.2.2. *Model building.* The travel guide authors focus on three aspects of basic information, behavioral information, and the content of information in user data and send vectorized travel user review data matrix to the circulatory network for training to get a good and negative view of the product, performance data are then used for similar calculations [18]. The structure of the tourism permit is shown in Figure 4.

The basic information of tourist users is expressed as follows:

$$P = \alpha_1 \text{age} + \alpha_2 \text{sex} + \alpha_3 \text{place}. \quad (2)$$

The behavior information of tourist users is expressed as follows:

$$S = \beta_1 \text{demand} + \beta_2 \text{prefer} + \beta_3 \text{consume}. \quad (3)$$

The context information of tourist users is expressed as follows:

$$Q = \gamma_1 \text{time} + \gamma_2 \text{location} + \gamma_3 \text{interact}. \quad (4)$$

Therefore, the travel recommendation feature information is expressed as follows:

$$TR = \alpha P + \beta S + \gamma Q, \quad (5)$$

where α is the weight of basic information, $\alpha = [\alpha_1, \alpha_2, \alpha_3]$; β is the weight of behavior information, $\beta = [\beta_1, \beta_2, \beta_3]$, γ is the weight of context information, $\gamma = [\gamma_1, \gamma_2, \gamma_3]$.

The unstructured data mentioned above are processed, in which the age below 18 is recorded as 1, the age of 18 to 25 is recorded as 2, the age of 26 to 35 is recorded as 3, and the age of 36 to 45 is recorded as 4, 46 to 55 years old is recorded

as 5, 56 years old and above is recorded as 6; the gender is recorded as 0 for male and 1 for female; the same location is recorded as 1, and the difference is recorded as 0; according to the order of the above-given travel modes, they are represented by 1~7, respectively; consumption below 1000 yuan is recorded as 1, 1000~2000 yuan is recorded as 2, 2001~3000 yuan is recorded as 3, 3001~4000 yuan is recorded as 4, 4001~5000 yuan is recorded as 5, and over 5000 yuan is recorded as 6; the time is divided into spring, summer, autumn, and winter, the months from March to May are recorded as 1, the months from June to August are recorded as 2, the months from September to November are recorded as 3, and the months from December to February are recorded as 4. Use formula (1) to calculate the similarity of features between users. Since different user features have different effects on user similarity, the calculation of user similarity needs to assign corresponding weights to different features, and find similar user groups through.

$$\text{SIM}(a, b) = \alpha \text{sim}(a_p, b_p) + \beta \text{sim}(a_s, b_s) + \gamma \text{sim}(a_Q, b_Q). \quad (6)$$

After the vector data is input into the convolutional neural network, the inner product is calculated with the convolution kernel in the convolution layer, the convolution layer contains multiple convolution kernels, and each attribute element that constitutes the convolution kernel has its own weight coefficient and offset when the size of the processed tourism vector data is smaller than the original tourism vector data, zero can be used to fill the sample boundary. The eigenvalues of the convolutional neural network can be calculated by the following equation:

$$c_i = f(w \cdot \text{vec}_i + b). \quad (7)$$

In formula (7), w is the convolution weight value; vec_i is the word vector; b is the bias term.

Select the commonly used nonlinear sigmoid activation function to complete the convolution calculation and the adjustment of the weight offset, the activation function is

$$\text{sigmoid}(x) = \frac{1}{1 + e^{-x}}. \quad (8)$$

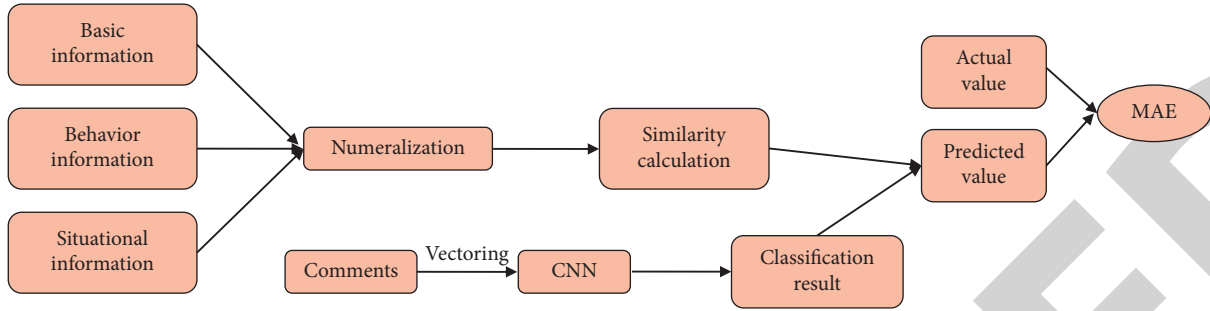


FIGURE 4: Recommendation model structure.

The data after convolution calculation enters the pooling layer, and the maximum pooling method is used to obtain the result. There are no separate weight coefficients in the pooling layer. Assuming that the tourist user data obtained by the convolutional layer is $U = \{u_1, u_2, \dots, u_s\}$, the pooling result P is

$$P = \max(U) = \max\{u_1, u_2, \dots, u_s\}. \quad (9)$$

After the pooling result reaches the fully connected layer, through the ReLU activation function, the final tourist user implicit feature information TR and the adjusted weight coefficient and deviation are obtained, and then the result is output, the calculation formula (10) is as follows:

$$TR = \text{ReLU}(w \cdot \text{vec}_i + b). \quad (10)$$

$\text{ReLU}(x) = \max(0, x)$ in formula (10).

The convolutional neural network classifies the positive and negative of the reviews by whether there are direct classifiers that express emotional factors in the tourist reviews, according to the proportion of positive and negative word vectors, sort from high to low, and rate it. 100% of the positive words in the comments are scored as 5 points, 99% of the positive words are scored as 4.9 points, and so on, until 1 point, and then the predicted users are recommended according to the ranking order.

4. Results and Discussion

4.1. Experimental Data and Processing. The author records travel information to 32 scenic spots of grades 5A and 4A with specialized software and credit scores listed on the Ctrip website. First, it removes duplicate files, blank files, and inaccurate files from useless areas in the file; I data are then placed in a sound filter, i.e., indirect markings are removed; the quoted data is then filtered and segmented by *Python's* jieba keywords and stopwords. Since the union neural network has some requirements for the length of the input vector, the length of the sentence must be combined after segmenting the word. The length of the data segmentation points is usually about 50, so sentences as long as 50 are selected, and the background or pattern can be used if the length is insufficient or too long. Integration of information affects all aspects of tourism and recreation; Then use word2vec to vector the file sharing of word segmentation;

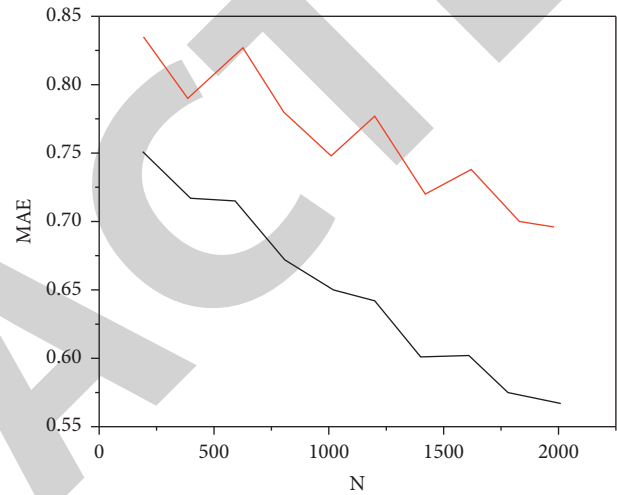


FIGURE 5: Comparison of experimental results.

send vectorized multidimensional data to the neural network to decompose operations [19].

4.2. Experimental Results and Analysis. To better understand the benefits of a combination of neural network and cofiltering techniques, the author compares this model with a conventional cofiltering technique, which only measures the users and products, and the experimental results can be seen in the figure [20]. Figure 5 shows that the MAE cost of the collection method is lower than that of the filtration process, which shows the sensitivity of the data in the data of tourists, status information, and assumptions can improve the accuracy of the recommendations. As the value of the data in the rating increases, the value of MAE increases, but this shows that one preference decreases altogether, which means that the quality of the structure will deteriorate when data is large more certification.

5. Conclusion

Given the inadequacy of natural travel information, the author presents models of travel information based on the interconnectedness of neural networks. The design uses a circulatory neural network to divide the positive and negative emotions that exist in the analysis by analyzing and studying tourist information, behavioral data, information

Retraction

Retracted: Intelligent Application of Data Mining Model in Chinese International Education

Mathematical Problems in Engineering

Received 8 August 2023; Accepted 8 August 2023; Published 9 August 2023

Copyright © 2023 Mathematical Problems in Engineering. This is an open access article distributed under the Creative Commons Attribution License, which permits unrestricted use, distribution, and reproduction in any medium, provided the original work is properly cited.

This article has been retracted by Hindawi following an investigation undertaken by the publisher [1]. This investigation has uncovered evidence of one or more of the following indicators of systematic manipulation of the publication process:

- (1) Discrepancies in scope
- (2) Discrepancies in the description of the research reported
- (3) Discrepancies between the availability of data and the research described
- (4) Inappropriate citations
- (5) Incoherent, meaningless and/or irrelevant content included in the article
- (6) Peer-review manipulation

The presence of these indicators undermines our confidence in the integrity of the article's content and we cannot, therefore, vouch for its reliability. Please note that this notice is intended solely to alert readers that the content of this article is unreliable. We have not investigated whether authors were aware of or involved in the systematic manipulation of the publication process.

Wiley and Hindawi regrets that the usual quality checks did not identify these issues before publication and have since put additional measures in place to safeguard research integrity.

We wish to credit our own Research Integrity and Research Publishing teams and anonymous and named external researchers and research integrity experts for contributing to this investigation.

The corresponding author, as the representative of all authors, has been given the opportunity to register their agreement or disagreement to this retraction. We have kept a record of any response received.

References

- [1] F. Wu, "Intelligent Application of Data Mining Model in Chinese International Education," *Mathematical Problems in Engineering*, vol. 2022, Article ID 9171551, 7 pages, 2022.

Research Article

Intelligent Application of Data Mining Model in Chinese International Education

Feng Wu 

College of International Education, Minzu University of China, Beijing 100081, China

Correspondence should be addressed to Feng Wu; 20170817347@mail.sdufe.edu.cn

Received 17 July 2022; Accepted 10 August 2022; Published 28 August 2022

Academic Editor: Hengchang Jing

Copyright © 2022 Feng Wu. This is an open access article distributed under the Creative Commons Attribution License, which permits unrestricted use, distribution, and reproduction in any medium, provided the original work is properly cited.

In order to improve the effect of intelligentization of Chinese international education, this paper puts forward the application method of the data mining model. Through the collection, transformation, processing, mining, and analysis of a large number of random data generated in education and teaching, this method provides learning suggestions for learners, realizes evaluation and prediction, presents knowledge information for educators, realizes educational decision-making, and realizes the continuous optimization of the teaching process. The experimental results show that the relationship between teachers' teaching and students' scores is obtained through the analysis of association rules in data mining technology. The support and confidence of students' scores taught by teacher B are 28.57% and 72%, respectively, and the support and confidence of students' scores taught by teacher C are 19.05% and 70.59%, respectively. The two rules are established to a great extent through data association. Data mining technology can effectively optimize the effect of intelligentization of Chinese international education.

1. Introduction

In recent years, Chinese international education has been booming at home and abroad. The number of Confucius Institutes and Confucius Classrooms around the world is increasing. Chinese has entered the national education system of some countries. Some private language education institutions teach Chinese courses. The number of practitioners in this field is growing. By December 31, 2016, 512 Confucius Institutes and 1073 Confucius Classrooms had been established in 140 countries (regions) around the world. As of September 2015, there were 363 colleges and universities nationwide offering undergraduate programs in Chinese international education, with 63933 students. There are 108 institutions offering professional master's degrees, with 10133 students. 104 colleges and universities offer master's degrees in Chinese Linguistics and Philology, and 95 colleges and universities offer master's degrees in Linguistics and applied linguistics. There are 14 colleges and universities that enroll doctoral degrees in Chinese international education and 35 colleges and universities that train doctoral degrees in Chinese International Education at

doctoral programs in linguistics and applied linguistics. Many graduates of these colleges and universities will find jobs in Chinese international education. On the surface, international Chinese education is developing rapidly from talent training to teaching research. The annual global Confucius Institute Conference has more than 1000 participants, and the number of members of the world Chinese language teaching association has also increased significantly. By 2013, the number of members has grown from more than 270 in 16 countries and regions at the beginning of its establishment to 4415 from 69 countries and regions at present. However, the basic research and applied research of Chinese international education are far from meeting the needs of diversified teaching. The demand for resources for Chinese teaching in the world is unprecedented, and the supply of resources obviously cannot keep up [1, 2].

The expansion of Chinese international education needs to innovate information technology, shift the focus from technological innovation to technological application, improve information construction, promote the Chinese language and culture internationally, give play to the important role of Chinese in international exchanges, and enhance the

national cultural soft power. In today's information-based and globalized society, with the improvement of China's comprehensive strength, the state attaches great importance to language development, and the information-based development of Chinese international education is increasingly valued. With the cooperation between linguistics, informatics, sociology, psychology, communication, and other related disciplines, we can make use of the research results of more disciplines to devote ourselves to the international education of Chinese and its promotion. At present, more and more overseas people realize that Chinese is an important tool to understand China and its language and culture. The international promotion of Chinese is developing rapidly, and Confucius Institutes are blooming everywhere. The number of overseas learners of Chinese as a second language is rising, and the gap among teachers in Chinese international education is growing. Therefore, it is of great strategic and practical significance to study and develop the technical theory of Chinese International Education and to think about its information construction methods and significance.

2. Literature Review

As human society enters the information age, education also enters the information age with human society, that is, the education information age. In the information age, the introduction of new educational technology has promoted the rapid growth of educational informatization, and a large amount of data have been generated and accumulated in the database. However, understanding these data has gone far beyond the scope of people's ability. Finally, a large amount of data cannot be effectively used, forming the phenomenon of information island, data explosion but poor knowledge [3]. In response to this challenge, data mining technology came into being and showed strong vitality. It can find hidden and ignored rules and patterns from the vast ocean of data, so as to better support decision-making. The application of data mining in education informatization aims to find useful information from the massive data collected by the electronic education system. The ultimate purpose is to benefit all participants in the education system, provide a basis for solving the semistructured and unstructured decision-making problems in the field of education, and better promote the development of education informatization. Traditional data mining in the solution side is rarely considered from the perspective of users' use. It pays more attention to professional issues, such as algorithms and system design. It is oriented by the data mining system. Such a system has very high requirements for professionals. It is generally only applicable to professionals, and it is not very applicable to nonprofessionals. Therefore, many enterprises need additional development costs for such a data mining system with high professional technology content [4].

3. Research Methods

3.1. Overview of Data Mining. Data mining is a process of discovering the relationship between models and data in massive data by using various analysis tools and revealing

meaningful connections, patterns, and trends by carefully analyzing a large amount of data; it is a knowledge mining process that uses pattern cognition, statistics, and mathematics to extract unknown and operable information from large databases. Synonyms similar to data mining include knowledge mining, knowledge extraction, pattern analysis, and data fusion [5].

3.2. Research on Data Mining Model

3.2.1. Data Mining and Knowledge Discovery. Knowledge retrieval and data retrieval is a combination of intellectual, machine learning, and database technology. Knowledge exploration (KDD) is considered as the whole process of extracting the necessary knowledge from the data, and the data extraction is considered as a special stage in the KDD layer. Process uses a special process to delete patterns from a file. Discovery is a discussion topic that covers a wide range of areas, including technology education, style knowledge, information intelligence, knowledge, information representation, high performance, and expert [6]. KDD is an advanced process of extracting standards that is reliable, cost-effective, and understandable by big data. "Garim" can be considered as the foundation of knowledge that creates knowledge after examination and improvement [7].

As shown in Figure 1, the data mining process consists of the following steps:

- (1) Data cleaning: remove data noise and data obviously irrelevant to the mining topic;
- (2) Data integration: in the future, the related data in the white multi data sources will be combined together;
- (3) Data selection: extract data related to analysis tasks from the database;
- (4) Data conversion: convert the data into a data storage form that is easy for data mining;
- (5) Data mining: this is an important step in developing knowledge. Its function is to apply data structures or intelligent processes to the extraction of knowledge permanently;
- (6) Pattern evaluation: select meaningful patterns and knowledge from the mining results according to certain evaluation criteria;
- (7) Knowledge representation: its function is to use visualization and knowledge expression technology to show the relevant knowledge mined to users.

Data mining steps can interact with users or knowledge bases, provide interesting patterns to users, or store them in knowledge bases as new knowledge [8]. Data mining is used to discover hidden patterns, which is the most important step in the whole process of knowledge discovery.

Based on the data mining process shown in Figure 2, a typical data mining system is shown in Figure 2, which mainly includes the following main components:

- (1) Database, data warehouse, or other databases: this indicates that data mining objects contain one or

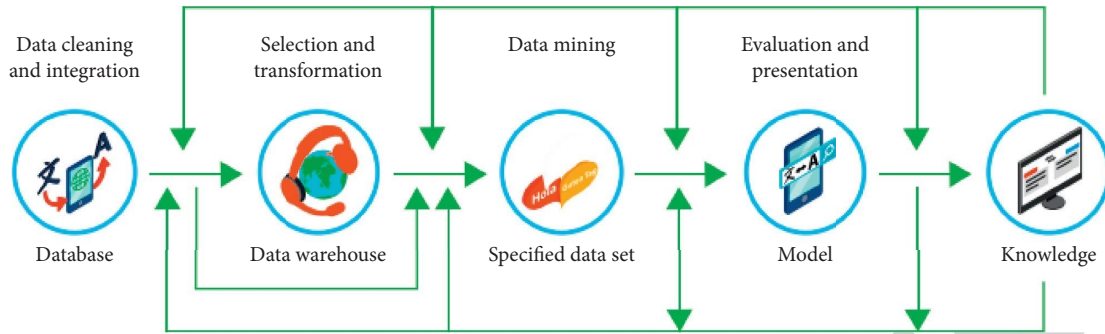


FIGURE 1: Schematic diagram of the whole process of data mining.

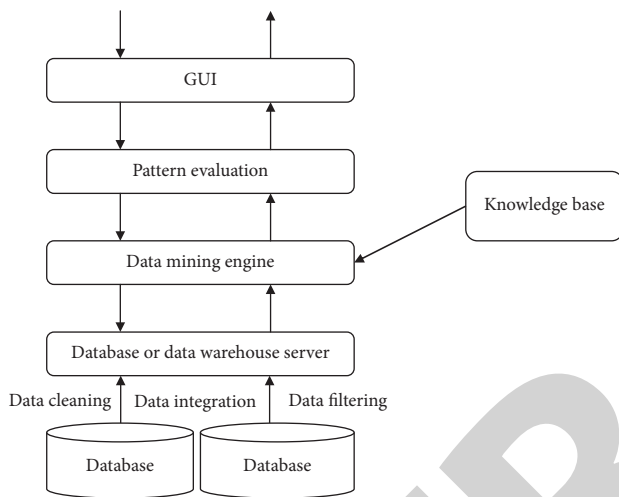


FIGURE 2: Overall structure of data mining system.

more databases, data warehouses, data tables, or other databases. In general, data processing and data aggregation should be done prior to the implementation of the equipment.

- (2) Database or data storage server: this type of server is responsible for reading the affected data as per the user's data extraction request;
- (3) Basic knowledge: it is used to store the registry knowledge needed for data retrieval. This knowledge can help guide data mining processes or measure mining profits.
- (4) File deletion: this is the most important part of file deletion. It usually consists of a group of mining functional modules to perform mining functions such as qualitative induction, organizational analysis, distribution induction, evolutionary arithmetic, and deviation analysis [9].

3.2.2. Task Model of Data Mining

(1) *Concept Type Description: Qualitative and Comparative.* A concept is often an overview of the overall situation of a data set containing a large amount of data. Data are associated with categories or conceptual models, a large number

of data sets are summarized, and concise and accurate descriptions are obtained. Such descriptions are called conceptual descriptions. This description is called conceptual description. There are mainly two methods to obtain the concept description: one is to use more generalized attributes to summarize the analyzed data, which the analyzed data are called the target data set. The other compares the characteristics of two types of data analysis and provides a summary of the results, and the two types of data analysis are called plan data and comparison data.

(2) *Association Analysis.* Association analysis is used to discover association rules that show the condition that attribute values frequently appear together in a given data set. Association analysis is widely used in transaction data analysis. It is more formally described as follows: association rules are rules in the form of $X \Rightarrow Y$, that is, $A_1 \wedge \dots \wedge A_m \Rightarrow B_1 \wedge \dots \wedge B_n$ where $A_i (i \in \{1, \dots, m\}), B_j (j \in \{1, \dots, n\})$ is an attribute value pair. Association rules are interpreted as "data tuples that meet the conditions in X also meet the conditions in Y ". Correlation analysis is widely used in marketing, transaction analysis, and other application fields. Association rule mining first finds out the frequent item sets in the data, for example, sets a and B meet the minimum support threshold and then generate association rules like $A \Rightarrow B$ from them. These rules also satisfy the predefined minimum confidence threshold of the probability of satisfying B under the condition of satisfying A [10].

(3) *Cluster Analysis.* The methods of cluster analysis and classification prediction are obviously different. The classification prediction model uses the data of known categories, which belongs to the teacher-supervised learning method. However, the data processed by cluster analysis are non-categorical, which belongs to the nonteacher supervised learning method. In cluster analysis, first of all, according to the basic cluster analysis principle of "maximizing the similarity of data objects in each cluster, minimizing the similarity of data objects in each cluster," and using the calculation formula to measure the similarity of data objects, the data objects are divided into several data groups. Therefore, the similarity of data objects in one group is greater than that of data objects in different groups. Each group obtained by group analysis can be considered as a

collection of data items that fall into the same category. From this similar data, we can obtain the appropriate patterns of distributed theory by studying classification. It is also possible to obtain hierarchical models of old data that are organized by extension to the receiving group as shown in Figure 3 [11].

(4) *Heterogeneous Analysis*. Heterogeneous analysis can be described as follows: given the set of N data points or objects and the expected number of outliers K , it is found that objects are incompatible and exceptional compared with the remaining data. The problem of heterogeneous analysis can be regarded as two problems: (1) define what kind of data in a given data set can be considered inconsistent; (2) find an effective method to mine such outliers [12, 13].

3.3. *Structure and Implementation of Data Mining Model*. Data mining is an integration that affects many sectors. As shown in Figure 4, it includes database procedures, statistics, technology training, training courses, data science research, and other disciplines. In addition, depending on the data extraction process used, technology in other places may be used, such as neural networks, dim/coarse light theory, representation, inductive logic programming, or high performance. Depending on the type of data to be extracted or the data to be extracted, the data can be combined and integrated with spatial data analysis, data extraction, data acquisition design, graphic analysis, signal processing, computer graphics, web technology, economics, and psychology and participated in data research [14].

3.4. Application of Data Mining Technology in Education

3.4.1. *Selection of Teachers' Teaching Methods*. In the teaching process, teachers can use a variety of teaching methods to complete their teaching tasks such as teaching method, discussion method, experimental method, computer-assisted teaching method, visiting method, investigation method, and practice method. In general, one or several methods can be adopted. Therefore, it is possible to use data mining to determine which method to use in the next step to extract data from the data and meet the needs of learning, making it easier for students to understand knowledge [15]. For example, the evaluation of all learners in the teaching method, the evaluation of the results of learning from different teaching methods, and the process of regression linear analysis and the rules of correlation language will be used to determine which students and classes fit into these teaching methods so that further training scores can be achieved [16].

3.4.2. *Learning Evaluation and Student Feature Mining*. Learning evaluation is one of the important responsibilities of educators. Assessing students' learning behavior not only plays a role in information feedback and stimulating students' learning motivation but also means to check the curriculum plan, teaching procedures, and teaching purposes, or a way to examine students' individual differences and facilitate

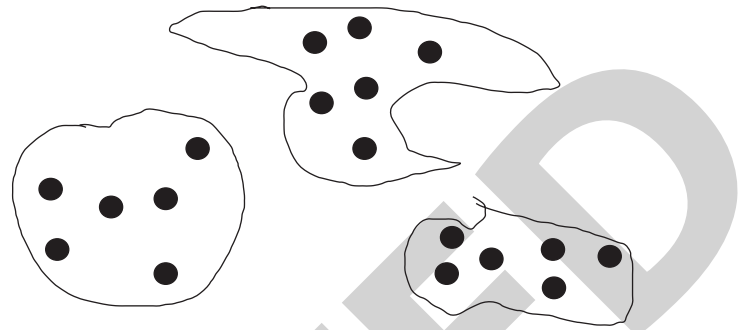


FIGURE 3: Schematic description of cluster analysis.

teaching in accordance with their aptitude. The evaluation should follow the principle of “comprehensive evaluation contents, diversified evaluation methods, multiple evaluation times, and the organic combination of self-evaluation and mutual evaluation.” By using data mining tools to analyze and process students' academic performance, behavior records, and reward and punishment databases, we can get students' evaluation results in time and correct students' bad learning behaviors in time. At the same time, it can reduce the workload of teachers and overcome the unfairness and objectivity of teachers' subjective evaluation [17].

3.4.3. *Intervention on Teacher-Student Behavior*. The school teaching management database records the learning, work, social activities, rewards, and punishments of students and teachers in each session and uses the association analysis of data mining to find the internal relationship between teachers and students' various behavior activities. For example, the rule “C can be deduced when there are a and B,” that is, when there are a behavior and B behavior, there will be C behavior. In the actual situation, if students or teachers are found to have a and B behaviors, they can immediately analyze the possibility of producing C behavior and timely formulate strategies to promote or stop the occurrence of C behavior [18].

3.4.4. *Reasonable Course Setting*. The course learning of students in school is gradual, and there is a certain relationship and order between courses. Before learning a higher-level course, you must take some precourses first. If the precourse is not well studied, it will inevitably affect the study of subsequent courses. In addition, different classes in the same grade learning the same course sometimes have great differences in the overall scores of students in the class due to different teachers and class cultures. By using the examination results of previous students in various disciplines stored in the school teaching database, combined with the related functions of data mining, such as association analysis and time series analysis, we can mine useful information from these massive data, help analyze the correlation, regression, and other properties of these data, get some valuable rules and information, and finally find the reasons that affect

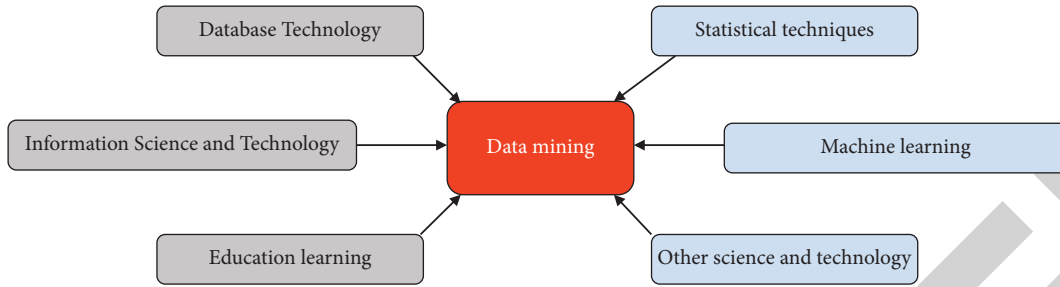


FIGURE 4: Schematic diagram of close integration of data mining and related disciplines.

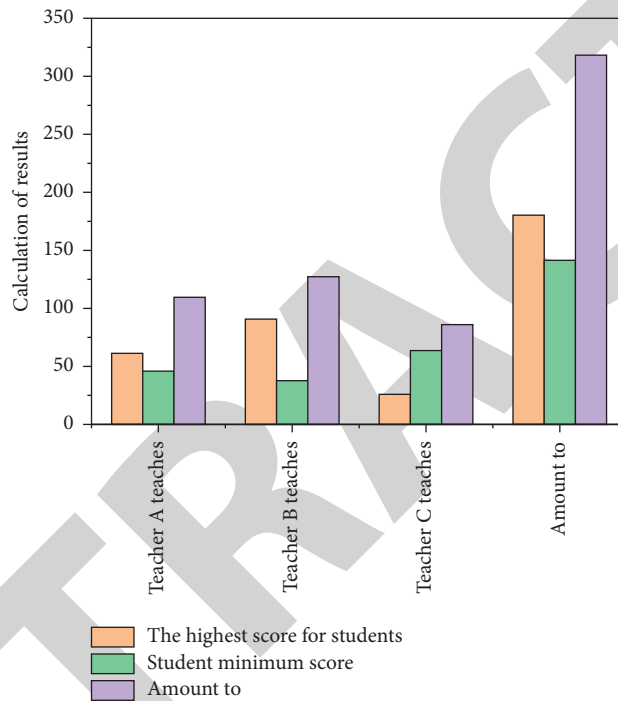


FIGURE 5: Statistical chart of final test scores.

students’ performance. On this basis, we make reasonable arrangements for the curriculum [19].

3.4.5. Examination. Examination is the test of teaching and learning effect, and it is one of the indispensable links in teaching. Although we can generally evaluate the achievements made in a certain period from the point of view of score, it does not effectively explain in which factors the score is related to, and we cannot know the key factors of success and failure in teaching, which cannot promote teaching and learning. Moreover, the level of students’ scores is also closely related to the quality of test questions. Therefore, exploring effective methods to evaluate the quality of test questions (difficulty of test questions, comprehensiveness of knowledge points, etc.) is also of great significance in the actual teaching process. If the association rules in data mining are applied to the test paper analysis database, and then, indicators such as difficulty, discrimination, and relevance of each question are analyzed according to the student’s scores, and teachers can

make a more accurate evaluation of the quality of the test questions and then can be used to check their own teaching situation and students’ mastery and provide guidance for future teaching.

4. Result Analysis

Classroom teaching evaluation not only regulates, controls, guides, and promotes teaching but also has strong guidance. It is an important part of school teaching management and the main means to evaluate teaching achievements [20]. The school conducts a classroom teaching evaluation survey every semester, accumulating a large amount of data. By using data mining technology and applying association rules to teaching evaluation data, we can mine some useful data, reasonably configure class teachers and enable students to better maintain a good learning attitude, so as to provide decision support information for teaching departments, promote better teaching work, and improve teaching quality.

TABLE 1: Table of support and confidence.

	Teacher A	Teacher B	Teacher C	Teacher A	Teacher B	Teacher C
	\geq Maximum score	\geq Maximum score	\geq Maximum score	\geq Minimum score	\geq Minimum score	\geq Minimum score
Support	19.05%	28.57%	7.94%	14.29%	11.11%	19.05%
Confidence level	57.14%	72.00%	29.41%	42.86%	28.00%	70.59%

For example, the final test scores of students taught by different teachers are shown in Figure 5.

It is advisable to set “teacher A’s teaching \geq student’s high score” as $X \Rightarrow Y$, and then, the support and confidence of the association rule “teacher A’s teaching \geq student’s high score” are (1) and (2), respectively.

$$\text{Support}(X \Rightarrow Y) = \frac{60}{315} = 19.05\%, \quad (1)$$

$$\text{Confidence}(X \Rightarrow Y) = \frac{60}{105} = 57.14\%. \quad (2)$$

By analogy, calculate the support and confidence of other associations, as shown in Table 1.

The support and confidence of “teacher B teaching \geq - students get high scores” are 28.57% and 72%, respectively, and the support and confidence of “teacher C teaching \geq - students get low scores” are 19.05% and 70.59%, respectively, indicating that these two rules are tenable to a large extent.

5. Conclusion

This article introduces the use of data mining technology to improve the learning experience. Gaining the necessary knowledge from a wide range of documents can not only support further refinement, improvement, and refinement of the study but also address issues. Of learning, analysis of the rules of the data mining technology organization provides a correlation between the faculty and the scores of the students. The support and confidence of students’ scores taught by teacher B are 28.57% and 72%, respectively, and the support and confidence of students’ scores taught by teacher C are 19.05% and 70.59%, respectively. After data association, the two rules are established to a large extent. Therefore, data mining technology can effectively optimize the effect of intelligentization of Chinese international education.

Data Availability

The data used to support the findings of this study are available from the corresponding author upon request.

Conflicts of Interest

The authors declare no conflicts of interest.

References

- [1] J. Gonondo, “Confucius institute and the development of Chinese language teaching in Cameroon,” *Journal of Education and Practice*, vol. 12, no. 3, pp. 34–39, 2021.
- [2] A. Cun and M. Mcvee, “Experiences of Chinese international students within higher education: a narrative study,” *Pedagogies*, vol. 17, no. 3, pp. 1–22, 2020.
- [3] C. Wei and L. Zhong, “Research on the problems and countermeasures of higher education management informatization development in the computer internet era,” *Journal of Physics: Conference Series*, vol. 1992, no. 2, Article ID 022126, 4 pages, 2021.
- [4] A. A. Jalal and B. H. Ali, “Text documents clustering using data mining techniques,” *International Journal of Electrical and Computer Engineering*, vol. 11, no. 1, pp. 664–670, 2021.
- [5] S. A. Wulandari, H. Kuswara, and N. Palasara, “Analisis penerapan data mining pada penjualan kerupuk rambak menggunakan metode naïve bayes classifier untuk optimasi strategi pemasaran,” *Jurnal SITECH: Sistem Informasi dan Teknologi*, vol. 3, no. 2, pp. 83–94, 2021.
- [6] Z. J. Wang, J. Wang, X. Zeng, and Y. Xing, “Knowledge discovery and data mining-based garment size selection for mass customization,” *Journal of Fiber Bioengineering and Informatics*, vol. 13, no. 3, pp. 113–128, 2020.
- [7] B. Zhu, L. Zhang, and Y. Zhang, “The early warning method of drug adverse reaction monitoring based on data mining algorithm was studied,” *Journal of Physics: Conference Series*, vol. 1852, no. 3, Article ID 032052, 2021.
- [8] M. Liao, J. Patton, R. Yan, and H. Jiao, “Mining process data to detect aberrant test takers,” *Measurement Interdisciplinary Research and Perspectives*, vol. 19, no. 2, pp. 93–105, 2021.
- [9] B. S. Ahmed, M. L. Ben Maâti, and M. Al-Sarem, “Predictive data mining model for electronic customer relationship management intelligence,” *International Journal of Business Intelligence Research*, vol. 11, no. 2, pp. 1–10, 2020.
- [10] H. Lu, H. Shinzawa, and S. G. Kazarian, “Intermolecular interactions in the polymer blends under high-pressure co2studied using two-dimensional correlation analysis and two-dimensional disrelation mapping,” *Applied Spectroscopy*, vol. 75, no. 3, pp. 250–258, 2021.
- [11] M. Hourqueig, G. Bouzille, M. Mirabel et al., “Risk of atrial fibrillation in hypertrophic cardiomyopathy: a clustering analysis based on the French registry on hypertrophic cardiomyopathy (remy),” *Archives of Cardiovascular Diseases Supplements*, vol. 13, no. 1, pp. 21–22, 2021.
- [12] J. Wang and J. Yu, “Train performance analysis using heterogeneous statistical models,” *Atmosphere*, vol. 12, no. 9, p. 1115, 2021.
- [13] V. Oleshko, “Phase evolution analysis during real-time solid-state chemical lithiation of crystalline thin window silicon membranes using low-loss stem-eels imaging,” *Microscopy and Microanalysis*, vol. 27, no. S1, pp. 2728–2730, 2021.
- [14] Y. Li, H. Zhang, and S. Liu, “Applying data mining techniques with data of campus card system,” *IOP Conference Series: Materials Science and Engineering*, vol. 715, no. 1, Article ID 012021, 2 pages, 2020.
- [15] Y. Zhang, X. Kou, Z. Song, Y. Fan, M. Usman, and V. Jagota, “Research on logistics management layout optimization and real-time application based on nonlinear programming,” *Nonlinear Engineering*, vol. 10, no. 1, pp. 526–534, 2021.

Retraction

Retracted: Trajectory Tracking of Soccer Motion Based on Multiobject Detection Algorithm

Mathematical Problems in Engineering

Received 26 September 2023; Accepted 26 September 2023; Published 27 September 2023

Copyright © 2023 Mathematical Problems in Engineering. This is an open access article distributed under the Creative Commons Attribution License, which permits unrestricted use, distribution, and reproduction in any medium, provided the original work is properly cited.

This article has been retracted by Hindawi following an investigation undertaken by the publisher [1]. This investigation has uncovered evidence of one or more of the following indicators of systematic manipulation of the publication process:

- (1) Discrepancies in scope
- (2) Discrepancies in the description of the research reported
- (3) Discrepancies between the availability of data and the research described
- (4) Inappropriate citations
- (5) Incoherent, meaningless and/or irrelevant content included in the article
- (6) Peer-review manipulation

The presence of these indicators undermines our confidence in the integrity of the article's content and we cannot, therefore, vouch for its reliability. Please note that this notice is intended solely to alert readers that the content of this article is unreliable. We have not investigated whether authors were aware of or involved in the systematic manipulation of the publication process.

Wiley and Hindawi regrets that the usual quality checks did not identify these issues before publication and have since put additional measures in place to safeguard research integrity.

We wish to credit our own Research Integrity and Research Publishing teams and anonymous and named external researchers and research integrity experts for contributing to this investigation.

The corresponding author, as the representative of all authors, has been given the opportunity to register their agreement or disagreement to this retraction. We have kept a record of any response received.

References

- [1] Y. Xie, "Trajectory Tracking of Soccer Motion Based on Multiobject Detection Algorithm," *Mathematical Problems in Engineering*, vol. 2022, Article ID 3602074, 8 pages, 2022.

Research Article

Trajectory Tracking of Soccer Motion Based on Multiobject Detection Algorithm

Yuping Xie 

Chengdu Vocational & Technical College of Industry, Chengdu 610213, Sichuan, China

Correspondence should be addressed to Yuping Xie; 2018212646@mail.chzu.edu.cn

Received 27 June 2022; Accepted 9 August 2022; Published 27 August 2022

Academic Editor: Hengchang Jing

Copyright © 2022 Yuping Xie. This is an open access article distributed under the Creative Commons Attribution License, which permits unrestricted use, distribution, and reproduction in any medium, provided the original work is properly cited.

In order to improve the tracking ability of soccer robot in the complicated static and dynamic environment, a method of soccer trajectory tracking based on multiobject detection algorithm is proposed. This method makes use of the advantages of convenient polar coordinate calculation and realistic path simulation and puts the path coding of the soccer robot in two-dimensional polar coordinates. Then, the distance relationship between the current path point, the next path point, and the obstacle point is used to judge whether to carry out path planning. When the obstacle is encountered, the improved PSO algorithm with nonlinear inertia weight is called to carry out path planning. The simulation results show that under two obstacles, when the number of iterations is $T = 19$, the soccer robot starts to avoid obstacles and intercept. When iteration number $T = 10$, the soccer robot starts to avoid obstacles and intercept side by side. Under multiple obstacles, when $T = 19$, the soccer robot starts to avoid obstacles and intercept in front. When $T = 30$, the soccer robot reaches the target point. The convergence of the improved PSO algorithm and the effectiveness of path planning are verified.

1. Introduction

Soccer robot not only contains all the contents of multiagent system but also contains a more demanding dynamic environment and real-time requirements than the general system. First of all, soccer robot competition is a distributed multirobot system in which a group of robots fight against another group of robots, in which each robot is an intelligent body with decision-making ability [1]. In the course of the game, each robot can not only exert its individual ability but also exert its collective strength through coordination and cooperation. Second, the robots of each team on the playing field run everywhere for shooting or defending, making it a very complex dynamic environment that changes from moment to moment. Third, in order to defeat the other side, the robot teams of both sides must understand the dynamic changes of their own and the enemy camps in real time and make behavioral decisions based on the dynamic changes, namely, strategic issues such as overall attack, partial attack, or defense [2]. At the same time, in order to implement this decision, all agents must solve the problem of coordination

and cooperation through communication [3]. Similarly, path planning has a wide range of applications, such as cruise missile path planning, aircraft path planning, robot manipulator path planning, TSP and its derivation of virtual assembly path planning and vehicle (VRP) path planning, road network based path planning, routing problems, electronic map GPS navigation path search and planning. In recent years, the research on robot path planning has made great progress in the depth and scope of the problem and formed a multidimensional research integrating theory, algorithm, and application. At the same time, some new intelligent algorithms have made significant breakthroughs with the gradual deepening of people's research on natural phenomena and biological populations. Intelligent algorithm is the focus and hotspot of current path planning method research. Many new intelligent optimization algorithms have been applied in path planning, such as immune algorithm, immune genetic algorithm, immune chaos algorithm, particle swarm algorithm, ant colony algorithm, hybrid optimization algorithm, and heuristic search method. The emergence of these new intelligent optimization

algorithms that simulate or refer to biological behaviors further stimulates the enthusiasm of researchers for theoretical and applied research on intelligent information processing systems and improves the development speed of highly intelligent information processing systems. Figure 1 shows a robust target tracking method and process that integrates detection processes.

2. Literature Review

The early work on mobile robot path planning mainly focused on mobile robot obstacle avoidance in a static obstacle environment, which has been very mature. At present, the research focuses on dynamic path planning of mobile robots in a complex environment, including obstacle avoidance between mobile robots and static obstacles and collision avoidance between dynamic obstacles. To solve these problems, scholars at home and abroad have proposed a variety of dynamic path planning methods and achieved some results. Huang et al. proposed the method of rectangular wave transmission in the path planning process. In the transmission process, it is assumed that the wave reaches the grid cells of eight adjacent positions at the same time, which is easy to realize, but it is easy to cause the generated actual path is not the shortest path [4]. Therefore, Liu et al. proposed to replace a rectangular wave with the circular wave, assuming that the wave first reaches four grid units in horizontal and vertical directions and then four grid units on diagonal lines during transmission [5]. The circular wave solves the problem of the arrival of grid waves in different directions but increases the complexity of implementation. Kim et al. proposed the double-wave propagation algorithm, which reduced the time and space costs, and also took into account the influence of different terrain environments on path planning [6]. Aharonov et al. discussed the wave propagation path planning algorithm based on a fan-shaped grid map in polar coordinates and solved the problem of circular wave propagation radius by introducing the concepts of ring channel and ring region [7]. Zhang et al. proposed a multirobot global path planning algorithm combining an improved genetic algorithm and coevolution mechanism, which solved the local optimal problem in genetic algorithm path planning and achieved faster convergence speed [8]. Hong et al. proposed an immune genetic algorithm to complete path exploration in the complex environment [9]. Nabavi et al. proposed a static path planning method combining gravity search and particle swarm optimization, which transformed the multiobjective optimal solution problem into the optimal solution problem of a single objective, ensuring the maximum distance between the path and obstacles [10]. Malik et al. used the greedy algorithm to carry out path planning. When there were obstacles on the optimal path, they sought a new path through a turning point setting to reduce the system resources consumed by the algorithm. As the demand for robot intelligence increases, the environment it faces becomes more and more complex, and the focus of path planning research gradually turns to application research in the complex dynamic environment [11].

At present, there are several common algorithms that can be used for the path planning of soccer robot. The basic idea of the artificial potential field method is to design an abstract virtual force field to deal with the movement of robot. The target produces “gravitation” to the robot, and the obstacle produces “repulsion” to the robot. The combined force of the target can be used to control the robot’s action, which can be applied to the path planning, but the problems of local minimum and unreachable target will occur. Ant colony algorithm is a global path planning algorithm, which can search the optimal path. However, the ant colony algorithm is affected by the location of the starting and ending points and the distribution of obstacles. When the environment space of the mobile robot is complex, the optimization convergence speed of the ant colony algorithm slows down, and the ants tend to fall into the infeasible point, and even the problem of path derouting and locking appears, which reduces the efficiency of path planning. Particle swarm optimization algorithm (Particle Swarm Optimization) due to the search ability and convergence speed and higher efficiency, in the industrial production process and theory study, is widely used. It has great advantages in optimization problems, but the algorithm will converge to the local optimal solution prematurely in the process of search mechanism and optimization [12]. Static obstacle avoidance of the robot is carried out by adding dynamic inertial weights. The improved particle swarm optimization (PSO) algorithm is applied to dynamic and static obstacle avoidance of robots, which overcomes some shortcomings of pSO in the application field, such as nonconvergence, premature algorithm, and algorithm not adapting to the dynamic environment, and achieves good results.

3. The Research Methods

3.1. Soccer Robot Environment Modeling

3.1.1. Idea of Modeling. In the path planning of a soccer robot, the robot should anticipate every advance. If there is an obstacle between the current point and the next point, the PSO algorithm is used to plan the path; otherwise, the robot continues to advance along the straight line of the target point according to the specified step size (ρ) [13].

In order to make the calculation more convenient, the reciprocal formula of polar coordinates and Cartesian coordinates is shown as follows:

$$\begin{cases} x = \rho \cos \theta, \\ y = \rho \sin \theta, \\ x^2 + y^2 = \rho^2. \end{cases} \quad (1)$$

3.1.2. Obstacle Judgment. Given a polar coordinate radius ρ and its moving step is equal to ρ , the circle with the current point as the center and radius ρ will judge whether there is an obstacle. If so, it will judge whether there is an obstacle between the current point and the next point. If so, the PSO algorithm will be called. The mathematical description of the judgment criteria is as follows.

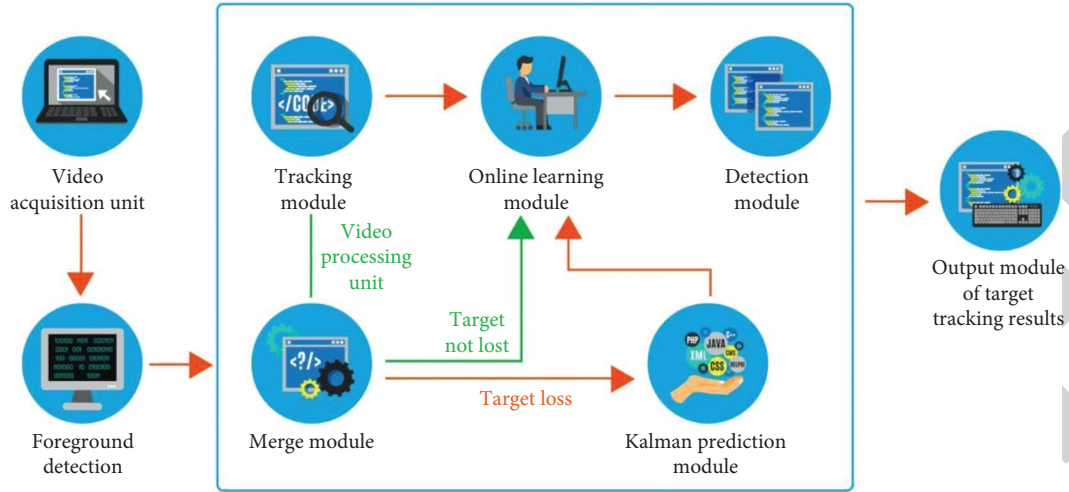


FIGURE 1: A robust target tracking method and process integrating detection process.

First, it is assumed that the robot is a small ball with radius r , the moving step size is ρ , the current point is (A_1, B_1) , the next point is (A_2, B_2) , and the obstacle point is (C_1, D_1) . Then, when $(r + \rho) > \sqrt{(A_1 - C_1)^2 + (B_1 - D_1)^2}$, it means that there are obstacles in the moving range. If $\sqrt{(A_1 - A_2)^2 + (B_1 - B_2)^2} = \sqrt{(A_1 - C_1)^2 + (B_1 - D_1)^2} + \sqrt{(A_2 - C_1)^2 + (B_2 - D_1)^2}$ indicates that the obstacle is on the line between the current point and the next point, then the PSO algorithm is called to carry out path planning; otherwise, the obstacle walks along a straight line.

3.1.3. PSO Path Planning. The current point and the next point are divided into N equal parts, each with width P/N , and a point is connected on the bisector, namely, a path L_j is obtained. Then, L_j is a particle j ($1 \ll j \ll M$, M , particles), and the dimension of the particle is, namely, a particle swarm of $M \times N$ is generated to solve the global optimal solution, namely, the optimal path.

3.2. Improved PSO Algorithm

3.2.1. Fitness Function (Fit). On the basis of taking the path length as a fitness function, the safety degree was added, and all parameters were weighted and averaged. The objective function of the shortest path length is shown in the following formula:

$$Y_{fit1} = \sum_{i=1}^n \sqrt{(x_{ji} - x_{ji-1})^2 + (y_{ji} - y_{ji-1})^2}, \quad (2)$$

(x_{ji}, y_{ji}) is the coordinates of point i on path j , and (x_{ji-1}, y_{ji-1}) is the coordinates of a point (x_{ji}, y_{ji}) on path j . At this point, the coordinate of the next point predicted by robot path planning is (x_{jn}, y_{jn}) , and this point and target point (g_1, g_2) need to be connected to calculate the path. The length function of the entire path is shown in the following formulas:

$$Y_{fit2} = \sqrt{(x_{jn} - g_1)^2 + (y_{jn} - g_2)^2}, \quad (3)$$

$$Y = Y_{fit1} + Y_{fit2}. \quad (4)$$

Degree of avoiding obstacles—degree of safety (assuming that regional robots are all circles with radius r , then the critical safety distance is $2r$)—is shown in the following formula:

$$OB(i) = \min \left\{ 0, \left[\sqrt{(x_{ji} - x_k)^2 + (y_{ji} - y_k)^2} - 2r \right] \right\}. \quad (5)$$

3.2.2. Constraint Function. If all the obstacles fall outside the circular area with robot center O as the center and radius of $2r$, the soccer robot can directly generate a straight path from the starting point to the end point. Similarly, the range of this path can be approximated as a rectangular area with a width of $4r$ and two boundary functions as the upper and lower limits. The function is shown in the following formula:

$$\begin{cases} y = kx, \\ kx - 2r\sqrt{1+k^2} \geq y, \\ kx + 2r\sqrt{1+k^2} \leq y. \end{cases} \quad (6)$$

Based on the above fitness functions, $F = A \times Y + B \times OB(i)$ can be obtained, where A and B are the weighting factors of the two functions and are any real numbers greater than or equal to zero [14]. The proportion of Y and $OB(i)$ in the fitness function can be adjusted by adjusting the size of A and B . For example, $A=1$ and $B=0$ represent the fitness function of path length only. In order to completely avoid obstacles, generally $B < A$.

3.2.3. PSO Algorithm for Nonlinear Dynamic Adjustment of Inertia Weight. The iterative formula of particle swarm velocity is shown in the following equation:

$$V_{i,j}(t+1) = wV_{i,j}(t) + c_1r_1(P_{i,j}(t) - x_{i,j}(t)) + c_2r_2(P_{g,j}(t) - x_{i,j}(t)), \quad (7)$$

where r_1, r_2 are random real numbers greater than 0 and less than 1, c_1 and c_2 are learning factors, $P_{i,j}$ is the optimal location of particle i so far, and $P_{g,j}$ is the global optimal location.

According to Equation (7), the inertia weight factor (Weight) is used to control the influence of the velocity of the previous iteration on the current velocity and has the ability to balance the global search and local search of particles: the larger the w value is, the larger the global search ability is, and the weaker the local search ability is. The smaller the w value is, the stronger the local search capability is, and the weaker the global search capability is [15]. Theoretically, as the number of iterations increases, the inertia factor of weight should gradually decrease, so that the PSO algorithm has a strong global search ability at the beginning and strong local convergence ability at the later stage.

Therefore, experts put forward the particle swarm optimization algorithm with linear decreasing law to change the inertia weight, as shown in the following formula:

$$w = w_{\max} - (w_{\max} - w_{\min}) \times \frac{K}{K_{\max}}. \quad (8)$$

However, the optimal effect of Equation (8) in PSO is not obvious. According to the idea of decreasing inertia weight, a particle swarm optimization algorithm of dynamic nonlinear decreasing inertia weight is proposed, as shown in the following equation:

$$w_{k+1} = w_{\min} + (w_k - w_{\min}) \times \left(\frac{(K_{\max} - k)}{K_{\max}} \right)^n, \quad (9)$$

where w_k is the value obtained in the current iteration, and its initial value is w_{\max} ; k represents the current iteration number; K_{\max} indicates the maximum number of iterations. The inertia weight w_{k+1} decreases nonlinearly from the initial value w_{\max} with the different value of n and the iteratively varying value of w_k [16, 17]. When $k=0$, $w_{k+1} = w_{\max}$, it goes down to a minimum of w_{\min} at $k = K_{\max}$. According to the different regions of individual particles and particle swarm, the inertia weight can decrease by different nonlinear exponents. When the individual particle and particle swarm are in the central region far from the individual extreme value and the global extreme value, take $n = 1.1$. According to Equation (9), it can be seen that the inertia weight decreases slowly, so that the inertia weight has A large value in this stage, and the particle swarm will fly to the optimal position of the swarm at A fast speed. When individual particles and particle swarm gradually approach the target optimal value, $n = 0.9$ can be taken after entering the central range. It can be seen from Equation (9) that the inertial weight drops faster, and particles conduct a more detailed search for the optimization target in the region where the optimal value is located [18].

In order to verify the convergence of the improved algorithm, Ackley function was used for testing, as shown in the following formula:

$$f(x) = 20 + e - 20 \times \exp\left(-0.2 \times \sqrt{0.5 \times (x^2 + y^2)}\right) - \exp(0.5 \times (\cos 2\pi x + \cos 2\pi y)), \quad (10)$$

where $e = 2.71282$

Function at (0,0,0, ..., 0) has a minimum value of 0. As shown in Figure 2, it can be seen that the global optimal value of the Ackley function converges to 0. After adding dynamic nonlinear inertia weight, the global optimal value converges from 120 times to 70 times. In general, the improved algorithm converges faster and more accurately.

3.3. Improve PSO Path Planning Algorithm Flow. Algorithm flow chart can be described as follows:

- (1) Set the maximum value of inertia weight w_{\max} and minimum value w_{\min} , learning factor c_1 and c_2 , group D , and maximum iteration number D_{\max} . If constraint conditions are not met, take the current point as the origin and ρ as the radius for polar coordinates and carry out ρ equal portions; otherwise, generate a linear path from the starting point to the next path point.
- (2) Randomly generate m particles and their positions X_i and velocity V_i . Set the current optimal position $P_i = (p_{i1}, p_{i2}, \dots, p_{id})$, form the initial population t_0 , P_{best_i} represents the optimal value searched by the i th particle, and G_{best} represents the optimal value searched by the whole cluster.
- (3) The initial population fitness value was calculated, and the global optimal value P_g was updated [19].
- (4) A new particle swarm t_1 was generated according to the velocity and position iterative formula.
- (5) Calculate the fitness value of t_1 . If it is better than the previous generation, the next generation particle swarm t_2 will be generated; otherwise, it will be converted to Cartesian coordinates [20].
- (6) The algorithm is over. If the maximum number of iterations is reached or the accuracy requirements are met, the constraint conditions are judged again; otherwise, the loop is continued to iterate to update the particle swarm.

4. Results Analysis

4.1. Static Obstacle Avoidance with Particle Swarm Optimization. Particle swarm optimization algorithm with dynamic nonlinear inertial weights was used for robot path planning (static obstacles) [21].

Simulation parameters are starting point [5, 5], target point [25, 25], polar radius = 5, obstacle point [20, 20], [8, 10], [10, 10], [12, 10], [24, 20], [18, 20]; learning factor $c_1 = c_2 = 1.4962$; inertia weight $w_{\max} = 0.9$; $w_{\min} = 0.4$; dimension of

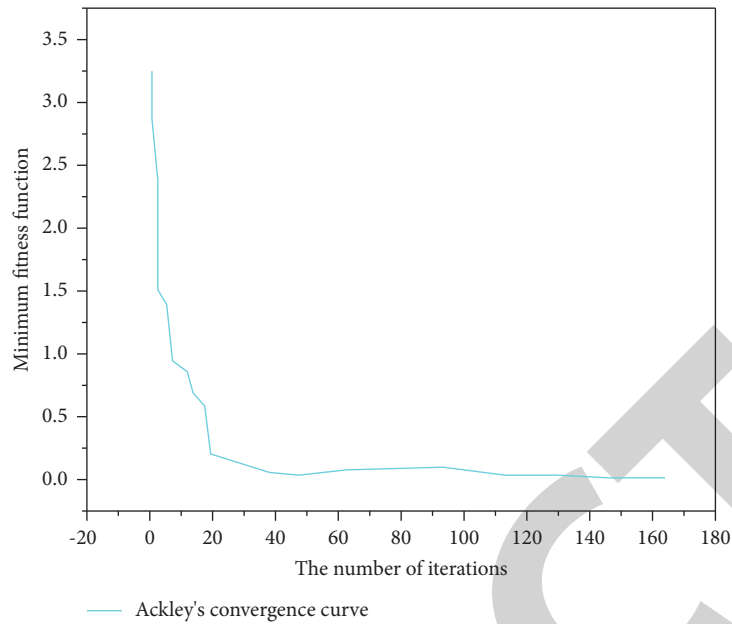


FIGURE 2: Convergence curve of Ackley function.

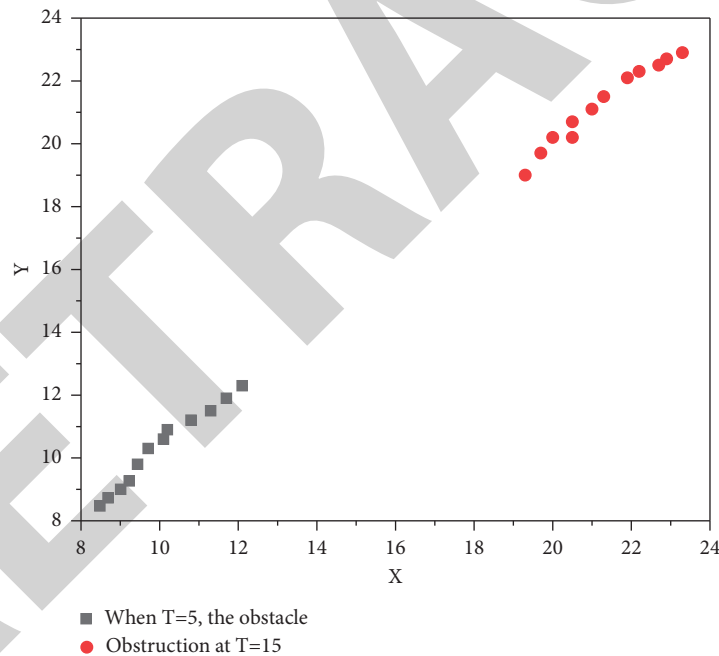


FIGURE 3: Robot path planning diagram of PSO algorithm before improvement.

search space $m = 10$; population number $N = 30$, iteration number T , maximum iteration number $DT_{\max} = 2000$;

As can be seen in Figure 3, when $T = 5$, the football robot starts to avoid the obstacle point $[10, 10]$. When $T = 15$, the football robot starts to avoid the obstacle point $[20, 20]$. The inertia weight changes according to the linear decreasing law, and the path planned by PSO can avoid obstacles, but the effect is not very obvious [22]. As can be seen in Figure 4, when $T = 5$, the football robot starts to avoid the obstacle point $[10, 10]$. When $T = 16$, the football robot starts to avoid the obstacle point $[20, 20]$. Inertial weights

change according to nonlinear dynamic laws, and the path planned by PSO can not only avoid obstacles but also have obvious effects [23].

4.2. Dynamic Obstacle Avoidance with Particle Swarm Optimization. Particle swarm optimization (PSO) with dynamic nonlinear inertial weights is used for robot path planning (dynamic obstacles).

Simulation parameters are starting point $[0,0]$, target point $[30, 30]$, polar radius $\rho = 2$, learning factor $c_1 = c_2$

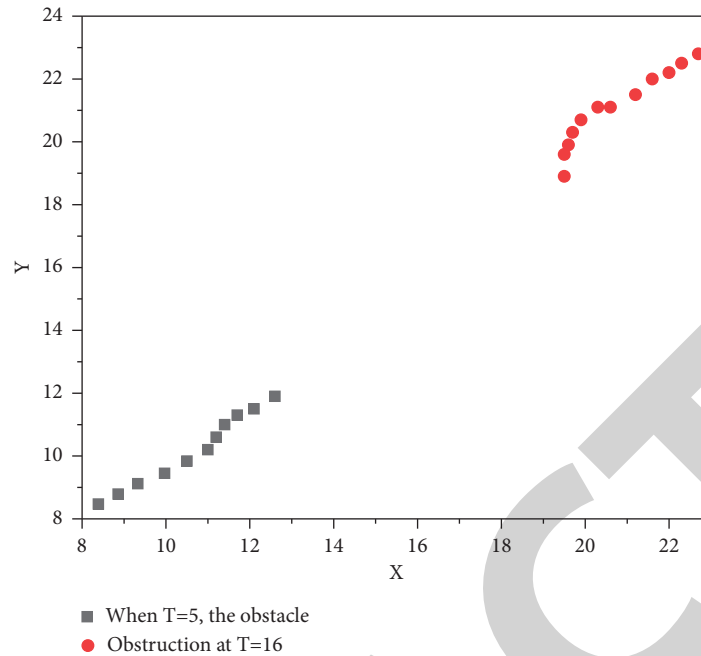


FIGURE 4: Improved PSO algorithm robot path planning diagram.

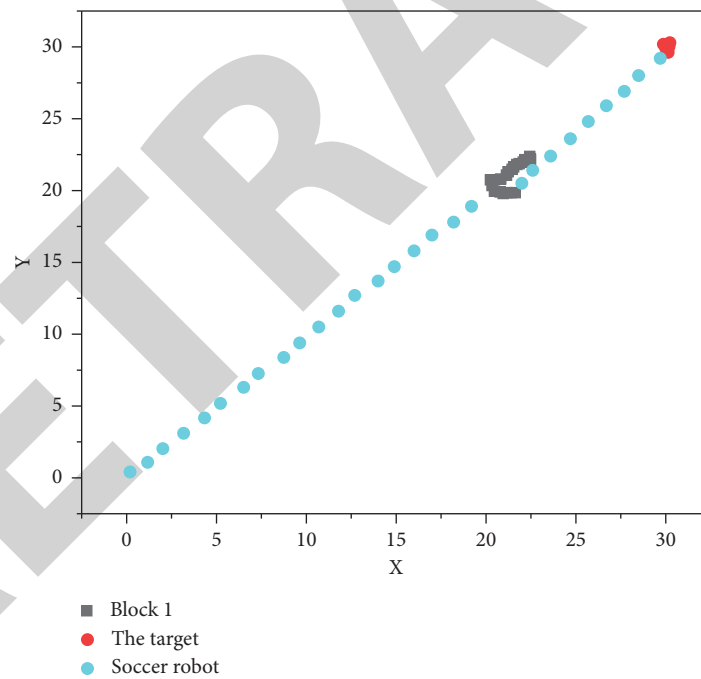


FIGURE 5: Frontal intercept obstacle avoidance.

=1.4962; inertia weight $w_{max}=0.9$; $w_{min}=0.4$; dimension of search space $m=10$; population number $N=30$, iteration number T , maximum iteration number $DT_{max}=2000$; robot speed $V_r=(1.5, 1.5)$;

Figure 5 shows 1 (22, 22), $V_o=(-0.06, -0.06)$.

Figure 6 shows 1 (10, 12), 2 (22, 22), and $V_{o1}=(-0.06, -0.06)$, $V_{o2}=(-0.1, 0.1)$.

Figure 7 shows 1 (20, 10), 2 (22, 22), 3 (24, 20), and $V_{o1}=(-0.35, 0.35)$, $V_{o2}=(-0.1, -0.1)$, $V_{o3}=(0, 0.23)$, $V_g=(-0.04, 0.04)$.

In Figure 5, when the iteration times $T=19$, the soccer robot starts to avoid obstacles and intercept in front. In Figure 6, when the iterations times $T=10$, the football robot starts to avoid the side intercept of obstacles, and when $T=19$, the football robot starts to avoid the front intercept of obstacles [24]. In Figure 7, when $T=30$, the soccer robot reaches the target point. As can be seen from Figures 5–7, the football robot can avoid obstacles in real time when facing moving obstacles in front and side interception, and chasing target points, with obvious effects [25].

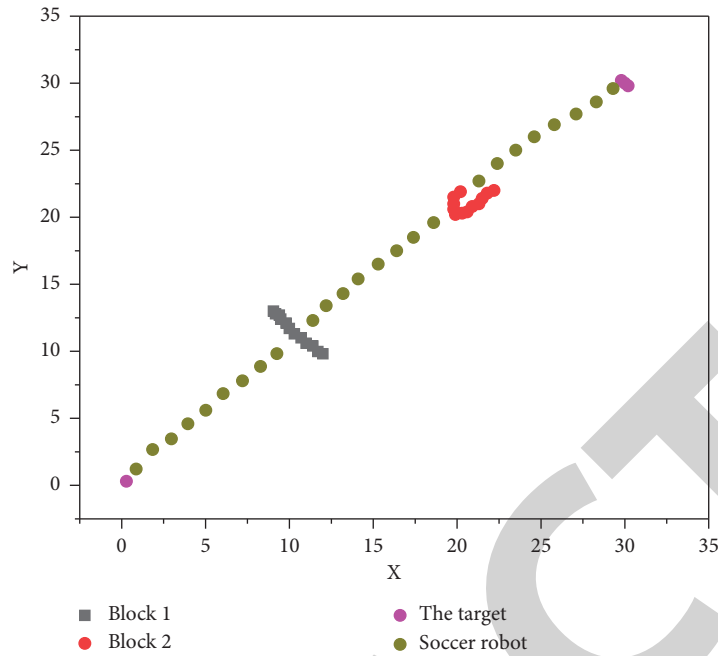


FIGURE 6: Frontal side intercept obstacle avoidance.

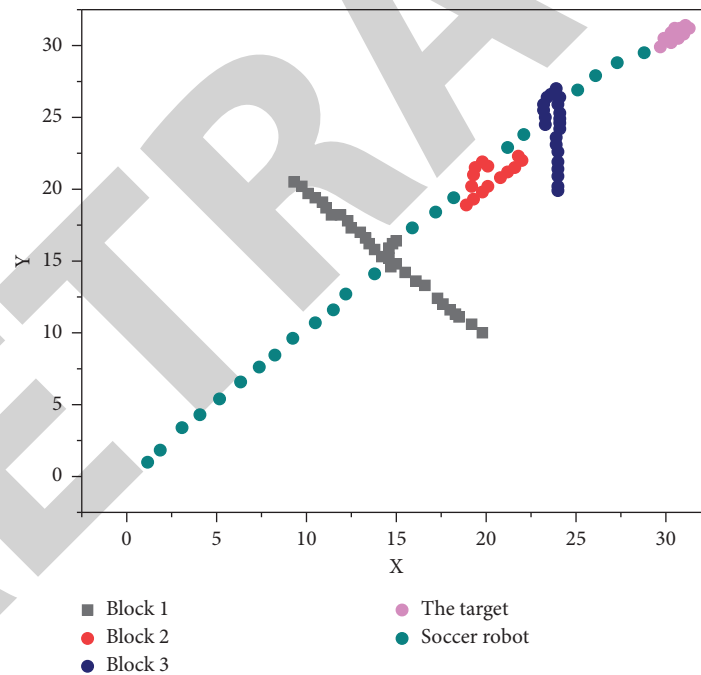


FIGURE 7: Multiple obstacles intercept obstacle avoidance chase and target.

5. Conclusion

In this essay, the path planning of soccer robot is accomplished by using the polar coordinate modeling method and improved particle swarm optimization algorithm with dynamic noninertial weights. The convergence of the algorithm is verified by the Ackley function, and the optimal path for obstacle avoidance is obtained in the face of static and dynamic obstacles. Static obstacle avoidance of the robot is carried out by adding dynamic

inertial weights. The improved particle swarm optimization (PSO) algorithm is applied to dynamic and static obstacle avoidance of robots, which overcomes some shortcomings of pSO in the application field, such as nonconvergence, premature algorithm, and algorithm not adapting to the dynamic environment, and achieves good results. The simulation results show that the improved algorithm theory achieves the research purpose, and the data fitting can meet the real-time requirements in practical application.

Retraction

Retracted: Application of Sensor-Based Intelligent Wearable Devices in Information Physical Education

Mathematical Problems in Engineering

Received 8 August 2023; Accepted 8 August 2023; Published 9 August 2023

Copyright © 2023 Mathematical Problems in Engineering. This is an open access article distributed under the Creative Commons Attribution License, which permits unrestricted use, distribution, and reproduction in any medium, provided the original work is properly cited.

This article has been retracted by Hindawi following an investigation undertaken by the publisher [1]. This investigation has uncovered evidence of one or more of the following indicators of systematic manipulation of the publication process:

- (1) Discrepancies in scope
- (2) Discrepancies in the description of the research reported
- (3) Discrepancies between the availability of data and the research described
- (4) Inappropriate citations
- (5) Incoherent, meaningless and/or irrelevant content included in the article
- (6) Peer-review manipulation

The presence of these indicators undermines our confidence in the integrity of the article's content and we cannot, therefore, vouch for its reliability. Please note that this notice is intended solely to alert readers that the content of this article is unreliable. We have not investigated whether authors were aware of or involved in the systematic manipulation of the publication process.

In addition, our investigation has also shown that one or more of the following human-subject reporting requirements has not been met in this article: ethical approval by an Institutional Review Board (IRB) committee or equivalent, patient/participant consent to participate, and/or agreement to publish patient/participant details (where relevant).

Wiley and Hindawi regrets that the usual quality checks did not identify these issues before publication and have since put additional measures in place to safeguard research integrity.

We wish to credit our own Research Integrity and Research Publishing teams and anonymous and named external

researchers and research integrity experts for contributing to this investigation.

The corresponding author, as the representative of all authors, has been given the opportunity to register their agreement or disagreement to this retraction. We have kept a record of any response received.

References

- [1] W. Chen, "Application of Sensor-Based Intelligent Wearable Devices in Information Physical Education," *Mathematical Problems in Engineering*, vol. 2022, Article ID 5075425, 7 pages, 2022.

Research Article

Application of Sensor-Based Intelligent Wearable Devices in Information Physical Education

Wanjun Chen 

Software Engineering Institute of Guangzhou, Guangzhou 510990, Guangdong, China

Correspondence should be addressed to Wanjun Chen; 201823252501039@zcmu.edu.cn

Received 11 July 2022; Accepted 10 August 2022; Published 27 August 2022

Academic Editor: Hengchang Jing

Copyright © 2022 Wanjun Chen. This is an open access article distributed under the Creative Commons Attribution License, which permits unrestricted use, distribution, and reproduction in any medium, provided the original work is properly cited.

In order to solve the heavy work tasks of teachers and improve the efficiency of classroom teaching, a sensor-based intelligent wearable device method is proposed. The method is divided into four stages: generalization-differentiation-solidification-automation. At the stage of generalization and differentiation, teachers should first demonstrate and drill the correct movements and brief notes for attention. It is not appropriate to emphasize the details of movements too much. In the movement exercise of the differentiation and solidification stage, attention should be paid to guiding students to experience the process of coordinating and generating force, and to enhance the experience of muscle sensation and perception. In the solidification stage, students' mastery of technical movements tends to be stable, and they should strengthen the combination with other mastered technical movements. In this stage, attention should be paid to the cultivation of individual technical style. The results showed that 46% of the students in the experimental group thought badminton special learning was interesting, while only 15% of the students in the control group held the same attitude. 39% of the students in the experimental group thought badminton special learning interesting, and 31% of the students in the control group; in the experimental group, 15% of students thought that their interest in badminton became average after a semester of special courses, while in the control group, 39% students should be interested in badminton. None of the students in the experimental group thought badminton learning was less interesting, while 15% of the students in the control group still felt badminton learning became less interesting. *Conclusion.* The method can effectively solve the heavy work of teachers and improve the efficiency of class.

1. Introduction

With the in-depth development of economic globalization in the twenty-first century, various high-tech information technologies have gradually developed vigorously [1]. The rapid development of information technology promotes the reform and innovation of university teaching. The trend of educational informatization and efficient utilization of resources is becoming more and more prominent. The application of intelligent wearable devices in college physical education teaching practice is a beneficial attempt to combine high-end information equipment and teaching. The successful docking of the two is conducive to improving the teaching mode, tracking mode, and evaluation mode of college physical education teaching practice, accurately docking students' practice and mastery of physical education

practice and promoting the overall good development of teaching [2].

School physical education as a basic stage of physical education is gradually being paid attention to. How to perfect the school physical education better to realize the integration of inside and outside class, making the physical education teaching process no longer limited to the classroom, and how to explore the effective extension path are the problems in front of physical education workers.

In this context, physical education in colleges and universities is gradually moving towards the direction of combining diversification, flexibility, and informatization [3]. In recent years, innovative research on wearable devices and other emerging information technologies has been frequently mentioned in various academic reports. Scholars have expounded on the development of wearable technology

in different fields from different perspectives. At present, the concept of combining wearable devices with sports has taken shape, and more and more applications and promotions combining with sports are also in progress. In the context of the rapid development of information technology, combined with previous studies on wearable technology, this article carries out a teaching experiment design for the daily teaching of badminton elective courses in colleges and universities. It tries to find new methods and means of wearable device-assisted teaching, stimulate students' enthusiasm for participation, improve the controllability and accuracy of college badminton elective teaching, and achieve the goal of steadily improving the teaching effect of college badminton elective teaching [4].

2. Literature Review

At the present stage, physical education teaching in colleges and universities in China is still relatively traditional. Through "spoon-feeding" teaching means, the preliminary mastery of skills and the attainment of students' physical fitness test are achieved, but the teaching objective of cultivating students' interest in learning and improving their subjective initiative in learning is not fully considered [5]. After the "sweet period of teachers and students", most students lack follow-up learning enthusiasm and motivation, resulting in absent-minded students in class, decreased executive ability, teachers' teaching weakness, poor teaching effect, and other phenomena. Some scholars have shown that the most significant characteristic of motor skill acquisition is that it is improved based on practice. With the progress of effective practice, the practitioner can achieve more accurate and punctual target movements. The effective practice here includes two aspects: "repetition" and "feedback." Sufficient repetitions will solidify the movements and make them proficient. Accurate feedback helps practitioners find and correct deviations in movements and achieves refinement of technical movements. The traditional teaching mode of badminton technique in colleges and universities mainly adopts teachers' explanation and demonstration and students' repeated practice. In the early stage of technical movement teaching, there are many imitation exercises, and it is difficult for students with a weak ability to construct movement representation to find the correct movement experience. However, when students make mistakes in the process of practice, they often only rely on the feedback form of the teacher's language description and demonstration to guide students to correct them. This kind of simple language description can not make students clearly recognize and understand the accuracy of their own actions, and it is easy to increase the probability of repeated guidance and correction by teachers, resulting in heavy work for teachers and greatly reducing the efficiency of classroom teaching.

An intelligent sensor is used as a novel teaching aid. The realization of its functions is based on the formation of rules of motor skills. The main task is to provide intuitive and effective information feedback for practitioners and deepen their representation cognition through the application of modern detection devices, such as intelligent sensors, in the

process of technical movement learning and practice in class [6]. Through the sensor device attached to the bottom of the badminton racket handle, the intelligent mobile terminal is connected to realize real-time monitoring of students' movements in the process of badminton practice [7]. Each swing action of students is recorded in the form of a movement track, and numerical display of swing speed, strength, radian, and other indicators, so as to replace the simple language description of teachers in the past, so that the teaching feedback information will be directly and specifically present. The teacher's explanation is optimized and the student's practice experience is enhanced.

3. Methods

3.1. The Process of Traditional Teaching Methods in Badminton Teaching. As shown in Figure 1, the traditional teaching mode is still adopted in PE technology teaching in most colleges and universities in China. It is mainly reflected in the educational thought represented by the Herbart school, which advocates that teachers are the main body of classroom teaching. Teachers mainly explain and demonstrate and students imitate and practice, showing a relatively single teaching mode. From the process guidance in the figure above, we can see that in this mode, teachers are easy to control and organize badminton classes. Using conventional teaching methods and means to teach basic skills to students, students can repeat and imitate until they master the movements. This teaching mode can help students to complete the acquisition of basic skills. However, in the teaching process, it is not conducive to give full play to students' subjective initiative and does not play a good role in promoting the improvement of students' interest in learning and the cultivation of their learning initiative.

3.2. The Process of Intelligent Sensor-Assisted Badminton Teaching. As shown in Figure 2, the use of intelligent sensors to assist badminton teaching requires teachers to actively create research-based learning modes and try to achieve simple guided teaching. Teachers are required to encourage students to make full use of real-time numerical information feedback provided by sensors (such as hitting speed, strength, and arc) and standard degree evaluation of movements in the process of practice, to form a conscious self-evaluation, and to explore standard badminton technical movements, appropriate power generation and timing. Through the effective collection of kinematic parameters in the swing process, students can be promoted to discuss and communicate with each other, deepen their understanding and grasp of correct badminton technical movements, and return to the principal status of students in class [8].

3.3. Teaching Experiment Steps of Sensor-Assisted Traditional Classroom Teaching. The main goal of badminton technology teaching is to let students master basic badminton technology and skills. When the sensor-assisted teaching mode is switched, the role of teachers is more inclined to be teaching assistant and guide.

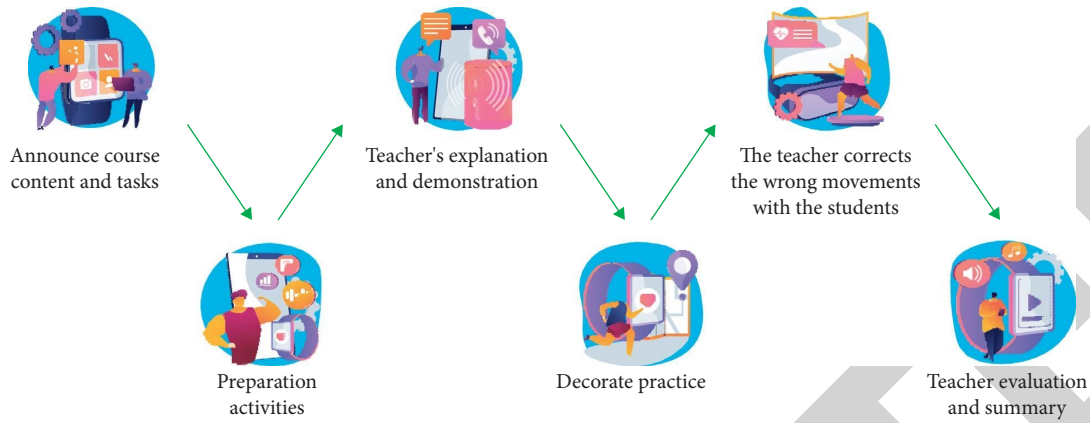


FIGURE 1: Flow chart of traditional badminton teaching in class.

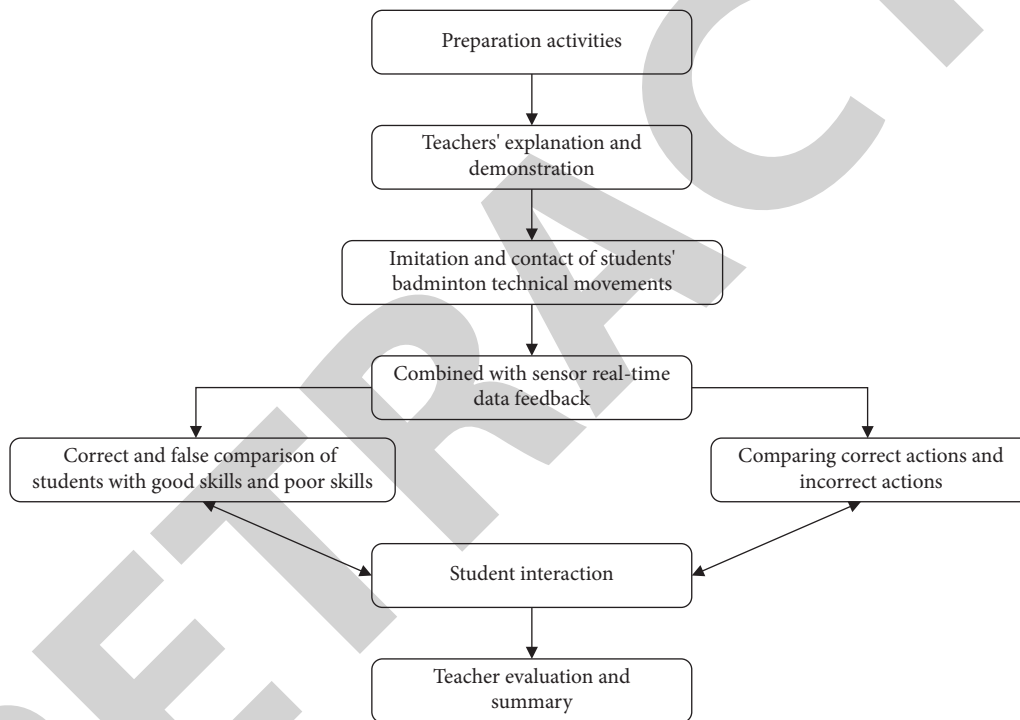


FIGURE 2: Flowchart of intelligent sensor-assisted badminton teaching.

3.3.1. *The Beginning of the Lesson.* Centering on the course, the operation method, main function and use purpose of the sensor equipment were introduced to the students in the experimental group, so as to deepen their behavioral ability and thinking consciousness, guide students to have subjective analysis and judgment of their own behaviors in the process of using the equipment, and then improve their research and practice ability.

3.3.2. *The Progress of the Lesson.* The guidance of intelligent sensor-assisted teaching to badminton technical action teaching is carried out according to the four stages of “generalization-differentiation-solidification-automation.”

Forehand overhand hitting a lob is taken as an example. At the stage of generalization and differentiation, teachers

should first demonstrate and drill the correct movements and brief notes for attention. It is not appropriate to emphasize the details of movements too much. In the training session of classroom technical movements are arranged immediately, students are guided to form a complete impression of technical movements by using sensor information feedback, and students are not directly evaluated for their exercises, so as to stimulate their thirst for knowledge and active awareness of inquiry [9]. As far as possible to meet the students’ freedom to exercise, the students are required to learn to improve themselves for each exercise movement.

In the movement practice of the differentiation-solidification stage, students should be guided to experience the process of coordinating force and enhance the experience of muscle sensation and perception. Group cooperation mode was established to promote students to cultivate their ability

of independent thinking, problem finding, and problem solving in helping each other, mutual assistance, and mutual learning.

In the solidifying stage, students' mastery of technical movements tends to be stable, so they should strengthen the combination with other mastered technical movements for flexible application in actual combat. At this stage, attention should be paid to the cultivation of personal technical style [10].

3.3.3. The End of the Lesson. By observing students' practice in class, the teacher points out common mistakes in the course of students' practice at the end of each class and does not take the initiative to propose solutions. Instead, the students are encouraged to analyze and discuss the phenomena. After class, students are required to reflect on their own shortcomings and improvement direction.

3.4. Comparison between Traditional Teaching and Intelligent Assisted Teaching. Let's take an overhand forehand hit as an example.

In the traditional mode, after the completion of technical movement teaching, teachers will focus on requiring students to improve the proficiency and stability of movements, and the word "efficient force generation" will often come out [11]. Indeed, as a sport with strong resistance across the net, the mastery of every single action of badminton technology ultimately serves the high-quality hitting effect. However, as far as practitioners and teachers are concerned, there is no objective evaluation standard to analyze and judge the effect of this exercise.

With the aid of intelligent teaching, we can easily show the actual effect and mastery of the badminton technical action to the practitioners through the speed and strength curve recorded by the sensor [12].

In the speed-force curve part, the dashed line represents the power curve, which records the power state of the practitioner of this action behavior; the solid line represents the speed curve, which records the waving speed state of this action behavior. The more similar the peak values of the two curves are, the more the stroke is completed in the same direction and the fluctuation in the power curve, which reflects the kinetic energy loss in the swing process. The zigzagging fluctuation of the speed curve is used to explain whether the force is consistent in the swing process (if there is an obvious fluctuation before the first peak of the speed curve, it indicates that the lead beat is incoherent and there is a phenomenon of repeated force) [13]. In the actual swing application, the occurrence of downward acute Angle shows the existence of reverse power, which is reflected in misleading, limiting power, and affecting the shot timing. The smoother the movement, the more calm the recorded curve tends to be, and the more regular it tends to be, without drastic fluctuations.

The traditional badminton teaching is mainly guided by the verbal feedback of the action by the teacher. For the students with a weak ability of representation construction, it is difficult to find the correct technical action experience.

The use of intelligent sensing equipment to assist teaching is to form digital intuitive feedback on the arc of swing, hitting power, hitting speed, and other related indicators through the specific restoration of the image of various badminton technical actions in the process of students' practice, so as to deepen students' experience of technical actions in a guided way [14]. With the cycle of "exercise-feedback-self-analysis-targeted repractice", students can master and perfect their technical movements and finally finalize them correctly. It effectively solves the disadvantages of poor understanding ability and slow mastery of skills of students in traditional badminton teaching method. In addition, the number of students' active practice after class increases, which further promotes the students' mastery of badminton skills.

4. Results and Discussion

Interest is an important factor for the success of badminton teaching. Only when students are interested in badminton can they keep a positive and conscious attitude towards badminton for a long time [15]. As shown in Table 1, in order to verify the influence of intelligent sensor-assisted teaching methods on students' interest in learning badminton, students were investigated in the form of questionnaires after the experiment. The subjective self-evaluation of the students in the experimental group and the control group (combined with the objective reality of badminton technique practice frequency, self-learning time, learning initiative and enthusiasm, etc.) was counted, and the results were shown in Figure 3.

Figure 3 shows the comparison of the two groups of students' learning interest in badminton after the experiment. After one semester's study, 46% of the students in the experimental group thought badminton special learning was interesting, while only 15% of the students in the control group held the same attitude. 39% of the students in the experimental group thought badminton special learning interesting, 31% of the students in the control group; In the experimental group, 15% of students thought that their interest in badminton became average after a semester of special courses, while in the control group, 39% students should be interested in badminton. None of the students in the experimental group thought badminton learning was less interesting, while 15% of the students in the control group still felt badminton learning became less interesting. From the overall situation, the students in the experimental group are more interested in learning badminton than the control group. The two groups of students learned badminton special courses on the basis of the same teachers, venues, teaching tasks, and time schedule. The only difference was that the experimental group used sensor equipment to assist routine teaching in the learning process. According to the statistics in Table 1, the attitude of using sensors in the badminton learning process of the experimental group was evaluated after the experiment, and the students in the experimental group all took the initiative to use the sensors. The use of intelligent sensing equipment to assist teaching is more conducive to stimulate students' interest in learning

TABLE 1: Comparison of badminton skills between the two groups before the experiment.

Technical actions	Experimental group \bar{X}	Control group \bar{X}	T	P
Forehand long serve technique	4.62	4.69	-0.221	0.829
Forehand technique	5.38	5.15	0.898	0.387

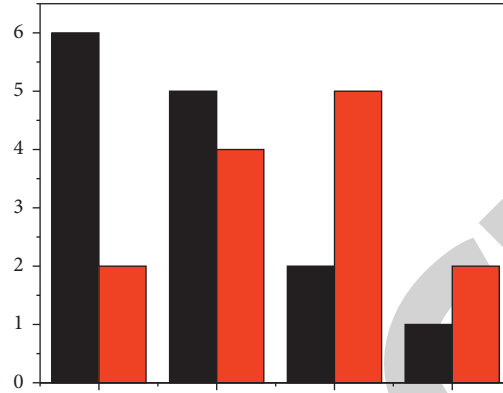


FIGURE 3: Comparison of badminton learning interest between the experimental group and the control group after the experiment.

badminton and mobilize their learning enthusiasm [16] as shown in Figure 4.

According to Figure 4, students in the experimental group actively participated in after-class exercises every week, while the control group still showed that 15% of students did not actively participate in after-class exercises. 23% of the experimental group practiced once or twice a week after class, while 46% of the control group did. 46% of the experimental group practiced three to four times a week after class, compared with 23% of the control group. Nearly 46 percent of the experimental group participated in self-directed exercises at least five times a week after class, compared with 15 percent of the control group. From the figure above, it can be seen that the initiative of students in the experimental group is significantly better than that in the control group.

After the control experiment, part of the questionnaire of students' interest reflected more real. Combined with the investigation of students' interest in badminton and the reasoning analysis of badminton practice in their spare time, in the process of physical education classroom teaching, the use of intelligent sensors to assist traditional classroom teaching is conducive to creating a good training atmosphere for students and stimulating their learning enthusiasm [17]. This device can provide objective feedback and suggestions for the current technical actions in real time, which is the icing on the cake for the cultivation of interest in badminton and the improvement of initiative in after-class practice as shown in Table 2.

Formula (1) was used to calculate the data in Table 2.

$$\bar{X} = \sum Xi/N. \tag{1}$$

After the experiment, the scoring method combining standard and technical evaluation was adopted. The

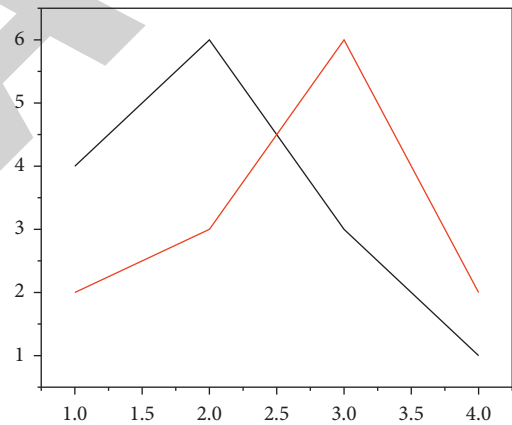


FIGURE 4: After the experiment, the experimental group and the control group actively practiced badminton times after class every week.

experimental data showed that students in the experimental class scored higher than those in the control group in the four technical tests of forehand lob, backhand lob, forehand lob, and forehand lob [18]. T test analysis showed that the students in the experimental group were significantly different from the control group in the four technical movements such as forehand high shot ($P < 0.01$).

The analysis of the reason is that the intelligent sensor auxiliary teaching can be more effective in accordance with the actual situation of students, formulate scientific and reasonable training, accelerate the understanding and master of various badminton skills. The cognitive process of motor skills includes three stages: motor perception, motor representation, and motor concept [19]. Motor imagery plays an important part in the formation of motor skills, and

TABLE 2: Influence of different teaching methods on students' badminton skills.

Projects	Experimental group \bar{X}	Control group \bar{X}	T	P
A long forehand serve	7.76	6.81	5.839	0.000
Backhand ball at the net	7.69	6.50	3.484	0.005
A forehand hit a long shot	7.73	6.80	5.482	0.000
Lob	7.15	6.31	4.247	0.001

Note. $P < 0.01$ has a very significant difference, $P < 0.05$ has a significant difference.

the clarity of motor imagery largely determines the speed and accuracy of motor skill formation [20]. Therefore, the sensor-assisted teaching method is significantly better than the traditional teaching method in promoting students' mastery of badminton technology.

5. Conclusion

This paper proposes a sensor-based approach to intelligent wearable devices. The method guides students to form a complete impression of technical movements by using sensor information feedback and does not directly evaluate students' movements, so as to stimulate students' thirst for knowledge and active awareness of inquiry. Students' freedom of exercise should be satisfied as much as possible, and students are required to learn to improve themselves for each exercise. Through the control group experiment and the analysis of the experimental results, it can be seen that compared with the traditional teaching method, the number of students' active practice after class has increased, which has more promoted the students' mastery of badminton skills. Therefore, it is feasible to apply this method to badminton teaching in colleges and universities.

Data Availability

The data used to support the findings of this study are available from the author upon request.

Conflicts of Interest

The author declares that there are no conflicts of interest.

Acknowledgments

The study was supported by University-level Project of Guangzhou Software University: Exploration and Practice of Sports School-based Curriculum Construction in Universities under the Background of Education Informatization (Grant no. JYJG202106).

References

- [1] O. Fedorovich, O. Uruskiy, Y. Pronchakov, and M. Lukhanin, "Method and information technology to research the component architecture of products to justify investments of high-tech enterprise," *RADIOELECTRONIC AND COMPUTER SYSTEMS*, no. 1, pp. 150–157, 2021.
- [2] E. Lee and C. Y. Lee, "Ppg-based smart wearable device with energy-efficient computing for mobile health-care applications," *IEEE Sensors Journal*, vol. 21, no. 12, pp. 13564–13573, 2021.
- [3] X. Shi, X. Li, and Y. Wu, "The application of computer-aided teaching and mobile internet terminal in college physical education," *Computer-Aided Design and Applications*, vol. 18, no. S4, pp. 163–174, 2021.
- [4] R. R. Mohanty and V. R. Krishnamurthy, "Kinesthetic metaphors for precise spatial manipulation: a study of object rotation," *Journal of Computing and Information Science in Engineering*, vol. 21, no. 2, pp. 1–25, 2020.
- [5] D. M. Gelfman, "Changing the learning objectives for teaching physical examination at the medical school level," *The American Journal of Medicine*, vol. 133, no. 3, pp. e77–e78, 2020.
- [6] A. Jolfaei, V. G. Menon, C. Lv, A. K. Bashir, Y. K. Tan, and K. Kant, "Guest editorial advanced sensing and sensor fusion for intelligent transportation systems," *IEEE Sensors Journal*, vol. 21, no. 14, pp. 15425–15426, 2021.
- [7] N. Yang, S. Xu, and Z. Quan, "An Efficient Public Key Searchable Encryption Scheme for mobile Smart Terminal," *IEEE Access*, no. 99, p. 1, 2020.
- [8] Y. N. Li, Y. Xu, Z. J. Yu, X. P. Chen, and J. A. Hu, "Discussion on teaching reform of oral histopathology in multiple classes," *Zhonghua kou qiang yi xue za zhi = Zhonghua kouqiang yixue zazhi = Chinese journal of stomatology*, vol. 55, no. 9, pp. 673–676, 2020.
- [9] K. Saho, K. Sugano, M. Kita, K. Uemura, and M. Matsumoto, "Classification of health literacy and cognitive impairments using higher-order kinematic parameters of the sit-to-stand movement from a monostatic Doppler radar," *IEEE Sensors Journal*, vol. 21, no. 8, pp. 10183–10192, 2021.
- [10] S. I. Bross, "Message and causal asymmetric state transmission over the state-dependent degraded broadcast channel," *IEEE Transactions on Information Theory*, vol. 66, no. 6, pp. 3342–3365, 2020.
- [11] V. Vijayalakshmi, S. Patchainayagi, S. Rajkumar, and A. Tilahun, "Augmenting inter-personal skills in elt classrooms using digital tools augmenting inter-personal skills in elt classrooms using digital tools," *Turkish Online Journal of Qualitative Inquiry*, vol. 12, no. 3, pp. 2692–2712, 2021.
- [12] A. Chowdhury, G. Verma, C. Rao, A. Swami, and S. Segarra, "Unfolding wmmse using graph neural networks for efficient power allocation," *IEEE Transactions on Wireless Communications*, vol. 20, no. 9, pp. 6004–6017, 2021.
- [13] J. Li, J. Yan, K. Huang et al., "A modeling and measuring method for armature muzzle velocity based on railgun current," *IEEE Transactions on Plasma Science*, vol. 49, no. 7, pp. 2272–2277, 2021.
- [14] S. A. Voinova, "The technical objects' efficiency control by their renewal," *Automation of technological and business processes*, vol. 12, no. 3, pp. 29–33, 2020.
- [15] W. Daniel, "A new age of photography: diy digitization' in manuscript studies," *Anglia*, vol. 139, no. 1, pp. 71–93, 2021.
- [16] M. Fan and A. Sharma, "Design and implementation of construction cost prediction model based on svm and lssvm in industries 4.0," *International Journal of Intelligent Computing*

Retraction

Retracted: Design of English Translation Model Based on Recurrent Neural Network

Mathematical Problems in Engineering

Received 8 August 2023; Accepted 8 August 2023; Published 9 August 2023

Copyright © 2023 Mathematical Problems in Engineering. This is an open access article distributed under the Creative Commons Attribution License, which permits unrestricted use, distribution, and reproduction in any medium, provided the original work is properly cited.

This article has been retracted by Hindawi following an investigation undertaken by the publisher [1]. This investigation has uncovered evidence of one or more of the following indicators of systematic manipulation of the publication process:

- (1) Discrepancies in scope
- (2) Discrepancies in the description of the research reported
- (3) Discrepancies between the availability of data and the research described
- (4) Inappropriate citations
- (5) Incoherent, meaningless and/or irrelevant content included in the article
- (6) Peer-review manipulation

The presence of these indicators undermines our confidence in the integrity of the article's content and we cannot, therefore, vouch for its reliability. Please note that this notice is intended solely to alert readers that the content of this article is unreliable. We have not investigated whether authors were aware of or involved in the systematic manipulation of the publication process.

Wiley and Hindawi regrets that the usual quality checks did not identify these issues before publication and have since put additional measures in place to safeguard research integrity.

We wish to credit our own Research Integrity and Research Publishing teams and anonymous and named external researchers and research integrity experts for contributing to this investigation.

The corresponding author, as the representative of all authors, has been given the opportunity to register their agreement or disagreement to this retraction. We have kept a record of any response received.

References

- [1] X. Wang, "Design of English Translation Model Based on Recurrent Neural Network," *Mathematical Problems in Engineering*, vol. 2022, Article ID 5177069, 7 pages, 2022.

Research Article

Design of English Translation Model Based on Recurrent Neural Network

Xiaohui Wang 

School of Foreign Language, Xuzhou University of Technology, Xuzhou 221000, Jiangsu, China

Correspondence should be addressed to Xiaohui Wang; 201811110911115@stu.hubu.edu.cn

Received 27 June 2022; Accepted 3 August 2022; Published 25 August 2022

Academic Editor: Hengchang Jing

Copyright © 2022 Xiaohui Wang. This is an open access article distributed under the Creative Commons Attribution License, which permits unrestricted use, distribution, and reproduction in any medium, provided the original work is properly cited.

In order to improve the accuracy and stability of English translation, this paper proposes an English translation model based on recurrent neural network. Based on the end-to-end encoder-decoder architecture, a recursive neural network (RNN) English machine translation model is designed to promote machine autonomous learning features, transform the distributed corpus data into word vectors, and directly map the source language and target language through the recurrent neural network. Selecting semantic errors to construct the objective function during training can well balance the influence of each part of the semantics and fully consider the alignment information, providing a strong guidance for the training of deep recurrent neural networks. The experimental results show that the English translation model based on recurrent neural network has high effectiveness and stability. Compared with the baseline system, it has improved about 1.51–1.86 BLEU scores. *Conclusion.* The model improves the performance and quality of English machine translation model, and the translation effect is better.

1. Introduction

Since the machine translation task was put forward, a large number of resources have been put into related research, and a wealth of research results have been produced. Machine translation systems have also developed from rule systems based on dictionaries and manual rules, case-based translation systems to statistical machine translation systems. Statistical machine translation can quickly learn translation knowledge from a large amount of data [1]. It has obvious advantages in robustness and translation quality compared with rule-based and case-based methods. It has become the mainstream in machine translation research (as shown in Figure 1). Over the last 10 years, statistical machine translation systems have been intensively studied and a variety of statistical translation models have been proposed, the most important of which is the suggestion of phrase-based translation models. A word-based statistical translation system begins with a lexical correspondence between languages and extracts parts of the translated language from the data as the basic unit of machine translation because a translated phrase pair can directly record a rich translation phenomenon

compared to the lexical level. The machine translation system and translation performance have improved significantly [2]. However, phrase-based translation systems also face some problems. Machine translation researchers have done a series of in-depth exploration work. An important attempt is to introduce a large number of lexical and syntactic features to better describe translation phenomena. Vocabulary-based feature is a sparse high-dimensional feature, which is difficult to obtain accurate estimation and prone to overfitting in the case of limited bilingual data, and its ability to describe long-distance, phrase-level translation is limited. Although syntactic features can describe the recursive structure in language to a certain extent, syntactic features depend on the results of syntactic analysis. However, the current syntactic analysis technology is not robust enough to achieve the desired results. In recent years, deep neural network technology has received extensive attention in natural language processing. Deep neural network can automatically learn new representations of various objects in natural language, which puts forward a new idea to solve the problem that sparse features are easy to overfit and lack the ability to describe language structures in natural language processing.

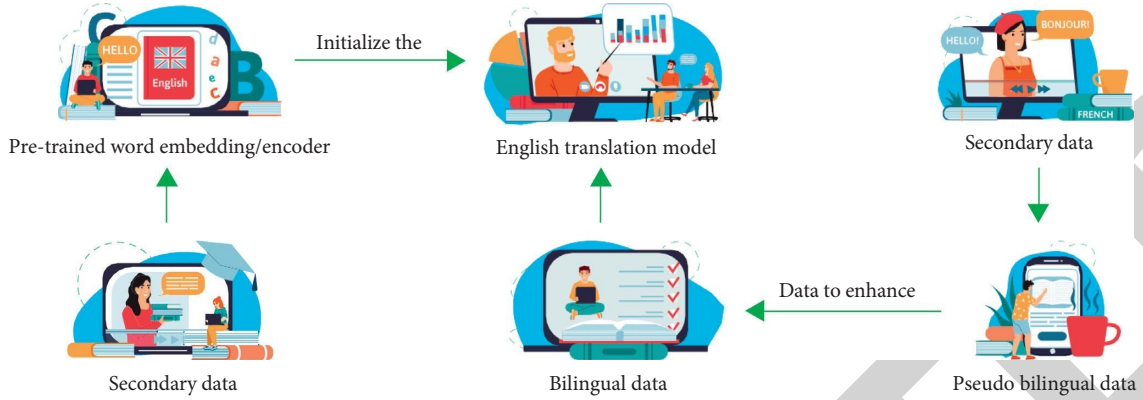


FIGURE 1: Design of English translation model.

2. Literature Review

Li and others created the IBM 701 computer to complete the research on English-Russian machine translation. The IBM 701 computer accepted the test of the world's first machine translation machine and translated several simple Russian sentences into English. This simple test showed the feasibility of people using computers to translate at that time. Since then, people began to study machine translation [3]. Abebe and others deepened the reform of Halliday system grammar and proposed the SCHRDLU model. These new theories and methods of machine translation in the 1970s have opened up a new way of thinking for machine translation [4]. Li and others put forward machine translation models based on statistics and examples, which are based on large-scale real text processing and use corpus processing means to transform corpus into language knowledge base. This is an important revolution in the history of machine translation and also pushes natural language processing to a new stage of rapid development [5]. Aziz and others believe that the basis of language is rules, and the sentences of a language can be derived from its grammar, sentence pattern, and other rules. Therefore, Chomsky gave the theoretical principle of generating sentences from rules. From then on to the 1990s, rule-based machine translation has been the mainstream of machine translation research. Rule-based methods include literal translation, transformational translation, and inter-language translation [6]. Marquez and others put forward the case-based machine translation method [7]. Its basic idea is to build a case sentence base corresponding to the source language and the target language. For the sentence to be translated, the sentence with the closest distance is matched from the source language corpus, then the target sentence corresponding to the sentence is found, and the target sentence is appropriately modified according to the sentence to be translated, and thus the target sentence of the sentence to be translated is obtained. Kumar and others proposed to integrate the case-based machine translation method with the rule-based method, which greatly improved the translation performance [8].

3. Research Methods

3.1. Recurrent Neural Network Analysis. In the context of in-depth training, neural networks have unique advantages and play an important role in solving many problems, such as distribution, but neural network transmission has its limitations. The human brain is involved in energy, and distribution is a small part of it [9]. In addition to identifying events, people are able to determine the physical relationship between information resources and information resources, and the length of the data varies. Only a normal neural network can solve these problems.

The recursive neural network model is shown in Figure 2.

If the intermediate closed-loop link is deleted, it becomes the input layer, potential layer, and release layer in the neural network.

v_k represents the input at time k ; h_k represents the hidden form at k time; W_k represents k -time output; U represents the weight matrix from input layer to hidden layer; M represents the weight matrix from hidden layer to hidden layer; and N represents the weight matrix from hidden layer to output layer [10, 11]. When k is 1, set h_k to 0, and the specific calculation process is as follows:

$$\begin{cases} r_1 = Uv_1 + Mh_0, \\ h_1 = f(r_1), \\ w_1 = g(Nh_1), \end{cases} \quad (1)$$

where f and g represent the activation function.

With the time gradually advancing, the memory state h_1 of time 1 participates in the next prediction activity, as shown in the following formula:

$$\begin{cases} r_2 = Uv_2 + Mh_1, \\ h_2 = f(r_2), \\ w_2 = g(Nh_2). \end{cases} \quad (2)$$

Thus, the specific state at time t is obtained, as shown in the following formula:

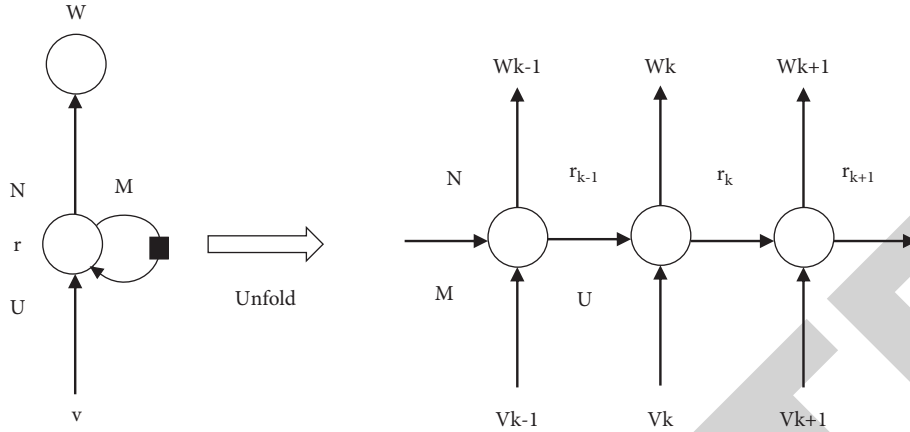


FIGURE 2: Recurrent neural network model.

$$\begin{cases} r_k = Uv_k + Mh_k, \\ h_k = f(r_k), \\ w_k = g(Nh_k). \end{cases} \quad (3)$$

During training, recurrent neural network is prone to gradient explosion or disappearance, which leads to the fact that the gradient cannot be transmitted continuously in a long sequence, finally making it difficult for the model to capture a long distance. Under normal conditions for gradient bursts, the gradient threshold can be scientifically determined based on model parameter training and can be stopped immediately if the gradient exceeds a specified threshold [12]. For the missing gradient, several methods can be used to solve this problem. For example, initiate the weight value scientifically so that the whole brain does not select the maximum or minimum to avoid gradient disappearance area; sigmoid and tanh can be replaced by relu function according to function; design with integrated protocols such as long short-term memory (LSTM) or GRU.

3.2. Framework of English Translation Model Based on Recurrent Neural Network. Figure 3 shows the range of standard English translators based on neural network reconstruction.

The process uses an organic mix of Nginx and web servers to improve developer’s scalability and reliability. When multiple users request, Nginx not only transmits the request results to the server but also completes multiple requests equal to the maximum number of visits against failure. Intermediate processes include intermediate programs and memory database modules [13]. The data sent by the user are processed on average, and the random data are transferred efficiently and quickly through the memory database. Improving the management and coordination of strategic plans can improve the security and high efficiency of data transmission. The decryption process has two identifiers, the GPU and the CPU. In order to reduce the delay of the model response according to many methods of parallel modeling and

hybrid decoding, the parallel response of the model is optimized, and each model has a high degree of parallelism and low lag.

3.3. English Machine Translation Model Based on LSTM Attention Embedding. According to the analysis of LSTM network model (as shown in Figure 4), the output vector of LSTM network model encoding phase is constant. Therefore, a parallel vector is used to encode the source sentence. In actual English machine translation, the input English sequence is a sequence of indefinite length, which leads to the problem that the model cannot fully match the English input sequence when the standard LSTM model is used for machine translation of English, which makes the translation effect unsatisfactory. In addition, because of the different meanings in the translation, showing the sequence of designs in constant numbers with the same amount of attention to the sequence does not help improve the quality of translation [14]. Therefore, in order to solve the above problems, we are studying the LSTM network and carrying out the design of English translation technology based on the LSTM network. First, a set of vectors is used instead of the length to indicate the order of the terms. Then, by dynamically selecting the background vector while creating the temporary object, the translation model pays more attention to the objects that are related to the language during the translation, thus improving the interpretation of the model. The English LSTM translator, built into the monitoring process, consists of three parts: the encoder, the decoder, and the monitoring process. The procedure for calculating the state of the next hidden process of the objective of the model is the same as for the LSTM decoder section, as shown in the following equation:

$$Z_i + 1 = \sigma(c_i, u_i, z_i), \quad (4)$$

where u_i represents the i -th word in the target language sequence and c_i represents the background vector of the word i . The back vector of the LSTM model embedded in the face mechanism is not a continuous one but a set of multiple vectors. Therefore, each word in the target language sequence can see its own origin vector.

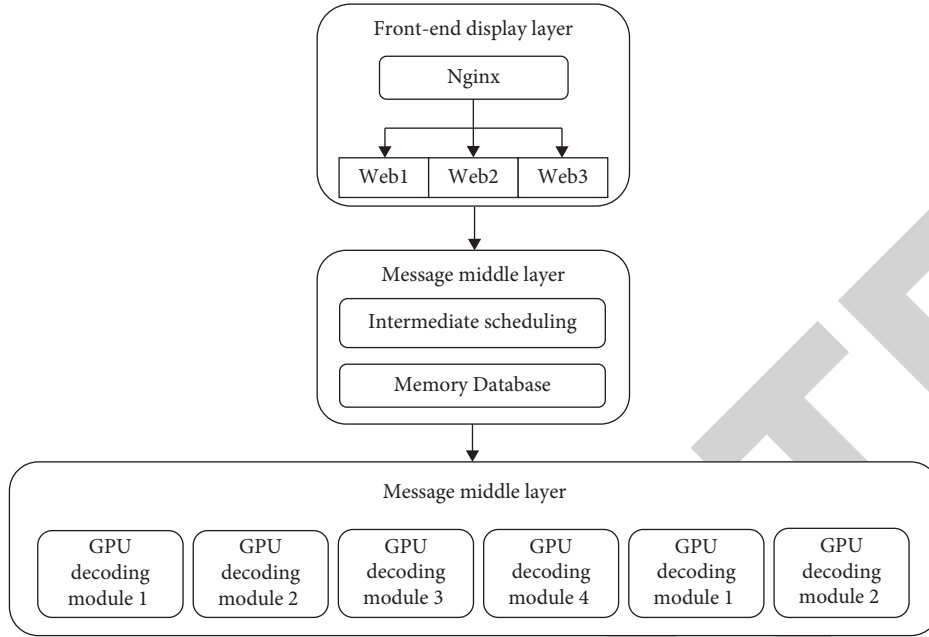


FIGURE 3: Model framework.

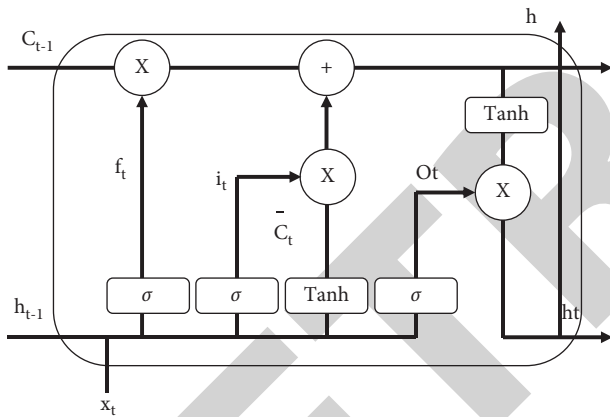


FIGURE 4: Schematic diagram of LSTM network structure.

If the hidden layer state of the encoder at time j is h_j , the corresponding background vector can be calculated by

$$C_i = \sum_{j=1}^T a_{ij} h_j, \quad (5)$$

where a_{ij} represents the weight, i.e., the value of attention to the i -th word of the first language sequence of the i -th word of the sequence of words, which can be calculated by equations (6) and (7).

$$a_{ij} = \frac{\exp(e_{ij})}{\sum_{k=1}^T \exp(e_{ik})}, \quad (6)$$

$$e_{ij} = a(z_i, h_j), \quad (7)$$

where a is a function used to measure the current lag process of the target language and the comparison of word order lag states, and it can be calculated by

$$e_{ij} = v^T \tanh(W_z z_i + W_h h_j), \quad (8)$$

where v , W_z , and W_h represent the model parameters to be learned. By improving the monitoring procedures in the LSTM network, the model can measure the weight difference at the end of the language, which solves the problem of distance from the LSTM model and improves the standard performance [15, 16].

4. Result Analysis

4.1. Experimental Environment and Parameter Setting. To measure the performance of standardized English translation translators based on the advanced level of LSTM. The evaluation system based on tensorflow framework is developed. Among them, LSTM neural network includes 30,000 large words, 512 large vector word and hidden number, 2 LSTM network set number, 3 general search line, and 128 large package. To improve the quality, the measurements were optimized using the stochastic gradient drop method, the decomposition phase algorithm, and the column search algorithm [17].

4.2. Dataset Source and Preprocessing. The study selected 2019 data from the International Speech Language and Translation Assessment Competition (IWSLT) as test data with 220,000 Chinese-English pair sentences, 3 pairs of tests, and 1 pair of small file data [18]. It should be noted that the LSTM English translator cannot be trained directly from the IWSLT 2019 documentation, so the documentation must be converted to word vectors [19]. The study used the term segmentation of data and then applied CBOW to vector segmented data.

4.2.1. Word Segmentation. IWSLT 2019 data contain two parallel sentences in Chinese and English, and the study segmented the experimental data in Chinese and English because of the different ways of segmenting words in Chinese and English. Chinese lexicon uses word segmentation based on statistics [20]. Firstly, according to the composition form of Chinese words, a word is regarded as a combination of multiple fixed words; then, according to the size of the co-occurrence frequency between words in the context of the sentence, the probability of word generation is judged, that is, the credibility of the word. Finally, set the threshold according to the credibility of the word, form the condition of word formation, and determine the word segmentation. For English segmentation, the basic unit of English is the word, so it only needs to be divided directly by space. However, because English has a semicolon, it is necessary to remove semicolons when segmenting words. There are three simple steps you can take to stay away from English. First, rewrite the uppercase and lowercase letters, separating the words and characters at the end of the sentences with spaces, and finally, following the English language completely, write the general sentences using a special template.

4.2.2. Word Vector Representation. Word vectorization refers to the digitization of language symbols, so that language symbols can be input into the model for training and learning. CBOV is used to vectorize words [21]. Assuming that the dictionary size is $|v|$, the index set $v = \{0, 1, \dots, |v| - 1\}$ with one-to-one correspondence between the word and the integer in the dictionary is established, and the integer corresponding to the word in the dictionary is the index of the word [22]. If there is a text sequence with a length of T , a time window size of m , and a word at time t of J , the probability of CBOV maximizing the generation of the center word from the background word is as follows:

$$J = \prod_{t=1}^T P(w^{t-m}, \dots, w^{t-1}, w^{t+1}, \dots, w^{t+m}). \quad (9)$$

By taking the negative logarithm of the above equation, the loss function can be obtained, i.e., the maximum value of (9) can be calculated by

$$J = \sum_{t=1}^T \log P(w^t | w^{t-m}, \dots, w^{t-1}, \dots, w^{t+m}). \quad (10)$$

Assuming that the background word vector is expressed as v and the center word vector is expressed as u , then through CBOV training, for the words indexed as i in the dictionary, the vector v_i of the word as the background word can be obtained, and the vector as the center word can represent u_i .

4.3. Evaluation Indicators. This study selected the BLEU value as a measure for the mean quality of the translation

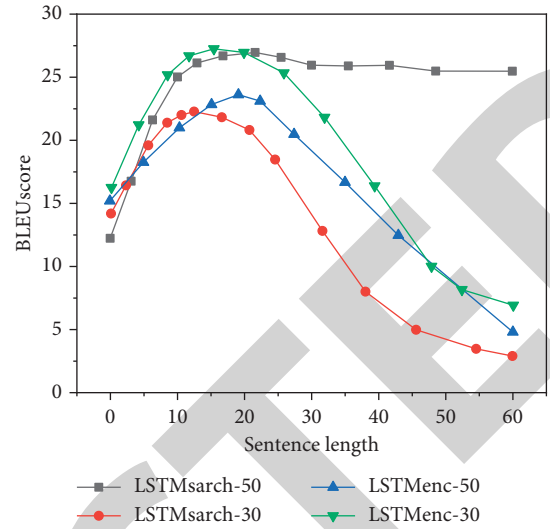


FIGURE 5: Performance of attention mechanism (RNN changed to LSTM).

design. The greater the cost, the better the translation. The way to calculate BLEU is as follows:

$$\text{BLEU} = \text{BP} \times \exp\left(\sum_{n=1}^N w_n \log_{10} p_n\right), \quad (11)$$

where BP represents the penalty factor; N represents the longest tuple length, usually 4; n represents the number of tuples; w_n represents the weight of tuple n ; and p_n represents the ratio of tuple n .

4.4. Model Validation. To measure the effectiveness of the translation standards according to the LSTM color scale, the LSTM model and the LSTM color scale were used to train the experimental data, and the results are shown in Figure 5. In Figure 5, the value of BLEU centralized LSTM model is higher than that of the standard LSTM model, which shows that the middle LSTM model has better translation values in longer sentences and demonstration performance. Performance is improving [23].

4.5. Model Comparison. To learn about the effectiveness of LSTM standard English translators, learn how to use LSTM English translator models, RNN English translator models, and GRU-attention English translator models and apply translation. An English translation compares the test data. The training packages and results are shown in Figure 6. As shown in Figure 6, the BLEU value of the standard English translator with LSTM is analyzed on machine development. During the test, it is found that the Bleu value of the English translation model based on LSTM is higher than that of the English translation model based on the traditional RNN. The GRU-attention and recursion-based neural network translation model is efficient and stable and improves the score from 1.51 to 1.86 BLEU compared to the core standard.

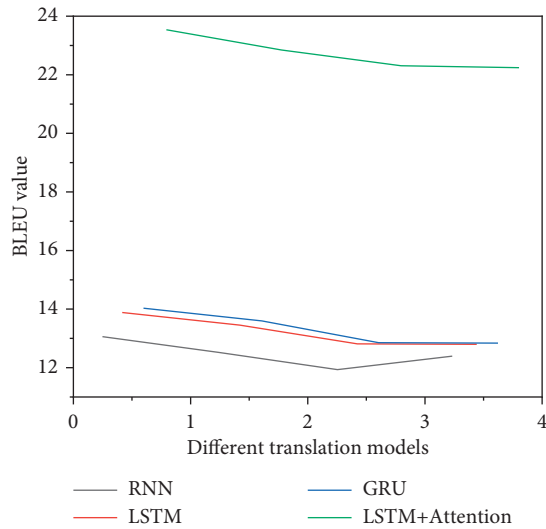


FIGURE 6: BLEU values of different translation models on the experimental dataset.

5. Conclusion

In conclusion, the new concept of English machine translation template recursion and LSTM color-level innovation is the introduction of a focused mechanism of the standard design of LSTM English translation to improve the presentation content language of native language information, thereby improving the translation and interpretation efficiency of the English translation system. Compared with other English translators, LSTM standard English translation system has better performance and can perform more efficient translation.

Data Availability

The data used to support the findings of this study are available from the corresponding author upon request.

Conflicts of Interest

The author declares that there are no conflicts of interest.

Acknowledgments

This study was funded by the Research Project of Philosophy and Social Science in Colleges and Universities of Jiangsu Provincial Department of Education (Research on Ecological View in American Romantic Literature) (Project No. 2021SJA1121).

References

- [1] S. Gautam, A. K. Patra, J. Brema et al., "Prediction of various sizes of particles in deep opencast copper mine using recurrent neural network: a machine learning approach," *Journal of the Institution of Engineers: Series A*, vol. 103, no. 1, pp. 283–294, 2022.
- [2] L. Ehrlich, D. Ledbetter, M. Aczon, E. Laksana, and R. Wetzel, "966: continuous risk of desaturation within the next hour prediction using a recurrent neural network," *Critical Care Medicine*, vol. 49, no. 1, p. 480, 2021.
- [3] W. Y. Li, A. Takata, H. Nabae, G. Endo, and K. Suzumori, "Shape recognition of a tensegrity with soft sensor threads and artificial muscles using a recurrent neural network," *IEEE Robotics and Automation Letters*, vol. 6, no. 4, pp. 6228–6234, 2021.
- [4] H. B. Abebe, C. L. Hwang, B. S. Chen, F. Wu, and C. Jan, "Recurrent neural network with fractional learning-based fixed-time formation tracking constrained control for a group of quadrotors," *IEEE Access*, vol. 9, no. 99, pp. 81399–81411, 2021.
- [5] V. M. Jape, H. M. Suryawanshi, J. P. Modak, and J. P. Modak, "An efficient grasshopper optimization with recurrent neural network controller-based induction motor to replace flywheel of the process machine," *Transactions of the Institute of Measurement and Control*, vol. 43, no. 1, pp. 151–166, 2021.
- [6] E. N. Aziz, A. Kasem, W. S. Suhaili, and P. Zhao, "Convolution recurrent neural network for daily forecast of pm10 concentrations in Brunei Darussalam," *Chemical Engineering Transactions*, vol. 83, no. 1, pp. 355–360, 2021.
- [7] J. Puentes Marquez, C. De Oliveira Ribeiro, E. Ruelas Santoyo, and V. Figueroa Fernandez, "Ethanol fuel demand forecasting in Brazil using a lstm recurrent neural network approach," *IEEE Latin America Transactions*, vol. 19, no. 4, pp. 551–558, 2021.
- [8] R. G. Kumar and R. Shriram, "Sentiment analysis using bi-directional recurrent neural network for Telugu movies," *International Journal of Innovative Technology and Exploring Engineering*, vol. 9, no. 2, pp. 241–245, 2019.
- [9] M. Picozzi and A. G. Iaccarino, "Forecasting the preparatory phase of induced earthquakes by recurrent neural network," *Forecasting*, vol. 3, no. 1, pp. 17–36, 2021.
- [10] A. Pimpalkar, M. Singh, S. Sheikh, K. Gedam, and A. Khadgi, "Fake news classification using bi-directional lstm-recurrent neural network," *Journal of Huazhong University of Science and Technology*, vol. 50, no. 6, pp. 1–9, 2021.
- [11] S. Raj, S. Tripathi, and K. C. Tripathi, "Ardho-deep rnn: autoregressive deer hunting optimization based deep recurrent neural network in investigating atmospheric and oceanic parameters," *Multimedia Tools and Applications*, vol. 81, no. 6, pp. 7561–7588, 2022.
- [12] T. Verma and S. Dubey, "Prediction of diseased rice plant using video processing and lstm-simple recurrent neural network with comparative study," *Multimedia Tools and Applications*, vol. 80, no. 19, pp. 29267–29298, 2021.
- [13] J. Matayoshi, E. Cosyn, and H. Uzun, "Are we there yet? evaluating the effectiveness of a recurrent neural network-based stopping algorithm for an adaptive assessment," *International Journal of Artificial Intelligence in Education*, vol. 31, no. 2, pp. 304–336, 2021.
- [14] S. P. Yadav, S. Zaidi, A. Mishra, and V. Yadav, "Survey on machine learning in speech emotion recognition and vision systems using a recurrent neural network (rnn)," *Archives of Computational Methods in Engineering*, vol. 29, no. 3, pp. 1753–1770, 2021.
- [15] S. Baldev and K. K. Anumandla, R. Peesapati, Scalable wavefront parallel streaming deblocking filter hardware for hevcd decoder," *IEEE Transactions on Consumer Electronics*, vol. 66, no. 1, pp. 41–50, 2020.
- [16] F. Ercan, T. Tonnellier, and W. J. Gross, "Energy-efficient hardware architectures for fast polar decoders," *IEEE Transactions on Circuits and Systems I: Regular Papers*, vol. 67, no. 1, pp. 322–335, 2020.

Retraction

Retracted: Application of Neural Network Sample Training Algorithm in Regional Economic Management

Mathematical Problems in Engineering

Received 8 August 2023; Accepted 8 August 2023; Published 9 August 2023

Copyright © 2023 Mathematical Problems in Engineering. This is an open access article distributed under the Creative Commons Attribution License, which permits unrestricted use, distribution, and reproduction in any medium, provided the original work is properly cited.

This article has been retracted by Hindawi following an investigation undertaken by the publisher [1]. This investigation has uncovered evidence of one or more of the following indicators of systematic manipulation of the publication process:

- (1) Discrepancies in scope
- (2) Discrepancies in the description of the research reported
- (3) Discrepancies between the availability of data and the research described
- (4) Inappropriate citations
- (5) Incoherent, meaningless and/or irrelevant content included in the article
- (6) Peer-review manipulation

The presence of these indicators undermines our confidence in the integrity of the article's content and we cannot, therefore, vouch for its reliability. Please note that this notice is intended solely to alert readers that the content of this article is unreliable. We have not investigated whether authors were aware of or involved in the systematic manipulation of the publication process.

Wiley and Hindawi regrets that the usual quality checks did not identify these issues before publication and have since put additional measures in place to safeguard research integrity.

We wish to credit our own Research Integrity and Research Publishing teams and anonymous and named external researchers and research integrity experts for contributing to this investigation.

The corresponding author, as the representative of all authors, has been given the opportunity to register their agreement or disagreement to this retraction. We have kept a record of any response received.

References

- [1] Y. He, "Application of Neural Network Sample Training Algorithm in Regional Economic Management," *Mathematical Problems in Engineering*, vol. 2022, Article ID 7666331, 7 pages, 2022.

Research Article

Application of Neural Network Sample Training Algorithm in Regional Economic Management

Yan He 

College of Plant Science, Tibet Agricultural and Animal Husbandry University, Nyingchi, Tibet 860000, China

Correspondence should be addressed to Yan He; 20121510@stumail.hbu.edu.cn

Received 1 July 2022; Accepted 5 August 2022; Published 24 August 2022

Academic Editor: Hengchang Jing

Copyright © 2022 Yan He. This is an open access article distributed under the Creative Commons Attribution License, which permits unrestricted use, distribution, and reproduction in any medium, provided the original work is properly cited.

In order to solve the limitations of the traditional method of determining expert weights in AHP and improve the level of the regional economy, this paper proposes a neural network algorithm based on AHP. This paper first calculates the interest correlation coefficient among experts, then obtains the comprehensive evaluation value of all experts according to the evaluation value matrix, and then determines the evaluation weight of each expert in the expert group. Finally, the comprehensive weight of each index is obtained by weighting the index weight obtained from the traditional AHP and the expert evaluation weight. Then, the evaluation value obtained by the improved AHP is used as a prior sample to train and test the BP neural network, and a classifier that can be popularized is obtained. The experimental results show that the overall evaluation value of circular economy of 9 construction enterprises is at a medium level, only 2 enterprises have an evaluation value of more than 50, and one enterprise has an evaluation value of only 35, indicating that the overall implementation of circular economy of these 9 construction enterprises is still at a low level, with great room for development and improvement. *Conclusion.* The economic management method based on a neural network algorithm can make the evaluation results more accurate and reliable and has high popularization and application value.

1. Introduction

With the increasingly severe situation of resource shortage, the circular economy has attracted more and more attention from all walks of life. It has become one of the effective models to alleviate the contradiction between resource shortage and economic development and achieve sustainable development. With the continuous development of computer technology and scientists' in-depth research on human brain science, it will play an important role to use a neural network to imitate human thinking to deal with problems in economic management [1]. The neural network is a complex dynamic system. The future development direction of the artificial neural network is to connect neural network with traditional technology, reduce its complexity and make it easy to understand and operate, as shown in Figure 1. Using an artificial neural network to deal with the scientific prediction and optimal decision-making of

economic management has broad prospects for development. The application and development of the artificial neural network method in the field of economic management is mainly reflected in the expansion of the application field and the combination with other economic management research methods. As an important force to promote the rapid development of the national economy, the development level of its circular economy determines the sustainable development ability of China's economy to a certain extent [2]. The artificial neural network method is suitable for dealing with nonlinear mapping relations, nonlinear simulation computing ability, self-learning, and self-organization functions, which makes it have a wide range of adaptability and capacity. It has unique advantages in dealing with qualitative indicators and hierarchical relationship variables. When combined with other quantitative analysis methods, the application range of the artificial neural network method is broader. Therefore, an in-depth

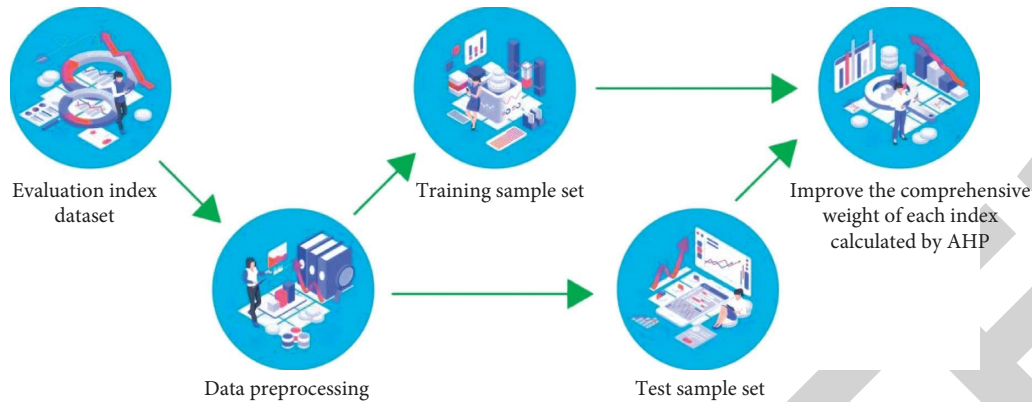


FIGURE 1: Neural network sample training.

study on the development of economic management and evaluation of its development status is of great significance to improve the efficiency of the circular economy of construction enterprises and the development level of the circular economy in China.

2. Literature Review

The background of neural network research can be traced back to the end of the 19th century and the interdisciplinary research on physics, psychology, and neurophysiology at the beginning of the 20th century [3]. These early studies systematically analyzed the general theories of learning, sensation, and reflex based on biological neural networks but did not make a mathematical generalization of the working mechanism of biological neurons. After Khalimon and others proposed the analytic hierarchy process (AHP) in 1980, Chinese and foreign scholars have carried out a series of studies using this method, and the results are quite rich. Due to the strong subjectivity of this method, scholars have also improved and innovated on the basis of AHP [4]. In foreign studies, Ma and others took an information technology service industry as an example and combined fuzzy logic theory with AHP to evaluate the importance of each component of human capital [5]. Vizzaccaro and others corrected the AHP by determining the expert evaluation weight through the projection method and obtained a good improvement effect [6]. Bakshi and others used the improved AHP for natural disaster assessment. Their innovation is mainly reflected in that they do not directly construct a judgment matrix based on expert scores but obtain a judgment matrix by comparing it with the highest score of the index set in advance, avoiding the subjectivity of the assessment to a certain extent [7]. Xu and others combined fuzzy AHP with the fuzzy TOPSIS method to evaluate the quality of medical services and concluded that medical services should be improved from the aspects of specialization, interactivity, and service accuracy [8]. Blanco-Urrejola and others studied the location of solar energy in a region by calculating the weights of various indicators in combination with GIS and AHP [9]. In terms of research on the evaluation of the circular economy, there are mainly lifecycle assessment (LCA), energy analysis,

materials flow analysis (MFA), ecological footprint, comprehensive evaluation methods, etc. Qian and others used the life cycle method to evaluate building energy, providing effective information for decision makers to make energy repair decisions [10]. Kuo and others studied the material circulation mode of the French copper industry through the dynamic material flow analysis model, focusing on the impact of the economic system, resource consumption, product manufacturing, and waste generation on pollution [11]. Bradha and others used the ecological footprint method to evaluate the existing resource protection policies. The sensitivity analysis of the calculation results shows that the ecological footprint method has a good ability to evaluate the negative impact of policies [12]. Boboshko and others used the emergy analysis method to accumulate the total input of raw materials, labor, and resources through emergy equivalents and evaluated the resource utilization and transfer efficiency in the industrial ecological economy [13]. On the basis of current research, this paper proposes a method based on an improved AHP-BP neural network algorithm. Firstly, the interest correlation coefficient among experts is calculated, then the comprehensive evaluation value of all experts is obtained according to the evaluation value matrix, and then the evaluation weight of each expert in the expert group is determined. Finally, the comprehensive weight of each index is obtained by the weighted average of the index weight obtained from the traditional AHP and the expert evaluation weight. Then, the evaluation value obtained by the improved AHP is used as a prior sample to train and test the BP neural network, and a classifier that can be popularized is obtained. It is of great significance to improve the circular economy efficiency of construction enterprises and the development level of the circular economy.

3. Research Methods

3.1. Improved AHP Method Based on Stakeholder Perspective. The traditional AHP method scores the evaluation objects by multiple experts and then simply takes the mean value of the score to build a judgment matrix to calculate the weight of indicators at all levels. However, when there is an interesting relationship between experts and the evaluation object, they

will strive for more say by improving their own advantages and suppressing competitors, resulting in the loss of fairness in the calculation of index weights [14]. Therefore, based on the perspective of stakeholders, this paper proposes an improved AHP method to give different weights to experts who may score as common stakeholders and potential competitors, and then weighted average the index weights obtained from their scores to obtain the comprehensive weights of each index, making the weight calculation more fair.

3.1.1. Calculate Expert Evaluation Weight Based on Stakeholder Perspective. In the multi-index evaluation system composed of N experts o_1, o_2, \dots, o_n and selected M indexes x_1, x_2, \dots, x_m , set $x_{ij} = x_j(o_i)$ ($i = 1, 2, \dots, n, j = 1, 2, \dots, m$) as the value of expert o_i under the index x_j . The evaluation data matrix can be expressed as follows:

$$A = [x_{ij}]_{n \times m} = \begin{bmatrix} x_{11} & x_{12} & \cdots & x_{1m} \\ x_{21} & x_{22} & \cdots & x_{2m} \\ \cdots & \cdots & \cdots & \cdots \\ x_{n1} & x_{n2} & \cdots & x_{nm} \end{bmatrix}. \quad (1)$$

Without losing generality, assume that M indicators are extremely large (benefit type), and assume that the data in A is the normalized data. It can be seen from the evaluation data matrix A that the closer the values of the evaluation indicators (row vectors in matrix A) given by the two experts are, the more likely they are to have common interests.

3.1.2. BP Neural Network Model. This paper adopts BP neural network, which is a multilayer feedforward neural network. The conversion function of its neurons is a non-linear sigmoid function. In this paper, $f(x) = 1/(1 + e^{-x})$ function is used. The basic idea of the BP neural network is to minimize the sum of squares of errors in the output layer of the network by adjusting the weights and thresholds of the network so that the output value is as close to the target value as possible.

The learning process of the BP neural network is the process of constantly changing weights and thresholds to minimize the error value [15].

The specific steps of the improved AHP-BP neural network algorithm in the evaluation of circular economy are shown in Figure 2.

- (1) Establish the evaluation index system of circular economy and collect data
- (2) Data preprocessing, dividing the data into the training set and test set
- (3) Calculate the evaluation weight of each expert based on the perspective of stakeholders
- (4) Calculate the weight of each index of AHP by using the scores of each expert

- (5) Weighted average of the expert evaluation weight and AHP index weight obtained in steps (3) and (4) to calculate the comprehensive weight of each index
- (6) The evaluation value of the circular economy is obtained by multiplying the index data of the evaluation object and the comprehensive weight of the index
- (7) Taking the results obtained in step (6) as input, the BP neural network model is trained with training set samples
- (8) The BP neural network model is used to verify the test set samples and analyze the results, which is popularized and applied

3.2. Case Study

3.2.1. Index Data of Circular Economy. Before training the neural network, this paper first standardized the sample data to eliminate the dimensional influence. When the larger the index value is, the better the evaluation is, the data standardization method adopted is: $x^* = 0.1 + (x_i - x_{i\min}) / (x_{i\max} - x_{i\min}) \times 0.9$; when the smaller the index value, the better the evaluation, the data standardization method adopted is: $x^* = 0.1 + (x_{i\max} - x_i) / (x_{i\max} - x_{i\min}) \times 0.9$. x^* represents the standardized value of index x_i , $x_{i\min}$ represents the minimum value of the i -th index, and $x_{i\max}$ represents the maximum value of the i -th index [16].

See Table 1 for the dimensionless index data after processing the original data.

3.2.2. Calculation of AHP Index Weight. For the evaluation index, compare the scores of experts in pairs to obtain the index judgment matrix of each expert at all levels. Taking one expert as an example, the judgment matrix of the first level index is

$$U = \begin{bmatrix} 1 & \frac{1}{3} & \frac{1}{5} & 3 & 5 \\ & 3 & 1 & \frac{1}{3} & 5 & 7 \\ & & 5 & \frac{1}{3} & 1 & 7 & 9 \\ & & & \frac{1}{3} & \frac{1}{5} & \frac{1}{7} & 1 & 3 \\ & & & & \frac{1}{5} & \frac{1}{7} & \frac{1}{9} & \frac{1}{3} & 1 \end{bmatrix}. \quad (2)$$

The approximate eigenvectors of the judgment matrix are [0.156, 0.322, 0.413, 0.066, 0.043], as shown in Table 2.

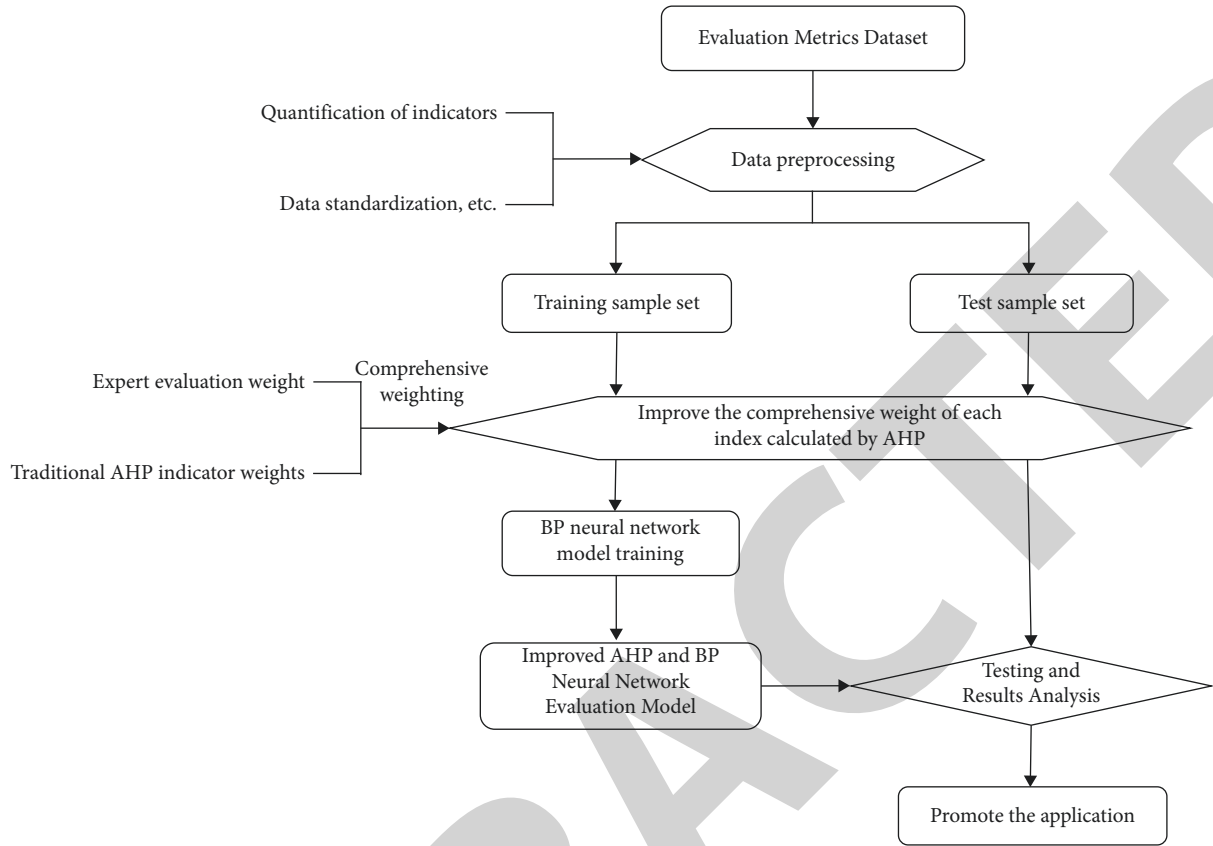


FIGURE 2: Steps of improving AHP-BP neural network algorithm.

TABLE 1: Sample data of circular economy evaluation indicators of construction enterprises.

Number/index	1	2	3	4	5	6	7	8	9	10
U_{11}	0.1	0.413	0.747	0.742	0.584	0.755	0.9	0.882	0.872	0.893
U_{12}	0.1	0.146	0.232	0.254	0.267	0.393	0.566	0.686	0.862	0.9
U_{13}	0.129	0.1	0.208	0.231	0.282	0.366	0.512	0.717	0.854	0.9
U_{14}	0.541	0.734	0.9	0.249	0.194	0.1	0.172	0.272	0.266	0.437
U_{21}	0.48	0.686	0.48	0.417	0.393	0.1	0.116	0.374	0.398	0.9
U_{22}	0.111	0.1	0.204	0.244	0.271	0.464	0.530	0.807	0.773	0.9
U_{23}	0.107	0.1	0.194	0.23	0.26	0.432	0.532	0.875	0.769	0.9
U_{24}	0.127	0.125	0.189	0.1	0.236	0.317	0.188	0.9	0.748	0.800
U_{31}	0.1	0.161	0.153	0.227	0.354	0.56	0.678	0.861	0.668	0.9
U_{32}	0.209	0.33	0.324	0.453	0.58	0.336	0.45	0.9	0.337	0.1
U_{33}	0.13	0.1	0.406	0.507	0.49	0.798	0.777	0.9	0.596	0.612
U_{34}	0.220	0.848	0.838	0.374	0.452	0.475	0.1	0.9	0.871	0.795
U_{35}	0.245	0.1	0.630	0.384	0.295	0.63	0.9	0.554	0.524	0.429
U_{36}	0.197	0.196	0.1	0.282	0.237	0.363	0.61	0.517	0.727	0.9
U_{37}	0.404	0.521	0.1	0.268	0.381	0.521	0.699	0.308	0.525	0.9
U_{41}	0.1	0.369	0.724	0.726	0.514	0.702	0.9	0.679	0.854	0.801
U_{42}	0.115	0.125	0.145	0.1	0.196	0.253	0.445	0.585	0.747	0.9
U_{43}	0.222	0.312	0.483	0.434	0.327	0.1	0.9	0.884	0.816	0.874
U_{44}	0.169	0.265	0.458	0.202	0.35	0.418	0.9	0.32	0.301	0.1
U_{45}	0.109	0.1	0.335	0.486	0.404	0.809	0.792	0.9	0.697	0.772
U_{46}	0.597	0.9	0.779	0.361	0.477	0.381	0.843	0.1	0.358	0.222
U_{47}	0.325	0.639	0.541	0.1	0.667	0.616	0.668	0.696	0.719	0.9
U_{51}	0.607	0.74	0.9	0.106	0.1	0.555	0.591	0.697	0.438	0.516
U_{52}	0.1	0.541	0.74	0.321	0.379	0.382	0.886	0.485	0.748	0.534
U_{53}	0.486	0.9	0.539	0.365	0.414	0.838	0.184	0.345	0.669	0.612

$$\lambda_{\max} = \sum_{i=1}^n \frac{\sum_{j=1}^n a_{ij} w_j}{n w_i} = 5.0634,$$

$$CI = \frac{\lambda_{\max} - n}{n - 1} = 0.01268, \quad (3)$$

$$RI = \frac{CI}{CR} = \frac{0.01268}{1.12}$$

$$= 0.0113 < 0.10.$$

The consistency ratio is less than 0.10. Through the consistency test, the expert's AHP level-1 index weight w_i can be obtained. Similarly, the AHP level-1 index weight of the other 9 experts can be obtained.

By weighted averaging the AHP primary index weight and its evaluation weight of the above-given 10 experts, the primary index weight of the index system can be obtained as $u = (0.12, 0.31, 0.38, 0.11, 0.08)$. According to the same method, the secondary index weight can be obtained, and then the comprehensive weight can be determined [17].

After calculation, the overall ranking of the comprehensive evaluation hierarchy has passed the overall consistency test. It can be considered that the index weights at all levels are reasonable and effective, and the comprehensive weights of the indicators at all levels of the evaluation index system can be obtained.

Comprehensive evaluation results of circular economy of construction enterprises. Calculate through the formula $Y = W \times X$, where y is the evaluation result vector; W is the weight vector of 25 evaluation indexes; X is the dimensionless sample data [18]. Therefore, the circular economy evaluation value of 59 construction enterprises is [0.1738, 0.2256, 0.3168, 0.4059, 0.3445, 0.3510, 0.4962, 0.6077, 0.6891, 0.6606, 0.7608, 0.2096, 0.319, 0.4018, 0.4923, 0.4528, 0.4486, 0.5857, 0.6903, .7191, 0.7359, 0.7972, 0.6597, 0.7608, 0.2126, 0.3148, 0.3985, 0.4904, 0.4376, 0.4502, 0.5820, 0.8002, 0.6597, 0.7608, 0.5807, 0.6943, 0.7191, 0.7400, 0.7972, 0.6591, 0.7608, 0.2107, 0.3237, 0.3927, 0.5014, 0.4535, 0.5872, 0.7958, 0.7608, 0.5835, 0.5608, 0.4835, 0.3881, 0.5370, 0.4941, 0.4990, 0.4559, 0.4634, 0.4128].

3.2.3. Establishment of BP Neural Network Model

(1) *Determine Network Hierarchy.* Any given continuous function $\Phi = X \rightarrow Y$, $X \in R^n$, $Y \in [0, 1]^m$, then Φ can be accurately implemented by a three-layer network. Therefore, the BP neural network constructed in this paper has three layers, including input layer, middle hidden layer, and output layer.

(2) *Determine the Number of Network Output Input Nodes.* In this paper, the number of nodes n in the input layer of the BP neural network is the same as the number of evaluation indicators, i.e., 25; the output of the BP neural network is the evaluation value of circular economy for construction enterprises, so the number of nodes in the output layer is $m = 1$.

(3) *Determine the Number of Hidden Layer Neurons.* At present, there is no clear theoretical basis for how to determine the number of hidden layer nodes. It is generally believed that too few hidden layer elements will lead to insufficient fitting, and too many will lead to overfitting and reduce the generalization of the network [19]. The following methods are usually used to determine the number of hidden layer nodes j : $j = \sqrt{m+n+a}$; $j = \log_2 n$; $j = \sqrt{mn}$. Where n is the number of input nodes, M is the number of output nodes, and a is a constant between 1 and 10. Based on experience, $j = 10$ is selected in this paper.

(4) *Training Sample Data.* The first 50 of the sample data of 59 construction enterprises are selected as the training set, that is, the input vector $X = [X_1, X_2, \dots, X_{50}]^T$. The circular economy evaluation value of construction enterprises numbered 1–50 obtained by the improved AHP method in the sample is used as the output target value of the neural network, that is, the target output vector t training = $[t_1, t_2, \dots, t_{50}]^T$, t test = $[t_{51}, t_{67}, \dots, t_{59}]^T$, and then the BP neural network is created through the Matlab toolbox and trained.

(5) *Parameter Setting of Training Function.* Select "TRAINRP" for training function; the adaptive function is "LEARNGDM," the executive function is "MSE," the transfer function is "LOGSIG," the number of neurons is "10," and the training accuracy is $e = 0.00001$; training times $N = 10000$ (default values are selected for other parameters).

(6) *Training Results.* The training results show that after 10 steps of training, the square sum of network training error MSE meets the requirements of target error. The output value of the network after training is very close to the expected value. If the accuracy requirements are met, the network can be used for simulation [20]. According to the above steps, the neural network evaluation test was conducted on 50 construction enterprise samples in the training set, and the relative error of the training results is shown in Table 3.

4. Result Analysis

Click "Simulate" in the Matlab toolbox and input the index sample data of construction enterprises numbered 51–59. The evaluation results are [0.5200, 0.4457, 0.3538, 0.5398, 0.4815, 0.4776, 0.40945, 0.4477, 0.4610]. Compared with the expected output value, the error is shown in Table 4. It can be seen that the maximum relative error between the output value and the expected value obtained by BP neural network simulation is 0.0482, which is completely acceptable in the evaluation of the circular economy. It can be seen that the neural network has high evaluation efficiency and small error and can be popularized and applied in the evaluation of circular economy in construction enterprises in the future. Save the trained neural network. When evaluating the circular economy of other construction enterprises in the future, just input the index data of the enterprise and start the network to obtain the evaluation results.

TABLE 2: Normalization and eigenvector of a primary index judgment matrix.

Criterion layer U judgment matrix	U_1	U_2	U_3	U_4	U_5	Sum of lines (\bar{W}_i)	Feature vector ($W_i = (\bar{W}_i / \sum_{j=1}^n \bar{W}_j)$)
U_1	0.105	0.166	0.112	0.184	0.200	0.767	0.156
U_2	0.315	0.498	0.186	0.306	0.280	1.585	0.322
U_3	0.524	0.166	0.560	0.429	0.360	2.039	0.413
U_4	0.035	0.100	0.080	0.061	0.120	0.324	0.066
U_5	0.021	0.070	0.062	0.020	0.040	0.213	0.043

TABLE 3: Training results of BP neural network.

Sample no	1	2	3	4	5	6	7	8	9	10
Expected value	0.1738	0.2256	0.3168	0.4059	0.3445	0.351	0.4962	0.6077	0.6891	0.6606
Training value	0.23748	0.22203	0.23114	0.38759	0.30415	0.32826	0.50822	0.64775	0.75898	0.69606
Relative error	-0.06368	0.00357	0.08566	0.01831	0.04035	0.02274	-0.01202	-0.04005	-0.06988	-0.03546
Sample No	11	12	13	14	15	16	17	18	19	20
Expected value	0.7608	0.2096	0.3196	0.4018	0.4923	0.4528	0.4486	0.5857	0.6903	0.7191
Training value	0.77443	0.233772	0.307	0.37077	0.46253	0.4293	0.4181	0.5959	0.71117	0.7409
Relative error	-0.01363	-0.02417	0.0126	0.03103	0.02977	0.0235	0.0305	-0.0102	-0.02087	-0.0218
Sample No	21	22	23	24	25	26	27	28	29	30
Expected value	0.7359	0.7972	0.6597	0.7608	0.2126	0.3148	0.3985	0.4904	0.4376	0.4502
Training value	0.77573	0.8262	0.67036	0.77176	0.25621	0.34043	0.4536	0.47815	0.42223	0.4739
Relative error	-0.03983	-0.029	-0.01066	-0.01096	-0.04361	-0.02563	-0.0551	0.01225	0.01537	-0.0237
Sample no	31	32	33	34	35	36	37	38	39	40
Expected value	0.582	0.8002	0.6597	0.7608	0.5807	0.6943	0.7191	0.74	0.7972	0.6591
Training value	0.54904	0.83352	0.6667	0.78486	0.59568	0.64858	0.73067	0.78783	1.0003	0.70266
Relative error	0.03296	-0.03332	-0.007	-0.02406	-0.01498	0.04572	-0.01157	-0.04783	-0.2031	-0.04356
Sample no	41	42	43	44	45	46	47	48	49	50
Expected value	0.7608	0.2107	0.3237	0.3927	0.5014	0.4535	0.5872	0.7958	0.7608	0.5835
Training value	0.77505	0.22493	0.34543	0.46647	0.47214	0.47	0.62417	0.81485	0.80576	0.5976
Relative error	-0.01425	-0.01423	-0.02173	-0.07377	0.02926	-0.0165	-0.03697	-0.01905	-0.04496	-0.0141

TABLE 4: Test results of BP neural network.

Number	51	52	53	54	55	56	57	58	59
Expected value	0.5608	0.4835	0.3881	0.537	0.4941	0.499	0.4559	0.4634	0.4128
Output value	0.5200	0.4457	0.3538	0.5398	0.4815	0.4776	0.4095	0.4477	0.4610
Relative error	0.0408	0.0378	0.0343	-0.0028	0.0126	0.0214	0.0464	0.0157	-0.0482

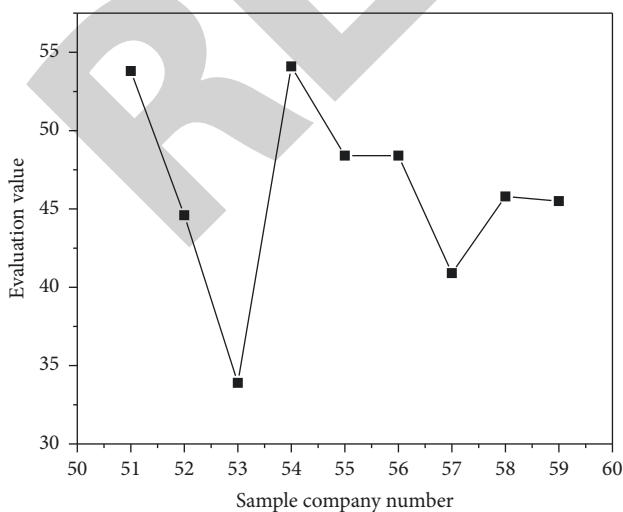


FIGURE 3: Comprehensive evaluation value of circular economy of construction enterprises numbered 51-59.

In order to understand the evaluation results more intuitively, the comprehensive evaluation values of the circular economy obtained from the above simulation are multiplied by 100. The results are shown in Figure 3. It can be seen that the overall evaluation value of the circular economy of the nine construction enterprises is at the medium level, only two of them have an evaluation value of more than 50, and one of them has an evaluation value of only 35. Therefore, the implementation of a circular economy in these nine construction enterprises is still at a low level, with great room for development and improvement.

5. Conclusion

This paper creatively puts forward an improved AHP method. Firstly, the expert evaluation weight is calculated from the perspective of stakeholders, and then the AHP weight of each index is obtained according to the scores of each expert, and the comprehensive weight of each index is

Retraction

Retracted: Parameter Identification of 3D Elastic-Plastic Model for Tunnel Engineering Based on Improved Genetic Algorithm

Mathematical Problems in Engineering

Received 8 August 2023; Accepted 8 August 2023; Published 9 August 2023

Copyright © 2023 Mathematical Problems in Engineering. This is an open access article distributed under the Creative Commons Attribution License, which permits unrestricted use, distribution, and reproduction in any medium, provided the original work is properly cited.

This article has been retracted by Hindawi following an investigation undertaken by the publisher [1]. This investigation has uncovered evidence of one or more of the following indicators of systematic manipulation of the publication process:

- (1) Discrepancies in scope
- (2) Discrepancies in the description of the research reported
- (3) Discrepancies between the availability of data and the research described
- (4) Inappropriate citations
- (5) Incoherent, meaningless and/or irrelevant content included in the article
- (6) Peer-review manipulation

The presence of these indicators undermines our confidence in the integrity of the article's content and we cannot, therefore, vouch for its reliability. Please note that this notice is intended solely to alert readers that the content of this article is unreliable. We have not investigated whether authors were aware of or involved in the systematic manipulation of the publication process.

Wiley and Hindawi regrets that the usual quality checks did not identify these issues before publication and have since put additional measures in place to safeguard research integrity.

We wish to credit our own Research Integrity and Research Publishing teams and anonymous and named external researchers and research integrity experts for contributing to this investigation.

The corresponding author, as the representative of all authors, has been given the opportunity to register their agreement or disagreement to this retraction. We have kept a record of any response received.

References

- [1] X. Dong and L. Chen, "Parameter Identification of 3D Elastic-Plastic Model for Tunnel Engineering Based on Improved Genetic Algorithm," *Mathematical Problems in Engineering*, vol. 2022, Article ID 8305175, 8 pages, 2022.

Research Article

Parameter Identification of 3D Elastic-Plastic Model for Tunnel Engineering Based on Improved Genetic Algorithm

Xiaoma Dong  and Lifei Chen

Yangzhou Polytechnic Institute, Yangzhou, Jiangsu 225127, China

Correspondence should be addressed to Xiaoma Dong; 2016123730@jou.edu.cn

Received 28 June 2022; Accepted 29 July 2022; Published 23 August 2022

Academic Editor: Hengchang Jing

Copyright © 2022 Xiaoma Dong and Lifei Chen. This is an open access article distributed under the Creative Commons Attribution License, which permits unrestricted use, distribution, and reproduction in any medium, provided the original work is properly cited.

In order to overcome the deficiencies of the existing intelligent displacement back analysis methods, the authors propose a parameter identification method for the 3D elastic-plastic model of tunnel engineering based on an improved genetic algorithm. An improved SVR algorithm is introduced, which solves this problem by transforming the multidimensional output variable regression into a multilayer standard one-dimensional output variable regression; combined with the decimal-coded genetic algorithm, an improved GA-SVR algorithm is formed, and genetic algorithm is used to search for optimal SVR model parameters, in order to establish the optimal nonlinear mapping relationship between the parameters to be identified and the displacement. The genetic algorithm is used to carry out the optimal identification of the parameters to be identified. In order to compare the effect of this improved GA-SVR algorithm, the genetic algorithm is combined with the BP neural network to form the GA-BP algorithm and compile the corresponding calculation program. The two algorithms are applied to the intelligent identification of the parameters of the 3D elastic-plastic model of the same tunnel engineering. The experimental results show that the maximum relative error of the 6 parameters to be identified is 18.51%, only 2 are over 15% and 14 are within 10%, and the average relative error of the 6 parameters is only 10.32%, the minimum is 2.63%; for the GA-BP algorithm, the maximum relative error of identification is 22.73%, 4 are more than 15% and 9 are within 10%, and the average relative error of 6 parameters' identification is up to 13.91%, and the minimum is 4.64%. The improved GA-SVR algorithm can achieve higher identification accuracy and better calculation efficiency than the GA-BP algorithm and can be used in the identification of similar geotechnical engineering parameters.

1. Introduction

With the development of the economy and the progress of the society, many people's behaviors, such as mining production, water conservancy development, national defense construction, and transportation, have an increasingly close relationship with the stability of the caverns in the rock mass and the surrounding rock of the tunnel. Underground engineering has played a pivotal role in water conservancy and hydropower, road traffic, and mining engineering [1]. Various engineering geological problems caused by the interaction between the rock and soil mass and engineering activities, which are the occurrence environment of various projects, have also received more and more attention; the stability of large-scale underground engineering caused by a

large number of rock and soil excavation has become an important problem faced by human engineering activities [2]. Because of the complexity and diversity of natural rock mass structures, people's understanding of the stability of surrounding rocks has encountered great obstacles; therefore, the research on the stability of the surrounding rock and its influencing factors is of great significance to the in-depth understanding of human engineering activities and the stability of the surrounding rock.

The study of rock mass structural plane characteristics is a complex and hot issue in the field of rock mechanics and has always been paid close attention by academic circles and engineering application units. The rock mass structural plane is a geological interface or zone with a certain direction, relatively low mechanical strength, and two-way

extension (or a certain thickness) in the rock mass formed in the long geological history development process. Because of the existence of the structural plane, it not only destroys the integrity of the rock mass but also directly affects the mechanical properties and stress distribution state of the rock mass and greatly affects the penetration path and failure mode of the rock mass. The existence of structural planes affects the stability of rock mass engineering [3]. Therefore, at present, in the fields of engineering geology, rock mechanics, and hydrogeology, much attention is paid to the study of rock mass structure.

2. Literature Review

Li et al. conducted detailed research on the elastic-plastic damage constitutive model of rock and other materials [4]. Namazi et al. used the transverse isotropic constitutive relation to simulate the local deformation behavior of geomaterials in triaxial symmetric compression test, which considered the case of shear zone and pure compression zone [5]. Raghavan et al. established an elastic-plastic damage model of geological materials under the framework of continuous thermodynamics, the tensile stress damage is considered in the model, the plastic potential function is based on the Drucker–Prager criterion, and the damage is a function of volumetric strain [6]. Anirban has conducted a lot of systematic research on the elastic-plastic damage constitutive model of rock materials; considering the hydraulic properties of rock under saturated and unsaturated states, an elastic-plastic damage coupled constitutive model of semibrittle materials is established and compared with the experimental results [7]. Arbabsiar et al. proposed a statistical damage constitutive model for rock softening based on the Weibull distribution of mesoscopic element strength, in order to describe the entire continuous change process of microcracks from damage to fracture, and the influence of strength criterion and residual strength on the softening-type statistical damage model was studied [8]. Tushavina et al. established an elastic damage model based on fracture mechanics theory, which can be used to describe the stress-strain relationship of rock-like materials under uniaxial compression, since macroscopic plastic deformation is not considered in the model establishment process; therefore, the effect of confining pressure on rock plasticity cannot be reflected [9].

The parameter identification of geotechnical numerical calculation model based on the displacement inverse analysis method has been paid more and more attention. However, based on the research results at home and abroad, the current displacement inverse analysis still has the following problems: (1) the inverse analysis model is generally concentrated on the homogeneous material and the linear elastic model, although it can achieve good results, is obviously still a little bit deviated from the actual situation; (2) the direct optimization and inversion of the current stage all use two-dimensional plane calculation to shorten the calculation time to meet the engineering requirements, but many projects cannot actually be approximated as two-dimensional problems (Figure 1); (3) whether the adopted

optimization method can guarantee the convergence to the optimal solution in the parameter search interval; (4) the mechanical behavior of geotechnical engineering is affected by many uncertain factors, and the relationship between these factors and the basic information of back analysis is also highly uncertain and nonlinear; errors are difficult to avoid with any definite computational model; (5) the complexity of geotechnical materials and the harsh construction environment of geotechnical engineering bring two problems: ① the information obtained from monitoring is inaccurate; ② large-scale and high-density monitoring is also impossible.

The author applied this improved support vector regression algorithm to the inverse analysis of the three-dimensional elastic-plastic displacement of the tunnel in order to overcome the shortcomings of the existing intelligent displacement inverse analysis methods.

3. Research Methods

3.1. Improved GA-SVR Algorithm. The so-called improved GA-SVR algorithm refers to the use of genetic algorithm to optimize the network parameters of the improved SVR algorithm; in order to establish the optimal nonlinear mapping relationship between the parameters to be inverted and the displacement, the following descriptions will be made separately.

3.1.1. Improved GA-SVR Algorithm. The improved GA-SVR algorithm draws on the idea of the support vector multiclass classification algorithm and converts the multidimensional output regression problem into a multilayer standard one-dimensional SVR algorithm to solve. The same tunnel shotcrete support design comparison shows that this improved algorithm is better than BP neural network. The network generalization performance is better and the prediction accuracy is higher, which verifies its effectiveness in the field of geotechnical engineering [10]. Some people have elaborated on the standard one-dimensional SVR algorithm. The flowchart of the improved SVR algorithm is shown in Figure 2.

The training steps are as follows:

- (1) The input parameter X of the learning sample is used as the training input of the network, and the sample value y_1 of the first output parameter is used as the training output of the network; after machine learning, predict the input variable X' of the test sample to obtain the first output parameter y'_1 of the test sample, denoted as $j = 1$.
- (2) Judge whether j reaches the number n of regression output parameters; if so, output the y'_1 of the test sample, otherwise the calculation goes to Step (3), and record $j = j + 1$.
- (3) Take X and y_1 as the training input of the network and the sample value y_2 of the second output parameter as the training output of the network; after machine learning, the input variables X' and y'_1 of

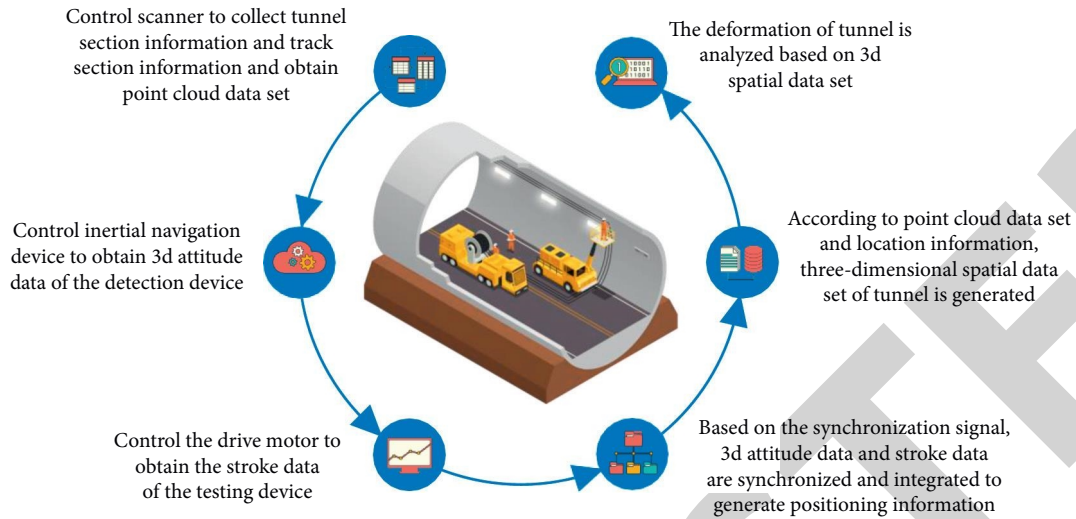


FIGURE 1: The 3D identification of tunnel engineering.

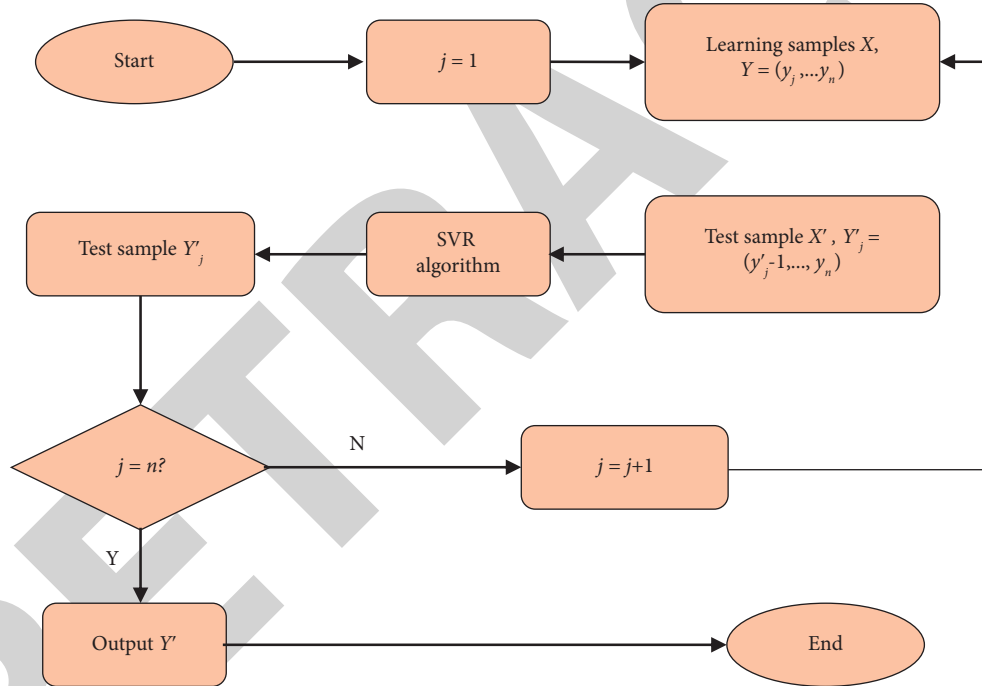


FIGURE 2: Flowchart of the improved SVR algorithm.

the test sample are predicted to obtain the second sample value of the test sample, an output parameter y'_2 .

- (4) X , y_1 , and y_2 are used as the training input of the network, and the sample value y_3 of the third output parameter is used as the training output of the network; after machine learning, predict the input variables X' , y'_1 , and y'_2 of the test sample to obtain the third output parameter y'_3 of the test sample.
- (5) Repeat the above steps in the same way until the condition of Step (2) is satisfied.

3.1.2. Genetic Algorithm. In order to speed up the searching speed of genetic algorithm, the author adopts decimal coding genetic algorithm, and its genetic operation operator is described below.

(1) *Selection Operator.* Using the queuing selection method, after calculating the fitness of each individual, the individuals are sorted in the group according to the size of the fitness, and then the predesigned probability table is assigned to the individuals in sequence as their respective selection probabilities. According to the standard geometric distribution selection method, the selection probability of each individual is defined as the following formula:

$$P = q'(1 - q)^{r'-1}, \quad (1)$$

where

$$q' = \frac{q}{1 - (1 - q)^P}. \quad (2)$$

In the formula, q is the probability of selecting the best individual; r' is the rank of the individual, 1 is the best; P is the population size.

(2) *Hybrid Operator.* Using arithmetic crosses, let P_c be the probability of the crossover operation, and to determine the parent of the crossover operation, repeat the following process from $i = 1$ to P : a uniform random number r is generated from $(0, 1)$, if $r < P_c$ is selected as a parent, X_i is selected as a parent, and \bar{X}, \bar{Y} is used to represent the parent selected above. The hybrid operation is carried out as follows, and two offspring are generated, that is, the following formula:

$$\left. \begin{aligned} \bar{X}' &= r\bar{X} + (1 - r)\bar{Y} \\ \bar{Y}' &= (1 - r)\bar{X} + r\bar{Y} \end{aligned} \right\}. \quad (3)$$

Check whether the newly generated offspring are feasible solutions; if feasible, use them to replace the parent; otherwise, keep the feasible ones, then generate new random numbers, and repeat the crossover operation until two feasible offspring are obtained [11].

(3) *Mutation Operator.* Using nonuniform mutation, the mutation method is for real number coding. Suppose x_i is an individual in the group and x'_i is the offspring produced by mutation, then we obtain the following formula:

$$x'_i = \begin{cases} x_i + (b_i - x_i)f(G), & (r_1 < 0.5), \\ x_i - (x_i - a_i)f(G), & (r_1 \geq 0.5). \end{cases} \quad (4)$$

Among them,

$$f(G) = \left[r_2 \left(1 - \frac{G}{G_{\max}} \right) \right]^b. \quad (5)$$

In the formula, r_1 and r_2 are uniform random numbers between $(0, 1)$, G is the current generation, G_{\max} is the maximum number in the generation, and b is the shape parameter.

3.1.3. *Adaptation Function.* In the training stage of the improved SVR network, the total relative error is used as the objective function as shown in the following formula:

$$f(x) = \min \left(\sum_{j=1}^m \sum_{i=1}^n \left| \frac{y'_i - y_i}{y_i} \right| \times 100\% \right), \quad (6)$$

where m is the number of network output variables, n is the number of test samples during network training, and y_i and y'_i are the sample value and network prediction value of the i -th test sample during network training, respectively.

When using the genetic algorithm to optimize the parameters of the support vector machine network, the fitness function adopts the following nonlinear acceleration form:

$$g(x) = \exp[-0.005f(x)]. \quad (7)$$

It can be seen from equations (6) and (7) that when the prediction error is 0, that is, when the prediction result is completely consistent with the sample value, the adaptation function reaches the maximum value of 1, since the objective function is nonnegative, the adaptation function cannot be greater than 1; the closer the fitness function value is to 1, the higher the accuracy of the network training.

3.1.4. *Improved GA-SVR Algorithm.* The implementation steps of this algorithm are as follows:

- (1) Divide the training samples into two parts: one part is used as a learning sample to improve the GA-SVR network, and the other part is used as a test sample to test the network training ability.
- (2) Initialize the genetic algorithm, randomly generate an initial population of SVR network parameters (kernel parameters, C and ϵ) with a population size of N_p , and the counter is denoted as $g = 0$.
- (3) The improved GA-SVR algorithm reads in the training samples and test samples, and at the same time, it reads the individual network parameters in the initial population for network training and prediction.
- (4) The prediction result of each individual is passed to the genetic algorithm, the fitness of each individual is calculated by the fitness function of the genetic algorithm, and the fitness is evaluated.
- (5) Determine whether the prespecified evolutionary algebra is reached; if so, the algorithm ends and the individual with the highest fitness is returned to decode to obtain the optimal SVM network parameters. If the evolutionary algebra is not reached, go to the next step.
- (6) The selection operator selects individuals with higher fitness in the initial population and performs replication, crossbreeding, and mutation operations to generate a progeny population of SVR network parameters whose number of individuals is N_p , and the counter is recorded as $g = I + 1$.
- (7) Repeat Steps (3)–(6) until the specified evolutionary algebra is reached. The algorithm ends, and the optimal SVM network parameters are returned. The flowchart of the improved GA-SVR algorithm is shown in Figure 3.

3.2. Intelligent Identification of Parameters of Tunnel Engineering 3D Elastic-Plastic Model Based on Improved GA-SVR Algorithm

3.2.1. *Acquisition of Training Samples: Numerical Experiments.* Since the calculation model is axisymmetric, only half of it is considered in modeling, and the length of

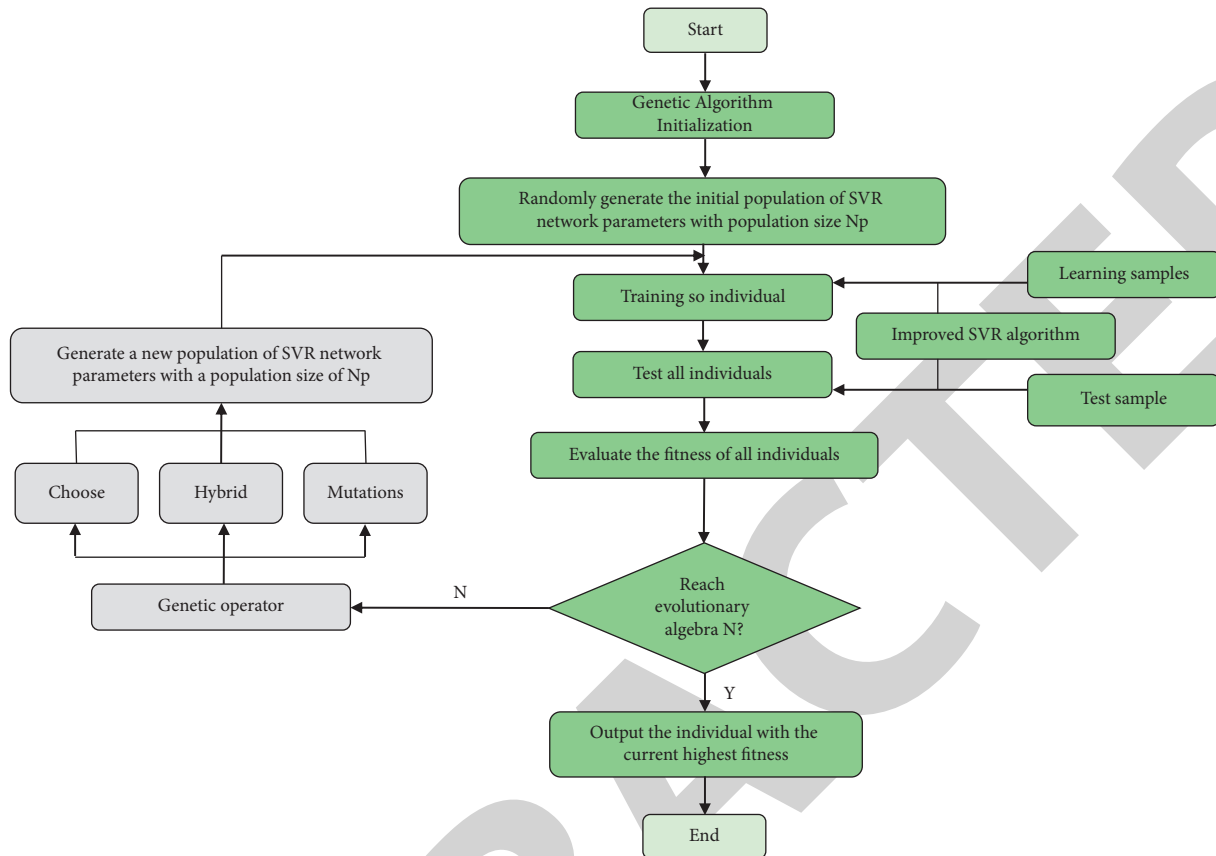


FIGURE 3: Flowchart of the improved GA-SVR algorithm.

the calculation model from top to bottom and from left to right is 60 m. The axial length of the model is set at 50 m [12, 13].

The tunnel is constructed in sections with upper and lower steps, the cycle footage is 1 m, and the upper section is excavated 6 m ahead of the lower section. The excavation range of the upper section is above the line segment to the vault, and the vertical coordinate is -0.75 to 4.55 ; after the excavation of the upper section is completed, immediately hit the bolt and spray concrete. When the distance between the upper and lower sections exceeds 6 m, the lower section is excavated and supported, and then the upper and lower sections are excavated at the same time [14]. Considering that the tunnel is excavated in II–V grade surrounding rock, the IV~V grade surrounding rock tunnel has a buried depth of 20–145 m, a shotcrete thickness of 8–20 cm, an anchor bolt length of 2–3 m, and a dilatation angle of 1° – 13.5° . The burial depth of grade II-III surrounding rock tunnel is 20–220 m, the thickness of shotcrete is 2–6 cm, the length of bolt is 1.5–2 m, and the dilatation angle is 10° – 18° . The horizontal side pressure coefficient is taken as 0.5~1.5, the bolt spacing is taken as 1 m, the bolt diameter is taken as 18~22 mm, the surrounding rocks of grades II-III are divided into 11 levels, and the surrounding rocks of grades IV-V are divided into 26 levels; according to the uniform experimental design method, 37 numerical test schemes are combined [15, 16].

Numerical simulation of excavation process is done using FLAC3D software and the Mohr–Coulomb constitutive model. In this paper, the author randomly selects the calculated absolute displacement of each measuring point in each test on the monitoring surface $Y = 16$ m when the face is advanced to $Y = 16$ m; the absolute displacement of each measuring point is converted into the relative convergence value of measuring lines EA, EB, AC, and BD, evenly and randomly. 6 test results were selected from 37 numerical tests as test samples, the last three samples of the test sample set are regarded as the “specific projects” to be inverted, and the parameters to be identified are cohesion, internal friction angle, deformation modulus, lateral pressure coefficient, Poisson’s ratio, and dilatancy angle [17].

3.2.2. Intelligent Identification of Three-Dimensional Elastic-Plastic Parameters of Tunnel Engineering Based on Improved GA-SVR Algorithm. The direct optimization method is used for intelligent identification of elastic-plastic parameters, in order to compare the effect of the improved GA-SVR algorithm proposed by the author on the three-dimensional elastic-plastic inversion; here, the GA-BP algorithm is used for the same inverse analysis, except that the regressor is changed to BP neural network [18]. The genetic algorithm uses the same real number coding and the same fitness function. In order to improve the generalization ability of the BP network, the input data are normalized. The

TABLE 1: Optimal model parameters.

Improved SVR model			BP model		
C	σ	ε	M	lr	Epochs
8207.5	171.7	0.2	14	0.6185	43

TABLE 2: Identification results of the improved GA-SVR algorithm.

Side pressure coefficient		Deformation modulus relative error (%)	Poisson's ratio		Poisson's ratio relative error (%)	Dilation angle (°)		Relative error of dilation angle (%)
Actual value	Identification value		Actual value	Identification value		Actual value	Identification value	
0.82	0.86	4.88	0.42	0.48	14.29	3.5	3.42	2.29
0.50	0.45	10.00	0.24	0.28	16.67	14.8	14.99	1.28
1.40	1.24	11.43	0.22	0.22	0.00	16.4	15.69	4.33
		8.77			10.32			2.63

TABLE 3: Identification results of GA-BP algorithm.

Cohesion (MPa)		Cohesion relative error (%)	Internal friction angle (°)		Relative error of internal friction angle (%)	Deformation modulus (GPa)	
Actual value	Identification value		Actual value	Identification value		Actual value	Identification value
0.20	0.18	10.00	23.8	20.05	15.76	2.0	2.08
1.54	1.33	13.64	51.6	45.09	12.62	22.2	18.11
1.82	1.89	3.85	55.8	48.35	13.35	27.6	31.77
Average relative error (%)		9.16			13.91		

Levenberg–Marquardt algorithm is used to adjust the weights, and the weight adjustment rate is as follows:

$$\Delta W = (J^T J + \mu I)^{-1} J^T e. \quad (8)$$

In the formula, J is the Jacobian matrix of the error differential to the weight, e is the error vector, I is the identity matrix, and μ is a scalar. The introduction of μI is to ensure the positive definiteness of the inverse matrix; when μ is large, equation (8) is close to the gradient method, and when μ is small, equation (8) is changed to Gauss–Newton method. In this method, μ is also adaptively adjusted. Because of the use of approximate second derivative information, the algorithm has a faster convergence rate than the standard BP algorithm. A 3-layer BP neural network is used, the number of nodes in the input layer is 12, the number of nodes in the output layer is 4, and the neurons in the hidden layer use the Sigmoid transformation function. Its expression is as follows:

$$f(x) = \frac{1}{1 + e^{-x}}. \quad (9)$$

The neurons in the output layer adopt a linear transformation function [19, 20]. The network training convergence accuracy is 0.01. The number of neurons in the hidden layer m , the learning rate lr , and the number of iterations' epochs are obtained by the genetic algorithm search. The BP network computing program borrows the neural network toolbox that comes with MATLAB software [21]. The learning sample set and the first three test samples in Table 1 are read into the improved GA-SVR and GA-BP algorithm

programs. The SVR kernel function adopts the RBF kernel function, the program predicts the three test samples while learning knowledge, and the network parameters are continuously adjusted by genetic algorithm, until the network parameters that can minimize the prediction error of the three test samples are found within the specified evolutionary algebra; after the network training is over, the optimal mapping relationship between the parameters to be inverted and the displacement has been established [22]. After obtaining the optimal network parameters, the displacement and weight, using the same fitness function and genetic operator, 100 generations of evolution and a population size of 30, within the search range of the parameters to be inverted, search for the values of the parameters to be inverted that can make the predicted displacements closest to the calculated displacements of the next three samples. The identification results of the improved GA-SVR algorithm and GA-BP algorithm are shown in Tables 2 and 3, respectively.

4. Analysis of Results

For the improved GA-SVR algorithm, the maximum relative error of the 6 parameters to be identified is 18.51%, only 2 parameters exceed 15% and 14 parameters are within 10%. The average relative error of 6 parameters' identification is only 10.32% at maximum and 2.63% at minimum. For the GA-BP algorithm, the maximum relative error of identification is 22.73%, 4 are over 15% and 9 are within 10%, and the average relative error of 6 parameters' identification is

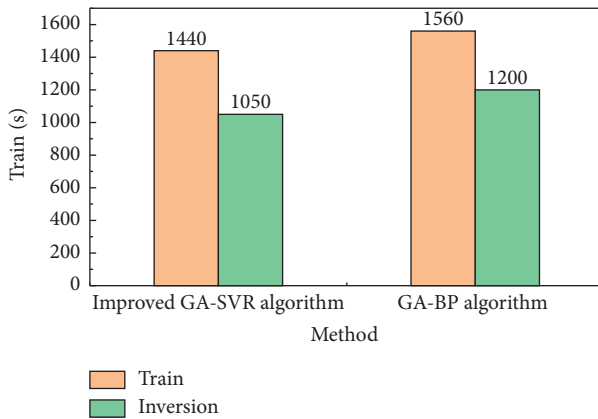


FIGURE 4: Comparison of the calculation time of the two algorithms.

13.91% at maximum and 4.64% at minimum. Overall, the identification results of these two algorithms are satisfactory, but in contrast, the improved GA-SVR algorithm has better identification results than the GA-BP algorithm, especially for the ones that have a significant impact on numerical calculation; the first 4 parameters are more obvious [23].

According to the predicted displacement situation of the subsequent excavation inversion results, under the condition that the convergence itself is small, the prediction result of the improved GA-SVR algorithm is significantly better than that of the GA-BP algorithm, and the other two examples are not much different [24]. The calculation time of the two algorithms is shown in Figure 4 (P4 dual-core 2.8 G, 256 M memory PC). It can be seen from Figure 4 that the calculation time of the improved GA-SVR algorithm is slightly shorter, that is, the improved GA-SVR algorithm has higher computational efficiency than the GA-BP algorithm [25].

5. Conclusion

After comparative research, the following conclusions can be drawn:

- (1) It is feasible to apply the improved GA-SVR algorithm to the 3D elastic-plastic parameter identification of tunnel engineering, and the author's example proves this.
- (2) Whether it is the improved GA-SVR algorithm or the GA-BP algorithm, applying it to the identification of three-dimensional elastic-plastic parameters of tunnel engineering can achieve good results, but in contrast, the improved GA-SVR algorithm is slightly better than the GA-BP algorithm in terms of identification accuracy, computational efficiency, and convergence; it can be popularized and applied in similar projects.

Data Availability

The data used to support the findings of this study are available from the corresponding author upon request.

Conflicts of Interest

The authors declare no conflicts of interest.

References

- [1] T. Li, J. Zhan, C. Li, and Z. Tan, "Evaluation of the adaptability of an EPB TBM to tunnelling through highly variable composite strata," *Mathematical Problems in Engineering*, vol. 2021, no. 12, pp. 1–14, 2021.
- [2] J. Wu, H. Chen, N. Yang et al., "High tunnelling electro-resistance in a ferroelectric van der waals heterojunction via giant barrier height modulation," *Nature Electronics*, vol. 3, no. 8, pp. 466–472, 2020.
- [3] R. Chanana, "Diffusion current after ionisation of thermal sio 2 in a mos device forms the fowler-nordheim electron tunnelling current showing wave-particle duality of electrons," *IOSR Journal of Electrical and Electronics Engineering*, vol. 16, no. 1, pp. 50–54, 2021.
- [4] Z. C. Li, G. H. Wang, J. W. Hao et al., "The influence of construction scheme of asymmetric three-cabin utility tunnelling on the surface settlement behaviour," *KSCE Journal of Civil Engineering*, vol. 25, no. 9, pp. 3568–3582, 2021.
- [5] E. Namazi, M. Hajihassani, S. Gilani, and S. Zolfegharifar, "Risk assessment of building damage induced by tunnelling through a gene expression programming model," *Geotechnical & Geological Engineering*, vol. 40, no. 4, pp. 2357–2370, 2022.
- [6] A. Raghavan, P. Rao, J. Neuzil, D. Pountney, and S. Nath, "Oxidative stress and rho gtpases in the biogenesis of tunnelling nanotubes: implications in disease and therapy," *Cellular and Molecular Life Sciences*, vol. 79, no. 1, pp. 36–15, 2022.
- [7] A. Anirban, "40 years of scanning tunnelling microscopy," *Nature Reviews Physics*, vol. 4, no. 5, 291 pages, 2022.
- [8] M. Arbabsiar, M. Ebrahimi Farsangi, and H. Mansouri, "Fuzzy logic modelling to predict the level of geotechnical risks in rock tunnel boring machine (tbm) tunnelling," *Rudarsko-Geolosko-Naftni Zbornik*, vol. 35, no. 2, pp. 1–14, 2020.
- [9] O. Et al, "Numerical calculation of heat and mass transfer processes in the adsorbers of the air purification system," *Turkish Journal of Computer and Mathematics Education (TURCOMAT)*, vol. 12, no. 2, pp. 2714–2718, 2021.
- [10] Q. Guo, L. Gao, X. Chu, and H. Sun, "Parameter identification for static var compensator model using sensitivity analysis and improved whale optimization algorithm," *CSEE Journal of Power and Energy Systems*, vol. 8, no. 2, pp. 535–547, 2022.
- [11] R. Boukellif, A. Ricoeur, and M. Oxe, "Parameter identification of crack-like notches in aluminum plates based on strain gauge data," *Structural Health Monitoring*, vol. 20, no. 6, pp. 3227–3238, 2021.
- [12] D. Li and Y. Wang, "Parameter identification of a differentiable bouc-wen model using constrained extended kalman filter," *Structural Health Monitoring*, vol. 20, no. 1, pp. 360–378, 2021.
- [13] C. Che, H. Wang, X. Ni, and Q. Fu, "Performance degradation prediction of aeroengine based on attention model and support vector regression," *Proceedings of the Institution of Mechanical Engineers - Part G: Journal of Aerospace Engineering*, vol. 236, no. 2, pp. 410–416, 2022.
- [14] T. Sananmuang, K. Mankong, S. Ponglowhapan, and K. Chokeshaiusaha, "Support vector regression algorithm modeling to predict the parturition date of small - to medium-

Retraction

Retracted: Application of Multimedia Tilt Photogrammetry Technology Based on Unmanned Aerial Vehicle in Geological Survey

Mathematical Problems in Engineering

Received 5 December 2023; Accepted 5 December 2023; Published 6 December 2023

Copyright © 2023 Mathematical Problems in Engineering. This is an open access article distributed under the Creative Commons Attribution License, which permits unrestricted use, distribution, and reproduction in any medium, provided the original work is properly cited.

This article has been retracted by Hindawi, as publisher, following an investigation undertaken by the publisher [1]. This investigation has uncovered evidence of systematic manipulation of the publication and peer-review process. We cannot, therefore, vouch for the reliability or integrity of this article.

Please note that this notice is intended solely to alert readers that the peer-review process of this article has been compromised.

Wiley and Hindawi regret that the usual quality checks did not identify these issues before publication and have since put additional measures in place to safeguard research integrity.

We wish to credit our Research Integrity and Research Publishing teams and anonymous and named external researchers and research integrity experts for contributing to this investigation.

The corresponding author, as the representative of all authors, has been given the opportunity to register their agreement or disagreement to this retraction. We have kept a record of any response received.

References

- [1] W. Li, "Application of Multimedia Tilt Photogrammetry Technology Based on Unmanned Aerial Vehicle in Geological Survey," *Mathematical Problems in Engineering*, vol. 2022, Article ID 4616119, 6 pages, 2022.

Research Article

Application of Multimedia Tilt Photogrammetry Technology Based on Unmanned Aerial Vehicle in Geological Survey

Wenyu Li 

Baotou Railway Vocational & Technical College, Baotou 014060, China

Correspondence should be addressed to Wenyu Li; 201701350206@lzpcc.edu.cn

Received 29 May 2022; Revised 21 June 2022; Accepted 21 July 2022; Published 21 August 2022

Academic Editor: Hengchang Jing

Copyright © 2022 Wenyu Li. This is an open access article distributed under the Creative Commons Attribution License, which permits unrestricted use, distribution, and reproduction in any medium, provided the original work is properly cited.

In order to better investigate the geological research, a tilt photogrammetry technology based on the unmanned aerial vehicle is proposed. This paper makes use of UAV tilt photogrammetry technology to make geological macroscopic analysis and establishes 3d color digital ground model, forming a set of technical methods for geological survey assisted by UAV. The experimental results show that the coordinate calculation is significantly improved, and the root mean square error of plane coordinates reaches 0.2 m, which can meet the requirements of later cartography and spatial measurement. The feasibility and efficiency of carrying out a geological survey based on the unmanned aerial vehicle are verified by the practical application in landslide hazard geological survey. It is proved that DEM and DOM data obtained based on oblique photogrammetry data can form various thematic maps by superimposing them with vector GIS data, which will provide a basic data model for subsequent engineering investigation, site management, and image display.

1. Introduction

The UAV tilt photography technology refers to the images obtained by the UAV shooting at a certain angle. By installing multiple sensors on the UAV, data information is collected from different angles, and relatively clear and complete ground object information is obtained [1]. The most useful data images are mainly satellite images with the smallest inclination angle and vertical angle. However, the information from these two angles can only get local information, and the whole physical model and scene cannot be constructed. Inclination photography is an airborne photography monitoring technology taken from multiple angles, which perfectly combines aerial photography technology of unmanned aerial vehicles with data and information collection technology on the ground. Information images of the ground are collected from different angles by multiple sensors on the same platform. This technology changes the limitation that the traditional aerial photography technology can only shoot from the vertical direction and can more clearly reflect the actual situation of real objects on the ground. UAV tilt photography technology can

truly reflect the situation of the photographed target. With the support of advanced positioning technology, rich image data can be obtained, and the photography process does not consume a lot of manpower and material resources [2]. The UAV oblique photography can detect the situation of the measured area from multiple angles, truly reflect the local actual situation, and make up for the shortcomings of traditional photogrammetry. In addition, the UAV tilt photography technology can analyze a single image through corresponding software. The length, height, area, and other information of the photographed target are inferred. The UAV tilt photography technology can combine the image data from various angles to build a 3D real scene model, which can not only improve the comprehensiveness and systematicness of data information but also effectively reduce the aerial photography cost. UAV tilt photography technology has the advantages of flexibility, unlimited flight, and low aerial photography cost. Especially, the advantage of being able to build a three-dimensional real-life model has greatly expanded the application range of this technology, making this technology have a very broad development prospect [3].

With the development of unmanned aerial vehicle (UAV) and real-time positioning technology, tilt photogrammetry technology is becoming more and more mature. It can obtain high-resolution all-element geographic information in the survey area by taking photos at low altitude by UAV, can quickly and efficiently obtain the side and top information of the target object, and generate a real 3D model by combining real-time positioning technology and 3D reconstruction technology. In recent years, this technology has been widely used in land, water conservancy, urban planning, and other industries and achieved remarkable results [4]. Moon et al. [5] studied the method of building damage assessment based on UAV tilt photography [5]. Xu et al. [6] applied oblique photogrammetry to waterway engineering and put forward the operation flow of UAV spatial data acquisition for waterway engineering [6]. The feasibility of oblique photogrammetry technology in the application of waterway engineering is verified. Yang et al. [7] explored the influence of oblique photogrammetry on traditional cadastral management and its improved technology and pointed out that oblique photogrammetry technology can significantly reduce the cost of geographic information collection and promote the transformation of urban land management from 2D to 3D [7]. With the growth of computer computing power and UAV performance, inclination photogrammetry technology is bound to play a more and more important role in the planning and construction of various types of projects. Therefore, the application of UAV tilt photogrammetry technology in the geological survey is put forward. Three-dimensional reconstruction of various ground features and landforms on the construction site is realized by using oblique photogrammetry technology. On this basis, a standardized process of spatial information collection that can meet the management needs of the construction site is established, and a set of technical methods for assisting geological survey with unmanned aerial vehicles are formed. This method can not only obtain the image data of the survey area but also obtain the geological information which is more concerned by the geological survey through geological interpretation and analysis. Real-time images of the disaster area are carried out through the oblique photogrammetry technology of drones. After filming, it will be transmitted to the commander, which will help to formulate preventive measures against geological disasters. At the same time, because of the advantages of portable, fast maneuvering, and low risk, the small UAV has obvious advantages in the rapid emergency geological survey under extremely complex terrain conditions, extremely poor traffic conditions, and extremely dangerous environment [8].

2. Image Data Acquisition

Aerial survey image data of UAV are obtained by field flight shooting in the investigation area. Through a series of work, such as investigation task analysis and research, field reconnaissance, UAV type selection, flight altitude and flight path design, ground image control point planning, equipment parameter setting, aerial photography of field flight

operations, result inspection and corresponding supplementary measurement, aerial photogrammetry covering the whole investigation area with certain overlap rate, high pixel, high resolution, and high definition is obtained [9]. The workflow of image data acquisition in field aerial survey is shown in Figure 1.

3. Image Data Postprocessing

The aerial survey image data obtained from the aerial survey of unmanned aerial vehicles in the field and POS information of air routes combined with a proper amount of ground image control point measurement results can be used to form DEM (digital elevation model), DOM (digital orthophoto map), DLG (digital line map), and other basic products through postprocessing software (such as Pix4D-mapper and photoscan). At the same time, it can also form three-dimensional color surface models and Google tiles which are composed of polygonal Mesh nets in the whole survey area. The result of UAV postprocessing is to integrate multiple debris images, and the resulting image becomes a part of the observation area image. It reflects all the information in a topographic map, a picture, or a model, so that geological investigators can understand the overall macro information of the survey area and further analyze the work [10].

4. Geological Interpretation and Geological Information Elements Collection Methods

The traditional topographic map surveying and mapping requires a large amount of investment to ensure the operation of complex and diverse disaster forms. Compared with the established scale map, the UAV performs aerial photography through multiple angles and completes the multidirectional aerial map setting according to the actual needs, thereby providing a guarantee for the investigation of disasters.

As shown in Figure 2, geological interpretation and collection of geological information are mainly to identify, measure, analyze, and collect the coordinate information, spatial geometric parameters, and geological information of geological objects such as geological points, lines, planes, and bodies concerned in the geological survey by means of indoor interpretation and preliminary geological analysis of UAV-related products. It mainly includes the spatial position coordinates of various geological objects, formation lithology, geological boundary, joint and plane occurrence, plane distribution range of geological bodies, spreading area, volume, feasibility, and key points, so as to provide more comprehensive and abundant geological information for the fieldwork of geological survey and geological analysis [11].

Geological interpretation and geological information collection are mainly based on field aerial photographs combined with image control points to form a three-dimensional color surface model of the investigation area through postprocessing in the industry. This model is used as the basis of the information collection platform, and the image, color, and texture of the model are combined with

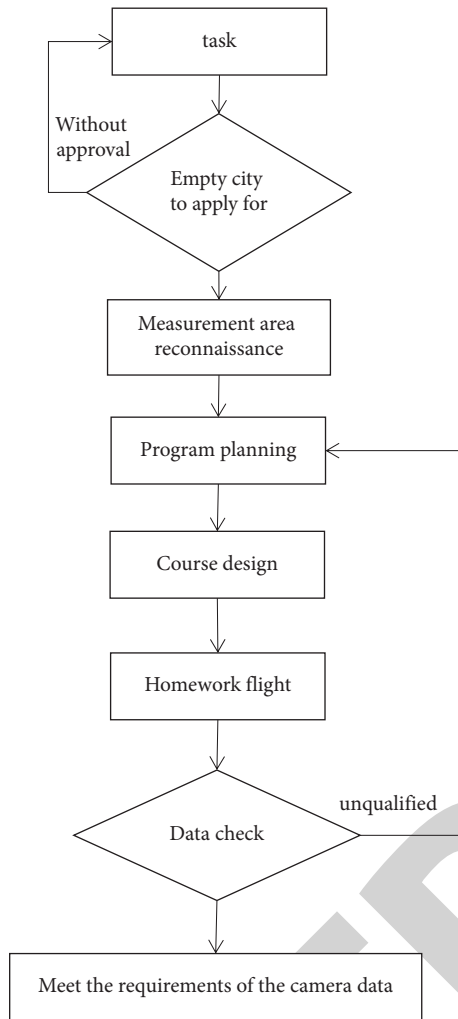


FIGURE 1: Aerial photography process of UAV.

vector coordinate information and three-dimensional relative position information of the model. Interpreting and identifying the position coordinates, formation lithology, geological boundary, joint and plane occurrence, plane distribution range, spreading area, and volume of the geological body involved in the geological survey and obtained information [12].

4.1. Selection of Geological Information Collection Platform.

Through the comparison of UAV-related achievements, the 3D color surface model is a 3D vectorized digital model, which contains not only spatial coordinate information but also real and rich color information, landform, and ground object information. It can not only reproduce the scene of the field work target area but also help geological engineers deepen their observation and understanding of the investigation site. At the same time, it can also preliminarily identify and interpret geological information such as rock and soil characteristics, foundation covering boundary, boundary of unfavorable geological body, surface cracks, joint structure, and hydrology based on surface color change and image information [13]. Meanwhile, the 3D surface

model is editable, searchable, and open. It can realize the editing of any concerned geological object in the model, such as identification and convenient outline, and can use its query function to quickly obtain the coordinate information and geometric parameter information of geological objects. The openness of the model also ensures that the obtained information is stored in a common general format of geological work, which is convenient for further analysis and operation in the later period. Therefore, the three-dimensional surface model can be selected as the working platform for geological information collection to realize a series of functions such as capturing, identifying, collecting, analyzing, judging, and storing the information of geological objects of interest [14].

4.2. Geological Point Information Collection Method.

Geological point information mainly includes the coordinate information of the geological point and the relevant geological information of the position where the geological point is located. The traditional method is to select the key parts of the survey work area as geological points for on-site recording through a field geological survey. The workflow of collecting geological point information by UAV is mainly divided into several steps. First, the locations where important geological phenomena are exposed are marked and numbered on the 3D surface model to form identification points, and then, the locations of geological points are accurately checked from multiple angles with the help of functions such as model rotation and amplification, and corresponding adjustments are made, so that the selected identification points are taken as indoor preliminary geological points; second, the coordinates and elevation information of geological points are automatically extracted by using the spatial coordinate information contained in the three-dimensional vectorized surface model with the help of related postprocessing software; third, according to the surface color and image information restored by the high-altitude scene combined with geological experience, preliminary indoor analysis is carried out to extract relevant geological attribute information such as topography, stratum lithology, structural characteristics, hydrological characteristics, physical geological phenomena, adverse geological phenomena, and the like of geological points. Finally, obtaining the working conditions, traffic conditions, safety conditions, investigation routes, and investigation priorities of the site where the geological points are located, then forming the comprehensive information of the geological points, intercept 3D models from different perspectives instead of plane photos and section photos, and achieving the preliminary indoor analysis results based on aerial survey geological points [15].

4.3. Geological Boundary Identification and Information Collection Methods.

Identification and collection of geological boundaries are mainly to identify and outline linear geological objects such as lithologic boundary, structural trace, geological hazard boundary, hazard zoning boundary,

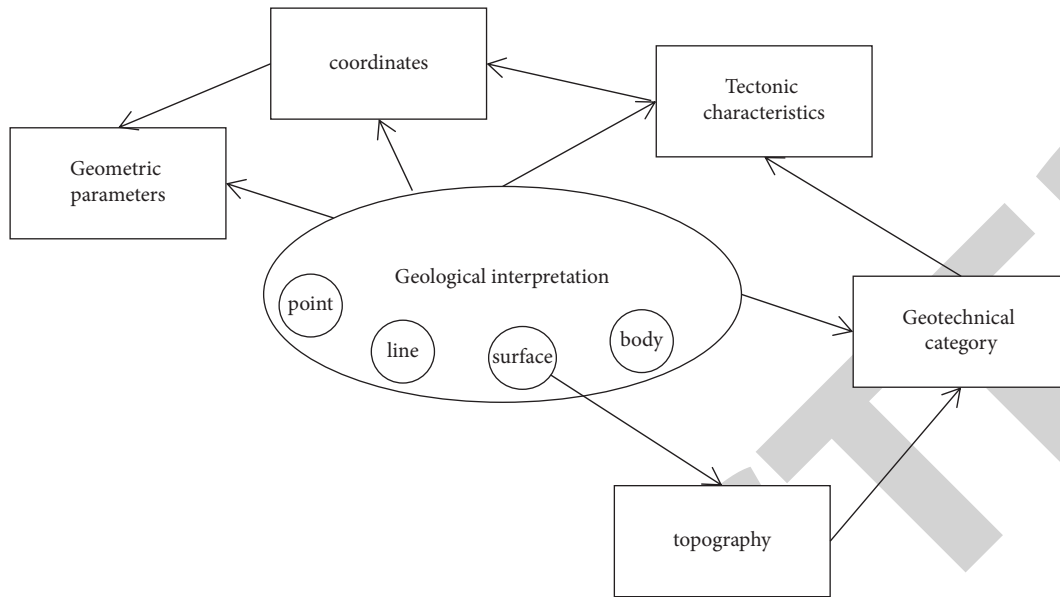


FIGURE 2: Composition of information elements.

and surface cracks. The analysis and data collection of geological boundary by 3D models are usually based on the changes of surface area, color data, and images. Geological information is confirmed through analysis. In the model, lines are manually described and sketched along the distribution trace of linear geological objects [1].

4.4. Collection Method of Geological Interface Information.

The geological interface information mainly includes the geological attribute, undulation, surface adhesion, and distribution occurrence of the interface. Due to the limitation of resolution and clarity of aerial photos and models, information can only be obtained from geological interfaces with large exposure scales and good air conditions.

The geological interface information collection based on the 3D surface model formed by UAV is mainly based on the color, image, and texture development characteristics of the geological interface, combined with geological experience to judge the geological attributes, undulation, and surface attached materials of the interface. The acquisition and calculation method of its distribution occurrence is mainly obtained by using the spatial analytic geometry knowledge on the basis of obtaining the coordinates of more than three points on the interface. The calculation process can be realized by programming [16].

4.5. Geological Body Information Collection Method. The collection of geological body information mainly includes the distribution location, plane area, section shape, thickness estimation, and volume calculation of different types of geological bodies.

First, the boundary of the geological body can be identified in the 3D surface model, and the boundary distribution coordinates and plane distribution area can be obtained by using the calculation function of the software.

Then, the plane position information and elevation distribution range can be obtained after the coordinate statistics. The section shape can be drawn in any part of the model, and the surface relief characteristics of the section line can be easily obtained. On the basis of obtaining the profile shape, the thickness can be estimated according to the profile shape combined with geological analysis or by using the relevant exploration data. Combined with the plane distribution area information, the volume of the geological body is estimated [17].

5. Application Cases

Among the selected hillsides, a large number of residents, houses, and cultivated land are distributed on the landslide mass, and township governments, schools, and gas stations are distributed on the opposite bank. The landslide has caused great potential safety hazards to life and property safety. Due to its large scale and sensitive hazard objects, the landslide has been listed as a key investigation project by the land and resources department. Considering the tight time, heavy task, difficult field operation, high safety risk, and no topographic map and other basic data, the geological survey was carried out with UAV in this project. Based on this requirement, the aerial photography equipment is selected as follows: Dajiang T600 UAV “Wu” series products. The model of carrying lens is fc350, with a total pixel of 12.76 million and an effective pixel of 12.4 million. The maximum resolution of the image is 4000×3000 pixels. In the field test, 4 sorties were flown, and 23 routes were photographed. The working base station was the GPS CORS positioning base station in Xinyi, Jiangsu Province. The coordinate system is the national geodetic coordinate system 2000 (CGCs 2000), the relative flight height of the flight line is 35 m, the down-looking resolution is 0.05 m, and the focal length is

20 mm. The effective area of aerial photography is about 0.3 km^2 , 15 control points are set in the area, and the mean square error of the plane is 0.199 M. After data collection, in order to keep consistent with the existing GIS platform, the data were transformed into Xi'an 80 coordinate system [3].

As shown in Table 1, Smart 3D capture software was used to realize automatic and rapid modeling of test data. It mainly includes four stages: data preprocessing, aerial triangulation, 3D modeling, and accuracy evaluation. The detection control points are set in the field, and the accuracy of the model is evaluated by GPS coordinates.

In this paper, the measurement of spatial geometric parameters of the geological body is mainly introduced by taking the volume estimation of the landslide as an example. First, on the basis of landslide boundary delineation, the boundary coordinates, perimeter, and distribution area of the landslide are directly obtained by using the software query function. The perimeter of the landslide is about 2 km, and the plane distribution area is about $23 \text{ km} \times 104 \text{ m}^2$. Then, the section shape of the landslide is obtained. The thickness of the landslide is preliminarily estimated by using the profile morphology and geological knowledge. As shown in Figure 3, through the analysis of the profile morphology and the preliminary geological judgment, the thickness of the landslide mass is about 50 m. Finally, the volume of the landslide is estimated, and the initially estimated landslide volume is about $1000 \times 10^4 \text{ m}^3$.

By synthesizing the above preliminary geological interpretation information and reflecting it in the form of mapping, the preliminary engineering geological plan sketch can be generated, which can be used as the preliminary results of a geological survey. At the same time, combined with the macro and microdetailed images, the final analysis is carried out to form the preliminary geological comprehensive analysis conclusion of the survey area. With the help of the UAV, the sketch of the geological plan was formed rapidly in the landslide of the ladder groove. At the same time, it is concluded that the landslide is a large overburden high landslide, mainly distributed in the relatively gentle slope between 2475 m and 2100 m, with an area of about $23 \times 10^4 \text{ m}^2$ and with a volume of about $1000 \times 10^4 \text{ m}^3$. Surface cracks appeared in the back edge, and local shear failure deformation occurred in the front edge. The stability of the landslide is poor.

Compared with the review results in a later stage, the plane position and elevation of the landslide boundary based on the UAV survey are basically consistent with the actual boundary. The plane error is only cm decimeter level, and the elevation error is in meter level. The occurrence error is within 5° . The error is less than 10%. The main reason is that it is difficult to accurately judge the landslide thickness based on the terrain profile characteristics and geological experience by using the UAV aerial survey results, which often lags behind the actual exploration results, resulting in the error of volume estimation. But it fully meets the accuracy requirements of the preliminary survey [18].

TABLE 1: Calculation quality results of space three.

	Point	15
Before air three solution	Average reprojection error	2.72
	Root mean square error of reprojection	19.46
	Root mean square error of three-dimensional coordinates	0.3
	Root mean square error of horizontal coordinates	0.2
	Root mean square error of vertical coordinate	0.002
After air three solution	Average retransmission error	5.88
	Root mean square error of reprojection	18.22
	Root mean square error of three-dimensional coordinates	0.2
	Root mean square error of horizontal coordinates	0.2
	Root mean square error of vertical coordinate	0.01

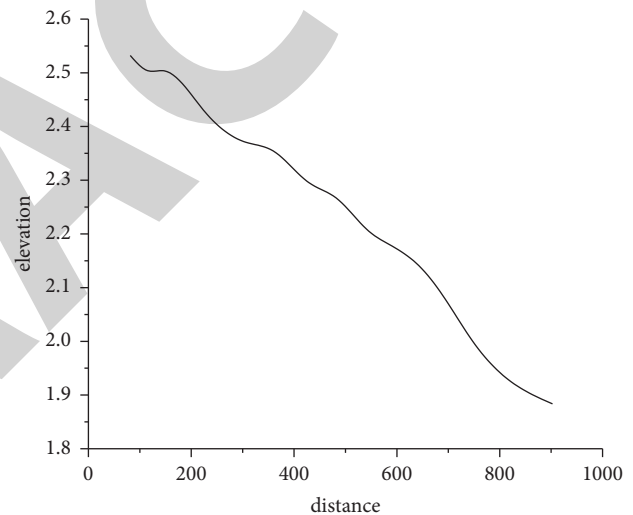


FIGURE 3: Section shape and thickness estimation.

6. Conclusion

In this paper, UAV can be used to obtain the whole and microimage data needed for geological survey, which can provide reliable data for geological survey and geological analysis, especially in the case of few people, extremely complex terrain conditions and extremely bad natural environment. The use of UAV can further obtain the geological information and spatial position information of geological objects such as geological points, lines, planes, and bodies, which can provide more powerful help for field investigation. The practical application shows that the UAV tilt photogrammetry technology is feasible in the construction site and has a significant guiding role for the field survey. Through reasonable and standard UAV field information collection and internal data processing calculation process, it can be rapidly applied in different project departments of engineering construction enterprises. Combined with 3s technology to establish an efficient geographic information service platform and introduce GIS spatial analysis tools, the

Research Article

Application of Deep Learning Intelligent Laser Scanning Technology in Mural Digitization

Zhiming Dong ^{1,2}

¹*Xi'an Jiaotong University, Xi'an 710115, China*

²*Xi'an Technological University, Xi'an 710021, China*

Correspondence should be addressed to Zhiming Dong; dongzm@stu.xjtu.edu.cn

Received 16 June 2022; Accepted 19 July 2022; Published 19 August 2022

Academic Editor: Kai Guo

Copyright © 2022 Zhiming Dong. This is an open access article distributed under the Creative Commons Attribution License, which permits unrestricted use, distribution, and reproduction in any medium, provided the original work is properly cited.

Ancient Chinese murals have a long history and a large number of types. They are witnesses to the development of ancient Chinese civilization. They still have important historical, artistic, and scientific values, as well as other values such as cultural relics, economy, and missionary education. Yet, the clear and smooth images of earlier have been damaged and covered by fog after the ancient murals were destroyed by human being and the nature. Therefore, the ancient murals that exist till now have been bothered by different damages and sickness. Protection and prevention are needed the most. In recent years, the application of scientific and technological means has played a role in the protection of ancient murals, making the work methods of cultural relics protection more scientific and diverse. In the context of the increasingly rich digital protection of cultural relics, the protection of murals requires more innovative work. However, at present, the resolution of ancient murals is low and the texture details are ambiguous, which leads to the problems of insufficient viewing and low research value. This paper focuses on ancient Chinese murals and conducts exploration on the phenomenon of mural damage and blurred colors. The deep learning intelligent laser scanning technology is used to extract the damaged ancient mural images. In this thesis, the images of murals have been restored using the new-super resolution technology to achieve the optimal mural images so that the mural images are more beautiful and artistic, which provides new ideas for the protection of murals.

1. Introduction

Murals are the textured paintings on the wall made of materials such as clay, woods, bricks, and stones. The pigment employed in the murals shows a great diversity, and so do the greasypaint and pigment of traditional drawings. The form and theme of the murals are decided by the style and content of the buildings and also should be in line with the space environment of buildings.

After the long history, there have been artistic classics that are still astonishing like the Dunhuang murals [1]. They still have important historical, artistic, and scientific values, as well as other values such as cultural relics, economy, and missionary education [2]. Therefore, the protection of mural images is urgent. The digital protection of cultural heritage is not only a major national demand for the protection and

promotion of cultural heritage but also a frontier research topic for multidisciplinary integration [3]. The technologies including digital museum collections and digital communication are used by the digital preservation for the culture heritage, which can change and restore the nonmaterial cultural heritage into the digital form featured by sharing and reproduction.

Each iteration of the image propagates that the pixel information of the image goes in the line of the iso-illumination to the missing area [4]. Yizhen Chen said a super-resolution algorithm gets rooted in generative adversarial network. However, this method has poor adaptability, and the processing scene is relatively simple, and there are often problems of edge blurring and loss of high-frequency details [5]. The emergence of 3D laser scanning technology can solve this problem very effectively. 3D laser scanning technology

has the characteristics of high efficiency, speed, and accuracy. It can effectively reconstruct image elements in murals [6].

This paper improves the previous image restoration method through the deep learning laser scanning technology, completes the initial restoration of the mural image, and then further conducts laser scanning on the mural image [7]. Through 3D laser scanning, we can directly obtain the image information in the murals, instead of traditional manual drawing, which will save a lot of manpower, material resources, and time [8].

2. Related Theories

2.1. Deep Learning. The deep learning can accomplish matrix counting with large scale and trigger the development of image recognition. This field has a great potential in application and development. Neural network structure contains multiple hidden layers, which can describe the characteristics of the target object more abstractly and at a deeper level [9].

In the process of supervised learning, the relationship of the characteristics of the data, which is trained, and the tags will be discovered [10]. The training data of unsupervised learning are not labeled, a deep belief network (DBN), etc. [11]. The best model is trained by the supervision learning training, and the experiment employs the model to reflect all the information into a certain output. The judgment should be made for the output for the purpose of classification. The learning is the imitation of human beings no matter it is a supervision learning or a machine learning.

The generative model G can present the features of the data [12]. The discriminative model D is a classifier that estimates the possibility that an input sample maybe from the training one [13]. Where X represents the real image information, Z represents the noise image information, XP represents the probability distribution of the real image information, $ZP(z)$ represents the probability distribution of the generated data, $G(z)$ represents the reconstructed image data, $D(x)$ represents the reconstructed image data, and $D(g(z))$ represents the possibility of judging whether the reconstructed image information is real through the discrimination network. $\log D(x)$ represents the judgment of the discrimination network on the real image data $D(g(z))$ represents the judgment on the reconstructed image information [14]. It is shown in Figure 1:

$$\min_G \max_D V(D, G) = E_{X \sim P_x} [\log D(X)] + E_{Z \sim P_z} [\log(1 - D(G(z)))] \quad (1)$$

2.2. The Application of DL. The traditional recognition algorithm cannot meet the high recognition requirements of remote sensing image processing because it relies heavily on artificial feature extraction. Deep learning technology can fully utilize the spatial structure information of 3D laser scanning technology [15]. The combination of 3D laser scanning technology and deep learning technology can effectively extract useful features of images [16].

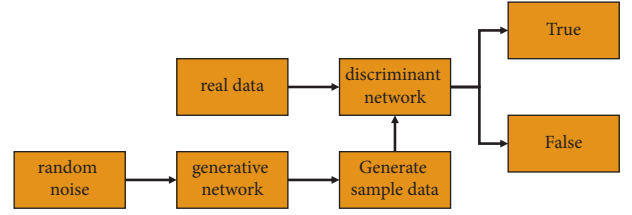


FIGURE 1: Generative adversarial network structure diagram.

2.3. Application of 3D LST. Since the 2D laser radar and the PTZ device are to be upgraded, therefore, in order to make the acquisition process easier and the acquisition results more precise, a 3D laser scanner acquisition device is designed [17]. After many experiments, it has been proved that the system can be well adapted to complex 3D scenes, and the point cloud technology can be used to obtain better model reconstruction effect [18].

2.4. Image Super-Resolution Reconstruction. In view of the problem that the aesthetic value of mural images decreases due to the rough details in the mural image processing, an ultra-high-resolution mural image optimization method is provided. Using deep learning ideas and a phased approach to network models better mural image optimization is achieved. Through different methods, learning the improvement ideas of different methods will provide new inspiration for super-resolution reproduction of mural images [19]. Jianfang came up with an enhanced super-resolution way, which is stable and can solve problems in ancient murals with low resolution and blurred texture details. Based on GAN, the method is improved to extract images using dense residual blocks. Finally, it is found that the method is better than the other related algorithms [20].

Deep learning-based MRI super-resolution reconstruction techniques have attracted attention due to their resolution over traditional super-resolution reconstruction techniques [21].

3. Technology

3.1. 3D Laser Scanning Technology. In the implementation process, a variety of high-tech surveying and mapping instruments are integrated. On this basis, based on the non-contact high-speed laser measurement method, calculate the distance between the target and the center by recording the time difference, as shown in the following equation:

$$d = \frac{c \times \Delta t}{2}, \quad (2)$$

where D is the measured distance; C is the light speed; t is the variation. Laser scanner system using laser scanning technology is mainly composed of hardware system and software system, as shown in Figure 2. The computer system records the emission time t_1 and the optical scanning system. Location and angle information (X): when the optical receiving system receives the light signal reflected by the target, the computer system records the receiving time t_2 and controls

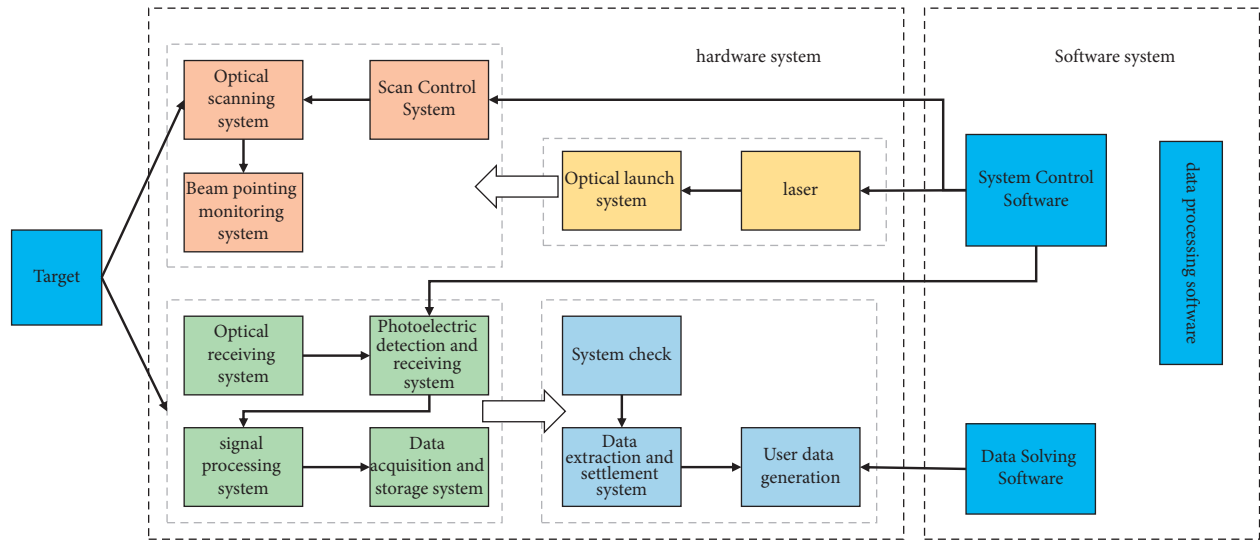


FIGURE 2: 3D Laser scanning system.

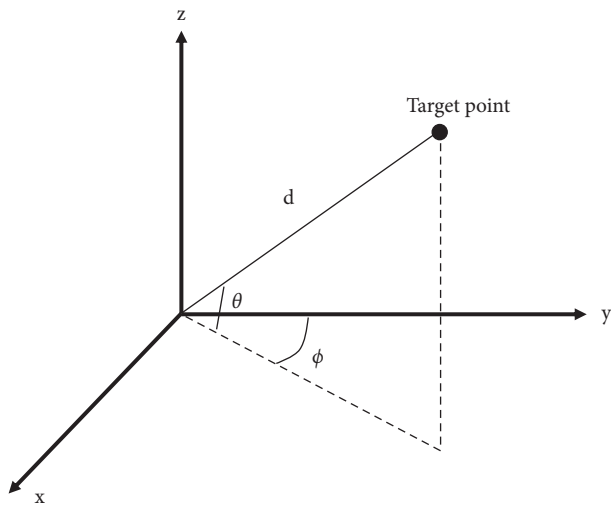


FIGURE 3: Schematic diagram of 3D laser measurement.

the laser to emit light from different angles through the scanning control system.

The coordinate center defined by the laser scanner is the original part, and X and Y are perpendicular to each other. The results of measurements are shown in Figure 3.

During the 3D laser scanning process, the ranging observation value S is mainly obtained by the 3D laser scanner through the data acquisition system. When using the ground laser scanning 3D measurement technology in 3D laser scanning for soil and water conservation monitoring, the coordinate system usually used is the internal coordinate system of the instrument; among them, the X axis is in the lateral scanning plane, and the Y axis and Z axis are, respectively, in the lateral scanning plane. Inner and X-axis and the horizontal one are vertical to each other, and formula (3) for the coordinates of the 3D laser foot point is obtained as follows:

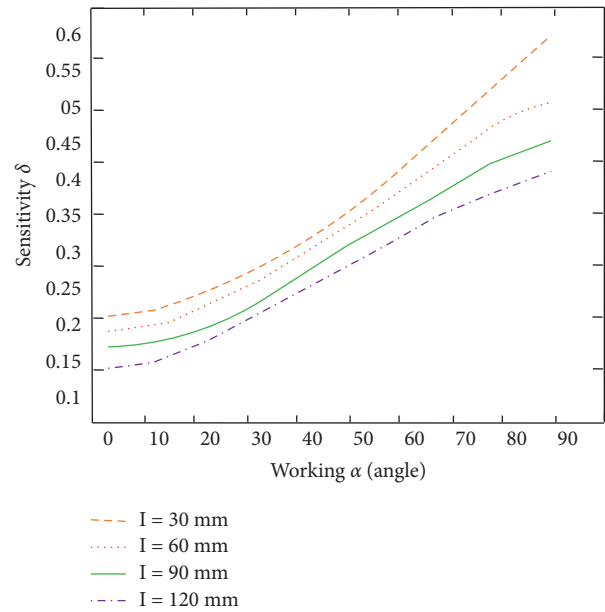


FIGURE 4: Relationship between working angle α and measurement sensitivity δ .

$$\begin{aligned} X &= D \cos \beta \cos \alpha, \\ Y &= D \cos \beta \sin \alpha, \\ Z &= D \sin \beta. \end{aligned} \tag{3}$$

In this formula, the three-dimensional coordinates of the measured object are represented by the variables “X, Y, and Z”; the distance between the measured object and the instrument is represented by D; the horizontal and vertical scanning angles are represented by α and β , respectively.

In addition to the object displacement Δ , the measurement sensitivity is also related to several other parameters such as α , β , f , and l . A is the angle between the

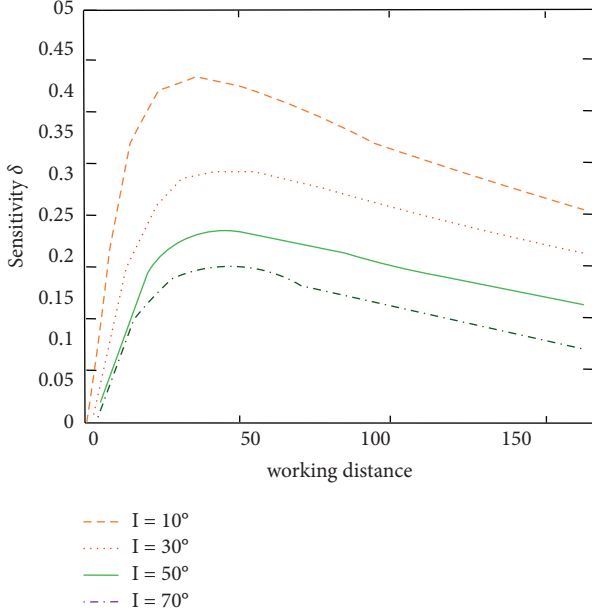


FIGURE 5: Relationship between working distance l and measurement sensitivity δ .

incident laser beam and the surface normal of the measured object, that is, the incident angle, and we define this parameter as the working angle. l is the distance between the spot where the laser irradiates the surface of the object to be measured and the main plane of the receiving lens, and we define this parameter as the working distance of the system. We select the optimal incident angle of the system laser projection by observing the changing trend of the working angle α and the measurement sensitivity δ at the positions of 30 mm, 60 mm, 90 mm, and 120 mm, respectively, as shown in Figure 4.

When the measurement range and working angle of the system are determined, the relationship between the working distance l and the measurement sensitivity δ is known. For angles of 10° , 20° , 30° , 40° , 50° , 60° , 70° , and 80° , the changing trends of the working distance l and the measurement sensitivity δ are shown in Figure 5.

3.2. Network Structure Design

3.2.1. Generative Network Design. The generation system adopts the FCN structure and the decoder decoder structure. The result of the mural image is set as only the image information of the mask area, while the image information of other areas remains unchanged. The result of generating a network is usually a size of 128×128 preprocessed mural pictures. When an image having 24 to 36 pixel values is randomly obtained and the mask is completed, and the pixel value of the mask area is set to zero in the input image, the mask mural image is obtained. The FCN network obtains the image feature signal through the convolution layer, restores the feature map signal to the size image of the original pixel through the deconvolution layer calculation, and outputs the image value of the image restoration non mask area, and

TABLE 1: Generate network details information table.

Type	Kernel	Dilation	Stride	Outputs
Conv	5×6	1	1×2	64
Conv	3×2	1	2×1	32
Conv	3×1	1	1×1	128
Conv	3×1	1	2×2	256
Conv	3×1	1	1×2	128
Dilated conv	3×3	2	1×1	256
Dilated conv	3×3	3	1×3	256
Dilated conv	3×1	6	1×3	64
Conv	3×1	1	1×1	256
Conv	4×1	1	$1/2 \times 2$	128
Deconv	3×1	1	1×2	128
Conv	4×3	1	$2 \times 1/2$	64
Deconv	3×3	1	1×2	32
Output	3×3	1	2×1	3

saves the restored mask area image information, and outputs the final restored image value. The generated network details are shown in Table 1.

In order to better generate close to the real repair effect, this paper proposes to improve the model by using the MSE and adversarial loss function. The MSE and the adversarial are optimized simultaneously with the different network, and the GNM and the DNM are optimized.

The function is used to measure the quality of their built image. The final loss function calculation formula (4) can be expressed as follows, in which the coefficients employed to balance different losses are symbolized by input 1, 2.

$$l_G = l_{MSE}^{SR} + \lambda_1 l_{VGG}^{SR} + \lambda_2 l_{adv}. \quad (4)$$

The pixel-level MSE loss calculation formula (5) is as follows:

$$l_{MSE}^{SR} = \frac{1}{r^2 W H} \sum_{x=1}^{rW} \sum_{y=1}^{rH} \left(I_{x,y}^{HR} - G_{\theta_G}(I_{x,y}^{LR}) \right)^2. \quad (5)$$

W and H are the width and height, respectively, and represent Euclidean distance between real image pixels and the generated pixels.

The MSE loss can make the reconstructed graphics have extremely high peak signal-to-noise ratios, but usually lack high-frequency content. We calculate the MSE by summing all squared losses for each sample and the formula is shown as

$$MSE = \frac{1}{N} \sum_{(x,y) \in D} (y - \text{prediction}(x))^2, \quad (6)$$

where N represents the total number of samples; (x, y) represents data, wherein represents the attribute set in the exercise data; and y represents the true value of the exercise data. The prediction (x) is the expected value of the exercise data X .

Based on the same principle, the main purpose of the judgment system is to make the output of the power generation system approximately zero, while the output of the judgment system of the real data is approximately one. The resistance loss formula is shown as follows:

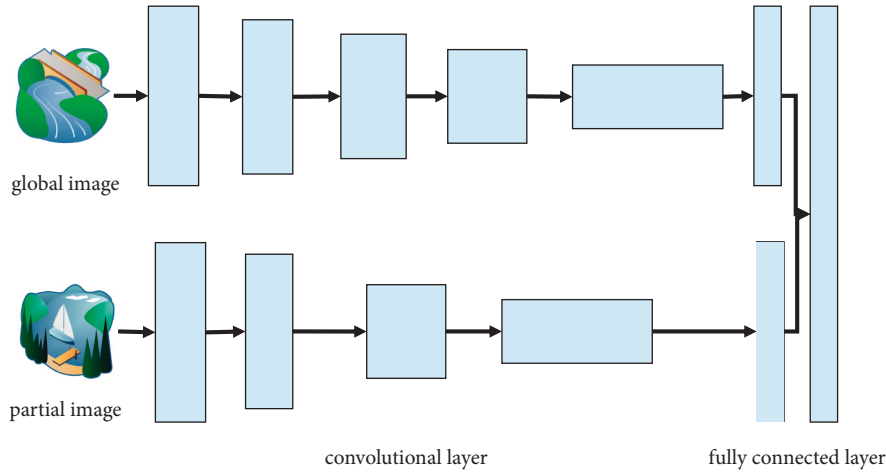


FIGURE 6: Discriminant network structure diagram.

$$\min_G \max_D V(D, G) = E_{X \sim P_{\text{data}(x)}} [\log D(X)] + E_{Z \sim P_z} [\log(1 - D(G(z)))] \quad (7)$$

Here, x refers to the real data, while z indicates the other data, and $P_{\text{data}(x)}$ is the probability of real data, P_z represents the probability distribution of synthetic data. Such combined data result represents the data result combined by the generation network, and $D(x)$ represents the discrimination method, and represents the probability of judging the statistics of the true number to be true. $D(g(z))$ is a probability that the computer network determines whether the synthesized data generated by the computer network is actual. $\log D(x)$ represents the determination of the real data by the discriminating computer network. $D(g(z))$ represents the determination of the comprehensive information.

Loss function of WGAN (8) is like this

$$L(D) = E_{x \sim P_r} [D(x)] - E_{x \sim P_g} [D(x)]. \quad (8)$$

Gradients of the discriminator $D(x)$ are not greater than a finite constant K by adding the Lipschitz limit, as shown in

$$\|\nabla_x D(x)\| \leq K. \quad (9)$$

Generally, K is equal to 1, and adversarial loss calculation formula (10) may be obtained by weighted combination with the original discriminator loss as follows:

$$l_{\text{adv}} = -E_{x \sim P_r} [D(x)] + E_{x \sim P_g} [D(x)] + \lambda E_{x \sim P_x} \left[\left(\|\nabla_x D(x)\|_p - 1 \right)^2 \right], \quad (10)$$

rp shows different data in the model. P_x is the distribution obtained by randomly sampling the real and generated data.

3.2.2. Discriminant Network Design. The network structure basically adopts the CNN design, that is, the image is

TABLE 2: Global discriminant network.

Type	Kernel	Stride	Outputs
Conv	5×5	2×2	64
Conv	5×5	2×2	128
Conv	5×5	2×2	156
Conv	5×5	2×2	512
Conv	5×5	2×2	512
FC	-	-	1024

obtained through the convolution layer to obtain the local signal of the image, then the signal is filtered and filtered by the pool layer, and then linked to the full connection layer to integrate the local image signal into the feature vector, and finally the image is classified. The two discriminant networks respectively output feature vectors of the same dimension, and then connect the two feature vectors to output the feature vectors. The basic structure of the discrimination network is shown in Figure 6.

The global discriminant network can take all the images as input, including the real mural images and the synthesized images in the generation network. Each convolution layer can pass through 2×2 to deepen the feature map so as to obtain more abundant graphic signals in the graph. The most detailed global feature discrimination network structure is shown in Table 2.

3.3. Super-Resolution Reconstruction to Get the Mural More Artistic. In order to reduce the aesthetic value of the painting effect, a super-resolution reconstruction method is invented to improve the painting effect. Super-resolution reconstruction is a kind of image processing method that computer processes the pixel sequence of low resolution image to restore the high-resolution image.

This method is based on the generated network. First, the reconstructed high-resolution image is output to the generated network, and then it is judged as a real high-resolution network. Then, through the transfer learning method, the high batch uniformity is gradually removed, and the

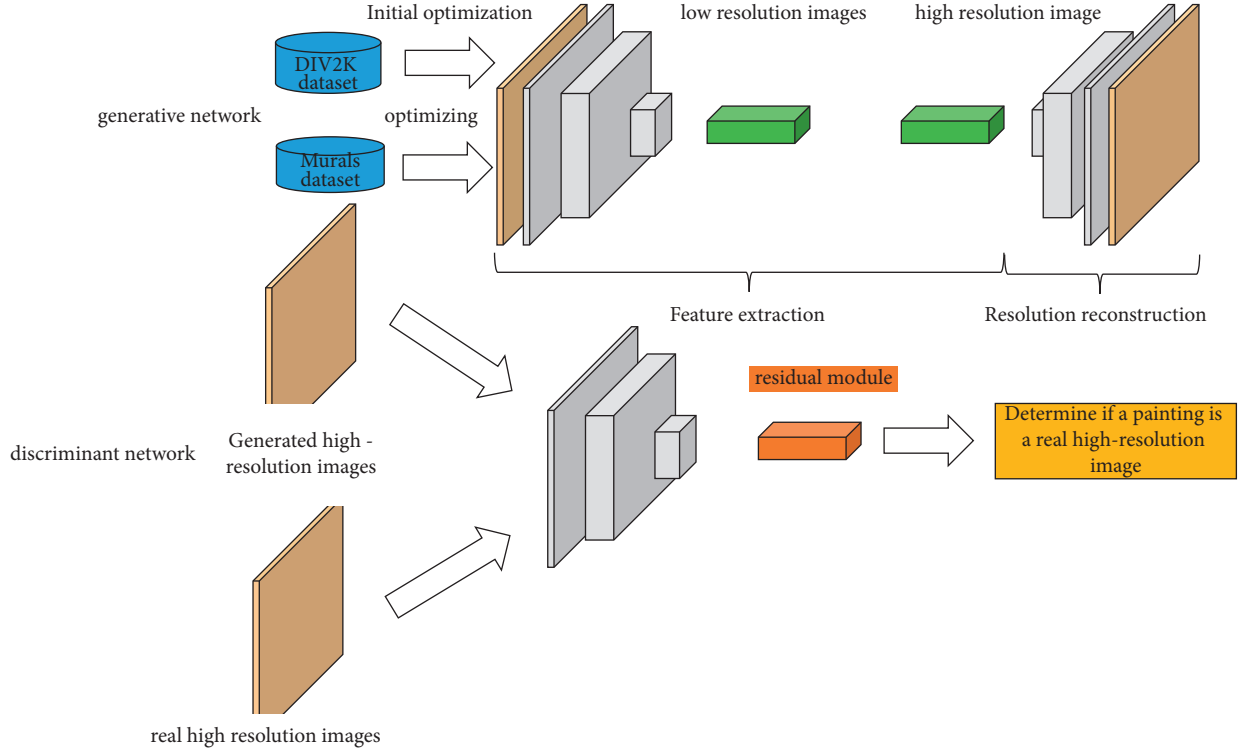


FIGURE 7: Network structure diagram of super-resolution reconstruction ways for enhanced Chinese mural images.

network model is established in stages, so as to achieve further high mural image optimization.

The super-resolution reconstruction method of the enhanced art mural pictures is based on the computer network and follows the basic construction method of generating the confrontation network system. The discrimination system judges whether the output image in the generation system and the real image are true or false. The network structure of the super-resolution reconstruction method for art painting images is shown in Figure 7.

4. Results and Analysis

4.1. Experimental Environment and Experimental Design. The hardware environment built in this experiment: CPU is Inter Core i7-7700K, memory is 16 GB, graphics card is NVIDIA Ge Force GTX 1080Ti, has 3D laser scanner, CCD camera, and GPS receiver; the software environment built: CUDA version is 9.0, cu DNN version is 7.0, and operating system is Windows 10; it uses Python 3.6, using the PyTorch framework to write test experiments. The compiled software used is the device. The training set of the data used in this experiment has 800 DIV2K images, 2650 Flickr2K images, and 90 murals. The test dataset has 30 murals. The factor for the high-resolution and low-resolution images in this paper is 4. Finally, the mural dataset is sent to the network to continue training, and the generator and discriminator are renewed alternately. The model is converged, and finally the following experimental analysis is carried out on the obtained results.

4.2. Evaluation Index of 3D Laser Scanning Results. Using two commonly used nonsubjective assessment indexes: the two indicators judge quality of image reconstruction. The higher the PSNR number of the two images, the less the contortion between scanned images and high-resolution images, that is, the more effective the scanned results; the way judges reconstructed image. The more similar the points of the two images, the closer the SSIM value is to 1, which is more consistent with the public's visual sensory effect. The specific calculation expression of PSNR is shown in formula (11), and the specific calculation expression of SSIM is shown in (12).

$$\text{PSNR} = 10 \times \log_{10} \frac{225^2 \times W \times H}{\sum_{i=1}^W \sum_{j=1}^H [\bar{x}(i, j) - x(i, j)]^2}. \quad (11)$$

$$\text{SSIM}(X, Y) = \frac{(2\mu_X\mu_Y + C_1)(2\sigma_{XY} + C_2)}{(\mu_X^2 + \mu_Y^2 + C_1)(\sigma_X^2 + \sigma_Y^2 + C_2)}. \quad (12)$$

W and H represent the width and height in the model, respectively, $x(i, j) - x(i, j)$ indicates the Euclidean distance between pixels of the two images; μ_X and μ_Y indicate the context of the images X and Y , respectively, σ_X and σ_Y represent the standard deviation of the images X and Y , respectively, σ_{XY} represents the variables of the images X and Y , which are linearly transformed, and C_1 and C_2 are constant XY numbers.

It can be concluded that the response curve changes sharply at the pixel values near both ends, and the data fit is poor. In order to better restore the response curve, a weight function is introduced to increase the proportion of

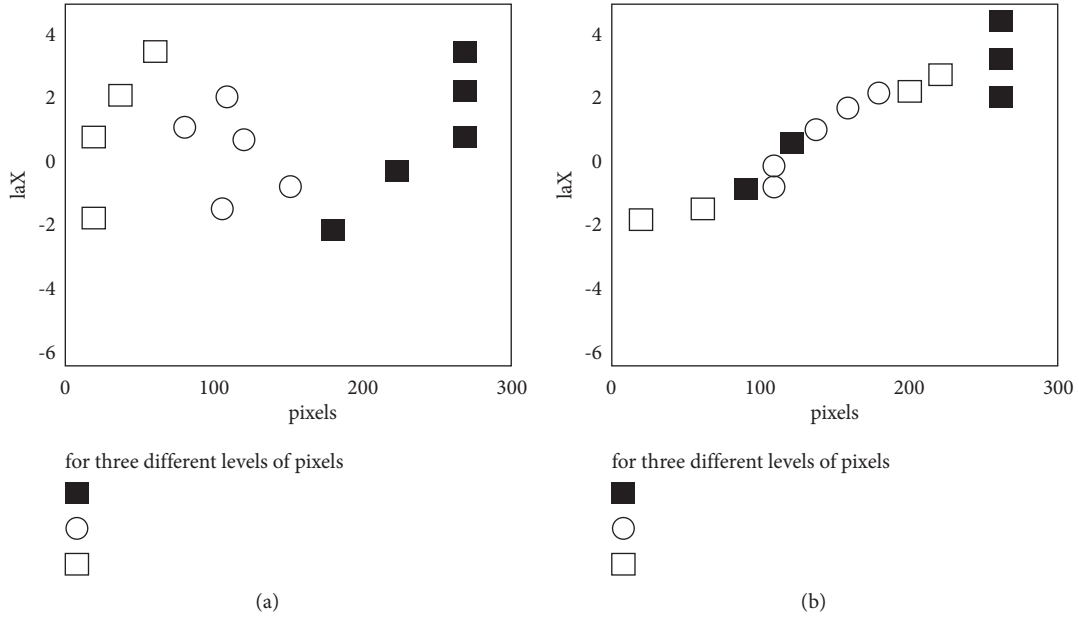


FIGURE 8: Schematic diagram of the response curve solution process. (a) Collected pixels; (b) response curve.

exposure data located in the middle part of the response function. As shown in (13), it is the response curve closest to the actual response curve, and the fitting process is shown in Figure 8:

$$w(z) = \begin{cases} z - z_{\min}, & z \leq \left(\frac{1}{2}\right)(z_{\max} + z_{\min}), \\ z_{\max} - z, & z > \left(\frac{1}{2}\right)(z_{\max} + z_{\min}). \end{cases} \quad (13)$$

The horizontal axis in Figure 8(a) corresponds to the pixel value Z of the image, and the vertical axis is the logarithm of the exposure $\ln X$. Select 3 pixels in 5 images with different exposures to restore the response curve g , the 3 symbols in the figure represent 3 pixels at different positions of an image, and 3 points are selected for 5 images corresponding to 3-curve fragment. According to the constraint condition $g(Z_{mi}) = 0$, the three curve segments are combined into one by moving up and down, thus expressing the corresponding curve between exposure and pixel value, as shown in Figure 8(b).

4.3. Analysis of Data. In order to prove the effect of laser scanning technology in rebuilding old frescoes, 4 images are chosen in the rebuilt 4x high-resolution frescoes at random and compared with the corresponding low-resolution frescoes, and the PSNR and SSIM of the two groups of images were mainly compared. The exploration consequences are clearly presented in Table 3. It will be known from the consequences in Table 3 that reconstructed murals also get good PSNR and SSIM values.

In order to further study the characteristics of laser scanning technology from image texture information, overall brightness, and clarity, 50 professional evaluators were selected to subjectively score the reconstruction results

TABLE 3: SSIM and PSNR after reconstruction of murals.

Image	a	b	c	d
PSNR	25.71	30.01	25.04	30.11
SSIM	0.676	0.772	0.816	0.718

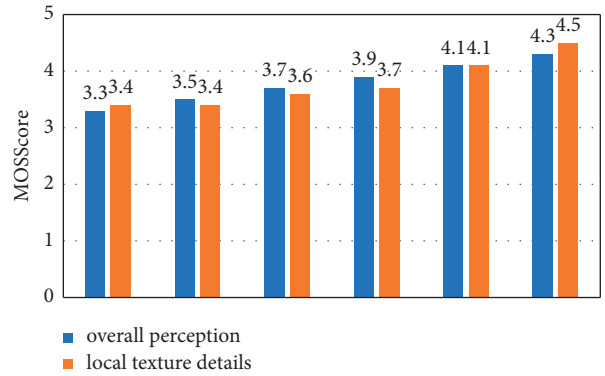


FIGURE 9: Subjective scoring map of the reconstructed murals.

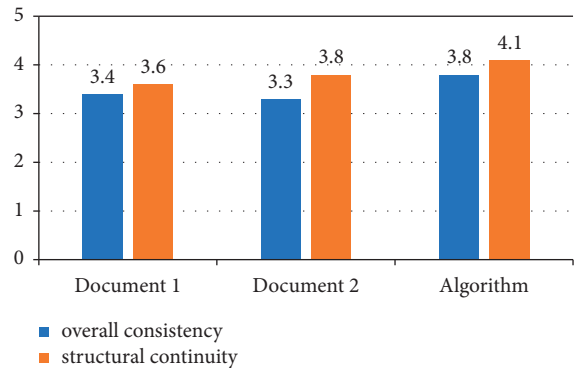


FIGURE 10: Comparison of subjective scores under different algorithms.

TABLE 4: PSER values under different algorithms.

Sample	Document 1	Document 2	Algorithm
1	38.63	37.69	40.53
2	36.94	38.34	42.67
3	36.58	38.21	41.95
4	42.67	41.18	45.36
5	37.93	38.06	42.67
6	38.28	38.09	43.62
7	39.94	38.33	42.88
8	41.23	42.58	45.95
9	42.63	42.39	45.23
10	38.15	38.97	41.36

TABLE 5: SSIM values under different algorithms.

Sample	Document 1	Document 2	Algorithm
1	0.853	0.875	0.853
2	0.776	0.812	0.931
3	0.865	0.850	0.871
4	0.766	0.790	0.831
5	0.848	0.827	0.901
6	0.773	0.831	0.889
7	0.732	0.838	0.851
8	0.758	0.763	0.862
9	0.816	0.794	0.847
10	0.798	0.828	0.863

of conventional images of murals of different styles and mural maps of 3D laser scanning technology, as shown in Figure 9.

After statistics, the overall consistency and structural continuity scores of the three different algorithms are averaged, respectively. To visually compare the specific information of satisfaction evaluation, a histogram is made as shown in Figure 10. By comparison, the score, which is consistent with the previous ones and consecutive in structure, is 3.3–3.8 under the first and second algorithm, and the mentioned algorithms are 3.8 and 4.1.

10 test mural images were randomly selected as samples through experiments, and the objective comparison of the restoration effect of artificially destroyed mural images was carried out by two methods. The comparison of PSER under different algorithms is shown in Table 4. It analyzes the similar aspects from three perspectives including the brightness, comparison, and the structure. The SSIM values under the different algorithms are shown in Table 5.

We calculated the average value of PSNR and SSIM corresponding to each image under the three algorithms. Compared with the literature [1] algorithm, the algorithm in this paper has obvious improvement in visual continuity because the algorithm in this paper adopts the idea of confrontation generation. Repairing murals has better repair effect for larger damaged areas, and the distortion compared to the original image is smaller, and the final PSNR value is increased by 3~5 dB on average. The use of two discriminant networks has played a role in promoting the optimization of the generative network model; at the same time, the local consistency of the image has been greatly improved, which makes the SSIM value increase by 0.05~0.07 on average.

5. Conclusion

The ancient murals are damaged badly due to the history and environment factors. The application of digital images technology in the protection for the ancient culture relics is considered. For the problem, the thesis has put forward an adversarial network based on the deep learning with 3D technology to restore the resolution of the murals. After the reconstruction, the high-resolution murals are clear and bright and retain rich textured details. Moreover, the ornamental value and research value of murals have been improved to a certain extent, and the loss of ancient murals has been further protected [14].

Data Availability

The labeled dataset used to support the findings of this study is available from the author upon request.

Conflicts of Interest

The author declares that there are no conflicts of interest.

References

- [1] A. Nurunnabi, F. N. Teferle, and J. Li, "An efficient deep learning approach for ground point filtering in aerial laser scanning point clouds," *ISPRS - international archives of the photogrammetry, Remote Sensing and Spatial Information Sciences*, vol. 431, no. 7, pp. 66–70, 2021.
- [2] M. Valizadeh, M. R. Sohrabi, and F. Motiee, "Application of intelligent models and spectrophotometry method for simultaneous determination of Dorzolamide and Timolol in ophthalmic dosage form," *Optik*, vol. 217, Article ID 164870, 2020.
- [3] L. I. Venturott and P. M. Ciarelli, "Application of data augmentation techniques for hate speech detection with Deep Learning," *Progress in Artificial Intelligence*, Springer, Berlin/Heidelberg, Germany, 2021.
- [4] N. E. Khalifa, M. Loey, and S. Mirjalili, "A comprehensive survey of recent trends in deep learning for digital images augmentation," *Artificial Intelligence Review*, vol. 55, no. 2, pp. 99–104, 2021.
- [5] J. Y. Lee, "Experimental evaluation of deep learning methods for an intelligent pathological voice detection system using the saarbruecken voice database," *Applied Sciences*, vol. 11, no. 15, pp. 7149–8106, 2021.
- [6] S. R. Fahim, S. K. Sarker, and S. M. Muyeen, "A deep learning based intelligent approach in detection and classification of transmission line faults," *International Journal of Electrical Power & Energy Systems*, vol. 133, no. 3, pp. 117–122, 2021.
- [7] M. Luca, A. Ciobanu, and T. Barbu, "Artificial intelligence and deep learning," *Important Tools in Assisting Gastroenterologists*, vol. 5, no. 6, pp. 212–220, 2022.
- [8] M. Peker, B. Nci, and E. Musaolu, "An efficient deep learning framework for people detection in overhead images," vol. 17, no. 5, pp. 199–204, 2022.
- [9] A. Sj, B. Dks, and C. Tj, "Real time analysis of Intelligent placing system for vehicles using IOT with," *Deep learning*, vol. 51, no. 1, pp. 339–343, 2022.
- [10] O. V. Druzhinina, O. N. Masina, A. A. Petrov, and S. V. Shcherbatykh, "Application of intelligent technologies and neural network modeling methods in the development of

- a hybrid learning environment,” *Journal of Physics: Conference Series*, vol. 1691, no. 1, Article ID 012125, 2020.
- [11] I. Al-Omari, S. Hadayeghparast, and H. Karimipour, “Application of deep learning on IoT-enabled smart grid monitoring,” *Journal of European Economy*, vol. 14, no. 3, pp. 89–97, 2021.
- [12] K. Kreitmair, “Digital Behavioral Technology,” *Deep Learning, and Self-Optimization*, vol. 6, no. 1, pp. 55–67, 2021.
- [13] J. Min, “Research on the application of computer intelligent proofreading system in college English teaching,” *Journal of Physics: Conference Series*, vol. 1915, no. 3, Article ID 032078, 2021.
- [14] A. Mm, B. Gm, and A. Ha, “Deep learning-based intelligent face recognition in IoT-cloud environment,” *Computer Communications*, vol. 152, pp. 215–222, 2020.
- [15] D. A. Gura, Y. V. Dubenko, and I. G. MarkovskiY, “The development of the intelligent data processing unit concept in the bridge monitoring system is realized by using the scanning technology,” *Journal of European Economy*, vol. 3, no. 7, pp. 21–28, 2020.
- [16] B. Zhang, Z. Zhao, Y. Huang et al., “Correlation between quantitative perfusion histogram parameters of DCE-MRI and PTEN, P-Akt and m-TOR in different pathological types of lung cancer,” *BMC Medical Imaging*, vol. 21, no. 1, pp. 73–78, 2021.
- [17] S. Khan, A. Goodarzi, and J. Taron, “Application of deep learning lstm and arima models in time series forecasting: a methods paper for comparative analysis of Canadian and Swedish radon data,” *Journal of European Economy*, vol. 9, no. 12, pp. 144–150, 2021.
- [18] N. Zaini, L. W. Ean, and A. N. Ahmed, “A systematic literature review of deep learning neural network for time series air quality forecasting,” *Journal of European Economy*, vol. 3, no. 9, pp. 57–62, 2022.
- [19] D. Kim, C. J. Chung, and K. Eom, “Measuring online public opinion for decision making: application of deep learning on political context,” *Sustainability*, vol. 14, no. 3, pp. 155–160, 2022.
- [20] J. Cao, Y. Jia, and M. Yan, “Superresolution reconstruction method for ancient murals based on the stable enhanced generative adversarial network,” *EURASIP Journal on Image and Video Processing*, vol. 2021, no. 1, pp. 1–23, 2021.
- [21] A. K. Haghighat, V. Ravichandra-Mouli, and P. Chakraborty, “Applications of deep learning in intelligent transportation systems,” *Journal of Big Data Analytics in Transportation*, vol. 2, no. 11, pp. 88–94, 2020.

Retraction

Retracted: Monitoring and Analysis of Cotton Planting Parameters in Multiareas Based on Multisensor

Mathematical Problems in Engineering

Received 26 September 2023; Accepted 26 September 2023; Published 27 September 2023

Copyright © 2023 Mathematical Problems in Engineering. This is an open access article distributed under the Creative Commons Attribution License, which permits unrestricted use, distribution, and reproduction in any medium, provided the original work is properly cited.

This article has been retracted by Hindawi following an investigation undertaken by the publisher [1]. This investigation has uncovered evidence of one or more of the following indicators of systematic manipulation of the publication process:

- (1) Discrepancies in scope
- (2) Discrepancies in the description of the research reported
- (3) Discrepancies between the availability of data and the research described
- (4) Inappropriate citations
- (5) Incoherent, meaningless and/or irrelevant content included in the article
- (6) Peer-review manipulation

The presence of these indicators undermines our confidence in the integrity of the article's content and we cannot, therefore, vouch for its reliability. Please note that this notice is intended solely to alert readers that the content of this article is unreliable. We have not investigated whether authors were aware of or involved in the systematic manipulation of the publication process.

Wiley and Hindawi regrets that the usual quality checks did not identify these issues before publication and have since put additional measures in place to safeguard research integrity.

We wish to credit our own Research Integrity and Research Publishing teams and anonymous and named external researchers and research integrity experts for contributing to this investigation.

The corresponding author, as the representative of all authors, has been given the opportunity to register their agreement or disagreement to this retraction. We have kept a record of any response received.

References

- [1] Z. Fan, N. Zhang, D. Wang, J. Zhi, and X. Zhang, "Monitoring and Analysis of Cotton Planting Parameters in Multiareas Based on Multisensor," *Mathematical Problems in Engineering*, vol. 2022, Article ID 7013745, 8 pages, 2022.

Research Article

Monitoring and Analysis of Cotton Planting Parameters in Multiareas Based on Multisensor

Zehua Fan,¹ Nannan Zhang,¹ Desheng Wang,² Jinhu Zhi,² and Xuedong Zhang¹ 

¹College of Information Engineering, Tarim University, Alar, Xinjiang 843300, China

²College of Plant Sciences, Tarim University, Alar, Xinjiang 843300, China

Correspondence should be addressed to Xuedong Zhang; 41818058@xs.ustb.edu.cn

Received 15 June 2022; Accepted 25 July 2022; Published 17 August 2022

Academic Editor: Hengchang Jing

Copyright © 2022 Zehua Fan et al. This is an open access article distributed under the Creative Commons Attribution License, which permits unrestricted use, distribution, and reproduction in any medium, provided the original work is properly cited.

In order to realize cotton growth monitoring, a cotton planting monitoring system based on image processing technology was proposed. The system requires camera to collect cotton canopy images, leaf areometer to detect the leaf area index, and spectrometer to detect the normalized vegetation index (NDVI) and the vegetation index (RVI). Due to different types of data, based on the establishment of the output transmission system, the canopy coverage was calculated by the image processing method, and there was a linear relationship between canopy coverage NDVI and RVI. The leaf area index (LAI) of *N* content was established, and the model of dry matter accumulation and canopy coverage was exponential. The experiment result shows that the linear and exponential coefficients of the model *k* and *b* increased with the increase of the nitrogen application rate. The fitting determination coefficient remained high under different nitrogen application rates. The fitting coefficient *R*² of the three models in the two test fields ranged from 0.83 to 0.923, which also met the needs of model evaluation. The system was used to detect the cotton field with good accuracy.

1. Introduction

Agriculture is the basic industry of a country. It is the basic principle and law of agricultural production to develop agriculture according to local conditions, rationally utilize agricultural resources, and give play to regional advantages according to the regional distribution law of agriculture. Precision agriculture represents the direction of agricultural development and is also the focus of agricultural research. Compared with traditional agriculture, precision agriculture is characterized by the maximum saving of natural resources and the minimum pollution of the ecological environment in exchange for high-tech and scientific management [1]. Its core is to divide the whole field appropriately into a number of small pieces, timely access to small pieces of land information. Decisions are made on a plot basis, taking into account differences in natural conditions, and farming operations are carried out accurately on each plot, that is, real-time diagnosis of spatial differences in soil properties and crop growth conditions. On this basis, the timed, positioned, and

prescription farming can be achieved to make full use of modernized and mechanical technique to achieve intensive farming and obtain high economic benefits [2, 3].

At present, due to the lack of farmland information acquisition technology with low cost, high density, high accuracy, and high reliability, field information acquisition has become a bottleneck restricting the development of precision agricultural technology. Remote sensing technology, with its macrocharacteristics of rapid, real-time, accurate, and economical, provides the possibility to solve this problem.

Remote sensing technology is an important key technology to implement precision agriculture, which can obtain accurate information of crop growth and development, disease, insect, grass, water, and fertilizer, and corresponding environmental conditions in real time. It is an important tool to obtain field information of precision agriculture. In recent decades, remote sensing technology has made an important contribution in monitoring crop yield and forecasting crop conditions in large areas of agricultural resources.

2. Literature Review

Remote monitoring technology of crop growth monitoring mainly uses CCD camera to collect remote image data and transmits the remote image captured by the camera to the control center through the wired wireless network or the mobile network. The control center processes the image and extracts relevant variable parameter values, currently uses CCD camera remote monitoring plant growing appearance information study which is also less and mostly uses the crop remote physiological monitoring technology PRPMT (plant remote physiological monitoring technique), through the various sensors installed in the plant body probes, monitoring of environmental factors, and crop. Changes in physiological indicators, soil moisture content, etc. [4, 5], Fouzi et al. developed a static image network real-time acquisition system, which consists of a camera support system and two subsystems. The camera support system enables network users to control the camera orientation and focal length and obtain a still image in real time [6]. Database support system server is to provide users with collected images. Database support system and camera support system work in coordination, regularly automatically obtained field images in the form of remote database provided to users, and users can retrieve the collected images according to the shooting time. Kük and Öveçoğlu monitored the environmental factors such as atmospheric temperature, humidity, soil humidity, light intensity, atmospheric vapor pressure difference, and tree physiological indexes such as fruit growth and leaf temperature in litchi orchard by using the plant dialogue monitoring system [7]. Moraes et al. studied the greenhouse environmental information acquisition system based on GPRS and WEB, and successfully realized the remote detection of the temperature, humidity, CO₂ concentration, and light intensity of the air and soil in the greenhouse by using ASP.NET technology and the B/S mode. It is pointed out that the accuracy and deviation of detection data mainly depend on the accuracy and error of sensors [8]. Caro-Ruiz et al. studied a static image acquisition technology based on WEB and built a crop image acquisition and a management system based on WEB [9]. Wang et al. combined the idea of network technology, computer vision technology, image processing, and data analysis technology to establish the prototype of the corn growing information remote monitoring system based on the B/S mode [10]. At present, the mainstream cotton growth monitoring methods are laboratory spectral analysis and image analysis [11].

On the current basis of this article in laboratory spectral analysis, NDVI and RVI were detected by spectrometer, and then the growth status model was established to evaluate the growth status. Image analysis is to establish the cotton growth model, with the characteristics of fast detection speed, but the model establishment process did not consider many factors, the accuracy is often poor that this system uses image processing and a spectral analysis method, establishes the cotton growth model, while introducing spectral analysis and leaf analysis, and improves

the accuracy of the model. Because of the difference between cotton image acquisition, incoming spectral analysis, and leaf analysis data acquisition, IMS technology is adopted to establish a network system that can realize the transmission of various data types. The test results show that the system has higher detection accuracy.

3. Research Method

3.1. System Composition. In order to realize the real-time evaluation of cotton growth status, the leaf area index (LAI) of surface plant N content and dry matter accumulation of surface plant were used as standards to establish the cotton growth status model based on IMS multiarea technology [12]. The system collects cotton canopy images by the camera and transmits them to the application service layer through the IMS system for canopy image processing and canopy coverage calculation. Then, with canopy coverage as the variable, the leaf area index (LAI) of N content and dry matter accumulation on the surface as the stress variables, three growth index models were established. The leaf area index (LAI) was collected by the LAI instrument, and the normalized vegetation index (NDVI) and the vegetation index (RVI) were collected by the spectrometer to test the feasibility of the model. After the growth model was established, the camera collected the canopy image of the cotton field to be tested, calculated the canopy coverage, and then calculated the three growth model indicators of the cotton field to be tested to evaluate the growth status of the cotton field. The system terminals include cameras, leaf areometers, and spectrometer. The output of the camera is image continuous data, and the output of leaf areometers and spectrometer is Atlas data, as shown in Figure 1 [13].

Application services include canopy image processing, growth model establishment, target cotton field canopy image detection, and other functions in the process of transmitting detection data from system terminals to application services. Due to different data forms at the terminal layer, the IMS system should be used to build models. MRCP and MRPF are relay servers and control servers, respectively. MPT-SCF is the execution point of the media multipath transmission function supported by IMS and can complete tasks such as registration session establishment and multipath transmission service authorization, and complete the allocation and release of the relay path in the interaction with the relay server control server.

3.2. Canopy Image Coverage Calculation. Timely intervention is very important to improve cotton quality and yield when cotton growth is not good. Canopy area is closely tied to the cotton growth state, the cotton canopy image captured by the camera, and image processing calculation of cotton coverage C , and then set up on the Earth's surface and plant N content of the leaf area index, dry matter accumulation of cotton plant growth parameters, and model between cotton canopy coverage, an effective evaluation of the current cotton growth situation.

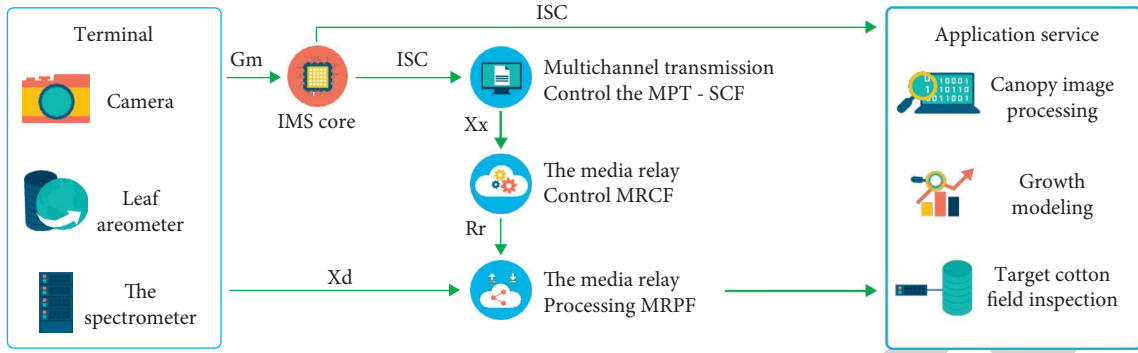


FIGURE 1: System composition.

3.2.1. Picture Processing. The image of the cotton canopy is collected by the camera, and the binary image of the cotton canopy is obtained by image enhancement processing to realize the calculation of the cotton coverage rate [14]. Image processing includes the following steps: canopy image enhancement. When the camera is collecting the cotton canopy image, it is affected by light intensity at different times, so it is necessary to suppress the influence of light conditions on the cotton canopy image. Image gray processing combines the information of R , G , and B channels into the same gray intensity. Binary processing: the pixel value of cotton canopy leaves is 255, and the rest is 0. Image filtering processing is carried out for the spot-like salt and pepper clutter in the binary image, and finally a clear cotton canopy binary image is obtained.

When the camera head shoots the cotton canopy image, it will be affected by different environmental light, resulting in different image clarity. In order to effectively eliminate the influence of illumination and other environmental factors on the image, an algorithm is designed to suppress stray light [15]. Cotton canopy image is taken at 7:00 and it is known that the image $I(x, y)$ obtained includes cotton canopy $R(x, y)$ image and stray light. Now, the stray light is suppressed, and formula (1) can be obtained as

$$R_{n,i}(x, y) = \log \left[\frac{I(x, y)}{I(x, y) * N e^{-(x+y)^2/\delta_i^2}} \right], \quad (1)$$

N is the normalized parameter of Gaussian function; δ is the Gaussian standardization deviation, which affects the local contrast of the image. Three scales, 15, 90, and 250, are used for calculation δ .

In the three channels, the intensity of the first channel is

$$R_{MSR,i}(x, y) = \sum_{n=1}^3 W_n R_{n,i}(x, y). \quad (2)$$

w_n is the weight coefficient of three scales.

The intensity of the three channels is adjusted again, and the final intensity $R_{MSR,i}(x, y)$ of the three channels is calculated as

$$R_{MSRCR,i}(x, y) = C_i R_{MSR,i}(x, y). \quad (3)$$

C_i is the secondary adjustment coefficient of 3 channels.

$$C_i = \log[\alpha I_i(x, y)] - \log \sum_{i=1}^3 I_i(x, y). \quad (4)$$

Among them, the value range of α is 0.5~2. After image enhancement, the edge of ridges and cotton leaves becomes clear.

Grayscale processing and binary processing are carried out on the image after enhanced processing. The grayscale processing adopts index MExG - ExR, then, formula (5) is obtained as

$$\text{MExG} - \text{ExR} = 2G - 1.9R - B. \quad (5)$$

G , B , and R are the three channel intensities of the enhanced images, respectively, which are transformed into gray images, and then binarization processing is carried out by the maximum variance method. There are discrete interference points in the ridge of the cotton field, and there are also discrete interference points in the leaf area. Now, the median filtering method is used to remove the interference points in the binary image.

3.2.2. Calculation of Canopy Coverage. After image enhancement, the binary image of separation between the cotton canopy and the field ridge was obtained, and the canopy coverage was calculated by the statistical method to prepare for the establishment of cotton growth parameters and the canopy coverage model, such as surface plant N content, leaf area index, and surface plant dry matter accumulation.

Canopy coverage is the ratio of the canopy leaf area to the area of the whole image. It is known that the size of the canopy binary image is $m \times n$ pixel and the gray scale $R(i, j)$ is 255 pixels, so canopy coverage C is the following formula:

$$C = \frac{\sum_{j=1}^m \sum_{i=1}^n R(i, j)}{m \times n}. \quad (6)$$

3.3. Model of the Cotton Growth State. N is an important component of chlorophyll, which determines the photosynthetic capacity of plants. Leaf growth is also related to photosynthesis and transpiration of nutrient elements transport. Material accumulation can indicate the current

plant material accumulation degree. Normalized vegetation index (NDVI) and the vegetation index (NDVI) of the cotton canopy are the current mature evaluation parameters of the cotton growth state, which can be detected by the spectrometer. The research ideas are as follows: to explore the relationship between canopy coverage C , NDVI, and RVI, and to determine the feasibility of using canopy coverage C to characterize the cotton growth state; leaf area index (LAI) C and canopy coverage N were used to model dry matter accumulation of plants on the surface [16].

3.3.1. The Relationship between CC, NDVI, and RVI.

Vegetation index RVI has been widely used to evaluate the growth condition of vegetation qualitatively and quantitatively, and NDVI can represent the content of N elements in vegetation, and then evaluate whether plants need to apply nitrogen fertilizer. The two parameters are mature and can be detected by the spectrometer. The relationship between canopy coverage rate C and canopy coverage rate RVI, NDVI is studied, and the feasibility of the canopy coverage rate to characterize the plant growth state is discussed [17].

The relationship between different canopy coverage rates and their corresponding NDVI relationships is established, as shown in Figure 2. On the whole, canopy coverage rates and NDVI show a linear distribution.

$$\text{NDVI} = 0.91C + 0.093. \quad (7)$$

The linear determination coefficient is 0.95, indicating a good linear correlation between the canopy coverage rate and canopy coverage rate NDVI, and the linear fitting performance is high in the range [0.3–0.6]. With the increase of canopy coverage, the accuracy of the model decreased, indicating that canopy coverage can effectively represent the N element content in plants.

The relationship between the canopy coverage rate and RVI is also linear, showing that the canopy coverage rate RVI gradually decreases with the increase. The linear fitting result is shown in the following equation

$$\text{RVI} = -0.736C + 0.664. \quad (8)$$

The linear correlation coefficient $R2$ was 0.96, and the fitting degree was the best in the range [0.45–0.7]. The results showed that both canopy coverage and RVI, NDVI had good linear correlation, so it was feasible to characterize the growth state of cotton by canopy coverage C .

3.3.2. Establishment of the Cotton Growth Model. Leaf area index (LAI) of plant N content and dry matter accumulation on the ground surface were selected as the growth characteristic parameters of cotton. The N content of plant could effectively represent chlorophyll content, the leaf surface index could represent the growth state of plant leaves, and dry matter accumulation on the ground surface could represent the matter accumulation of cotton. Canopy coverage was used as a variable; the leaf area index (LAI) of plant N content and dry matter accumulation on the ground were used as stress variables to establish models [18, 19].

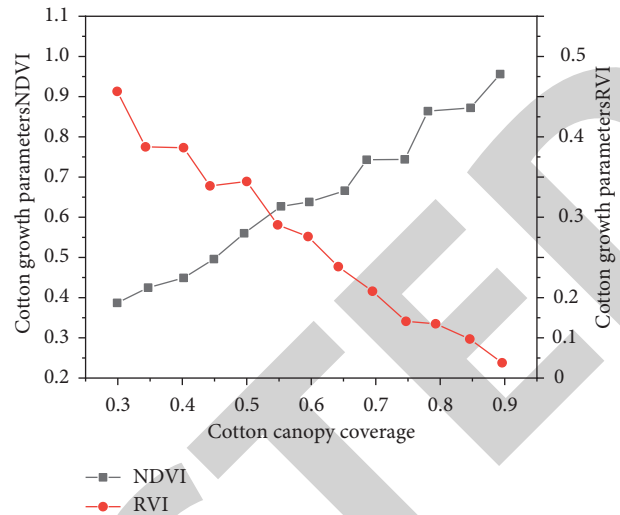


FIGURE 2: Relationship between canopy coverage and RVI, NDVI.

In the experiment, plant N content was detected by the Kjeldahl nitrogen determination method. Leaf area index was determined by the digital leaf area meter to measure the leaf area index (LAI) of a single cotton plant [20]. The cotton leaf area index (LAI) per plant was multiplied by the number of cotton plants per unit area to determine the cumulative amount of dry matter on the surface of the plant: separate the single cotton sample, dry it in 105°C oven for 30 min, dry it in 80°C oven until the quality is not reduced, and then weigh it. The dry matter mass per plant was multiplied by the number of plants per unit area to obtain the dry matter mass of the upper part of the ground.

Figures 3(a)–3(c) were, respectively, used to fit the canopy coverage with the plant N content and the leaf area index (LAI) with the plant dry matter accumulation on the surface.

Figure 3(a) shows the fitting results of canopy coverage and plant N content, which are distributed in exponential form, and the fitting determination coefficient is 0.94, i.e.:

$$y = 0.712e^{4.187C}. \quad (9)$$

Figure 3(b) shows the fitting results of canopy coverage and the leaf area index, the distribution is exponential, and the fitting determination coefficient is 0.89, i.e.:

$$y = 0.462e^{2.564C}. \quad (10)$$

Figure 3(c) shows the fitting results of canopy coverage and cumulative dry matter amount of plants on the surface, which are distributed in an exponential form, and the fitting determination coefficient is 0.92, i.e.:

$$y = 0.769e^{4.245C}. \quad (11)$$

Comprehensive analysis showed that the growth index and canopy coverage of three kinds of cotton were exponential distribution. And the lowest model fitting determining coefficient is 0.89, showing that the fitting model has high precision.

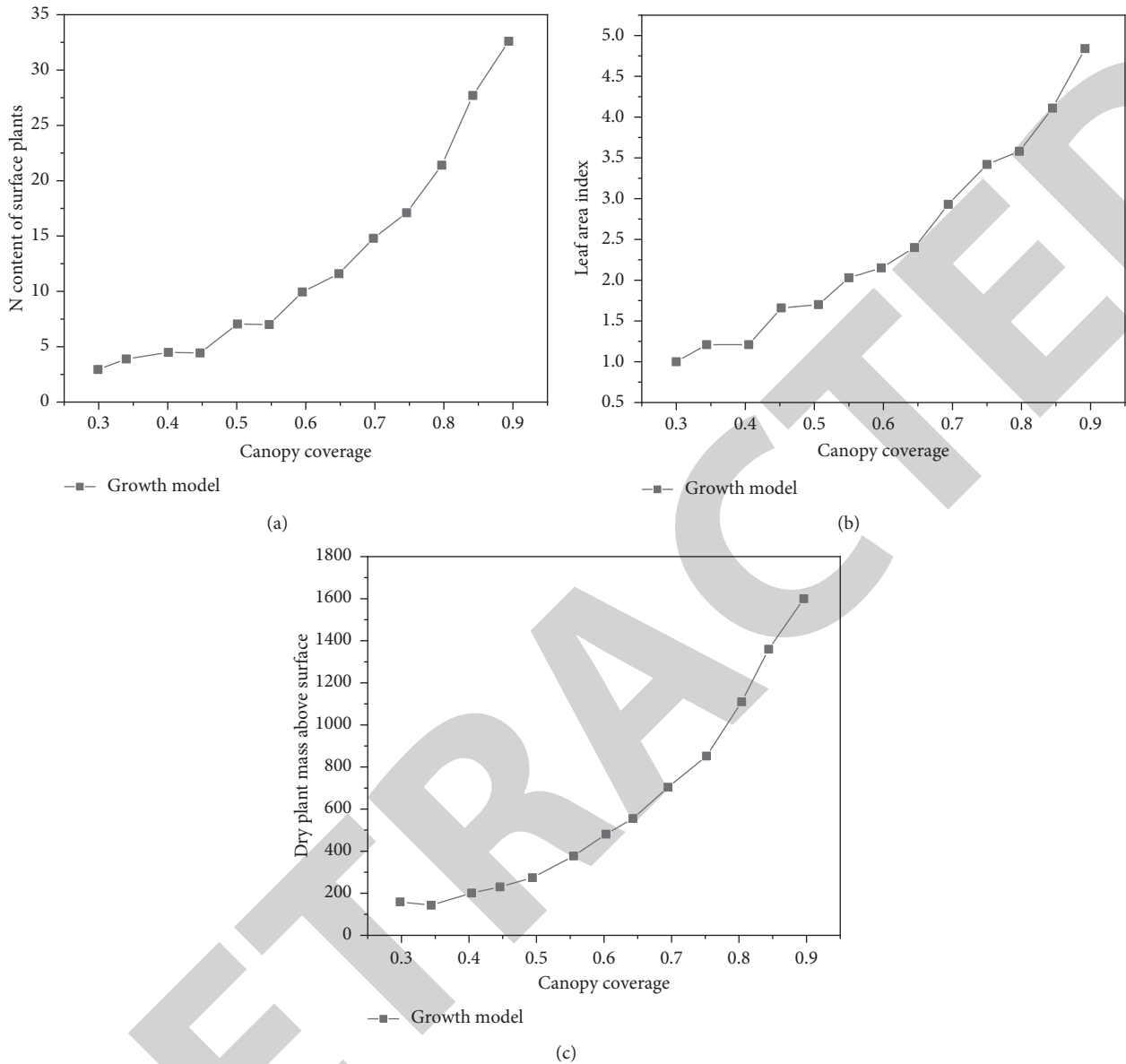


FIGURE 3: (a-c) Cotton growth model.

3.4. Effect of N Fertilizer Dosage on Cotton Growth. Nitrogen is a component of chlorophyll, under the action of chlorophyll plants will be water and CO₂ into sugar; sugar is the plant growth and accumulation of raw materials. At the same time, the effect of nitrogen on plant growth and development is very obvious, plants can use nitrogen to synthesize more protein, promote cell division and growth, and then grow more leaves, generate more chlorophyll, to achieve stable and sustainable growth of cotton. In this paper, cotton images with different nitrogen application rates were tested to calculate canopy coverage, and then the leaf area index (LAI) of plant N content and dry matter accumulative amount of plants on the surface were calculated through the model to evaluate the current growth status of cotton and guide nitrogen topdressing.

3.4.1. N Fertilizer Dosage and the Cotton Growth Index Model. According to the cotton growth model, the leaf area index (LAI) of plant N content and the cumulative dry matter amount of plant on the surface are both exponential relationships with canopy coverage, i.e.:

$$y = ke^{bc} \tag{12}$$

The effects of N fertilizer dosage on the leaf area index of plant N content and dry matter accumulation of plants on the ground surface were analyzed. The method was to fit the cotton canopy coverage and growth index *k* under different N fertilizer dosage, and the linear coefficient is shown in Figure 4. In general, the linear coefficient of the fitting model of the three indexes increased with the increase of nitrogen

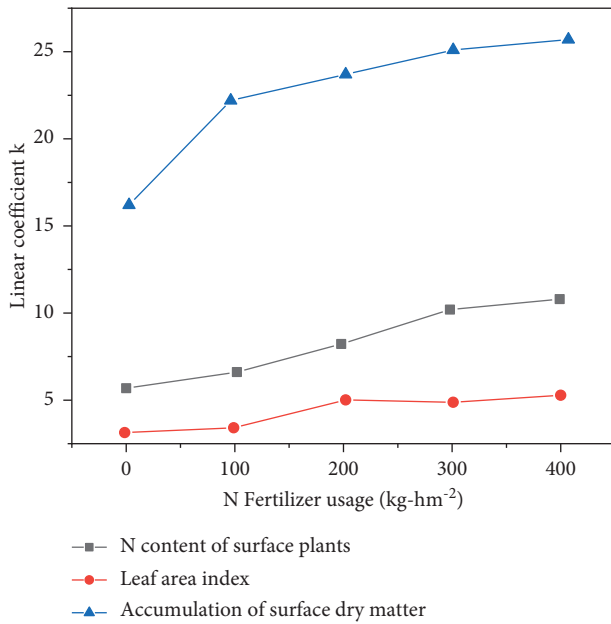


FIGURE 4: Effects of nitrogen dosage on cotton growth.

content: the linear coefficient k of the plant N content model increased from 0.49 to 0.8. The linear coefficient of the LAI model increased from 0.385 to 0.481. The linear coefficient k of dry matter accumulation model increased from 23.5 to 28.74. The effects of nitrogen application rate on the three growth indexes from high to low were dry matter accumulation and leaf area index, respectively.

3.4.2. Effect of N Fertilizer Dosage on Model Fitting Accuracy. Nitrogen application is ranged from 0 to 400 kg/hm². The fitting accuracy of three growth models under different nitrogen application rates was tested, and the changing trend of model accuracy under different nitrogen content was tested. Under different nitrogen application rates, the models between plant N content, leaf area index (LAI), plant dry matter accumulation on the surface, and canopy coverage were fitted, and the corresponding fitting determination coefficients were calculated. As shown in Figure 5, the fitting determination coefficients R^2 of the three models were all greater than 0.84, indicating that the above three models had high reliability [21]. Among them, the fitting accuracy of N content in surface plants was the highest, and the distribution range was 0.949–0.978, which showed a trend of increasing first and then decreasing, and reached the maximum value when the N application rate was 300 kg/hm². The fitting accuracy of the foliar index was next, with a distribution range of 0.846–0.938, which increased first and then decreased, and reached the maximum value at 300 kg/hm². The fitting determination coefficient of plant dry matter accumulation on the surface was the lowest, which showed a trend of increasing first, then decreasing and then increasing, and also reached the maximum value when the N fertilizer amount was 300 kg/hm². The analysis of fitting determination coefficient showed that nitrogen fertilizer dosage had a certain influence on the model accuracy and

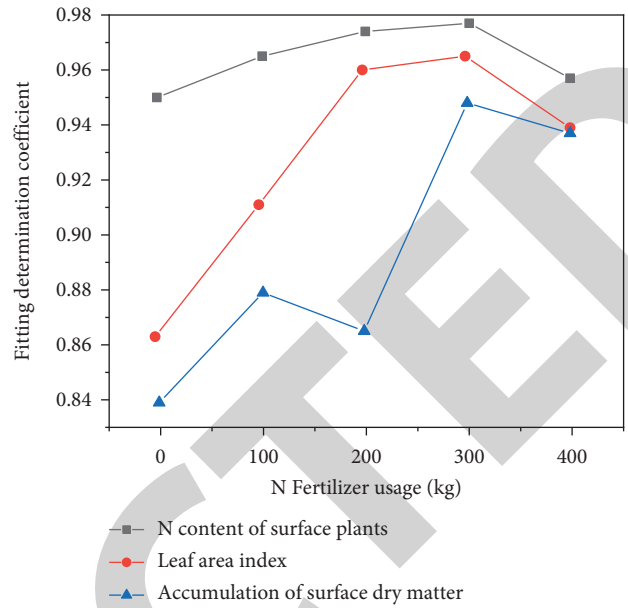


FIGURE 5: Effect of N fertilizer dosage on model accuracy.

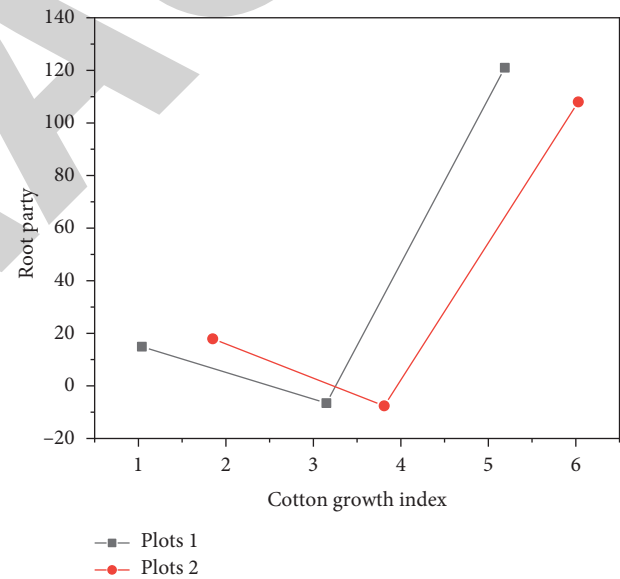


FIGURE 6: System testing.

reached the maximum value when N fertilizer dosage was 300 kg/hm², and the whole model met the accuracy requirement [22].

4. Interpretation of Result

The leaf area index (LAI) of plant N content and dry matter accumulation on the ground surface were used as plant growth parameters. The cotton canopy image was extracted by the image analysis method, and the canopy coverage was calculated, as shown in Figure 6. The cotton growth model with canopy coverage as independent variable and three growth parameters as dependent variables was established [23]. In the collection of cotton growth data, the camera leaf

area and spectral analyzer are used, and the data collection forms are different. Therefore, the IMS data transmission system is adopted to realize data transmission. Now, this system is used to establish the cotton growth model, and the growth state of the two test fields is analyzed, and RMSE of root square difference between the two test fields is tested [24]. The N content and the RMSE value of surface plants in the two experimental fields were 1.62 and 1.7, leaf area indexes were 0.675 and 0.65, and dry matter accumulative amounts of surface plants were 170 and 168, respectively. Therefore, the system could effectively evaluate the current growth status of cotton [25].

5. Conclusion

In order to realize the monitoring of cotton growth condition, a monitoring system was designed based on IMS network technology and image processing technology. The image processing technology was used to extract cotton canopy coverage, and the spectrometer collected the normalized vegetation index (NDVI) and the vegetation index (RVI) to test the feasibility of the model. Leaf area meter was used to detect the leaf area index. Firstly, the relationship between cotton canopy coverage and the normalized vegetation index (NDVI) and the vegetation index (RVI) was linear, and the fitting determination coefficient was greater than 0.95, indicating the feasibility of establishing the cotton growth model based on cotton canopy coverage. Secondly, the leaf area index (LAI) and dry matter accumulation of surface plants were established as dependent variables. Taking cotton canopy coverage as an independent variable, a cotton growth model was established. All three models are exponential and the fitting determination coefficient R^2 are all above 0.89. The effects of N fertilizer dosage on three growth indexes were discussed: with the increase of N fertilizer dosage, the linear coefficient k and exponential coefficient b of the three models showed an increasing trend, and the three models had high precision under different N fertilizer dosage. Two experimental fields were tested by using this system. RMSE of root square mean difference of three index models met the design requirements, and R^2 of the fitting determination coefficient was between 0.83 and 0.923, indicating that the system can effectively evaluate cotton growth status.

Data Availability

The data used to support the findings of this study are available from the corresponding author upon request.

Conflicts of Interest

The authors declare that there are no conflicts of interest.

Acknowledgments

This study is funded by the National Natural Science Foundation of China (31960503) and the “two districts” construction plan project of Xinjiang Production and Construction Corps (2021bb023-02).

References

- [1] T. Weng, Y. Xie, G. Chen et al., “Load frequency control under false data inject attacks based on multi-agent system method in multi-area power systems,” *International Journal of Distributed Sensor Networks*, vol. 18, no. 4, pp. 155013292210904–155013292214618, 2022.
- [2] B. Tomšič, D. Marković, V. Janković et al., “Biodegradation of cellulose fibers functionalized with $\text{CuO/Cu}_2\text{O}$ nanoparticles in combination with polycarboxylic acids,” *Cellulose*, vol. 29, no. 1, pp. 287–302, 2022.
- [3] Z. Wu, X. Li, X. Liu et al., “Membrane shell permeability of rs-198 microcapsules and their ability for growth promoting bioactivity compound releasing,” *RSC Advances*, vol. 10, no. 2, pp. 1159–1171, 2020.
- [4] A. Feng, J. Zhou, E. D. Vories, K. A. Sudduth, and M. Zhang, “Yield estimation in cotton using uav-based multi-sensor imagery,” *Biosystems Engineering*, vol. 193, no. 3, pp. 101–114, 2020.
- [5] S. Ale, N. Omani, S. K. Himanshu, J. P. Bordovsky, K. R. Thorp, and E. M. Barnes, “Determining optimum irrigation termination periods for cotton production in the Texas high plains,” *Transactions of the American Society of Agricultural and Biological Engineers*, vol. 63, no. 1, pp. 105–115, 2020.
- [6] M. Fouzi, M. Thimma, M. Binsabt, A. A. Husain, and S. Aouabdi, “Stem cell growth and proliferation on rgd bio-conjugated cotton fibers,” *Bio-Medical Materials and Engineering*, vol. 32, no. 1, pp. 39–52, 2021.
- [7] M. Küçük and M. L. Öveçoğlu, “Fabrication of $\text{SiO}_2\text{-ZnO}$ np/zno nr hybrid coated cotton fabrics: the effect of zno nr growth time on structural and uv protection characteristics,” *Cellulose*, vol. 27, no. 3, pp. 1773–1793, 2020.
- [8] C. A. Moraes, L. W. de Oliveira, E. J. de Oliveira, D. F. Botelho, A. N. de Paula, and M. F. Pinto, “A probabilistic approach to assess the impact of wind power generation in transmission network expansion planning,” *Electrical Engineering*, vol. 104, no. 2, pp. 1029–1040, 2021.
- [9] C. Caro-Ruiz, A. S. Al-Sumaiti, S. Rivera, and E. Mojica-Nava, “A mdp-based vulnerability analysis of power networks considering network topology and transmission capacity,” *IEEE Access*, vol. 8, no. 1, pp. 2032–2041, 2020.
- [10] Y. Wang, J. Wang, L. Yao, and W. Y. Yin, “Emi analysis of multiscale transmission line network using a hybrid fdtd method,” *IEEE Transactions on Electromagnetic Compatibility*, vol. 63, no. 4, pp. 1202–1211, 2021.
- [11] W. Zhou, Y. Wang, and Z. Chen, “Impedance-decoupled modeling method of multiport transmission network in inverter-fed power plant,” *IEEE Transactions on Industry Applications*, vol. 56, no. 1, pp. 611–621, 2020.
- [12] J. Ponocko and J. V. Milanovic, “Multi-objective demand side management at distribution network level in support of transmission network operation,” *IEEE Transactions on Power Systems*, vol. 35, no. 3, pp. 1822–1833, 2020.
- [13] D. Bose, C. K. Chanda, and A. Chakrabarti, “Vulnerability assessment of a power transmission network employing complex network theory in a resilience framework,” *Microsystem Technologies*, vol. 26, no. 8, pp. 2443–2451, 2020.
- [14] E. Hernández-Rodríguez, L. H. Escalera-Vázquez, E. Mendoza, D. García-Ávila, and M. Montoro Girona, “Reduced-impact logging maintain high moss diversity in temperate forests,” *Forests*, vol. 12, no. 4, pp. 383–419, 2021.
- [15] S. Timilsina, J. Aryal, and J. B. Kirkpatrick, “Mapping urban tree cover Changes using object-based convolution neural

Retraction

Retracted: Application of Cloud Computing Combined with GIS Virtual Reality in Construction Process of Building Steel Structure

Mathematical Problems in Engineering

Received 8 August 2023; Accepted 8 August 2023; Published 9 August 2023

Copyright © 2023 Mathematical Problems in Engineering. This is an open access article distributed under the Creative Commons Attribution License, which permits unrestricted use, distribution, and reproduction in any medium, provided the original work is properly cited.

This article has been retracted by Hindawi following an investigation undertaken by the publisher [1]. This investigation has uncovered evidence of one or more of the following indicators of systematic manipulation of the publication process:

- (1) Discrepancies in scope
- (2) Discrepancies in the description of the research reported
- (3) Discrepancies between the availability of data and the research described
- (4) Inappropriate citations
- (5) Incoherent, meaningless and/or irrelevant content included in the article
- (6) Peer-review manipulation

The presence of these indicators undermines our confidence in the integrity of the article's content and we cannot, therefore, vouch for its reliability. Please note that this notice is intended solely to alert readers that the content of this article is unreliable. We have not investigated whether authors were aware of or involved in the systematic manipulation of the publication process.

Wiley and Hindawi regrets that the usual quality checks did not identify these issues before publication and have since put additional measures in place to safeguard research integrity.

We wish to credit our own Research Integrity and Research Publishing teams and anonymous and named external researchers and research integrity experts for contributing to this investigation.

The corresponding author, as the representative of all authors, has been given the opportunity to register their

agreement or disagreement to this retraction. We have kept a record of any response received.

References

- [1] Y. Dong, H. Sui, and L. Zhu, "Application of Cloud Computing Combined with GIS Virtual Reality in Construction Process of Building Steel Structure," *Mathematical Problems in Engineering*, vol. 2022, Article ID 4299756, 8 pages, 2022.

Research Article

Application of Cloud Computing Combined with GIS Virtual Reality in Construction Process of Building Steel Structure

Yugang Dong , Haozhi Sui, and Lei Zhu

Weifang Engineering Vocational College, Qingzhou 262500, Shandong, China

Correspondence should be addressed to Yugang Dong; 41818061@xs.ustb.edu.cn

Received 26 June 2022; Accepted 28 July 2022; Published 17 August 2022

Academic Editor: Hengchang Jing

Copyright © 2022 Yugang Dong et al. This is an open access article distributed under the Creative Commons Attribution License, which permits unrestricted use, distribution, and reproduction in any medium, provided the original work is properly cited.

In order to ensure that the steel structure of the building can meet the requirements of the strength of the building structure and the strict requirements in the fields of earthquake resistance, fire protection, energy saving, and environmental protection in the construction process, a method based on virtual reality supply chain cloud computing collaborative management technology is proposed. This method analyzes the main technology of building steel structure and establishes personalized cloud computing collaborative management technology based on virtual reality supply chain. Based on the analysis of industry characteristics and personalized service characteristics, the virtual reality control mechanism of personalized data mining is proposed by considering the service time cost and user experience quality. Based on cloud computing and VIRTUAL reality GIS, a collaborative management and control system architecture is proposed to optimize user personalized needs and solve the impact of differentiation on the supply chain. Experimental results show that compared with the noncollaborative management scheme, the collaborative management algorithm proposed by this method reduces the interference of personalized differences on supply chain management by 25%. The experimental results show that this method can greatly guarantee the satisfaction of steel structure construction process.

1. Introduction

According to the general code of Chinese civil building, the building with steel structure as structure is called steel structure building [1]. Compared with traditional concrete materials, steel structure materials have strong advantages in energy saving and environmental protection. On the premise of meeting the quality and safety requirements of high-rise buildings, steel structural materials can meet the requirements of national building energy-saving development and improve the building aesthetics, which is significantly better than traditional building structural materials. In architectural design and construction, the application of steel structure is important, not only can meet the needs of super high-rise building structure strength, in the field of earthquake resistance, fire protection, energy saving, and environmental protection, steel structure is superior to the traditional concrete structure [2]. And as the cloud computing technology began to gradually enter people's vision,

the concept of "cloud" was put forward, by the academic and industrial circles of various countries great attention. Cloud refers to the Internet here, and there is no unified conclusion on the specific meaning of cloud computing so far. But its original meaning belongs to the Internet computing environment. As an interdisciplinary subject applying virtual reality technology, geographic information system (GIS) has been gradually developed with the deepening of human technology research. With the idea of open-source software gradually prevailed, open-source GIS is also beginning to emerge. In the face of vast amounts of geographic information data, how to properly store and manage them is now a hot issue. At the same time, the development of cloud computing technology has given this question a reasonable and high esteemed solution. Storage of GIS data in cloud platform is not only low cost but also high security. At the same time, processing of massive GIS data using cloud computing technology is much more efficient than processing on a stand-alone platform.

Therefore, using cloud computing GIS and other technologies to analyze the construction technology and requirements of building steel structure and develop relevant construction technology can help achieve high-quality development of building construction.

2. Literature Review

In view of the research on the construction process of building steel structure, Luo et al proposed that the application of BIM technology in the construction of building steel structure can not only control the actual construction cost but also achieve a comprehensive understanding of the overall construction of steel structure, which can fundamentally improve the construction quality of construction projects [3]. Yin et al. proposed to reduce the occurrence probability of reverse logistics by analyzing and processing big data, subdividing logistics demand, and combining correlation analysis [4]. Prusov proposed to use virtual reality technology to establish three-dimensional cloud simulation of enterprise field environment, which enhanced users' actual experience of field operation. They proposed to use cloud computing to transform all network resources into services, and users can access these services online to achieve on-demand computing and collaboration [5]. Liu et al. proposed the establishment of a cloud service platform about GIDS in order to simplify the installation and management of GIS applications, reduce the investment and operating cost of GIS, and improve the variability of GIS applications and underlying facilities [6]. Kim and Kang et al. proposed that cloud GIS is a service platform for collaborative processing of information data for users. Through cloud GIS, users do not need to know the position of the application in the system but only need to use PC or mobile phone and connect to the Internet to query data information through the cloud anytime and anywhere to achieve distributed cross-platform spatial data integration management and processing [7]. Ortega et al. put forward the virtual technology system based on cloud computing. Through the discussion of key technologies, existing resources can be effectively virtualized into services, and 3D cloud simulation of enterprise field environment can be established through virtual reality technology, enhancing users' actual experience of field operation [8].

Based on the collaborative supply chain system of cloud computing combined with GIS virtual reality technology, the characteristics of the industry and personalized service are firstly analyzed. At the same time, the characteristics of service time cost and user experience quality are comprehensively considered, and the virtual reality control mechanism of personalized data mining is proposed. Implementation includes the management and supervision of construction steel structure construction process, the equipment material selection to the last in the construction process of prophase planning and design to ensure the safety of the building just materials used. Joint virtual reality based on cloud computing and GIS collaborative management control system architecture is presented to optimize the user

personalized needs and solve differential effects on supply chain.

3. Research Method

3.1. Technology Platform. The overall platform architecture of cloud GIS is a Hadoop-based cloud GIS platform, in which mass data storage and high-performance computing are based on Hadoop high-performance distributed parallel processing architecture. The platform uses map resynchronization distributed parallel computing architecture to disperse spatial data processing and analysis tasks to each node in the cloud to reduce data computing time [9]. This kind of high-performance computing is especially suitable for the processing of sea data and the analysis and processing of GIS. The specific framework of the platform is shown in Figure 1, which consists of four layers: physical layer, cloud platform layer, service layer, and application layer.

3.1.1. Physical Layer. This layer is located at the lowest level of the architecture and consists of computer servers and network resources.

3.1.2. Cloud Layer. Cloud platform layer is the core of the entire system architecture, which is divided into four layers, namely, operating system layer, cloud platform, environment data layer, and management-layer Cloud platform environment. Distributed storage and computing environment is based on Hadoop, including distributed storage, management, and processing of massive spatial data. In this layer, distributed data storage and management use HBASE and HDFS functional modules in Hadoop to establish corresponding spatial data tables based on HBASE and store multiresolution image data vector data and service data. The final processing result data are stored in HDFS, and HBASE data can be accessed using SQL-like languages, such as Pig Hive and Zookeepe, which are responsible for coordinating services [10]. The data layer includes multiresolution image data vector data metadata and other related service data. Image data of various resolutions can be stored in different modes. Image tile data of various resolutions are stored in corresponding tables of HBASE, while unsegmented large-scale image data are directly stored in HDFS. Vector data are directly stored in HBASE tables. Metadata consists of two parts: cloud data such as vector raster data. Second, various service metadata are stored in HBASE tables [11]. In this way, Hadoop Distributed File System (HDFS) solves the problem of inconvenient management of small files. Meanwhile, HBASE timestamp can be used to achieve data version control.

The management layer is the core layer and is responsible for managing all the data and other information that need to be scheduled and managed. The management layer provides distributed data storage interfaces, high-performance distributed computing management interfaces, and cloud platform function aggregation interfaces [12]. Distributed storage interface including transparent storage interface based on data sharing, multiresolution image map

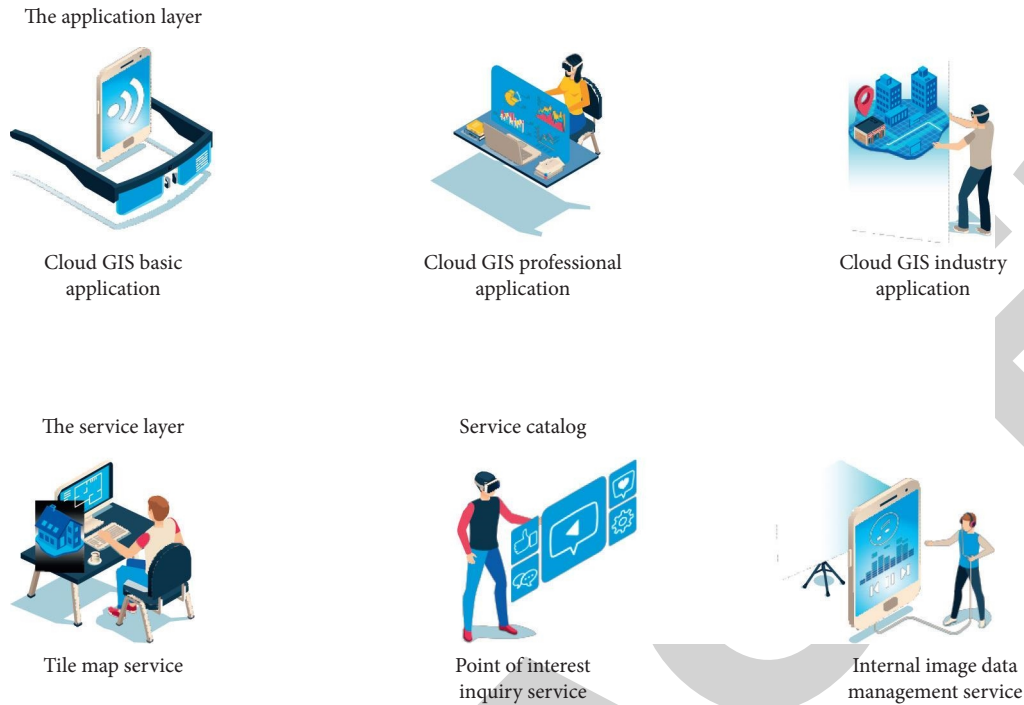


FIGURE 1: Cloud GIS overall platform architecture: the function and design scheme of each floor.

service, and image pyramid storage interface. In addition, it also includes multiresolution image data distributed storage interface, vector data distributed storage interface, cloud data storage interface, and other business data storage interfaces for high-performance distributed computing.

3.1.3. Service Layer. According to the characteristics of cloud computing, cloud computing resources are provided to users in the form of network services [13]. Cloud computing services include LaaS, Paas, SaaS, and DaaS. Generally, cloud GIS only provides Paas, SaaS, and DaaS layer services. The service layer provides service catalogs for applications, mainly including tile-land country service, query service for points of interest, and internal image management service, class H basic service. As your application expands, you can also provide an interface to add new services.

3.1.4. Application Layer. The application layer provides users with one-stop services directly; all resources and GIS functions are provided to users in the form of basic application services, professional application services, and industrial application services. The application layer mainly combines different services through Mashup data sets and service sets to form application services for different purposes to meet the needs of different users. For clients, cloud GIS can provide different services for different client systems, including C\S architecture desktop, GIS B\S architecture, WebGIS mobile GIS, and so on [14].

In the construction of steel structure, information management framework needs to pay attention to the following problems:

- (1) The construction process of the message management framework should ensure that the construction party of the project is involved in it. According to the different parts of the project construction, the steel structure project should be designed first, and the production of the prefabricated parts of the shrinkage agent in the steel structure should be constructed [15].
- (2) For steel structure construction process to use the technology to the actual data in real-time to share in the whole process of construction, in the process of data transmission to reduce the error rate of information data, the construction management framework is to fully comply with the principle of the steel structure construction period, to achieve the centralized management of data information, ensure the construction project involves more than one unit can be involved, to facilitate Focus on giving reasonable suggestions and opinions.
- (3) In the process of the construction of steel structure message management framework, it is necessary to use technology to collect a number of data information displayed in the construction in real time, so as to facilitate the relevant construction party to have a comprehensive understanding of the construction situation, and to formulate a scheme for the problems existing in the monitoring process, so as to improve the safety of construction [16].

3.2. Personalized Virtual Reality Data Mining Model.

Virtual reality technology is a brand-new comprehensive information technology that emerged at the end of the 20th century. It integrates digital image processing, computer graphics, multimedia technology, sensor technology, and other information technology branches. Virtual reality is based on computer technology as the core, realistically build a virtual environment that integrates vision, hearing, touch, and so on. VRML is short for virtual reality modeling language [17].

VRML is not equal to virtual reality completely, but it has an important influence on virtual reality technology. As a modeling language to describe virtual environment on the Web, VRML exists independently. As an independent real-time interactive 3D modeling and rendering tool for distributed multimedia integration platform, VRML provides technology that can effectively integrate 2D and 3D text and multimedia materials into a virtual environment, so that users are immersed in it.

VRML is a modeling language; its basic goal is to build interactive three-dimensional multimedia on the Internet, that is, it is used to describe three-dimensional objects and their behavior, and can build virtual realm [18]. Using VRML to realize the interaction with Internet, virtual reality has the following advantages: enrich the media expression form, visual management of collaborative role, improve the user interface of collaborative environment, and enhance the interaction of collaborative environment. It can be seen that the integration of VRML into the development process of online virtual laboratory can not only enhance the expressive force and user acceptance but also achieve a better collaborative work virtualization environment.

The supply chain personalized data mining system is designed into four submodules, which are user-driven module, data storage module, data mining module, and feedback module, respectively. The user-driven module takes management users as the main body and inputs various supply chain information according to user management requirements. The user information must be set with an upload field, which serves as the weight factor for activating the upper module and is also the most important basis for decision-making for the upper module. The data storage module determines the supply chain data storage mode according to the weight factor of the lower module and sets the database scale and the fields in the table combined with the user scale. The storage module is the hardware platform of personalized data mining and logical processing core; it is the embodiment of the space complexity of personalized data mining model of data mining module focus on the whole the computational complexity of personalized data mining model and logic relation, personalized data, how to accurately draw a supply chain need to choose reasonable mining algorithm. At the top is the feedback module, which not only decides what form to use to feed back personalized data to supply users but also feeds back control information to the three lower modules to further optimize the personalized data mining model, as shown in Figure 2:

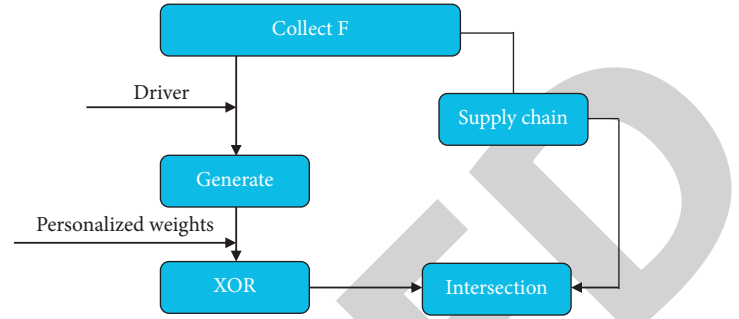


FIGURE 2: Data mining model.

The following is the function definition and execution process of the four modules. The functions required by the user-driven module include supply chain user data collection, classification, and polling. To facilitate personalized data storage, it is necessary to accommodate multiple input data types and transparently handle the differences of data types, as shown in the following formula:

$$D = \sum_{j=1}^N \sum_{i=1}^N P_D(i, j). \quad (1)$$

P_D represents the supply chain user data set, M represents the number of data types, N represents the data dimension, and D represents the data source set provided to the data storage module after transparent processing. The personalized characteristics of user data need to be set in real time and diversified based on supply chain requirements. The supply chain management demand is obtained according to user demand, and the personalized data mining evaluation ability is carried out according to the information of the uppermost feedback module, so that the personalized mining model has self-renewal and repairability. To accurately locate system preferences, the system has the personalized data polling function according to the user's personalized needs and establishes cross-layer interaction mechanism with the uppermost feedback module. Supply chain management users' evaluation of personalized data mining can be generated in various forms: according to the effectiveness feedback record of users, users can use the conclusion of personalized data mining to set the record evaluation key points of supply chain, personalized satisfaction information group, user evaluation information collection, and personalized satisfaction information of groups.

Data storage module is the data basis of personalized data mining. It optimizes data sources and addresses before data mining, improves the efficiency of personalized data mining, and optimizes computational complexity while reducing spatial complexity [19]. In this module, data storage needs to consider the following factors:

- (1) User personalized demand preference.
- (2) The difference between the relevant supply catalog and the personalized preference is to select the most matched and least matched line catalog.

(3) Evaluation and statistics of personalized differences between group users and some individual users of the group. Data mining module as the key module of personalized data mining model, the static data mining system, it is difficult to solve the personalized needs of users of individual and group conflict, so according to individual differences in evaluation and statistics, a real-time dynamic scheduling the following data mining algorithm improve the robustness of personalized data mining model [20].

- (1) When the personalized difference is small, that is, less than 0.5, the line product catalog is analyzed based on the characteristics of individual user needs.
- (2) When the personalized difference is lower than 0.5, based on the personalized needs of individual users and group users that maximize part of the difference, the output of personalized preference is maximized from the aspects of the supply chain background, behavior, scenic spot characteristics, and so on.
- (3) When the individuation difference is greater than 0.5, it indicates that the individuation contradiction between individual users and group users is large, which is difficult to be solved in a single individual. Based on the analysis of user needs and the linear mapping of supply chain, the preevaluation of product matching is given, and the individuation data mining of group decomposition is carried out.

The feedback module can feed back information to the lower three functional modules in the following ways:

- (1) Modify the weight factor and pass it to the user drive module through the feedback channel.
- (2) The personalized difference statistical information is modified and transmitted to the data storage module and the data mining module, so that the two modules can obtain the relationship between the four functional modules in the personalized data mining model established by the user's evaluation information of the supply chain established by the personalized data mining in real time, as shown in Figure 3.

3.3. Design of Cloud Computing Coordination System for Building Steel Structure. In the personalized data mining model established in the previous section, the contradiction between the personalized needs of individual users and group users, namely, the personalized difference, has a great influence on the data reliability of personalized data mining. Therefore, this model is deployed on cloud platform, cloud computing is added between data storage module and data mining module, and collaborative management of supply chain is implemented through collaboration between cloud servers and writing between personalized data mining submodules, as shown in Figure 4.

The collaboration steps in Figure 4 are detailed as follows:

- (1) Collaborative management of data mining: in the personalized data mining model, collaborative execution is carried out among the four submodules according to the time sequence. Based on pipeline technology, the delay of information transmission between module ports is shortened here. This paper defines the personalized multidimensional matrix of data mining, called $d*c*m$ multidimensional matrix, where dimension D represents the mining data result set driven by personalized supply chain, dimension C represents the cloud computing demand set driven by personalized, and dimension M represents the interface set used for collaborative management. The data mining and analysis results of each layer are the elements of the multidimensional matrix. The length of the multidimensional matrix reflects the supply chain scale of the pipeline. The scale of dimension M represents the timing sequence and delay of signals transmitted on the information transmission interface. The scale of dimension C records the collaborative execution force and execution efficiency of the cloud platform. The scale of dimension D can represent the collaborative weight among the four submodules in the personalized data mining model.
- (2) Cloud computing collaborative management: cloud-to-cloud computing collaboration between different supply chain personalized data mining modules is established to weaken the interference of differentiation level on supply chain management.

The following two points need to be noted:

- (1) The mapping relationship between the pipeline scale of supply chain and the dimension of data mining matrix must be considered when applying multidimensional matrix to the computing collaboration between cloud. Based on this, a cloud platform with high dimensional integration can be obtained between different personalized data mining modules of the supply chain. The cloud platform can obtain the management demand of each assembly line of the supply chain in real time. Then, through the clouds to initialize the d , c , and m parameters, thus multidimensional matrix from multiple instantiation personalized choose collaborative management needs the strongest of the multi-dimensional matrix elements and their mapping of the cloud, on the basis of further optimization between the cloud and the cloud computing collaborative process. For these collaborative process, cloud platform can optimize data points associated polling of the multidimensional matrix.
- (2) For the interference of personalized supply chain management generated in the collaborative management process of cloud computing, the cloud platform weakens the elements of each

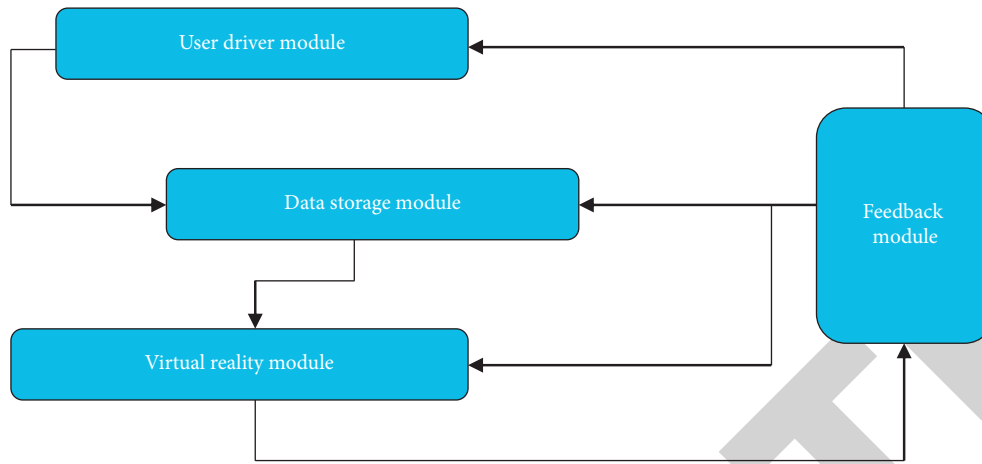


FIGURE 3: Soft decision factor roaming graph.

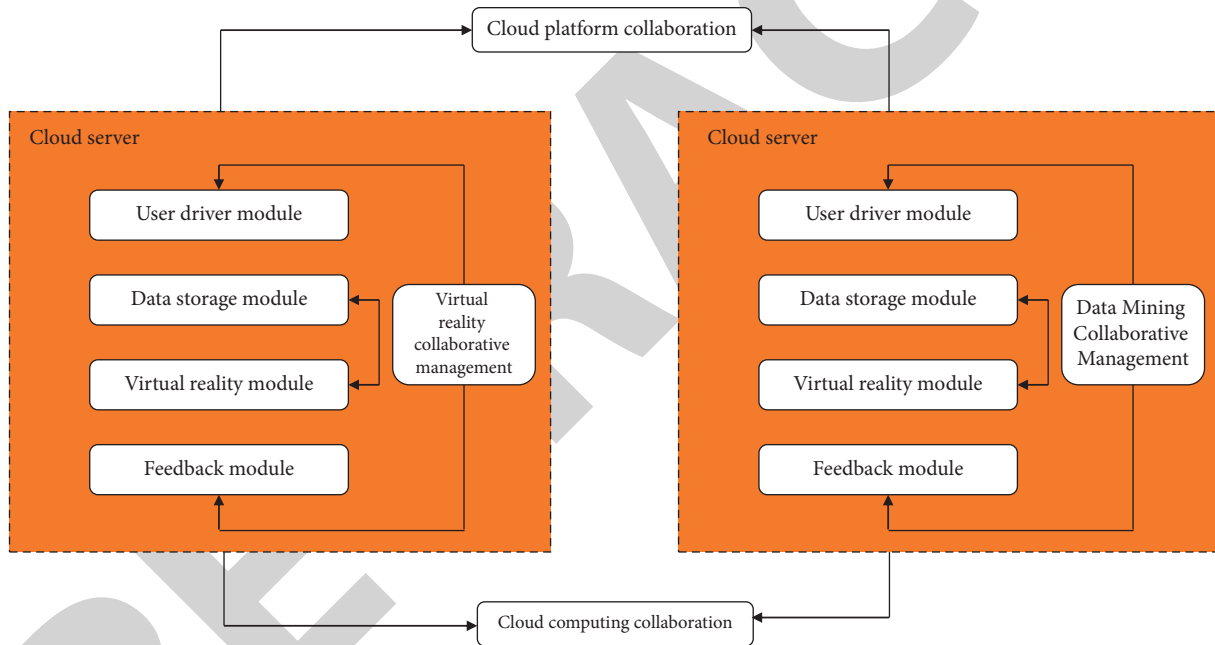


FIGURE 4: Supply chain cloud computing collaborative management architecture.

multidimensional matrix, which is defined as the closed-loop graph representation of personalized attributes of data mining. The closed loop defines multiple inflection points according to the element scale and value of the multidimensional matrix. These inflection points tend to cause multipoint interference to personalized supply chain management. Therefore, weakening the differential strength of a closed-loop edge is beneficial to the mapping and consistency guarantee of the multidimensional matrix.

- (3) On the cloud platform, cloud servers can allocate computing tasks and coordinate resource management to improve resource utilization and personalized data mining efficiency of the cloud platform.

Among them, the storage data of the server of the cloud platform are bound in the closed loop [21]. The resources consumed by the computing task data mining process of closed loop and cloud server will restrict the resource utilization and data mining efficiency of cloud platform. Therefore, multiple closed-loops are used to organically integrate the result set of multidimensional matrix data mining and personalized supply chain management requirements and follow the closed-loop mapping rules, which can optimize the computing process of cloud servers and the resource consumption of collaborative management and help ensure the stability of collaborative supply chain management [22]. The collaborative management efficiency of supply chain cloud computing is shown as follows:

TABLE 1: Experiment parameter.

Parameter	Value
The user types	10 kinds
Difference evaluation factor	[0.1, 0.9]
The cloud number	[2, 5]
User satisfaction factor	[1, 5]
User data scale	[0.1, 10]GB

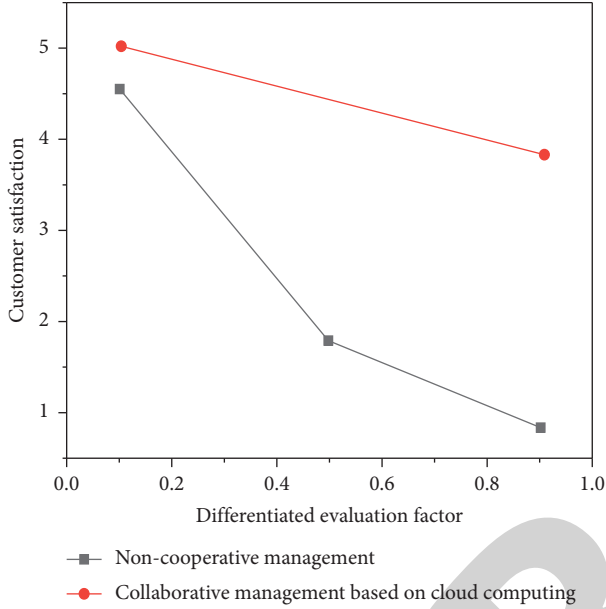


FIGURE 5: Comparative analysis of satisfaction.

$$E = \frac{1}{2} \alpha \left(\sum_{i=1}^{\sqrt{M \cdot N}} t_i - P_D(\beta, i) \right). \quad (2)$$

E represents management efficiency, α represents the weight of game personalized difference optimization, and β represents the weight of collaborative interaction of personalized data model.

4. Interpretation of Result

The core of the collaborative management mechanism based on cloud computing virtual reality technology established in this paper is to optimize users' personalized needs and solve the impact of differentiation on the supply chain through personalized data mining and collaborative management architecture using virtual reality technology. Therefore, based on the experimental environment shown in Table 1 and from the point of differentiation, the user satisfaction of the proposed scheme and the noncollaborative scheme was compared and analyzed, and the results are shown in Figure 5. All experiments in this paper are completed on a PC, and virtual reality modeling language (VRML) technology is adopted. As can be seen from Figure 5, the satisfaction of the two management schemes in the case of low differentiation.

When the differentiation evaluation factor is greater than 0.5, user satisfaction is lower than 2, indicating that users are dissatisfied with the products in the supply chain. In contrast, the proposed collaborative management scheme significantly weakens the interference of differentiation level on supply chain management by fully considering the contradiction of differentiation of supply chain through collaborative management of data mining and computing collaboration between cloud computing and personalized data mining modules.

5. Conclusion

In this paper, a supply chain cloud computing collaborative management technology based on personalized data mining is proposed. In order to effectively guarantee the accuracy and feedback satisfaction of users' personalized demand, based on the analysis of industry characteristics and personalized service characteristics, and based on the multi-objectives such as service time cost and user experience quality, the collaborative management technology of supply chain cloud computing based on personalized data mining is established. The core of the collaborative management mechanism is to optimize user's personalized needs and solve the impact of differentiation on the supply chain through personalized data mining and collaborative management architecture. The experimental results show that the proposed collaborative management scheme can effectively weaken the interference of personalized differences on supply chain management, significantly improve customer satisfaction, and further guarantee the satisfaction of steel structure construction process requirements.

Data Availability

The data used to support the findings of this study are available from the corresponding author upon request.

Conflicts of Interest

The authors declare no conflicts of interest.

References

- [1] V. K. Bansal, "Use of GIS to consider spatial aspects in construction planning process," *International Journal of Construction Management*, vol. 20, no. 3, pp. 207–222, 2020.
- [2] R. Kumar and A. Sharma, "Risk-energy aware service level agreement assessment for computing quickest path in computer networks," *International Journal of Reliability and Safety*, vol. 13, no. 1-2, p. 96, 2019.
- [3] H. Y. Luo, L. M. Zhang, H. J. Wang, and J. He, "Process of building collapse caused by the po Shan road landslide in Hong Kong on 18 June 1972," *Landslides*, vol. 18, no. 12, pp. 3769–3780, 2021.
- [4] C. Yin, Z. Chen, Y. Feng, W. Zhu, Y. Zhao, and L. Chen, "The mechanism of fire resistance of a low carbon high-strength multi-functional steel for building construction," *Journal of Materials Science*, vol. 57, no. 15, pp. 7706–7718, 2022.
- [5] D. Prusov, "Scientific substantiation of engineering preparation measures due to the influence of construction in the

Retraction

Retracted: Construction of Heritage Digital Resource Platform Based on Digital Twin Technology

Mathematical Problems in Engineering

Received 26 September 2023; Accepted 26 September 2023; Published 27 September 2023

Copyright © 2023 Mathematical Problems in Engineering. This is an open access article distributed under the Creative Commons Attribution License, which permits unrestricted use, distribution, and reproduction in any medium, provided the original work is properly cited.

This article has been retracted by Hindawi following an investigation undertaken by the publisher [1]. This investigation has uncovered evidence of one or more of the following indicators of systematic manipulation of the publication process:

- (1) Discrepancies in scope
- (2) Discrepancies in the description of the research reported
- (3) Discrepancies between the availability of data and the research described
- (4) Inappropriate citations
- (5) Incoherent, meaningless and/or irrelevant content included in the article
- (6) Peer-review manipulation

The presence of these indicators undermines our confidence in the integrity of the article's content and we cannot, therefore, vouch for its reliability. Please note that this notice is intended solely to alert readers that the content of this article is unreliable. We have not investigated whether authors were aware of or involved in the systematic manipulation of the publication process.

Wiley and Hindawi regrets that the usual quality checks did not identify these issues before publication and have since put additional measures in place to safeguard research integrity.

We wish to credit our own Research Integrity and Research Publishing teams and anonymous and named external researchers and research integrity experts for contributing to this investigation.

The corresponding author, as the representative of all authors, has been given the opportunity to register their agreement or disagreement to this retraction. We have kept a record of any response received.

References

- [1] H. Jia and J. Yan, "Construction of Heritage Digital Resource Platform Based on Digital Twin Technology," *Mathematical Problems in Engineering*, vol. 2022, Article ID 4361135, 8 pages, 2022.

Research Article

Construction of Heritage Digital Resource Platform Based on Digital Twin Technology

Haomei Jia ¹ and Jing Yan²

¹Department of Computer Science, Tangshan Normal University, Tangshan, Hebei 063000, China

²Experimental Management Center, Tangshan Normal University, Tangshan, Hebei 063000, China

Correspondence should be addressed to Haomei Jia; 1112050427@st.usst.edu.cn

Received 15 June 2022; Accepted 27 July 2022; Published 17 August 2022

Academic Editor: Hengchang Jing

Copyright © 2022 Haomei Jia and Jing Yan. This is an open access article distributed under the Creative Commons Attribution License, which permits unrestricted use, distribution, and reproduction in any medium, provided the original work is properly cited.

In order to preserve and inherit material cultural heritage, the author proposes a method for digital construction of the Great Wall's cultural heritage based on digital twin. This method discusses the connotation of the whole life cycle of the Great Wall digital twin, proposes the research path and content of the digital twin construction of the Great Wall cultural heritage, and conducts the application of the Great Wall digital twin to evaluate the application effect. The evaluation results show that users' overall satisfaction with Great Wall's digital twin application is relatively high, and the average score of each indicator is above 4, and the functional experience is slightly poor. *Conclusion.* This method can provide full life cycle visualization services for the digital archiving, application, and decision-making of the Great Wall cultural heritage and provide theoretical and methodological references for the preservation and inheritance of material cultural heritage.

1. Introduction

The early digital display was widely used in the field of film art and was considered to be a display method including projection technology and transmission technology, with extensive and convenient dissemination advantages [1]. With the wide application of many new technologies such as Internet technology, multimedia technology, and virtual reality technology, the concept of digital display has been endowed with richer connotations and extensions. The so-called "digital display" is to display the content as the main body, with digital technology as the means of realization. Through various new media and digital media technologies, the digital presentation of the display content is realized [2]. The application of new media technology provides a new display method and means of expression for digital display. It is not limited by national borders, regions, time, and space and integrates and innovates various media information to form a new platform for information dissemination.

The digital display method of material cultural heritage, according to the characteristics of different types of heritage,

classifies and stores information through various digital technologies and uses various new media technologies to achieve digital display. It not only fully mobilizes the various sense organs of the human body but also lets the audience have a more systematic and comprehensive understanding of the displayed content.

2. Literature Review

Countries applied digital technology to cultural heritage protection earlier, and the related theoretical research was relatively mature. Most of the research content revolves around the theoretical construction of digital protection, the development of key technologies, or the application and practice of digital technology in the display and dissemination of cultural heritage. Singh et al. pointed out that emerging technologies such as VR and AR have the potential and advantages of efficient and low-cost ways to preserve and disseminate cultural information [3]; Rhee et al. applied AR and 3D computer graphics technology to the cultural relics enhanced display system and analyzed its usability [4];

Jahanger et al. used a technology acceptance model to analyze the cultural heritage movement and the acceptance of augmented reality applications [5]; Karimi et al. proposed an augmented reality-based interactive virtual guide for visiting archaeological sites [6]; Karmakar et al. explored in their doctoral dissertation the application of augmented and virtual reality technology in museum education through computer-supported collaborative learning [7]. In the “double wall dialogue,” Dy et al. introduced the research results of the archaeological demonstration of Bodward Fortress using airborne laser scanning technology and described the motion recovery structure technology for accurately generating 3D data [8].

In recent years, the development of digital technology has been booming. Although China’s research on its application in cultural heritage protection is booming, there are still certain limitations. Specifically, intangible cultural heritage is the main focus of most researches, and there is relatively little research on tangible cultural heritage. The research purposes are mostly based on the protection of intangible cultural heritage and the development and construction of museums. Research related to the protection of intangible cultural heritage focuses on the digital preservation and inheritance of intangible cultural heritage, and research related to the development of museums more focuses on the improvement of the guide system in the museum and the development and design of derivative cultural and creative products. There are many studies on cultural heritage itself or cultural institutions such as museums, and there are few studies on public cognition and user experience.

At present, there is much digital twin research in various countries in aerospace, machinery manufacturing, and other fields, and less research in cultural heritage, other humanities, and social sciences. At the same time, the digital construction of the Great Wall cultural heritage also lacks research and application in the field of digital twins. The digital construction of the Great Wall in China has more single-level studies such as 3D models, platform R&D, and AR/VR multiterminal displays, but there are fewer closed-loop comprehensive studies integrating “lightweight modeling, IoT communication, data processing, and application services” [9-10]. The existing digital research of the Great Wall cultural heritage in China has made great breakthroughs in “image recording, partial restoration, and archaeological demonstration.” However, there is a lack of research on “full life cycle” content such as historical process evolution and future construction simulation. This paper analyzes the research status of digital twin theory and technology in various countries and the digital construction of the Great Wall cultural heritage and proposes that digital twins should be used in the Great Wall National Cultural Park, with theoretical and practical significance for the digital construction of the Great Wall cultural heritage.

3. Research Methods

3.1. Significance of Digital Twin for the Construction of Great Wall National Cultural Park. The significance of the Great Wall is mainly manifested in promoting the development of the Chinese nation. The historical and cultural value of the

Great Wall is mainly reflected in its contribution to human civilization. Therefore, the rich cultural relics of the Great Wall have extremely high cultural and historical value. However, with natural wind erosion, several wars, the rapid development of China’s urbanization in recent years, and the serious lack of awareness of the cultural heritage of the Great Wall, as a result, the defense system of the Great Wall has been seriously threatened. According to the 2009 National Cultural Relics Directorate City Resources Survey and Identification Results, only 8.2% of the Ming Great Wall artificial walls are well-preserved, nearly three-quarters of the walls are in poor condition, and even no relics exist [11].

The Great Wall digital twin can digitally restore its historical construction process, important historical time and space, and real-time status quo, providing reliable digital resources and strong data support for the protection, restoration, and display of the Great Wall. At the same time, AI computing is performed on the Great Wall and its surrounding environment through massive data, providing a visual intelligent simulation for the future construction of the Great Wall [12]. Therefore, the construction of the digital twin of the Great Wall cultural heritage is not only a new exploration of digital twin technology in the field of cultural heritage but also an innovative supplement to the existing theoretical system of digital construction of the Great Wall cultural heritage. After inducting and deducting the relevant research results from China and other countries, it is believed that the common theoretical system and common characteristics of digital twin and material cultural heritage digitization are shown in Figure 1 [13].

3.2. Research on the Connotation of the Whole Life Cycle of the Great Wall Digital Twin. Virtual simulation is a simulation technology that simulates the physical world by converting physical models into software. The characteristics and parameters of the physical world are reflected through 3D high-fidelity modeling [14, 15]. A digital twin is based on virtual simulation, real-time perception, diagnosis, and prediction of the state of physical objects through actual measurement, simulation, and data analysis; regulation of the behavior of physical objects through optimization and instructions; and self-evolution through mutual learning between related digital models. This enables simultaneous improvement in stakeholder decision-making during the life cycle of physical entity objects. It can be said that virtual simulation is part of many key technologies for realizing digital twins. In addition, the formation of digital twins also requires various IoT and Internet technologies such as sensors, data transmission, data analysis, drives, and cloud platforms.

In recent years, under the background of vigorously promoting the development of scientific and technological innovation industries and advocating the protection of cultural heritage, the digital research and practice of China’s tangible and intangible heritage have made great progress. Virtual simulation is the first generation of digital simulation technology with high-reduction 3D models as the core technical feature, from manual modeling using 3D Max,

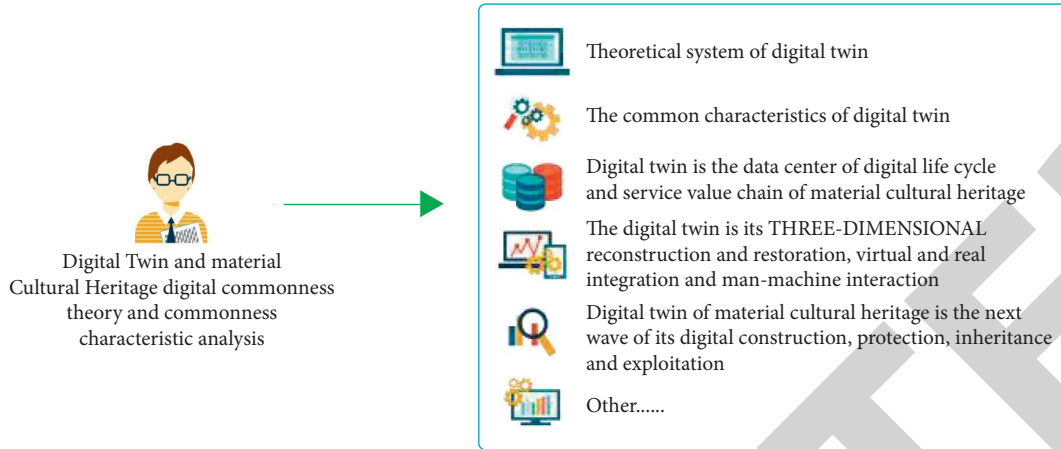


FIGURE 1: Analysis of common theory and common characteristics.

Unity, and other software to intelligent modeling using scanned point cloud data to generate models. From the physical display using 3D printing molding technology to the virtual display using VR/AR/XR technology, different concepts and technologies have created different application scenarios and interaction methods [16].

With the development of information technology and the advent of the Internet of everything era, digital twin, as the second generation of digital simulation technology with the whole life cycle as the core feature, highly integrates virtual simulation with the new generation of Internet of things, Internet, blockchain, artificial intelligence, etc. Electronics and Information technology: its application fields have gradually shifted from aerospace, military, and other fields to modeling and processing, design and manufacturing, smart city management, and other fields. With forward-looking concepts and technical advantages, digital twins will provide new methods and new tools for cultural heritage in various application scenarios such as digital protection, monitoring, simulation development, and display.

As a key technology to realize intelligent construction, digital twin can realize information fusion and interaction between virtual space and physical space. Therefore, combining with the characteristics of complex construction projects and many-elements information, referring to the five-dimensional model of digital twin, a multidimensional model of intelligent construction based on digital twin is proposed, as shown in the following equation [17]:

$$M_{BDT} = (B_{PE}, B_{VE}, B_{SS}, B_{DD}, B_{CN}). \quad (1)$$

In the formula, B_{PE} represents the physical construction entity, B_{VE} represents the virtual construction model, B_{SS} represents the intelligent construction service for the whole life cycle of the building, B_{DD} represents the data of the whole life cycle of the construction object, and B_{CN} represents the connection between the modules.

In terms of the entire life cycle, digital twins in the fields of aerospace, machinery production, and smart city management are iteratively updated in the process of physical entity simulation; the starting point of its life cycle is the present state of the physical entity. Material cultural heritage

is different from the former. As an important material cultural heritage in China, the Great Wall is a large-scale military defense project built in different historical periods. Therefore, the digital twin of the Great Wall should be composed of three parts: history, current situation, and future in terms of twin structure (see Figure 2).

The first part is a retro-twin to the Great Wall's defense system. Through the review and demonstration of a large number of documents, combined with virtual simulation technology and artificial intelligence algorithm simulation technology, we can really restore the construction process of the Great Wall defense system and the changes in different historical periods. Its purpose is to sort out and digitize the construction history and war history of the Great Wall defense system. The second part is the twin management of the status quo of the Great Wall and its surrounding environment [18]. On the basis of BIM, GIS, and other model data, through the application of multitype distributed sensing equipment and safe and high-speed network transmission, the purpose is to restore the 1:1 status of the Great Wall, not only the visual 1:1 restoration but also a 1:1 restoration of changes in the real world such as climate, human flow, and geological changes, so that the inside and outside are the same, holographic mirroring. The third part is the future development twin of the Great Wall that contains AI calculation predictions and manual design changes. AI calculation prediction is a simulation of the environmental changes of the Great Wall by computer through data collection and operation of the real physical world. Artificial design changes can be redesigned through artificial digital models, which change and present the Great Wall and its surrounding environment. The purpose is to "trial and error" through the simulation of the digital environment and provide more reasonable countermeasures for the environmental protection construction of the Great Wall.

Therefore, the digital twin of the Great Wall is to recreate a corresponding "virtual Great Wall" in cyberspace, forming a physical Great Wall in the physical dimension and a digital Great Wall in the information dimension (historical information, status quo information) and coexisting and blending the virtual and the real pattern, through real-time

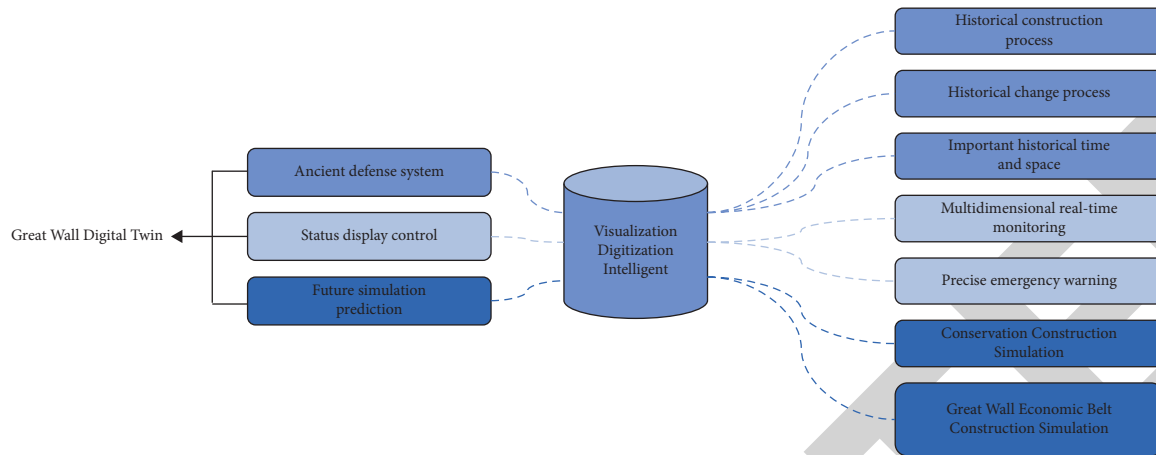


FIGURE 2: The twin structure of the Great Wall digital twin in the full life cycle.

feedback of multiple types of sensors to the digital world, intelligent, consistent, and complete visual mapping, and simulation can be realized [19].

4. Analysis of Results

The construction path of the Great Wall digital twin consists of three parts, namely, literature and data research, framework and key technology research, and visual terminal and application research, and the structural relationship is shown in Figure 3 [20].

4.1. Literature and Data Research on Multitype Great Wall Cultural Heritage. By arranging and analyzing the material and intangible cultural heritage, the construction process, change process, and important historical temporal and spatial data of the Great Wall can be demonstrated. It is a technical data study on the construction of the digital twin of the Great Wall cultural heritage. The data research on the material cultural heritage of the Great Wall includes the content of the documents and data of the Great Wall ontology buildings, military settlements, public buildings, and relics in different historical periods. The data research on the intangible cultural heritage of the Great Wall includes the content of the documents and data of the defense of the Great Wall in different historical periods, folk culture, and major historical events. Zhang et al. mentioned the tangible heritage of the Great Wall cultural heritage in the construction of the Ming Great Wall cultural heritage database, including the Great Wall body building, military settlements, public buildings, related relics, and all the tools and utensils contained in it. Among them, the main buildings include the walls, enemy towers, wall towers, beacon towers, piers, and battle towers of the Great Wall; military settlements include towns, road cities, acropolis, Suocheng, Baocheng, Guancheng, posts, and outposts; public buildings include official residences, storage pastures, temples and ancestral halls, school academies, archways, and towers; relics include water kilns, residential sites, smoke stoves, fire pools, and other relics.

4.2. Research on the Great Wall Digital Twin Framework and Key Technologies. First, research is conducted on the theoretical framework of the Great Wall digital twin system. We research on the application strategy of digital twin technology in tangible and intangible cultural heritage and propose the theoretical concept, construction connotation, and technical framework, as well as the contents and functions of each part of the digital twin of the Great Wall cultural heritage. Second, we research on the construction of the Great Wall lightweight virtual entity library and the construction methods of the Great Wall virtual entity with different precision levels and realize the construction of the Great Wall virtual entity library based on this. It includes the restoration of construction in different historical stages; the reproduction of special historical node scenarios; the real mapping of the current environment; and the base of the future development model. Third is the application research of multitype sensors in the data interaction layer. We research on the network architecture and perception acquisition methods of different types of distributed sensors and study the near real-time data flow method between the digital domain and the physical domain based on Firefly [21], and based on this, the methods and paths of real-time data acquisition of the Great Wall and its surrounding environment are studied. Fourth, we research on the transmission and processing methods of the Great Wall's multitype data. We research on the transmission methods of data of the Great Wall cultural heritage, geology, ecological environment, social economy, and human environment, including communication protocols, data fusion, interface services, and other research contents.

4.3. Research on the Visualization of the Great Wall Cultural Heritage and the Multiterminal Application of Digital Twin. The visualization of the Great Wall cultural heritage consists of three-dimensional digital visualization, information and data visualization, and other contents. The former is mainly aimed at the Great Wall virtual entity, and the latter is mainly aimed at the visual design of information and data in system association, functional interaction, interface

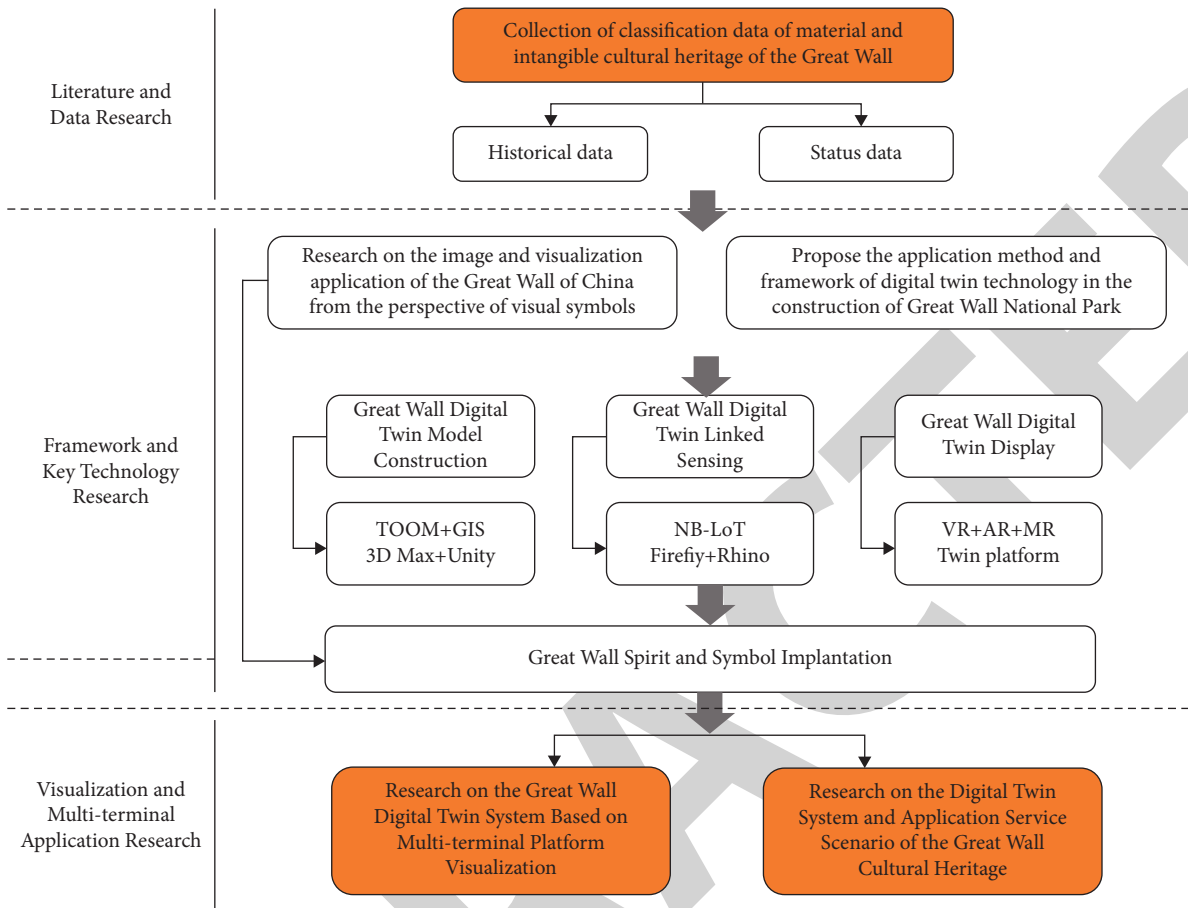


FIGURE 3: Research path for the construction of the Great Wall digital twin.

experience, structural navigation, media communication, and technical aesthetics. At the same time, based on the research on the spirit and cultural symbols of the Great Wall, the application method and content of the cultural heritage of the Great Wall in the national cultural park online platform, offline exhibition hall, various management platforms, and other multiterminal scenarios are studied. A multidimensional interactive approach to culture, art and technology has also been explored.

4.4. Test Results and Analysis. In order to evaluate the usability, functionality, and acceptability of the overall interactive system of the Great Wall digital twin application and to verify the user experience satisfaction and dissemination effect based on the digital display and dissemination strategy of cultural heritage, for target users, two evaluation items, namely, task test and filling in subjective evaluation scale, were carried out, respectively. The description of the indicators is shown in Table 1.

The user task test is divided into two parts: interface operation and functional actual experience. The task design revolves around the core functions of the application, the specific task design is shown in Table 2.

After sorting through the task test results, it is found that the users have completed various tasks well; most

users can complete all tasks independently, and some users can also successfully complete the tasks after being briefly prompted by the main test staff. In terms of the specific operations of the application, it has been observed that during the test of task 2, the number of misoperations by users is high, and it generally occurs when switching between the functions of floor plan navigation and real-scene navigation, which one is the live tour function. In addition, it was also observed that during the completion of task 4, it is a common practice of the user to click the “More” button to display the hidden menu instead of swiping right on the screen. Based on the above observations, the design of ambiguous icons should be optimized in subsequent application iterations until it is convenient for users to understand, and various gesture-guided designs should be improved before users use them for the first time.

Figure 4 shows the average scores of each index in the user’s subjective evaluation scale. From the data, it can be seen that the user’s overall satisfaction with the Great Wall digital twin application is relatively high, and the average score of each index is above 4 points. Among them, the interactive operation scores are more prominent, and users are more satisfied with various gesture designs, which are in line with daily usage habits. About lower functional scores, the reason is mainly limited by its own

TABLE 1: User's subjective evaluation scale.

First-level indicator	Secondary indicators	Indicators	Indicator score
Interface usability	Visual style	The overall style is harmonious and unified, beautiful, and applicable	5 4 3 2 1
		Icons are well-designed and easy to understand	5 4 3 2 1
	Interaction	The function level is clear and the operation process is reasonable	5 4 3 2 1
		Gesture operation conforms to daily usage habits	5 4 3 2 1
	Emotional experience	I am satisfied with the overall experience	5 4 3 2 1
Experiential	Feature	I can see the details of the artifacts clearly, as expected	5 4 3 2 1
	Availability	Easy to operate, can get started quickly	5 4 3 2 1
	Pleasure	I enjoyed the experience, it was immersive	5 4 3 2 1
Digital communication	Cognition	The content presented is informative, interesting, and easy to understand	5 4 3 2 1
		Novel and interesting display of cultural relics	5 4 3 2 1
	Mentality and attitude	I would like to be exposed to such a form of communication	5 4 3 2 1
		I think such a form has artistic appeal and has a positive effect on cultural dissemination	5 4 3 2 1
		I think this form has a strong sense of participation	5 4 3 2 1
Behavior	I would like to take the initiative to pay attention to relevant information	5 4 3 2 1	

TABLE 2: User testing tasks.

Task theme	Serial number	Detailed description of the task
Interface usability	Task 1	Task description: reserve museum tickets Task start status: go to the home page and look for the appointment entry Task end status: complete the appointment, return to the home page
	Task 2	Task description: choose a theme route of interest to start the tour and experience the AR live tour Task start status: enter the navigation page and operate according to the prompts Mission end status: open AR real-world tour or plan route diagram
	Task 3	Task description: turn on the camera to participate in the AR treasure hunt and collect a treasure of the town hall Mission start status: enter the AR camera page and look for the treasure hunt entrance Task end status: complete collection and return to AR camera page
	Task 4	Task description: learn about the specific introduction of a collection of cultural relics and listen to its audio commentary Task start status: enter the home page and click on more entries When the task is over, enter the audio commentary page to complete the listening
	Task 5	Task description: enter my page to see which exhibitions have participated Task start status: go to my page Task end status: complete the search and return to the home page
AR experience	Task 6	Task description: use the camera to scan the identification map of the terracotta beast-shaped pot and view the cultural relic model Mission start status: turn on the AR camera, ready to scan Mission end status: artifact models appear on the screen
	Task 7	Task description: open the AR application, generate the cultural relic model, place it on the recognition plane, and appreciate the details Task start state: open AR app and try to tap the screen Mission end status: after the model is successfully generated, use two fingers/single finger to rotate and move the cultural relic
	Task 8	Mission description: pick a fun cultural relic sticker and complete a selfie Mission start status: open AR camera and select a sticker Mission end status: successful selfie

technical level, the functional experience cannot be combined with the interactive prototype of the application interface, and the display method is relatively simple. On the whole, the Great Wall digital twin application basically meets the user's expectations and visually achieves a beautiful atmosphere while satisfying the basic display of cultural relics in terms of functions. The user experience

has been improved to a certain extent with pleasure and immersion through technology, and the digital display and dissemination of cultural resources in the collection have been better achieved. However, the richness of functions and the accuracy of icon recognition remain to be improved. In terms of performance, it still needs to be further optimized.

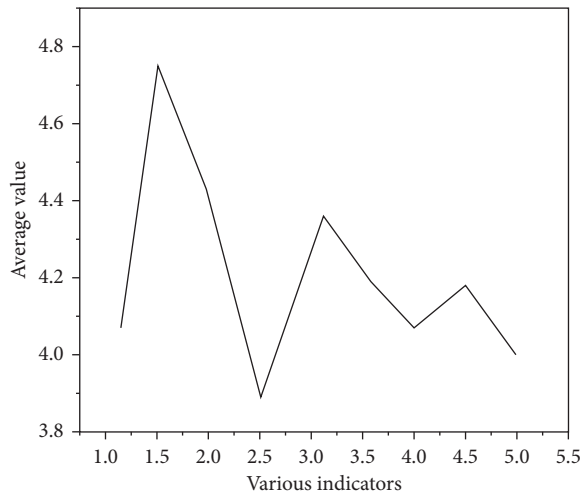


FIGURE 4: The average score of each index of the subjective evaluation scale.

5. Conclusion

The research on the construction of the digital twin of the Great Wall is an innovative study of forward-looking digital technology in the field of cultural heritage protection and inheritance, which is of great significance to the digital construction of the Great Wall National Cultural Park in China.

For the overall system structure, the establishment of the Great Wall digital twin includes five dimensions. They are the physical entity dimensions of the Great Wall, composed of material and intangible cultural heritage data. The virtual entity dimension of the Great Wall is composed of multitype and multilevel virtual simulation models of the Great Wall. The Great Wall twin application dimension consists of multiterminal application service scenarios. The twin communication connection dimension consists of data connection and processing. The twin platform dimension consists of core data centers.

Aiming at the innovation of research, from the perspective of research, it can provide full life cycle visualization services for the digital archiving, application, and decision-making of the Great Wall cultural heritage and provide a new vision and new path for the digital construction of the Great Wall National Cultural Park. In terms of research content, in view of the shortcomings of the research status of various countries in China, combined with the characteristics of digital twin technology, it innovatively proposes a comprehensive research on the closed-loop application of the physical entity, virtual entity, and twin application scenarios of the Great Wall. At the same time, it is a combination of art and technology, providing new research directions and footholds.

Data Availability

The data used to support the findings of this study are available from the corresponding author upon request.

Conflicts of Interest

The authors declare no conflicts of interest.

Acknowledgments

This study was funded by the Scientific Research Fund of Tangshan Normal University, Research on the Application of Digital Twin Technology in Tangshan Industrial Heritage Protection (project no. 2022C46).

References

- [1] P. Tichá, M. Domonkos, J. Trejbal, P. Demo, and Z. Prošek, "Electrospun sio2 nanotextiles for preservation of a tangible cultural heritage," *Key Engineering Materials*, vol. 868, pp. 86–91, 2020.
- [2] L. Lisienkova, T. Shindina, and T. Lisienkova, "Development of a methodology for assessing the technical level of cultural heritage objects in construction," *Civil Engineering Journal*, vol. 7, no. 4, pp. 662–675, 2021.
- [3] R. K. Singh, A. Singh, L. Ksherchokpa et al., "Grassroots approaches for sustaining biocultural diversity and livelihood security: insights from indian eastern himalaya," *Environmental Management*, vol. 68, no. 1, pp. 17–37, 2021.
- [4] B. Rhee, F. Pianzola, N. Oh, G. Choi, and J. Kim, "Remediating tradition with technology: a case study of from tangible to intangible: a media showcase of kisa chin p'yori chinch'an uigwe," *Digital Creativity*, vol. 32, no. 1, pp. 56–70, 2021.
- [5] Q. K. Jahanger, J. Louis, C. Pestana, and D. Trejo, "Potential positive impacts of digitalization of construction-phase information management for project owners," *Journal of Information Technology in Construction*, vol. 26, pp. 1–22, 2021.
- [6] S. Karimi and I. Iordanova, "Integration of bim and gis for construction automation, a systematic literature review (slr) combining bibliometric and qualitative analysis," *Archives of Computational Methods in Engineering*, vol. 28, no. 7, pp. 4573–4594, 2021.
- [7] A. Karmakar and V. S. K. Delhi, "Construction 4.0: what we know and where we are headed?" *Journal of Information Technology in Construction*, vol. 26, pp. 526–545, 2021.
- [8] A. Dy, A. Dw, A. Hz, W. A. Ye, B. Ssa, and A. Qd, "A novel application integration architecture for the education industry - sciencedirect," *Procedia Computer Science*, vol. 176, pp. 1813–1822, 2020.
- [9] A. Sharma and R. Kumar, "A framework for pre-computed multi- constrained quickest QoS path algorithm," *Journal of Telecommunication, Electronic and Computer Engineering*, vol. 9, no. 3-6, p. 897, 2017.
- [10] T. Marcher, G. H. Erharter, and M. Winkler, "Machine learning in tunnelling - capabilities and challenges," *Geomechanics and Tunnelling*, vol. 13, no. 2, pp. 191–198, 2020.
- [11] G. Uggla and M. Horemuz, "Identifying roadside objects in mobile laser scanning data using image-based point cloud segmentation," *Journal of Information Technology in Construction*, vol. 25, pp. 545–560, 2020.
- [12] J. Jayakumar, B. Nagaraj, S. Chacko, and P. Ajay, "Conceptual implementation of artificial intelligent based E-mobility controller in smart city environment," *Wireless Communications and Mobile Computing*, vol. 2021, Article ID 5325116, 8 pages, 2021.
- [13] A. Zarinwall, T. Waniek, R. Saadat, U. Braun, H. Sturm, and G. Garnweitner, "Comprehensive characterization of aptes

Retraction

Retracted: Optimization of Plane Image Color Enhancement Processing Based on Computer Vision Virtual Reality

Mathematical Problems in Engineering

Received 5 December 2023; Accepted 5 December 2023; Published 6 December 2023

Copyright © 2023 Mathematical Problems in Engineering. This is an open access article distributed under the Creative Commons Attribution License, which permits unrestricted use, distribution, and reproduction in any medium, provided the original work is properly cited.

This article has been retracted by Hindawi, as publisher, following an investigation undertaken by the publisher [1]. This investigation has uncovered evidence of systematic manipulation of the publication and peer-review process. We cannot, therefore, vouch for the reliability or integrity of this article.

Please note that this notice is intended solely to alert readers that the peer-review process of this article has been compromised.

Wiley and Hindawi regret that the usual quality checks did not identify these issues before publication and have since put additional measures in place to safeguard research integrity.

We wish to credit our Research Integrity and Research Publishing teams and anonymous and named external researchers and research integrity experts for contributing to this investigation.

The corresponding author, as the representative of all authors, has been given the opportunity to register their agreement or disagreement to this retraction. We have kept a record of any response received.

References

- [1] R. Xue, M. Liu, and Z. Lian, "Optimization of Plane Image Color Enhancement Processing Based on Computer Vision Virtual Reality," *Mathematical Problems in Engineering*, vol. 2022, Article ID 9404874, 7 pages, 2022.

Research Article

Optimization of Plane Image Color Enhancement Processing Based on Computer Vision Virtual Reality

Renzheng Xue , Ming Liu, and Zuozheng Lian

School of Computer and Control Engineering, Qiqihar University, Qiqihar 161006, China

Correspondence should be addressed to Renzheng Xue; 19401109@smail.cczu.edu.cn

Received 23 May 2022; Revised 21 June 2022; Accepted 4 July 2022; Published 5 August 2022

Academic Editor: Hengchang Jing

Copyright © 2022 Renzheng Xue et al. This is an open access article distributed under the Creative Commons Attribution License, which permits unrestricted use, distribution, and reproduction in any medium, provided the original work is properly cited.

In order to solve the problems of low brightness contrast of a color image, hiding a large amount of detail information, and deviation of color information in the process of image acquisition, an optimization method of plane image color enhancement processing based on computer vision virtual reality is proposed. In this method, the input RGB image is converted into the image represented by the HSI color model, and its adaptive brightness is adjusted to improve the overall brightness of the image. For the local detail enhancement of the color image, the three-dimensional Gaussian model perceived by retinal neurons is introduced into the illuminance image estimation of the MSR algorithm to enhance the image color. The results are as follows: from the perspective of objective parameter evaluation, the mean, standard deviation, information entropy, and average gradient of example images 1 and 2 are improved by about 70%; this algorithm not only enhances the brightness and contrast of the image but also maintains the detailed edge information of the image and the color characteristics of the object itself. The average enhancement rate is the highest among various algorithms, up to 95%. The algorithm proposed in this paper maintains the edge detail information of the image, optimizes the defects of the combination of traditional bilateral filtering and Retinex algorithm, and the color is also well restored, which makes the monitoring image easier to identify, more conducive to criminal investigation and solving cases, and lays a foundation for subsequent image processing.

1. Introduction

Human beings obtain external information mainly through vision and hearing, and scientific research shows that the proportion of information obtained through vision is higher than 75%. As one of the main sources of visual information, image is a vital information transmission medium [1]. In recent years, with the increasing popularity of portable digital cameras, people have more opportunities to obtain images in the open air. However, in the process of image acquisition, due to the influence of many factors such as hardware equipment configuration, lighting conditions, weather conditions, objective environment, and so on, there may be a series of problems in the actually obtained image. In particular, the brightness and contrast of the color image acquired at night will be significantly low, and the color information and local detail information are easy to be hidden, which makes the computer vision system unable to

conduct more in-depth research on the acquired night color image. There are many application fields of computer vision technology, such as visual tracking, intelligent vehicle, anomaly detection and recognition, and so on. In particular, the in-depth study of night color image enhancement technology is also one of the research hotspots of computer vision technology [2, 3]. In general, the brightness and contrast of color images at night will be significantly low, and a large number of local detail information and color information are easy to be hidden. However, clear images are the key prerequisite for understanding the real scene. Therefore, night color image enhancement has broad research prospects in the fields of public social security, urban traffic law enforcement, and so on [4]. Processing the target image through image enhancement technology is mainly to enhance the information concerned by people in the image according to the actual needs, which is conducive to the specific analysis and practical application in the future [5].

According to the actual needs, the image enhancement system designed by people needs to have the ability to deal with different environments adaptively. At present, researchers at home and abroad are still constantly engaged in the research of night color image enhancement technology and have achieved good results, but they are far from reaching the mature stage. Because of this, there is still a large research space in this field [6]. Figure 1 is a processing device and a processing method for enhancing the color of a plane image.

2. Literature Review

On dark nights, there is only a small amount of natural light, such as starlight and moonlight, which is very little compared with sunlight. Due to the lack of visible light at night, ordinary cameras can not be fully exposed, so the brightness and contrast of the obtained image are low, and the color and detail information are largely hidden. In recent years, with the continuous development of night vision technology, people pay more and more attention to color night vision technology. The current hardware instrument achievements mainly include low light night vision instrument, laser night vision instrument, and infrared thermal imager. They use a large number of invisible light bands to obtain more information sources for the night environment, such as medium wave infrared, near infrared, long wave infrared, short wave infrared, ultraviolet, and other light sources [7]. However, these instruments are relatively expensive, mainly used in the military field and have not been popularized. Therefore, we need to use some image enhancement methods to improve the image quality. Natural color effect and clear object details are the ultimate goal of night color image enhancement. The existing technical solutions mainly include multiple image fusion and single image enhancement. This paper aims at the research of image enhancement [8].

Image enhancement technology, one of the important parts of digital image processing, has been widely used. Traditional image enhancement techniques mainly include spatial processing and frequency domain processing [9]. The spatial processing method is to directly process the pixels of the image, which mainly includes the histogram equalization method, specified return method, gray transformation method, and Retinex method. Among them, the histogram equalization method mainly converts the gray range of the gray histogram of the original image into uniform distribution, which improves the visual effect of the image, but this method is easy to lose the detailed information of the original image. Mi and others proposed an improved histogram equalization algorithm, which can effectively improve the problem of easy loss of detail information in traditional histogram equalization methods, but color images are prone to color distortion. The operation speed of the gray-scale transformation method is relatively fast, but it is difficult to determine the parameters, so different images cannot achieve the effect of adaptive adjustment, and there may be over enhancement [10]. Huang and others proposed a new method, which can improve the overall brightness and

local contrast at the same time and effectively solve the adaptive problem in the gray transformation method, but the effect is not ideal for the image with low illumination [11]. The frequency domain method is to filter the image based on Fourier transform, which mainly includes high-pass filtering, low-pass filtering, and other processing methods. Low-pass or high-pass filtering can only smooth or sharpen the image. At present, many image enhancement processing techniques for filling traditional image enhancement methods have been proposed. Overall, the most effective method is the image enhancement technology based on the Retinex theoretical model [12].

Night image enhancement is a special problem involving images with variable illumination conditions. The Retinex algorithm is an effective theory, which aims to simulate the human visual system (HVS) to achieve color constancy and dynamic range compression [13]. Kim and others put forward the final version of Retinex theory, that is, the so-called color constancy theory. Land believes that the color information obtained by the visual system is only related to the reflection essence of the object, but has nothing to do with the light intensity on the surface of the object [14]. The theory divides the image into two parts: one is the low-frequency part of the image, which corresponds to the brightness component of the object; the second is the high-frequency part of the image, which corresponds to the reflection component of the object surface [15]. Among the various improved algorithms based on Retinex theory, aiming at the different estimation methods of incident light components, they mainly include Retinex algorithm of random walk, Retinex algorithm based on iterative path, and Retinex algorithm of center/surround. In comparison, the center/surround Retinex algorithm is not only easy to implement and run but also has significantly improved running speed and better processing effect. It is the most widely used in practical application [16].

Based on the current research, this paper proposes an improved MSR image enhancement algorithm based on the problems and defects of the existing Retinex image enhancement algorithm and enhances the night color image.

3. Research Methods

3.1. Color Model. The color model is an abstract mathematical model, also known as color space or color system. It is a model that uses a set of values to define color [17]. In essence, the color model is a way to explain the coordinate system and subspace, in which all colors are represented by a single point. The typical color model is generally divided into three dimensions, namely vector space. The corresponding points are used to represent a color in the color space, and the position coordinates are vectors with three components [18]. It can be seen that color space can quantify the ability of abstract color perception, so a color model is a powerful means to study color information [19]. At present, the commonly used color model is three-dimensional, because three different coordinate axes can be used to represent different characteristics [20]. There are many kinds of commonly used three-dimensional color models, and

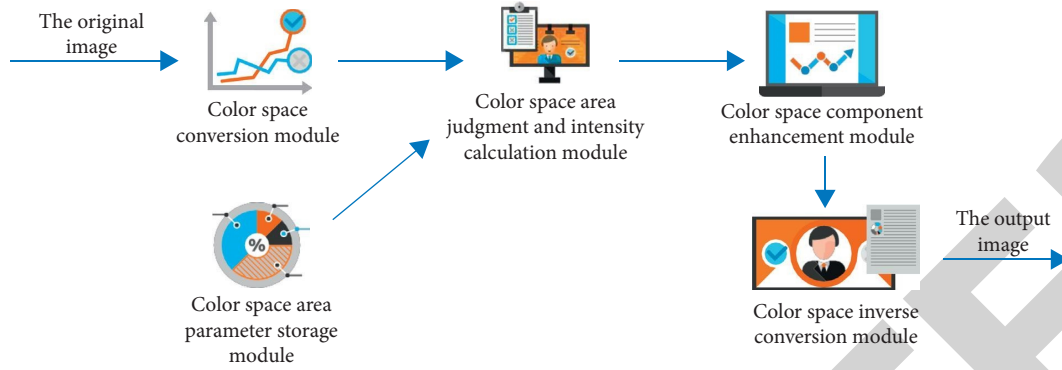


FIGURE 1: Enhancement processing device and processing method of plane image color.

different color models also have great differences. For different research purposes of various problems, it is very necessary to select the appropriate color space before processing color images.

At present, most color models are either hardware oriented or application-oriented. In digital image processing, hardware oriented RGB (red, green, and blue) color space is the most widely used at present. This model is usually used in color cameras and color monitors; in addition, CMY (cyan, magenta, and yellow) and CMYK (cyan, magenta, yellow, and black) models are mainly used for color printers; HSI (hue, saturation, and brightness) color space is more in line with human’s interpretation of color. It can also process the color information and gray information in the image separately. In the application of image enhancement, it can achieve good color retention and enhancement performance at the same time [21, 22]. HSI color model is completely different from the above two color models based on physics or process, which is - a perception based color model [23]. This color model can not only avoid the phenomenon of color deviation but also simplify the processing of color images to a great extent. The HSI color model proposed by Munsell is natural and intuitive for human beings because it is in line with human understanding of color [24].

When processing color images, if the three components of R, G, and B are processed separately, their correlation will be destroyed, resulting in the problem of color deviation. HSI color model can effectively solve this problem: first, convert the RGB image into the image represented by HSI color space, then keep the chroma component unchanged, only enhance the brightness component, and finally convert it into the image represented by RGB color space [25]. The flow chart of this process is shown in Figure 2.

3.2. Retinex Algorithm. In the related research of image processing, image enhancement is a very popular research field at present. Because the existing image enhancement technology has not formed a unified theoretical method, there are many enhancement methods and research results, especially the image enhancement method based on Retinex theory. In 1964, the Retinex theoretical model was proposed

by Edwin hland. Because Retinex is an abbreviation for the combination of retina and cortex, it is also called retina cerebral cortex theory. Retinex theoretical model explains the adjustment mode of the human visual system to the color and brightness of external objects and the color constancy of objects under different lighting conditions. According to Retinex theory, the color of the object seen by our eyes is actually the effect of the interaction between the incident light on its surface and the object. It has little to do with the spectral properties of the incident light received by our eyes but is closely related to the reflection characteristics of the object itself.

Since the advent of the Retinex theoretical model, researchers in different periods have proposed many different versions of Retinex algorithms on the basis of it. Which can be roughly divided into the following categories: random walk Retinex algorithm, homomorphic filtering Retinex algorithm, Poisson equation method, Retinex algorithm based on iterative operation, and center/surround Retinex algorithm. The classification of the Retinex algorithm is mainly based on different illumination image estimation principles, so the overall process framework of the Retinex algorithm can be represented in Figure 3.

Assuming that the starting point and ending point of the random path generated in an image are A and B, respectively, and the number of pixels on this path is n, and the gray values of each point are $d_1, d_2, d_3, \dots, d_n$, then the relative light dark relationship between A and B is expressed as formulas (1) and (2):

$$\frac{B}{A} = \log \left[T \left(\frac{d_2}{d_1} \right) \times T \left(\frac{d_3}{d_2} \right) \times T \left(\frac{d_4}{d_3} \right) \times \dots \times T \left(\frac{d_n}{d_{n-1}} \right) \right], \quad (1)$$

$$T(x) = \begin{cases} x & x \leq 1, \\ 1 & x > 1, \end{cases} \quad (2)$$

where $T(x)$ is a threshold function; if the neighborhood pixel value of the current image cable is within the threshold range, it is considered that the light dark relationship between the two pixels has not changed.

The Retinex algorithm has the following advantages: on the whole, the brightness of the image is less affected by the illumination; for extremely bright or dark images, it can

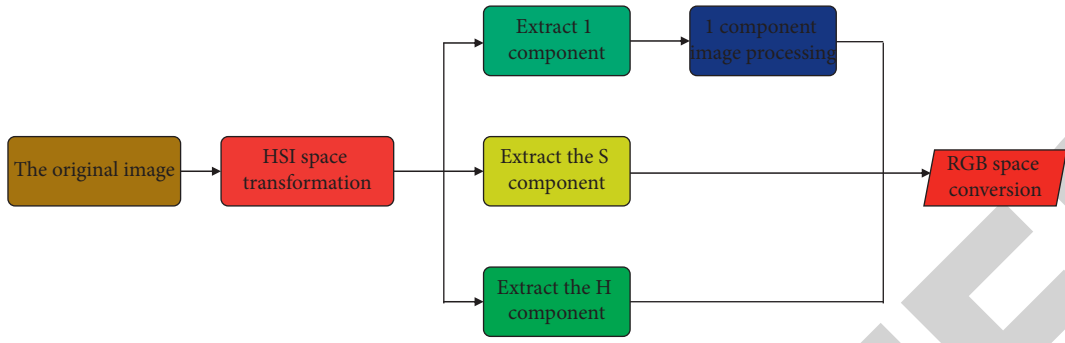


FIGURE 2: Flow chart of color image processing based on monochrome technology.

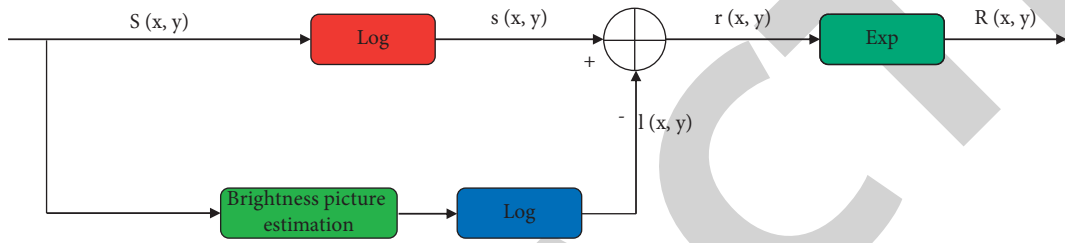


FIGURE 3: Overall block diagram of Retinex algorithm.

eliminate the influence of lighting conditions, improve image contrast and improve image color distortion to a certain extent.

3.3. Improved MSR Image Enhancement Algorithm. For color image enhancement, this paper proposes an improved MSR image enhancement method based on the MSR algorithm, and its specific process is shown in Figure 4. Because the traditional center/surround Retinex algorithm enhances the three color channels of R , G , and B , respectively, resulting in obvious color deviation in the enhanced synthetic RGB image, this algorithm first converts the input RGB image into the image represented by HSI color space, and separately enhances its brightness component I ; nighttime images usually contain a large number of dark connected areas or local highlight areas. In this paper, an adaptive adjustment function is proposed to nonlinearly adjust the brightness component I of the image, improve the brightness of the dark area of the image, suppress the “halo” phenomenon that may be caused by the local highlight area, and compress its dynamic range; in addition, for the local detail enhancement of night color image, the bilateral filtering of three Gaussian model with neuron receptive field is introduced into the illuminance image estimation of MSR algorithm. The model can effectively maintain the edge characteristics of the image while enhancing the image contrast; finally, the color information of the enhanced RGB image is restored, and the final result image is output.

For the RGB image enhanced by the brightness component I , in order to recover the color information of the image, the R' , G' , and B' component values of the resulting image can be calculated by using the proportional values of the R , G , and B components of the original image and the brightness component. Assuming the enhanced luminance component, the mathematical expression is as follows fd3:

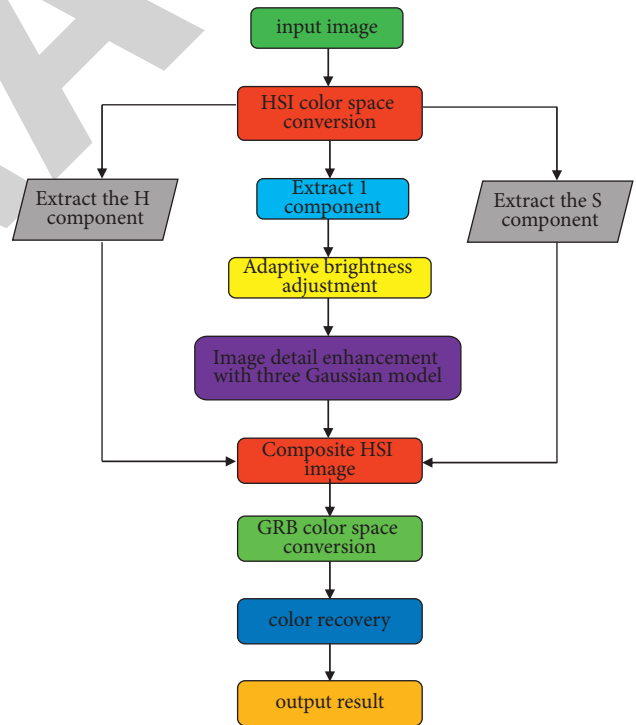


FIGURE 4: Flow chart of improved MSR algorithm.

$$R' = \frac{R}{I} * I', G' = \frac{G}{I} * I', B' = \frac{B}{I} * I'. \quad (3)$$

Equation (3) can be obtained from equation (2):

$$\frac{R'}{R} = \frac{G'}{G} = \frac{B'}{B} = \frac{I'}{I}, \quad (4)$$

TABLE 1: Comparison of objective evaluation criteria of various algorithms in example image 1.

	Mean value	Standard deviation	Information entropy	Average gradient
Original image	20.2462	12.5662	5.5247	2.7235
SSR algorithm	169.6584	70.1196	7.5582	33.3834
MSR algorithm	26.6572	32.7919	5.8444	12.4666
MSRCR algorithm	169.0295	25.8485	6.5276	6.8076
Retinex algorithm for bilateral filtering	71.7219	34.8577	7.0068	3.7907
Algorithm in this paper	88.9657	39.4950	7.1387	7.1070

TABLE 2: Comparison of objective evaluation criteria of each algorithm of example image 2.

	Mean value	Standard deviation	Information entropy	Average gradient
Original image	32.8601	36.6571	6.1261	4.2972
SSR algorithm	143.8501	88.4418	7.4842	19.8124
MSR algorithm	20.8233	46.9176	4.3890	7.8242
MSRCR algorithm	158.3715	19.3082	6.1948	5.0900
Retinex algorithm for bilateral filtering	80.7702	38.2703	7.1300	5.5405
Algorithm in this paper	103.3802	39.8945	7.2301	7.4264

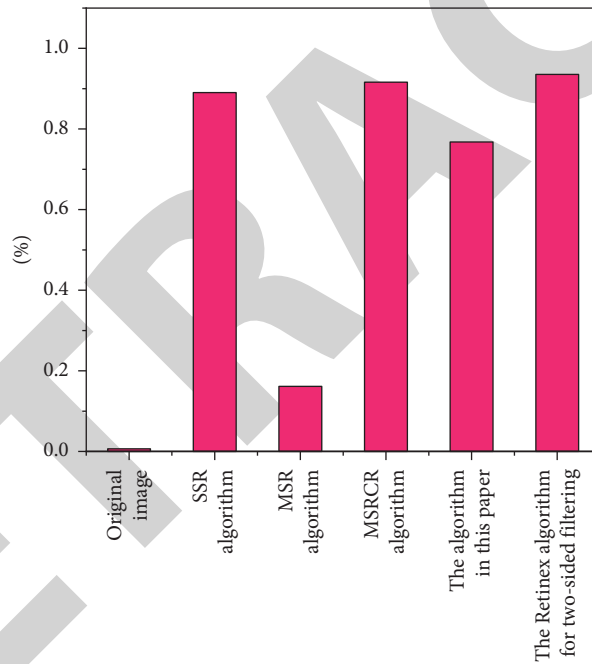


FIGURE 5: Average enhancement rate of the image by the algorithm.

It can be seen that the R , G , and B color components of the original image and the enhanced image in the RGB color space are directly proportional because after image enhancement for the brightness image of the original image, the pixels corresponding to the R , G , and B color components have the same color, but the brightness is different. This method can overcome the problem of color distortion in the Retinex algorithm.

4. Result Analysis

4.1. Performance Verification of Improved MSR Algorithm. In order to verify the enhancement effect of this algorithm when applied to night color image enhancement, SSR algorithm, MSR algorithm, MSRCR algorithm, bilateral

filtering Retinex algorithm, and this algorithm are compared. The original image selects the color image with a local light source or a large number of dark areas. The results are shown in Tables 1 and 2 and Figure 5.

From the perspective of objective parameter evaluation, the average value, standard deviation, information entropy, and average gradient of example images 1 and 2 are improved by about 70%. Although individual parameters are lower than other algorithm parameters, on the whole, each parameter has been comprehensively improved. This algorithm not only enhances the brightness and contrast of the image but also maintains the detailed edge information of the image and the color characteristics of the object itself. The average enhancement rate is the highest among various algorithms, up to 95%.

5. Conclusion

In this paper, an improved MSR image enhancement algorithm is proposed. For the night color image, especially the night image with a local light source or a large number of dark connected areas, an adaptive brightness adjustment function is proposed according to the brightness and darkness of the image so that the details of the dark area and highlight area of the image can be significantly enhanced. In addition, this paper introduces the bilateral filtering with three Gaussian model of retinal neuron receptive field into the illuminance image estimation of MSR algorithm, which enhances the brightness and contrast of the image, maintains the edge detail information of the image, optimizes the defects of the combination of traditional bilateral filtering and Retinex algorithm, and the color is also well restored, which makes the monitoring image easier to identify and more conducive to a criminal investigation. It also lays a foundation for the followup image processing work.

Although the algorithm based on Retinex can improve the brightness of the image one by one, the image quality of the other four algorithms based on Retinex can still be improved better:

- (1) In the process of image enhancement based on computer vision virtual reality-based flat image color enhancement algorithm, it is necessary to separate the detail layer image and the base layer image from the brightness image, and then enhance the two layers of images. Reconstruction is performed to obtain an enhanced luminance image, and the computation speed is reduced in the process.
- (2) The enhancement effect of the improved and reconstructed plane image color enhancement algorithm for images with uneven brightness distribution needs to be further strengthened, and the enhancement applicability of the algorithm to most images needs further research and exploration.

Data Availability

The data used to support the findings of this study are available from the corresponding author upon request.

Conflicts of Interest

The authors declare that there are no conflicts of interest.

Acknowledgments

The study was supported by Heilongjiang Province Education Department Scientific Research Project (Project nos. 135309465, 135409224).

References

- [1] T. H. Park and I. K. Eom, "Sand-dust image enhancement using successive color balance with coincident chromatic histogram," *IEEE Access*, vol. 9, no. 99, p. 1, 2021.
- [2] J. Feng and S. Qi, "Motion deblurring in image color enhancement by wgan," *International Journal of Optics*, vol. 2020, no. 6, pp. 1–15, Article ID 1295028, 2020.
- [3] T. Sato, "Txi: texture and color enhancement imaging for endoscopic image enhancement," *Journal of Healthcare Engineering*, vol. 2021, no. 9, pp. 1–11, Article ID 5518948, 2021.
- [4] K. Srinivas, A. K. Bhandari, and A. Singh, "Low-contrast image enhancement using spatial contextual similarity histogram computation and color reconstruction," *Journal of the Franklin Institute*, vol. 357, no. 18, pp. 13941–13963, 2020.
- [5] X. Shen, X. Zhang, and Y. Wang, "Color enhancement algorithm based on daltonization and image fusion for improving the color visibility to color vision deficiencies and normal trichromats," *Journal of Electronic Imaging*, vol. 29, no. 5, pp. 53004–53011, 2020.
- [6] C. Li, S. Anwar, J. Hou, R. Cong, C. Guo, and W. Ren, "Underwater image enhancement via medium transmission-guided multi-color space embedding," *IEEE Transactions on Image Processing*, vol. 30, no. 99, pp. 4985–5000, 2021.
- [7] S. Bianco, C. Cusano, F. Piccoli, and R. Schettini, "Personalized image enhancement using neural spline color transforms," *IEEE Transactions on Image Processing*, vol. 29, no. 99, pp. 6223–6236, 2020.
- [8] D. Li, J. Bao, S. Yuan, H. Wang, L. WangWang, and W. Liu, "Image enhancement algorithm based on depth difference and illumination adjustment," *Scientific Programming*, vol. 2021, no. 1, pp. 1–10, Article ID 6612471, 2021.
- [9] C. Peng, L. Cai, X. Huang, J. Xu, Z. Fu, and X. Li, "Cnn-based suppression of false contour and color distortion in bit-depth enhancement," *Sensors*, vol. 21, no. 2, pp. 416–421, 2021.
- [10] Z. Mi, Y. Li, Y. Wang, and X. Fu, "Multi-purpose oriented real-world underwater image enhancement," *IEEE Access*, vol. 8, no. 99, pp. 112957–112968, 2020.
- [11] W. Huang, Y. Zhu, and R. Huang, "Low light image enhancement network with attention mechanism and retinex model," *IEEE Access*, vol. 8, no. 99, p. 1, 2020.
- [12] F. Wang, B. Zhang, C. Zhang, W. Yan, Z. Zhao, and M. Wang, "Low-light image joint enhancement optimization algorithm based on frame accumulation and multi-scale retinex," *Ad Hoc Networks*, vol. 113, no. 4, Article ID 102398, 2021.
- [13] B. Wang, R. An, T. Jiang, F. Xing, and F. Ju, "Image spectral resolution enhancement for mapping native plant species in a typical area of the three-river headwaters region, China," *Remote Sensing*, vol. 12, no. 19, p. 3146, 2020.
- [14] B. H. Kim, C. Bohak, K. H. Kwon, and Y. K. Min, "Cross fusion based low dynamic and saturated image enhancement for infrared search and tracking systems," *IEEE Access*, vol. 8, no. 99, p. 1, 2020.
- [15] Z. A. Ameen, "Contrast enhancement of digital images using an improved type-ii fuzzy set-based algorithm," *Traitement du Signal*, vol. 38, no. 1, pp. 39–50, 2021.
- [16] F. Fang, T. Wang, Y. Wang, T. Zeng, and G. Zhang, "Variational single image dehazing for enhanced visualization," *IEEE Transactions on Multimedia*, vol. 22, no. 10, pp. 2537–2550, 2020.
- [17] M. A. H. Arellano, H. P. Barreto, and I. T. Villalobos, "Visible-nir image fusion based on top-hat transform," *IEEE Transactions on Image Processing*, vol. 30, no. 99, pp. 4962–4972, 2021.
- [18] H. W. Jang and Y. J. Jung, "Deep color transfer for color-plus-mono dual cameras," *Sensors*, vol. 20, no. 9, p. 2743, 2020.
- [19] X. Cao, S. Rong, Y. Liu, T. Li, Q. Wang, and B. He, "Nuicnet: non-uniform illumination correction for underwater image

Research Article

Analysis of China's Regional Economic Competitiveness, Regionalization, and Spatial Aggregation Characteristics Based on Density Clustering Algorithm

Jinglin He ¹ and Rixing Liu²

¹College of Economics and Management, Hubei University of Automotive Technology, Shiyan, Hubei 442002, China

²Western Jiangxi Regional Economic and Social Development Research Center of Yichun University, Yichun University, Yichun, Jiangxi 336000, China

Correspondence should be addressed to Jinglin He; 20190013@huat.edu.cn

Received 25 May 2022; Revised 16 June 2022; Accepted 27 June 2022; Published 3 August 2022

Academic Editor: Kai Guo

Copyright © 2022 Jinglin He and Rixing Liu. This is an open access article distributed under the Creative Commons Attribution License, which permits unrestricted use, distribution, and reproduction in any medium, provided the original work is properly cited.

Regional development disparities, especially in developing countries, have traditionally been one of the central issues of empirical research in regional economics. However, this rapid change is accompanied by profound changes in the spatial distribution of economic activities in China, the formation of regional economic “blocks,” the widening of regional disparities, and the geographical concentration of economic growth efficiency are important issues highlighted in this change. Therefore, it is important to explore the spatial clustering characteristics and patterns of regional economic growth to provide a scientific basis for relevant government departments to formulate reasonable regional development strategies and promote the balanced and stable development of economic growth. Clustering analysis is an important research topic in the field of data mining, which is used to discover unknown object classes in large-scale data sets. This paper proposes a density-clustering algorithm based on the regional economic competitiveness of China and analyzes its spatial aggregation characteristics. From the perspective of spatial structure theory, economic development is a dynamic process, and to optimize the spatial pattern of China's regional economic development and improve the efficiency of economic interaction between regions, it is necessary to fully exploit the diffusion and trickle-down effects of important growth poles in the region to the surrounding areas. The experimental results show that the error rate of KSNM is very small, and the error rate of K-means and PSO has increased to a certain extent. Therefore, it can be obtained that the density-clustering algorithm based on the regional economic competitiveness zoning method in China can find out the correct clustering results without the given clustering individual cases. Thus, it is important to grasp the current situation of regional economic agglomeration and reveal the driving factors of agglomeration formation to promote the coordinated development of regional economy and guide the spatial layout of economic development.

1. Introduction

Regional economic activities will produce agglomeration within a certain range due to the flow of production factors; otherwise, they will be increasingly fragmented [1]. In a market economy, a country, an industry, and a region face a competitive environment [2]. The country has to participate in competition, the industry has to participate in competition, and the region also has to participate in competition [3]. The development of market economy system and

industrial structure adjustment is uneven, while the eastern region is gradually converging with the international standards, the central and western regions are slow in adjusting their ownership structure and industrial structure [4]. When decomposing the composition and sources of regional differences, we only examined the impact of the three major zones and interprovincial differences on the overall regional differences in China, but failed to refine them to the level of intraprovincial differences, ignoring the unevenness of regional economies within provinces [5].

Economic growth refers to the sustainable growth of national wealth or social wealth, which is generally expressed as the growth of gross domestic product (GDP) [6]. To solve the problem of regional equity, it is necessary to accelerate the pace of economic development while needing to simultaneously take into account the coordinated relationship between developed and less-developed regions [7]. The earlier hierarchical and mesh database systems have failed to meet the market demand, and the research and development of relational database systems have led to a new era of database systems [8]. At the same time, the development of data modeling tools and indexing and access methods have further driven the progress of database systems [9]. Under the impetus of knowledge-based economy, especially in the context of the bottleneck of global manufacturing development, the world economy, especially developing countries and regional economies, needs to change the economic growth mode and upgrade the industrial structure [10]. The density-clustering algorithm makes it easier to understand why things happen and find out the difference between whether (good and bad) history repeats itself [11]. Because trends are now changing very fast, automatic analysis and specialized algorithms that identify trends, identify anomalies, and predict the future also make the difference between winning and just competing [12].

Two significant features of the globalized world economy are the global flow of resources, and the global market economy. When external disturbances occur, Chinese provinces differ in their industrial structure, economic openness, and flexibility in adjusting their economic activities due to the differences [13]. Provinces face different combinations of unemployment-inflationary pressures and have widely varying states of economic performance [14]. Factors such as slow economic development and unbalanced regional economic development have seriously constrained China's economic construction [15]. Thus, it is necessary to adhere to the principle of practical approach, analyze in depth the historical process and current situation of economic development of each region, and implement the principle of adapting to the time and place. Therefore, it is important for governments to consider how to improve the competitiveness of national regions, create regional advantages, and strengthen their attractiveness to global resources. Due to the long-standing deep-seated structural contradictions and the unconventional mode of economic growth, institutional, institutional, and legal barriers to land management still exist. The formulation of policies to enhance the competitiveness of national regions has become an important part of the strategies and policy systems of regional governments.

The innovative points of this paper are as follows:

- (1) The article applies competitiveness zoning and spatial aggregation characteristics to regional economic analysis, which intuitively and quantitatively realizes regional economic analysis in a spatial manner.
- (2) In view of the deficiency that the density-clustering algorithm relies on the decision map generated in the

algorithm when the clustering centers are selected, which is difficult to accurately determine the clustering centers, the spatial aggregation feature analysis is proposed.

- (3) The dynamics of the spatial clustering characteristics of regional economic growth is explored and applied to a multiregional and multiscale empirical study.

The research framework of this paper contains five major parts, which are organized as follows:

The first part of this paper introduces the research background and significance, and then introduces the main work of this paper. The second part imports the work related to regional economic competitiveness zoning and spatial aggregation characteristics of China, and density-clustering algorithm. In the third part, we present an overview of economic growth efficiency measurement methods and regional economic competitiveness zoning methods so that the readers of this paper can have a more comprehensive understanding of China's regional economic competitiveness zoning methods based on density-clustering algorithm. The fourth part is the core of the thesis, which completes the description of the spatial aggregation analysis based on density-clustering algorithm and spatial aggregation feature analysis. The last part of the paper is the summary of the whole work.

2. Related Work

2.1. Regional Economic Competitiveness Division and Spatial Agglomeration Characteristics in China. The research on regional development disparities in China consists of two aspects: first, an empirical study on the change of the East–West gap, mainly using economic statistical indicators to examine the current situation and dynamic trajectory of the gap between regions in China; second, an explanation of the causes of the gap formation. On the one hand, regional economic growth depends on regional human capital, natural resources, capital stock, and the level of regional science and technology and the speed of technological progress. On the other hand, regional economic growth is closely related to regional industrial agglomeration. By analyzing the spatial pattern of regional economic growth and spatial agglomeration results in different time periods, we analyze the spatial agglomeration pattern of regional economic growth, and then provide theoretical basis and important support for the spatial restructuring of economic growth and policy formulation in the country and five regions.

Deng et al. started to apply a new approach to decompose the composition and sources of regional differences in order to reveal some of the main factors that cause the variation of regional differences [16]. Based on the understanding that the technology spillover effect decreases gradually with geographical distance and thus technology spillover is localized, Chen et al. theoretically concluded that spatial agglomeration drives regional economic growth through technology spillover [17]. Obomeghie and Ugbohmhe decomposed the Gini coefficient to analyze the differences in the income of the population between rural areas [18]. A study on the dynamics of spatial agglomeration

characteristics and regional comparisons of regional economic growth in multiple study areas was conducted to explain the spatial differences in regional economic growth in China. Goli and Joksimovi used spatial density to represent agglomeration and argued that agglomeration affects labor productivity in US states through three ways: transportation costs, externalities from knowledge spillovers, and pecuniary externalities [19]. The empirical results found that employment density and labor productivity and the Bai et al. used a weighted coefficient of variation to decompose the industrial or sectoral composition of regional differences [20].

Based on this reviewing of the theoretical and empirical studies on regional disparities and China's regional disparities under the framework of economic growth theory, spatial economics, and the combination of both, the characteristics, progress, and further issues to be addressed in these studies are analyzed and summarized.

2.2. Density-Clustering Algorithm. We adopt different management strategies and methods for regional economies at different stages of development. We can correctly grasp the law of China's economic development, identify the weak points of economic development and the unbalanced areas of economic development, and give macroscopic inclined policy regulation to promote China's rapid economic development. The current domestic research focuses more on the difference of development level and less on the difference of regional economic development status. Density-clustering algorithm is to solve this problem, and the maturity of database technology and the development of artificial intelligence technology provides the basis for the research of density-clustering algorithm, and the researchers from various disciplines came together to study the density-clustering algorithm technology.

Chen et al. proposed a hybrid genetic clustering algorithm by using K-means operator instead of crossover operator in genetic operator [21]. Kumar and Kumar introduced the improved idea of having the distance from the sample point of density maximum to the sample point of density minimum as the truncated reference value [22]. Ma et al. adopted the floating point encoding of clustering center and designed the floating-point crossover and variation algorithm [23]. Gungor and Ozmen obtained the I-DBSCAN adaptive clustering algorithm with the help of two main factors in discriminating the clustering results, the trend of the number of clusters and the trend of the number of noise points [24]. Lu and Zhu proposed a K-means clustering algorithm using particle swarm optimization algorithm. It improves the global search capability of K-means and also has local search capability [25].

Density clustering algorithm brings together researchers from different fields, especially scholars and engineers in database, artificial intelligence, mathematical statistics, visualization, parallel computing, etc. Therefore, density-clustering algorithms are a broad interdisciplinary discipline involving various technologies such as artificial intelligence techniques, statistical techniques, and database techniques.

3. Regional Economic Competitiveness Division Method of China Based on Density-Clustering Algorithm

3.1. Measurement Method of Economic Growth Efficiency. For the country, the relational database formed by the data information accumulated in its daily business is an important data source for intelligence mining, so it is especially important to choose a good clustering algorithm to get a good clustering effect and find out the hidden valuable information [26]. As a result, the country is facing a series of economic and social development problems, and the issue of regional economic disparities in China has thus increasingly become one of the central issues of empirical research in regional economics [27]. Regional economic disparities are mainly measured by comparing GDP or national income in a per capita sense across geographic regions [28]. Division of labor is the source of economic agglomeration, while externalities and increasing payoffs have to be the link between the role of division of labor and economic agglomeration. Based on this, the path of economic growth efficiency agglomeration formation can be summarized in Figure 1.

First, the frontier surface of production is derived by data envelopment analysis. Since the results of spatial exploratory data analysis of the regional economy are related to the scale of the regional study unit, the spatial agglomeration of regional economic growth will be influenced by both spatial and temporal scales [29]. Therefore, its simulation process is based on random numbers, which are generated mainly by using random sampling data tables, by using physical methods, and by using data methods to generate pseudorandom numbers. Column j in matrix U is sample X_j , which is relative to the membership function of C subset, so the hard partition space of X is

$$M_{be} = \{U \in R^{cn} | \mu_{ik} \in \{0, 1\}, \forall i, k; \forall k\}. \quad (1)$$

Therefore, a country should pay attention to study the essential characteristics of these four different stages and formulate corresponding development countermeasures in order to maintain a sustainable competitive advantage. Each productivity change requires solving four linear programs including two current environmental technical efficiencies and two mixed environmental technical efficiencies. The spatial weight matrix is introduced to estimate the parameters of the regional spatiotemporal process model more effectively. The objective is to search for the cluster centers with the best clustering partitioning effect, even though the criterion function is minimal, so the fitness function should be taken as $1/E$, i.e. the fitness function:

$$f(x) = \frac{1}{E} = \frac{1}{\sum_{i=1}^K \sum_{x \in C_i} |x - c_i|^2}. \quad (2)$$

Economic growth and regional disparity, simultaneously as products in development, are interdependent and mutually transformed in the presence of a critical point of efficiency agglomeration. However, in

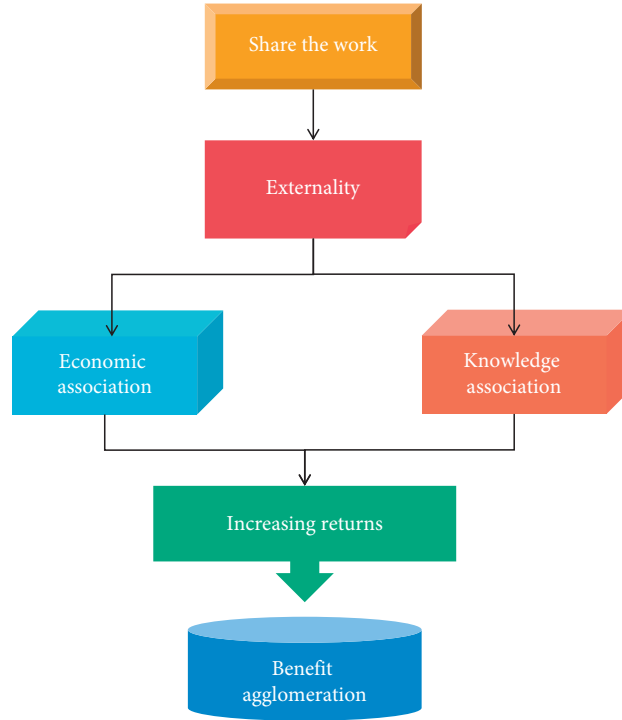


FIGURE 1: The formation path of long-term economic efficiency agglomeration.

order for the transformation to be successfully completed, attention must be paid to the satisfaction of the corresponding transformation conditions. Therefore, the impact and mechanism of efficiency agglomeration on economic growth and regional disparity can be shown in Figure 2.

Second, technical efficiency and productivity are measured by directional distance functions. Monte Carlo simulation analysis is used to test the local spatial autocorrelation indicators and obtain the empirical pseudosignificance level. Thus, it is determined whether the observations of a spatial target are arranged in the overall region with significant local correlation, and the specific pattern of regional economic growth spatial agglomeration is analyzed. In order to facilitate a convenient and rational analysis, the various categories of the country can be classified into several strategic business units according to their strategic relevance. Classification is built by providing a training data set with labels, acquiring data features through pretraining, and then using the model to predict data categories. To measure the quality of the clusters, an error sum of squares reference function is used, defined as follows:

$$E = \sum_{i=1}^k \sum_{x \in C_i} \|x - \bar{x}_i\|^2. \quad (3)$$

\bar{x}_i —The average value of the cluster, that is, the cluster center.

Since the regional economic information and analysis model is based on polygons such as counties and cities, provinces and countries, we have to try to generate the

spatial weight matrix of spatial polygons. The prefecture-level cities are selected as the basic research unit, with moderate geographical area and large enough cities, especially the central cities are mostly large- and medium-sized cities, which can become the growth poles with strong ability to gather and diffuse economic factors. If the variance of the cost function is negative, the original center of mass is replaced by the noncentral center of mass at the current location; otherwise, the center of mass remains unchanged. The degree of adaptation is appropriately extended by the simulated annealing algorithm, and the degree of adaptation stretching method is as follows:

$$f_i = \frac{e^{f_i/T}}{\sum_{i=1}^M e^{f_i/T}}. \quad (4)$$

f_i —Adaptation of the i th individual.

However, not all methods can satisfy the monotonicity requirement due to the different types of clustering methods chosen. In this paper, the correlation coefficient is calculated based on the Euclidean distance using the variational method with the following recursive expressions:

$$D_{kr}^2 = \frac{1+\beta}{2} [D_{kp}^2 + D_{kq}^2] + \beta D_{pq}, G_r = \{G_r, G_q\}. \quad (5)$$

Finally, the further decomposition of ML index can obtain the situation of technological progress, technical efficiency, and scale effect. According to the factors influencing regional economic spatial agglomeration, combined with the existing research results, it can be

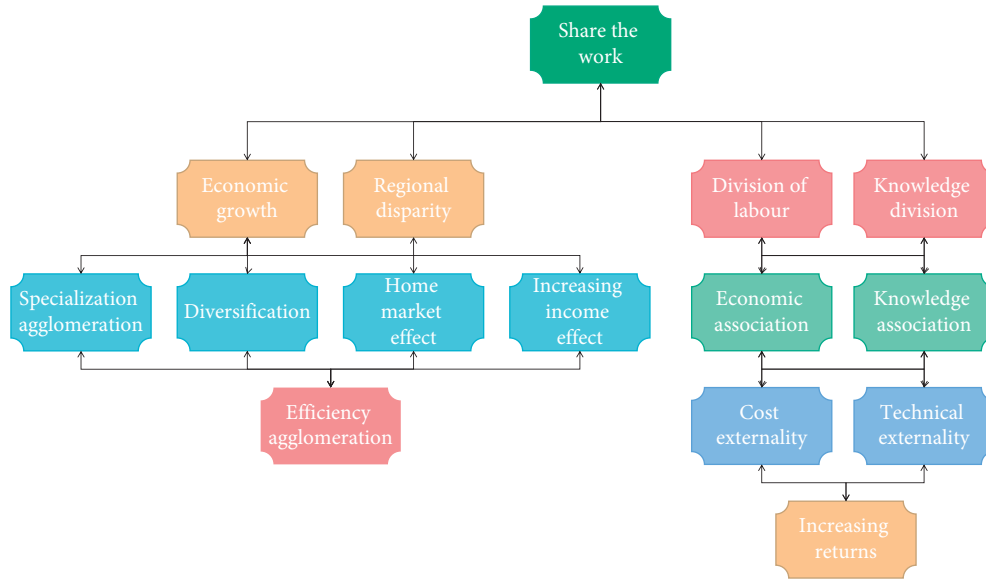


FIGURE 2: Origin, formation, and influence of efficiency agglomeration.

seen that the index system is mainly constructed from several aspects, such as factor endowment, human resources, transportation cost, knowledge, and capital. These indicators mainly reflect the economic correlation between a certain region and other regions, and the strength of the connection between the region and other regions. The distance-based spatial weight matrix assumes that the strength of spatial interactions is determined by the distance between regions in the center of mass or the distance between the locations of regional administrative centers. Exploratory spatial data analysis is often the first step in spatial analysis. It is a method that integrates GIS, graphics, and statistics to describe the spatial distribution of study objects and geographic units, thereby revealing spatial connections, agglomerative properties, identifying singular observations, and discovering other consistent features.

3.2. Regional Economic Competitiveness Zoning Method. The indicators of the delineated residential, commercial, and industrial functional areas are consistent with the principles of functional area delineation and can be used as an object for evaluating the level of intensive use within Chinese cities [30]. Different data types of data sets require different types of clustering algorithms for calculation. Density-clustering algorithms usually involve more complex mathematical methods and information technology, and in order to facilitate users to understand and use such techniques, it is necessary to instruct the operation, guide the mining, and express the results, etc., figuratively with the help of graphics, images, animations, etc., otherwise, it is difficult to promote the popularization of density-clustering algorithms. Therefore, it is not only necessary to study numerical data but also requires the method of cluster analysis to be adapted to the change of data types. The natural conditions mainly consider the slope and topographic relief in the region, while the

natural resources mainly consider the distribution of water resources and mineral resources in the region. The flow chart of the locational directional model is shown in Figure 3 below.

First, statistical data can be spatialized through spatial analysis methods. The project goals and requirements are understood from a business perspective, converted into a problem definition of a density-clustering algorithm, and an initial plan to reach the goals is designed. Commonly used criterion functions are the error sum-of-squares criterion and the weighted average sum-of-squares distance criterion. Call the whole C fuzzy division space of X . If it contains degenerate division, then it is called degenerate C fuzzy division space. Let

$$V = i \frac{\sum_{j=1}^n (u_{ij})^m x_j}{\sum_{j=1}^n (u_{ij})^m}. \quad (6)$$

In the division of functional areas, there are three types of functional areas: residential, commercial, and industrial, so it is necessary to classify the land-use types of residential, commercial, and industrial land. We use data range normalization here. The method is to first find the range of each variable and then calculate the mean of each variable:

$$X = \frac{X_{ij}' \overline{X_j'}}{\text{mix}\{X_{ij}'\} - \text{mix}\{X_j'\}}. \quad (7)$$

The initial point has a large influence on it, and it is even difficult to achieve the global optimum, furthermore, it can only dispose of the clustering cases where hyperspherical cluster structures exist, and it does not have the ability to identify the clustering structures of arbitrary shapes. Therefore, in the actual cluster analysis, different types of attributes are combined in the same difference degree matrix for calculation. Data

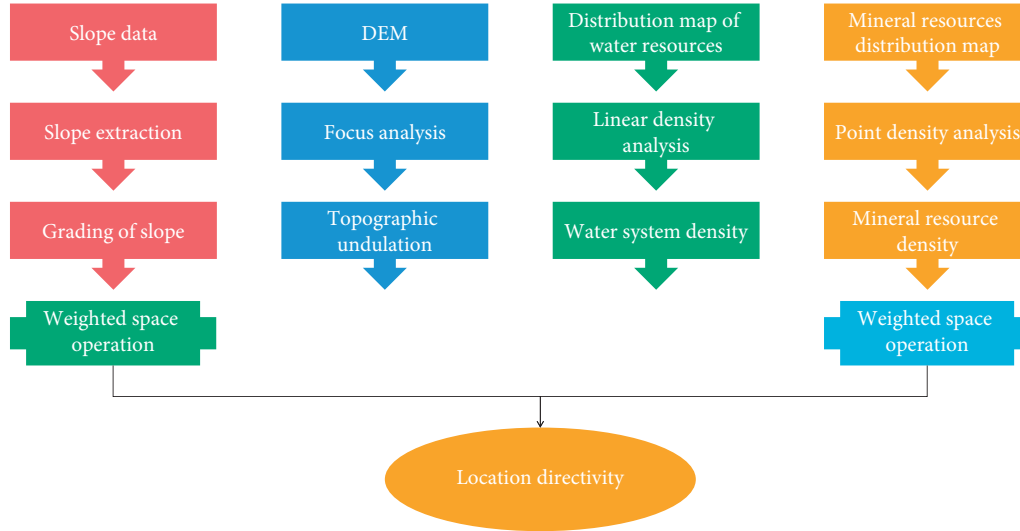


FIGURE 3: Flow chart of location directivity model.

preprocessing techniques as a step in knowledge discovery can improve the quality of data, and thus can enhance the accuracy and quality of the density clustering algorithm process. When the absolute value of the data is compared with the specified threshold, the soft threshold noise is removed because the part less than or equal to the threshold is zero and the part greater than or equal to the threshold is the difference from the specified threshold, with the following equation:

$$\omega\lambda = \begin{cases} [\text{sign}(\omega)](|\omega| - \lambda), & |\omega| \geq \lambda, \\ 0, & |\omega| < \lambda. \end{cases} \quad (8)$$

Second, overlay analysis is applied to reflect the combined effects of various factors on economic spatial agglomeration from a spatial perspective and to explain the occurrence of spatial agglomeration. The initial raw data are constructed into a data set that is eventually suitable for processing by modeling tools. Urban single residential land and urban mixed residential land are all residential type land, while commercial land, financial and insurance land, supplementary business and financial, restaurant and hotel land, and supplementary wholesale and retail land are commercial type land. Therefore, it is necessary to preprocess the data before density clustering and transform the data into suitable data for mining. Assume a mixed data $X(k)$, which consists of m dimensional observation signal vectors:

$$x(k) = [x_1(k), x_2(k), \dots, x_m(k)]^T. \quad (9)$$

A similarity measure of the gaps is defined for the actual problem, and then certain objects are assigned to belong to a certain cluster according to the nearest neighbor rule. The results of economic region classification are shown in Table 1.

Finally, the impact of various factors on locational directionality is considered, and then the relative

magnitude of the factors' influence is simulated. The model is evaluated more thoroughly and each step of constructing the model is checked to confirm whether it actually achieves the intended business purpose. The commonly used Hemming distance between fuzzy sets, let A and B be two fuzzy subsets of $U = \{u_1, u_2, \dots, u_n\}$, is found as follows:

$$D(A, B) = \frac{1}{n} \sum_{i=1}^n |\mu_A(u_i) - \mu_B(u_i)|. \quad (10)$$

Since clustering is the combination of objects for classification to maximize the separability of categories, the clustering criterion should be a function reflecting the similarity or dissimilarity between categories. It seeks the optimal combination and relative position of various economic objects in space from their clustering degree in space and their interaction relationship, and examines the dynamic change law of them in interaction over time. Spatial correlation is multidimensional, so when measuring spatial correlation, it is necessary to judge the expression of geographic space, indicating the neighboring relationship of each unit, thus introducing the spatial weight matrix to quantify the position of each unit as a prerequisite for spatial measurement analysis. The contradiction between the demand for differentiated macrocontrol policies and the uniform supply of central macrocontrol policies is more prominent in each province, and it is necessary to implement differentiated macrocontrol.

4. Analysis of Spatial Aggregation Characteristics Based on Density-Clustering Algorithm

4.1. Analysis of Density-Clustering Algorithm. The density-clustering algorithm has the advantage of automatically discovering the class cluster centers of dataset samples and can satisfy the efficient clustering of arbitrarily shaped

TABLE 1: Division results of economic regions.

Name of economic zone	North economic zone	Yangtze river basin economic zone	Southeast economic zone	Southwest corner economic zone	Northwest economic region
Provinces included	Beijing, Tianjin, Hebei, ...	Shanghai, Jiangsu, Anhui, ...	Guangdong, Guangxi, Hainan, ...	Chongqing, Sichuan, Yunnan, ...	Gansu, Ningxia, Xinjiang, ...
Number of provinces	10	7	5	4	4

dataset samples. Spatial clustering refers to the study area's economy exhibiting specific spatial patterns, and the economic effects in this paper emphasize the externalities that clustered areas have on the economic development of other regions. The density-clustering algorithm has a high density in the center, surrounded by neighbors whose densities are below it, and the density of surrounding data points continuously decreases. The error rates of KSNM, K-means, and PSO algorithms are compared using the public data set iris, and the results are shown in Figures 4 and 5.

The error rate of KSNM is very small, and the error rate of K-means and PSO has increased to a certain extent. Therefore, it can be concluded that the density-clustering algorithm is based on China's regional economic competitiveness zoning method can find the correct clustering results without the given clustering individual cases.

First, the clustering centers are established based on the present-day characteristics of the class centers. This can be determined by regression, inference-based tools using Bayesian formalism, or decision tree induction. Gini coefficient calculations by population groups are performed on sample data to examine the status of per capita income differences between and within groups, and also to examine the degree of per capita income crossover between groups. The purpose is to analyze the neighboring spatial clustering relationships, spatial instability, and spatial structural framework of the values taken by a certain spatial object, especially when the global correlation analysis is not able to detect the spatial distribution patterns within the region. This type of clustering is often called minimum variance partitioning, and it is suitable for situations where the classes of objects are dense and similar in number, while the objects between the different classes are clearly separated. For each object that constitutes a cluster, there must be no less than a given value, that is, the density of its domain must be no less than a certain threshold. The clustering continues as long as the number of density samples in the adjacent regions exceeds a certain threshold value. The interclass priority and intraclass priority can be obtained using the method of authority value and hub value used by hits algorithm. KSNM and SNN, respectively, are calculated for the above three data sets to obtain the values of J_c . Table 2 shows the results of comparing the convergence ability of KSNM with SNN.

Second, the other data points are drawn to the class of data points with the smallest proximity and higher density than their current class. The smoothed data are

obtained by examining the "near neighbors" of the data, and the smoothed values include box mean, box median, and box boundary, etc. The larger the box width, the better the smoothing effect. Based on the results, the spatial distribution of the coordination between economic development and resources and environment in each region of China is analyzed and based on this, and the relevant influencing factors of economic growth efficiency are proposed from the perspective of spatial economics, and the strength and mode of action of these factors are further examined. That is, for each sample in a given cluster, at least a certain number of samples must be included in a given range of regions. The nodes are ranked using the authority values to generate intracluster priorities and intercluster priorities, which are analyzed separately. Local spatial correlation analysis can effectively detect the spatial differences caused by spatial correlation, determine the spatial hotspot areas, or high incidence areas of spatial object attribute values, and thus make up for the shortcomings of global spatial correlation analysis.

Finally, the decision diagram of sample distance relative to sample density is established to achieve the effect of presenting the class cluster center of arbitrary dimensional data set through two-dimensional plane, thus completing the clustering analysis of arbitrary dimensional data. The data attributes are divided into intervals by equal distance, and then the data falling within the intervals are mapped to equal discrete values. Using priority as the similarity measure can effectively avoid the effect of distance vector failure in clustering of high-dimensional data sets. Using provinces as the study unit will lead to the failure to truly reflect the spatial clustering characteristics and changes of economic growth within the study unit, while using counties as the study unit will compare urban areas with counties on the same scale.

The location of economic activities is mainly influenced by natural conditions and distribution of natural resources and tends to be more spatially distributed in places with better natural conditions and more concentrated natural resources. Therefore, the factor analysis method was applied to measure the scores of each factor and the overall competitiveness score of high-tech service industry in each province and city. The global type is mainly used to judge whether there are clustering characteristics of the whole regional economic phenomenon, and it does not reflect the specific places where the clusters are located, while the factor analysis can point out the range of clusters.

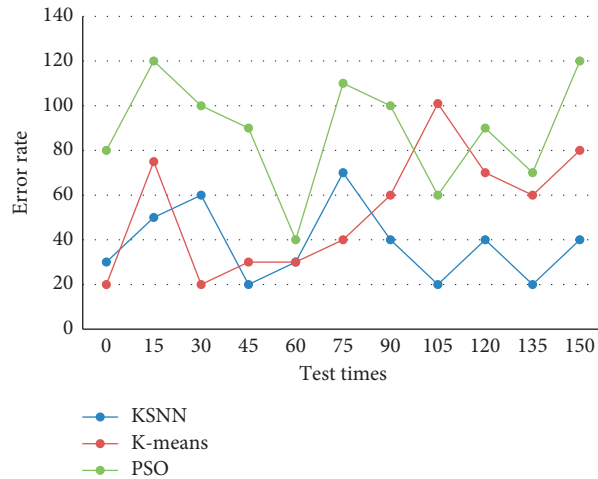


FIGURE 4: Comparison of error rates of KSNN, K-means, and PSO.

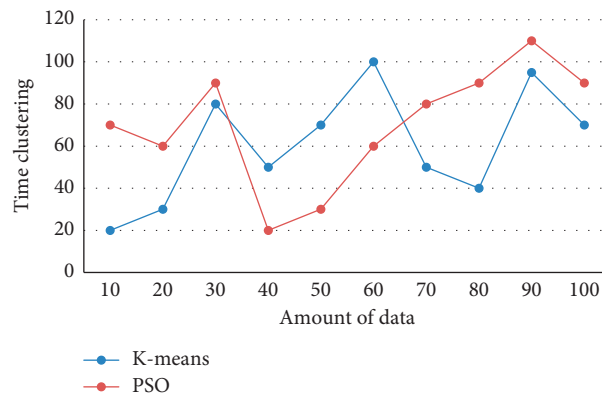


FIGURE 5: Performance analysis of K-means and PSO algorithms.

4.2. Analysis of Spatial Aggregation Characteristics. Although the high-, medium-, and low-economic growth efficiencies do not correspond exactly to the zoning structure of East, Central, and West. However, most of the regions with high environmental technical efficiency, i.e. high-economic growth efficiency, are indeed concentrated in the eastern regions of China, while most of the regions with low-environmental technical efficiency are concentrated in the western regions of China. The absorption of labor from other regions by developed regions is selective, and developed regions need a large amount of higher-quality labor such as skills and talents, skilled labor, and entrepreneurs, rather than general labor. It is difficult to discover potential local spatial association patterns by applying global indicators, and when global statistics cannot provide evidence of global spatial association, it is more necessary to use local indicators to discover potential locally significant spatial association. The comparison of priorities among nodes in the dataset at $k = 10$, and $k = 20$, respectively, was utilized. The comparison results are shown in Figure 6.

First of all, the central city has strong agglomeration power. Indicators and methods to measure the degree of spatial agglomeration of a regional economy are concentration rate, geographic linkage rate, and locational entropy method. Under the conditions of modern market economy, economic growth depends on the degree of possession of resources and markets; therefore, the competition for resources and markets is the main expression of competition, which is the soul of market economy. Concentration index is the proportion of the population of the area where half of a geographical factor is concentrated to the total population, reflecting the degree of concentration of the geographical factor in the area. The core objects will be increasing in this process, and the unprocessed objects are kept in the memory. If there are huge clusters in the database, a large amount of memory will be required to store the core object information, and its demand is unpredictable. Since the fusion operation is performed only for one convex hull functional area range at a time, and the distance between polygons in that range is not

TABLE 2: Comparison of convergence ability between KSNM and SNN.

J_c	KSNM	SNN
Fac	769.25	885.62
Iris	42.87	47.91
Artificial data set	673.95	681.83

too large, a larger distance is sufficient for the built-in distance parameter here. The density ratio determines the size of the clusters expanded from the centroid, and when the density ratio is larger, the class is expanded only to the relatively denser regions in the cluster, making the less-dense regions separated out, so the results of the impact of density radius change on the clustering results are shown in Figure 7.

Second, the economic volume of the border areas is small. The geographical linkage rate index mainly reflects the geographical distribution of the two factors in the region. To achieve the goal of coordinated regional economic development, a reasonable division of economic regions is a prerequisite. For the clustering operation of the dataset, the correlation between the nodes in different clusters is weak, and even there is no dependency between the nodes in the clusters. The radius ratio restricts the search from the core point to the ratio of the core point to its nearest neighbor distance, but it also causes the elimination of candidate core points, which affects the clustering accuracy. The effects of different radius ratio variations on clustering results are shown in Figure 8.

Meanwhile, any kind of changes in GDP growth rate and inflation rate can be attributed to the effects of external supply disturbances and external demand disturbances. Because of the possible crossover between the convex hull functional areas, the unwanted convex hull functional areas can be removed by the delete operation function. However, the algorithm has obvious limitations, namely, it is sensitive to the user-defined parameters, and subtle differences may lead to widely varying results, while the selection of parameters is irregular and can only be determined empirically.

Finally, the economic support of coastal areas is weak. The GDP growth rate and inflation rate are directly observable, and the supply disturbance and demand disturbance exist only in theoretical assumptions and are unobservable, but they are the main basis for implementing regulatory policies. Therefore, the priority within different clusters is greatly influenced by the nodes within this cluster and little influenced by the nodes within other clusters, or even not influenced by any nodes from other clusters. The coastal areas should develop high precision industries, speed up the construction of coastal ports, and energy development in areas with better resources, and vigorously develop agriculture, while the inland areas should speed up the construction of energy, transportation, and raw material

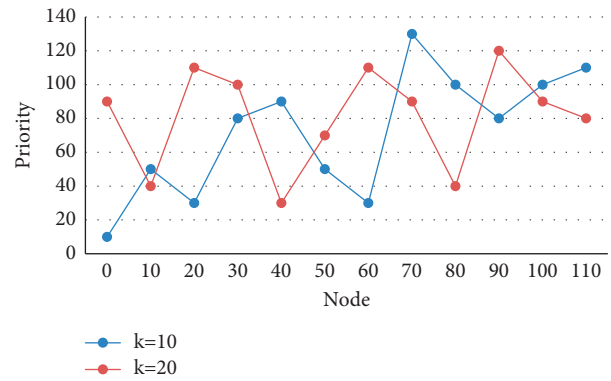


FIGURE 6: Priority comparison among data set nodes.

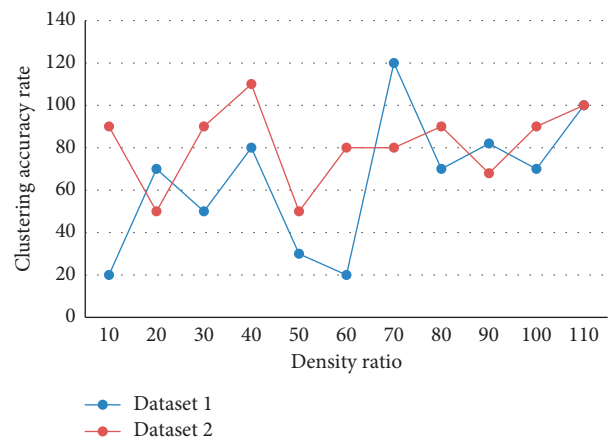


FIGURE 7: Influence of density radius change on clustering results.

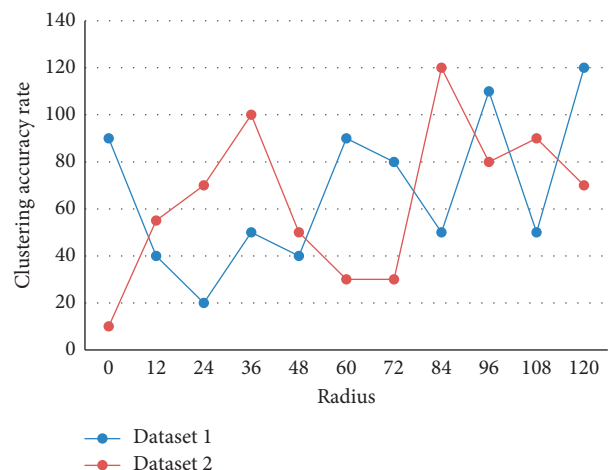


FIGURE 8: Influence of radius ratio change on clustering results.

industries, adjust and transform the existing machinery industry, develop consumer goods industries in a planned manner, and give full play to the potential of agricultural production.

5. Conclusions

In recent years, China's economy has been growing rapidly at nearly double-digit rates, and the economic and social landscapes have been greatly transformed, a phenomenon that academics at home and abroad call the "Chinese miracle." Although the results of interprovincial analysis show the changes in the regional economic landscape better, there is still the drawback of too large a spatial unit of analysis. The agglomeration of economic growth is very obvious in the historical process of economic development of industrialized countries. The analysis of this huge amount of information has become a difficult problem for national economic competition. Traditional methods of regional economic analysis assume that regions are independent of each other, while in reality, regions are interconnected as well as influenced by each other, and different regional environments have different effects on the economy. Density-clustering algorithm is a technique to mine knowledge and intelligence from massive digital information, so using density-clustering technology can improve the depth of intelligence analysis and the efficiency of national economic competition. In this paper, we propose a density clustering algorithm-based zoning method for China's regional economic competitiveness and analyze the spatial aggregation characteristics in detail to reveal the spatial autocorrelation and spatial heterogeneity of the economic development level of each province and region in China and its spatial dynamic evolution pattern. This provides favorable conditions for the creation of "growth poles" in the inland areas; the creation of "dual growth poles" in the eastern coastal growth poles and inland areas not only has a realistic basis but also has important practical significance for the improvement of the pace of regional gap reduction. It is also possible to incorporate geographic spatial effects into the model framework to detect and measure the impact of economic growth spillover from spatially adjacent regions on regional economic growth.

Data Availability

The labeled dataset used to support the findings of this study is available from the corresponding author upon request.

Conflicts of Interest

The authors declare that they have no conflicts of interest.

Acknowledgments

This research was supported by the Science and Technology Research Project of Hubei Education Department (Grant no. D20201801) and the Doctoral Scientific Research Foundation of Hubei University of Automotive Technology (Grant no. BK201907).

References

- [1] J. Jiang, D. Hao, Y. Chen, M. Parmar, and K. Li, "GDPC: gravitation-based density peaks clustering algorithm," *Physica A: Statistical Mechanics and Its Applications*, vol. 502, Article ID S0378437118301705, 2018.
- [2] Z. Xue and H. Wang, "Effective density-based clustering algorithms for incomplete data," *Big data mining and analysis*, no. 3, p. 12, 2021.
- [3] Z. Xue and H. Wang, "Effective density-based clustering algorithms for incomplete data," *Big Data Mining and Analytics*, vol. 4, no. 3, pp. 183–194, 2021.
- [4] Y. Zhou and Z. Lu, "Research on evaluation of regional economic competitiveness based on fuzzy analytic hierarchy process," *Region - Educational Research and Reviews*, vol. 1, no. 2, p. 24, 2020.
- [5] X. Cheng, R. Long, H. Chen, and Q. Li, "Coupling coordination degree and spatial dynamic evolution of a regional green competitiveness system – a case study from China," *Ecological Indicators*, vol. 104, no. SEP, pp. 489–500, 2019.
- [6] E. Kot, T. Kruzhkova, O. Rushitskaya, A. Ruchkin, and V. Kukhar, "The problem of improving the competitiveness of enterprises in the system of socio-economic relations," *IOP Conference Series: Earth and Environmental Science*, vol. 699, no. 1, Article ID 012058, 2021.
- [7] D. Zhao, Z. Zhao, and Z. Chen, "Construction of regional economic vitality model," *Journal of Economic Science Research*, vol. 3, no. 2, p. 5, 2020.
- [8] X. Wang, "Comprehensive evaluation on regional economic competitiveness of suzhou, wuxi and changzhou in jiangsu province," *Statistics and Applications*, vol. 09, no. 3, pp. 386–392, 2020.
- [9] I. Triyani, K. Adam, and D. Kristina, "Strengthening rural and regional economic competitiveness triggering purworejo regency economic growth through tourism-based kutoarjo transit node development," *The Indonesian Journal of Planning and Development*, vol. 4, no. 1, p. 19, 2019.
- [10] L. Nazarova, "The development of the regional economic system competitiveness policy," *Modern Economics*, vol. 20, no. 1, pp. 162–166, 2020.
- [11] D. Novita, M. Asaad, L. Tanjung, D. Hendrawan, and A. Hasibuan, "The regional investment competitiveness in binjai city," *International Journal of Pure and Applied Mathematics*, vol. 119, no. 17, p. 1983, 2020.
- [12] Y. A. Fridman, G. N. Rechko, and A. G. Pimonov, "Competitive positions of a region in innovative economic development," *Regional Research of Russia*, vol. 7, no. 4, pp. 333–341, 2017.
- [13] D. D. Burkaltseva, I. N. Voronin, and A. M. Lisitsky, "Assessing the effects of investments into innovative activity as a regional competitiveness factor," *International Journal of Applied Business and Economic Research*, vol. 15, no. 8, pp. 11–27, 2017.
- [14] S. T. Okutayeva, M. S. Bauer, A. K. Jussibaliyeva, and K. Bodaughan, "Development of regional livestock cluster in Kazakhstan as a method to improve competitiveness," *International Journal of Economic Research*, vol. 14, no. 7, pp. 223–237, 2017.
- [15] H. Dawid, P. Harting, and M. Neugart, "Fiscal transfers and regional economic growth," *Review of International Economics*, vol. 26, no. 3, pp. 651–671, 2017.
- [16] C. Deng, J. Song, R. Sun, S. Cai, and Y. Shi, "GRIDEN: an effective grid-based and density-based spatial clustering

- algorithm to support parallel computing,” *Pattern Recognition Letters*, vol. 109, no. JUL.15, pp. 81–88, 2018.
- [17] X. Chen, X. Wang, and H. K. Chan, “Manufacturer and retailer coordination for environmental and economic competitiveness: a power perspective,” *Transportation Research Part E: Logistics and Transportation Review*, vol. 97, no. JAN, pp. 268–281, 2017.
- [18] M. A. Obomeghie and U. O. Ugbomhe, “Globalization and its brunt on Nigeria global economic competitiveness: the need for holistic and dynamic strategies,” *International Journal of Social Sciences and Economic Review*, pp. 1–06, 2021.
- [19] R. Goli and M. Joksimovi, “Regionalization of Serbia as an instrument of balanced regional development and reduction of regional inequalities,” *Zbornik radova - Geografski fakultet Univerziteta u Beogradu*, vol. 2017, no. 65-1a, pp. 209–226, 2017.
- [20] L. Bai, X. Cheng, J. Liang, H. Shen, and Y. Guo, “Fast density clustering strategies based on the k-means algorithm,” *Pattern Recognition*, vol. 71, pp. 375–386, 2017.
- [21] J. Chen, H. He, J. Chen, S. Yu, and Z. Shi, “Fast density clustering algorithm for numerical data and categorical data,” *Mathematical Problems in Engineering*, vol. 2017, Article ID 6393652, 15 pages, 2017.
- [22] A. Kumar and S. Kumar, “Density based initialization method for K-means clustering algorithm,” *International Journal of Intelligent Systems and Applications*, vol. 9, no. 10, pp. 40–48, 2017.
- [23] J. Ma, X. Jiang, and M. Gong, “Two-phase clustering algorithm with density exploring distance measure,” *CAAI Transactions on Intelligence Technology*, vol. 3, no. 1, pp. 59–64, 2018.
- [24] E. Gungor and A. Ozmen, “Distance and density based clustering algorithm using Gaussian kernel,” *Expert Systems with Applications*, vol. 69, no. mar, pp. 10–20, 2017.
- [25] J. Lu and Q. Zhu, “An effective algorithm based on density clustering framework,” *IEEE Access*, vol. 5, pp. 4991–5000, 2017.
- [26] J. Xu, L. C. Fang, M. Gen, and S. E. Ahmed, “Proceedings of the twelfth international conference on management science and engineering management,” in *Proceedings of the International Conference on Management Science and Engineering*, Phuket Thailand, May 2019.
- [27] B. J. Lakshmi, K. B. Madhuri, and M. Shashi, “An efficient algorithm for density based subspace clustering with dynamic parameter setting,” *International Journal of Information Technology and Computer Science*, vol. 9, no. 6, pp. 27–33, 2017.
- [28] G. Pistilli, A. Campagna, L. Persia, and M. R. Saporito, “Regionalization of Ports as a strategic leverage to improve competitiveness: a study on central Italy ports and related hinterland,” *International Journal of Transport Development and Integration*, vol. 4, no. 1, pp. 51–61, 2020.
- [29] V. Bondarenko, O. Kurey, E. Derdi, and O. Butusov, “Monitoring of a region’s competitiveness as a mechanism of a state regional policy implementation,” *Regional Economy*, vol. 2, no. 2(96), pp. 33–43, 2020.
- [30] J. M. C. Díaz, L. Martínez-Bernabéu, and F. Flórez-Revelta, “Automatic parameter tuning for functional regionalisation methods,” *Papers in Regional Science*, vol. 96, no. 4, pp. 859–879, 2017.

Retraction

Retracted: Research and Implementation of Association Analysis of Agricultural Insurance Based on Data Mining Algorithm

Mathematical Problems in Engineering

Received 5 December 2023; Accepted 5 December 2023; Published 6 December 2023

Copyright © 2023 Mathematical Problems in Engineering. This is an open access article distributed under the Creative Commons Attribution License, which permits unrestricted use, distribution, and reproduction in any medium, provided the original work is properly cited.

This article has been retracted by Hindawi, as publisher, following an investigation undertaken by the publisher [1]. This investigation has uncovered evidence of systematic manipulation of the publication and peer-review process. We cannot, therefore, vouch for the reliability or integrity of this article.

Please note that this notice is intended solely to alert readers that the peer-review process of this article has been compromised.

Wiley and Hindawi regret that the usual quality checks did not identify these issues before publication and have since put additional measures in place to safeguard research integrity.

We wish to credit our Research Integrity and Research Publishing teams and anonymous and named external researchers and research integrity experts for contributing to this investigation.

The corresponding author, as the representative of all authors, has been given the opportunity to register their agreement or disagreement to this retraction. We have kept a record of any response received.

References

- [1] W. Shao, "Research and Implementation of Association Analysis of Agricultural Insurance Based on Data Mining Algorithm," *Mathematical Problems in Engineering*, vol. 2022, Article ID 3690346, 8 pages, 2022.

Research Article

Research and Implementation of Association Analysis of Agricultural Insurance Based on Data Mining Algorithm

Wen Shao 

School of Finance and Taxation, Dongfang College Shandong University of Finance and Economics, Taian, Shandong 271000, China

Correspondence should be addressed to Wen Shao; 201811111121711@stu.hubu.edu.cn

Received 16 May 2022; Revised 26 June 2022; Accepted 4 July 2022; Published 30 July 2022

Academic Editor: Hengchang Jing

Copyright © 2022 Wen Shao. This is an open access article distributed under the Creative Commons Attribution License, which permits unrestricted use, distribution, and reproduction in any medium, provided the original work is properly cited.

In order to establish the comprehensive competitive intelligence system of agricultural insurance companies, the process model of agricultural insurance competitive intelligence is constructed by combining data mining and process mining. The model is based on the relationship between data mining, process mining, and competitive intelligence based on analytic hierarchy process, and combines the current agricultural insurance subsidy policy, and the demand characteristics of competitive intelligence of agricultural insurance companies. Experimental results show that, among 11 secondary indicators, 6 indicators are rated above 4.0, that is, good grade or above, and 5 indicators score below 4.0, and still need to be improved. Prove data mining and the AHP algorithm can effectively improve the sustainability of agricultural insurance.

1. Introduction

Data mining, also known as knowledge discovery in databases, is a process of extracting useful information from massive data using various analytical methods and tools and analyzing and discovering potential relationships between models and data [1]. The content is very extensive, and association analysis, statistical analysis, cluster analysis, decision tree method, genetic algorithm, neural network algorithm, Bayesian network, fuzzy set, and rough set theory are all commonly used analysis and processing methods. Since the reform and opening up, the country's insurance business has grown rapidly, the service field has been continuously expanded, the market system has been gradually improved, the laws and regulations have been gradually improved, the supervision level has been continuously improved, and the overall strength has been significantly enhanced. The "Several Opinions of the State Council on the Reform and Development of the Insurance Industry" issued in 2006 clearly pointed out that insurance has the functions of economic compensation, financing, and social management which is the basic means of risk management in the market economy and is an important component of the

financial system and social security system. Part of it plays an important role in the construction of a socialist harmonious society. This dissertation solves the problem of the insurance industry's orientation in building a harmonious society and perfecting the socialist market economic system theoretically and in practice and elevates the function and role of insurance to a new height.

Since the insurance industry is an important part of the national economy, it is necessary to promote financial market stability, develop financial markets, promote trade and business development, promote savings growth, improve the efficiency of social risk management, promote social loss reduction, and promote more efficient social allocation of funds. Having played an irreplaceable role, all countries have spared no effort to promote the reform of the insurance industry and strengthen supervision. With the deepening reform and reorganization of the domestic insurance industry, the market environment of the insurance industry has undergone tremendous changes. China's insurance market has changed from a monopoly of individual companies to a number of large insurance companies dominated by a number of small and medium-sized insurance

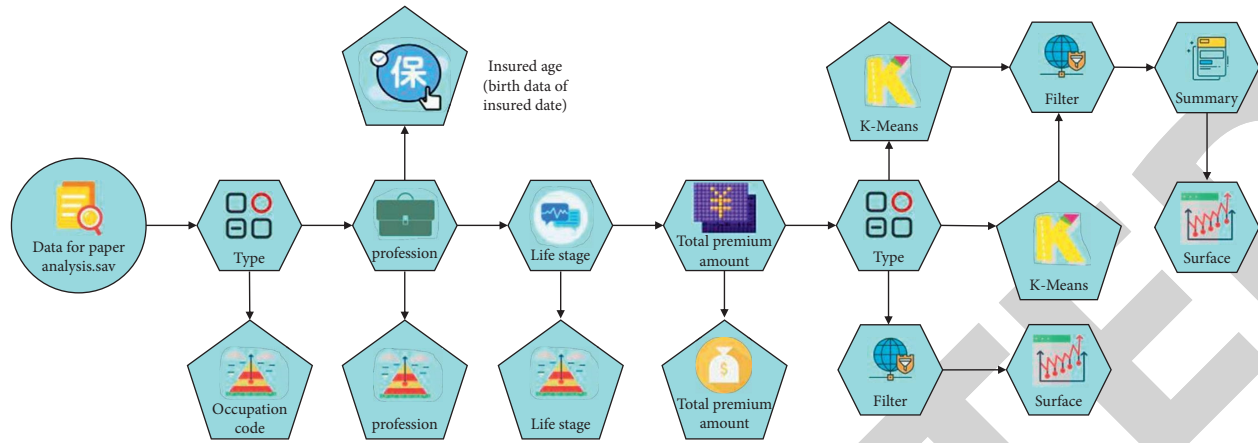


FIGURE 1: Overall mining process.

companies, the competitive landscape that companies are constantly entering. At the same time, since China's accession to the WTO, China's insurance market has been fully opened from the previous closed form to the current full opening. Foreign insurance companies have entered the Chinese insurance market on a large scale, making the balanced market pattern continue to differentiate. Therefore, insurance companies are facing a new and fiercely competitive market environment in which insurance profits are declining and forcing insurance companies to consider and develop new profit models and management methods to enhance their competitiveness. With the attention of various insurance companies, the agricultural insurance market will face increasingly fierce competition, and agricultural insurance companies will pay more and more attention to establishing a complete competitive intelligence system (CIS). As shown in Figure 1, this paper introduces two important information processing technologies: data mining and process mining, into the construction process of agricultural insurance competitive intelligence system. According to the characteristics of agricultural insurance itself, an integrated competitive intelligence system model is established and analyzed in detail. The specific working process of agricultural insurance comprehensive competitive intelligence system is also analyzed [2].

On the basis of this research, this paper proposes a research and implementation of agricultural insurance correlation analysis based on the data mining algorithm. On the basis of studying the relationship between data mining, process mining, and competitive intelligence, the comparative method based on the AHP method is used to scientifically evaluate the poverty alleviation efficiency evaluation research of agricultural insurance subsidy policy at this stage. Combined with the demand characteristics of agricultural insurance companies' competitive intelligence, the integrated data are constructed. The agricultural insurance competitive intelligence process model of mining and process mining has established an integrated competitive intelligence system model for agricultural insurance companies.

2. Literature Review

Based on association rules and neural network technology in data mining, Vyas et al. carried out the mining of insurance business data and found out the use of traditional statistical theories, undiscoverable potential operating rules, and business forms of the insurance industry [3]. Xu et al. proposed to talk about data mining technology and used to help life insurance companies improve their business management; They used the marketing data of relevant life insurance products of Swiss life insurance companies to conduct an empirical study, and concluded that OLAP technology can effectively assist the operation and management of life insurance companies [4]. Ahmed and Serra used neural network technology in data mining technology and combined relevant data to predict the price sensitivity of life insurance company customers, reprice insurance products, and help life insurance companies prevent customer risks [5]. Leidig and Teeuw think that the insurance industry has accumulated a large number of customers, products, and competing companies in the development process and socioeconomic environment data. It is necessary to integrate data mining theory and methods, apply in research in the insurance industry, And further analyze the homogeneity of data and the impact of different processing methods of information extraction on the application environment of data mining [6]. Zhang et al. elaborated on three types of models in data mining: decision trees, multiple adaptive, and hybrid models. They are the feasibility and ideas of insurance risk modeling [7]. Deng et al. use data warehouse and data mining technology to analyze the data of Hong Kong insurance agents and discuss how to choose an insurance agent [8]. Wei and Dan use the data mining tool Mineset from the insurance business data to find out the association rules that guide insurance companies and help insurance companies and control investment risks [9]. Khiareddine et al. through comparative research ideas, explain data mining methods, statistical analysis, data warehouse, and other fields, respectively; discuss their pros and cons and come to the data mining technology; and analyze the cost and income of the customer throughout the life

cycle. It is possible to mine high loyal customers and predict the conclusion of the product offering time [10]. Pelka et al. used data mining technology to analyze the customer experience survey data of automobile insurance telemarketing, in order to explore the part of automobile insurance telemarketing and insurance process that customers most want to optimize and improve, so as to help insurance companies improve the success rate of automobile insurance telemarketing with low investment cost [11]. According to Fang et al., based on data mining technology, the analysis summarizes the current situation of fraud prevention in the life insurance industry and the shortcomings of the antifraud system currently used by domestic and foreign life insurance companies, and using data provided by a central branch of China Pacific Life Insurance Co., Ltd., designed the various modules of the enterprise antifraud system. The modules include system business modules, system logic modules, and system physical model modules, and the author also combines the characteristics of each business model, the SPRINT algorithm in data mining. It has been successfully applied to the fraud prevention system of life insurance companies [12]. Kirubakaran and Ilangkumaran, using cluster analysis method to group Pacific Insurance Company's customer base, determined the strong business of different customer groups, used it in practice, and improved the sales success rate of old customers [13]. Wang et al. introduced the ant colony optimization algorithm into data mining and used six public data sets to compare the classification effect of the ant colony algorithm and the CN2 classification algorithm. In terms of association rule discovery, the resulting association rules are simpler than those obtained by the CN2 classification algorithm [14]. Jiang proposed an improved K-means classification algorithm, K-modes, which can handle categorical data. The main idea is to replace the mean with the pattern and to continuously update the pattern type in the clustering process based on the frequency to reduce the loss of clustering information. And in a database of millions of health insurance records, based on 34 categorical variables for data mining, the results show that the K-modes algorithm has good scalability in both categorical and numerical variable clustering [15].

3. Analysis of Efficiency Evaluation Software System Based on AHP Method

The author tried to build a software system for evaluating the efficiency of poverty alleviation in agricultural insurance operations, collect effective data information, perform empirical analysis using analytic hierarchy process (AHP), and draw research conclusions.

3.1. Sources of Sample Data Indicators. In order to better evaluate the operational poverty alleviation efficiency implemented by the subsidy policy, various indicators of the poverty alleviation efficiency evaluation system of policy-based agricultural insurance operations, regarding the efficiency of agricultural insurance operations as the target level, based on the three levels of macro, meso, and micro,

designed the first-level indicators of the poverty alleviation efficiency evaluation system of China's agricultural insurance operations. Then, decompose layer by layer according to the main content and logical relationship of each first-level indicator and decompose the 3 first-level indicators into 13 second-level indicators. Thus, a relatively complete evaluation system of poverty alleviation efficiency of agricultural insurance operations is obtained [14].

3.2. Evaluation of the Software Process. Setting up an evaluation set based on agricultural insurance efficiency evaluation indicators refers to a language description of various levels of indicators. It is an evaluation collection of each evaluation index. $U = \{u_1, u_2, \dots, u_n\}$, in this model, if $n = 5$, the evaluation set is as follows:

$$U = \{u_1, u_2, \dots, u_5\} = \{\text{excellent, good, medium, poor}\}. \quad (1)$$

Weight set refers to the weight coefficient of the target layer occupied by each indicator. Among $\sum_{i=1}^m b_i = 1$, the weight set of the first-level indicators is $B = (b_1, b_2, \dots, b_m)$, $m = 4$, and $\sum_{j=1}^k b_j = 1$, the weight set of the secondary indicators is $B = (b_{i1}, b_{i2}, \dots, b_{ik})$, $k = 4, 5$.

The author uses analytic hierarchy process (AHP), that is, the subjective assignment method of weight set, and the weight is obtained by the expert based on subjective judgment of experience. The weight of each indicator is determined [15].

On the basis of establishing a hierarchy, for each layer of structure and the elements of the next layer under the structure constitute subareas, for each element in this subregion, the Saaty1-9 scale method is adopted to construct the judgment matrix. That is, suppose that the element B_1, B_2, \dots, B_n in the B level is related to the upper element A, then it can be represented by the following judgment matrix formula:

$$S = (B_{ij})_{n \times n} = \begin{bmatrix} b_{11} & b_{12} & \dots & b_{1n} \\ b_{21} & b_{22} & \dots & b_{2n} \\ \dots & \dots & \dots & \dots \\ b_{n1} & b_{n2} & \dots & b_{nn} \end{bmatrix}. \quad (2)$$

The value of b_{ij} is determined by the Saaty1-9 scaling method.

Use MATLAB software to find the maximum eigenvalue λ_{\max} and standard eigenvector ω of the judgment matrix; among them, the value of ω element is the index of this level, the relative importance ranking weight value of a factor relative to the superior index is shown in the following formula:

$$CI = \frac{(\lambda_{\max} - n)}{(n - 1)}. \quad (3)$$

According to the order, n of the judgment matrix can find the corresponding consistency index RI. Figure 2 shows the value of Saaty's RI for 1-9 [16].

The formula for calculating the consistency ratio is $CR = CI/RI$. When $CR < 0.1$, the judgment matrix has good

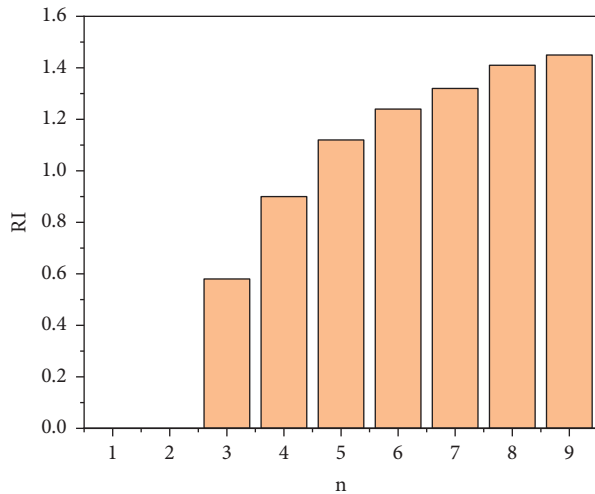


FIGURE 2: Consistency index RI.

consistency, reasonable judgment. When $CR = 0.1$, the judgment matrix has better consistency and the judgment is more reasonable. When $CR > 0.1$, the judgment matrix does not conform to the principle of consistency, and it needs to be revised again until the consistency check is met. The standard vector ω corresponds to λ_{\max} after meeting the consistency check, and it is the weight value of this level index to the upper level index. As a result, the software can calculate indicators at all levels in turn, relative to the absolute weight of the target layer [17].

Comprehensive scoring of software evaluation indicators and evaluation of China Agricultural Insurance's operational poverty alleviation efficiency can be achieved by scoring 13 secondary indicators. The author uses expert scoring and self-evaluation scoring to improve the accuracy and effectiveness of its scoring and, using the average weight method, both account for 1/2 each. After the weighted average, the scores of each index of the evaluation object are obtained, respectively, denoted as p_i , the score value of each indicator is multiplied by the corresponding weight U_i , that is, the evaluation result R of the poverty alleviation efficiency of agricultural insurance operations can be obtained.

Excellent: the poverty alleviation efficiency of agricultural insurance operations is very high, and there is no need for improvement; good: the poverty alleviation efficiency of agricultural insurance operations is relatively high, but there are still problems, the problem has been found, measures have been found, and the desired effect has been achieved; moderate: the poverty alleviation efficiency of agricultural insurance operations is not high, the problem has been found, and measures have been formulated but the desired effect has not been achieved; poor: agricultural insurance operations are inefficient in poverty alleviation, the problem has been found, but no specific improvement measures have been formulated; poor: the poverty alleviation efficiency of agricultural insurance operations is low, and the problem has not been found yet [18].

The evaluation model of the poverty alleviation efficiency of agricultural insurance operations is shown in the following formula:

$$R = \sum_{i=1}^n (P_i \times U_i), \quad (4)$$

where R is the evaluation value of the poverty alleviation efficiency of China's agricultural insurance operation; p_i is the scoring value of each evaluation index; and U_i is the weight of each evaluation index.

3.3. Agricultural Insurance Competitive Intelligence Collection Module. The main functions of the competitive intelligence collection module are to collect, sort, and classify the relevant information of agricultural insurance companies, and the classified information is then stored in the intelligence information database. The information processed by this module is first divided into two main sources, that is, the internal information system of the enterprise and the outside of the enterprise. At the same time, the information, it processes can also be divided into two types: data information and process information. The data information includes the operation of agricultural insurance companies; the decisive catastrophe loss data, compensation data; expense data for policy acquisition; indirect claims and policy maintenance, as well as the regulatory fee rate, market fee rate, and sales fee commission level data on market information, respectively, from regulatory information, market research, and peer analysis reports; external information and core business systems of enterprises, such as agricultural production, geography and meteorology; reinsurance business system; and financial management system and other internal enterprise information systems. Process information includes work lists and process logs about sales management and underwriting claims process, and these process information, mainly from internal information systems such as customer management, administrative management systems, and procurement management systems within the enterprise. The above data information and process information, data file converters, and process encoders that will navigate through categories, for conversion and collection, are imported into the intelligence information database [19].

3.4. Agricultural Insurance Competitive Intelligence Storage Module. Intelligence knowledge storage module, mainly composed of intelligence information database and competitive intelligence knowledge base, is used to store the intelligence information obtained by the intelligence collection module and the competitive intelligence knowledge obtained by the intelligence analysis and production module. Different from traditional competitive intelligence systems, information in the intelligence information base and intelligence knowledge base, according to their characteristics, is divided into two categories: data and process. The data information in the intelligence information database, obtained by the intelligence collection module, will be passed to the data mining submodule of the intelligence analysis production module, through traditional statistical mining and cutting-edge intelligent mining technology, and

obtain static data intelligence with application value. The process information in the intelligence information database, obtained by the intelligence collection module, will be passed to the process mining submodule of the intelligence analysis production module. Through semantic integration and mining engine processing, we obtain dynamic process intelligence with application value. Analyze the static data intelligence and dynamic process intelligence, obtained by the production module, which will be imported into the intelligence knowledge base for storage [20].

4. Experimental Results and Analysis

The following solves the AHP model for evaluating the poverty alleviation efficiency of agricultural insurance operations in a certain province and gets the weights of indicators at all levels. The model calculation is as follows.

- (1) Matrix judgment: find the weight value of each primary and secondary index relative to the target layer

Set first-level indicators $A_i = \{A_1, A_2, A_3\} = \{\text{farmers, insurance companies, and government departments}\}$, construct a first-level index judgment matrix, and solve to get the weight value of each level index relative to the target layer in the following formula:

$$S = (A_{ij})_{3 \times 3} = \begin{bmatrix} 0 & \frac{1}{2} & \frac{1}{3} \\ 0 & 0 & \frac{1}{2} \\ 0 & 0 & 0 \end{bmatrix} \quad (5)$$

The calculated maximum eigenvalue $\lambda_{\max} = 3.01032$, corresponding to the standard vector $\omega = (0.1638, 0.2972, 0.5390)$. Calculate the consistency index $CI = \lambda_{\max} - 3/3 - 1 = 0.00516$.

$CI = \lambda_{\max} - 3/3 - 1 = 0.00516$ shows that the matrix has good consistency and reasonable judgment. Therefore, the first-level weights (u) of China's agricultural insurance operation efficiency evaluation are as follows:

$$u_1 = 0.1638, u_2 = 0.2972, u_3 = 0.5390. \quad (6)$$

Judging from the results of the evaluation, in the evaluation index system for the efficiency of business poverty alleviation, the efficiency of poverty alleviation by government departments is the most critical, followed by the operating capacity of insurance companies and finally the insurance of farmers [4].

In the same way, the weight of each secondary index to the target layer can be solved. The weight $U_{ij} = u_i \times u_{ij}$ of each secondary index to the target layer is where $i = \{1, 2, 3\}$ and $j = \{1, 2\}/\{1, 2, 3, 4\}/\{1, 2, 3, 4, 5\}$. At the microfarmer level, calculate matrix $A_1 = (B_{ij})_{5 \times 5}$, the largest eigenvalue

$\lambda_{\max} = 5.4376$, corresponding to the standard vector $\omega = 0.071, 0.132, 0.52, 0.217, 0.06$, and then calculate consistency index $CI = 0.1094$ and $CR = 0.0977$ and $CR < 0.1$, with good consistency and reasonable judgment. Therefore, the weights of the secondary evaluation indicators are $u_{11} = 0.071, u_{12} = 0.132, u_{13} = 0.52, u_{14} = 0.217$, and $u_{15} = 0.06$. At the level of Zhongguan insurance company, calculate matrix $A_2 = (B_{ij})_{4 \times 4}$, the largest eigenvalue $\lambda_{\max} = 4.223$, corresponding to the standard vector $\omega = (0.248, 0.123, 0.569, 0.061)$ and then calculate the consistency index $CI = 0.0742$, $CR = 0.0824$, and $CR < 0.1$, with good consistency, the judgment is reasonable [13, 21]. Therefore, the weights of the secondary evaluation indicators are $u_{21} = 0.248, u_{22} = 0.123, u_{23} = 0.569$, and $u_{24} = 0.061$.

According to the above calculation principle, it can also be calculated that the weights of the secondary indicators of macro government departments are $u_{31} = 0.833$ and $u_{32} = 0.167$.

In the process of scoring 11 indicators, two scoring methods are used comprehensively, the scoring subject will quantify each evaluation object according to the scoring standard and obtain their respective scores. After weighted average, the evaluation score p_i is obtained.

On the basis of calculating the weights (U_i) and scoring results (P_i) of indicators at all levels, multiply the score of each indicator with its corresponding weight, that is, the evaluation result (R) of the poverty alleviation efficiency of China's agricultural insurance operation is obtained, and the calculation is as follows:

$$R = \sum_{i=1}^n (P_i \times U_i). \quad (7)$$

The reference standard for the evaluation result R is $0 < R < 2.9$, indicating poor poverty alleviation efficiency, need to find out where the problem lies and make effective adjustments and improvements; $2.9 < R < 3.5$, indicating that the efficiency of poverty alleviation is poor, and the problems found need to be addressed and develop practical measures to improve; $3.5 < R < 4.0$, indicating that the poverty alleviation efficiency is moderate, and the rectification measures need to be revised and make the improvement of the problems to achieve the desired effect; $4.0 < R < 4.5$, indicating that the poverty alleviation efficiency is good, due to effective rectification and improvement of the problem, and the expected effect has been achieved; $4.5 < R < 5.0$, indicating that the efficiency of poverty alleviation is excellent and no improvement is needed [21]. In order to be able to visually see the changing trend of the data over the years and in order to facilitate analysis and research, we have reflected the above data in the icon, and the details are shown in Figures 3–6 and 7.

It is not difficult to see from Figure 3 that, from 2015 to 2020, agricultural insurance premium income in a certain province shows a steady increase and a significant growth rate from 2.31778 billion yuan in 2015 to 4.63987 billion yuan in 2017, almost doubled. Compared with the premium

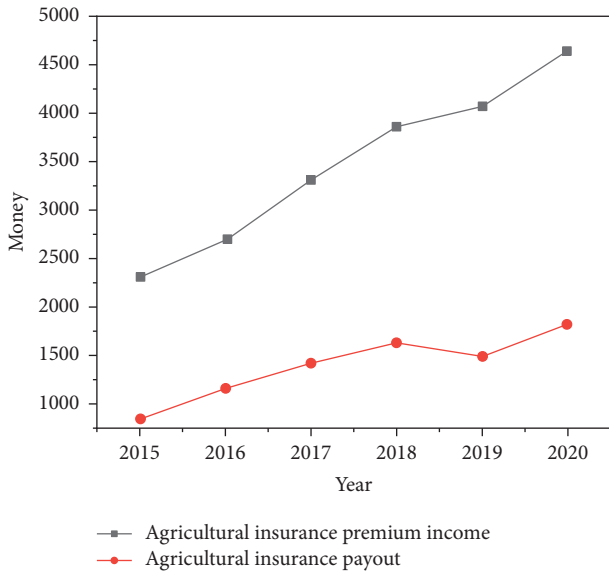


FIGURE 3: 2015–2020 agricultural insurance premium income and compensation expenditure in a certain province.

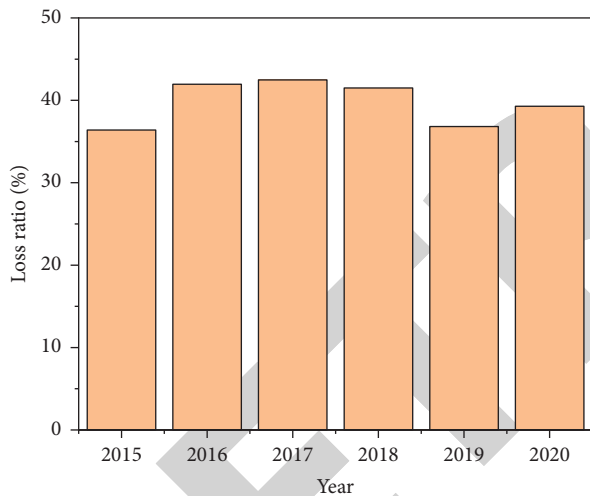


FIGURE 4: The average annual loss rate of agricultural insurance in a certain province from 2015 to 2020.

income, although the compensation expenditure has also increased correspondingly, but relatively speaking, the increase rate is not so obvious. In 2019, there is even a downward trend compared to 2018 [22].

As can be seen from Figure 4, from 2015 to 2020, the proportion of agricultural insurance premiums in a certain province in property insurance shows an upward trend; although in 2019 it has decreased slightly, but it does not affect the overall trend much, and this country's high and continuous emphasis on agricultural insurance for poverty alleviation has a lot to do with [23].

Because of the agricultural insurance management costs here, it is roughly estimated at 30% of the premium income,

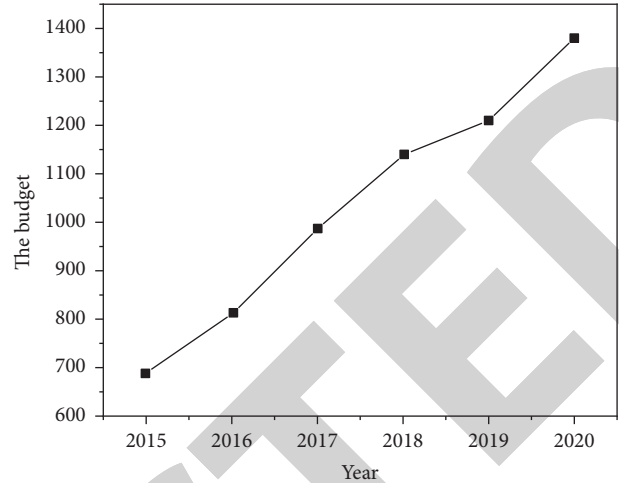


FIGURE 5: A province's agricultural insurance management cost budget from 2015–2020.

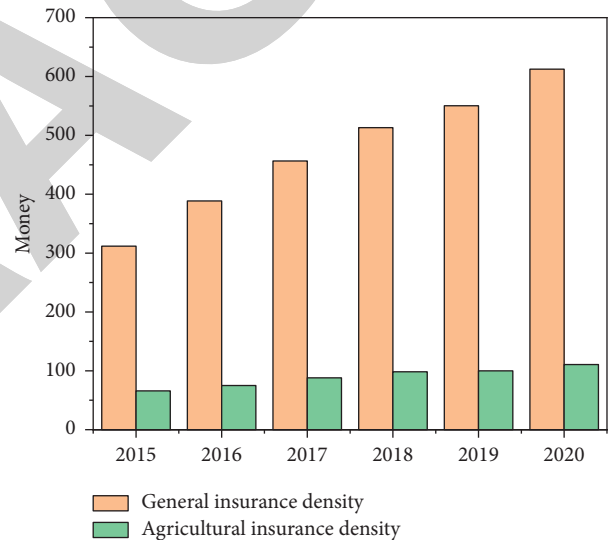


FIGURE 6: The density of property and agricultural insurance in a province from 2015 to 2020.

so the trend of change is the same as the trend of premium income.

As can be seen from Figure 7, between 2015 and 2020, although the density of agricultural insurance in a certain province follows the density of property insurance, showing an upward trend; however, the increase in agricultural insurance density is obviously not as fast as property insurance. In recent years, the depth of agricultural insurance has changed with the depth of property insurance, it is almost the same direction and the same speed. However, even if it is showing an increasing trend and it is also among the fast-growing ranks in various provinces and cities, it is still far from the average level in developed countries.

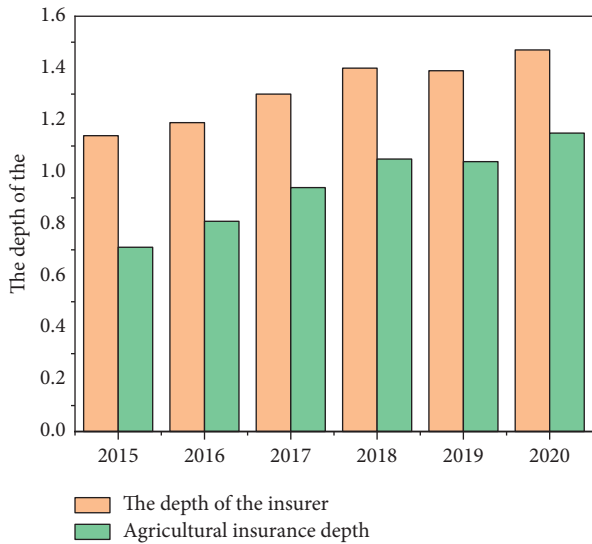


FIGURE 7: The depth of property and agricultural insurance in a province from 2015 to 2020.

5. Conclusion

The author, based on the research of data mining, process mining, and competitive intelligence theory, combines the demand characteristics of competitive intelligence of agricultural insurance companies and demonstrates the important significance of integrated data mining and process mining in the competitive intelligence work of agricultural insurance companies. The author refined and upgraded the general competitive intelligence process, constructed an agricultural insurance competitive intelligence process model integrating data mining and process mining, and analyzed its four main processes. Use the comparative method based on the AHP method to scientifically evaluate this stage, research on the evaluation of poverty alleviation efficiency of agricultural insurance subsidy policy, and put forward the agricultural insurance subsidy services in our province, the optimization mechanism, and guarantee measures for precise poverty alleviation.

Data Availability

The data used to support the findings of this study are available from the corresponding author upon request.

Conflicts of Interest

The author declares that there are no conflicts of interest.

References

- [1] H. Zhou, Y. Li, and Y. Gu, "Research on evaluation of airport service quality based on improved ahp and topsis methods," *Transport*, vol. 174, no. 3, pp. 1–36, 2018.
- [2] Yang and Ruihua, "Agricultural insurance: theory, empirical research and experience – based on farmers household data," *China Agricultural Economic Review*, vol. 10, no. 1, pp. 173–175, 2018.
- [3] S. Vyas, T. Dalhaus, M. Kropff, P. Aggarwal, and M. P. M. Meuwissen, "Mapping global research on agricultural insurance," *Environmental Research Letters*, vol. 16, no. 10, Article ID 103003, 19 pages, 2021.
- [4] J. Xu, P. Feng, and P. Yang, "Research of development strategy on China's rural drinking water supply based on swot-topsis method combined with ahp-entropy: a case in hebei province," *Environmental Earth Sciences*, vol. 75, no. 1, p. 58, 2016.
- [5] O. Ahmed and T. Serra, "Economic analysis of the introduction of agricultural revenue insurance contracts in Spain using statistical copulas," *Agricultural Economics*, vol. 46, no. 1, pp. 69–79, 2015.
- [6] M. Leidig and R. M. Teeuw, "Quantifying and mapping global data poverty," *PLoS One*, vol. 10, no. 11, Article ID e0142076, 2015.
- [7] Y. y. Zhang, G. w. Ju, and J. t. Zhan, "Farmers using insurance and cooperatives to manage agricultural risks: a case study of the swine industry in China," *Journal of Integrative Agriculture*, vol. 18, no. 12, pp. 2910–2918, 2019.
- [8] X. Deng, D. Zeng, and H. Shen, "Causation analysis model: based on ahp and hybrid apriori-genetic algorithm," *Journal of Intelligent and Fuzzy Systems*, vol. 35, no. 1, pp. 767–778, 2018.
- [9] C. Wei and L. Dan, "Market fluctuation and agricultural insurance forecasting model based on machine learning algorithm of parameter optimization," *Journal of Intelligent and Fuzzy Systems*, vol. 37, no. 5, pp. 6217–6228, 2019.
- [10] A. Khiareddine, C. Ben Salah, and M. F. Mimouni, "Power management of a photovoltaic/battery pumping system in agricultural experiment station," *Solar Energy*, vol. 112, pp. 319–338, 2015.
- [11] N. Pelka, O. Musshoff, and R. Finger, "Hedging effectiveness of weather index-based insurance in China," *China Agricultural Economic Review*, vol. 6, no. 2, pp. 212–228, 2014.
- [12] L. Fang, R. Hu, H. Mao, and S. Chen, "How crop insurance influences agricultural green total factor productivity: evidence from Chinese farmers," *Journal of Cleaner Production*, vol. 321, no. 7, Article ID 128977, 2021.
- [13] B. Kirubakaran and M. Ilangkumaran, "Selection of optimum maintenance strategy based on fahp integrated with gra-topsis," *Annals of Operations Research*, vol. 245, no. 1–2, pp. 285–313, 2016.
- [14] P. Wang, Z. Zhu, and S. Huang, "The use of improved topsis method based on experimental design and Chebyshev regression in solving mcdm problems," *Journal of Intelligent Manufacturing*, vol. 28, no. 1, pp. 229–243, 2017.
- [15] S. Jiang, "Research on big data audit based on financial sharing service model using fuzzy ahp," *Journal of Intelligent and Fuzzy Systems*, vol. 40, no. 4, pp. 8237–8246, 2021.
- [16] J. L. Zhou, Q. Q. Xu, and X. Y. Zhang, "Water resources and sustainability assessment based on group ahp-pca method: a case study in the jinsha river basin," *Water*, vol. 10, no. 12, p. 1880, 2018.
- [17] Z. An, L. Song, S. Mahalingam, G. Xiao-Zhi, and V. N. Hamed, "Research on the role of ahp- entropy method in the identification and evaluation of China tariff source risk," *Journal of Intelligent and Fuzzy Systems*, vol. 34, no. 2, pp. 1053–1060, 2018.
- [18] G. Wang, M. Liao, and J. Jiang, "Research on agricultural carbon emissions and regional carbon emissions reduction strategies in China," *Sustainability*, vol. 12, no. 7, p. 2627, 2020.

Retraction

Retracted: Application of 3D Laser Virtual Imaging Technology in Combined Building Interactive Modeling

Mathematical Problems in Engineering

Received 26 September 2023; Accepted 26 September 2023; Published 27 September 2023

Copyright © 2023 Mathematical Problems in Engineering. This is an open access article distributed under the Creative Commons Attribution License, which permits unrestricted use, distribution, and reproduction in any medium, provided the original work is properly cited.

This article has been retracted by Hindawi following an investigation undertaken by the publisher [1]. This investigation has uncovered evidence of one or more of the following indicators of systematic manipulation of the publication process:

- (1) Discrepancies in scope
- (2) Discrepancies in the description of the research reported
- (3) Discrepancies between the availability of data and the research described
- (4) Inappropriate citations
- (5) Incoherent, meaningless and/or irrelevant content included in the article
- (6) Peer-review manipulation

The presence of these indicators undermines our confidence in the integrity of the article's content and we cannot, therefore, vouch for its reliability. Please note that this notice is intended solely to alert readers that the content of this article is unreliable. We have not investigated whether authors were aware of or involved in the systematic manipulation of the publication process.

Wiley and Hindawi regrets that the usual quality checks did not identify these issues before publication and have since put additional measures in place to safeguard research integrity.

We wish to credit our own Research Integrity and Research Publishing teams and anonymous and named external researchers and research integrity experts for contributing to this investigation.

The corresponding author, as the representative of all authors, has been given the opportunity to register their agreement or disagreement to this retraction. We have kept a record of any response received.

References

- [1] X. Ma, G. Shang, D. Liu, and D. Ju, "Application of 3D Laser Virtual Imaging Technology in Combined Building Interactive Modeling," *Mathematical Problems in Engineering*, vol. 2022, Article ID 8048269, 8 pages, 2022.

Research Article

Application of 3D Laser Virtual Imaging Technology in Combined Building Interactive Modeling

Xiaoqiu Ma , Ge Shang, Dandan Liu, and Donglei Ju

¹Department of Basic Science, Jilin Jianzhu University, Jilin, Changchun 130000, China

Correspondence should be addressed to Xiaoqiu Ma; 2016123712@jou.edu.cn

Received 23 May 2022; Revised 21 June 2022; Accepted 29 June 2022; Published 22 July 2022

Academic Editor: Hengchang Jing

Copyright © 2022. This is an open access article distributed under the Creative Commons Attribution License, which permits unrestricted use, distribution, and reproduction in any medium, provided the original work is properly cited.

In order to solve the problem of panoramic stitching of combined building facade images, the illuminance at the junction is reduced, resulting in the problem of vignetting, the author proposes a vignetting correction method based on 3D laser virtual imaging technology for surface fitting of modular buildings. By calculating the corner points, analyzing the correlation between the image coordinate system and the world coordinate system, obtaining the unit coordinate data of the corner points in the world coordinate system, and constructing a combined three-dimensional interactive model of the camera imaging; The ORB feature matching algorithm is used to perform image matching, by decomposing the homography matrix, the projection transformation matrix, rotation matrix and translation matrix of the camera's internal parameters are calculated, and the cylindrical coordinate projection method is used to complete the panoramic stitching of building facade images; Using the image grayscale correction method based on two-dimensional surface fitting, calculate the correlation coefficient of the Hesse matrix, and use the Hesse matrix to iteratively converge, obtain 2D surface parameter values to eliminate image vignetting. Simulation results show: The vignetting correction time of the combined building facade panoramic image using the vignetting correction method of surface fitting, compared with the common vignetting correction method, the vignetting correction time of the combined building facade panoramic image is shorter, and it is stable at about 5 seconds. Conclusion: The proposed method can effectively correct the vignetting of the combined building facade panoramic image, and the gray distribution of the corrected image is uniform, which shortens the image vignetting correction time.

1. Introduction

In the field of computer vision and computer graphics, the reconstruction of 3D models of buildings has always been a research hotspot; this research direction has a wide range of applications in the fields of smart city construction, virtual reality, and digital protection of cultural relics [1]. For modeling methods that require professional modeling knowledge, they cannot meet the modeling needs of ordinary users. Traditional 3D building modeling methods mainly include procedural modeling, point cloud-based building modeling, and image-based building modeling. Compared with the first two methods, the image-based 3D reconstruction technology, model reconstruction by extracting and calculating 3D information from the input image, it effectively avoids the geometric complexity of 3D scenes, but at the same time there are defects and limitations in geometric accuracy and 3D information integrity, this

brings many difficulties to the reconstruction of 3D buildings. In recent years, the research on the reconstruction method of building models based on a single image is more meaningful and challenging than the previous two methods [2]. Figure 1 shows the principle of holographic imaging. In building modeling based on a single image, existing methods mainly use information, such as feature points and feature lines provided in the input image, or the symmetry of geometry and repeated structural constraints [3], by solving the scene camera parameters, the calibration is completed or the 3D information is recovered according to the geometric constraints of the building surface.

2. Literature Review

In the modeling process, the shape grammar in architecture is successfully used in the design and analysis of buildings, and the assembly and construction of buildings are realized through

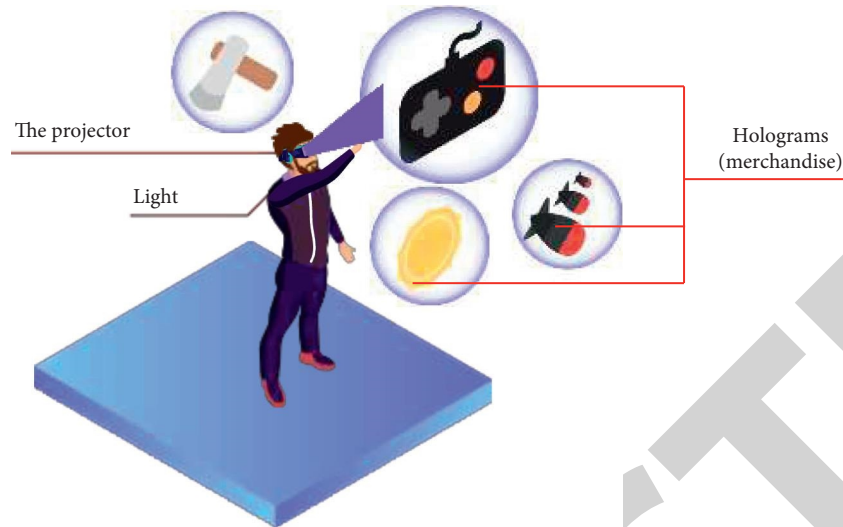


FIGURE 1: The principle of holographic imaging.

specific grammar rules. With the help of shape grammars, Feng et al. proposed a procedural modeling system for modeling architectural surfaces. According to the building appearance layout given by the user [4], using a heuristic search algorithm, several building models are generated semiautomatically that approximate the given exterior layout [5]. Bui et al. proposed a component-based multilayer parameter modeling method [6], using a probabilistic network to describe the high-level parameters of buildings and components as a user interaction interface, and using a rule base to describe the low-level parameters of components, and combined with the construction template to describe the building construction process. Procedural building modeling using shape grammar usually requires users to have specialized knowledge, and it is difficult to effectively extend the grammar rules. In the building modeling based on point cloud or aerial photography data, the building surface is scanned with a 3D laser scanner to obtain the point cloud data of the building objects, and the point cloud data is processed to realize the 3D modeling of the building. Shan et al. proposed an optimization-based tracking algorithm to achieve 3D modeling of buildings [7]. Based on vehicle-mounted LiDAR scan data, Hizam et al. proposed an interactive SmartBox tool [8], which enables users to construct building models directly on the acquired 3D point cloud data of large-scale urban scenes. Combining aerial data with ground-acquired data, Vu et al. proposed an automatic generation of photo-realistic 3D city models with complex surface details [9]. The modeling method based on point cloud or aerial data usually acquires a large amount of data, and the cost of effective data processing is high, which limits the practicality of the method.

In order to improve the imaging quality of the panoramic image of the combined building facade, it is necessary to prevent the occurrence of image vignetting. Thus, the author proposes a vignetting correction method based on surface fitting. Firstly, we construct a 3D interactive model of a combined building, associate the cuboid as a geometric

constraint, and obtain the 3D data of the building inside the image [10, 11], we analyze the correlation between the relative corner points in the image coordinate system and the world coordinate system, and then we establish a camera imaging model, IAC representation is used to solve the internal parameters of the camera, so that the visual imaging effect of the combined building facade is better, and the correctness of the panoramic image stitching is maintained. Secondly, the panorama image stitching method is adopted, the ORB matching method is used to extract the adjacent image matching points, the homography matrix is calculated according to the matching points, and the wave correction processing is performed on the camera shake to prevent the image from being deformed, and realize the panoramic stitching of the building facade image. Finally, the surface fitting vignetting correction method is used, and the steepest descent method is combined with the two-dimensional surface fitting to obtain the global change trend of the image gray level, and complete the correction of the vignetting phenomenon of panoramic images. The simulation results confirmed that the author's method has good applicability and can be widely used in real scenarios.

3. Research Methods

3.1. 3D Interactive Modeling of Modular Buildings. In the process of constructing the 3D model of the modular building, building objects to be constructed are generally constructed from regular cuboid parts. Therefore, the author regards the cuboid set primitive as the basic factor for the construction of the combined architectural model. Using the geometric convergence of the cuboid itself, the three-dimensional data of the building target in the input image can be obtained, and the vertices of the original component cuboid target projected in the two-

dimensional image can be marked, it is used in the geometric primitives of the three-dimensional geometry contrast relationship [12]. Due to the large target area of the building, projection into a two-dimensional image often produces distortion, so the corners that need to be marked must cover the six faces of the cuboid.

For the marked six corner points and regions, the goal of camera calibration is to match the cuboid part model and the region-free two-dimensional image contour $p_0 p_1 p_2 p_3 p_4 p_5$ with each other, after calculating the corner points, analyzing the correlation between the image coordinate system and the world coordinate system, the internal and external parameters of the camera are obtained, and a combined three-dimensional interactive model of camera imaging is constructed. First, the camera imaging matrix is described as the following formula [13]:

$$M = K[R|t]. \quad (1)$$

In the formula,

$$K = \begin{pmatrix} f_x & s & u_0 \\ 0 & f_y & v_0 \\ 0 & 0 & 1 \end{pmatrix}. \quad (2)$$

In the formula, K represents the projection transformation matrix; R and $t \in R^3$ represent the camera rotation matrix and the translation matrix in turn. The orientation and pose of the camera depend on the parameter sizes of these two matrices. Since there is no distortion behavior when the building is photographed, the distortion parameter s is equal to zero, and the world coordinate system is a symmetrical coordinate system, then $f_x = f_y = f$, which represents the focal length. We set the coordinates of the principal point to (u_0, v_0) ; according to the homogeneous coordinates, it can be known that the camera projection matrix irradiated to each cuboid vertex P_i and the two-dimensional point q_i in the building image are in a mutual contrast relationship, then

$$p_i = Mq_i. \quad (3)$$

We analyze the dual relationship between the geometric convergence of the parallelepiped on the surface of the 3D cuboid part and the camera's internal parameters, and we calculate it [14]. $\tau = f_x/f_y$ represents the aspect ratio of the camera, because $f_x = f_y = f$, so $\tau = 1$. We use the IAC notation to solve the camera's internal parameters, which is defined as the following formula:

$$\omega = K^{-T}K^{-1} = \begin{pmatrix} 1 & 0 & -u_0 \\ 0 & 1 & -v_0 \\ -u_0 & -v_0 & f^2 + u_0^2 + v_0^2 \end{pmatrix}. \quad (4)$$

Taking the world coordinate system in the scene as the center of the bottom surface of the cuboid, the projection of

the cuboid component in the image is realized by the orientation of the camera. We denote the corresponding vertex of the cuboid as the following formula:

$$\mu = L^{-T}\tilde{L} = \begin{pmatrix} l_1^2 & 0 & 0 \\ 0 & l_2^2 & 0 \\ 0 & 0 & 1 \end{pmatrix}. \quad (5)$$

In the formula, \tilde{L} represents the upper left matrix of L , and l_1 and l_2 represent the Euclidean morphological data of the cuboid. Assuming that C_i is the homogeneous coordinate $(\pm 1, \pm 1, \pm 1, 1)^T$ of the vertices in the cuboid space, after the camera calibration is completed, the unit coordinate data of the corner points in the world coordinate system can be deduced according to the formula (3), thereby constructing a three-dimensional interactive model of a combined building imaged by the camera, and its expression is the following formula:

$$\begin{aligned} F_i &= Mp_i\mu \\ &= K\omega LC_i \\ &= K\omega \begin{bmatrix} \tilde{L} & 0 \\ 0^T & 1 \end{bmatrix} C_i. \end{aligned} \quad (6)$$

The constructed 3D model of the building target can make the combined building facade clearer and more intuitive, and further ensure the accuracy of panoramic image stitching.

The process of constructing a 3D model of a building [15] is shown in Figure 2.

Since the building subject in a single building image captured by the camera occupies most of the area in the image [16], the imaging projected on the two-dimensional image often has perspective distortion, in order to resolve the ambiguity, the user needs to mark the 6 corners that can cover the 6 faces of the cuboid. In the camera calibration, set the origin of the world coordinate system as the center of the bottom surface of the cuboid, and the coordinate axes are aligned with the sides of the cuboid, in order to match the user's marked area with the two-dimensional projected image area of the cuboid component in the world coordinate system, using the camera model based on the geometric constraints of the parallelepiped, the internal and external parameters of the camera and the size parameters l_1 and l_2 of the cuboid are calculated.

3.2. Panoramic Stitching of Building Facade Images. In order to stitch a group of continuously shot building images into a panoramic image of building facade, the features of the overlapping area images should be matched first. Here, the ORB feature matching method is used, and the key points are analyzed by binary bit strings [17].

The basic principle of ORB descriptor is to use a small number of grayscale comparisons of image block characteristics to achieve accurate feature matching, with feature points as the center, the criterion for the $S \times S$ image block p is described as the following equation:

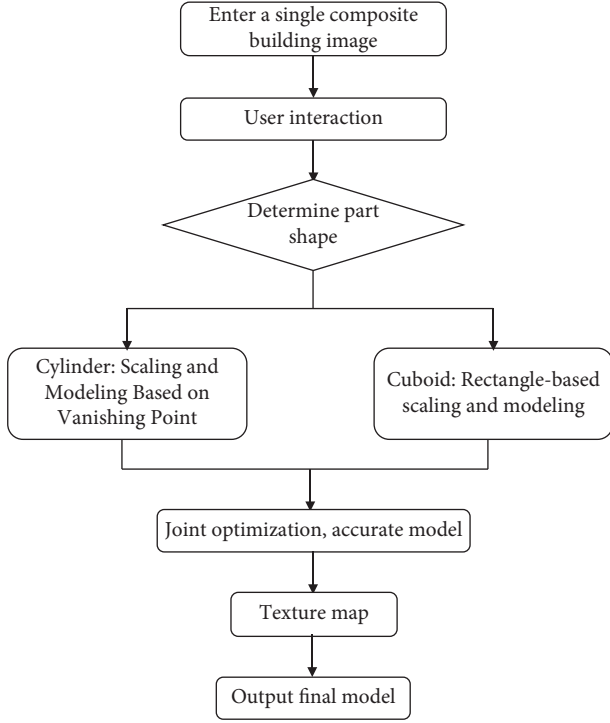


FIGURE 2: Method flow chart.

$$\tau(p; x, y) = \begin{cases} 1, & p(x) < p(y) \\ 0, & p(x) \geq p(y) \end{cases}. \quad (7)$$

In the formula, $p(x)$ is the pixel gray value of the image block p at the $x = (u, v)^T$ position by smoothing. If the binary feature quantities of $o(x, y)$ \bar{a} orientations are arbitrarily selected in the image block p , the analytical formula of the ORB feature function is the following formula:

$$f_o(p) = \sum_{1 \leq i \leq n} 2^{i-1} \tau(p; x_i, y_i) F_i. \quad (8)$$

Considering many factors, such as speed and precision, the value of o is set to 256.

Key points of measurement using the above process: a 256-bit string of binary bits can be obtained, where each bit has a value of 0 or 1. If D_1 and D_2 are binary bit strings of two key points, the following formulas

$$D_1 = x_0 x_1 x_2 \cdots x_{256}, \quad (9)$$

$$D_2 = y_0 y_1 y_2 \cdots y_{256}. \quad (10)$$

The plane homography represents the projection mapping from one plane to another, and the key includes three parts: the projection transformation matrix of the camera's internal parameters, the rotation matrix R , and the translation matrix t between the planes.

$M = (x, y, z)^T$ and $M' = (x', y', z')^T$ in turn represent the spatial coordinates of three-dimensional space points in

different viewpoint coordinate systems, $m = (x, y, 1)^T$ and $m' = (x', y', 1')^T$ represent the relative matching points of the two images in turn, then

$$\begin{aligned} m &\cong KM, \\ m' &\cong KM'. \end{aligned} \quad (11)$$

We mark the canonical vector of the plane π as n , then all the space points are $M \in \pi$, because of $n^T M = 1$, equations (12)~(14) can be obtained:

$$\begin{aligned} M' &= RM + t \\ &= (R + tn^T)M f_o(p), \end{aligned} \quad (12)$$

$$K^{-1}m' = (R + tn^T)K^{-1}M f_o(p), \quad (13)$$

$$m' = K(R + tn^T)K^{-1}m f_o(p). \quad (14)$$

In an environment with an open field of view, when the camera is rotated to capture images, it can be determined that the camera is doing pure rotation activities, and then the camera is calibrated from a set of overlapping images [18]. First, the homography matrix H_{ij} between all the coincident images is calculated, according to the correlation principle of the plane homography matrix, assuming that the camera performs pure rotation activities, the following formula can be obtained:

$$H_{ij} \cong K_i R_{ij} K_j^{-1}. \quad (15)$$

According to the orthogonality criterion of the rotation matrix R_{10} , equations (16) and (17) are obtained:

$$h_{00}^2 + h_{01}^2 + f_0^{-1} h_{02}^2 = h_{10}^2 + h_{11}^2 + f_0^{-1} h_{12}^2, \quad (16)$$

$$h_{00} h_{10} + h_{01} h_{11} + f_0^{-2} h_{02} h_{12} = 0, \quad (17)$$

where h is the height of the image. Since the image rotation matrix derived from the homography transformation between images is a correspondence matrix, the stitched images will be wavy. In order to make the final stitched image vertical, it is necessary to construct an overall rotating coordinate system.

We reflect the three-dimensional space point x_i to the point x_{ik} in the two-dimensional image, because in the process of capturing the image, the camera will produce irregular motion [19], but usually the horizontal edge of the camera is kept parallel to the ground. In order to build an overall rotating coordinate system, we need to set up a matrix r_g , multiply it by r_k to the right, and make sure that the overall y -axis is perpendicular to the x -axis. We combine the convergence conditions of all images into a set and transform it into a least squares problem:

$$\begin{aligned} r_{gl} &= \arg \min_r \sum_k (r^T r_{k0})^2 \\ &= r g \min_r r^T \left[\sum_k r_{k0} r_{k0}^T \right] r. \end{aligned} \quad (18)$$

The author uses the cylindrical coordinate projection method to map the image on the cylindrical surface. The point in the cylinder is determined by the angle θ and the height h parameter, and its relative correlation is the following formula:

$$(\sin\theta, h, \cos\theta) \propto (x, y, f). \quad (19)$$

Because the cylinder is a surface that can be unfolded, the image can be moved and rotated in the cylindrical coordinates to maintain the same shape, so the panoramic stitching of the building facade image is performed, and its expression is the following formula:

$$x = f \tan\theta = f \tan \frac{x'}{s}, \quad (20)$$

$$y = h \sqrt{x^2 + f^2} = \frac{y'}{s} f \sqrt{1 + \tan^2 \frac{x'}{s}} = f \frac{y'}{s} \sec \frac{x'}{s}.$$

Through the above process, the problem of insufficient viewing angle of the equipment can be effectively solved, a wide-field panoramic image can be obtained, and the real scene of the combined building facade can be fully displayed.

3.3. Realization of Vignetting Correction Based on the Surface Fitting. In the actual scene where the camera captures images, some light beams cannot be imaged at the splicing intersection due to the cover of the mirror, resulting in a decrease in the illumination at the junction, this phenomenon is the vignetting phenomenon formed by the splicing of camera mirrors [20, 21]. Since the reflection edge of the mirror and the optical axis are at an angle of 45° , the distance between the reflection point and the receiving screen is constantly changing, therefore, the vignetting distribution in the image plane also changes with the distance between the mirror and the receiving screen and produce corresponding changes. In addition, straight-edge diffraction is also one of the causes of camera mirror vignetting [22].

Traditional vignetting correction methods include look-up table method, progressive scan method, and function approximation method [23, 24]. The table look-up method needs to use the standard image to obtain the corresponding table of the vignetting coefficient in advance, so the same convergence must be met every time you shoot, and it is not suitable for panoramic shooting of combined building facades. The progressive scanning method uses the real image data to achieve line-by-line fusion, fuses the grayscale change of the full image, and then repairs it; if the grayscale of the two adjacent lines of the real image changes a lot, this method will generate linear fringes, which cannot guarantee the reliability of the final vignetting correction result. The function approximation method is to use multiple calibrations, the compensation elements of a single pixel under each illumination are calibrated, and then the compensation elements of each pixel are fused to obtain the vignetting repair analytical formula of the pixel, but the operation process of this method is relatively complicated.

The author proposes an image grayscale correction method based on the two-dimensional surface fitting, which can effectively improve many deficiencies of traditional methods. Specifically, it is described as the following formula:

$$f(x, y) = \tanh(r_x(x - x_0) + r_y(y - y_0)) + c. \quad (21)$$

In the formula, $x' = 1, 2, \dots, m, y' = 1, 2, \dots, n, r_x$ and r_y represent the attenuation rates along the x and y axis of the image, respectively, and (x_0, y_0) is the brightness center point of the reference image, which is also the normalized pixel coordinate; c is a constant offset value. As long as the appropriate x and y axis decay rates are obtained, the direction of its brightness change can be clearly defined, and the gray value of the pixel point, within the vignetting threshold, can also be corrected.

The author uses the steepest descent method to calculate the surface parameters, and obtains the relevant coefficients of the Hesse matrix, the Hesse matrix is used to gradually adopt iterative convergence, and finally the relevant parameter values of the surface are obtained. Based on this, a more accurate parameter estimation value is calculated, which meets the needs of vignetting correction of panoramic images in real scenes.

According to the degraded state of the real vignetting image, we use the two-dimensional curved surface of formula (21) to fit the degraded image. Using the same feature of vignetting as the correction basis, the image brightness attenuation will change with the change of the distance from each pixel to the image brightness center, but in actual operation, the known reference image brightness center is not the image center, so when solving the parameters, the formula (21) should be converted into a Column function, which is specifically defined as the following formula:

$$F(X) = \sum_{y=1}^n \sum_{x=1}^m [f(x, y) - f_{xy}]^2. \quad (22)$$

In the formula, f_{xy} represents the pixel value of the real image.

Because the gradient of the direct let is equal to zero, the solution process of the equations $x_0, y_0, r_x, r_y,$ and c will be very difficult, so the steepest descent method is used to solve the minimum value of F , satisfying $\varepsilon F^0 = F(X^0), g^0 = g(X^0) = \nabla F(X^0)k = 0$, then the gradient of the objective function $F(x_0, y_0, r_x, r_y, c)$ at point x is described as the following formula:

$$\begin{aligned} g(X) &= \nabla F(X) \\ &= \left(\frac{\partial F}{\partial x_0}, \frac{\partial F}{\partial y_0}, \frac{\partial F}{\partial r_x}, \frac{\partial F}{\partial r_y}, \frac{\partial F}{\partial c} \right)^T \\ &= (g_1, g_2, g_3, g_4, g_5)^T. \end{aligned} \quad (23)$$

Because the arctangent function contains the row function, that is, the e^x term, and the Taylor series is used for calculation, then the row function is recorded as formula

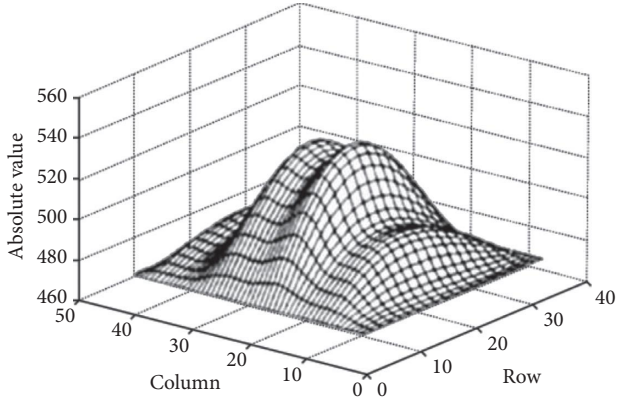


FIGURE 3: Grayscale distribution of the original vignetting image.

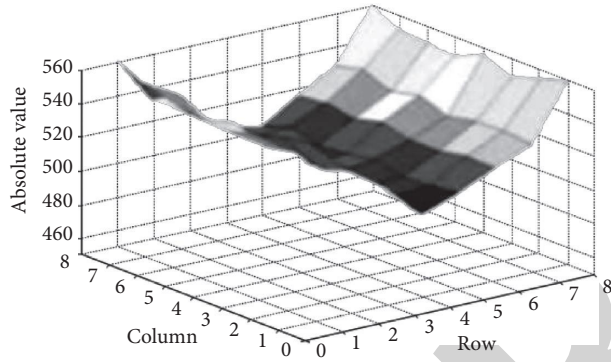


FIGURE 4: Vignetting surface fitting results.

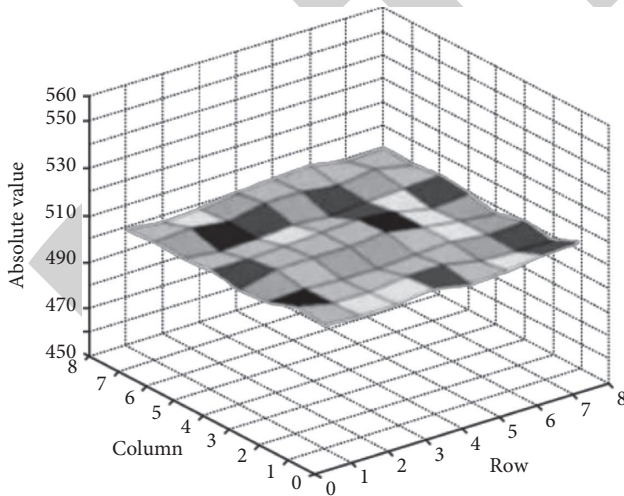


FIGURE 5: Grayscale distribution after surface correction.

(24). Considering the complexity of the method, only the first three items are selected to represent the row function.

$$e^x = 1 + x + \frac{1}{2}x^2. \quad (24)$$

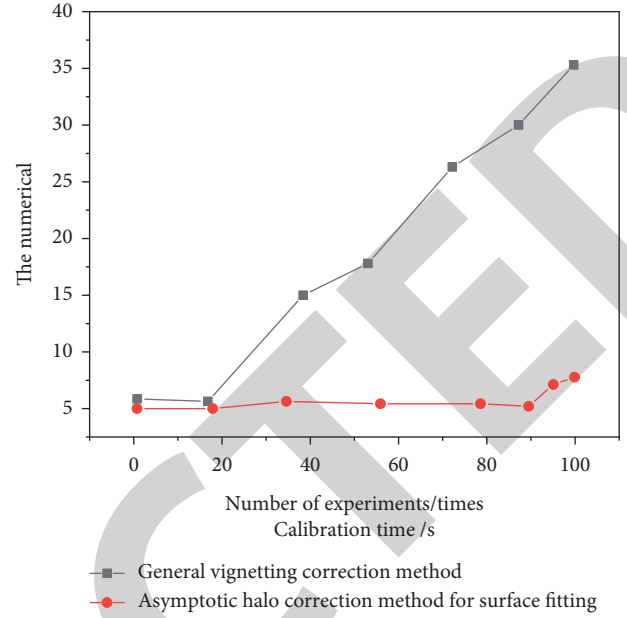


FIGURE 6: Comparison of vignetting correction time for panoramic images of building facades.

The above is the analysis of the vignetting correction principle of the proposed method, and it will be used in the actual correction process to simulate the vignetting correction, the calculation process is as follows:

First of all, in a theoretical sense, the steepest descent method can converge on random original values, if the original values are not selected properly, the convergence rate will be too slow, because in the real vignetting correction operation, in order to meet the convergence conditions $-0.5 < x_0 < 0.5$, $-0.5 < y_0 < 0.5$, therefore, the original value x_0 of X can be approximately selected as $v = \bar{f}_{xy}$, both x_0 and y_0 are located in the center of the image, and satisfy the correlation of equation (25). In this way, the original value can be iterated, and the convergence time is short, and accurate estimation results can be obtained.

$$\begin{aligned} r_x &= r_y \\ &= \sum_{x=1}^n \sum_{y=1}^m (f_{xy} - \bar{f}_{xy})^2. \end{aligned} \quad (25)$$

Then, we calculate the values corresponding to the following formulas:

$$t_k = \frac{(g^k)^T g^k}{(g^k)^T H^k g^k}, \quad (26)$$

$$X^{k+1} = X^k - t_k g(X^k), \quad (27)$$

$$F^{k+1} = F(X^{k+1}), \quad (28)$$

$$g^{k+1} = g(X^{k+1}). \quad (29)$$

If the corresponding value satisfies the convergence condition, then we end the calculation process and finally complete the vignetting correction of the panoramic image, effectively remove the vignetting phenomenon of the image, and further enhance the image quality. The convergence condition is the following formula:

$$\|g\| = \sqrt{g_1^2 + g_2^2 + g_3^2 + g_4^2 + g_5^2} < \varepsilon. \quad (30)$$

4. Results Analysis

In order to verify the effectiveness of the vignetting correction method of the combined building facade panoramic image proposed by the author, a simulation is carried out. The experimental environment is a Window10 operating system computer, the dual-core Intel second-generation Core processor OPTIPLEX3010 is the main frequency, the system is Win7 flagship 32-bit, and is implemented by MatlabR2014a programming. The author took aerial panoramic images of building facades as the experimental objects, and the test images were taken on the spot to collect image data, the environmental parameters of the camera used in the experiment are Sony A6000, with 24.3 million pixels, a 3-inch display screen, and 920,000 pixels, and a total of 4 photos were taken.

Due to the influence of camera vignetting, the brightness of the middle area of the data collected by the actual camera is obviously different, the image vignetting phenomenon is more serious, and its gray level change is shown in Figure 3.

Using the vignetting correction method based on surface fitting proposed by the author, the original vignetting image is processed, the surface parameters are calculated by the steepest descent method, and the vignetting surface is fitted according to the degradation state of the real vignetting image, and the fitting results as shown in Figure 4.

Using the surface fitting method, the vignetting surface of the combined building facade panoramic image is corrected, and the correction result is shown in Figure 5.

As can be seen from Figure 5, the overall distribution of image vignetting correction is basically uniform, and the vignetting phenomenon disappears.

Using the method proposed by the author, the vignetting phenomenon of the actual combined building facade panoramic image can be effectively removed, and the grayscale distribution of the corrected image is uniform and the effect is ideal. It can be seen that the correction accuracy of the author's method is high, and the curve trend is relatively stable, which can meet the high standard imaging of actual panoramic images. It is because the author's method for vignetting correction, considering the accuracy of panoramic image stitching, has good applicability [25].

In order to further verify the effectiveness of the author's method, the vignetting correction method of the surface fitting and the ordinary vignetting correction method are used, the vignetting correction of the combined building facade panoramic image is carried out, and the correction

time of the two methods is compared, the comparison results are shown in Figure 6.

According to Figure 6, it can be seen that the vignetting correction time of the combined building facade panoramic image using the vignetting correction method of the surface fitting is compared with the common vignetting correction method; the vignetting correction time of the combined building facade panoramic image is shorter, and it is stable at about 5 seconds.

5. Conclusion

In order to effectively enhance the imaging quality of panoramic images of combined building facades, the author proposes a vignetting correction method based on the surface fitting, corrects vignetting in panoramic images of combined building facades. By establishing a 3D interactive model, we can intuitively understand the facade form of the combined building and ensure the accuracy of panoramic image stitching. Using the panoramic image stitching method, we improve the problem of the insufficient viewing angle of equipment and obtain a wide-field panoramic image. We use the surface fitting method to solve the image vignetting phenomenon, shorten the image vignetting correction time, and realize high-quality imaging of combined building facade panoramic images. In the follow-up work, various geometric primitives, such as sphere and cone, can be added to realize more complex combined building model reconstruction.

Data Availability

The data used to support the findings of this study are available from the corresponding author upon request.

Conflicts of Interest

The authors declare that there are no conflicts of interest.

Acknowledgments

This work was supported by the Jilin Jianzhu University 2021 First-Class Undergraduate Course Construction Project "Advanced Drawing Technology (Architecture) Double Innovation Training, No. 2021050."

References

- [1] Y. Wu and Y. Chen, "Influence of virtual imaging technology based on html5 technology on digital painting," *Microprocessors and Microsystems*, vol. 82, no. 9, Article ID 103855, 2021.
- [2] H. Nghiem, "An efficient method for yield and failure surfaces of the steel i-section," *Advanced Steel Construction*, vol. 16, no. 3, pp. 246–254, 2020.
- [3] Z. C. Li, G. H. Wang, J. W. Hao et al., "The influence of construction scheme of asymmetric three-cabin utility tunnelling on the surface settlement behaviour," *KSCE Journal of Civil Engineering*, vol. 25, no. 9, pp. 3568–3582, 2021.
- [4] G. L. Feng, X. T. Feng, B. R. Chen et al., "Characteristics of microseismicity during breakthrough in deep tunnels: case

Retraction

Retracted: Video Image Processing Method Based on Cloud Platform Massive Data and Virtual Reality

Mathematical Problems in Engineering

Received 26 September 2023; Accepted 26 September 2023; Published 27 September 2023

Copyright © 2023 Mathematical Problems in Engineering. This is an open access article distributed under the Creative Commons Attribution License, which permits unrestricted use, distribution, and reproduction in any medium, provided the original work is properly cited.

This article has been retracted by Hindawi following an investigation undertaken by the publisher [1]. This investigation has uncovered evidence of one or more of the following indicators of systematic manipulation of the publication process:

- (1) Discrepancies in scope
- (2) Discrepancies in the description of the research reported
- (3) Discrepancies between the availability of data and the research described
- (4) Inappropriate citations
- (5) Incoherent, meaningless and/or irrelevant content included in the article
- (6) Peer-review manipulation

The presence of these indicators undermines our confidence in the integrity of the article's content and we cannot, therefore, vouch for its reliability. Please note that this notice is intended solely to alert readers that the content of this article is unreliable. We have not investigated whether authors were aware of or involved in the systematic manipulation of the publication process.

Wiley and Hindawi regrets that the usual quality checks did not identify these issues before publication and have since put additional measures in place to safeguard research integrity.

We wish to credit our own Research Integrity and Research Publishing teams and anonymous and named external researchers and research integrity experts for contributing to this investigation.




The corresponding author, as the representative of all authors, has been given the opportunity to register their agreement or disagreement to this retraction. We have kept a record of any response received.

References

- [1] M. Liu, R. Xue, and X. Li, "Video Image Processing Method Based on Cloud Platform Massive Data and Virtual Reality," *Mathematical Problems in Engineering*, vol. 2022, Article ID 2802901, 7 pages, 2022.

Research Article

Video Image Processing Method Based on Cloud Platform Massive Data and Virtual Reality

Ming Liu , Renzheng Xue , and Xiaoye Li 

School of Computer and Control Engineering, Qiqihar University, Qiqihar 161006, China

Correspondence should be addressed to Renzheng Xue; 19401109@smail.cczu.edu.cn

Received 23 May 2022; Revised 20 June 2022; Accepted 4 July 2022; Published 22 July 2022

Academic Editor: Hengchang Jing

Copyright © 2022 Ming Liu et al. This is an open access article distributed under the Creative Commons Attribution License, which permits unrestricted use, distribution, and reproduction in any medium, provided the original work is properly cited.

In order to solve the practical problem that the massive video data generated by monitoring equipment cannot be processed efficiently temporarily, this paper proposes a framework for face recognition of massive video data based on distributed environment. Combined with the application features of face recognition, this method designs a strategy for fast reading of massive video data and optimizes the feature data obtained by the cloud platform, so as to speed up the retrieval speed of face features. The results are as follows: the compression rate of the proposed compression method is higher than that of the traditional matrix triple and binary methods, which is increased by about 65%; the data optimization method in this paper greatly reduces the amount of feature data, which is 7.08 times less than that in the nonoptimization state. At the same time, the process of face recognition is reduced from 12.6 seconds to 2.73 seconds, and the time of feature decompression is only 0.75 seconds more than the original; the experiment shows that it takes 10180 seconds for the system to process 200 GB pictures with 9 computing nodes, and the total running time of the system is 4737 seconds longer than that of a single node, accounting for about 5.45% of the total time of a single node system. At the same time, the experimental data show that the system is 8.53 times faster than that of a single node with 9 computing nodes. It is proved that this framework has certain research significance in dealing with massive unstructured data. It not only provides theoretical reference value for the research of massive video processing but also makes a contribution to the actual industry.

1. Introduction

With the development of the Internet and the doubling of Internet data, the Internet has entered the era of big data. The four characteristics of big data can be summarized as “4V”: Massive data scale (VAST), fast data flow (Velocity), rich data types (Variety), and huge data value (Value). In terms of data scale alone, it took about one year for the global Internet to generate data of 1ep in 2001, one day in 2013, and only half a day in 2016. Moreover, the world produces new data at a growth rate of 40% every year. So far, the total amount of global information can double every two years. In 2012, the total amount of global data has reached 1.87 zb, and this number will double every two years [1]. By 2020, the total amount of data in the world will reach 35 to 40 zb.

Big data not only refers to massive data but also has a variety of structures, including all kinds of structured data

and unstructured data (such as video files, audio files, and pictures). In addition, the massive data may also include missing data and incomplete data, which pose severe challenges to data processing [2].

The emergence of big data technology makes it possible to quickly process massive data. Effectively mining the information in big data will greatly promote the development of society. In practical application, social security or public security criminal investigation often need to obtain face information from video. In the face of massive video data, it has become impossible to manually find or borrow the processing capacity of a single machine. With the help of big data computing framework deployed on cheap machine cluster or cloud platform, face recognition of massive video can effectively reduce the labor cost of traditional methods. This framework for fast processing massive video needs to be highly scalable, fast

processing massive data, and timely responding to user needs [3].

2. Literature Review

On the one hand, with the rapid growth of Internet data, relying on high-performance computing to complete data processing has encountered a bottleneck. The reason is that high-performance computers are confined to the existing hardware technology. With the improvement of processing speed, the cost for performance improvement research will also increase significantly, but the performance improvement is often not very significant. The traditional way of processing massive data cannot meet the explosive demand of the Internet. On the other hand, since 2003, big data processing platforms for massive data have been put forward continuously. So far, there has been a very rich ecosystem of big data processing technology. This provides another idea for the processing of big data to improve the computing power vertically. By expanding the ordinary PC horizontally, the processing of massive data can be completed [4]. In recent years, with the continuous development of cloud computing technology, cloud computing technology is known as the third wave of science and technology after personal computer technology and Internet technology. Cloud computing integrates heterogeneous computing resources, virtualizes computing resources, and provides users with an on-demand charging mode. Cloud computing technology greatly improves the efficiency of dynamic management of computing resources in big data services. Many Internet companies in the world are also popular with cloud computing technology and provide convenient PAAS services or SaaS services. The combination of big data processing platform and cloud computing technology makes big data processing technology more convenient and easy to use in terms of computing resources such as network, storage, and CPU, which also leads to the research frenzy of international companies and research institutions in the fields related to cloud computing technology and big data, which also greatly promotes the rapid development of big data and finally forms a complete and rich big data ecological environment [5].

It has been ten years since Google put forward the concept of cloud computing in 2006. Cloud computing plays an important role in big data processing. Similarly, from the release of distributed file system GFS and distributed processing frame MapReduce by Google in 2003 to the big data processing platform, after more than ten years of accumulation, big data processing technology has made great strides. Today's big data ecosystem has developed components of various computing services centered on Hadoop. The whole big data ecosystem has covered all aspects of big data application [6].

Based on the current research, this paper designs a framework for face recognition of massive video data. Combined with the characteristics of face recognition task, a reading model for unstructured data such as video is proposed, and the face feature data is optimized while extracting face features, which makes the distributed computing

platform process massive video with high scalability and rapidity, and provides a feasible framework for the application of massive video face recognition. Through the implementation and testing on spark platform, the feasibility of the framework proposed in this paper is proved. The framework in this paper is suitable for the task of finding a target character from massive videos in the context of big data. It provides an idea for distributed computing platform to read massive videos, and provides an optimization method of face image feature data in the context of big data [7].

3. Research Methods

3.1. Distributed Computing Platform. After Google put forward GFS and MapReduce technology, it implemented it and opened source to form today's Hadoop ecosystem components. The initial open source projects were HDFS and MapReduce as distributed file system and distributed computing framework, respectively. On this basis, many rich big data applications have been established. Hadoop distributed system is mainly divided into two parts: HDFS distributed file system and MapReduce computing framework [8].

3.1.1. HDFS Distributed File System. The function of distributed file system is to transfer file information to other nodes through sharing among multiple servers. This method is very important for distributed system. Moreover, in terms of function, the distributed file system should allow users to access file services. On this basis, it should ensure that the quality of service of the whole system can approach or exceed the performance of the local file system. The distributed file system is implemented on the basis of cloud computing and provides users with remote file system services. However, this design should also ensure the transparency of the distributed file system, so that users cannot feel the existence of the distributed file system, and cannot be inferior to the local file system in operation and service quality. This transparency is a key, which is directly related to the user experience. In addition, in the implementation of the distributed file system, the distributed file system should ensure its high availability, that is, to provide users with a convenient, available, and secure file system. At the same time, the distributed file system should consider more problems than the local file system, such as the support of concurrent access to the file system and the consistency of multiple copies, writes, and modifications of data [9].

The system architecture of HDFS is a typical master-slave framework. The architecture diagram of HDFS file system is shown in Figure 1. The whole HDFS cluster consists of one NameNode, one SecondaryNameNode, and several DataNode. NameNode is the central control node, which is responsible for the management of files in the whole file system. The NameNode responds to the file access request sent by the client and returns the file storage location on the NameNode to the client. The NameNode controls the DataNode through the control command on the

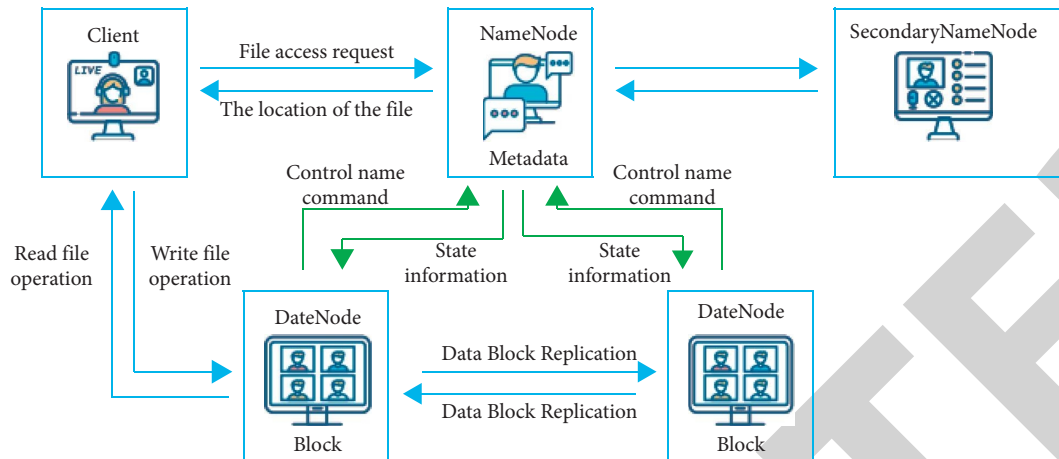


FIGURE 1: Framework of HDFS file system.

management file system. The DataNode sends the status information on the local node to the NameNode through the heartbeat mechanism. When the heartbeat stops, the NameNode will deal with the stopped node accordingly [10]. In this master-slave mode system, the shutdown of the master node will cause the collapse of the whole system. Therefore, the SecondaryNameNode backs up the data on the NameNode. When the NameNode fails and stops working, the SecondaryNameNode can use the previous backup data to provide services for the slave node.

3.1.2. MapReduce Computing Model. MapReduce is an important basic computing model in the Hadoop system. Other plugins in Hadoop ecology usually take MapReduce as the basic framework. When processing massive datasets, MapReduce abstracts the whole calculation process into two processes: map and reduce. Map processes the datasets of K/V key value pairs, and reduce regulates the processing results [11].

When implementing MapReduce programming, mapper function and reducer function need to be implemented. Mapper function is to process the input K/V key value pair. When dealing with key value pairs, MapReduce does not require too many input and output types of K/V. MapReduce provides many implementation interfaces. Users can customize different data K/V types according to their own needs. Mapper function is to process the data fragments generated when the MapReduce framework calls jobs. Each mapper corresponds to a data fragment, and the output of map does not require one-to-one correspondence with the input. The job execution process of MapReduce is shown in Figure 2.

3.2. Spark Distributed Computing System. Spark was born in AMPLab at the University of California, Berkeley, in 2009. At present, spark has become a project level opensource project under the Apache Software Foundation [12]. Spark can be regarded as an alternative to MapReduce. It can be compatible with HDFS and hive distributed storage layers, and can be integrated into Hadoop ecosystem to make up for the shortcomings of MapReduce.

Spark is a big data parallel computing framework based on memory computing. Based on memory computing, spark improves the real-time performance of data processing in the big data environment, ensures high fault tolerance and high scalability, and allows users to deploy spark on a large number of cheap hardware to form a cluster [13]. Spark's architecture also adopts the master-slave model in distributed computing. Master is the node running the master process in the cluster, and slave is the node running the worker process in the cluster. The role of master is the same as that of JobTracker in MapReduce, which controls the operation of the whole cluster and is responsible for the normal operation of the whole cluster; the worker is the same as the TaskTracker in MapReduce. As a computing node in the cluster, it receives commands from the master node and reports the status of its own node to the master node. The executor is responsible for task execution: the client is mainly used as a client for users to submit applications, while the driver controls the execution of the whole application and prints the log of control results. The architecture of spark is shown in Figure 3.

3.3. Machine Learning Face Recognition Method. There are many kinds of traditional machine learning methods for face recognition: knowledge-based method, feature invariant method, template matching method, and appearance-based method. This paper mainly deals with the massive video carried out by spark without too much discussion on the technology of face recognition [14].

The Eigenface method reduces the dimension of the pixel matrix through PCA and finally determines whether it is the same person by calculating the distance of pixels in the low dimensional space. The algorithm is described as follows:

Let $X = \{x_1, x_2, \dots, x_n\}$ represent a random feature, where $x_i \in R^d$.

- (1) First, calculate the mean vector μ , as shown in formula (1):

$$\mu = \frac{1}{n} \sum_{i=1}^n x_i. \quad (1)$$

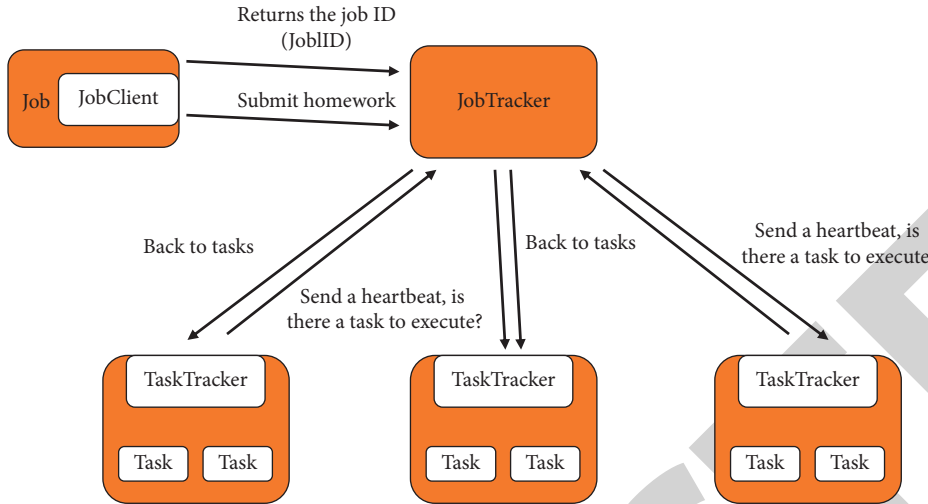


FIGURE 2: MapReduce job execution flowchart.

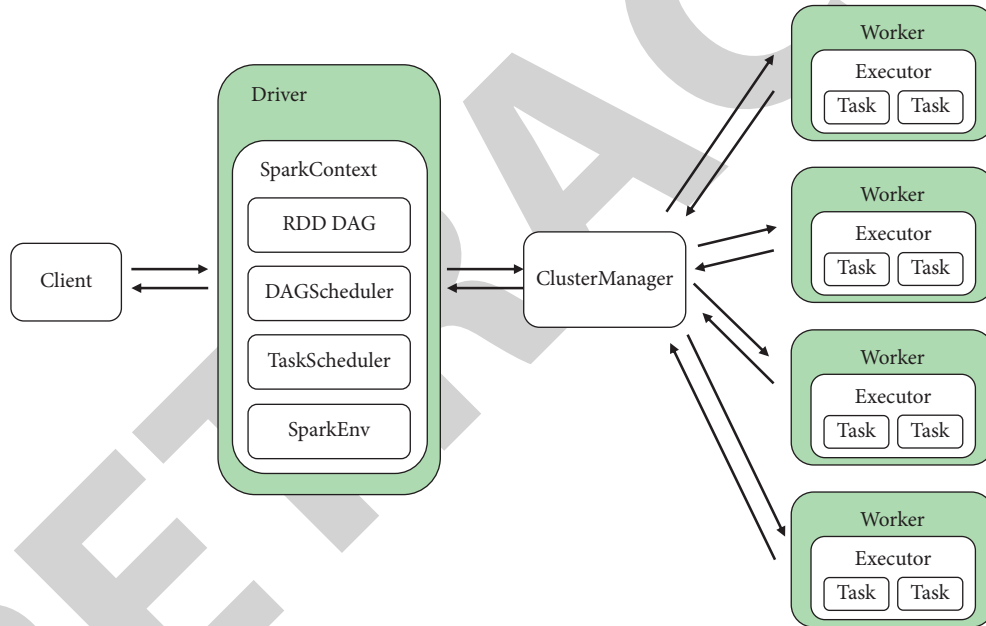


FIGURE 3: Spark structure frame.

(2) Calculate the covariance matrix S , as shown in formula (2):

$$S = \frac{1}{n} \sum_{i=1}^n (x_i - \mu)(x_i - \mu)^T. \quad (2)$$

(3) Calculate the eigenvalue of S and the corresponding eigenvector, as shown in equation (3):

$$Sv_i = \lambda_i v_i, \quad i = 1, 2, \dots, n. \quad (3)$$

(4) The eigenvalues and their corresponding eigenvectors are sorted in descending order, and the K principal components are the eigenvectors corresponding to the largest feature. The K principal components y of X are shown in formula (4):

$$y = W^T(x - \mu), \quad W = v_1, v_2, \dots, v_k. \quad (4)$$

(5) Reconstruct feature x , as shown in equation (5):

$$x = Wy + \mu. \quad (5)$$

After PCA dimensionality reduction, the feature quantity encodes the face features and illumination.

3.4. Massive Video Face Recognition Technology. A video processing method implemented on HBase is proposed by scholars. The video is transformed into video frame image, which is processed by the coprocessor of HBase. Coprocessor is similar to a database trigger, which triggers the action when

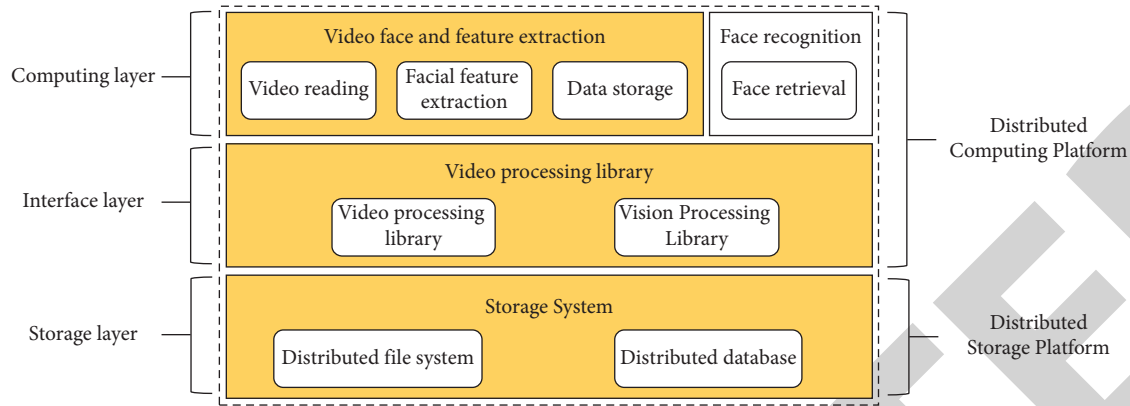


FIGURE 4: Distributed massive video face recognition framework.

operating the table. The data table, face table, and keypoint table are designed on HBase to store the image, the extracted face, and face features, respectively. When processing video frame images, the face detection and feature extraction are completed in coprocessor, and the matching of face features by HBase is used to find the face in a specific image [15]. However, because the extracted frame video pictures are extracted from continuous frames, even if the contents of the pictures are not different, they are processed, which produces redundant information. The processing is not only time consuming, but also the amount of data information is often larger than the amount of original video data. This paper proposes a method to extract the key frames of video pictures on the basis of solving the problem of increasing the amount of data after video decompression [16].

Therefore, in the implementation of massive video face recognition framework, the face recognition data processing scene is different from the application of massive video transcoding. The data segmentation granularity of video data transcoding is larger than that of video face processing. The method used for video transcoding is not suitable for massive video face recognition [17]. In the aspect of video data reading, the smaller granularity of video data processing can transform video processing into picture processing.

The process of massive video face and feature extraction is shown in Figure 4. This framework includes a distributed file system for storing massive video files, a distributed computing framework for processing massive video, and a distributed database for storing processing results. The distributed database has the ability to store massive data and provides reliable security. For example, in the implementation part of this paper, massive video data is stored in HDFS, and HDFS completes the fault-tolerant storage of data. The default number of backups of HDFS is 3. In the cloud computing environment, HDFS ensures the fault-tolerant and disaster tolerant ability of data by storing the same data in any server, servers in the same rack, and servers in different racks [18].

4. Result Analysis

4.1. Comparison of Algorithm Compression. The two designed feature extraction and optimization methods are tested, respectively. Firstly, the proposed compression

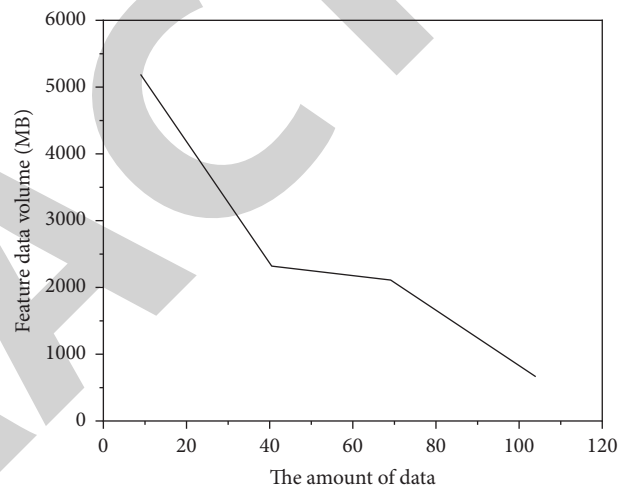


FIGURE 5: Comparison of data volume of different compression methods.

method is compared with the traditional triple and binary methods [19]. In this paper, a total of 82,060 face features are extracted, and the amount of data achieved by the three methods is compared. However, because the implementation of the algorithm may be different, the running time is not compared is shown in Figure 5 [20].

After comparison, it is found that the compression rate of the compression method proposed in this paper is higher than that of the traditional matrix triple and binary methods.

4.2. Comparison of Operation Time. In order to test whether the optimization of LBP feature vector in this paper reduces the execution time of the framework, this paper carries out compression and non compression experiments on 144,880 face feature data obtained from 200 GB video data processing [21]. The experimental platform consists of 10 Intel-i3-4130 quad core processors, 8 GB memory, Ubuntu14.01 operating system, one master node, and nine slave nodes, as shown in Table 1.

The experimental results are shown in Table 1. The data optimization method in this paper greatly reduces the amount of feature data, which is 7.08 times less than the data

TABLE 1: Results of compressed and uncompressed characteristic data.

	Compressed	Uncompressed	Proportion
Characteristic data volume	1269 MB	8996 MB	1 : 7.08
Retrieval time	2.73 s	12.60 s	1 : 4.62
Feature processing time	2.31 s	1.56 s	1.48 : 1

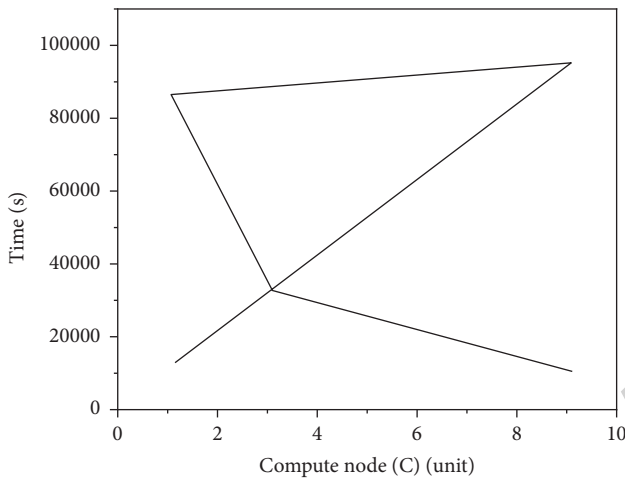


FIGURE 6: Scalability of spark face recognition for massive video faces.

in the non optimization state. At the same time, the process of face recognition is reduced from 12.6 seconds to 2.73 seconds, and the time of feature decompression is only 0.75 seconds more than the original. Experiments show that the data optimization method in this paper greatly reduces the amount of feature data and the total running time of the framework [22].

4.3. Extensibility Verification of Spark Face Recognition for Massive Video Faces. In order to verify the scalability of the framework for processing video data, the system sets the worker nodes to 1, 3, 5, 7, and 9, respectively, in Spark's standalone mode. The scalability of video processing in this framework is tested by measuring the time taken to process 200 GB data [23]. The experimental results are shown in Figure 6.

The experiment shows that it takes 10180 seconds for the system to process 200 GB pictures with 9 computing nodes, and the total running time of the system is 4737 seconds longer than that of a single node, accounting for about 5.45% of the total time of a single node system. At the same time, the experimental data show that the system is 8.53 times faster than that of a single node with 9 computing nodes. Therefore, with the increase of processing nodes, the acceleration ratio of the system basically increases linearly, the total running time of the system increases less, and the system has good scalability [24, 25].

5. Conclusion

With the extensive application of monitoring equipment in the field of social security, the video data generated by monitoring equipment gradually exceed the traditional storage, management, and analysis ability. The massive video data generated by these equipment is of great significance to social security and public security criminal investigation. At the same time, it also has high requirements for the timeliness of these data processing. Since entering the new century, with the continuous development of computer technology, cloud computing technology has been applied. This provides convenient and easy-to-use computing, storage, network, and other resources for massive data processing. With the development of the times and the popularity of intelligent devices, massive big data is in urgent need of an effective method for processing. The massive video data processing technology developed on the basis of cloud computing is applied. The big data processing platform represented by Hadoop Spark provides a technology that integrates storage, processing, query, and other general functions for massive data. These technologies not only have the computing power to deal with massive video but also have a good guarantee in aspects not involved in traditional technologies such as data fault tolerance. This paper designs a framework for face recognition of massive video data in a distributed environment, which provides an application that can query the target characters in massive surveillance video in a short time for the fields of public security and criminal investigation.

Data Availability

The data used to support the findings of this study are available from the corresponding author upon request.

Conflicts of Interest

The authors declare no conflicts of interest.

Acknowledgments

Heilongjiang Province Education Department Scientific Research Project (Project no. 135309465).

References

- [1] P. Liu, J. Wang, Z. Wang, Z. Zhang, and D. G. Dorrell, "Cloud platform-oriented electrical vehicle abnormal battery cell detection and pack consistency evaluation with big data: devising an early-warning system for latent risks," *IEEE Industry Applications Magazine*, vol. 28, no. 99, pp. 2–13, 2021.
- [2] X. Feng, F. Yan, X. Y. Liu, and Q. Jiang, "Development of IoT cloud platform based intelligent raising system for rice seedlings," *Wireless Personal Communications*, vol. 122, no. 2, pp. 1695–1707, 2021.
- [3] N. Zhang, "A cloud-based platform for big data-driven CPS modeling of robots," *IEEE Access*, vol. 9, no. 99, p. 1, 2021.
- [4] R. KumarKumar and A. SharmaSharma, "Risk-energy aware service level agreement assessment for computing quickest

Retraction

Retracted: Application of Data Image Encryption Technology in Computer Network Information Security

Mathematical Problems in Engineering

Received 8 August 2023; Accepted 8 August 2023; Published 9 August 2023

Copyright © 2023 Mathematical Problems in Engineering. This is an open access article distributed under the Creative Commons Attribution License, which permits unrestricted use, distribution, and reproduction in any medium, provided the original work is properly cited.

This article has been retracted by Hindawi following an investigation undertaken by the publisher [1]. This investigation has uncovered evidence of one or more of the following indicators of systematic manipulation of the publication process:

- (1) Discrepancies in scope
- (2) Discrepancies in the description of the research reported
- (3) Discrepancies between the availability of data and the research described
- (4) Inappropriate citations
- (5) Incoherent, meaningless and/or irrelevant content included in the article
- (6) Peer-review manipulation

The presence of these indicators undermines our confidence in the integrity of the article's content and we cannot, therefore, vouch for its reliability. Please note that this notice is intended solely to alert readers that the content of this article is unreliable. We have not investigated whether authors were aware of or involved in the systematic manipulation of the publication process.

Wiley and Hindawi regrets that the usual quality checks did not identify these issues before publication and have since put additional measures in place to safeguard research integrity.

We wish to credit our own Research Integrity and Research Publishing teams and anonymous and named external researchers and research integrity experts for contributing to this investigation.

The corresponding author, as the representative of all authors, has been given the opportunity to register their agreement or disagreement to this retraction. We have kept a record of any response received.

References

- [1] L. Li, "Application of Data Image Encryption Technology in Computer Network Information Security," *Mathematical Problems in Engineering*, vol. 2022, Article ID 8963756, 7 pages, 2022.

Research Article

Application of Data Image Encryption Technology in Computer Network Information Security

Li Li 

Teacher's College, Xi'an University, Xi'an 710065, China

Correspondence should be addressed to Li Li; 18404202@masu.edu.cn

Received 22 May 2022; Revised 22 June 2022; Accepted 29 June 2022; Published 21 July 2022

Academic Editor: Hengchang Jing

Copyright © 2022 Li Li. This is an open access article distributed under the Creative Commons Attribution License, which permits unrestricted use, distribution, and reproduction in any medium, provided the original work is properly cited.

In order to solve the practical problem that the security of computer network information cannot be guaranteed, which seriously affects the network performance, the author proposes a public key data encryption system based on PKI. The system proposed by the author is based on the public key cryptographic algorithm RSA, including implementation of data encryption and digital signature and key distribution, an improved RSA algorithm is proposed for the slow speed of RSA. The result obtained is as follows: after reasonable selection of parameters and the use of optimized algorithms (also known as combined algorithms), the RSA algorithm is about 1.0% to 2% more efficient than the traditional algorithm, to a certain extent, the operation efficiency of the RSA algorithm is improved, and the purpose of improving the RSA algorithm is achieved. It is proved that the public key data encryption system is of great significance for modern computer network information encryption and maintaining a green and secure network environment.

1. Introduction

In recent years, the Internet has penetrated more and more deeply into people's lives due to its simplicity, convenience, and low cost, it has become the main means of the people's information exchange [1]. The original traditional information media such as paper, film, and tape have given way to electronic media. People can inquire about information on the Internet through network portals, or exchange information on the Internet through e-mail and BBS, all of which greatly improve people's work efficiency [2].

The Internet can not only provide people with information but also make it possible to develop online e-commerce such as online shopping and online bookstores, which greatly affects people's lives. At the same time, the emergence of e-commerce marks the expansion of the Internet from a network that mainly provides information services to the commercial field, which can attract more funds to invest in the construction of the Internet, thereby promoting the development of the network [3].

The development of the network has brought unprecedented convenience to people, but also brought new challenges to people [4, 5]. A large amount of data is

transmitted on the Internet every day, including web content with relatively low security requirements, emails with relatively high security requirements, and e-commerce transaction data requiring high confidentiality. All of these have put forward higher requirements for data security on the Internet [6, 7]. Due to the openness of the Internet itself, every user who surfs the Internet becomes both a beneficiary of the network and a destroyer of the network [8]. Also due to the disorder of the current Internet network, the network order is basically in an unreliable state. Therefore, it is required to perform encryption/decryption, signature/verification, and other work on the data transmitted by online users to ensure their own online security.

The rapid development of computer networks has brought mankind into the information age. The transparent transmission characteristics of the network bring people a lot of conveniences and high efficiency, but at the same time, it also brings many information security problems. An important problem to be solved urgently in the development, among them, how to ensure the safe transmission of information in the network, is a very important subject of network security. Through the analysis of computer network security and cryptographic

technology, it can be determined that cryptographic technology is a basic technology in information security technology, and encrypting files transmitted through the network is an effective way to ensure file security. Based on the in-depth study of the current most advanced data encryption technology, this subject proposes an application of data image encryption technology in computer network information security. The system fully combines a symmetric key encryption algorithm, a public key encryption algorithm, and data signature technology to provide a feasible operation mode for fast and safe transmission of confidential documents, and also for the establishment of a perfect and strict computer network security mechanism. Preliminary lay the foundation for practice. This network file encryption system is mainly designed for some specific departments and enterprises and has a relatively important practical application value.

2. Literature Review

With the vigorous development of computer networks, the increasing number of network services, and the in-depth and extensive development of e-commerce, the confidentiality, integrity, and availability of information has never been more important. Cryptography is an old and young science [9]. Say it is ancient; it is because humans used simple cryptography thousands of years ago, in order to preserve and transmit classified political and military information. But the cryptographic ideas and technologies of this period were not so much a science as an art [10] because at this time, when cryptographers design and analyze cryptographic algorithms, they mainly rely on intuition and manual calculations, and there is no strict theory as the basis.

Rani and others laid the theoretical foundation of information theory, which gave birth to the new science of cryptography [11]. However, during this period, due to the restrictions of various governments, and the application of cryptography was generally limited to the government and military departments, the research on cryptography did not achieve much. Liu et al. have well summarized the previous development of cryptography, thus widely spreading the idea of cryptography [12].

Kanwal et al. led a revolution in cryptography, proving for the first time that secure communication without a shared key between the sender and the receiver is possible, thus ushering in a new era of public key cryptography [13]. The cryptosystems used before this all belong to the private key cryptosystem, that is, the sender and the receiver of information use the same or similar key, and the key needs to be negotiated and transmitted before information is transmitted, as shown in Figure 1 for the data encryption system model [14, 15]. Subsequently, the first practical public key cryptosystem, RSA, was proposed. Today, RSA is still one of the most popular public key cryptosystems. At the same time, the US National Bureau of Standards (NBS) recognized the important commercial use of cryptography, so it solicited and published the US data encryption standard DES in 1977 [16]. The publication of the DES

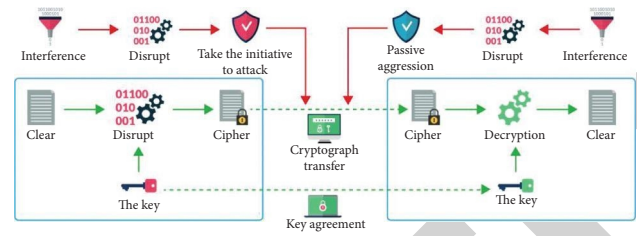


FIGURE 1: Data encryption system model.

encryption standard was quickly recognized and adopted by many companies and institutions and was then widely used in many industrial and commercial fields [17]. However, with the rapid improvement of computing technology (software and hardware) and the in-depth development of cryptography research, DES was broken in 1998 [18]. In October 2000, the United States solicited the AES (Advanced Encryption Standard) cipher algorithm [19] instead of DES.

In recent years, with the proposal and implementation of the action plan for establishing a public key infrastructure (PKI), the idea of automatic key distribution based on the PKI layered structure has also been born. This is a safer and faster automatic key distribution system [20]. In order to solve the security problem of the Internet, countries all over the world have carried out research on it for many years and initially formed a complete set of Internet security solutions, that is, the currently widely used PKI architecture. PKI architecture adopts the certificate management public key and binds the user's public key and the user's other identification information (such as name, e-mail, and ID number), on the Internet, verifying the user's identity; PKI architecture combines public key cryptography and symmetric cryptography to realize automatic key management on the Internet to ensure the confidentiality and integrity of online data [21].

Based on the current research, the author proposes a scheme to improve the RSA algorithm, and the scheme is based on RSA parameter selection and the optimization algorithm itself to achieve the improvement of the RSA algorithm and has been verified in the experiment: compared with the traditional RSA algorithm, the improved RSA algorithm has higher encryption speed.

3. Research Methods

3.1. Symmetric Key Encryption. The symmetric algorithm is sometimes called the traditional cryptographic algorithm, that is, the encryption key can be deduced from the decryption key, and vice versa [22]. In most symmetric algorithms, the encryption/decryption keys are the same. These algorithms are also called secret-key algorithms or single-key algorithms, which require the sender and the receiver to agree on a key before secure communication [23]. Symmetric algorithms rely on keys, and revealing the key means that anyone can encrypt/decrypt messages. As long as the communication needs to be kept secret, the key must be kept secret.

Some parameters are explained as follows: M: plaintext; C: ciphertext; E: encryption algorithm; D: decryption algorithm; k: key.

The encryption and decryption of the symmetric cryptographic algorithm is expressed as

$$E_k(M) = C, \quad (1)$$

$$D_k(C) = M. \quad (2)$$

Symmetric algorithms can be divided into two categories. A class of algorithms that operate only on a single bit (sometimes a byte) in the plaintext is called a sequence algorithm or sequence cipher [24]. Another type of algorithm is to operate on a group of bits of the plaintext, these groups of bits are called blocks, and these corresponding algorithms are called block algorithms or block ciphers. Typical block lengths for modern computer cryptographic algorithms are 64 bits, 128 bits, and 256 bits.

3.2. Public Key Cryptography. The key to designing a public key cryptosystem is to find a suitable one-way function first, and most public key cryptosystems are established based on the difficulty of computing the inverse of a one-way function [25]. For example, the RSA system is a typical implementation based on the one-way function model.

Among all the public key cryptosystems so far, the RSA system is the most famous one. This algorithm has been recommended as the public key data encryption standard by the data encryption technology subcommittee SC20 of ISO/TC97. The security of the RSA algorithm is based on a characteristic fact in number theory: combining two large prime numbers into one large number is easy, but the reverse process is very difficult. Under today's technical conditions, when n is large enough, in order to find d , it is extremely difficult or even impossible to find p and q corresponding to d from n through prime factorization. It can be seen that the security of RSA depends on the digit length of the large number n as the public key. In order to ensure sufficient security, it is generally believed that current personal applications need to use 384 or 512 bits of n , companies need to use 1024 bit n , and in extremely important cases, 2048 bit n .

In practical applications, users can ensure the confidentiality of data transmission by using encryption and decryption. When the reverse operation is used, the data can be authenticated, at this time, the encryption is actually a digital signature, and the decryption is the verification of the signature. Considering factors such as security and a large amount of plaintext information, the HASH operation is generally performed first. See Table 1 for a summary of the RSA algorithm.

3.3. PKI (Public Key Infrastructure). PKI is a public key infrastructure, which is a new security technology, it uses public key encryption technology to provide a set of security basic platforms, and users can use the services provided by the PKI platform to communicate securely.

The basis for users of the PKI system to establish a secure communication trust mechanism is: any communication on

TABLE 1: Summary of the RSA algorithm.

Public key	$n = p \cdot q$ (p, q keep secret), e and $(p-1)(q-1)$ coprime
Private key	$d = e^{-1} \pmod{(p-1)(q-1)}$
Encryption	$C = M^e \pmod{n}$
Decrypt	$M = C^d \pmod{n}$

the Internet that requires security services is based on the public key, and the private key is only in the hands of the other party that the communication trusts. The basis of trust is achieved through the use of public key certificates. A public key certificate is the combination of a user's identity and the public key held by him before the combination, a trusted authority CA verifies the user's identity, and then the certificate combines the user's identity and the corresponding public key, and the digital sign to prove the validity of its certificate.

3.4. Improved RSA Algorithm. The specific description of the RSA algorithm is as follows:

- (1) Arbitrarily select two different large prime numbers p and q to calculate the product $n = pq$, $\phi(n) = (p-1)(q-1)$
- (2) Arbitrarily select a large integer e that satisfies $\gcd(e, \phi(n)) = 1$, and the integer e is used as the encryption key (note: the selection of e is very easy, for example, all prime numbers greater than p and q are available);
- (3) The determined decryption key d , if you know e and $\phi(n)$, it is easy to calculate d
- (4) The integers n and e are made public, and d is kept secret
- (5) Encrypt plaintext m ($m < n$ is an integer) into ciphertext c , and the encryption algorithm is $c = E(m) = m^e \pmod{n}$;
- (6) Decrypt the ciphertext c into plaintext m , and the decryption algorithm is $m = D(c) = c^d \pmod{n}$;

However, it is impossible to calculate d from only n and e (note: not p and q). Therefore, anyone can encrypt the plaintext, but only authorized users (who know d) can decrypt the ciphertext.

After analyzing the security of the RSA algorithm, the author proposes some improvements to the RSA algorithm to make it more secure and faster. First of all, there are many parameters in the RSA algorithm, the selection of these parameters directly affects the security and operation speed of the RSA algorithm, the selection of RSA parameters is very important, and the optimization of the algorithm itself is also very critical.

Technically, the security of the RSA algorithm is equivalent to the difficulty of solving the inverse of the RSA one-way function. However, in practical applications, attacks are often caused by loopholes in algorithm implementation details, therefore, when using the RSA algorithm to construct a cryptosystem, in order to ensure the security of the system, each parameter must be carefully selected. RSA has three main parameters: modulus n , encryption key e , and decryption key d .

In modern cryptography, a public key cryptosystem occupies an important position, as the representative of the public key cryptosystem, the RSA cryptosystem is widely used in various fields of modern information security technology. However, the power residual calculation adopted by this algorithm is time-consuming, which has always been a bottleneck restricting its wide application. Both encryption and decryption in RSA involve raising an integer to the power, modulo n . If you do the exponentiation on the integer first, then modulo n , the intermediate result will be huge. Fortunately, there is a feature of modulo arithmetic that can be exploited:

$$[(a \bmod n) * (b \bmod n)] \bmod n = (a * b) \bmod n. \quad (3)$$

Thus, a modulo n operation can be performed on the intermediate result, which can make the calculation practical.

3.5. System Structure. The integer limit that can be represented by a 32-bit computer is 64 bits, and the large prime number required in the RSA algorithm used by the author is at least 100 bits. Therefore, in the realization of this program, the first thing that comes to mind is how to store these large numbers, and how to establish the operation library of these large numbers. Generally, a large array is used to represent this large number. During operation, the array can be regarded as a binary stream, and the purpose can be achieved by different bit operations. Currently, on 32-bit systems, an array of unsigned long can be defined. Because unsigned long is 32 bits. If you want to generate a 1024-bit key, you need to set the dimension of this array to 32. Figure 2 is the main flowchart of this program.

In order to figure out how to get n , e , and d , basically the program first generates a large prime number e , then it generates a prime number q , and ensures that e and $q-1$ are relatively prime, and also generates a large prime number p , ensures that e and $p-1$ are relatively prime, and then calculate $n = p * q$, after obtaining n , we compare the sizes of n and e . If $e \geq n$ then we go back to the beginning, if $e < n$, then n and e are successfully found. As for calculating d , can be based on formula $d = e^{-1} \bmod (p-1) * (q-1)$. Figure 3 is a flowchart of how to get these numbers.

So, what is the specific process of GET e , GET q , and GET p in Figure 3, because they are all large prime numbers generated randomly, one algorithm can be used uniformly. First, randomly generate a large number, and then you can set this large number to ensure that it is large enough and odd. Then you can judge whether the number is prime or not. As for the method for judging prime numbers, the Rabin–Miller probabilistic primality test is used because only prime numbers can pass all the tests. Figure 4 roughly describes this process.

4. Analysis of Results

4.1. System Operation Results. Test text file test.txt, the text content is 1234567890test, because there may be machine factors that affect the encryption speed, the optimized RSA algorithm, and the algorithm combined with the SMM

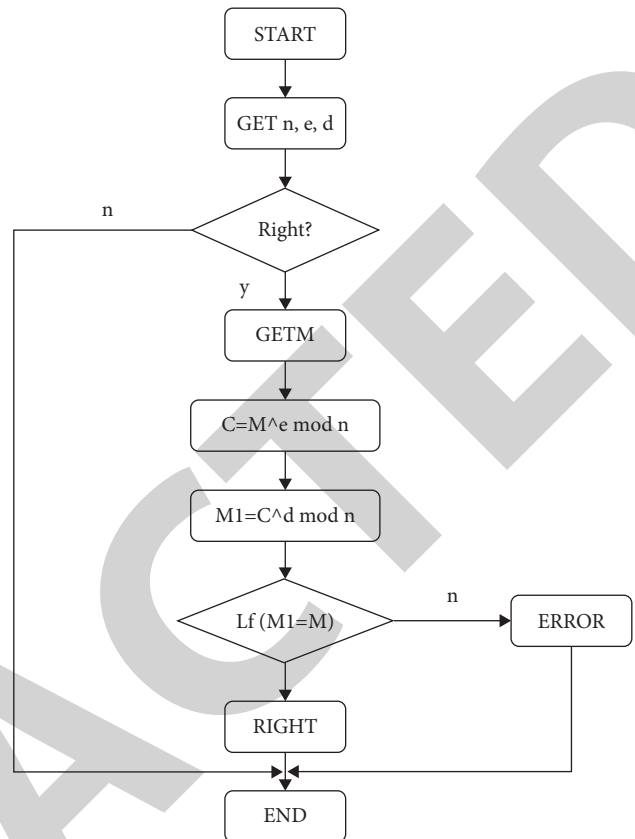


FIGURE 2: Main program flowchart.

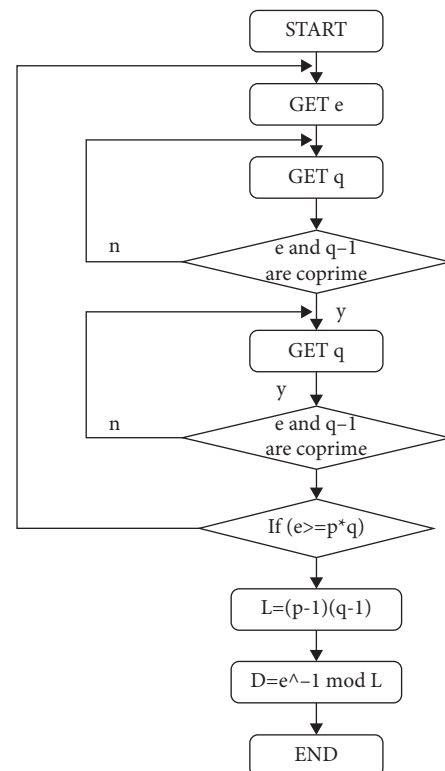


FIGURE 3: GET n, e, d flowchart.

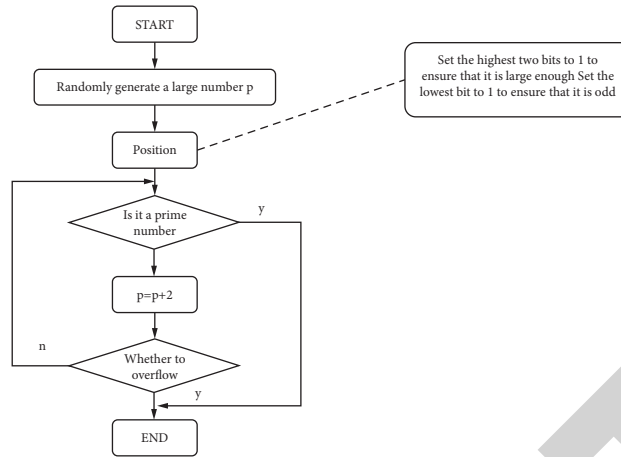


FIGURE 4: Flowchart of generating large prime numbers.

TABLE 2: 40-bit modulus experimental results.

Operation time (select 40-bit modulo)	Time required for traditional algorithm (s)		Time required for combining algorithms (s)	
	Encryption operation	Decryption operation	Decryption operation	Decryption operation
First	2.754	2.884	2.694	2.794
The second time	2.754	2.905	2.694	2.884
The second time	2.754	2.914	2.784	2.884
The fourth time	2.764	2.914	2.704	2.794
The fifth time	2.754	2.884	2.684	2.886
Average time	2.765	2.898	2.694	2.894

TABLE 3: Experimental results of 80-bit modulus.

Operation time (select 80-bit modulo)	Time required for traditional algorithm (s)		Time required for combining algorithms (s)	
	Encryption operation	Decryption operation	Decryption operation	Decryption operation
First	17.895	18513	17.635	18.496
The second time	17.958	18.503	17.815	18.496
The second time	17.881	18.582	17.831	18.492
The fourth time	17.705	18.503	17.759	18.492
The fifth time	17.928	18.572	17.822	18.482
Average time	17.862	18.533	17.762	18.493

TABLE 4: Experimental results of 100-bit modulus.

Operation time (select 100-bit modulo)	Time required for traditional algorithm (s)		Time required for combining algorithms (s)	
	Encryption operation	Decryption operation	Decryption operation	Decryption operation
First	35.474	39.658	35.468	39.588
The second time	35.424	39.782	34.589	39.536
The second time	35.485	39.698	34.986	39.552
The fourth time	35.492	39.724	34.765	39.568
The fifth time	35.485	39.756	35.269	39.562
Average time	35.476	39.731	35.083	39.569

method (now called the combined algorithm for the time being). The traditional algorithm and the combined algorithm are tested three times, and the average time is used to compare the running efficiency of these algorithms. Considering the performance of the computer used in the

experiment, we did not use an excessively large number to conduct the experiment, the comparison between the traditional algorithm of 40, 80, and 100-bit modulus and the combined algorithm is given below, the results are shown in Table 2–4 and Figure 5.

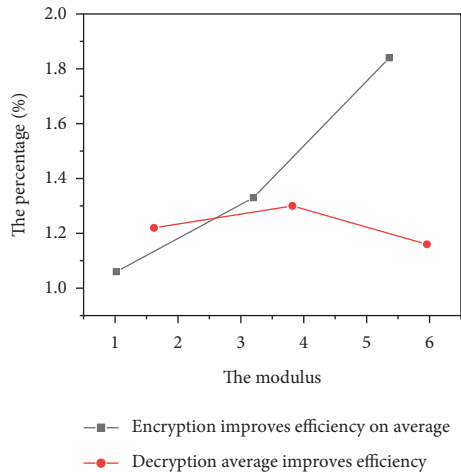


FIGURE 5: Encryption and decryption increase efficiency on average.

From the above data, it can be seen that, after reasonable selection of parameters and the use of optimized algorithms (also called combined algorithms), the RSA algorithm is about 1.0% to 2% more efficient than the traditional algorithm, which improves the operational efficiency of the RSA algorithm to a certain extent, the purpose of improving the RSA algorithm is achieved.

5. Conclusion

This subject mainly studies the application of the public key cryptosystem in the network information security system, the algorithm used is the representative algorithm RSA in the public key cryptosystem. The author establishes the network information security model based on PKI, considering that the PKI technology is based on the public key cryptosystem. The public key cryptosystem meets the requirements for information security in today's era, and the RSA algorithm in public key cryptography plays an important role in cryptography. The obtained results are as follows: an improved RSA algorithm is implemented, and the algorithm is applied in data encryption and digital signature, which improves the running speed of the system to a certain extent. A comprehensive understanding of PKI is presented. In order to meet the needs of network development, the author proposes a linear, an RSA-based (n, n) -oriented group signature scheme, this scheme reduces network overhead, it also prevents blind signatures. From the current point of view, in order to meet the actual needs, digital image encryption technology will further improve the confidentiality, encryption and decryption speed, and compression ratio, at the same time, the direction of reducing the computational complexity is developed. The research on image encryption technology is still in its infancy, and there are still a lot of problems to be further explored and developed. Practice has proved that this scheme can realize the fast and secure transmission of data and information, and provides an effective means for

the transmission of confidential documents on the network, so it has a good application prospect.

Data Availability

The data used to support the findings of this study are available from the corresponding author upon request.

Conflicts of Interest

The authors declare that they have no conflicts of interest.

References

- [1] L. M. Jawad, T. Abbas, and D. W. Ahmed, "An effective color image encryption scheme based on double piecewise linear chaotic map method and rc4 algorithm," *Journal of Engineering Science & Technology*, vol. 16, no. 2, pp. 1319–1341, 2021.
- [2] A. T. Hashim, A. K. Jabbar, and Q. F. Hassan, "Medical image encryption based on hybrid aes with chaotic map," *Journal of Physics: Conference Series*, vol. 1973, no. 1, p. 13, Article ID 012037, 2021.
- [3] S. Roy, M. Shrivastava, U. Rawat, C. V. Pandey, and S. K. Nayak, "Iesca: an efficient image encryption scheme using 2-d cellular automata," *Journal of Information Security and Applications*, vol. 61, no. 5, Article ID 102919, 2021.
- [4] P. W. Khan and Y. Byun, "A blockchain-based secure image encryption scheme for the industrial internet of things," *Entropy*, vol. 22, no. 2, p. 175, 2020.
- [5] K. A. K. Patro and B. Acharya, "An efficient dual-layer cross-coupled chaotic map security-based multi-image encryption system," *Nonlinear Dynamics*, vol. 104, no. 3, pp. 2759–2805, 2021.
- [6] F. Yu, Z. Zhang, H. Shen, Y. Huang, S. Cai, and S. Du, "Fpga implementation and image encryption application of a new prng based on a memristive hopfield neural network with a special activation gradient," *Chinese Physics B*, vol. 31, no. 2, p. 10, Article ID 020505, 2022.
- [7] T. Sivakumar, M. Pandi, N. Senthil Madasamy, and R. Bharathi, "An image encryption algorithm with hermite chaotic polynomials and scan pattern," *Journal of Physics: Conference Series*, vol. 1767, no. 1, p. 12, Article ID 012044, 2021.
- [8] S. De, J. Bhaumik, and D. Giri, "A secure image encryption scheme based on three different chaotic maps," *Multimedia Tools and Applications*, vol. 81, no. 4, pp. 5485–5514, 2022.
- [9] C. Zou, X. Wang, and H. Li, "Image encryption algorithm with matrix semi-tensor product," *Nonlinear Dynamics*, vol. 105, no. 1, pp. 859–876, 2021.
- [10] N. Mahendiran and C. Deepa, "A comprehensive analysis on image encryption and compression techniques with the assessment of performance evaluation metrics," *SN Computer Science*, vol. 2, no. 1, pp. 1–12, 2021.
- [11] N. Rani, S. R. Sharma, and V. Mishra, "Grayscale and colored image encryption model using a novel fused magic cube," *Nonlinear Dynamics*, vol. 108, no. 2, pp. 1773–1796, 2022.
- [12] Y. Liu, J. Zhang, D. Han, P. Wu, Y. Sun, and Y. S. Moon, "A multidimensional chaotic image encryption algorithm based on the region of interest," *Multimedia Tools and Applications*, vol. 79, no. 25, pp. 17669–17705, 2020.
- [13] S. Kanwal, S. Inam, O. Cheikhrouhou, K. Mahnoor, A. Zaguia, and H. Hamam, "Analytic study of a novel color image encryption method based on the chaos system and color codes,"

Retraction

Retracted: Based on Virtual Reality Technology Research on Innovation and Design of Ceramic Painting Products

Mathematical Problems in Engineering

Received 8 August 2023; Accepted 8 August 2023; Published 9 August 2023

Copyright © 2023 Mathematical Problems in Engineering. This is an open access article distributed under the Creative Commons Attribution License, which permits unrestricted use, distribution, and reproduction in any medium, provided the original work is properly cited.

This article has been retracted by Hindawi following an investigation undertaken by the publisher [1]. This investigation has uncovered evidence of one or more of the following indicators of systematic manipulation of the publication process:

- (1) Discrepancies in scope
- (2) Discrepancies in the description of the research reported
- (3) Discrepancies between the availability of data and the research described
- (4) Inappropriate citations
- (5) Incoherent, meaningless and/or irrelevant content included in the article
- (6) Peer-review manipulation

The presence of these indicators undermines our confidence in the integrity of the article's content and we cannot, therefore, vouch for its reliability. Please note that this notice is intended solely to alert readers that the content of this article is unreliable. We have not investigated whether authors were aware of or involved in the systematic manipulation of the publication process.

Wiley and Hindawi regrets that the usual quality checks did not identify these issues before publication and have since put additional measures in place to safeguard research integrity.

We wish to credit our own Research Integrity and Research Publishing teams and anonymous and named external researchers and research integrity experts for contributing to this investigation.

The corresponding author, as the representative of all authors, has been given the opportunity to register their agreement or disagreement to this retraction. We have kept a record of any response received.

References

- [1] Y. Jiang, "Based on Virtual Reality Technology Research on Innovation and Design of Ceramic Painting Products," *Mathematical Problems in Engineering*, vol. 2022, Article ID 4421769, 7 pages, 2022.

Research Article

Based on Virtual Reality Technology Research on Innovation and Design of Ceramic Painting Products

Yong Jiang 

Nantong Vocational University, Nantong, Jiangsu 226007, China

Correspondence should be addressed to Yong Jiang; 20148432@stu.sicau.edu.cn

Received 22 May 2022; Revised 20 June 2022; Accepted 4 July 2022; Published 20 July 2022

Academic Editor: Hengchang Jing

Copyright © 2022 Yong Jiang. This is an open access article distributed under the Creative Commons Attribution License, which permits unrestricted use, distribution, and reproduction in any medium, provided the original work is properly cited.

In order to obtain the complete color point cloud data of traditional ceramic artworks and reconstruct them efficiently, a 3D digital reconstruction method of ceramic painting products based on virtual reality technology was proposed. By the method, the 3D color point cloud data of ceramic works were collected by the camera 3D scanning equipment. The new postprocessing methods such as fusion and repair were investigated and proposed so as to obtain the complete optimized color point cloud information. The high-fidelity 3D mesh model and simplified mesh of ceramic artworks were obtained through the mesh process and the digital display platform was developed by using virtual reality technology. The experiment results showed that the 3D color point cloud data of traditional ceramic artworks were obtained by +5 exposure blend methods on average in the 6 combined modes and point cloud optimization and repair were completed. High-precision color mesh model was generated and digital promotion and publicity were carried out. The proposed 3D reconstruction technology and virtual display method made a positive exploration for the protection, inheritance, and promotion of China's ceramic artworks and made a new attempt for the digital protection of cultural heritage by using modern science and technology.

1. Introduction

In the Neolithic period, human beings began to make and use pottery. After thousands of years of development and evolution, glazed pottery gradually emerged. Then, in the feudal society period when human beings mastered fire more skillfully, human beings were able to make ceramics with a more dense molecular arrangement and smoother surface glaze. In the early stage of ceramics development, ceramics were always developed to meet practicality first and then shape and decoration [1]. After the social productive forces gradually met the needs of human basic survival, the functions and application scenarios of ceramics also changed. From their original role as containers, they have developed into objects with ornamental collection value, even for funeral, marriage, and so on. The development of ceramic products design coincides with Maslow's Demand Theory.

People begin to pursue spiritual aesthetic needs when practicality is satisfied. Therefore, the evolution trajectory

of ceramics is determined and dominated by social productivity, human material life, and human spiritual needs [2].

Ceramics design methods are also changing with the changes of social productivity and technology, from traditional manual design to CAD software aided design. With the gradual maturity of VR technology, VR technology has also been applied to the design industry. Nowadays, the application of VR technology in the design industry includes interior, landscape, automobile, aircraft, electronic products, and other fields, but there are still very few cases and practices in the field of ceramics design [3].

Virtual Reality (VR for short) is a new technology in the middle of the twentieth century. This technology is pioneered in the United States. After half a century of exploration and practice in various laboratories and university research institutes, this technology has gradually been mature and gradually entered people's vision in production, entertainment, innovative research, and other aspects.

2. Literature Review

EA Filonova et al. developed SpmAR, a software with a very user-friendly interface for rapid 3D model building [4]. Demidov et al. focused on the visualization research of virtual reality and developed a virtual holographic system, which solved the limitations of current interaction technology [5]. Jijun et al. developed an olfactory simulator, which was a breakthrough in the research of virtual reality technology in the field of olfactory. Once the fruit in the virtual space was placed on the nose tip wearing the olfactory simulator, the user could smell the fragrance of the fruit emitted by the device at the nose tip [6]. Liu et al. provided a virtual reality demonstration environment by integrating distributed virtual environment, as well as a virtual reality system for pilot training, a 3D dynamic database, and a development platform for a virtual reality-based application system. They also focused on the representation and processing of physical characteristics of objects in the virtual environment and developed some hardware for visual interface in virtual reality [7]. Iijima et al. made a further progress in VR technology and found more foothold for the technology, such as education, design, and other fields, giving virtual reality technology more possibilities and greater development prospects [8]. Xu et al. focused their research in VR on the representation and processing of physical characteristics of objects in a VR environment [9]. Bounareli et al. established a desktop virtual building environment real-time roaming system [10]. Xie et al. carried out a 3D reconstruction of the pagoda to protect this world's cultural heritage in a digital form. Moreover, the Palace Museum in China completed the 3D digitalization of many cultural relics and displayed them on the online platform of "Digital Heritage Library," which was open to people to browse the 3D models of cultural relics [11].

In the above-given data acquisition method, 3D location information and surface color information are obtained separately. In the later texture mapping process, due to the influence of human factors, the accuracy of mapping location is inevitably not high, resulting in the matching degree of the 3D reconstruction model and original cultural relics being affected. At the same time, traditional ceramic artworks have their unique attributes, such as the complexity of the model and the high reflective property of the surface glaze, which inevitably leads to data missing and model holes in the data collection. In addition, the richness of the glaze color on the ceramics surface also poses a new challenge to the color reducibility of the 3D reconstruction model surface. On the basis of integrating the current 3D data acquisition technology, the technical route and implementation plan suitable for the 3D digital collection of ceramic cultural relics are proposed. Combined with the color point cloud overlapping algorithm and hole repair algorithm, the complete information reconstruction of ceramic cultural relics is realized. In cooperation with Guangdong Ceramic Museum, data collection of 115 ceramic artworks has been realized by using the proposed technology and methods and the promotion and inheritance of traditional cultural heritage has been innovatively realized by using virtual reality and other information means.

3. Research Methods

3.1. Artistic Features of Ceramics and 3D Reconstruction Scheme

3.1.1. The Artistic Characteristics of Ceramics. Ceramics originated in the late Neolithic Age. After a long period of development and accumulation, ceramics developed rapidly in the Tang and Song dynasties and reached prosperity in the Ming and Qing Dynasties [12]. According to the records, the Ming Dynasty pottery production had been "initially divided into eight processes" and firing technology and product quality were greatly improved. Traditional ceramics artists gave full play to the good plasticity of local clay to create a large number of vivid and modelling complex characters, such as animals, birds, flowers, fruits, and vegetables. They also made use of the plant ash, scrap metal, and jade residue by local people's workshops to produce ceramic glaze, forming a thick dignified, and colorful characteristics [13].

3.1.2. 3D Reconstruction of Ceramics. The first step of 3D reconstruction is to obtain accurate data information. According to the characteristics of ceramics, the best scheme is to obtain the 3D position information and color information of the object at the same time in this stage to ensure the authenticity and accuracy of the collected data. At present, the commonly used noncontact 3D scanning equipment includes laser, structured light, and photographic 3D scanners.

The laser 3D scanner can calculate the spatial information of the object by projecting the laser beam to the object and getting the reflected beam from the receiving sensor. It has the characteristics of a high data sampling rate and high precision. However, the reflectivity of the scanned object is easy to affect the reflection of the laser beam. And, the surface texture, environment, and structure are easy to make the data scanned by laser have a large number of noise points. In addition, the laser scanner can only collect 3D spatial data of objects, while texture and color data need to be processed by artificial mapping and texture mapping by digital camera shooting.

A structured light 3D scanner uses a raster projection unit to project a group of raster fringe with phase information onto the surface of the object. Using the principle of stereo camera measurement, it can quickly obtain high-density 3D data information on the surface of the object. It has the characteristics of fast scanning speed and high measurement accuracy. Also, this method still has data missing for surface highlights and cannot get the color information of the object.

Photographic 3D scanner (also called image modelling) is a more advanced technology products in recent years. The structured light and computer vision technology are fused to quickly get a series of images to calculate, the scanned object space position information is restored and the color of the object surface texture information is obtained at the same time. Because the reflectivity of the scanned object is less affected, relatively complete surface information can be

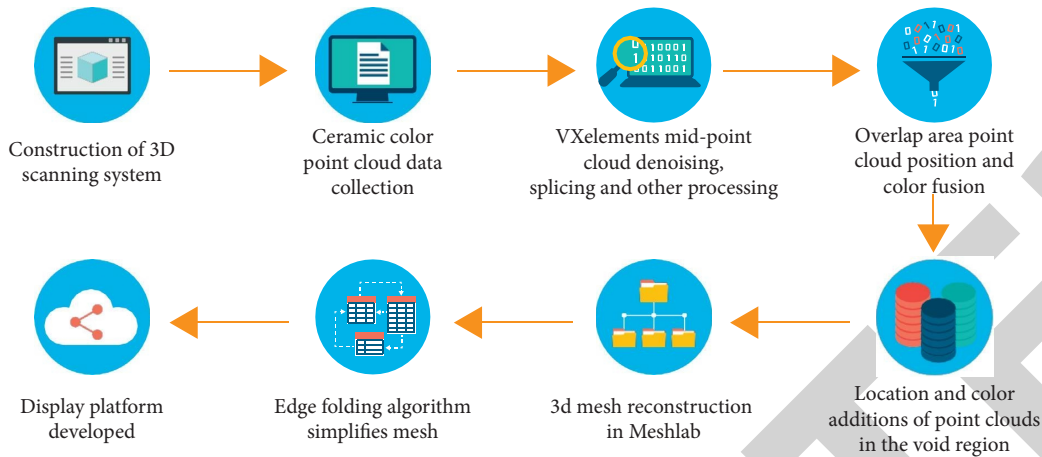


FIGURE 1: 3D reconstruction scheme.

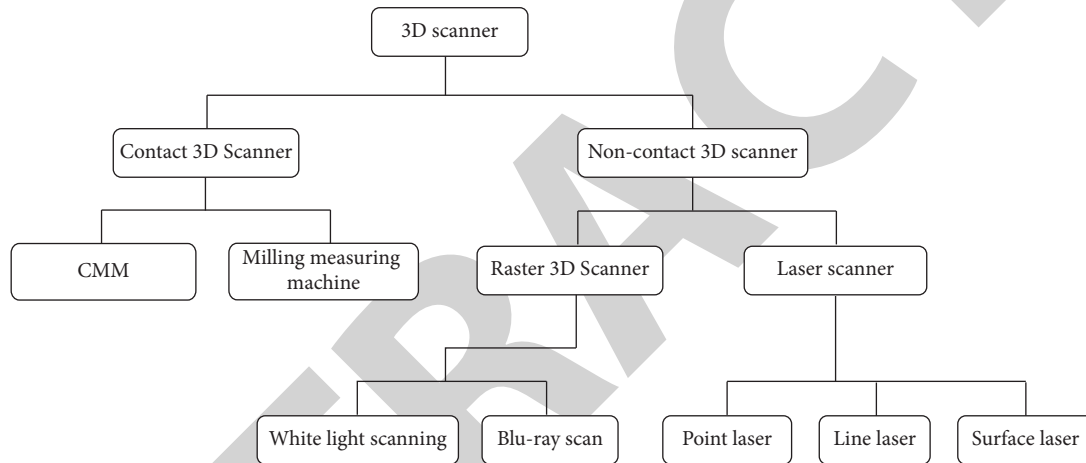


FIGURE 2: Classification of 3D scanners.

collected without spraying an imaging agent or other processing. As it is based on color digital image, 3D data with texture information can be obtained directly, which is very suitable for the digital collection of ceramic artworks.

Since it is impossible to scan the 3D information of each orientation of the same object at one time and most artworks have their own occlusion phenomenon, it is necessary to scan multiple times to obtain more comprehensive data in practical work. At the same time, 3D data acquired by scanning equipment still inevitably have problems such as noise points and data missing, which requires post-processing such as denoising, splicing, overlapping area fusion, and hole repair of the collected data. Finally, a complete 3D mesh model is obtained through meshing and the digital content is applied. Considering the above-given factors, the 3D reconstruction scheme of ceramic artworks is shown in Figure 1 [14].

3.2. 3D Data Acquisition and Processing

3.2.1. Acquisition of 3D Data of Ceramic Artworks. There are many kinds of 3D scanning equipment, which can be roughly

divided into two kinds: a contact scanner and a noncontact scanner. Contact scanner is mainly representative of the three coordinate measuring machine and milling measuring machine. Noncontact scanner has a raster 3D scanner and a laser scanner in two categories. Grating 3D scanner can also use white light scanning or blue-ray scanning two measurement methods. The laser scanner can be divided into point laser, line laser, and surface laser scanner according to the laser type [15] as shown in Figure 2.

The camera 3D scanner consists of two digital cameras, a color camera, a white light projector, and multiple LED white lights. It also uses two high-performance graphics workstations and is equipped with NVIDIA RTX graphics cards and special scan control software VX elements. During the scanning process, the ceramic artworks are placed on a disc-shaped rotating platform. In the process of acquisition, the 3D resolution of the collection point cloud is set as 0.2 mm and the accuracy of the 3D model obtained under this resolution is as high as 0.1 mm. In addition, the LED white light completely covers the scanning area and the acquisition work is carried out in a stable white light environment with no strong reflective objects around, which is conducive to accurately obtaining the color value of the

TABLE 1: Product parameters of the scanner.

Weight	950 g
Size	154 × 178 × 235 mm
Measuring rate	550,000 measurements per second
Scanning area	143 mm × 108 mm
Light source	White light (LED)
Resolution ratio	0.1 mm
Volume precision	0.3 mm/m
Locating method	Geometric shapes and/or colors and/or objects
Reference distance	380 mm
Depth of field	100 mm
Component size range (recommended)	0.05–0.5 m
Texture resolution	50–250 DPI
Texture color	24 bit
Software	VX elements

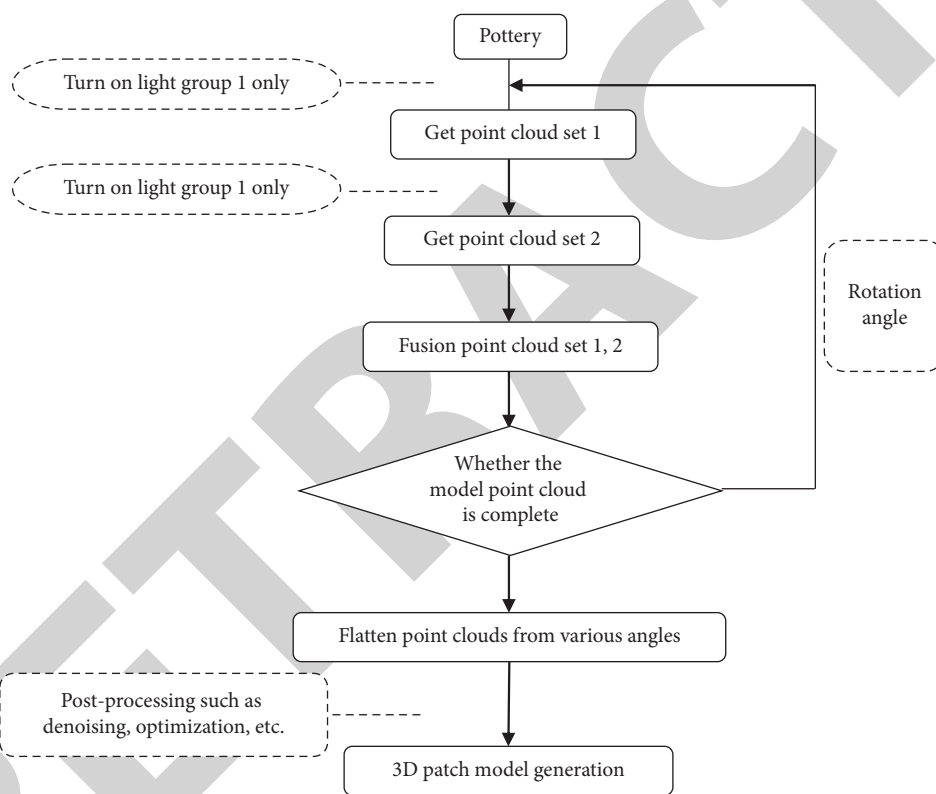


FIGURE 3: 3D model acquisition process.

surface of the ceramic artworks. The product parameters of the scanner are shown in Table 1.

3.2.2. Preprocessing of the Acquired Data. After the scanning and software calculation, 3D data still had some defects. It was mainly manifested as a large number of outliers. For the occluded parts, the data were lost inevitably so that holes appeared in some places. The 3D data obtained by fractional scanning needed to be spliced. Scanning control software VX elements was used to initially complete the removal of outliers, scanning data splicing, and hole repair. But the hole repair results were not ideal and overlapping data often existed in point cloud splicing, which required further fusion processing [16].

3.2.3. Point Cloud Acquisition Process. After determining the scanner model, the work of point cloud data acquisition of ceramic cultural relics began. The practice process was shown in Figure 3 [17]. First, with other environmental factors (the ceramic artwork placement position, scanner fixed position, etc.) unchanged, light group 1 and light group 2 were opened, respectively. The points from the same angle scanned under the two light groups were obtained successively and the point clouds of the two groups were aligned and fused. Then, it was judged whether the point cloud obtained in the above steps constituted a complete point gathering of the model. If not, the model was rotated at a certain angle (it varied according to the complexity of different ceramic models) and all the above-given steps were

repeated until the complete point gathering was obtained. The fused points obtained from various angles were gathered and spliced, denoised, optimized, and other postprocessing, and finally the 3D surface model of ceramic sculpture was obtained.

3.2.4. Alignment Fusion and Stitching Integration of Point Cloud Data. In order to align and fuse the two sets of point cloud data accurately, it was recommended to adopt the iterative nearest point algorithm, also known as the ICP algorithm. The ICP algorithm was simple and easy to implement iterative calculation. And, it could also achieve high matching accuracy, so it was an effective and fast algorithm. Figure 4 showed the flow chart of the ICP algorithm [18]. In practical application, the local extremum may fail to converge due to the improper initial point. The ICP algorithm was used mainly to calculate the matching relation between two sets of point gathering and the transformation parameter the rotation matrix R and the translation vector t of the two sets of point gathering through least square iteration. And, then the matching and alignment between two sets of point clouds were completed. The ceramic shapes were mainly characters, flowers, and birds, with prominent morphological characteristics, which was easy to define the corresponding marking points. In the experimental process, two groups of point cloud data were obtained under two groups of light sources with different directions according to the method proposed previously, namely, point gathering A and point gathering B . N pairs of identification points were determined in A and B as initial conditions. The least square method was used to calculate the minimum value of error function F . The formula was as follows. At this point, the rotation matrix R and the translation vector t were obtained [19].

$$F = \min \frac{1}{k} \sum_{i=1}^N B_i - (RA_i + t)^2. \quad (1)$$

4. Results and Analysis

4.1. Mesh Reconstruction of Color Point Cloud. The 3D ceramic data in the color point cloud form is in a discrete state, which requires surface mesh reconstruction. Namely, topological relations between points are established to obtain continuous surface characteristics so as to be applied to more development processes. The most commonly used mesh reconstruction methods include surface reconstruction algorithm based on the Poisson equation, Delaunay triangulation algorithm, and related optimization methods. Through the above-given work, ceramic color point cloud data can well maintain the uniform distribution law and retain normal information, providing an excellent data basis for Poisson mesh reconstruction [20].

Poisson mesh reconstruction can better mesh the original sharpness and angle characteristics of the ceramic and restore the shielding parts with a high degree of authenticity.

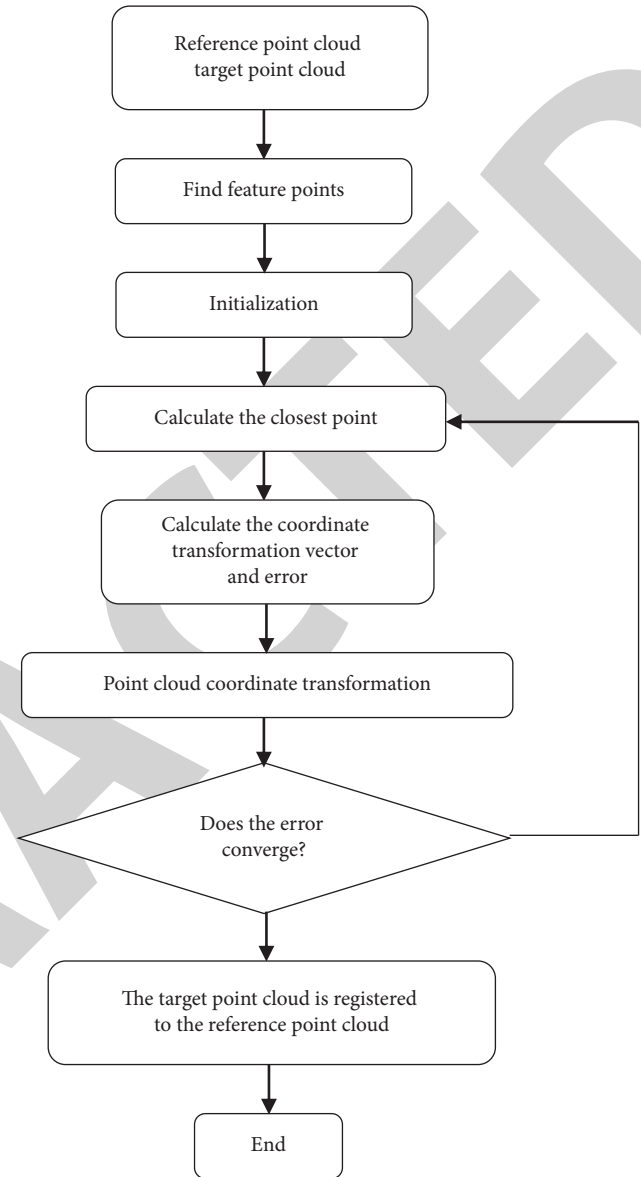


FIGURE 4: Flow chart of ICP algorithm.

4.2. Simplification of Color Mesh Model. The high-precision 3D mesh model obtained above records the detailed and complete information of ceramic works, which can not only provide professionals with the characteristics of ceramic sculpture techniques but also serve as the source data of 3D reproduction and physical restoration. However, due to its large amount of data and high resource occupation, it is not suitable for virtual display and Internet application directly, so simplifying the mesh complexity of the 3D model has become an essential link [21, 22].

The principle of model simplification is to reduce the number of model meshes as much as possible on the premise of ensuring information fidelity. Firstly, the vertex color information of the high-precision color mesh is mapped to the texture image by UV expansion, and the concave and convex information of the model surface is recorded into the normal map. Then, mesh simplification algorithms (such as

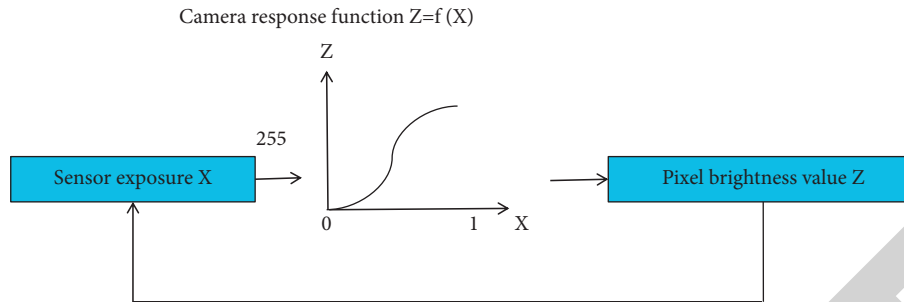


FIGURE 5: Camera response curve function.

Meshlab's edge folding simplification algorithm) are used to reduce the number of mesh faces and obtain the simplified low-precision mesh model. Finally, texture images and normal maps are baked onto low-precision mesh models to retain the visual effect of the original data to the maximum extent [23].

There are two software synthesis methods of HDR images, one is the pixel domain synthesis method and the other is the irradiated general image restoration and reconstruction method. The irradiance information content in natural scenes can be restored by solving the camera response function, synthesizing HDR images, and displaying HDR images [24]. The response function corresponding to the camera response curve can transform the radiation brightness of the real scene into the pixel value of camera imaging through the nonlinear system, as shown in Figure 5. The camera response function has the characteristics of propriety, smooth continuity, nonlinearity, and monotonicity. A sequence of Dharma images taken with multiple exposures are chosen and an exposure blend is selected, then Photomatix Pro allows you to choose +5 exposure blend methods on average in the 6 combined modes, each based on a different algorithm.

4.3. Development of Virtual Reality Application. The development of modern information technology and virtual reality opens up a new direction for the inheritance, activation, and popularization of cultural heritage. People do not have to spend the whole time on the museum and the exhibition hall and they can appreciate the artworks on a device in any place at any time.

Based on the previous research, a virtual display platform for ceramic artworks is developed including a computer terminal and mobile phone terminal. So the public can view ceramic artworks from a close distance and any angle and observe the rich glaze texture and morphological characteristics of ceramics from the details. In addition, the simplified mesh model of ceramics is also applied in the construction of a 3D ceramic display platform, and the tourism route with distinctive local cultural characteristics is jointly created with local museums so that people can know about ceramic artworks in advance [25].

5. Conclusion

With the development of science and technology and the progress of civilization, there will be more application

scenarios for the 3D digital reconstruction of cultural heritage, which plays a very positive role in promoting and inheriting traditional culture. Based on the characteristics of ceramic artworks, a 3D reconstruction method suitable for ceramic artworks with rich color information and complex shape was investigated and implemented. The method was efficient and convenient. And, the information was preserved completely. It was suitable for virtual reality application. At present, digital scanning and 3D reconstruction of 115 precious ceramic relics in the Ceramic Museum are completed. High-precision 3D ceramic mesh model is completed and related virtual reality applications are developed. With the continuous development of technology, this digital content will have more and more applications in the future. In general, the development of experimental software and hardware technology is still one of the reasons that restrict the wide application of this technology. The reconstruction and texture mapping of Shiwan ceramic relics by the existing 3D technology are difficult to be completely consistent with the original objects. However, problems such as the slow response speed of the virtual system and a lack of real-time operation still exist. But these problems can not prevent people from using digital technology to promote the process of digital protection of Shiwan ceramics.

Data Availability

The data used to support the findings of this study are available from the author upon request.

Conflicts of Interest

The author declares that there are no conflicts of interest.

References

- [1] D. Tejero-Martin, C. Bennett, and T. Hussain, "A review on environmental barrier coatings: history, current state of the art and future developments," *Journal of the European Ceramic Society*, vol. 41, no. 3, pp. 1747–1768, 2021.
- [2] N. Sata, F. Han, H. Zheng et al., "Development of proton conducting ceramic cells in metal supported architecture," *ECS Transactions*, vol. 103, no. 1, pp. 1779–1789, 2021.
- [3] G. Kordas, "Cuo (bromosphaerol) and cemo (8 hydroxyquinoline) microcontainers incorporated into commercial marine paints," *Journal of the American Ceramic Society*, vol. 103, no. 4, pp. 2340–2350, 2020.